Ioannis Doltsinis

Elements of Plasticity

Theory and Computation

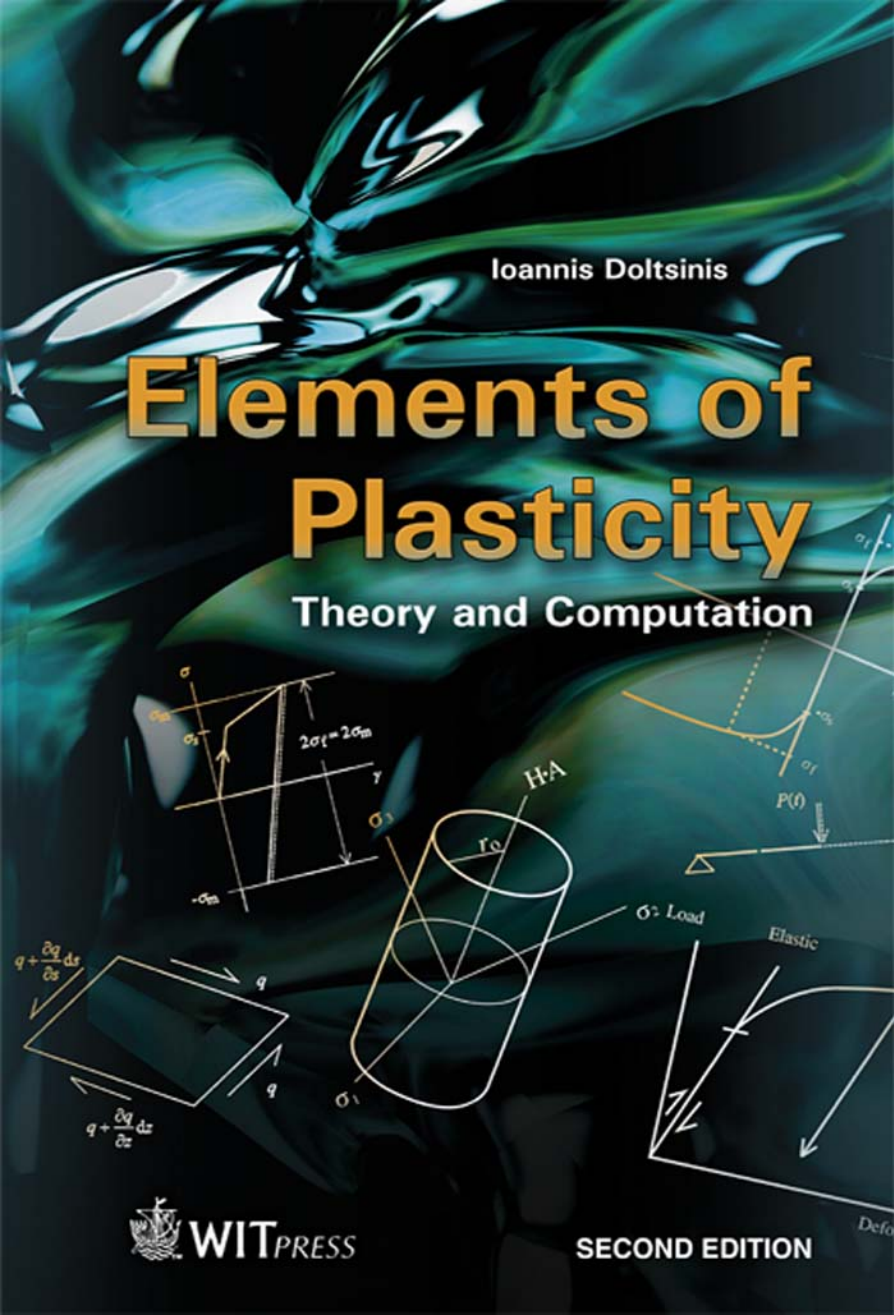

WIT PRESS

SECOND EDITION

Elements of Plasticity

Theory and Computation

WIT PRESS

WIT Press publishes leading books in Science and Technology.
Visit our website for the current list of titles.
www.witpress.com

WIT eLibrary

Home of the Transactions of the Wessex Institute, the WIT electronic-library provides the international scientific community with immediate and permanent access to individual papers presented at WIT conferences. Visit the WIT eLibrary at http://library.witpress.com

High Performance Structures and Materials

Objectives

The High Performance Structures and Materials series has been established to document the dynamic and rapid changes presently happening in the field of structural engineering. New concepts are constantly being introduced, and the series reflects the wide range of significant international research and development.

The series encompasses the following topics:

High Performance Structures
Nonlinear Structural Behaviour
Emerging Applications
Design Innovation
Smart Structures
Space Structures
Microstructures
Marine and Offshore Structures
Composite Structures
Retrofitting of Structures
Sustainability in Design
Shape and Topology Optimisation
Shock and Impact
Structural Capacity under Damage
Soil Structure Interaction
Material Technology
Dynamic Control of Materials
Smart Materials
Sensor Technology
Virtual Instrumentation
Numerical Methods
Computer Packages
Computer Modelling
Control Systems

Associate Editors

This page intentionally left blank

Elements of Plasticity

Theory and Computation

SECOND EDITION

Ioannis Doltsinis
Faculty of Aerospace Engineering and Geodesy
University of Stuttgart, Germany

WIT*PRESS* **Southampton, Boston**

Ioannis Doltsinis
Faculty of Aerospace Engineering and Geodesy
University of Stuttgart, Germany

The computer graphics of this volume and the original text processing in LaTex were carried out by Grethe Knapp Christiansen.

Published by

WIT Press
Ashurst Lodge, Ashurst, Southampton, SO40 7AA, UK
Tel: 44 (0) 238 029 3223; Fax: 44 (0) 238 029 2853
E-Mail: witpress@witpress.com
http://www.witpress.com

For USA, Canada and Mexico

WIT Press
25 Bridge Street, Billerica, MA 01821, USA
Tel: 978 667 5841; Fax: 978 667 7582
E-Mail: infousa@witpress.com
http://www.witpress.com

British Library Cataloguing-in-Publication Data

A Catalogue record for this book is available
from the British Library

ISBN: 978-1-84564-428-4

ISSN: 1469-0071

Library of Congress Catalog Card Number: 2009932305

Printed in Great Britain by Lightning Source UK Ltd., Milton Keynes

Contents

This page intentionally left blank

Preface to the second edition

The good reception to the first edition in academia as well as among practising engineers and the positive echo throughout the professional community have been understood as an obligation to continue caring about the contents of the book. Using *Elements of Plasticity* in the class as a companion textbook to the related course taught by the author at Stuttgart University revealed, over the years, space for improvements, now implemented in the second edition. It is anticipated that the readership will benefit even more from the revised text, which has been supplemented where advisable.

Apart from the impulses that came while teaching the subject, helpful suggestions have been contributed by readers of the book. As in the first edition, the author has pleasure in acknowledging the indispensable assistance of Grethe Knapp Christiansen in processing the text. Thanks are due to the Publishers for encouraging the project and for its efficient realization.

Ioannis Doltsinis
Stuttgart, Germany
January 2010

This page intentionally left blank

Preface to the first edition

Plasticity, the ability to undergo permanent deformations, is a property of metallic materials that has great significance for the load carrying behaviour of engineering structures, and for the manufacturing of structural components by forming processes. This book deals with the load carrying aspect of plasticity. In particular, deformations are considered infinitesimal and emphasis is placed on the distribution and intensity of stress and permanent strain. Unlike elasticity, under plastic conditions solutions are not scalable. Instead they evolve during the course of loading, as a result of the interaction between the structural system and the changing material characteristics. The storage of stress that may accompany plastic strain determines the behaviour upon unloading and subsequent loading cycles. At the same time, the stress limiting properties of plastic materials allow for the estimation of the load carrying capability of structures, and of failure limits under time varying conditions. This situation is of vital importance to the structural analyst and to the design engineer, who are forced to establish the strength of the structure for safety under the constraints of minimum material and weight, and thus have to account for plasticity.

For the purpose of an overview to this volume, two phases will be distinguished in the evolution of the research topic of plasticity. In the first phase, researchers explored plastic and elastoplastic material behaviour and set up mathematical formalisms for its description, investigated the behaviour of elastoplastic structures, developed analytical solutions and postulated general theorems, thus establishing the theoretical foundations of plasticity. However, one fact ought not to be overlooked when considering this phase of research: the difficulty in obtaining solutions, because of the complexity of the rigorous material description, which lead to various compromising but nonetheless interesting alternative approaches. A representative stage of that era is documented in the literature (*Proceedings of the Second Symposium on Naval Structural Mechanics*, Brown University, Rhode Island, April 5–7, 1960, E.H. Lee and P.S. Symonds (Eds), Pergamon Press, Oxford, 1960).

The second phase of research, in which the author was involved, is characterized by the development of computational methods of elastoplastic analysis. The use of computational methods in structural analysis began in the 1950s and evolved into the finite element method, the boundary element method, and the other numerical methods that are widely used today. These

are not only utilized for standard investigations of stress and deformation, but also as research tools in various branches of science and engineering. Initial steps in computer-based elastoplastic analysis were explorative in nature. They combined physical and numerical constituents mostly dependent on intuition. The author, then at the Institute for Statics and Dynamics of Aerospace Structures, University of Stuttgart, has actively experienced the initiating impulses, and from the late 1960s had the opportunity to shape the development of rigorous numerical techniques of elastoplastic analysis. The prime objective was to produce stable and accurate computation schemes for application in engineering practice. Their implementation in the general-purpose, finite element software ASKA (Automatic System for Kinematic Analysis) with Dipl.-Ing. (ETH) Hans Balmer from the early 1970s was exclusively guided by industrial demands. The algorithms, continuously extended with regard to the structural elements, on one hand, and the inelastic material options (thermoplasticity, creep, viscoplasticity, soil materials), on the other hand, have also become standard procedures in the other commercial software PERMAS. The latter was developed from ASKA and has since progressed independently.

The community of practising engineers has shown, from the beginning, an interest in the advantages offered by the computational techniques of elastoplastic analysis, but at the same time scientists also showed a hesitancy in adopting the novel approach, despite its firm grounding in the basics of plasticity. Numerous seminars and workshops held at the international level served audiences from both industry and academia, and have given rise to considerable published material on the subject. On the other hand, working with graduating students has revealed a tendency among them to simply apply computer software with little regard to the circumstance. This motivated the author to establish a university course, which stressed the most important elements of plasticity to improve the physical understanding, to correctly posing problems of elastoplastic analysis, solving problems with the aid of the computer and providing a sound interpretation of the numerical results. This course is being taught by the author at the Faculty of Aerospace Engineering, University of Stuttgart, for almost two decades now. Working with students over a long period has revealed a need for *written* background material. Although some excellent monographs on plasticity are available and are referred to in this volume, the conventional treatment of the subject does not appear well suited for the purpose of a computer-oriented approach.

As a result, the present volume has been produced by bridging conventional theory and the numerical analysis of elastoplastic systems. The text focuses on the most important elements of theory and computation using matrix notation. It avoids the development of analytical solutions except for the purpose of illustration and verification. The scope of the book goes much further than the time limitations of the original, one-semester university course. In particular, it answers a more general demand for the subject,

and includes results of research and development work by the author and his team in computational plasticity, compiled from unpublished notes and from papers in professional journals. Complementary to plasticity, some considerations on creep and viscoplasticity have been added in the book, and a number of selected applications from engineering practice demonstrate the usage of computational techniques. The book is aimed equally at graduate students, practising engineers and consultants, and can serve either to elucidate computational concepts and tools for the analysis of elastoplastic structures and solids, or to further advance the essential knowledge of the subject.

The author would like to express his appreciation to WIT Press for their cooperation in publishing the book and for the care taken with its production.

Ioannis Doltsinis
Stuttgart, Germany
November 1999

This page intentionally left blank

Preliminaries

Introduction

This text is concerned with the mechanical response of elastoplastic solids and their characteristic properties in the consideration of structural analysis. Whenever appropriate, plasticity will be established by pointing out differences from elasticity. The latter subject is assumed to be sufficiently familiar to the reader to serve as a background for the present purpose. In this connection we refer to the classical textbook on the theory of elasticity by Timoshenko and Goodier [1].

In common language the term elasticity is sometimes used as a synonym for the deformability of a solid. It implies, however, that deformations disappear completely after the removal of the applied forces. Elastic materials are therefore not formable; changes in shape can be maintained only under the continuous action of forces. Beyond elasticity certain materials exhibit the property of plasticity (i.e. formability).

In substance this work refers primarily to metals. As illustrated by the schematic force–deformation diagram for a metallic specimen in Fig. 1, the resistance of the specimen to deformation – its stiffness – diminishes once the elasticity limit is exceeded, and removal of the force then recovers deformation only partially. The development of permanent deformation under moderate additional forces beyond the elasticity limit is characteristic of plasticity. This property is the basis for a number of important manufacturing processes in metal forming (e.g. forging, rolling, upsetting and extruding), which shape the desired part by significantly changing the original geometry of the workpiece material. Plasticity is beneficial for the production of structural parts by materials processing. The mathematical modelling and the numerical analysis of material deformation processes make up the contents of a different volume [2].

This account rather deals with the response of structures and structural components to applied loads. The appearance of plastic deformation under service conditions will affect the stress and strain response to the loading programme and the load-carrying capacity in a manner not predictable by the elastic analysis of the structure. In order that stress and strain are reproducible under the loading conditions, the structure is, as a rule, not permitted to exceed the elasticity limit of the material during standard

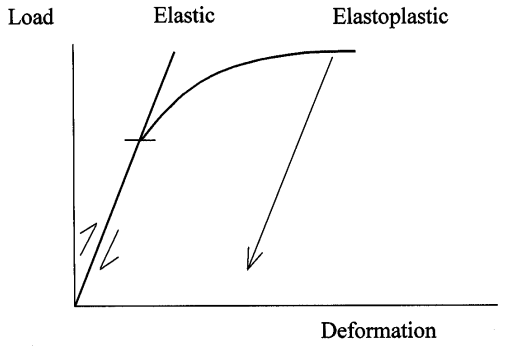

Figure 1: Elastoplastic vs elastic response.

operation. Structural design (specifying dimensions of load-carrying components) is not restricted, however, to service conditions, but also accounts for the safety of the system in critical situations. Keeping stress levels below the elasticity limit for both service and safety does not utilize the reserve capacity of the structure when deforming plastically. For an appropriate employment of the material, overloading at extreme situations is accommodated within the plastic range, thus helping to save weight. The safety of the structure then has to be proved on the basis of an elastoplastic analysis. If plastic deformation has to be tolerated even under service conditions, elastoplastic analysis is also necessary in this connection. Such situations can arise from stress concentrations at isolated locations in the structure, or from the diminution of the yield stress, the elasticity limit of the material, in parts operated at high temperature levels. In the present context, noticeable changes of the geometry of the structure may be considered as failure, and therefore the theoretical treatment refers to negligible effects of the deformation upon the geometrical shape and dimensions of the structure.

For an illustration of the design aspect of plasticity we consider the simple case of a beam with a rectangular cross-section under pure bending as described in Fig. 2. Let the elasticity limit of the material be defined by the stress σ_s, which is not altered by plastic deformation. The beam, subjected in its plane to the bending moment M under service conditions, must ultimately sustain a bending moment nM, where $n > 1$ denotes the safety factor. For an elastic design the ultimate bending moment is determined by the linear stress profile in the upper part of Fig. 2, defined by the stress magnitude $|\sigma| = \sigma_\mathrm{s}$ in the outmost fibres. It reads

$$nM = \frac{2}{3} b_\mathrm{e} h^2 \sigma_\mathrm{s} \tag{1}$$

and specifies the thickness b_e pertaining to the elastic design for an otherwise prescribed height $2h$ of the beam.

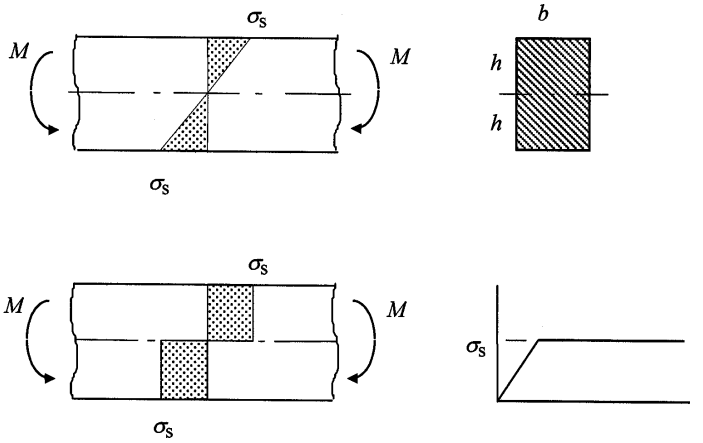

Figure 2: Elastic vs plastic design of beam.

Plasticity theoretically allows the magnitude of the stress to increase up to the elasticity limit σ_s across the entire beam, as shown in the lower part of Fig. 2. This tendency to smooth out the stress distribution on the penalty of plastic deformation is a consequence of the limitation of the stress level in the plastic range of the material, and may be considered characteristic of plasticity. The above remark on homogenization does not apply to the distribution of the strain, where the effect is reversed. From the ultimate stress profile in the cross-section of the plastic beam, we deduce for the bending moment the expression

$$nM = b_p h^2 \sigma_s, \tag{2}$$

which determines the beam thickness b_p pertaining to the plastic argument. Comparison of eqns (1) and (2) reveals that

$$b_p = \frac{2}{3} b_e \tag{3}$$

and indicates the superiority of the plastic design with respect to saving material resources and structure weight. Apart from the critical loading, operation under service conditions must be within the elastic range, i.e.

$$M = \frac{2}{3}\, b_p\, h^2\, |\sigma|\,, \qquad (|\sigma| \le \sigma_s). \tag{4}$$

Comparison with eqn (2) gives the safety factor in plasticity

$$n = \frac{3}{2}\,\frac{\sigma_s}{|\sigma|} \ge \frac{3}{2}. \tag{5}$$

The minimum value $n = 3/2$ corresponds to the case that the stress magnitude $|\sigma|$ in the outmost fibres attains the elasticity limit σ_s during service operation.

It is worth noting that, in the above considerations, the load-carrying capacity reserve in the plastic range is not provided by the material since it was not able to build up stresses beyond the elasticity limit. It is rather the beam (the structure component) which allows – by plastic deformation – the stress distribution to be adapted to an increasing loading. Conversely, if structures are not able to redistribute stresses, an increase of the loading above elasticity is only possible in conjunction with suitable material properties.

The text of this volume consists of three main parts: the description of elastoplastic material behaviour, the elastoplastic response of solids and structures, and the development and application of computational finite element techniques. The subject of the behaviour of elastoplastic solids and structures will be exposed in the present context from the point of view of the mechanics of structures and continua as applied to infinitesimal deformations. Throughout the main text, we assume isothermal conditions and a constant velocity of deformation or alternatively rate insensitivity of the material (i.e. absence of viscosity). Chapter 1 deals with the mathematical description of the constitutive response of elastoplastic materials. A discussion of the uniaxial stress–strain characteristic of the material reveals the particular type of the elastoplastic material law that is then established for uniaxial and multiaxial conditions. Chapter 2 performs the transition from the local considerations to the most essential issues regarding the response of elastoplastically deforming structures and to the description of field problems in elastoplasticity. In this connection, the equations governing quasistatic equilibrium are discussed along with appropriate solution methods. Chapter 3 addresses the load-carrying capacity of elastoplastic structures under monotonic loading conditions, whereas Chapter 4 considers limit behaviour under alternating loads. Each chapter comprises case studies introducing the subject or illustrating the presented material.

Chapter 5 summarizes finite element techniques for the numerical solution of elastoplastic problems with a digital computer. On the background of the enhanced solution capabilities offered by numerical techniques, extensions of inelastic material behaviour are considered in Chapter 6. They comprise temperature dependence, time and rate effects, the significance of inertia and pressure sensitive materials. Chapter 7 demonstrates the application of finite element techniques to the numerical solution of problems related to engineering practice.

This volume intends to provide the reader with a concise presentation of the most essential issues both of the theory of plasticity and of the computational analysis techniques as based on finite elements. It is worth mentioning that the main steps of the algorithmic procedure are applicable, however, to different discretization methods as well. The theoretical development should

be useful in understanding elastoplastic behaviour and suitably applying and interpreting numerical elastoplastic analysis. For additional physical insight and theoretical information, the reader is referred to the classical books by Nadai [3], Hill [4], Kachanov [5] and Kaliszky [6]. Concerning finite elements in plasticity, reference is made to the early book by Owen and Hinton [7]. A wide presentation of the finite element method is given by Zienkiewicz et al. in [8].

Matrix notation

This section introduces the matrix notation used in the text. It also explains the symbolic presentation of matrix operations encountered in the other chapters. Matrix algebra is assumed to be familiar to the reader, and therefore explanations are largely restricted to what might be considered of specific interest to our subject. More details can be found in specialized texts like the concise presentation by Marcus in [9] and the mathematical treatise by Serre in [10].

Definitions

A *matrix* is the arrangement of numbers or variables in a rectangular (or square) array structured in rows and columns. For example, the matrix

$$\mathbf{A} = \begin{bmatrix} a_{11} & a_{12} & a_{13} \\ a_{21} & a_{22} & a_{23} \end{bmatrix} \tag{6}$$

is a rectangular 2×3 matrix with elements a_{ij} $(i = 1, 2; j = 1, 2, 3)$. The first index specifies the row, the second refers to the columns of the scheme, thus positioning the element in the array. A short-term presentation of eqn (6) reads

$$\mathbf{A} = [a_{ij}] \qquad (m \times n), \tag{7}$$

and $(m \times n)$ is the size of a matrix with m rows and n columns as dimensions. The *transpose* of the matrix is defined as

$$\mathbf{A}^{\mathrm{t}} = \begin{bmatrix} a_{11} & a_{21} \\ a_{12} & a_{22} \\ a_{13} & a_{23} \end{bmatrix} \quad \text{or} \quad \mathbf{A}^{\mathrm{t}} = [a_{ji}]. \tag{8}$$

It is obtained by interchanging columns and rows in the original scheme. A square $(n \times n)$ matrix is *symmetric* if

$$\mathbf{A}^{\mathrm{t}} = \mathbf{A}. \tag{9}$$

A *diagonal* matrix is a square matrix possessing non-zero elements only on the diagonal. Display of zero elements is usually omitted:

$$\mathbf{D} = \begin{bmatrix} d_1 & & \\ & \ddots & \\ & & d_m \end{bmatrix} \quad \text{or} \quad \mathbf{D} = \lceil d_i \rfloor. \tag{10}$$

The *unity* matrix (or identity matrix) is defined as

$$\mathbf{I} = \begin{bmatrix} 1 & & \\ & \ddots & \\ & & 1 \end{bmatrix} \quad \text{or} \quad \mathbf{I} = \lceil 1 \rfloor, \tag{11}$$

and a zero matrix is a rectangular array occupied by zeros throughout. We shall use the symbol **0** for a zero array whether it is a matrix or a vector.

A *vector* is a matrix array with a single column:

$$\mathbf{a} = \begin{bmatrix} a_1 \\ \vdots \\ a_m \end{bmatrix} \quad \text{or} \quad \mathbf{a} = \{a_1 \cdots a_i \cdots a_m\}. \tag{12}$$

The alternative presentation of the vector in eqn (12) will be employed for typographical brevity. The braces are used in order to distinguish it from the row vector:

$$\mathbf{a}^{\mathrm{t}} = [a_1 \cdots a_i \cdots a_m] \quad \text{or} \quad \mathbf{b} = [b_1 \cdots b_j \cdots b_n]. \tag{13}$$

Vectors consisting of zero and unity elements are useful in summing up and/or distributing quantities. In connection with the state of stress or strain we shall encounter the vector

$$\mathbf{e} = \{1\,1\,1\,0\,0\,0\}, \tag{14}$$

but different patterns are also suitable for other situations.

A single real number is a *scalar* quantity in distinction to a vector or a matrix, which assemble scalar elements. *Hypermatrices* and *hypervectors* (also known as block matrices and block vectors, respectively) are assembled from matrices or vectors as their elements. The elements of such hyperschemes are called *submatrices* or *subvectors*.

In contrast to scalar quantities, matrices and vectors are denoted by bold face characters: matrices are preferably upper case, vectors lower case.

Matrix algebra

Elementary operations

Equality of two matrices (or vectors) implies that the dimensions are the same and elements in corresponding positions are equal:

$$\mathbf{A} = \mathbf{B}\,; \quad a_{ij} = b_{ij} \quad (i = 1, \ldots, m; j = 1, \ldots, n). \tag{15}$$

Sum and difference
The matrices (or vectors) must have the same dimensions, and their sum is found by adding elements in corresponding positions:

$$\mathbf{A} \pm \mathbf{B} = [a_{ij} \pm b_{ij}]. \tag{16}$$

Multiplication
The scalar product of two vectors of equal dimension (n) is defined as

$$\mathbf{a}^{\mathrm{t}}\mathbf{b} = a_1 b_1 + a_2 b_2 + \cdots + a_n b_n = \mathbf{b}^{\mathrm{t}}\mathbf{a}. \tag{17}$$

The symbolic notation for the sum in eqn (17) refers to column vectors. It has to be modified if $\mathbf{a}$ and/or $\mathbf{b}$ are row vectors.

The two vectors are considered *orthogonal* if their scalar product vanishes:

$$\mathbf{a}^{\mathrm{t}}\mathbf{b} = 0, \quad \text{e.g. } [1\,1\,1] \begin{bmatrix} 1 \\ 1 \\ -2 \end{bmatrix} = 0. \tag{18}$$

The scalar product of a vector with itself supplies the squared length (magnitude) of the vector:

$$\mathbf{a}^{\mathrm{t}}\mathbf{a} = a_1^2 + a_2^2 + \cdots + a_n^2. \tag{19}$$

The product of two rectangular matrices $\mathbf{B}$ and $\mathbf{A}$ with dimensions $m \times k$ and $k \times n$, respectively, is obtained as:

$$\mathbf{BA} = \begin{bmatrix} \mathbf{b}_1 \\ \mathbf{b}_2 \\ \vdots \\ \mathbf{b}_m \end{bmatrix} [\mathbf{a}_1\, \mathbf{a}_2 \cdots \mathbf{a}_n] = \begin{bmatrix} \mathbf{b}_1\mathbf{a}_1 & \mathbf{b}_1\mathbf{a}_2 & \cdots & \mathbf{b}_1\mathbf{a}_n \\ \mathbf{b}_2\mathbf{a}_1 & \mathbf{b}_2\mathbf{a}_2 & \cdots & \mathbf{b}_2\mathbf{a}_n \\ \vdots & & & \\ \mathbf{b}_m\mathbf{a}_1 & \mathbf{b}_m\mathbf{a}_2 & \cdots & \mathbf{b}_m\mathbf{a}_n \end{bmatrix}. \tag{20}$$

The row vectors $\mathbf{b}_1\, \mathbf{b}_2 \cdots \mathbf{b}_m$ represent the rows of the matrix $\mathbf{B}$, the vectors $\mathbf{a}_1\, \mathbf{a}_2 \cdots \mathbf{a}_n$ the columns of the matrix $\mathbf{A}$. Accordingly, the elements $\mathbf{b}_i\mathbf{a}_j$ of the product matrix are obtained as the scalar products of the respective vectors. The vector dimension must be unique (k), and the dimension of the matrix product $(m \times k)(k \times n)$ is $m \times n$. Obviously, $\mathbf{BA} \neq \mathbf{AB}$.

With reference to eqn (20), the matrix product of two (column) vectors $\mathbf{b}$ and $\mathbf{a}$ with dimension m and n, respectively, is a matrix of dimensions $m \times n$ obtained as

$$\mathbf{b}\mathbf{a}^{\mathrm{t}} = \begin{bmatrix} b_1 \\ b_2 \\ \vdots \\ b_m \end{bmatrix} [a_1\, a_2 \cdots a_n] = \begin{bmatrix} b_1 a_1 & b_1 a_2 & \cdots & b_1 a_n \\ b_2 a_1 & b_2 a_2 & \cdots & b_2 a_n \\ \vdots & & & \\ b_m a_1 & b_m a_2 & \cdots & b_m a_n \end{bmatrix}. \tag{21}$$

The matrix product of a vector with itself is seen to yield a symmetric matrix

$$\mathbf{b}\mathbf{b}^{\mathrm{t}} = \begin{bmatrix} b_1^2 & b_1 b_2 & \cdots & b_1 b_m \\ b_2 b_1 & b_2^2 & \cdots & b_2 b_m \\ \vdots & & & \\ b_m b_1 & b_m b_2 & \cdots & b_m^2 \end{bmatrix}. \tag{22}$$

It is noticed that the transpose of a product of matrices is related as follows to the transpose of the individual matrices:

$$(\mathbf{A}\mathbf{B}\mathbf{C})^{\mathrm{t}} = \mathbf{C}^{\mathrm{t}}\mathbf{B}^{\mathrm{t}}\mathbf{A}^{\mathrm{t}} \tag{23}$$

and thus $(\mathbf{b}\mathbf{b}^{\mathrm{t}})^{\mathrm{t}} = \mathbf{b}\mathbf{b}^{\mathrm{t}}$ in eqn (22).

For completeness, multiplication of a matrix by a scalar implies that every element of the matrix is multiplied by this scalar:

$$c\mathbf{A} = [ca_{ij}]. \tag{24}$$

Functions of quadratic matrices

The square of a quadratic matrix or more generally the nth power (integer n) is defined as the product

$$\mathbf{A}^2 = \mathbf{A}\mathbf{A} \quad \text{and} \quad \mathbf{A}^n = \mathbf{A}\mathbf{A}\cdots\mathbf{A} \qquad (n \text{ times}). \tag{25}$$

The following property of the powers of the matrix product of two vectors of the same dimension can easily be confirmed:

$$(\mathbf{a}\mathbf{b}^{\mathrm{t}})^2 = (\mathbf{b}^{\mathrm{t}}\mathbf{a})\mathbf{a}\mathbf{b}^{\mathrm{t}} \quad \text{and} \quad (\mathbf{a}\mathbf{b}^{\mathrm{t}})^n = (\mathbf{b}^{\mathrm{t}}\mathbf{a})^{n-1}\mathbf{a}\mathbf{b}^{\mathrm{t}}. \tag{26}$$

Accordingly, the nth power of the matrix $\mathbf{a}\mathbf{b}^{\mathrm{t}}$ is obtained by multiplying the matrix by the scalar quantity $(\mathbf{b}^{\mathrm{t}}\mathbf{a})^{n-1}$. If the vectors are orthogonal ($\mathbf{b}^{\mathrm{t}}\mathbf{a} = \mathbf{a}^{\mathrm{t}}\mathbf{b} = 0$), all higher powers of the product matrix $\mathbf{a}\mathbf{b}^{\mathrm{t}}$ vanish. In the particular case $\mathbf{b} = \mathbf{a}$ we have:

$$(\mathbf{a}\mathbf{a}^{\mathrm{t}})^2 = (\mathbf{a}^{\mathrm{t}}\mathbf{a})\mathbf{a}\mathbf{a}^{\mathrm{t}}, \quad (\mathbf{a}\mathbf{a}^{\mathrm{t}})^n = (\mathbf{a}^{\mathrm{t}}\mathbf{a})^{n-1}\mathbf{a}\mathbf{a}^{\mathrm{t}}. \tag{27}$$

The scalar factor is here the squared magnitude (or length) of the vector.

Polynomials of a square matrix can be defined as

$$P(\mathbf{A}) = c_0\mathbf{I} + c_1\mathbf{A} + c_2\mathbf{A}^2 + \cdots + c_n\mathbf{A}^n, \tag{28}$$

and analogously power series. In particular, we note the exponential form

$$\exp(t\mathbf{A}) = \mathbf{I} + t\mathbf{A} + \frac{t^2}{2!}\mathbf{A}^2 + \frac{t^3}{3!}\mathbf{A}^3 + \cdots$$

$$= \sum_{n=0}^{\infty} \frac{t^n}{n!}\mathbf{A}^n. \tag{29}$$

Inverse of a matrix
The *inverse* of a square matrix $\mathbf{A}$ is denoted by $\mathbf{A}^{-1}$ and is defined by the property that

$$\mathbf{A}\mathbf{A}^{-1} = \mathbf{A}^{-1}\mathbf{A} = \mathbf{I}. \tag{30}$$

For the inverse of a product of two square matrices we have

$$\mathbf{AB}(\mathbf{AB})^{-1} = \mathbf{I} \quad \text{and} \quad (\mathbf{AB})^{-1} = \mathbf{B}^{-1}\mathbf{A}^{-1}. \tag{31}$$

The reversed order in the second equation is obtained by multiplying from the left the first equation consecutively by $\mathbf{A}^{-1}$ and $\mathbf{B}^{-1}$. The inverse of a matrix of the particular form $\mathbf{I} + \mathbf{ab}^{\mathrm{t}}$ can be given explicitly:

$$[\mathbf{I} + \mathbf{ab}^{\mathrm{t}}]^{-1} = \left[\mathbf{I} - \frac{1}{1 + \mathbf{b}^{\mathrm{t}}\mathbf{a}}\mathbf{ab}^{\mathrm{t}}\right]. \tag{32}$$

Matrix inversion is encountered in the solution of linear systems

$$\mathbf{Ax} = \mathbf{b} \quad \text{and} \quad \mathbf{x} = \mathbf{A}^{-1}\mathbf{b}. \tag{33}$$

A solution of the system can be obtained if the determinant of the coefficient matrix does not vanish; $|\mathbf{A}| \neq 0$. If $|\mathbf{A}| = 0$, the solution of eqn (33) is not possible. At the same time, the matrix $\mathbf{A}$ is said to be singular. Conversely, if a square matrix is singular, its determinant is zero. The inverse of a singular matrix does not exist.

Eigenvalues and eigenvectors
For every square matrix $\mathbf{A}$, a scalar λ and a non-zero vector $\mathbf{y}$ can be found such that

$$\mathbf{Ay} = \lambda\mathbf{y}. \tag{34}$$

The scalar λ is called an *eigenvalue* and $\mathbf{y}$ an *eigenvector*. From eqn (34), we obtain the equations stating the eigenvalue problem

$$[\mathbf{A} - \lambda\mathbf{I}]\mathbf{y} = \mathbf{0} \quad \text{and} \quad |\mathbf{A} - \lambda\mathbf{I}| = 0. \tag{35}$$

The condition of a zero determinant in eqn (35) ensures non-trivial solutions of the matrix equation for $\mathbf{y}$. This condition establishes the characteristic equation $|\mathbf{A} - \lambda\mathbf{I}| = 0$. If the dimension of $\mathbf{A}$ is $m \times m$, the characteristic equation will have m roots (i.e. the matrix will have m eigenvalues $\lambda_1, \lambda_2, \ldots, \lambda_m$). The eigenvalues will not necessarily all be distinct or non-zero. With the eigenvalues λ_i known, the associated eigenvectors $\mathbf{y}_i$ can be determined from the matrix equation in eqn (35). It is easy to confirm that $\alpha\mathbf{y}_i$ are also eigenvectors, which means that the direction of eigenvectors is unique but not their magnitude (or length). Usually, eigenvectors are scaled so that $\mathbf{y}^{\mathrm{t}}\mathbf{y} = 1$.

The eigenvalues of a symmetric matrix are real numbers and the eigenvectors are mutually orthogonal. If $\mathbf{A}$ and $\mathbf{B}$ are square and have the same

dimensions, the eigenvalues of **AB** and **BA** are the same but not necessarily the eigenvectors.

The determinant of any square matrix **A** possessing the eigenvalues $\lambda_1, \lambda_2, \ldots, \lambda_m$, is given by the product

$$|\mathbf{A}| = \lambda_1 \lambda_2 \cdots \lambda_m = \prod_{i=1}^{m} \lambda_i. \tag{36}$$

The matrix is singular if one of the eigenvalues is zero.

For completeness, the trace of the matrix (the sum of its diagonal elements) is obtained as

$$\mathrm{tr}(\mathbf{A}) = a_{11} + \cdots + a_{mm} = \lambda_1 + \cdots + \lambda_m = \sum_{i=1}^{m} \lambda_i. \tag{37}$$

Spectral decomposition

The spectral decomposition of a quadratic $m \times m$ matrix **A** is given by the relationship

$$\mathbf{A} = \mathbf{C}\mathbf{\Lambda}\mathbf{C}^{-1}. \tag{38}$$

In eqn (38), $\mathbf{\Lambda}$ denotes the diagonal matrix of the eigenvalues λ_i (the spectrum) of **A**,

$$\mathbf{\Lambda} = \begin{bmatrix} \lambda_1 & & \\ & \ddots & \\ & & \lambda_m \end{bmatrix} = \lceil \lambda_i \rfloor,$$

and the matrix **C** is composed of the respective eigenvectors $\mathbf{y}_i$ as its columns:

$$\mathbf{C} = [\mathbf{y}_1\, \mathbf{y}_2 \cdots \mathbf{y}_m] = [\mathbf{y}_i].$$

We arrive at eqn (38) by considering the identity,

$$\mathbf{A} = \mathbf{A}\mathbf{C}\mathbf{C}^{-1} \qquad (\mathbf{C}\mathbf{C}^{-1} = \mathbf{I}).$$

In detail,

$$\begin{aligned} \mathbf{A} &= \mathbf{A}\,[\mathbf{y}_1\, \mathbf{y}_2 \cdots \mathbf{y}_m]\,\mathbf{C}^{-1} \\ &= [\mathbf{A}\mathbf{y}_1\, \mathbf{A}\mathbf{y}_2 \cdots \mathbf{A}\mathbf{y}_m]\,\mathbf{C}^{-1} \\ &= [\lambda_1\mathbf{y}_1\, \lambda_2\mathbf{y}_2 \cdots \lambda_m\mathbf{y}_m]\,\mathbf{C}^{-1} = \mathbf{C}\mathbf{\Lambda}\mathbf{C}^{-1}. \end{aligned}$$

The inverse transformation to eqn (38) is seen to diagonalize the matrix:

$$\mathbf{C}^{-1}\mathbf{A}\mathbf{C} = \mathbf{\Lambda}. \tag{39}$$

The spectral decomposition presumes that the eigenvalues and the eigenvectors of the matrix are known, and that the matrix $\mathbf{C}$ of the eigenvectors has an inverse. For a symmetric matrix $\mathbf{A}$, the eigenvectors $\mathbf{y}_i$ are mutually orthogonal ($\mathbf{y}_i^{\mathrm{t}}\mathbf{y}_j = 0\,,\ i \neq j$). Using normalized eigenvectors ($\mathbf{y}_i^{\mathrm{t}}\mathbf{y}_i = 1$), the matrix $\mathbf{C}$ is seen to be orthogonal ($\mathbf{C}^{\mathrm{t}}\mathbf{C} = \mathbf{C}\mathbf{C}^{\mathrm{t}} = \mathbf{I}$, and $\mathbf{C}^{\mathrm{t}} = \mathbf{C}^{-1}$). Thus, for a symmetric matrix,

$$\mathbf{A} = \mathbf{C}\mathbf{\Lambda}\mathbf{C}^{\mathrm{t}} \quad \text{and} \quad \mathbf{C}^{\mathrm{t}}\mathbf{A}\mathbf{C} = \mathbf{\Lambda}. \tag{40}$$

Differential forms

If $f(\mathbf{x})$ is a scalar function of the variables $x_1, x_2, \ldots, x_n$ collected in the vector $\mathbf{x}$, then the differential of the function f is given as:

$$\mathrm{d}f = \begin{bmatrix} \dfrac{\partial f}{\partial x_1} & \dfrac{\partial f}{\partial x_2} & \cdots & \dfrac{\partial f}{\partial x_n} \end{bmatrix} \begin{bmatrix} \mathrm{d}x_1 \\ \mathrm{d}x_2 \\ \vdots \\ \mathrm{d}x_n \end{bmatrix} = \frac{\mathrm{d}f}{\mathrm{d}\mathbf{x}}\mathrm{d}\mathbf{x}. \tag{41}$$

The row vector

$$\frac{\mathrm{d}f}{\mathrm{d}\mathbf{x}} = \begin{bmatrix} \dfrac{\partial f}{\partial x_1} & \dfrac{\partial f}{\partial x_2} & \cdots & \dfrac{\partial f}{\partial x_n} \end{bmatrix} \tag{42}$$

comprises the partial derivatives of the function f with respect to the variables x_i. In case that two (or more) groups of variables are involved constituting the vectors $\mathbf{x}$ and $\mathbf{y}$ respectively, we have $f(\mathbf{x}, \mathbf{y})$ and

$$\mathrm{d}f = \frac{\partial f}{\partial \mathbf{x}}\mathrm{d}\mathbf{x} + \frac{\partial f}{\partial \mathbf{y}}\mathrm{d}\mathbf{y} = \begin{bmatrix} \dfrac{\partial f}{\partial \mathbf{x}} & \dfrac{\partial f}{\partial \mathbf{y}} \end{bmatrix} \begin{bmatrix} \mathrm{d}\mathbf{x} \\ \mathrm{d}\mathbf{y} \end{bmatrix}. \tag{43}$$

In the collective hypervector notation the quantities $\partial f/\partial \mathbf{x}, \partial f/\partial \mathbf{y}$ represent subvectors, as do the quantities $\mathrm{d}\mathbf{x}$ and $\mathrm{d}\mathbf{y}$.

Next, we consider the vector

$$\mathbf{g}(\mathbf{x}) = \begin{bmatrix} g_1(x_1, \cdots, x_n) \\ \vdots \\ g_m(x_1, \cdots, x_n) \end{bmatrix}. \tag{44}$$

Its differential is defined as

$$\mathrm{d}\mathbf{g} = \begin{bmatrix} \mathrm{d}g_1 \\ \vdots \\ \mathrm{d}g_m \end{bmatrix} = \begin{bmatrix} \dfrac{\partial g_1}{\partial x_1} & \dfrac{\partial g_1}{\partial x_2} & \cdots & \dfrac{\partial g_1}{\partial x_n} \\ \vdots & & & \\ \dfrac{\partial g_m}{\partial x_1} & \dfrac{\partial g_m}{\partial x_2} & \cdots & \dfrac{\partial g_m}{\partial x_n} \end{bmatrix} \begin{bmatrix} \mathrm{d}x_1 \\ \vdots \\ \mathrm{d}x_n \end{bmatrix} = \frac{\mathrm{d}\mathbf{g}}{\mathrm{d}\mathbf{x}}\mathrm{d}\mathbf{x}. \tag{45}$$

The $m \times n$ matrix

$$\frac{\mathrm{d}\mathbf{g}}{\mathrm{d}\mathbf{x}} = \begin{bmatrix} \dfrac{\partial g_1}{\partial x_1} & \dfrac{\partial g_1}{\partial x_2} & \cdots & \dfrac{\partial g_1}{\partial x_n} \\ \vdots & & & \\ \dfrac{\partial g_m}{\partial x_1} & \dfrac{\partial g_m}{\partial x_2} & \cdots & \dfrac{\partial g_m}{\partial x_n} \end{bmatrix} \tag{46}$$

comprises the partial derivatives $\partial g_i/\partial x_j$ as its elements.

For two (or more) groups of variables $\mathbf{x}$ and $\mathbf{y}$, the functional dependence can be written as $\mathbf{g}(\mathbf{x}, \mathbf{y})$. The differential reads

$$\mathrm{d}\mathbf{g} = \frac{\partial \mathbf{g}}{\partial \mathbf{x}}\mathrm{d}\mathbf{x} + \frac{\partial \mathbf{g}}{\partial \mathbf{y}}\mathrm{d}\mathbf{y} = \begin{bmatrix} \dfrac{\partial \mathbf{g}}{\partial \mathbf{x}} & \dfrac{\partial \mathbf{g}}{\partial \mathbf{y}} \end{bmatrix} \begin{bmatrix} \mathrm{d}\mathbf{x} \\ \mathrm{d}\mathbf{y} \end{bmatrix}, \tag{47}$$

and $\partial \mathbf{g}/\partial \mathbf{x}, \partial \mathbf{g}/\partial \mathbf{y}$ enter the hypermatrix operation as submatrices.

Below, we list the derivatives of some special functional forms:

$$\begin{aligned} f &= \mathbf{a}^{\mathrm{t}}\mathbf{x}, \quad \frac{\mathrm{d}f}{\mathrm{d}\mathbf{x}} = \mathbf{a}^{\mathrm{t}}; \\ f &= \mathbf{x}^{\mathrm{t}}\mathbf{A}\mathbf{x}, \quad \frac{\mathrm{d}f}{\mathrm{d}\mathbf{x}} = \mathbf{x}^{\mathrm{t}}[\mathbf{A} + \mathbf{A}^{\mathrm{t}}] = 2\mathbf{x}^{\mathrm{t}}\mathbf{A} \qquad (\text{for } \mathbf{A}^{\mathrm{t}} = \mathbf{A}); \\ \mathbf{g} &= \mathbf{A}\mathbf{x}, \quad \frac{\mathrm{d}\mathbf{g}}{\mathrm{d}\mathbf{x}} = \mathbf{A}. \end{aligned} \tag{48}$$

We also notice the chain rule in the case where $f(\mathbf{y})$ and $\mathbf{y}(\mathbf{x})$:

$$\mathrm{d}f = \frac{\mathrm{d}f}{\mathrm{d}\mathbf{x}}\mathrm{d}\mathbf{x} = \frac{\mathrm{d}f}{\mathrm{d}\mathbf{y}}\frac{\mathrm{d}\mathbf{y}}{\mathrm{d}\mathbf{x}}\mathrm{d}\mathbf{x}\,, \quad \frac{\mathrm{d}f}{\mathrm{d}\mathbf{x}} = \frac{\mathrm{d}f}{\mathrm{d}\mathbf{y}}\frac{\mathrm{d}\mathbf{y}}{\mathrm{d}\mathbf{x}}.$$

Analogously,

$$\mathrm{d}\mathbf{g} = \frac{\mathrm{d}\mathbf{g}}{\mathrm{d}\mathbf{x}}\mathrm{d}\mathbf{x} = \frac{\mathrm{d}\mathbf{g}}{\mathrm{d}\mathbf{y}}\frac{\mathrm{d}\mathbf{y}}{\mathrm{d}\mathbf{x}}\mathrm{d}\mathbf{x}\,, \quad \frac{\mathrm{d}\mathbf{g}}{\mathrm{d}\mathbf{x}} = \frac{\mathrm{d}\mathbf{g}}{\mathrm{d}\mathbf{y}}\frac{\mathrm{d}\mathbf{y}}{\mathrm{d}\mathbf{x}}. \tag{49}$$

The second differential of a scalar function $f(\mathbf{x})$ of the vector $\mathbf{x}$ is obtained as:

$$\begin{aligned} \mathrm{d}^2 f &= \frac{\mathrm{d}}{\mathrm{d}\mathbf{x}}\left(\frac{\mathrm{d}f}{\mathrm{d}\mathbf{x}}\mathrm{d}\mathbf{x}\right)\mathrm{d}\mathbf{x} = \frac{\mathrm{d}}{\mathrm{d}\mathbf{x}}\left(\mathrm{d}\mathbf{x}^{\mathrm{t}}\frac{\mathrm{d}f}{\mathrm{d}\mathbf{x}^{\mathrm{t}}}\right)\mathrm{d}\mathbf{x} \\ &= \mathrm{d}\mathbf{x}^{\mathrm{t}}\frac{\mathrm{d}^2 f}{\mathrm{d}\mathbf{x}\mathrm{d}\mathbf{x}^{\mathrm{t}}}\mathrm{d}\mathbf{x}. \end{aligned} \tag{50}$$

The transpose of the row vector $\mathrm{d}f/\mathrm{d}\mathbf{x}$ has been denoted by

$$\left[\frac{\mathrm{d}f}{\mathrm{d}\mathbf{x}}\right]^{\mathrm{t}} = \frac{\mathrm{d}f}{\mathrm{d}\mathbf{x}^{\mathrm{t}}}$$

and is called the gradient of the scalar function f. The second-order differential quotient in eqn (50) can be detailed as

$$\frac{\mathrm{d}^2 f}{\mathrm{d}\mathbf{x}\mathrm{d}\mathbf{x}^{\mathrm{t}}} = \begin{bmatrix} \dfrac{\partial^2 f}{\partial x_1^2} & \dfrac{\partial^2 f}{\partial x_2 \partial x_1} & \cdots & \dfrac{\partial^2 f}{\partial x_n \partial x_1} \\ \vdots & & & \\ \dfrac{\partial^2 f}{\partial x_1 \partial x_n} & \dfrac{\partial^2 f}{\partial x_2 \partial x_n} & \cdots & \dfrac{\partial^2 f}{\partial x_n^2} \end{bmatrix}. \tag{51}$$

The matrix assembles the second-order partial derivatives of the function f with respect to the variables $x_1, x_2, \ldots, x_n$ as indicated. It is symmetric if the function depends continuously on the variables.

The matrix representation of the Taylor series expansion of the function $f(\mathbf{x})$ up to the second order reads

$$f(\mathbf{x} + \mathrm{d}\mathbf{x}) = f(\mathbf{x}) + \frac{\mathrm{d}f}{\mathrm{d}\mathbf{x}}\mathrm{d}\mathbf{x} + \frac{1}{2}\mathrm{d}\mathbf{x}^{\mathrm{t}}\frac{\mathrm{d}^2 f}{\mathrm{d}\mathbf{x}\mathrm{d}\mathbf{x}^{\mathrm{t}}}\mathrm{d}\mathbf{x}, \tag{52}$$

which utilizes the differential forms developed above.

References

[1] S. Timoshenko and J.N. Goodier, *Theory of Elasticity*, 3rd edn, McGraw-Hill, New York, 1970.

[2] I. Doltsinis, *Large Deformation Processes of Solids*, WIT Press, Southampton, 2004.

[3] A. Nadai, *Theory of Flow and Fracture of Solids*, Vol. I, 2nd edn, McGraw-Hill, New York, 1950.

[4] R. Hill, *Mathematical Theory of Plasticity*, Clarendon Press, Oxford, 1950.

[5] L.M. Kachanov, *Foundations of the Theory of Plasticity*, North-Holland, Amsterdam, 1971.

[6] S. Kaliszky, *Plasticity: Theory and Engineering Applications*, Elsevier, Amsterdam, 1989.

[7] R.D. Owen and E. Hinton, *Finite Elements in Plasticity*, Pineridge Press, Swansea, 1980.

[8] O.C. Zienkiewicz, R.L. Taylor and J.Z. Zhu, *The Finite Element Method: Its Basis and Fundamentals*, 6th edn, Elsevier, Amsterdam, 2005.

[9] M. Marcus, *Basic Theorems in Matrix Theory*, National Bureau of Standards, Applied Mathematics Series 57, U.S. Government Printing Office, Washington D.C., 1960.

[10] D. Serre, *Matrices: Theory and Applications*, Graduate Texts in Mathematics 216, Springer, New York, 2002.

This page intentionally left blank

CHAPTER 1

Elastoplastic material behaviour

1.1 The uniaxial case

1.1.1 Description of material response

We begin our considerations in the elastoplastic regime with the case of a rod specimen of metallic material under uniaxial tension. This simple case encompasses all the essential features of elastoplastic material response which are deduced directly from macroscopic experimental observations. Beyond the importance of the conventional tension test for obtaining material properties, the mathematical methodology of elastoplastic material description can be introduced herewith as a basis for the subsequent extension to multiaxial stress and strain states. For the tensile specimen with length l and cross-section A in Fig. 1.1, we define the uniaxial stress

$$\sigma = \frac{P}{A}, \tag{1.1}$$

where P denotes the axially applied force, and the longitudinal strain

$$\gamma = \frac{\delta}{l}, \tag{1.2}$$

where δ denotes the elongation of the specimen.

Stress–strain diagram
The specimen is considered originally undeformed. An increase of the tensile force from zero produces values of stress and strain lying along the solid line in the diagram of Fig. 1.2 (left). Inspection of the plot of the recorded stress and strain values indicates the deviation from the initial linear part – inherent to elastic response – at point L, the linearity limit. Beyond this point the stress–strain diagram is curvilinear with decreasing slope.

The above refers to monotonic loading conditions. If, in a different test programme, the specimen is first stressed to a state well beyond point L and is then unloaded, the strain follows the dashed line in the diagram. It is thereby observed that the removal of the stress restores the strain only

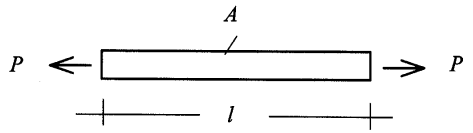

Figure 1.1: Rod specimen under uniaxial tension (schematic).

partially, while part of it adheres permanently to the specimen. Careful examination of the test data reveals that permanent, plastic deformation appears beyond point E, the elasticity limit. Reloading takes place along a slightly different path until the monotonic tensile characteristic is again reached. The latter is observed when the loading is increased further. The described behaviour is typical of any unloading and reloading operation in the elastoplastic regime of the test programme independently of the stress level. The path difference between unloading and reloading is known as the hysteresis loop.

The actual elastoplastic behaviour illustrated in Fig. 1.2 appears to be complex. Despite an increasing tendency to pay particular attention to secondary effects, reasonable simplifications are helpful for a suitable description of metal plasticity. The idealized behaviour in the elastoplastic regime depicted in the stress–strain diagram of Fig. 1.2 (right) is attributed to Ludwig Prandtl [1]. Accordingly, the elasticity limit is assumed to coincide with the linearity limit at A, the yield point of the material under uniaxial tension. We denote the associated stress by σ_s. The material response to stresses below the yield limit is elastic, and in this region unloading completely restores the deformation of the specimen.

Continuous loading beyond A follows the same curvilinear path as in Fig. 1.2 (left), but unloading from point B, for instance, is assumed here along a straight line parallel to the initial elastic one. Thereby, the elastic part ε of the strain is restored, while the plastic part η remains after the

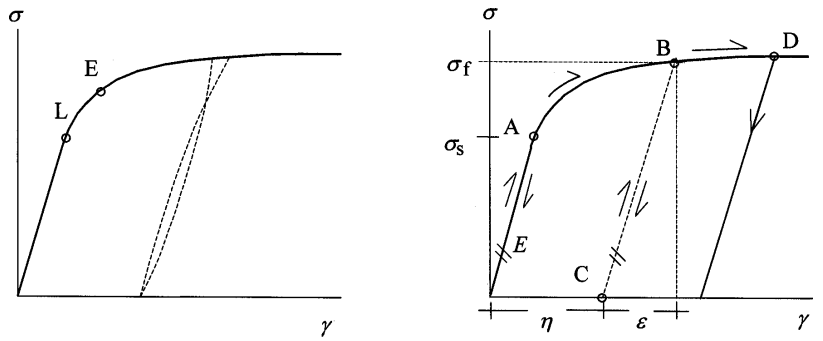

Figure 1.2: Elastoplastic stress–strain diagram and idealization (right).

removal of the stress. Reloading from point C takes place along the same elastic path as unloading, and the increase of the strain is purely elastic up to B, the state before unloading. Thus, the plastic strain at B and C is the same. For an increase of the stress beyond σ_f, the stress at state B, the material follows the monotonic loading diagram as if unloading had not occurred. Stress removal from a further advanced state D on the diagram indicates that this transition from B has been accompanied by additional plastic strain.

The appearance of a permanent plastic strain η in addition to the reversible elastic strain ε is characteristic of the elastoplastic regime. The total strain γ may be presented as

$$\gamma = \varepsilon + \eta. \tag{1.3}$$

The additive decomposition refers to the strain γ defined by eqn (1.2). Partition of the total elongation of the specimen δ into elastic and plastic terms specifies the respective strains ε and η for $l = \text{const}$.

The development of plastic strain along the tensile stress–strain diagram initially requires loading beyond the yield stress σ_s. The maximum stress once imposed under plastic deformation, however, is recorded by the material and becomes the actual yield limit σ_f for additional plastic straining. Thus σ_f takes the place of the original σ_s when the specimen is unloaded and later reloaded. A functional dependence

$$\sigma_\mathrm{f} = \sigma_\mathrm{f}(\eta) \qquad \text{with } \sigma_\mathrm{f}(0) = \sigma_\mathrm{s} \tag{1.4}$$

can be deduced from the tension test after subtraction of the elastic strain ε from the measured strain γ. Since the yield stress σ_f is increasing with plastic strain η, the material is said to (strain-)harden, and the function $\sigma_\mathrm{f}(\eta)$ describes the hardening characteristic.

Nature of the stress–strain relations

The additive composition of the strain as given by eqn (1.3) suggests the description of elastoplastic material behaviour by means of an elastic and a plastic constituent. This is demonstrated in Fig. 1.3 where the uniaxial stress–strain characteristic is split into two distinct diagrams pertaining to the parts ε and η of the strain γ. At a given stress level σ the elastic strain can be determined by Hooke's law as

$$\varepsilon = \frac{\sigma}{E}, \tag{1.5}$$

where E denotes the modulus of elasticity of the material. Equation (1.5) between stress and elastic strain may be considered an equation of state, relating ε uniquely to σ regardless of the particular loading sequence producing the actual stress. Any variation of the stress is accompanied by variations of the elastic strain along the straight path described by the law of elasticity.

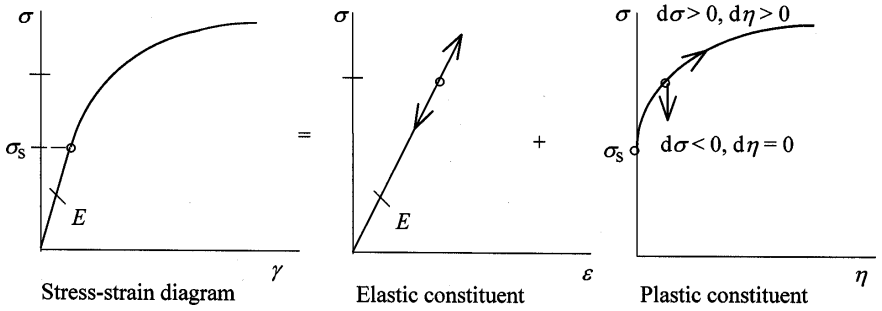

Figure 1.3: Elastic and plastic constituents.

Conversely, the stress may be considered to be a result of the elastic strain. Using eqn (1.3), we obtain from eqn (1.5)

$$\sigma = E\varepsilon = E(\gamma - \eta). \tag{1.6}$$

Determination of σ requires knowledge of the permanent strain η in addition to the measured strain γ. The stress–plastic strain diagram in Fig. 1.3 (right) represents the hardening characteristic $\sigma_{\mathrm{f}}(\eta)$ of the material. It is obtained from the original tensile stress–strain curve after reduction of the strain γ by the elastic strain ε from eqn (1.5). Simple knowledge of the momentary stress proves to be insufficient for a unique determination of the plastic strain. While the hardening characteristic provides us with a value for η at the given stress level, the same stress can be reached by unloading from any higher point of the hardening curve, and may therefore be associated with different values of the plastic strain unless the preceding loading history is specified.

For the above reason, we shall pay attention instead to the relations between incremental variations of stress and plastic strain along a prescribed stress path. For changes in plastic strain (plastic flow), the applied tensile stress σ must be raised to the state $\sigma_{\mathrm{f}}(\eta)$ ultimately attained in the past by the material. Then, an incremental increase of the stress by $\mathrm{d}\sigma > 0$ produces an increment $\mathrm{d}\eta$ in the plastic strain. Reduction of the stress by $\mathrm{d}\sigma < 0$ corresponds to elastic unloading and leaves the plastic strain unaffected, $\mathrm{d}\eta = 0$. In contrast to elasticity, an essential difference between loading and unloading becomes obvious in plasticity and introduces a nonlinear response even for incremental variations of the stress state.

1.1.2 Plastic flow and stress–strain relations

From the foregoing discussion of experimental observations, a mathematical description of uniaxial plastic flow will be based on the following three

postulates:

$$\begin{array}{lll} \text{(a)} \quad \text{Yield condition} & \phi = \bar{\sigma} - \sigma_{\mathrm{f}} \leq 0 & (\bar{\sigma} = |\sigma|); \\ \text{(b)} \quad \text{Hardening law} & \sigma_{\mathrm{f}} = \sigma_{\mathrm{f}}(\bar{\eta}) & (\bar{\eta} = |\eta|); \\ \text{(c)} \quad \text{Flow rule} & \mathrm{d}\eta = s\mathrm{d}\bar{\eta} & \left(s = \dfrac{\sigma}{|\sigma|} = \dfrac{\sigma}{\bar{\sigma}}\right). \end{array} \tag{1.7}$$

The yield condition in terms of the yield function $\phi(\sigma, \sigma_{\mathrm{f}})$ states that the momentary yield stress of the material, σ_{f}, cannot be exceeded by the applied stress σ. The absolute value of σ as an argument in the yield function aims at its use for compressive loading as well. This presumes that the magnitude σ_{f} of the yield stress is the same under tension or compression.

Hardening defines a material characteristic specifying the yield stress ($\sigma_{\mathrm{f}} > 0$) as a function of the plastic strain independently of the sign ($\bar{\eta} \geq 0$). Experimental evidence supports the hypothesis that the magnitude of the yield stress attains the same value under tension or compression. Strictly, this statement applies to separate tests under tensile or compressive action, not to combined loading sequences. Then, $\sigma(-\eta) = -\sigma(\eta)$ (see Fig. 1.4), and the material yield stress can be stated as a positive quantity $\sigma_{\mathrm{f}}(\bar{\eta})$ depending on the absolute value of the plastic strain, for tensile or compressive action. A more general definition of the quantity $\bar{\eta}$ is given by

$$\bar{\eta} = \int \mathrm{d}\bar{\eta}, \quad \mathrm{d}\bar{\eta} = |\mathrm{d}\eta| \tag{1.8}$$

which offers a measure for the accumulated plastic strain in alternating loading. Hardening in such a case will be discussed later in Section 1.3.

At this stage the formalism involves merely absolute values of the mechanical variables of the system. The direction of plastic flow is specified by the

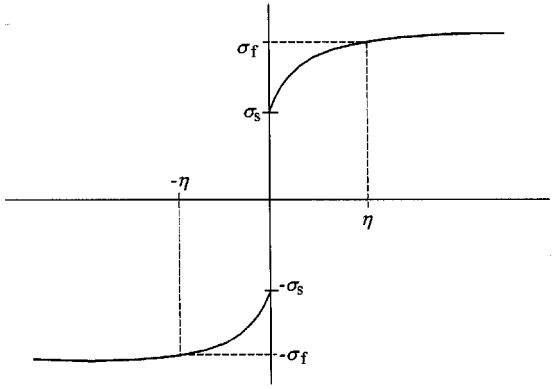

Figure 1.4: Yield stress under monotonic tension or compression.

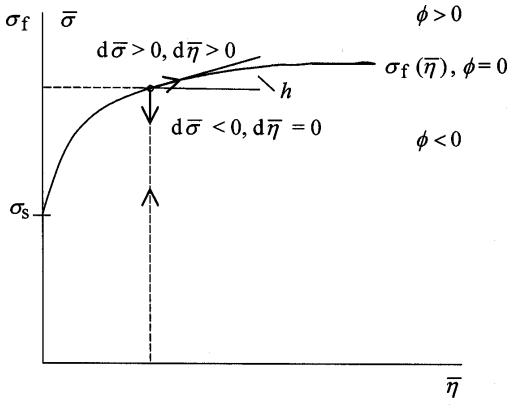

Figure 1.5: Yield condition and plastic loading.

flow rule. Thereby, the stress state at the occurrence of plastic flow defines the sign of changes in plastic strain. This can be stated as

$$\frac{d\eta}{|d\eta|} = \frac{\sigma}{|\sigma|} = s \tag{1.9}$$

and is reflected under (c) in eqn (1.7).

In the $\bar{\sigma}, \bar{\eta}$ - diagram of Fig. 1.5, the hardening characteristic $\sigma_f(\bar{\eta})$ is seen to separate two regions, one below the curve where $\phi < 0$, the other beyond it where $\phi > 0$, while $\phi = 0$ along the hardening curve. We consider a specimen which is unstressed, but may have been deformed plastically in a previous loading programme so that the actual yield stress σ_f is above the original σ_s. Increasing the stress $\bar{\sigma}$ from zero will not cause any additional plastic strain until the value σ_f is reached. Therefore, $\phi < 0$ defines the region where the material responds elastically to the applied stress. When $\bar{\sigma} = \sigma_f$, the material is said to be at a *plastic state*. This is a necessary condition for the occurrence of plastic flow, but the change in stress at this state is decisive. In particular, $d\bar{\sigma} < 0$ points into the elastic regime $\phi < 0$ and is associated with $d\bar{\eta} = 0$, while $d\bar{\sigma} > 0$ is accompanied by an increment of plastic strain $d\bar{\eta} > 0$, thus advancing the material state along the hardening characteristic $\phi = 0$. By this mechanism, the region $\phi > 0$ is not accessible to the material despite an increasing magnitude of stress.

Plastic flow requires that the yield function in eqn (1.7) is zero:

$$\phi = \bar{\sigma} - \sigma_f = 0. \tag{1.10}$$

Differentiation leads to the *consistency condition* during plastic flow

$$d\phi = d\bar{\sigma} - d\sigma_f = 0. \tag{1.11}$$

The increment of the yield stress can be related to the increment of plastic strain via the hardening law:

$$\mathrm{d}\sigma_\mathrm{f} = h\mathrm{d}\bar{\eta} \quad \text{with } h = \frac{\mathrm{d}\sigma_\mathrm{f}}{\mathrm{d}\bar{\eta}} \geq 0. \tag{1.12}$$

The parameter h is the local slope of the hardening curve. From eqns (1.11) and (1.12),

$$\mathrm{d}\bar{\eta} = \frac{1}{h}\mathrm{d}\bar{\sigma} \geq 0. \tag{1.13}$$

The requirement $\mathrm{d}\bar{\eta} \geq 0$ ensures that the quantity $\bar{\eta}$ can only increase and is satisfied by the *loading condition* for plastic flow,

$$\mathrm{d}\bar{\sigma} = s\mathrm{d}\sigma > 0. \tag{1.14}$$

The expression for $\mathrm{d}\bar{\sigma}$ in eqn (1.14) is deduced by differentiation of the equality $\bar{\sigma}^2 = \sigma^2$ and use of the definition of s in eqn (1.7). Substituting in eqn (1.13) and applying the flow rule, we obtain for the plastic strain increment:

$$\begin{aligned} &\mathrm{d}\eta = \frac{1}{h}ss\mathrm{d}\sigma = \frac{1}{h}\mathrm{d}\sigma \quad \text{if } \phi = 0 \text{ and } \mathrm{d}\bar{\sigma} = s\mathrm{d}\sigma > 0; \\ &\mathrm{d}\eta = 0 \quad \text{otherwise.} \end{aligned} \tag{1.15}$$

Incremental stress–strain relations

Whenever plastic flow occurs according to the conditions listed in eqn (1.15), $\mathrm{d}\eta$ supplements the incremental elastic strain $\mathrm{d}\varepsilon$ as from eqn (1.5) to give the strain increment:

$$\mathrm{d}\gamma = \mathrm{d}\varepsilon + \mathrm{d}\eta = \frac{E+h}{Eh}\mathrm{d}\sigma. \tag{1.16}$$

Equation (1.16) determines the change in strain $\mathrm{d}\gamma$ for a given incremental change in stress $\mathrm{d}\sigma$. For $h = 0$ (non-hardening material) this relation becomes meaningless, since eqn (1.15) is not applicable for the plastic strain. The non-hardening material is said to possess a *perfectly plastic* constituent. In this case of great theoretical significance the stress can be increased elastically from zero to the yield limit σ_s, but subsequent deformation takes place at constant stress (Fig. 1.6). As a consequence, we have

$$\mathrm{d}\sigma = E\mathrm{d}\varepsilon = 0 \tag{1.17}$$

and thus

$$\mathrm{d}\gamma = \mathrm{d}\varepsilon + \mathrm{d}\eta = \mathrm{d}\eta. \tag{1.18}$$

In the perfectly plastic case, once the yield limit is reached, the elastic part of the incremental strain vanishes and the latter is entirely of a plastic nature.

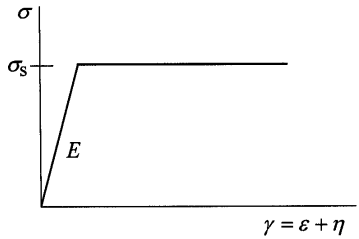

Figure 1.6: Elastic–perfectly plastic behaviour.

For an alternative description of the plastic strain increment, $\mathrm{d}\sigma$ in eqn (1.15) is expressed via the elastic relation, eqn (1.6), in terms of the difference $(\mathrm{d}\gamma - \mathrm{d}\eta)$. Solution for $\mathrm{d}\eta$ then gives the expression

$$\mathrm{d}\eta = \frac{E}{E+h}\mathrm{d}\gamma \tag{1.19}$$

for the incremental plastic strain, and the loading condition

$$s\mathrm{d}\gamma > 0 \tag{1.20}$$

in terms of the strain increment $\mathrm{d}\gamma$. In the case of a perfectly plastic material ($h = 0$) the above formulation implies eqn (1.18).

Subtraction of the plastic strain increment by eqn (1.19) from $\mathrm{d}\gamma$ gives the elastic part of the strain increment, and the stress change

$$\mathrm{d}\sigma = E\mathrm{d}\varepsilon = \frac{Eh}{E+h}\mathrm{d}\gamma \tag{1.21}$$

is as for hardening: $\mathrm{d}\sigma = h\mathrm{d}\eta$. Equation (1.21) determines in the elastoplastic material range the change in stress $\mathrm{d}\sigma$ for a given strain increment $\mathrm{d}\gamma$. It can be identified as the inverse relation to eqn (1.16).

1.2 Plastic yielding under multiaxial conditions

1.2.1 State of stress and strain

For a definition of stress and strain, we refer to the cubic element of the material in Fig. 1.7 which is oriented along the Cartesian axes. Stresses are defined by the Cartesian components of the force per unit area (traction) acting on each of the faces of the cubic element. Considering the face normal to the x-axis, for instance, we have the direct (or normal) stress σ_{xx} normal to the surface, and the shear (or tangential) stresses σ_{xy} and σ_{xz} tangential to it. The first stress index refers to the surface normal, the second specifies the direction of the component.

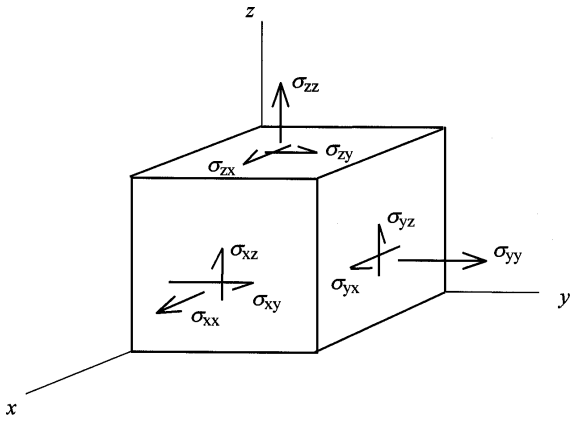

Figure 1.7: Definition of stress components.

Stresses are taken to be positive as indicated in Fig. 1.7. The nine components visible in the figure define the stress state at a point. They can be reduced to six by taking into account that shear stresses with reversed indices must be equal in order to ensure moment equilibrium. For a collective representation of the stress state we introduce the 6×1 matrix array (stress vector)

$$\boldsymbol{\sigma} = \left\{ \sigma_{xx}\, \sigma_{yy}\, \sigma_{zz}\, \sqrt{2}\sigma_{xy}\, \sqrt{2}\sigma_{yz}\, \sqrt{2}\sigma_{xz} \right\}. \tag{1.22}$$

The state of strain is characterized by the direct strains $\gamma_{xx}, \gamma_{yy}, \gamma_{zz}$, which are obtained as the extensions of a unit cube along the coordinate axes, and the shear strains $\gamma_{xy}, \gamma_{yz}, \gamma_{xz}$ representing the changes of the angles of the cube in the respective planes (Fig. 1.8). For a collective representation of

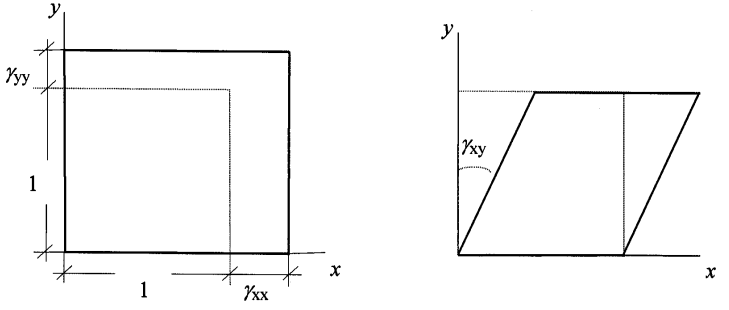

Figure 1.8: Definition of direct and shear strains.

the strain state, the 6×1 strain vector

$$\boldsymbol{\gamma} = \left\{ \gamma_{xx}\, \gamma_{yy}\, \gamma_{zz}\, \frac{1}{\sqrt{2}}\gamma_{xy}\, \frac{1}{\sqrt{2}}\gamma_{yz}\, \frac{1}{\sqrt{2}}\gamma_{xz} \right\} \tag{1.23}$$

is introduced in analogy to eqn (1.22) for the stress. The prefactors of the shear components in eqns (1.22) and (1.23) will help to simplify matrix operations [2].

Isotropic materials exhibit a markedly different response to normal stresses acting equally in all directions than to shear stresses. The so-called hydrostatic stress σ_H is defined as the mean value of the normal stress components,

$$\sigma_H = \frac{1}{3}(\sigma_{xx} + \sigma_{yy} + \sigma_{zz}) = \frac{1}{3}\mathbf{e}^t\boldsymbol{\sigma}, \tag{1.24}$$

where the indicated matrix operation makes use of the summation vector

$$\mathbf{e} = \{1\,1\,1\,0\,0\,0\}. \tag{1.25}$$

The single value of the hydrostatic stress is expanded to a hydrostatic stress state represented by the 6×1 stress vector

$$\boldsymbol{\sigma}_H = \{\sigma_H\, \sigma_H\, \sigma_H\, 0\, 0\, 0\}. \tag{1.26}$$

It consists of three direct components identical to σ_H and zero shear components, thus specifying the hydrostatic part of the stress state $\boldsymbol{\sigma}$. The matrix notation for the formation of $\boldsymbol{\sigma}_H$ reads

$$\boldsymbol{\sigma}_H = \sigma_H\mathbf{e} = \frac{1}{3}\mathbf{e}\mathbf{e}^t\boldsymbol{\sigma} \tag{1.27}$$

and defines the hydrostatic operator applied to the stress $\boldsymbol{\sigma}$.

The difference of the actual stress state $\boldsymbol{\sigma}$ to $\boldsymbol{\sigma}_H$ defines the deviatoric stress:

$$\boldsymbol{\sigma}_D = \boldsymbol{\sigma} - \boldsymbol{\sigma}_H = \left[\mathbf{I} - \frac{1}{3}\mathbf{e}\mathbf{e}^t\right]\boldsymbol{\sigma}, \tag{1.28}$$

where $\mathbf{I}$ denotes the identity matrix. The deviatoric stress components σ_{Dxx}, $\sigma_{Dyy}, \ldots$ are defined as in the array:

$$\boldsymbol{\sigma}_D = \left\{ (\sigma_{xx} - \sigma_H)\, (\sigma_{yy} - \sigma_H)\, (\sigma_{zz} - \sigma_H)\, \sqrt{2}\sigma_{xy}\, \sqrt{2}\sigma_{yz}\, \sqrt{2}\sigma_{xz} \right\}. \tag{1.29}$$

The deviatoric matrix operator applied to $\boldsymbol{\sigma}$ in eqn (1.28) modifies the direct stress components, while the shear stresses remain unaffected.

By definition, the deviatoric stress does not possess any hydrostatic component. Therefore, the condition

$$\mathbf{e}^t\boldsymbol{\sigma}_D = \sigma_{Dxx} + \sigma_{Dyy} + \sigma_{Dzz} = 0 \tag{1.30}$$

constrains the direct components of the deviatoric stress that cannot be varied independently. Hydrostatic and deviatoric constituents of the stress state are said to be orthogonal to each other in the sense that

$$\boldsymbol{\sigma}_{\mathrm{D}}^{\mathrm{t}}\boldsymbol{\sigma}_{\mathrm{H}} = \boldsymbol{\sigma}_{\mathrm{H}}^{\mathrm{t}}\boldsymbol{\sigma}_{\mathrm{D}} = 0, \tag{1.31}$$

which can be easily confirmed.

The strain state is partitioned in analogy to the stress. The volumetric strain γ_{V} is defined as

$$\gamma_{\mathrm{V}} = \frac{1}{3}(\gamma_{\mathrm{xx}} + \gamma_{\mathrm{yy}} + \gamma_{\mathrm{zz}}) = \frac{1}{3}\mathbf{e}^{\mathrm{t}}\boldsymbol{\gamma}. \tag{1.32}$$

A volumetric state of strain,

$$\boldsymbol{\gamma}_{\mathrm{V}} = \gamma_{\mathrm{V}}\mathbf{e} = \frac{1}{3}\mathbf{e}\mathbf{e}^{\mathrm{t}}\boldsymbol{\gamma}, \tag{1.33}$$

is obtained from the actual strain state by an application of the hydrostatic matrix operator of eqn (1.27). Analogously, the deviatoric strain

$$\boldsymbol{\gamma}_{\mathrm{D}} = \boldsymbol{\gamma} - \boldsymbol{\gamma}_{\mathrm{V}} = \left[\mathbf{I} - \frac{1}{3}\mathbf{e}\mathbf{e}^{\mathrm{t}}\right]\boldsymbol{\gamma} \tag{1.34}$$

follows as a result of the matrix operation defined in eqn (1.28). Deviatoric deformation conserves volume since

$$\mathbf{e}^{\mathrm{t}}\boldsymbol{\gamma}_{\mathrm{D}} = \gamma_{\mathrm{Dxx}} + \gamma_{\mathrm{Dyy}} + \gamma_{\mathrm{Dzz}} = 0. \tag{1.35}$$

In the elastoplastic regime each of the strain components in eqn (1.23) is considered to consist of two additive parts, the elastic strain and the plastic strain. The elastic part of the strain defines the 6×1 vector

$$\boldsymbol{\varepsilon} = \left\{\varepsilon_{\mathrm{xx}}\, \varepsilon_{\mathrm{yy}}\, \varepsilon_{\mathrm{zz}}\, \frac{1}{\sqrt{2}}\varepsilon_{\mathrm{xy}}\, \frac{1}{\sqrt{2}}\varepsilon_{\mathrm{yz}}\, \frac{1}{\sqrt{2}}\varepsilon_{\mathrm{xz}}\right\}, \tag{1.36}$$

and the plastic part of the strain defines the 6×1 vector

$$\boldsymbol{\eta} = \left\{\eta_{\mathrm{xx}}\, \eta_{\mathrm{yy}}\, \eta_{\mathrm{zz}}\, \frac{1}{\sqrt{2}}\eta_{\mathrm{xy}}\, \frac{1}{\sqrt{2}}\eta_{\mathrm{yz}}\, \frac{1}{\sqrt{2}}\eta_{\mathrm{xz}}\right\}. \tag{1.37}$$

The measured strain $\boldsymbol{\gamma}$ is then composed as

$$\boldsymbol{\gamma} = \boldsymbol{\varepsilon} + \boldsymbol{\eta}. \tag{1.38}$$

Volumetric and deviatoric states of $\boldsymbol{\varepsilon}$ and $\boldsymbol{\eta}$ are defined as for $\boldsymbol{\gamma}$. For instance, from eqn (1.33),

$$\boldsymbol{\gamma}_{\mathrm{V}} = \frac{1}{3}\mathbf{e}\mathbf{e}^{\mathrm{t}}[\boldsymbol{\varepsilon} + \boldsymbol{\eta}] = \boldsymbol{\varepsilon}_{\mathrm{V}} + \boldsymbol{\eta}_{\mathrm{V}}, \tag{1.39}$$

where $\boldsymbol{\varepsilon}_{\mathrm{V}}$ and $\boldsymbol{\eta}_{\mathrm{V}}$ result from the application of the hydrostatic operator to each of the constituents. Also, from eqn (1.34),

$$\boldsymbol{\gamma}_{\mathrm{D}} = \left[\mathbf{I} - \frac{1}{3}\mathbf{e}\mathbf{e}^{\mathrm{t}}\right][\boldsymbol{\varepsilon} + \boldsymbol{\eta}] = \boldsymbol{\varepsilon}_{\mathrm{D}} + \boldsymbol{\eta}_{\mathrm{D}}, \tag{1.40}$$

where $\boldsymbol{\varepsilon}_{\mathrm{D}}$ and $\boldsymbol{\eta}_{\mathrm{D}}$ denote the result of the deviator operation as applied to $\boldsymbol{\varepsilon}$ and $\boldsymbol{\eta}$, respectively. The condition of eqn (1.35) concerns each constituent separately:

$$\mathbf{e}^{\mathrm{t}}\boldsymbol{\varepsilon}_{\mathrm{D}} = 0, \quad \mathbf{e}^{\mathrm{t}}\boldsymbol{\eta}_{\mathrm{D}} = 0. \tag{1.41}$$

Elasticity

The partition of stress/strain into hydrostatic/volumetric and deviatoric constituents is utilized in forming the elasticity matrix for an isotropic material. In this case, hydrostatic stresses are proportional to volumetric strains:

$$\boldsymbol{\sigma}_{\mathrm{H}} = 3K\boldsymbol{\varepsilon}_{\mathrm{V}}. \tag{1.42}$$

The modulus of volume expansion K can be expressed in terms of the modulus of elasticity in tension (Young's modulus E) and the coefficient of lateral contraction (Poisson's ratio ν):

$$3K = \frac{E}{1-2\nu}. \tag{1.43}$$

Deviatoric stresses are set proportional to the deviatoric strains by the modulus of elasticity in shear G. The relationship between the respective vector arrays reads:

$$\boldsymbol{\sigma}_{\mathrm{D}} = 2G\boldsymbol{\varepsilon}_{\mathrm{D}}, \tag{1.44}$$

where

$$2G = \frac{E}{1+\nu}. \tag{1.45}$$

Superposition of eqns (1.42) and (1.44) gives the actual stress state, and expressing the parts $\boldsymbol{\varepsilon}_{\mathrm{D}}$ and $\boldsymbol{\varepsilon}_{\mathrm{V}}$ in terms of the entire $\boldsymbol{\varepsilon}$ in analogy to eqns (1.34) and (1.33) leads to the elastic stress–strain relationship:

$$\boldsymbol{\sigma} = 2G\boldsymbol{\varepsilon}_{\mathrm{D}} + 3K\boldsymbol{\varepsilon}_{\mathrm{V}} = 2G\left[\mathbf{I} + \frac{\nu}{1-2\nu}\mathbf{e}\mathbf{e}^{\mathrm{t}}\right]\boldsymbol{\varepsilon}. \tag{1.46}$$

In compact form, eqn (1.46) is written as

$$\boldsymbol{\sigma} = \boldsymbol{\kappa}\,\boldsymbol{\varepsilon}, \tag{1.47}$$

with the symmetric elasticity matrix (elastic material stiffness),

$$\boldsymbol{\kappa} = 2G\left[\mathbf{I} + \frac{\nu}{1-2\nu}\mathbf{e}\mathbf{e}^{\mathrm{t}}\right]. \tag{1.48}$$

The matrix relation in eqn (1.46) is easily inverted to determine the elastic strain for a given stress. Alternatively, the inverse form can be obtained directly using eqns (1.42) and (1.44). Superposition of the deviatoric and the volumetric part of strain from the above equations gives the elastic strain

$$\boldsymbol{\varepsilon} = \frac{1}{2G}\boldsymbol{\sigma}_{\mathrm{D}} + \frac{1}{3K}\boldsymbol{\sigma}_{\mathrm{H}} = \frac{1}{2G}\left[\mathbf{I} - \frac{\nu}{1+\nu}\mathbf{e}\mathbf{e}^{\mathrm{t}}\right]\boldsymbol{\sigma}. \tag{1.49}$$

Here, $\boldsymbol{\sigma}_{\mathrm{D}}$ and $\boldsymbol{\sigma}_{\mathrm{H}}$ have been expressed in terms of the stress $\boldsymbol{\sigma}$ by eqns (1.28) and (1.27), respectively. The inverse relation to eqn (1.47) becomes

$$\boldsymbol{\varepsilon} = \boldsymbol{\kappa}^{-1}\boldsymbol{\sigma} \tag{1.50}$$

with

$$\boldsymbol{\kappa}^{-1} = \frac{1}{2G}\left[\mathbf{I} - \frac{\nu}{1+\nu}\mathbf{e}\mathbf{e}^{\mathrm{t}}\right]. \tag{1.51}$$

1.2.2 Variation of the reference system: principal stresses

Prior to an analysis of the stress and strain components under transformations of the reference system, we consider a quantity which remains invariant: the work of the stresses on the strains. For this purpose, we refer to the volume element in Fig. 1.7 and assume the strain $\boldsymbol{\gamma}$ to be imposed on the material independently of an existing stress $\boldsymbol{\sigma}$. Since the stress components represent forces per unit area and strains may be interpreted as displacements per unit length, the expression

$$w = \sigma_{\mathrm{xx}}\gamma_{\mathrm{xx}} + \sigma_{\mathrm{yy}}\gamma_{\mathrm{yy}} + \sigma_{\mathrm{zz}}\gamma_{\mathrm{zz}} + \sigma_{\mathrm{xy}}\gamma_{\mathrm{xy}} + \sigma_{\mathrm{yz}}\gamma_{\mathrm{yz}} + \sigma_{\mathrm{xz}}\gamma_{\mathrm{xz}} = \boldsymbol{\sigma}^{\mathrm{t}}\boldsymbol{\gamma} \tag{1.52}$$

supplies the work of the stresses on the strains per unit volume of the material; it is invariant to transformations of the reference system.

Rotated reference system
Let the new reference system 0–$x'y'z'$ be rotated with respect to the original system 0–xyz. The coordinates of a point in the new system are obtained by the transformation

$$\begin{aligned} x' &= c_{\mathrm{x'x}}x \;+\; c_{\mathrm{x'y}}y \;+\; c_{\mathrm{x'z}}z \\ y' &= c_{\mathrm{y'x}}x \;+\; c_{\mathrm{y'y}}y \;+\; c_{\mathrm{y'z}}z \\ z' &= c_{\mathrm{z'x}}x \;+\; c_{\mathrm{z'y}}y \;+\; c_{\mathrm{z'z}}z. \end{aligned} \tag{1.53}$$

The coefficients in eqn (1.53) are the direction cosines of the rotated axes with respect to the original axes. For instance $c_{\mathrm{x'y}} = \cos(x', y)$ denotes the cosine of the new x'-direction to the original y-direction. Introducing the vectors

$$\mathbf{x}' = \{x'\ y'\ z'\}, \quad \mathbf{x} = \{x\ y\ z\} \tag{1.54}$$

and the transformation matrix,

$$\mathbf{C} = \begin{bmatrix} c_{\mathrm{x'x}} & c_{\mathrm{x'y}} & c_{\mathrm{x'z}} \\ c_{\mathrm{y'x}} & c_{\mathrm{y'y}} & c_{\mathrm{y'z}} \\ c_{\mathrm{z'x}} & c_{\mathrm{z'y}} & c_{\mathrm{z'z}} \end{bmatrix}, \tag{1.55}$$

one obtains a compact form of eqn (1.53) as

$$\mathbf{x}' = \mathbf{C}\mathbf{x}. \tag{1.56}$$

The inverse transformation reads

$$\begin{aligned} x &= c_{\mathrm{x'x}}x' + c_{\mathrm{y'x}}y' + c_{\mathrm{z'x}}z' \\ y &= c_{\mathrm{x'y}}x' + c_{\mathrm{y'y}}y' + c_{\mathrm{z'y}}z' \\ z &= c_{\mathrm{x'z}}x' + c_{\mathrm{y'z}}y' + c_{\mathrm{z'z}}z', \end{aligned} \tag{1.57}$$

and in matrix form

$$\mathbf{x} = \mathbf{C}^{\mathrm{t}}\mathbf{x}'. \tag{1.58}$$

From eqns (1.56) and (1.58), it follows that

$$\mathbf{C}^{\mathrm{t}}\mathbf{C} = \mathbf{C}\mathbf{C}^{\mathrm{t}} = \mathbf{I}. \tag{1.59}$$

Therefore, scalar multiplication of each column of $\mathbf{C}$ by itself gives unity, while multiplication by a different column yields zero; the same applies to the rows. The matrix $\mathbf{C}$ is orthogonal and its inverse is obtained by transposition.

For a transformation of the stress components, the infinitesimal tetrahedral element in Fig. 1.9 is considered to have the oblique face with area A normal to the new x'-direction. The areas of the three other faces are obtained as the projections of A onto the coordinate planes. These are

$$A_{\mathrm{x}} = Ac_{\mathrm{x'x}}, \quad A_y = Ac_{\mathrm{x'y}}, \quad A_z = Ac_{\mathrm{x'z}}. \tag{1.60}$$

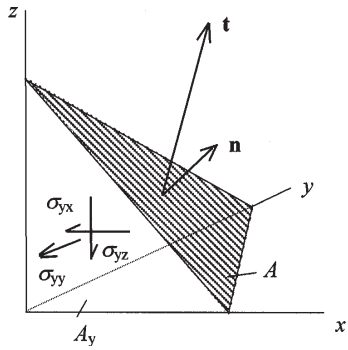

Figure 1.9: Transformation of stress components.

The force transferred by the oblique face to the tetrahedron is equilibrated by the stress resultants on the other three faces. Let $\mathbf{t} = \{t_\mathrm{x}\, t_\mathrm{y}\, t_\mathrm{z}\}$ denote the force transferred per unit area of the oblique face (traction). The component of the force along the x-direction is determined by

$$t_\mathrm{x} A = \sigma_{\mathrm{xx}} A_\mathrm{x} + \sigma_{\mathrm{yx}} A_\mathrm{y} + \sigma_{\mathrm{zx}} A_\mathrm{z}. \tag{1.61}$$

Analogously, two other equations are deduced for the y- and the z-directions. Substituting the areas $A_\mathrm{x}, A_\mathrm{y}, A_\mathrm{z}$ from eqn (1.60) in these three equations we obtain the component quantities $t_\mathrm{x}, t_\mathrm{y}, t_\mathrm{z}$ on the oblique face as

$$\begin{aligned} t_\mathrm{x} &= \sigma_{\mathrm{xx}}\, c_{\mathrm{x'x}} \;+\; \sigma_{\mathrm{yx}}\, c_{\mathrm{x'y}} \;+\; \sigma_{\mathrm{zx}}\, c_{\mathrm{x'z}} \\ t_\mathrm{y} &= \sigma_{\mathrm{xy}}\, c_{\mathrm{x'x}} \;+\; \sigma_{\mathrm{yy}}\, c_{\mathrm{x'y}} \;+\; \sigma_{\mathrm{zy}}\, c_{\mathrm{x'z}} \\ t_\mathrm{z} &= \sigma_{\mathrm{xz}}\, c_{\mathrm{x'x}} \;+\; \sigma_{\mathrm{yz}}\, c_{\mathrm{x'y}} \;+\; \sigma_{\mathrm{zz}}\, c_{\mathrm{x'z}}. \end{aligned} \tag{1.62}$$

Projection onto the new directions gives the direct and the shear stresses in the system 0–$x'y'z'$ for a plane normal to x' as

$$\begin{aligned} \sigma'_{\mathrm{xx}} &= c_{\mathrm{x'x}}\, t_\mathrm{x} \;+\; c_{\mathrm{x'y}}\, t_\mathrm{y} \;+\; c_{\mathrm{x'z}}\, t_\mathrm{z} \\ \sigma'_{\mathrm{xy}} &= c_{\mathrm{y'x}}\, t_\mathrm{x} \;+\; c_{\mathrm{y'y}}\, t_\mathrm{y} \;+\; c_{\mathrm{y'z}}\, t_\mathrm{z} \\ \sigma'_{\mathrm{xz}} &= c_{\mathrm{z'x}}\, t_\mathrm{x} \;+\; c_{\mathrm{z'y}}\, t_\mathrm{y} \;+\; c_{\mathrm{z'z}}\, t_\mathrm{z}. \end{aligned} \tag{1.63}$$

Both eqns (1.63) and(1.62) are interpreted as matrix multiplications and combined in the expression

$$\begin{bmatrix} \sigma'_{\mathrm{xx}} \\ \sigma'_{\mathrm{xy}} \\ \sigma'_{\mathrm{xz}} \end{bmatrix} = \begin{bmatrix} c_{\mathrm{x'x}} & c_{\mathrm{x'y}} & c_{\mathrm{x'z}} \\ c_{\mathrm{y'x}} & c_{\mathrm{y'y}} & c_{\mathrm{y'z}} \\ c_{\mathrm{z'x}} & c_{\mathrm{z'y}} & c_{\mathrm{z'z}} \end{bmatrix} \begin{bmatrix} \sigma_{\mathrm{xx}} & \sigma_{\mathrm{yx}} & \sigma_{\mathrm{zx}} \\ \sigma_{\mathrm{xy}} & \sigma_{\mathrm{yy}} & \sigma_{\mathrm{zy}} \\ \sigma_{\mathrm{xz}} & \sigma_{\mathrm{yz}} & \sigma_{\mathrm{zz}} \end{bmatrix} \begin{bmatrix} c_{\mathrm{x'x}} \\ c_{\mathrm{x'y}} \\ c_{\mathrm{x'z}} \end{bmatrix}. \tag{1.64}$$

The stress components on planes normal to the other two directions y' and z' are obtained analogously by considering elemental tetrahedra with an oblique face in the system 0–xyz normal to the new directions. Thereby, the denomination of the stresses on the left-hand side of eqn (1.64) has to be changed for the new normal direction considered. The latter is specified on the right-hand side. Summarizing, eqn (1.64) is completed as follows:

$$\begin{bmatrix} \sigma'_{\mathrm{xx}} & \sigma'_{\mathrm{yx}} & \sigma'_{\mathrm{zx}} \\ \sigma'_{\mathrm{xy}} & \sigma'_{\mathrm{yy}} & \sigma'_{\mathrm{zy}} \\ \sigma'_{\mathrm{xz}} & \sigma'_{\mathrm{yz}} & \sigma'_{\mathrm{zz}} \end{bmatrix} = \begin{bmatrix} c_{\mathrm{x'x}} & c_{\mathrm{x'y}} & c_{\mathrm{x'z}} \\ c_{\mathrm{y'x}} & c_{\mathrm{y'y}} & c_{\mathrm{y'z}} \\ c_{\mathrm{z'x}} & c_{\mathrm{z'y}} & c_{\mathrm{z'z}} \end{bmatrix} \begin{bmatrix} \sigma_{\mathrm{xx}} & \sigma_{\mathrm{yx}} & \sigma_{\mathrm{zx}} \\ \sigma_{\mathrm{xy}} & \sigma_{\mathrm{yy}} & \sigma_{\mathrm{zy}} \\ \sigma_{\mathrm{xz}} & \sigma_{\mathrm{yz}} & \sigma_{\mathrm{zz}} \end{bmatrix} \begin{bmatrix} c_{\mathrm{x'x}} & c_{\mathrm{y'x}} & c_{\mathrm{z'x}} \\ c_{\mathrm{x'y}} & c_{\mathrm{y'y}} & c_{\mathrm{z'y}} \\ c_{\mathrm{x'z}} & c_{\mathrm{y'z}} & c_{\mathrm{z'z}} \end{bmatrix}. \tag{1.65}$$

The first coefficient matrix in eqn (1.65) is $\mathbf{C}$, eqn (1.55), while the last is the transpose matrix $\mathbf{C}^\mathrm{t}$. With reference to eqn (1.59), the inverse relation to eqn (1.65) can be given explicitly.

Transformation of vector arrays
Transferring eqn (1.65) to the 6×1 stress vector $\boldsymbol{\sigma}$, eqn (1.22), we obtain instead

$$\boldsymbol{\sigma}' = \bar{\mathbf{C}}\boldsymbol{\sigma} \tag{1.66}$$

between the stress components in the original and the rotated system. The detailed form of the coefficient matrix in eqn (1.66) is

$$\bar{\mathbf{C}} = \begin{bmatrix} \bar{\mathbf{C}}_{\mathrm{nn}} & \sqrt{2}\bar{\mathbf{C}}_{\mathrm{ns}} \\ \sqrt{2}\bar{\mathbf{C}}_{\mathrm{sn}} & \bar{\mathbf{C}}_{\mathrm{ss}} \end{bmatrix}, \tag{1.67}$$

with the submatrices

$$\bar{\mathbf{C}}_{\mathrm{nn}} = \begin{bmatrix} c^2_{\mathrm{x'x}} & c^2_{\mathrm{x'y}} & c^2_{\mathrm{x'z}} \\ c^2_{\mathrm{y'x}} & c^2_{\mathrm{y'y}} & c^2_{\mathrm{y'z}} \\ c^2_{\mathrm{z'x}} & c^2_{\mathrm{z'y}} & c^2_{\mathrm{z'z}} \end{bmatrix},$$

$$\bar{\mathbf{C}}_{\mathrm{ss}} = \begin{bmatrix} c_{\mathrm{x'x}}\,c_{\mathrm{y'y}} + c_{\mathrm{x'y}}\,c_{\mathrm{y'x}} & c_{\mathrm{x'y}}\,c_{\mathrm{y'z}} + c_{\mathrm{x'z}}\,c_{\mathrm{y'y}} & c_{\mathrm{x'x}}\,c_{\mathrm{y'z}} + c_{\mathrm{x'z}}\,c_{\mathrm{y'x}} \\ c_{\mathrm{y'x}}\,c_{\mathrm{z'y}} + c_{\mathrm{y'y}}\,c_{\mathrm{z'x}} & c_{\mathrm{y'y}}\,c_{\mathrm{z'z}} + c_{\mathrm{y'z}}\,c_{\mathrm{z'y}} & c_{\mathrm{y'x}}\,c_{\mathrm{z'z}} + c_{\mathrm{y'z}}\,c_{\mathrm{z'x}} \\ c_{\mathrm{x'x}}\,c_{\mathrm{z'y}} + c_{\mathrm{x'y}}\,c_{\mathrm{z'x}} & c_{\mathrm{x'y}}\,c_{\mathrm{z'z}} + c_{\mathrm{x'z}}\,c_{\mathrm{z'y}} & c_{\mathrm{x'x}}\,c_{\mathrm{z'z}} + c_{\mathrm{x'z}}\,c_{\mathrm{z'x}} \end{bmatrix}, \tag{1.68}$$

$$\bar{\mathbf{C}}_{\mathrm{ns}} = \begin{bmatrix} c_{\mathrm{x'x}}\,c_{\mathrm{x'y}} & c_{\mathrm{x'y}}\,c_{\mathrm{x'z}} & c_{\mathrm{x'x}}\,c_{\mathrm{x'z}} \\ c_{\mathrm{y'x}}\,c_{\mathrm{y'y}} & c_{\mathrm{y'y}}\,c_{\mathrm{y'z}} & c_{\mathrm{y'x}}\,c_{\mathrm{y'z}} \\ c_{\mathrm{z'x}}\,c_{\mathrm{z'y}} & c_{\mathrm{z'y}}\,c_{\mathrm{z'z}} & c_{\mathrm{z'x}}\,c_{\mathrm{z'z}} \end{bmatrix},$$

$$\bar{\mathbf{C}}_{\mathrm{sn}} = \begin{bmatrix} c_{\mathrm{x'x}}\,c_{\mathrm{y'x}} & c_{\mathrm{x'y}}\,c_{\mathrm{y'y}} & c_{\mathrm{x'z}}\,c_{\mathrm{y'z}} \\ c_{\mathrm{y'x}}\,c_{\mathrm{z'x}} & c_{\mathrm{y'y}}\,c_{\mathrm{z'y}} & c_{\mathrm{y'z}}\,c_{\mathrm{z'z}} \\ c_{\mathrm{x'x}}\,c_{\mathrm{z'x}} & c_{\mathrm{x'y}}\,c_{\mathrm{z'y}} & c_{\mathrm{x'z}}\,c_{\mathrm{z'z}} \end{bmatrix}.$$

The transformation for the strain can be deduced from the invariance of the elementary work expression, eqn (1.52):

$$w = \boldsymbol{\sigma}^{\mathrm{t}}\boldsymbol{\gamma} = (\boldsymbol{\sigma}')^{\mathrm{t}}\boldsymbol{\gamma}' = \boldsymbol{\sigma}^{\mathrm{t}}\bar{\mathbf{C}}^{\mathrm{t}}\boldsymbol{\gamma}'. \tag{1.69}$$

Since the invariance of the elementary work to the reference system is independent of a particular stress state, there follows from eqn (1.69) for the strain

$$\boldsymbol{\gamma} = \bar{\mathbf{C}}^{\mathrm{t}}\boldsymbol{\gamma}'. \tag{1.70}$$

The inverse transformation to eqn (1.66) is found to be

$$\boldsymbol{\sigma} = \bar{\mathbf{C}}^{\mathrm{t}}\boldsymbol{\sigma}' \tag{1.71}$$

and implies the dual relation for the strain

$$\boldsymbol{\gamma}' = \bar{\mathbf{C}}\boldsymbol{\gamma}. \tag{1.72}$$

Comparison of eqns (1.71) and (1.72) with eqns (1.66) and (1.70), respectively, gives

$$\bar{\mathbf{C}}^{\mathrm{t}}\bar{\mathbf{C}} = \bar{\mathbf{C}}\bar{\mathbf{C}}^{\mathrm{t}} = \mathbf{I} \tag{1.73}$$

and therefore $\bar{\mathbf{C}}$ is an orthogonal matrix.

By virtue of eqn (1.73) it can be confirmed that the magnitude (length) of stress and strain vectors is invariant to rotations of the reference system:

$$\boldsymbol{\sigma}^{\mathrm{t}}\boldsymbol{\sigma} = (\boldsymbol{\sigma}')^{\mathrm{t}}\bar{\mathbf{C}}\bar{\mathbf{C}}^{\mathrm{t}}\boldsymbol{\sigma}' = (\boldsymbol{\sigma}')^{\mathrm{t}}\boldsymbol{\sigma}' \tag{1.74}$$

and

$$(\boldsymbol{\gamma}')^{\mathrm{t}}\boldsymbol{\gamma}' = \boldsymbol{\gamma}^{\mathrm{t}}\bar{\mathbf{C}}^{\mathrm{t}}\bar{\mathbf{C}}\boldsymbol{\gamma} = \boldsymbol{\gamma}^{\mathrm{t}}\boldsymbol{\gamma}. \tag{1.75}$$

Considering next the hydrostatic stress separately we obtain

$$\sigma_{\mathrm{H}} = \frac{1}{3}\,\mathbf{e}^{\mathrm{t}}\boldsymbol{\sigma} = \frac{1}{3}\mathbf{e}^{\mathrm{t}}\bar{\mathbf{C}}^{\mathrm{t}}\boldsymbol{\sigma}' = \frac{1}{3}\mathbf{e}^{\mathrm{t}}\boldsymbol{\sigma}', \tag{1.76}$$

which conforms with the identity for $\mathbf{e} = \{1\ 1\ 1\ 0\ 0\ 0\}$:

$$\bar{\mathbf{C}}\mathbf{e} \equiv \bar{\mathbf{C}}^{\mathrm{t}}\mathbf{e} \equiv \mathbf{e}. \tag{1.77}$$

The expression for σ_{H} is invariant to rotations of the reference system, and this is obviously reflected in the complete hydrostatic stress vector:

$$\boldsymbol{\sigma}'_{\mathrm{H}} = \bar{\mathbf{C}}\boldsymbol{\sigma}_{\mathrm{H}} = \boldsymbol{\sigma}_{\mathrm{H}}. \tag{1.78}$$

The deviatoric stress in the transformed system is obtained by

$$\boldsymbol{\sigma}'_{\mathrm{D}} = \boldsymbol{\sigma}' - \boldsymbol{\sigma}'_{\mathrm{H}} = \bar{\mathbf{C}}\boldsymbol{\sigma}_{\mathrm{D}}. \tag{1.79}$$

In analogy to the stress, the transformation by eqn (1.72) for the strain applies to the deviatoric part, while the volumetric strain is insensitive to it. The transformation is, of course, not affected by the physical nature of the strain, be it elastic or plastic.

Principal axes

Principal stress directions are defined by the requirement that only normal components exist on the plane element, while any tangential component is absent. Let the normal vector $\mathbf{n} = \{l\, m\, n\}$ specify a principal stress plane. The components of the traction $\mathbf{t} = \{t_{\mathrm{x}}\, t_{\mathrm{y}}\, t_{\mathrm{z}}\}$ on the associated plane element are obtained in analogy to eqn (1.62). In matrix form:

$$\mathbf{t} = \mathbf{T}^{\mathrm{t}}\mathbf{n}. \tag{1.80}$$

Here, the symbol $\mathbf{T}^{\mathrm{t}}$ stands for the arrangement of the stress components in the 6×6 matrix array as in eqn (1.64), and the normal vector $\mathbf{n}$ replaces the previous specification of the x'-direction. Since the traction $\mathbf{t}$ is now requested to

point along the principal axis, it can be represented as $\mathbf{t} = \sigma\mathbf{n}, \sigma$ being a scalar multiplier to the normal $\mathbf{n}$. Comparison with eqn (1.80) leads to the condition

$$[\mathbf{T}^{\mathrm{t}} - \sigma\mathbf{I}]\mathbf{n} = \mathbf{0} \tag{1.81}$$

for the principal direction $\mathbf{n}$, which defines an eigenvalue problem. Non-trivial solutions of the homogeneous linear system for $\mathbf{n}$ require that the determinant of the coefficient matrix vanishes. We write

$$|\mathbf{T}^{\mathrm{t}} - \sigma\mathbf{I}| = \begin{vmatrix} \sigma_{\mathrm{xx}} - \sigma & \sigma_{\mathrm{xy}} & \sigma_{\mathrm{xz}} \\ \sigma_{\mathrm{yx}} & \sigma_{\mathrm{yy}} - \sigma & \sigma_{\mathrm{yz}} \\ \sigma_{\mathrm{zx}} & \sigma_{\mathrm{zy}} & \sigma_{\mathrm{zz}} - \sigma \end{vmatrix} = 0. \tag{1.82}$$

The solution of eqn (1.82) for σ and eqn (1.81) for $\mathbf{n}$ specifies three principal directions for the considered stress state [3]. They are orthogonal to each other and associated with three values of the scalar σ, the principal stresses σ_1, σ_2 and σ_3. The principal directions thus define the axes of a reference system 0–$x_{\mathrm{I}}y_{\mathrm{I}}z_{\mathrm{I}}$ (or simply 0–1 2 3) in which the considered state of stress does not exhibit tangential components, but only the above normal components.

A principal stress vector is introduced as the 3×1 column array

$$\boldsymbol{\sigma}_{\mathrm{I}} = \{\sigma_1\ \sigma_2\ \sigma_3\}. \tag{1.83}$$

Given the principal directions, it can be obtained from the stress state by the transformation of eqn (1.66) to

$$\boldsymbol{\sigma}_{\mathrm{I}} = \bar{\mathbf{C}}_{\mathrm{I}}\boldsymbol{\sigma}. \tag{1.84}$$

The principal stress vector in eqn (1.83) allows the transformation to be accomplished with the reduced matrix

$$\bar{\mathbf{C}}_{\mathrm{I}} = [\bar{\mathbf{C}}_{\mathrm{nn}}\ \sqrt{2}\bar{\mathbf{C}}_{\mathrm{ns}}]_{\mathrm{I}}, \tag{1.85}$$

instead of the complete one in eqn (1.67). It can be easily verified that the inverse relation to eqn (1.84) reads

$$\boldsymbol{\sigma} = \bar{\mathbf{C}}_{\mathrm{I}}^{\mathrm{t}}\boldsymbol{\sigma}_{\mathrm{I}}, \tag{1.86}$$

and thus the three principal stresses completely define the stress state in conjunction with the principal directions. The transformation by eqn (1.84) also applies to the deviatoric part of the stress

$$\boldsymbol{\sigma}_{\mathrm{DI}} = \bar{\mathbf{C}}_{\mathrm{I}}\boldsymbol{\sigma}_{\mathrm{D}} \quad \text{and} \quad \boldsymbol{\sigma}_{\mathrm{D}} = \bar{\mathbf{C}}_{\mathrm{I}}^{\mathrm{t}}\boldsymbol{\sigma}_{\mathrm{DI}}. \tag{1.87}$$

The hydrostatic part is invariant to rotations of the reference axes.

In analogy to the principal stresses, principal strains

$$\boldsymbol{\gamma}_{\mathrm{I}} = \{\gamma_1\ \gamma_2\ \gamma_3\} \tag{1.88}$$

can be obtained for a given strain state independently of the stress. It is of interest, however, to consider strains associated with the stresses by the

constitutive law of the material. For the isotropic elastic material an imposition of stresses results in strains determined by eqns (1.42) and (1.44). In this case, principal deviatoric stresses $\boldsymbol{\sigma}_{\mathrm{DI}}$ lead to principal deviatoric strains:

$$\boldsymbol{\varepsilon}_{\mathrm{DI}} = \frac{1}{2G}\boldsymbol{\sigma}_{\mathrm{DI}} = \bar{\mathbf{C}}_{\mathrm{I}}\boldsymbol{\varepsilon}_{\mathrm{D}}. \tag{1.89}$$

The transition to the last expression uses eqn (1.87) for the principal stress transformation and observes the elasticity law. Since hydrostatic stresses cause volumetric elastic strains independently of coordinate rotations, the latter may be added unaltered to the deviatoric strain on both sides of eqn (1.89). As a result, we obtain for the complete strain state

$$\boldsymbol{\varepsilon}_{\mathrm{I}} = \bar{\mathbf{C}}_{\mathrm{I}}\boldsymbol{\varepsilon} \quad \text{and} \quad \boldsymbol{\varepsilon} = \bar{\mathbf{C}}_{\mathrm{I}}^{\mathrm{t}}\boldsymbol{\varepsilon}_{\mathrm{I}}, \tag{1.90}$$

which demonstrates that in isotropic elasticity the principal strains are co-axial to the associated principal stresses. The matrix $\bar{\mathbf{C}}_{\mathrm{I}}$ from the stress transformation also applies to the strain and vice versa.

1.2.3 Perfectly plastic material

Yield criterion and yield condition

In order to define combinations of stresses critical to plastic flow, we consider the elastic energy stored in a unit volume element of the material:

$$w_{\mathrm{e}} = \int_0^{\varepsilon} \boldsymbol{\sigma}^{\mathrm{t}}\mathrm{d}\boldsymbol{\varepsilon} = \frac{1}{2}\boldsymbol{\sigma}^{\mathrm{t}}\boldsymbol{\kappa}^{-1}\boldsymbol{\sigma}. \tag{1.91}$$

The integral in eqn (1.91) is evaluated for the stress using the elasticity law, eqn (1.50). With reference to deviatoric and hydrostatic or volumetric stress and strain, the energy expression is resolved into two parts:

$$\int \boldsymbol{\sigma}^{\mathrm{t}}\mathrm{d}\boldsymbol{\varepsilon} = \int \boldsymbol{\sigma}_{\mathrm{D}}^{\mathrm{t}}\mathrm{d}\boldsymbol{\varepsilon}_{\mathrm{D}} + 3\int \sigma_{\mathrm{H}}\mathrm{d}\varepsilon_{\mathrm{V}}. \tag{1.92}$$

As deviatoric stresses are orthogonal to volumetric strains (Section 1.2.1) the respective mixed scalar products vanish.

The first integral on the right-hand side of eqn (1.92) supplies the deviatoric strain energy, or energy of elastic distortion. Evaluation for the deviatoric stress $\boldsymbol{\sigma}_{\mathrm{D}}$ by utilizing the elastic relation for $\boldsymbol{\varepsilon}_{\mathrm{D}}$, eqn (1.44), gives

$$\int_0^{\varepsilon_{\mathrm{D}}} \boldsymbol{\sigma}_{\mathrm{D}}^{\mathrm{t}}\mathrm{d}\boldsymbol{\varepsilon}_{\mathrm{D}} = \frac{1}{2G}\int_0^{\sigma_{\mathrm{D}}} \boldsymbol{\sigma}_{\mathrm{D}}^{\mathrm{t}}\mathrm{d}\boldsymbol{\sigma}_{\mathrm{D}} = \frac{1}{4G}\boldsymbol{\sigma}_{\mathrm{D}}^{\mathrm{t}}\boldsymbol{\sigma}_{\mathrm{D}}. \tag{1.93}$$

The second integral on the right-hand side of eqn (1.92) supplies the energy of volume change. Utilizing the elastic relation between the volumetric strain

ε_{V} and the hydrostatic stress σ_{H}, eqn (1.42), we obtain:

$$3\int_0^{\varepsilon_{\mathrm{V}}}\sigma_{\mathrm{H}}\mathrm{d}\varepsilon_{\mathrm{V}} = \frac{1}{K}\int_0^{\sigma_{\mathrm{H}}}\sigma_{\mathrm{H}}\mathrm{d}\sigma_{\mathrm{H}} = \frac{1}{2K}\sigma_{\mathrm{H}}^2. \tag{1.94}$$

Metallic materials are found to be insensitive to plastic yielding when subjected to hydrostatic stress. The criterion for yielding is therefore based on the assumption that metals yield when the energy of elastic distortion attains a critical value independently of the particular combination of the stresses. When a uniaxial tensile specimen reaches the elastic limit stress σ_{s}, the deviatoric stress state is specified by the direct components $2\sigma_{\mathrm{s}}/3, -\sigma_{\mathrm{s}}/3, -\sigma_{\mathrm{s}}/3$. From eqn (1.93) the critical energy of distortion is then determined as

$$w_{\mathrm{s}} = \frac{\sigma_{\mathrm{s}}^2}{6G}. \tag{1.95}$$

For multiaxial stress states, the condition limiting the elastic range can be deduced by equating the expression for the energy of distortion in eqn (1.93) to its critical value from the uniaxial test, eqn (1.95). It reads

$$\frac{3}{2}\boldsymbol{\sigma}_{\mathrm{D}}^{\mathrm{t}}\boldsymbol{\sigma}_{\mathrm{D}} = \sigma_{\mathrm{s}}^2. \tag{1.96}$$

Equation (1.96) motivates the introduction of the *equivalent deviatoric stress* $\bar{\sigma}$ defined by

$$\bar{\sigma}^2 = \frac{3}{2}\boldsymbol{\sigma}_{\mathrm{D}}^{\mathrm{t}}\boldsymbol{\sigma}_{\mathrm{D}} = \frac{3}{2}\boldsymbol{\sigma}_{\mathrm{D}}^{\mathrm{t}}\boldsymbol{\sigma}, \tag{1.97}$$

as a *yield criterion*. This criterion was proposed by Huber [4] and later independently by von Mises [5]. The transition to the second expression in eqn (1.97) is possible because hydrostatic stresses in $\boldsymbol{\sigma}$ do not contribute to the scalar product with the deviatoric stresses. Since the equivalent stress is defined by a work expression, it is invariant to rotations of the reference system in which the stress components are specified, cf. also eqn (1.74).

The component form of $\bar{\sigma}^2$ is obtained with the entities of $\boldsymbol{\sigma}_{\mathrm{D}}$, eqn (1.29), as

$$\bar{\sigma}^2 = \frac{3}{2}\boldsymbol{\sigma}_{\mathrm{D}}^{\mathrm{t}}\boldsymbol{\sigma}_{\mathrm{D}} = \frac{3}{2}(\sigma_{\mathrm{xxD}}^2 + \sigma_{\mathrm{yyD}}^2 + \sigma_{\mathrm{zzD}}^2 + 2\sigma_{\mathrm{xy}}^2 + 2\sigma_{\mathrm{yz}}^2 + 2\sigma_{\mathrm{xz}}^2) \tag{1.98}$$

and interprets the equivalent stress as a measure of the magnitude of the deviatoric stress vector. The alternative expression for $\bar{\sigma}^2$ in eqn (1.97) appears to be advantageous when some components in the stress vector $\boldsymbol{\sigma}$ are zero, while present in the deviatoric $\boldsymbol{\sigma}_{\mathrm{D}}$. In the uniaxial case, for instance, the only non-zero stress is $\sigma_{\mathrm{xx}} = \sigma$ and therefore evaluation of $\bar{\sigma}^2$ requires merely a single deviatoric component: $\sigma_{\mathrm{Dxx}} = 2\sigma/3$. From eqn (1.97),

$$\bar{\sigma}^2 = \frac{3}{2}\boldsymbol{\sigma}_{\mathrm{D}}^{\mathrm{t}}\boldsymbol{\sigma} = \frac{3}{2}\sigma_{\mathrm{Dxx}}\sigma_{\mathrm{xx}} = \sigma^2. \tag{1.99}$$

For a two-dimensional stress state, the stress vector becomes

$$\boldsymbol{\sigma} = \{\sigma_{\mathrm{xx}}\ \sigma_{\mathrm{yy}}\ 0\ \sqrt{2}\sigma_{\mathrm{xy}}\ 0\ 0\} \tag{1.100}$$

and evaluation of the equivalent stress expression is reduced to the non-zero stress components in the x, y-plane. The normal components of the deviatoric stress in the plane are $\sigma_{\mathrm{Dxx}} = (2\sigma_{\mathrm{xx}} - \sigma_{\mathrm{yy}})/3$ and $\sigma_{\mathrm{Dyy}} = (2\sigma_{\mathrm{yy}} - \sigma_{\mathrm{xx}})/3$, while the third, $\sigma_{\mathrm{Dzz}} = -(\sigma_{\mathrm{xx}} + \sigma_{\mathrm{yy}})/3$, is not required for the present purpose. Then from eqn (1.97),

$$\bar{\sigma}^2 = \frac{3}{2}\boldsymbol{\sigma}_{\mathrm{D}}^{\mathrm{t}}\boldsymbol{\sigma} = \sigma_{\mathrm{xx}}^2 + \sigma_{\mathrm{yy}}^2 - \sigma_{\mathrm{xx}}\sigma_{\mathrm{yy}} + 3\sigma_{\mathrm{xy}}^2. \tag{1.101}$$

In a three-dimensional stress state the normal deviatoric stress components are obtained as $\sigma_{\mathrm{Dxx}} = (2\sigma_{\mathrm{xx}} - \sigma_{\mathrm{yy}} - \sigma_{\mathrm{zz}})/3$, $\sigma_{\mathrm{Dyy}} = (2\sigma_{\mathrm{yy}} - \sigma_{\mathrm{zz}} - \sigma_{\mathrm{xx}})/3$ and $\sigma_{\mathrm{Dzz}} = (2\sigma_{\mathrm{zz}} - \sigma_{\mathrm{xx}} - \sigma_{\mathrm{yy}})/3$. Together with the shear stress components they define the vector $\boldsymbol{\sigma}_{\mathrm{D}}$. Evaluation of eqn (1.97) gives

$$\begin{aligned}\bar{\sigma}^2 &= \frac{3}{2}\boldsymbol{\sigma}_{\mathrm{D}}^{\mathrm{t}}\boldsymbol{\sigma} \\ &= \frac{1}{2}\left[(\sigma_{\mathrm{xx}} - \sigma_{\mathrm{yy}})^2 + (\sigma_{\mathrm{yy}} - \sigma_{\mathrm{zz}})^2 + (\sigma_{\mathrm{zz}} - \sigma_{\mathrm{xx}})^2 + 6(\sigma_{\mathrm{xy}}^2 + \sigma_{\mathrm{yz}}^2 + \sigma_{\mathrm{xz}}^2)\right],\end{aligned} \tag{1.102}$$

in terms of the components of the complete stress vector.

Equation (1.96) in conjunction with the definition by eqn (1.97) suggests the introduction of a *yield function* $\phi(\boldsymbol{\sigma})$ such that

$$\phi(\boldsymbol{\sigma}) = \bar{\sigma} - \sigma_{\mathrm{s}} \leq 0. \tag{1.103}$$

The yield function ϕ compares the stress state $\boldsymbol{\sigma}$ with the uniaxial yield stress σ_{s} of the material via the equivalent stress $\bar{\sigma}$, and specifies the *yield condition* as in eqn (1.103). Thereby the value of the yield function limits elastic stress states to $\phi(\boldsymbol{\sigma}) < 0$ and defines plastic states at the yield limit $\phi(\boldsymbol{\sigma}) = 0$.

Plastic flow

Non-hardening, perfectly plastic materials are characterized by a constant yield stress and therefore the yield condition of eqn (1.103) remains the same as for initial yield independently of the amount of plastic deformation. The yield function ϕ for a certain material then depends solely on the stress, and once $\boldsymbol{\sigma}$ constitutes a plastic state $\phi(\boldsymbol{\sigma}) = 0$, stress changes *consistent with the yield condition* are restricted by the requirement

$$\mathrm{d}\phi = \frac{\mathrm{d}\phi}{\mathrm{d}\boldsymbol{\sigma}}\mathrm{d}\boldsymbol{\sigma} \leq 0. \tag{1.104}$$

The matrix notation of the differential operation implies the definitions

$$\frac{\mathrm{d}\phi}{\mathrm{d}\boldsymbol{\sigma}} = \left[\frac{\partial\phi}{\partial\sigma_{\mathrm{xx}}}\ \frac{\partial\phi}{\partial\sigma_{\mathrm{yy}}}\ \frac{\partial\phi}{\partial\sigma_{\mathrm{zz}}}\ \frac{1}{\sqrt{2}}\frac{\partial\phi}{\partial\sigma_{\mathrm{xy}}}\ \frac{1}{\sqrt{2}}\frac{\partial\phi}{\partial\sigma_{\mathrm{yz}}}\ \frac{1}{\sqrt{2}}\frac{\partial\phi}{\partial\sigma_{\mathrm{xz}}}\right] \tag{1.105}$$

and

$$\mathrm{d}\boldsymbol{\sigma} = \{\mathrm{d}\sigma_{\mathrm{xx}}\,\mathrm{d}\sigma_{\mathrm{yy}}\,\mathrm{d}\sigma_{\mathrm{zz}}\,\sqrt{2}\mathrm{d}\sigma_{\mathrm{xy}}\,\sqrt{2}\mathrm{d}\sigma_{\mathrm{yz}}\,\sqrt{2}\mathrm{d}\sigma_{\mathrm{xz}}\}.$$

In eqn (1.104) the negative sign leads to elastic states $\phi + \mathrm{d}\phi < 0$, while transitions to another plastic state $\phi + \mathrm{d}\phi = 0$ are governed by the equality sign and may be accompanied by plastic flow.

From eqn (1.103), changes of the yield function are given by $\mathrm{d}\phi = \mathrm{d}\bar{\sigma}$. With reference to eqn (1.97) for the equivalent deviatoric stress $\bar{\sigma}$, by differentiation,

$$2\bar{\sigma}\mathrm{d}\bar{\sigma} = \frac{3}{2}\left[\boldsymbol{\sigma}_{\mathrm{D}}^{\mathrm{t}}\mathrm{d}\boldsymbol{\sigma}_{\mathrm{D}} + \mathrm{d}\boldsymbol{\sigma}_{\mathrm{D}}^{\mathrm{t}}\boldsymbol{\sigma}_{\mathrm{D}}\right] \tag{1.106}$$

and since in scalar products factors can be interchanged, there follows

$$\mathrm{d}\bar{\sigma} = \frac{3}{2}\frac{1}{\bar{\sigma}}\boldsymbol{\sigma}_{\mathrm{D}}^{\mathrm{t}}\mathrm{d}\boldsymbol{\sigma}_{\mathrm{D}} = \frac{3}{2}\frac{1}{\bar{\sigma}}\boldsymbol{\sigma}_{\mathrm{D}}^{\mathrm{t}}\mathrm{d}\boldsymbol{\sigma}. \tag{1.107}$$

Thus the differential quotient in eqn (1.104) reads

$$\frac{\mathrm{d}\phi}{\mathrm{d}\boldsymbol{\sigma}} = \frac{\mathrm{d}\bar{\sigma}}{\mathrm{d}\boldsymbol{\sigma}} = \frac{3}{2}\frac{1}{\bar{\sigma}}\boldsymbol{\sigma}_{\mathrm{D}}^{\mathrm{t}}. \tag{1.108}$$

The yield function is not allowed to increase, and therefore admissible stress increments $\mathrm{d}\boldsymbol{\sigma}$ emanating from a plastic state build non-positive products with the deviatoric stress $\boldsymbol{\sigma}_{\mathrm{D}}$.

Plastic changes of the stress state at $\phi(\boldsymbol{\sigma}) = 0$ obey the consistency condition $\mathrm{d}\phi = \mathrm{d}\bar{\sigma} = 0$, which by eqn (1.107) implies

$$\boldsymbol{\sigma}_{\mathrm{D}}^{\mathrm{t}}\mathrm{d}\boldsymbol{\sigma}_{\mathrm{D}} = 2G\boldsymbol{\sigma}_{\mathrm{D}}^{\mathrm{t}}\mathrm{d}\boldsymbol{\varepsilon}_{\mathrm{D}} = 2G\boldsymbol{\sigma}_{\mathrm{D}}^{\mathrm{t}}\mathrm{d}\boldsymbol{\varepsilon} = 0. \tag{1.109}$$

The transition to the last expression documents that volumetric components do not contribute to the scalar product with the deviatoric stress. From eqn (1.109), the vanishing of $\mathrm{d}\bar{\sigma}$ is equivalent to a vanishing increment of the work of elastic distortion.

Expressing the elastic $\mathrm{d}\boldsymbol{\varepsilon}$ in eqn (1.109) by the difference between the total strain increment $\mathrm{d}\boldsymbol{\gamma}$ and the plastic part $\mathrm{d}\boldsymbol{\eta}$, results in

$$\boldsymbol{\sigma}_{\mathrm{D}}^{\mathrm{t}}\mathrm{d}\boldsymbol{\eta} = \boldsymbol{\sigma}_{\mathrm{D}}^{\mathrm{t}}\mathrm{d}\boldsymbol{\gamma} \geq 0. \tag{1.110}$$

In perfectly plastic flow, the incremental work of distortion is entirely converted into plastic work because the elastic part vanishes as a consequence of $\mathrm{d}\bar{\sigma} = 0$. Originally, the right-hand side of eqn (1.110) may be positive, negative or zero. We notice, however, that negative values diminish $\bar{\sigma}$ and are associated with elastic unloading. Therefore, the left-hand side, involving plastic flow, can only attain positive values or vanish. The inequality in eqn (1.110) states the *condition for plastic loading* in terms of the strain increment $\mathrm{d}\boldsymbol{\gamma}$.

In addition to the yield condition and the assumption of a non-hardening material discussed so far, we also need information on the direction of plastic deformation. Such information is provided by the *flow rule*. For metals,

from experimental evidence incremental plastic strains are set proportional (co-axial) to the deviatoric stress at which the flow occurs:

$$\mathrm{d}\boldsymbol{\eta} = \Lambda \boldsymbol{\sigma}_{\mathrm{D}}. \tag{1.111}$$

The flow rule stated by eqn (1.111) ensures that plastic deformation is isochoric; the volumetric part of the plastic strain vanishes:

$$\boldsymbol{\eta} \equiv \boldsymbol{\eta}_{\mathrm{D}}, \quad \eta_{\mathrm{V}} = \frac{1}{3}\mathbf{e}^{\mathrm{t}}\boldsymbol{\eta} = 0. \tag{1.112}$$

The scalar multiplier Λ in eqn (1.111) is determined by eqn (1.110) as a non-negative quantity. In this manner, yield condition, non-hardening assumption and flow rule establish an expression for the incremental plastic strain in perfectly plastic materials once the stress state at yield and the incremental change of strain are given.

For a rational interpretation of eqn (1.111) we introduce a positive scalar quantity $\mathrm{d}\bar{\eta}$, equivalent to the incremental plastic strain by means of the work equality:

$$\bar{\sigma}\mathrm{d}\bar{\eta} = \boldsymbol{\sigma}_{\mathrm{D}}^{\mathrm{t}}\mathrm{d}\boldsymbol{\eta}. \tag{1.113}$$

Substitution of eqn (1.111) for $\mathrm{d}\boldsymbol{\eta}$ gives the proportionality factor Λ as

$$\Lambda = \frac{3}{2}\,\frac{\mathrm{d}\bar{\eta}}{\bar{\sigma}}. \tag{1.114}$$

With the deviatoric stress $\boldsymbol{\sigma}_{\mathrm{D}}$ from eqn (1.111), eqn (1.113) defines the equivalent plastic strain increment as a measure of the magnitude of the incremental plastic strain:

$$\begin{aligned}\mathrm{d}\bar{\eta}^2 &= \frac{2}{3}\mathrm{d}\boldsymbol{\eta}^{\mathrm{t}}\mathrm{d}\boldsymbol{\eta} \\ &= \frac{2}{3}(\mathrm{d}\eta_{\mathrm{xx}}^2 + \mathrm{d}\eta_{\mathrm{yy}}^2 + \mathrm{d}\eta_{\mathrm{zz}}^2 + \frac{1}{2}\mathrm{d}\eta_{\mathrm{xy}}^2 + \frac{1}{2}\mathrm{d}\eta_{\mathrm{yz}}^2 + \frac{1}{2}\mathrm{d}\eta_{\mathrm{xz}}^2).\end{aligned} \tag{1.115}$$

Alternatively to eqn (1.111), the incremental plastic strain may be represented in terms of the magnitude $\mathrm{d}\bar{\eta}$ and the direction $\mathbf{s}$ of the plastic flow:

$$\mathrm{d}\boldsymbol{\eta} = \mathrm{d}\bar{\eta}\mathbf{s}. \tag{1.116}$$

Introduction of eqn (1.116) for $\mathrm{d}\boldsymbol{\eta}$ in the first eqn (1.115) gives

$$\mathbf{s}^{\mathrm{t}}\mathbf{s} = \frac{3}{2} \tag{1.117}$$

and confirms $\mathbf{s}$ as a direction vector of constant length. By comparison of eqn (1.116) with eqn (1.111) under consideration of eqn (1.114) the vector $\mathbf{s}$ becomes

$$\mathbf{s} = \frac{3}{2}\frac{1}{\bar{\sigma}}\boldsymbol{\sigma}_{\mathrm{D}} = \left[\frac{\mathrm{d}\bar{\sigma}}{\mathrm{d}\boldsymbol{\sigma}}\right]^{\mathrm{t}} = \left[\frac{\mathrm{d}\phi}{\mathrm{d}\boldsymbol{\sigma}}\right]^{\mathrm{t}}. \tag{1.118}$$

The equality to the differential quotients refers to eqn (1.108). We note an association of the flow rule with the yield condition in that the direction of plastic flow can be derived from the yield function $\phi(\boldsymbol{\sigma})$ by differentiation with respect to the stress.

With $\mathbf{s}$ from eqn (1.118) the increment of equivalent stress, eqn (1.107), becomes

$$\mathrm{d}\bar{\sigma} = \mathbf{s}^{\mathrm{t}}\mathrm{d}\boldsymbol{\sigma}_{\mathrm{D}} = \mathbf{s}^{\mathrm{t}}\mathrm{d}\boldsymbol{\sigma} \tag{1.119}$$

and must be non-positive for a perfectly plastic material. During plastic flow, vanishing of $\mathrm{d}\bar{\sigma}$ implies that

$$\mathbf{s}^{\mathrm{t}}\mathrm{d}\boldsymbol{\eta} = \mathbf{s}^{\mathrm{t}}\mathrm{d}\boldsymbol{\gamma} \geq 0, \tag{1.120}$$

in equivalence to eqn (1.110). With eqn (1.116) for $\mathrm{d}\boldsymbol{\eta}$, we obtain from eqn (1.120) the magnitude of the plastic strain increment as

$$\mathrm{d}\bar{\eta} = \frac{2}{3}\mathbf{s}^{\mathrm{t}}\mathrm{d}\boldsymbol{\gamma} \geq 0, \tag{1.121}$$

the inequality reflecting the plastic loading condition.

In turn, the incremental plastic strain reads

$$\begin{aligned} \mathrm{d}\boldsymbol{\eta} &= \frac{2}{3}\mathbf{s}\mathbf{s}^{\mathrm{t}}\mathrm{d}\boldsymbol{\gamma} \quad \text{if } \mathbf{s}^{\mathrm{t}}\mathrm{d}\boldsymbol{\gamma} > 0 \\ \mathrm{d}\boldsymbol{\eta} &= \mathbf{0} \quad \text{otherwise.} \end{aligned} \tag{1.122}$$

Equation (1.122) describes flow in a perfectly plastic material when a yield state $\phi(\boldsymbol{\sigma}) = 0$ has been reached.

A relation establishing co-axiality between strain rates and stresses in two-dimensional plastic flow (plane strain) was suggested by Saint Vénant [7] following the Tresca yield hypothesis [6] (see below at the end of Section 1.2.4). The generalization to three-dimensional conditions was performed by Lévy [8]. The association of the incremental plastic strain to a regular but otherwise general yield function (associated flow rule) goes back to von Mises [9].

In the absence of (or neglecting) elasticity, the flow rule as given by eqn (1.111) or eqn (1.116) (proportionality of the strain increment or rate to the deviatoric stress) describes the behaviour of a rigid–plastic solid. It is known as the Lévy–von Mises constitutive law.

The completion of the constitutive relation by the elastic constituent was given for plane problems by Prandtl [10]. Its extension to the three-dimensional case is due to Reuss [11]. The equations resulting for elastic–perfectly plastic solids are known as the Prandtl–Reuss equations. Incremental stress–strain relationships for elastoplastic solids will be presented subsequently in Section 1.3 discussing hardening materials.

1.2.4 Representation in principal space

Yield condition and plastic flow
Once the principal directions are known, the stress state can be represented by a vector $\boldsymbol{\sigma}_{\mathrm{I}}$ with components σ_1, σ_2 and σ_3 along the principal axes (Fig. 1.10). The hydrostatic stress $\boldsymbol{\sigma}_{\mathrm{H}}$ defines an axis with equal angular distances to each of the three principal directions, while the deviatoric stress $\boldsymbol{\sigma}_{\mathrm{DI}}$ lies in a plane perpendicular to the hydrostatic axis at distance $|\boldsymbol{\sigma}_{\mathrm{H}}| = \sqrt{3}\sigma_{\mathrm{H}}$ from the origin. The equivalent deviatoric stress

$$\bar{\sigma}^2 = \frac{3}{2}\boldsymbol{\sigma}_{\mathrm{DI}}^{\mathrm{t}}\boldsymbol{\sigma}_{\mathrm{DI}} = \frac{3}{2}(\sigma_{\mathrm{D1}}^2 + \sigma_{\mathrm{D2}}^2 + \sigma_{\mathrm{D3}}^2) \tag{1.123}$$

is proportional to the magnitude $|\boldsymbol{\sigma}_{\mathrm{DI}}| = (\boldsymbol{\sigma}_{\mathrm{DI}}^{\mathrm{t}}\boldsymbol{\sigma}_{\mathrm{DI}})^{1/2}$ of the deviatoric stress vector.

The yield condition is based on the distinction between stress states that can be attained elastically and those prone to plastic flow. In the principal stress space, the elasticity limit (yield locus) can be represented by a three-dimensional surface containing the elastic region of the material. For metals, with elasticity limit not depending on the hydrostatic stress, the yield surface has the shape of a cylinder of infinite extent inclined parallel to the hydrostatic axis.

By the yield condition of eqn (1.103) in conjunction with eqn (1.123), the cross-section of the cylinder in the deviatoric plane is a circle with the centre on the hydrostatic axis (Fig. 1.11). It is described by the equation $|\boldsymbol{\sigma}_{\mathrm{DI}}| = r_{\mathrm{o}}$ with radius $r_{\mathrm{o}} = \sqrt{2/3}\,\sigma_{\mathrm{s}}$. The space of elastic stress states is limited by

$$|\boldsymbol{\sigma}_{\mathrm{DI}}| \leq \sqrt{2/3}\,\sigma_{\mathrm{s}},$$

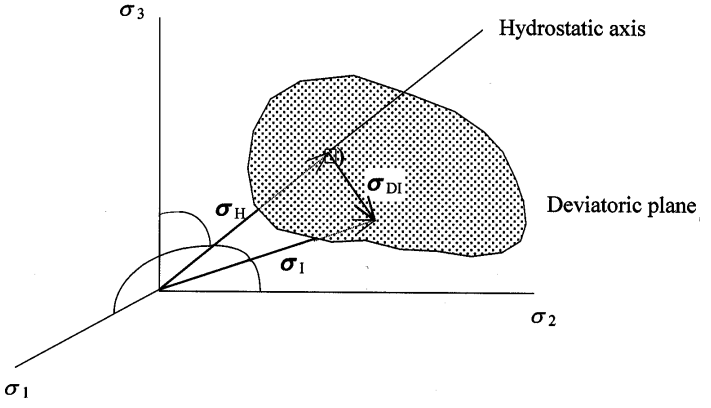

Figure 1.10: Vector representation of stress in principal space.

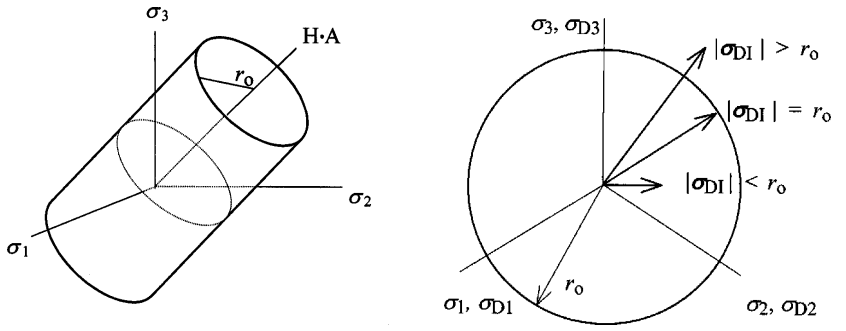

Figure 1.11: The von Mises yield surface in the principal stress space.

while the hydrostatic stress is not restricted. A view in the deviatoric plane perpendicular to the hydrostatic axis is depicted in Fig. 1.11 (right). Deviatoric stress vectors are directed along the radius. Those ending inside the circle are ascribed to elastic states. For a plastic state, the stress vector ends on the circle. Stress states outside the circle cannot be attained in the elastic–perfectly plastic material.

The yield surface is isotropic with respect to the direction of the deviatoric stress; it limits merely the magnitude $|\boldsymbol{\sigma}_{\mathrm{DI}}|$ of the deviatoric stress vector. The radius r_{o} can thus be adjusted to the experimental data from a single test, be it multiaxial or uniaxial. In the present context, r_{o} is adjusted to the uniaxial yield stress σ_{s} of the material in tension.

In perfect plasticity the stress vector ends on the yield surface, and changes in stress are consistent with the condition of non-increasing magnitude:

$$\mathrm{d}|\boldsymbol{\sigma}_{\mathrm{DI}}| = \mathbf{n}_{\mathrm{I}}^{\mathrm{t}}\mathrm{d}\boldsymbol{\sigma}_{\mathrm{DI}} \leq 0. \tag{1.124}$$

In the above expression for $\mathrm{d}|\boldsymbol{\sigma}_{\mathrm{DI}}|$, the unit vector

$$\mathbf{n}_{\mathrm{I}} = \frac{1}{|\boldsymbol{\sigma}_{\mathrm{DI}}|}\boldsymbol{\sigma}_{\mathrm{DI}} \tag{1.125}$$

defines the external normal to the yield surface (Fig. 1.12). Stress increments pointing inwards to the yield surface, $\mathbf{n}_{\mathrm{I}}^{\mathrm{t}}\mathrm{d}\boldsymbol{\sigma}_{\mathrm{DI}} < 0$, lead to elastic unloading, while for $\mathbf{n}_{\mathrm{I}}^{\mathrm{t}}\mathrm{d}\boldsymbol{\sigma}_{\mathrm{DI}} = 0$ another plastic state is approached on the yield surface. Changes with $\mathbf{n}_{\mathrm{I}}^{\mathrm{t}}\mathrm{d}\boldsymbol{\sigma}_{\mathrm{DI}} > 0$ are not admitted because of the fixed elasticity limit.

In the consistency condition, eqn (1.124), the incremental stress can be expressed by the incremental elastic strain ($\mathrm{d}\boldsymbol{\sigma}_{\mathrm{DI}} = 2G\mathrm{d}\boldsymbol{\varepsilon}_{\mathrm{DI}}$) and gives

$$\mathbf{n}_{\mathrm{I}}^{\mathrm{t}}\mathrm{d}\boldsymbol{\varepsilon}_{\mathrm{DI}} = \mathbf{n}_{\mathrm{I}}^{\mathrm{t}}\mathrm{d}\boldsymbol{\varepsilon}_{\mathrm{I}} \leq 0. \tag{1.126}$$

The second expression is due to the deviatoric nature of $\mathbf{n}_{\mathrm{I}}$, eqn (1.125). It follows that changes of the elastic strain in perfect plasticity are at most

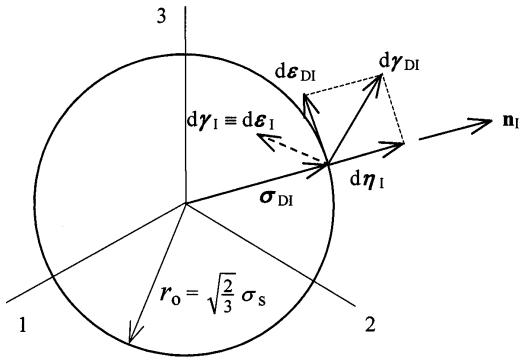

Figure 1.12: Plastic flow in perfect plasticity.

tangential to the yield surface, as also are the stress changes. With the elastic strain in the form $d\boldsymbol{\varepsilon}_I = d\boldsymbol{\gamma}_I - d\boldsymbol{\eta}_I$:

$$\mathbf{n}_I^t d\boldsymbol{\eta}_I = \mathbf{n}_I^t d\boldsymbol{\gamma}_I \geq 0. \tag{1.127}$$

Thus, the projections of the plastic and the total strain increment normal to the yield surface are equal.

In view of eqn (1.125) the co-axiality of the plastic strain increment and deviatoric stress in principal space can be written as

$$d\boldsymbol{\eta}_I = |d\boldsymbol{\eta}_I|\mathbf{n}_I = (\mathbf{n}_I^t d\boldsymbol{\eta}_I)\mathbf{n}_I. \tag{1.128}$$

Accordingly, plastic flow is directed along the exterior normal $\mathbf{n}_I$ to the yield surface and with eqn (1.127) there follows

$$\begin{aligned} d\boldsymbol{\eta}_I &= \mathbf{n}_I \mathbf{n}_I^t d\boldsymbol{\gamma}_I \quad \text{for } \mathbf{n}_I^t d\boldsymbol{\gamma}_I \geq 0 \\ d\boldsymbol{\eta}_I &= \mathbf{0} \quad \text{otherwise.} \end{aligned} \tag{1.129}$$

Assuming strains are referred to the same axes as stresses, plastic flow occurs if, at a stress state on the yield surface, the incremental strain vector $d\boldsymbol{\gamma}_I$ points outwards from the surface. From eqns (1.127) and (1.126), its decomposition normal and tangential to the yield surface then defines the incremental plastic strain and elastic strain, respectively (Fig. 1.12).

Tresca yield criterion

Tresca considered the maximum tangential stress at a point as characteristic of plastic yield [6]. A mathematical formulation of this hypothesis was given later by Saint Vénant for the case of plane strain [7].

The tangential stresses assume extremum values in the planes bisecting the angles between the principal planes (passing through the principal axes 1,2 and 3). They are called *principal tangential stresses* and are given by

$$\tau_1 = \frac{1}{2}(\sigma_2 - \sigma_3), \quad \tau_2 = \frac{1}{2}(\sigma_3 - \sigma_1), \quad \tau_3 = \frac{1}{2}(\sigma_1 - \sigma_2). \tag{1.130}$$

The normal stresses on the same planes are

$$\frac{1}{2}(\sigma_2+\sigma_3), \quad \frac{1}{2}(\sigma_3+\sigma_1), \quad \frac{1}{2}(\sigma_1+\sigma_2),$$

respectively. The above expressions for the principal tangential stresses and the associated normal components can be easily verified by utilizing the transformation of eqn (1.86) for the bisecting planes.

The maximum value in eqn (1.130) specifies the maximum tangential stress $\tau_{\max}$ at a point. If the (normal) principal stresses are ordered with respect to their value, the yield criterion reads

$$\tau_{\max} = -\frac{1}{2}(\sigma_3-\sigma_1) = -\tau_2 \quad \text{for } \sigma_1 \geq \sigma_2 \geq \sigma_3.$$

In the general case, where $\sigma_1 \geq \sigma_2 \geq \sigma_3$ does not need to be fulfilled, each one of the principal tangential stresses in eqn (1.89) is restricted by the yield condition:

$$\begin{aligned} |\tau_1| &= \frac{1}{2}|\sigma_2-\sigma_3| \leq \tau_s; \\ |\tau_2| &= \frac{1}{2}|\sigma_3-\sigma_1| \leq \tau_s; \\ |\tau_3| &= \frac{1}{2}|\sigma_1-\sigma_2| \leq \tau_s. \end{aligned} \tag{1.131}$$

Here, τ_s denotes the yield stress of the material under pure shear. The relation to the yield stress under uniaxial tension, σ_s, can be established by recalling that in the latter case $\sigma_1 = \sigma$ and $\sigma_2 = \sigma_3 = 0$. For the Tresca yield condition,

$$\tau_s = \frac{1}{2}\sigma_s.$$

In eqn (1.131), the inequality sign ensures that the stress state is elastic, while plastic states of stress satisfy the equality in one or two of the three conditions. In the principal stress space the conditions,

$$\sigma_2-\sigma_3 = \pm\sigma_s, \quad \sigma_3-\sigma_1 = \pm\sigma_s, \quad \sigma_1-\sigma_2 = \pm\sigma_s$$

are represented by pairs of planes parallel to those defined by the principal axes $1, 2$ and 3 and the hydrostatic axis $\sigma_1 = \sigma_2 = \sigma_3$. Thus, the Tresca yield surface is a prism with regular hexagonal cross-section in the deviatoric plane (Fig. 1.13).

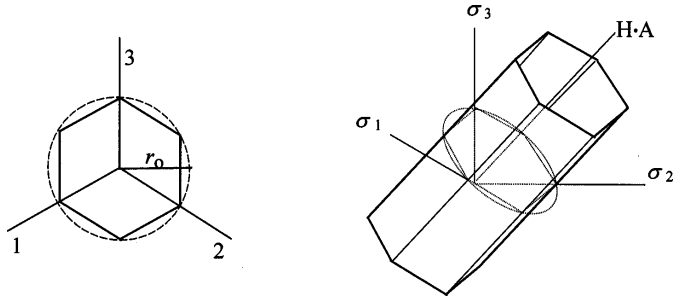

Figure 1.13: The Tresca yield limit.

The intersection of the planes with the axes of the principal stress is at a distance σ_s from the origin, and the projection of their distance on the deviatoric plane is $\sqrt{2/3}\sigma_s$. This defines the radius of the circle circumscribing the hexagon, and at the same time the von Mises yield locus.

Since the Tresca yield condition is linear between segments, it simplifies the solution of problems with stresses restricted within a single segment. Otherwise, the observance of three inequalities is inconvenient, and some difficulties regarding the direction of plastic flow arise at the corners of the hexagon. The subject of plasticity associated with a singular yield surface has been addressed in [18]. Under general conditions of stress and strain, plasticity as based on the smooth von Mises yield surface is suitable for numerical treatment using a computer.

1.2.5 Biaxial stress: rectangular plate under tension

The following example illustrates the theory of perfectly plastic flow for the case of plane stress. The rectangular plate shown in Fig. 1.14 has a constant thickness and is subjected to the uniaxial stress σ_1 while the strain in the lateral direction is suppressed ($\gamma_2 = 0$). Normal to its plane the plate is unconstrained and free of stress. The material is assumed elastic–perfectly plastic with Young's modulus E, Poisson's ratio ν and yield stress σ_s.

Without the lateral constraint, the homogeneous stress state in the plate is uniaxial and identical to the applied σ_1, which then can be increased only up to the yield stress σ_s. The kinematic constraint induces a lateral normal stress σ_2; shear stresses are absent. In the elastic range, the lateral constraint relates the stress components via Hooke's law:

$$\varepsilon_2 = \frac{1}{E}(\sigma_2 - \nu\sigma_1) = 0, \quad \text{and} \quad \sigma_2 = \nu\sigma_1. \tag{1.132}$$

The strain ε_1 in the direction of the loading thus reads

$$\varepsilon_1 = \frac{1}{E}(\sigma_1 - \nu\sigma_2) = \frac{1 - \nu^2}{E}\sigma_1. \tag{1.133}$$

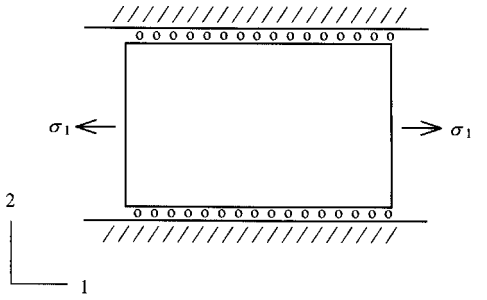

Figure 1.14: Rectangular plate under tension.

For the two-dimensional principal stress state σ_1, σ_2, the equivalent stress expression of eqn (1.101) reduces to

$$\bar{\sigma}^2 = \sigma_1^2 + \sigma_2^2 - \sigma_1\sigma_2, \tag{1.134}$$

and the elasticity limit is attained when $\bar{\sigma} = \sigma_s$. A graphical representation of the yield locus in the σ_1, σ_2-plane is given in Fig. 1.15. Equation (1.134), taken at $\bar{\sigma} = \sigma_s$, describes an ellipse with the longest axis inclined by 45° with respect to the σ_1-axis. The ellipse passes through the points $\sigma_1 = \pm\sigma_s, \sigma_2 = \pm\sigma_s$ on the axes, and $\sigma_2 = \sigma_1 = \pm\sigma_s, \sigma_2 = -\sigma_1 = \pm\sigma_s/\sqrt{3}$.

The elastic paths defined by eqn (1.132) are straight lines of slope ν, emanating from the origin. The lowest σ_1 on the ellipse is associated with $\nu = 0$, and the highest with $\nu = 1/2$. Substitution of σ_2 from eqn (1.132) in eqn (1.134) leads to

$$\bar{\sigma}^2 = (1 - \nu + \nu^2)\sigma_1^2 = \sigma_s^2 \tag{1.135}$$

and determines the stress σ_1 at the elasticity limit

$$\left(\frac{\sigma_1}{\sigma_s}\right)^2_{\text{elastic}} = \frac{1}{1 - \nu + \nu^2}. \tag{1.136}$$

Loading beyond elasticity induces plastic flow, while the perfectly plastic material imposes the restriction $\bar{\sigma} = \sigma_s$. Therefore eqn (1.134) becomes an equation for σ_2 in terms of σ_1. The quadratic equation has two roots

$$\sigma_2 = \frac{\sigma_1}{2} \pm \left(\sigma_s^2 - \frac{3}{4}\sigma_1^2\right)^{1/2}, \tag{1.137}$$

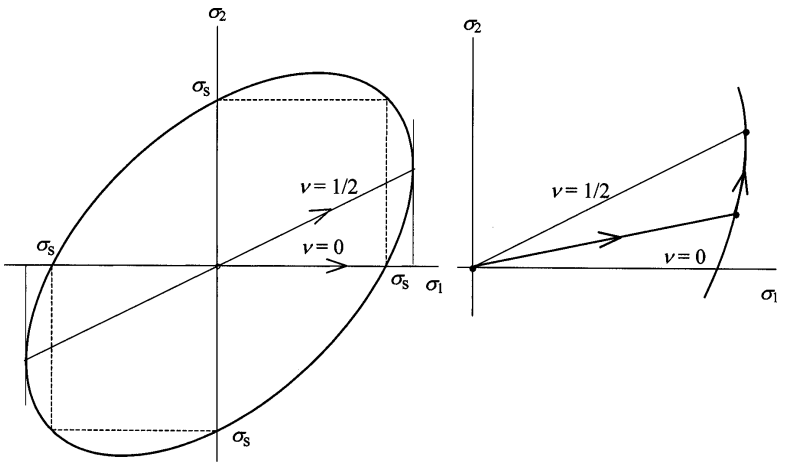

Figure 1.15: Elasticity limit (left) and stress path in elastic–perfectly plastic deformation of the plate (right).

but the one with the plus sign does not represent here an admissible solution: at the elasticity limit, eqn (1.136), the stresses σ_2 and σ_1 are still related by eqn (1.132), which is reproduced only for the minus sign. The above equation for σ_2 in the plastic state is meaningful as long as the discriminant is not negative. Vanishing of the discriminant determines the maximum applied stress σ_1 as

$$\left(\frac{\sigma_1}{\sigma_\mathrm{s}}\right)^2_{\max} = \frac{4}{3}. \tag{1.138}$$

The maximum applied stress σ_1 can alternatively be obtained as the outmost point of the limiting ellipse along the σ_1-direction. Differentiating eqn (1.134) at $\bar{\sigma} = \sigma_\mathrm{s}$ and setting $\mathrm{d}\sigma_1/\mathrm{d}\sigma_2 = 0$, we get the extremum σ_1 on the ellipse for $\sigma_2 = \sigma_1/2$, and the highest σ_1 as given by eqn (1.138). Equations (1.136) and (1.138) define the lower and the upper limit bounding the elastoplastic interval of the loading:

$$\frac{1}{1-\nu+\nu^2} \le \left(\frac{\sigma_1}{\sigma_\mathrm{s}}\right)^2 \le \frac{4}{3}. \tag{1.139}$$

Considering the strains, we notice that due to the lateral constraint,

$$\gamma_2 = \varepsilon_2 + \eta_2 = 0\,, \quad \text{and} \quad \eta_2 = -\varepsilon_2. \tag{1.140}$$

The elastic and plastic parts of this strain component compensate each other. The elastic strain ε_2 is related to the stresses σ_1 and σ_2 by means of the elastic relation

$$\varepsilon_2 = \frac{1}{E}(\sigma_2 - \nu\sigma_1) = \frac{1}{E}\left[\frac{1-2\nu}{2}\sigma_1 - \left(\sigma_\mathrm{s}^2 - \frac{3}{4}\sigma_1^2\right)^{1/2}\right], \tag{1.141}$$

where eqn (1.137) has been substituted for σ_2. Analogously for the strain ε_1 in the direction of the applied stress σ_1,

$$\varepsilon_1 = \frac{1}{E}(\sigma_1 - \nu\sigma_2) = \frac{1}{E}\left[\frac{2-\nu}{2}\sigma_1 + \nu\left(\sigma_\mathrm{s}^2 - \frac{3}{4}\sigma_1^2\right)^{1/2}\right]. \tag{1.142}$$

It still remains to determine the plastic strain component η_1. From the flow rule, eqn (1.111), all components of the incremental plastic strain exhibit the same proportionality to the components of the deviatoric stress. Therefore,

$$\frac{\mathrm{d}\eta_1}{\mathrm{d}\eta_2} = \frac{\sigma_{\mathrm{D}1}}{\sigma_{\mathrm{D}2}} = \frac{2\sigma_1 - \sigma_2}{2\sigma_2 - \sigma_1}. \tag{1.143}$$

The lateral plastic strain increment $\mathrm{d}\eta_2$ is determined by the elastic one $\mathrm{d}\varepsilon_2$, and from eqn (1.141) by differentiation

$$\mathrm{d}\eta_2 = -\mathrm{d}\varepsilon_2 = -\frac{1}{E}\left[\frac{1-2\nu}{2} + \frac{3}{4}\sigma_1\left(\sigma_\mathrm{s}^2 - \frac{3}{4}\sigma_1^2\right)^{-1/2}\right]\mathrm{d}\sigma_1. \tag{1.144}$$

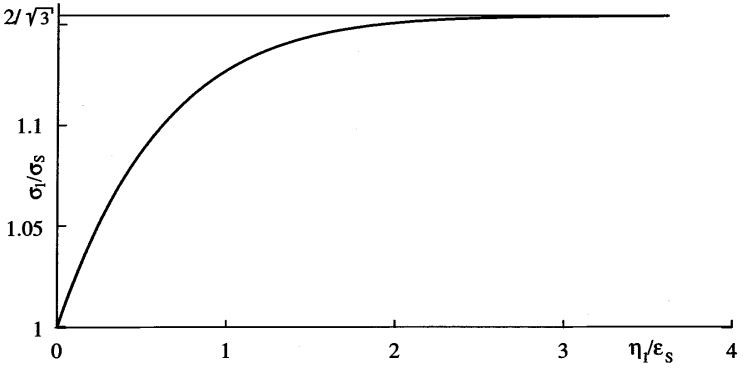

Figure 1.16: Axial stress–plastic strain diagram for the plate.

With eqn (1.137) for σ_2 and eqn (1.144) for $\mathrm{d}\eta_2$ we obtain from eqn (1.143) the relation

$$\mathrm{d}\eta_1 = \frac{1}{E}\left[\frac{1-2\nu}{4} + (1-4)B + B^2\right]\mathrm{d}\sigma_1 \tag{1.145}$$

between the differentials $\mathrm{d}\eta_1$ and $\mathrm{d}\sigma_1$. In eqn (1.145) we used the abbreviation

$$B = \frac{3}{4}\sigma_1\left(\sigma_\mathrm{s}^2 - \frac{3}{4}\sigma_1^2\right)^{-1/2}. \tag{1.146}$$

Integration of eqn (1.145) from the elasticity limit, eqn (1.136), gives the axial component of the plastic strain

$$\eta_1 = \frac{\sigma_\mathrm{s}}{E}\left[-\frac{1+\nu}{2}\frac{\sigma_1}{\sigma_\mathrm{s}} - (1-\nu)\sqrt{1-\frac{3}{4}\left(\frac{\sigma_1}{\sigma_\mathrm{s}}\right)^2} + \frac{\sqrt{3}}{4}\ln\frac{1+\frac{\sqrt{3}}{2}\frac{\sigma_1}{\sigma_\mathrm{s}}}{1-\frac{\sqrt{3}}{2}\frac{\sigma_1}{\sigma_\mathrm{s}}}\right]_{(\frac{\sigma_1}{\sigma_\mathrm{s}})_\mathrm{el}}^{\frac{\sigma_1}{\sigma_\mathrm{s}}} \tag{1.147}$$

as plotted in Fig. 1.16. The quantity σ_s/E is the strain ε_s at the yield stress σ_s of the material.

The thickness strain in the plate is also given for completeness. The plastic strain η_3 maintains the volume, and reads

$$\eta_3 = -(\eta_1 + \eta_2). \tag{1.148}$$

From $\sigma_3 = 0$, the elastic contraction as a consequence of ε_1 and ε_2 is

$$\varepsilon_3 = -\frac{\nu}{1-\nu}(\varepsilon_1 + \varepsilon_2). \tag{1.149}$$

In conclusion, we notice that application of a compressive stress σ_1 instead of the tensile one does not modify the results, but the sign. For the case of

an oblique applied stress which in addition to the axial stress σ also exhibits a shear component τ (see Chapter 2, Problem 4).

1.3 Hardening rules

Hardening describes the effect of plastic deformation on the yield condition. The isotropic hardening rule [12] and the kinematic hardening model [13] will be discussed in the following sections. Isotropic hardening is sufficient for plastic deformation under monotonic loading conditions, while cyclic plasticity is better described by the kinematic model. The combination of the kinematic and the isotropic rule is also considered, as a generalization. A recent discussion of the hardening issue is found in the monograph [19].

1.3.1 Isotropic hardening

In contrast to the perfectly plastic model, the yield criterion is affected by plastic deformation in the case of hardening materials. The stress–strain characteristic covers the description of monotonically applied uniaxial stress, but leaves space for different interpretations under more general loading conditions.

The *isotropic hardening* model assumes that plastic deformation modifies the yield condition independently of the direction of the inducing stress. In the principal stress space, the circular cylinder which represents the yield surface $\phi = 0$ is allowed to expand around the hydrostatic axis. In the deviatoric plane, the circle is specified by the radius $r = \sqrt{2/3}\sigma_\mathrm{f}$ from the origin. The radius r follows the increase of the flow stress σ_f with plastic deformation (Fig. 1.17). Accordingly, isotropic hardening modifies the yield condition, eqn (1.103), to

$$\phi(\boldsymbol{\sigma}, \sigma_\mathrm{f}) = \bar{\sigma} - \sigma_\mathrm{f} \leq 0. \tag{1.150}$$

The flow stress σ_f is defined as a function of the accumulated equivalent plastic strain $\bar{\eta} = \int \mathrm{d}\bar{\eta}$, a scalar measure of the plastic deformation experienced by the material in an arbitrary loading programme. The functional dependence $\sigma_\mathrm{f}(\bar{\eta})$ is considered a material characteristic. It can be deduced from any experiment on continuous plastic flow in the form $\sigma_\mathrm{f}(\bar{\eta}) = \bar{\sigma}(\bar{\eta})$. For the tensile test $\bar{\sigma} = \sigma$ and $\bar{\eta} = \eta$, so the relationship

$$\sigma_\mathrm{f}(\bar{\eta}) = \sigma(\eta) \tag{1.151}$$

can be derived from uniaxial test data.

Plastic states are defined by $\phi = 0$, and during plastic flow $\mathrm{d}\phi = 0$. In conjunction with eqn (1.150), the consistency condition gives

$$\mathrm{d}\phi = 0\colon \qquad \mathrm{d}\sigma_\mathrm{f} = h\mathrm{d}\bar{\eta} = \mathrm{d}\bar{\sigma} \quad \text{and}$$

$$\mathrm{d}\bar{\eta} = \frac{1}{h}\mathrm{d}\bar{\sigma} = \frac{1}{h}\mathbf{s}^\mathrm{t}\mathrm{d}\boldsymbol{\sigma} \geq 0, \tag{1.152}$$

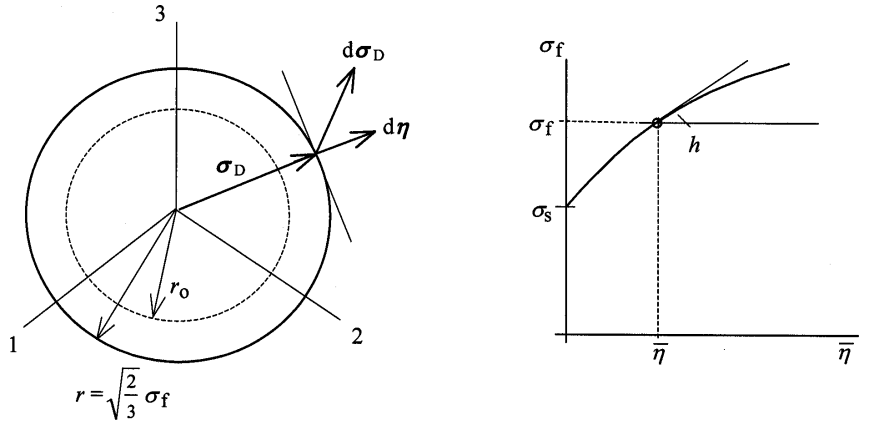

Figure 1.17: Isotropic hardening of the yield surface.

where eqn (1.119) has been used for $\mathrm{d}\bar{\sigma}$. The hardening parameter

$$h = \frac{\mathrm{d}\sigma_\mathrm{f}}{\mathrm{d}\bar{\eta}} = \frac{\mathrm{d}\sigma}{\mathrm{d}\eta} \tag{1.153}$$

can be specified by the slope of the uniaxial flow characteristic $\sigma(\eta)$.

The loading condition expressed by the inequality in eqn (1.152) associates plastic flow with an expansion of the yield surface. With $\mathbf{s}$ defined by eqn (1.118), the equivalent plastic strain increment is a consequence of a stress increment $\mathrm{d}\boldsymbol{\sigma}$ pointing outwards from the yield surface. Utilizing eqn (1.152) for $\mathrm{d}\bar{\eta}$ in the flow rule, eqn (1.116), the incremental plastic strain assumes the form

$$\mathrm{d}\boldsymbol{\eta} = \mathrm{d}\bar{\eta}\mathbf{s} = \frac{1}{h}\mathbf{s}\mathbf{s}^\mathrm{t}\mathrm{d}\boldsymbol{\sigma} \quad \text{for } \mathrm{d}\bar{\sigma} = \mathbf{s}^\mathrm{t}\mathrm{d}\boldsymbol{\sigma} > 0. \tag{1.154}$$

In extension of eqn (1.118) the direction of plastic flow is associated here with the yield surface pertaining to the actual state of hardening:

$$\mathbf{s} = \frac{3}{2}\frac{1}{\bar{\sigma}}\boldsymbol{\sigma}_\mathrm{D} = \left[\frac{\partial\phi}{\partial\boldsymbol{\sigma}}\right]^\mathrm{t}_{\sigma_\mathrm{f}=\mathrm{const.}}$$

Superposition of the incremental plastic strain on the elastic one, determines the strain increment for a given increment of stress:

$$\mathrm{d}\boldsymbol{\gamma} = \mathrm{d}\boldsymbol{\varepsilon} + \mathrm{d}\boldsymbol{\eta} = \boldsymbol{\kappa}^{-1}\left[\mathbf{I} + \frac{2G}{h}\mathbf{s}\mathbf{s}^\mathrm{t}\right]\mathrm{d}\boldsymbol{\sigma}. \tag{1.155}$$

If the incremental stress does not satisfy the condition for plastic loading, eqn (1.155) must be reduced to the elastic stress–strain relation.

The above formulation fails to describe perfectly plastic material with $h = 0$ because the stress cannot be varied arbitrarily in this case, but is restricted by the condition $\mathrm{d}\bar{\sigma} = \mathbf{s}^{\mathrm{t}}\mathrm{d}\boldsymbol{\sigma} = 0$. An alternative expression is obtained in terms of strain. With $\mathrm{d}\bar{\sigma} = 2G\mathbf{s}^{\mathrm{t}}[\mathrm{d}\boldsymbol{\gamma} - \mathrm{d}\boldsymbol{\eta}]$ from elasticity in eqn (1.152),

$$\mathrm{d}\bar{\eta} = \frac{2G}{h + 3G}\mathbf{s}^{\mathrm{t}}\mathrm{d}\boldsymbol{\gamma} \geq 0, \tag{1.156}$$

and with the flow rule, eqn (1.116), the plastic strain increment becomes

$$\mathrm{d}\boldsymbol{\eta} = \mathrm{d}\bar{\eta}\mathbf{s} = \frac{2G}{h + 3G}\mathbf{s}\mathbf{s}^{\mathrm{t}}\mathrm{d}\boldsymbol{\gamma} \quad \text{for } \mathbf{s}^{\mathrm{t}}\mathrm{d}\boldsymbol{\gamma} > 0. \tag{1.157}$$

The incremental stress follows:

$$\mathrm{d}\boldsymbol{\sigma} = \boldsymbol{\kappa}[\mathrm{d}\boldsymbol{\gamma} - \mathrm{d}\boldsymbol{\eta}] = \boldsymbol{\kappa}\left[\mathbf{I} - \frac{2G}{h + 3G}\mathbf{s}\mathbf{s}^{\mathrm{t}}\right]\mathrm{d}\boldsymbol{\gamma}. \tag{1.158}$$

This is the inverse relation to eqn (1.155), and must be reduced to the elastic one if the strain increment $\mathrm{d}\boldsymbol{\gamma}$ does not fulfil the plastic loading condition $\mathbf{s}^{\mathrm{t}}\mathrm{d}\boldsymbol{\gamma} > 0$. The perfectly plastic case is reproduced for $h = 0$.

1.3.2 Kinematic hardening and mixed model

The isotropy of the hardening rule implies that in the uniaxial case the yield stress σ_{f} induced under tension applies to subsequent compression as well, and vice versa. Thus, the yield condition, eqn (1.150), confines elastic variations of the uniaxial stress by $-\sigma_{\mathrm{f}} \leq \sigma \leq \sigma_{\mathrm{f}}$. The elastic region of the specimen for alternating sequences in tension and compression is enlarged from initially $2\sigma_{\mathrm{s}}$ to actually $2\sigma_{\mathrm{f}}$ by plastic deformation (Fig. 1.18).

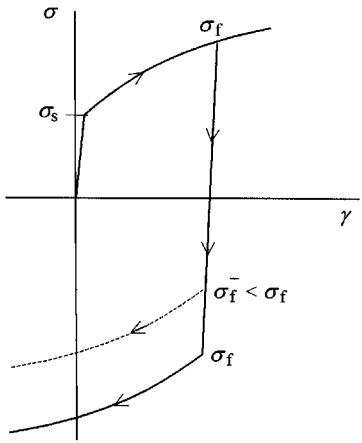

Figure 1.18: Demonstration of the Bauschinger effect.

Following experimental observations, load reversals are found to diminish the yield stress such that $\sigma_{\mathrm{f}}^{-} < \sigma_{\mathrm{f}}^{+}$, which is known as the Bauschinger effect. In order to account for this effect, the *kinematic hardening* rule proposed by Prager [13] assumes that the original yield surface remains rigid, but is displaced during the course of plastic deformation. In the principal stress space, the yield locus in the deviatoric plane is defined by the equation

$$[\boldsymbol{\sigma}_{\mathrm{DI}} - \boldsymbol{\alpha}_{\mathrm{I}}]^{\mathrm{t}}[\boldsymbol{\sigma}_{\mathrm{DI}} - \boldsymbol{\alpha}_{\mathrm{I}}] = r_{\mathrm{o}}^2.$$

This equation describes a circle of radius $r_{\mathrm{o}} = \sqrt{2/3}\sigma_{\mathrm{s}}$ with the centre displaced by $\boldsymbol{\alpha}_{\mathrm{I}}$ from the hydrostatic axis (Fig. 1.19). The vector $\boldsymbol{\alpha}_{\mathrm{I}}$ is by definition deviatoric in nature.

In terms of ordinary stress, the yield limit reads

$$[\boldsymbol{\sigma}_{\mathrm{D}} - \boldsymbol{\alpha}]^{\mathrm{t}}[\boldsymbol{\sigma}_{\mathrm{D}} - \boldsymbol{\alpha}] = \frac{2}{3}\sigma_{\mathrm{s}}^2. \tag{1.159}$$

Defining the equivalent quantity,

$$\bar{\sigma}_{\mathrm{K}}^2 = \frac{3}{2}\boldsymbol{\sigma}_{\mathrm{KD}}^{\mathrm{t}}\boldsymbol{\sigma}_{\mathrm{KD}} \tag{1.160}$$

with the 'kinematic' deviatoric stress given by the difference

$$\boldsymbol{\sigma}_{\mathrm{KD}} = \boldsymbol{\sigma}_{\mathrm{D}} - \boldsymbol{\alpha},$$

the yield condition can be stated analogously to eqn (1.150) as

$$\phi_{\mathrm{K}}(\boldsymbol{\sigma}, \boldsymbol{\alpha}) = \bar{\sigma}_{\mathrm{K}} - \sigma_{\mathrm{s}} \leq 0. \tag{1.161}$$

Equation (1.161) implies kinematic hardening of the yield surface by the deviatoric stress-type vector

$$\boldsymbol{\alpha} = \{\alpha_{\mathrm{xx}}\, \alpha_{\mathrm{yy}}\, \alpha_{\mathrm{zz}}\, \sqrt{2}\alpha_{\mathrm{xy}}\, \sqrt{2}\alpha_{\mathrm{yz}}\, \sqrt{2}\alpha_{\mathrm{xz}}\}, \tag{1.162}$$

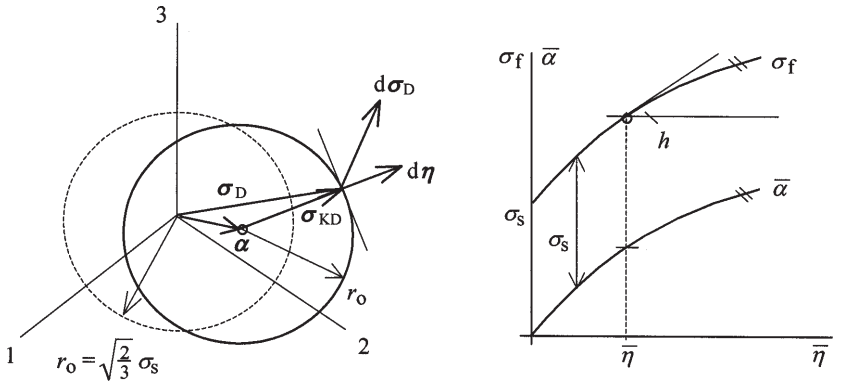

Figure 1.19: Kinematic hardening model.

which changes in proportion to the incremental plastic strain:

$$\mathrm{d}\boldsymbol{\alpha} = C\mathrm{d}\boldsymbol{\eta} = \frac{2}{3}h\mathrm{d}\boldsymbol{\eta}. \tag{1.163}$$

The vector $\boldsymbol{\alpha}$ accounts for the effect of *residual microstresses* in the material as a consequence of plastic deformation. The difference $\boldsymbol{\sigma}_{\mathrm{KD}} = \boldsymbol{\sigma}_{\mathrm{D}} - \boldsymbol{\alpha}$ is apparently the *active stress* in the present plasticity model [15]. In the case of uniaxial stress σ where

$$\boldsymbol{\sigma}_{\mathrm{D}} = \left\{ \frac{2}{3}\sigma \; -\frac{\sigma}{3} \; -\frac{\sigma}{3} \; 0 \; 0 \; 0 \right\}, \quad \boldsymbol{\alpha} = \left\{ \alpha \; -\frac{\alpha}{2} \; -\frac{\alpha}{2} \; 0 \; 0 \; 0 \right\}, \tag{i}$$

the equivalent stress quantity in eqn (1.161) becomes

$$\bar{\sigma}_{\mathrm{K}} = \left| \sigma - \frac{3}{2}\alpha \right|. \tag{ii}$$

The yield condition then bounds elastic stress states by

$$-\sigma_{\mathrm{s}} \leq \sigma - \frac{3}{2}\alpha \leq \sigma_{\mathrm{s}}, \tag{iii}$$

which fixes the span for elastic sequences in stress from tension to compression, and vice versa, to $2\sigma_{\mathrm{s}}$ (Fig. 1.19). If plastic deformation develops under tensile action, the stress follows the uniaxial hardening characteristic:

$$\sigma = \sigma_{\mathrm{s}} + \frac{3}{2}\alpha = \sigma_{\mathrm{f}}(\eta) \quad \text{and} \quad \frac{3}{2}\alpha = \sigma_{\mathrm{f}}(\eta) - \sigma_{\mathrm{s}}. \tag{iv}$$

In stress reversal, the elastic range is seen bounded by

$$\sigma_{\mathrm{f}} - 2\sigma_{\mathrm{s}} \leq \sigma \leq \sigma_{\mathrm{f}}. \tag{v}$$

From eqn (iv), for incremental changes in continuous loading,

$$\frac{3}{2}\mathrm{d}\alpha = h\mathrm{d}\eta = \frac{3}{2}C\mathrm{d}\eta \quad \text{and} \quad C = \frac{2}{3}h. \tag{vi}$$

In eqn (vi), the proportionality $\mathrm{d}\alpha = C\mathrm{d}\eta$ has been used between the axial components and specifies the proportionality factor C as employed in eqn (1.163).

The incremental plastic strain is presented in the form

$$\mathrm{d}\boldsymbol{\eta} = \mathrm{d}\bar{\eta}\mathbf{s}_{\mathrm{K}}. \tag{1.164}$$

The direction of plastic flow $\mathbf{s}_{\mathrm{K}}$ is defined by

$$\mathbf{s}_{\mathrm{K}} = \frac{3}{2}\frac{1}{\bar{\sigma}_{\mathrm{K}}}\boldsymbol{\sigma}_{\mathrm{KD}} = \left[\frac{\partial\bar{\sigma}_{\mathrm{K}}}{\partial\boldsymbol{\sigma}}\right]^{\mathrm{t}} = \left[\frac{\partial\phi_{\mathrm{K}}}{\partial\boldsymbol{\sigma}}\right]^{\mathrm{t}}, \tag{1.165}$$

and is thus associated with the yield condition in eqn (1.161).

The consistency condition during plastic flow is $\mathrm{d}\phi_{\mathrm{K}} = \mathrm{d}\bar{\sigma}_{\mathrm{K}} = 0$. With eqn (1.160) for $\bar{\sigma}_{\mathrm{K}}$:

$$\mathrm{d}\bar{\sigma}_{\mathrm{K}} = \mathbf{s}_{\mathrm{K}}^{\mathrm{t}}[\mathrm{d}\boldsymbol{\sigma} - \mathrm{d}\boldsymbol{\alpha}] = 0. \tag{1.166}$$

With eqn (1.163) for $\mathrm{d}\boldsymbol{\alpha}$ and eqn (1.164) for $\mathrm{d}\boldsymbol{\eta}$,

$$\mathbf{s}_{\mathrm{K}}^{\mathrm{t}}\mathrm{d}\boldsymbol{\alpha} = \frac{2}{3}h\mathbf{s}_{\mathrm{K}}^{\mathrm{t}}\mathrm{d}\boldsymbol{\eta} = h\mathrm{d}\bar{\eta}. \tag{1.167}$$

Substituting in eqn (1.166),

$$\mathrm{d}\bar{\eta} = \frac{1}{h}\mathbf{s}_{\mathrm{K}}^{\mathrm{t}}\mathrm{d}\boldsymbol{\sigma} \geq 0. \tag{1.168}$$

The incremental plastic strain of eqn (1.164) is then obtained as

$$\mathrm{d}\boldsymbol{\eta} = \frac{1}{h}\mathbf{s}_{\mathrm{K}}\mathbf{s}_{\mathrm{K}}^{\mathrm{t}}\mathrm{d}\boldsymbol{\sigma} \quad \text{for } \mathbf{s}_{\mathrm{K}}^{\mathrm{t}}\mathrm{d}\boldsymbol{\sigma} > 0, \tag{1.169}$$

the formalism being completely analogous to the previous isotropic hardening model. Similarly, the expression in terms of the strain increment $\mathrm{d}\boldsymbol{\gamma}$ instead of $\mathrm{d}\boldsymbol{\sigma}$ and the complete incremental stress–strain relations are analogous to those for isotropic hardening.

Equation (1.167) suggests introduction of the quantity

$$\mathrm{d}\bar{\alpha} = \mathbf{s}_{\mathrm{K}}^{\mathrm{t}}\mathrm{d}\boldsymbol{\alpha} = \mathrm{d}\sigma_{\mathrm{f}} \quad \text{and} \quad \bar{\alpha} = \int \mathrm{d}\bar{\alpha} = \sigma_{\mathrm{f}} - \sigma_{\mathrm{s}},$$

as a scalar measure of kinematic hardening. For completeness, we also notice the following relations:

$$\mathrm{d}\boldsymbol{\alpha} = \frac{2}{3}\mathrm{d}\bar{\alpha}\mathbf{s}_{\mathrm{K}}, \quad \mathrm{d}\bar{\alpha}^2 = \frac{3}{2}\mathrm{d}\boldsymbol{\alpha}^{\mathrm{t}}\mathrm{d}\boldsymbol{\alpha}.$$

Mixed hardening model

A combination of kinematic and isotropic hardening can be obtained by stating the yield condition in the form

$$\phi_{\mathrm{M}} = \bar{\sigma}_{\mathrm{K}} - \sigma_{\mathrm{is}} \leq 0. \tag{1.170}$$

In contrast to the fixed σ_{s} in eqn (1.161), the material parameter σ_{is} is allowed to vary with plastic deformation:

$$\sigma_{\mathrm{is}} = \sigma_{\mathrm{is}}(\bar{\eta}) \quad \text{and} \quad \mathrm{d}\sigma_{\mathrm{is}} = C_{\mathrm{is}}\mathrm{d}\bar{\eta}. \tag{1.171}$$

For uniaxial tension,

$$\sigma = \sigma_{\mathrm{is}}(\eta) + \frac{3}{2}\alpha = \sigma_{\mathrm{f}}(\eta), \tag{1.172}$$

as detailed in Fig. 1.20. By differentiation,

$$\frac{\mathrm{d}\sigma_{\mathrm{is}}}{\mathrm{d}\eta} + \frac{3}{2}\frac{\mathrm{d}\alpha}{\mathrm{d}\eta} = C_{\mathrm{is}} + \frac{3}{2}C_{\mathrm{K}} = h, \tag{1.173}$$

where C_{K} pertains to the kinematic constituent, eqn (1.163). For $C_{\mathrm{K}} = 0$, eqn (1.170) describes isotropic hardening, for $C_{\mathrm{is}} = 0$ it reduces to the kinematic hardening model.

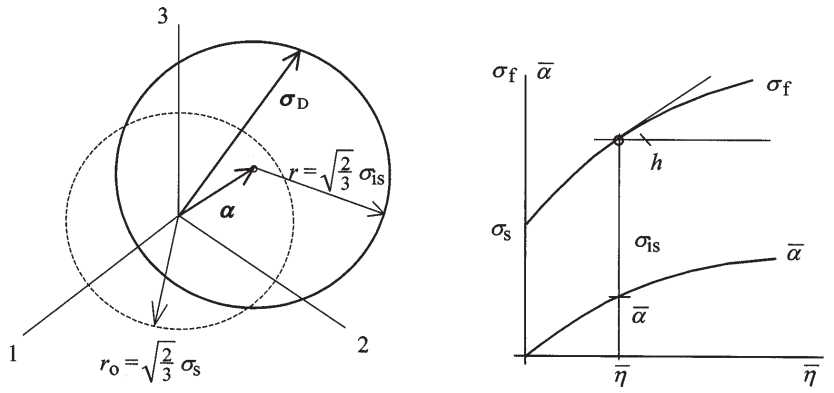

Figure 1.20: Mixed hardening model.

1.3.3 Thin-walled cylinder under tension and torsion

Experimental tests on plasticity under multiaxial stress are conveniently performed with thin-walled circular cylinders. In this case the state of stress can be controlled directly by the applied loading: axial force, internal pressure and torque. The particular experiment referred to here appears to be important to the hardening model. The loading sequence comprises torsion, torsion/tension and tension. It was observed that in the last step of the sequence, the plastic twist obtained before by tension under constant torsion decreases [14], which is contradictory to the isotropic hardening prediction. This observation has been explained by the assumption of a kinematic hardening model [15].

The thin-walled circular cylinder (Fig. 1.21) is subjected to a loading programme of torsion and tension. The load system induces a homogeneous stress state defined at each instant by the shear stress τ from torsion and the axial stress σ from tension. At each point the stress state with reference to a system $0\text{–}r\,\varphi\,z$ along the radial, circumferential and axial direction, respectively, specifies the vector:

$$\begin{aligned}\boldsymbol{\sigma} &= \{\sigma_{rr}\,\sigma_{\varphi\varphi}\,\sigma_{zz}\,\sqrt{2}\sigma_{r\varphi}\,\sqrt{2}\sigma_{\varphi z}\,\sqrt{2}\sigma_{rz}\}\\ &= \{\ 0\quad 0\quad \sigma\quad 0\quad \sqrt{2}\tau\quad 0\ \}.\end{aligned} \tag{1.174}$$

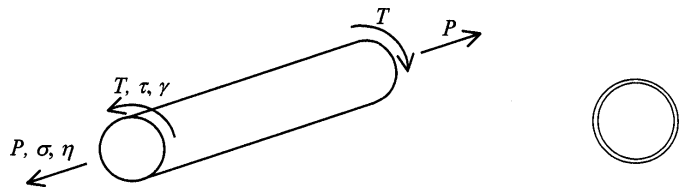

Figure 1.21: Thin-walled cylinder under tension and torsion.

Deviatoric stress and plastic strain are detailed as

$$\boldsymbol{\sigma}_{\mathrm{D}} = \left\{ -\frac{\sigma}{3} \; -\frac{\sigma}{3} \; \frac{2\sigma}{3} \; 0 \; \sqrt{2}\tau \; 0 \right\} \tag{1.175}$$

and

$$\boldsymbol{\eta} = \left\{ -\frac{\eta}{2} \; -\frac{\eta}{2} \; \eta \; 0 \; \frac{1}{\sqrt{2}}\gamma \; 0 \right\}, \tag{1.176}$$

where η denotes the plastic strain in the axial direction, and γ the shear strain.

The equivalent deviatoric stress (Section 1.2.3) is obtained as

$$\bar{\sigma}^2 = \frac{3}{2}\boldsymbol{\sigma}_{\mathrm{D}}^{\mathrm{t}}\boldsymbol{\sigma} = \sigma^2 + 3\tau^2 \tag{1.177}$$

and, therefore, during the course of plastic flow under isotropic hardening (Section 1.3.1),

$$\sigma^2 + 3\tau^2 = \sigma_{\mathrm{f}}^2. \tag{1.178}$$

Equation (1.178) can be represented by a circle centred in the $\sigma, \sqrt{3}\tau$-plane with radius σ_{f}, the actual yield stress (Fig. 1.22, left). Initially, $\sigma_{\mathrm{f}} = \sigma_{\mathrm{s}}$, the elasticity limit of the material.

From the flow rule $\mathrm{d}\boldsymbol{\eta} = \mathrm{d}\bar{\eta}\mathbf{s} = (3\mathrm{d}\bar{\eta}/2\bar{\sigma})\boldsymbol{\sigma}_{\mathrm{D}}$, we deduce the relationship

$$\frac{\mathrm{d}\gamma}{\mathrm{d}\eta} = \frac{3\tau}{\sigma} \tag{1.179}$$

between the shear and axial components of the incremental plastic strain.

The loading programme can be followed in Fig. 1.22 (left). The torque is applied first until the elasticity limit σ_{s} (path AB); no plastic flow occurs. At constant torque, the axial force is superposed increasing from zero (path BC). Thereby plastic flow occurs and contributes to both the elongation

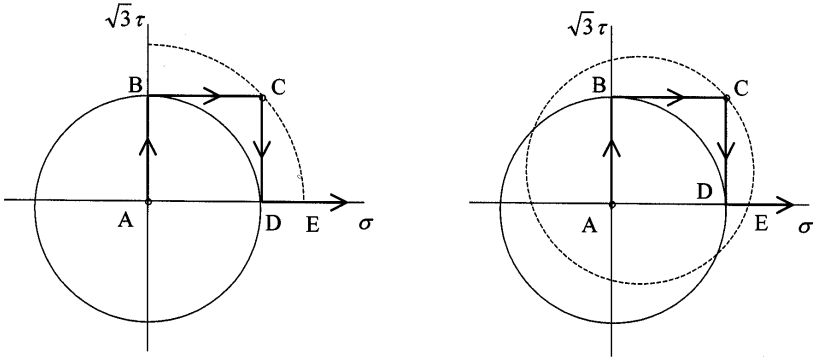

Figure 1.22: Isotropic hardening (left) and kinematic hardening (right).

and the twist. The strain components increase in proportion to the stress components as given by eqn (1.179), which determines the slope of the γ, η-diagram in Fig. 1.23. At point B ($\sqrt{3}\tau = \sigma_s, \sigma = 0$) we have $d\gamma/d\eta = 3\tau/\sigma = \infty$. As the axial stress σ increases, the slope diminishes. At point C ($\sqrt{3}\tau = \sigma = \sigma_s$) it is $d\gamma/d\eta = \sqrt{3}$. Removal of the torque at constant axial force (path CD) leaves plastic deformation unchanged. Further increase of the axial force beyond the expanded yield locus (point E) induces plastic flow only in the axial direction since the stress state ($\tau = 0, \sigma$) implies that $d\gamma/d\eta = 3\tau/\sigma = 0$ and therefore the shear strain γ remains constant. This disagrees with the experimental observation, where the plastic twist is seen to go back.

Next, considering kinematic hardening (Section 1.3.2) we introduce the deviatoric translation vector

$$\boldsymbol{\alpha} = \left\{ -\frac{\alpha}{2} \; -\frac{\alpha}{2} \; \alpha \; 0 \; \sqrt{2}\beta \; 0 \right\}. \tag{1.180}$$

The relative stress is

$$\begin{aligned} \boldsymbol{\sigma}_{\mathrm{KD}} &= \boldsymbol{\sigma}_{\mathrm{D}} - \boldsymbol{\alpha} \\ &= \left\{ -\frac{1}{3}\left(\sigma - \frac{3}{2}\alpha\right) \; -\frac{1}{3}\left(\sigma - \frac{2}{3}\alpha\right) \; \frac{2}{3}\left(\sigma - \frac{3}{2}\alpha\right) \; 0 \; \sqrt{2}(\tau - \beta) \; 0 \right\} \end{aligned} \tag{1.181}$$

and determines the equivalent stress quantity,

$$\bar{\sigma}_{\mathrm{K}}^2 = \frac{3}{2}\boldsymbol{\sigma}_{\mathrm{KD}}^{\mathrm{t}}\boldsymbol{\sigma}_{\mathrm{KD}} = \left(\sigma - \frac{3}{2}\alpha\right)^2 + 3\,(\tau - \beta)^2\,. \tag{1.182}$$

The yield locus is thus given by

$$\left(\sigma - \frac{3}{2}\alpha\right)^2 + 3(\tau - \beta)^2 = \sigma_s^2. \tag{1.183}$$

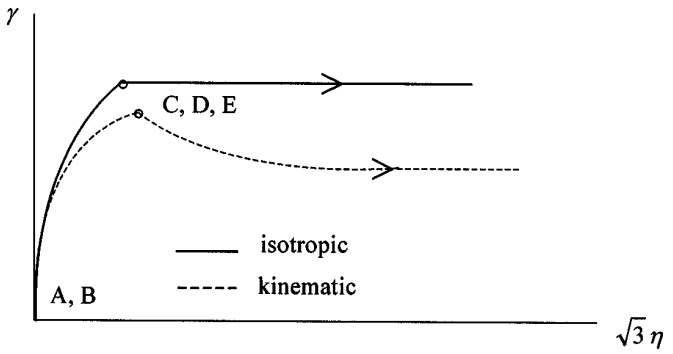

Figure 1.23: Effect of plastic extension upon twist (schematic).

It describes a circle in the $\sigma, \sqrt{3}\tau$-plane, of radius σ_s, with the centre at $\sigma = 3\alpha/2, \sqrt{3}\tau = \sqrt{3}\beta$. Initially, $\alpha = \beta = 0$ (Fig. 1.22, right).

From the flow rule: $\mathrm{d}\boldsymbol{\eta} = \mathrm{d}\bar{\eta}\mathbf{s}_K = (3\mathrm{d}\bar{\eta}/2\bar{\sigma}_K)\boldsymbol{\sigma}_{KD}$ we obtain for the components of incremental plastic strain

$$\frac{\mathrm{d}\gamma}{\mathrm{d}\eta} = \frac{3(\tau - \beta)}{\sigma - \frac{3}{2}\alpha}. \tag{1.184}$$

The loading sequence is identical to the previous case of isotropic hardening, but the yield locus is modified by the kinematic model (Fig. 1.22, right). Since $\mathrm{d}\boldsymbol{\alpha} = C\mathrm{d}\boldsymbol{\eta}$, the translation of the centre of the circle is directed along

$$\frac{\mathrm{d}\beta}{\mathrm{d}\alpha} = \frac{1}{2}\frac{\mathrm{d}\gamma}{\mathrm{d}\eta} = \frac{3}{2}\frac{\tau - \beta}{\sigma - \frac{3}{2}\alpha}. \tag{1.185}$$

Application of the torque (path AB) is an elastic process. Superposition of the axial force (path BC) induces plastic flow contributing to both deformation modes: elongation and twist. The proportion of the two components is given by eqn (1.184) in conjunction with eqn (1.185), and defines the slope of the related γ, η-diagram in Fig. 1.23. At point B ($\sqrt{3}\tau = \sigma_s, \sigma = 0; \beta = \alpha = 0$), we have $\mathrm{d}\gamma/\mathrm{d}\eta = \sqrt{3}\sigma_s/0 = \infty$ as for isotropic hardening. At point C ($\sqrt{3}\tau = \sigma_s, \sigma = \sigma_s$; β, α), the slope is less than in the isotropic model since with γ the quantity β rises faster than α to this point. Removal of the torque (path CD) is elastic; additional plastic flow occurs when the axial force increases beyond point E. Here ($\tau = 0, \sigma; \beta, \alpha$), the quotient $\mathrm{d}\gamma/\mathrm{d}\eta = -3\beta/(\sigma - 3\alpha/2)$ is seen to be negative. That means the plastic twist is going back with continuing extension of the tube. Since β is also diminishing with γ, the tendency decreases. Thus, the kinematic model correctly reproduces the effect of extension upon previous plastic twist. This result is particularly due to the association of the flow rule to the kinematic yield condition.

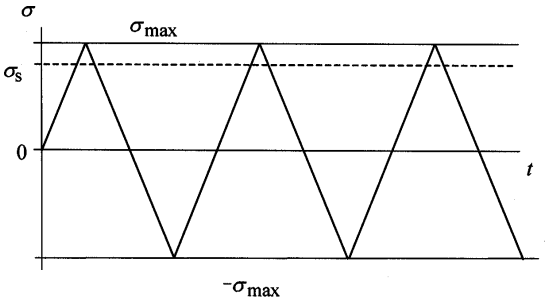

Figure 1.24: Cyclic loading programme.

1.3.4 Cyclic loading

The performance of the hardening models is discussed next for the case of cyclic loading. Figure 1.24 shows the loading programme for a uniaxial specimen subjected to alternating stress $-\sigma_m \leq \sigma \leq \sigma_m$ with amplitude beyond the elasticity limit: $\sigma_m > \sigma_s$.

The material exhibits a bilinear stress–strain characteristic. Figure 1.25 demonstrates the development of plasticity for isotropic (left) and kinematic hardening (right). In both cases the first loading induces an elastic strain up to σ_s, plastic flow occurs from σ_s to σ_m. Isotropic hardening thereby modifies the yield stress to $\sigma_f = \sigma_m$ and extends the span of the elastic region to $2\sigma_f = 2\sigma_m$ so that subsequent response to the loading programme is elastic. Kinematic hardening fixes the elastic region to $2\sigma_s < 2\sigma_m$. Therefore, stress reversal is accompanied by plastic flow after the elastic traversal of $2\sigma_s$. The same process is observed in all subsequent cycles, which produce alternating plastic strain.

Figure 1.26 refers to the behaviour of the two hardening models under cyclic strain $-\gamma_m \leq \gamma \leq \gamma_m$ with amplitude exceeding the elasticity limit: $\gamma_m > \sigma_s/E$. Isotropic hardening (left) enlarges the elastic region via the increasing yield stress σ_f, and therefore plastic strain production diminishes from cycle to cycle. Kinematic hardening (right) behaves as in the stress programme, following the same cycle in each sequence after the first straining to γ_m.

It is reported in [16] that the hardening observed in the early sequences of a cyclic strain programme is much less extensive than the prediction of the isotropic model. Saturation of hardening ultimately leads to stabilized stress–strain cycles in the material response as described by the kinematic model.

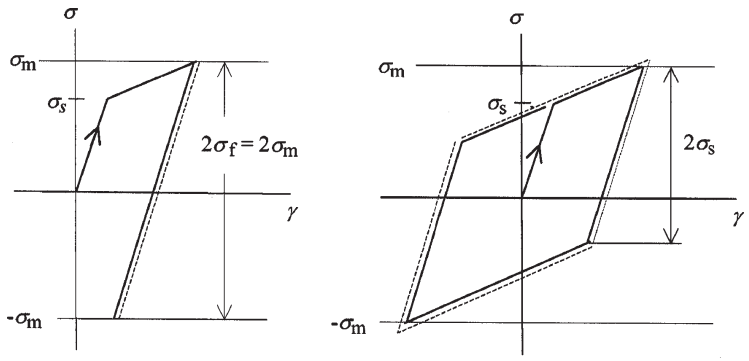

Figure 1.25: Response to cyclic stress.

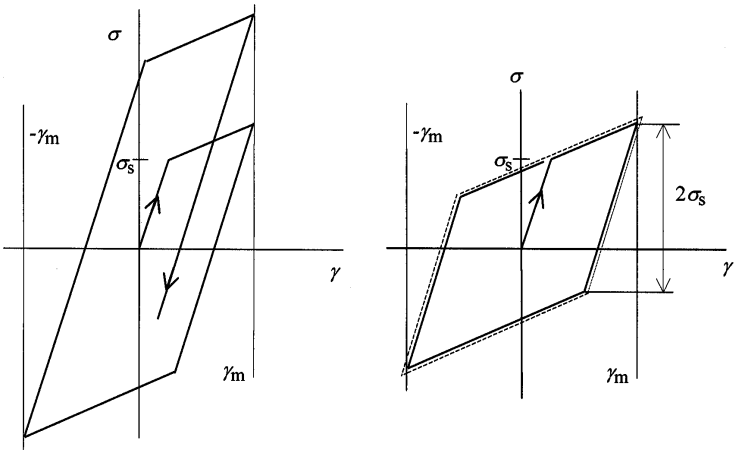

Figure 1.26: Response to cyclic strain.

1.4 A general view on elastoplastic constitutive description

In the regime of infinitesimal deformations the strain $\boldsymbol{\gamma}$ is assumed to be composed additively of an elastic part $\boldsymbol{\varepsilon}$ and an inelastic part $\boldsymbol{\eta}$. For incremental quantities:

$$\mathrm{d}\boldsymbol{\gamma} = \mathrm{d}\boldsymbol{\varepsilon} + \mathrm{d}\boldsymbol{\eta} = \boldsymbol{\kappa}^{-1}\mathrm{d}\boldsymbol{\sigma} + \mathrm{d}\boldsymbol{\eta}.$$

The elastic strain increment $\mathrm{d}\boldsymbol{\varepsilon}$ is associated with the stress increment $\mathrm{d}\boldsymbol{\sigma}$ by the law of elasticity. The variation $\mathrm{d}\boldsymbol{\eta}$ of the inelastic strain is the result of plastic flow.

Plasticity theory is based on the yield condition,

$$\phi(\boldsymbol{\sigma}, \mathbf{q}) \leq 0,$$

where the stress state $\boldsymbol{\sigma}$ enters the yield function ϕ as the argument, and $\mathbf{q}$ denotes a vector array of parameters describing the current plastic state of the material. It is not difficult to specify the parameters in the array $\mathbf{q}$ for the hardening models presented so far.

The equation $\phi(\boldsymbol{\sigma}, \mathbf{q}) = 0$ limits the elastic domain for the stress $\boldsymbol{\sigma}$ at the current state of hardening. It describes a convex surface in stress space with the hardening variables $\mathbf{q}$ as parameter. For stresses within the yield surface ($\phi(\boldsymbol{\sigma}, \mathbf{q}) < 0$) the material is in an elastic state, those on the yield surface are denoted as plastic. Plastic deformation does not occur, except from a plastic state.

Plastic flow affects the yield surface of hardening materials. A relation of the form

$$\mathrm{d}\mathbf{q} = \boldsymbol{\mathcal{H}}\mathrm{d}\boldsymbol{\eta}$$

is assumed between the variation of the hardening parameters and the plastic strain.

The flow rule defines the direction of plastic flow by the state of stress at $\phi(\boldsymbol{\sigma}, \mathbf{q}) = 0$. The associated flow rule derives from the yield function as

$$\mathrm{d}\boldsymbol{\eta} = \Lambda \left[\frac{\partial \phi}{\partial \boldsymbol{\sigma}}\right]^{\mathrm{t}} = \Lambda \frac{\partial \phi}{\partial \boldsymbol{\sigma}^{\mathrm{t}}} \qquad (\Lambda \geq 0).$$

It fulfils the normality condition with respect to the yield surface (see Chapter 3).

Continuous plastic flow is governed by the requirement $\mathrm{d}\phi = 0$, the consistency condition. Utilizing the hardening law and the flow rule,

$$\mathrm{d}\phi = \frac{\partial \phi}{\partial \boldsymbol{\sigma}}\mathrm{d}\boldsymbol{\sigma} + \frac{\partial \phi}{\partial \mathbf{q}}\mathrm{d}\mathbf{q} = \frac{\partial \phi}{\partial \boldsymbol{\sigma}}\mathrm{d}\boldsymbol{\sigma} + \Lambda \frac{\partial \phi}{\partial \mathbf{q}}\boldsymbol{\mathcal{H}}\frac{\partial \phi}{\partial \boldsymbol{\sigma}^{\mathrm{t}}} = 0$$

and

$$\Lambda = -\left(\frac{\partial \phi}{\partial \mathbf{q}}\boldsymbol{\mathcal{H}}\frac{\partial \phi}{\partial \boldsymbol{\sigma}^{\mathrm{t}}}\right)^{-1} \frac{\partial \phi}{\partial \boldsymbol{\sigma}}\mathrm{d}\boldsymbol{\sigma} \geq 0.$$

From the yield condition, the occurrence of plastic flow requires $\phi = 0$ and $(\partial\phi/\partial\boldsymbol{\sigma})\mathrm{d}\boldsymbol{\sigma} > 0$, which is termed the plastic loading condition. The change of state is otherwise elastic. It is noticed that the structure of the yield condition must be such that the convention $\Lambda > 0$ is observed in plastic loading. This requires that the scalar hardening factor is a positive quantity

$$-\frac{\partial \phi}{\partial \mathbf{q}}\boldsymbol{\mathcal{H}}\frac{\partial \phi}{\partial \boldsymbol{\sigma}^{\mathrm{t}}} > 0.$$

The determination of the plastic strain increment $\mathrm{d}\boldsymbol{\eta}$ in terms of the stress increment $\mathrm{d}\boldsymbol{\sigma}$ is now completed:

$$\mathrm{d}\boldsymbol{\eta} = \Lambda \frac{\partial \phi}{\partial \boldsymbol{\sigma}^{\mathrm{t}}} = -\left(\frac{\partial \phi}{\partial \mathbf{q}}\boldsymbol{\mathcal{H}}\frac{\partial \phi}{\partial \boldsymbol{\sigma}^{\mathrm{t}}}\right)^{-1} \frac{\partial \phi}{\partial \boldsymbol{\sigma}^{\mathrm{t}}}\frac{\partial \phi}{\partial \boldsymbol{\sigma}}\mathrm{d}\boldsymbol{\sigma}.$$

If the strain increment is given instead of the stress increment, it can be introduced in the equation of plastic flow by the law of elasticity. The consistency condition then reads

$$\mathrm{d}\phi = \frac{\partial \phi}{\partial \boldsymbol{\sigma}}\mathrm{d}\boldsymbol{\sigma} + \frac{\partial \phi}{\partial \mathbf{q}}\mathrm{d}\mathbf{q} = \frac{\partial \phi}{\partial \boldsymbol{\sigma}}\boldsymbol{\kappa}\mathrm{d}\gamma - \left[\frac{\partial \phi}{\partial \boldsymbol{\sigma}}\boldsymbol{\kappa} - \frac{\partial \phi}{\partial \mathbf{q}}\boldsymbol{\mathcal{H}}\right]\mathrm{d}\boldsymbol{\eta} = 0.$$

Employing the flow rule for $\mathrm{d}\boldsymbol{\eta}$ and solving for the scalar multiplier we obtain

$$\Lambda = \left(\frac{\partial \phi}{\partial \boldsymbol{\sigma}}\boldsymbol{\kappa}\frac{\partial \phi}{\partial \boldsymbol{\sigma}^{\mathrm{t}}} - \frac{\partial \phi}{\partial \mathbf{q}}\boldsymbol{\mathcal{H}}\frac{\partial \phi}{\partial \boldsymbol{\sigma}^{\mathrm{t}}}\right)^{-1} \frac{\partial \phi}{\partial \boldsymbol{\sigma}}\boldsymbol{\kappa}\mathrm{d}\gamma \geq 0,$$

which completes the determination of the incremental plastic strain in terms of the strain increment. The condition for plastic loading is $(\partial\phi/\partial\boldsymbol{\sigma})\boldsymbol{\kappa}\mathrm{d}\gamma > 0$.

In the above expression for Λ, the second term in the parentheses is a negative scalar quantity; the first is a positive one since it can be interpreted as an elastic energy. It is concluded that the plastic loading condition is compatible with the convention $\Lambda > 0$.

An alternative presentation of the flow rule reads

$$\mathrm{d}\boldsymbol{\eta} = \Lambda \frac{\partial \phi}{\partial \boldsymbol{\sigma}^{\mathrm{t}}} = \mathrm{d}\bar{\eta}\mathbf{s}.$$

The magnitude $\mathrm{d}\bar{\eta}$ of the incremental plastic strain is defined by

$$\mathrm{d}\bar{\eta}^2 = \frac{2}{3}\mathrm{d}\boldsymbol{\eta}^{\mathrm{t}}\mathrm{d}\boldsymbol{\eta}$$

and therefore the vector $\mathbf{s}$ possesses the property of a constant length

$$\mathbf{s}^{\mathrm{t}}\mathbf{s} = \frac{3}{2}.$$

With the associated flow rule for $\mathrm{d}\boldsymbol{\eta}$ the definition of $\mathrm{d}\bar{\eta}$ furnishes the relation

$$\mathrm{d}\bar{\eta} = \Lambda \left(\frac{2}{3} \frac{\partial \phi}{\partial \boldsymbol{\sigma}} \frac{\partial \phi}{\partial \boldsymbol{\sigma}^{\mathrm{t}}} \right)^{1/2} \geq 0,$$

and substitution in the alternative presentation gives the flow direction

$$\mathbf{s} = \left(\frac{2}{3} \frac{\partial \phi}{\partial \boldsymbol{\sigma}} \frac{\partial \phi}{\partial \boldsymbol{\sigma}^{\mathrm{t}}} \right)^{-1/2} \frac{\partial \phi}{\partial \boldsymbol{\sigma}^{\mathrm{t}}}.$$

Obviously, we obtain the identities $\mathrm{d}\bar{\eta} \equiv \Lambda$ and $\mathbf{s} \equiv \partial\phi/\partial\boldsymbol{\sigma}^{\mathrm{t}}$ if the yield function is defined such that $(\partial\phi/\partial\boldsymbol{\sigma})\partial\phi/\partial\boldsymbol{\sigma}^{\mathrm{t}} = 3/2$.

It is recalled now that we considered here the flow approach to plasticity and in the form most frequently employed. For a more detailed presentation the reader can consult the early review given in [17] and the précis in [18].

1.5 Problems

1. Given a nonlinear stress–strain diagram prove whether the material is elastoplastic or nonlinear elastic (unloading!).

2. An elastoplastic rod carries at the considered instant a tensile stress $\sigma_1 > \sigma_{\mathrm{s}}$. Mark on the stress–strain diagram (Fig. 1.27) at least three different paths leading to this stress and indicate the respective strain γ associated with σ_1.

3. Confirm that in a cycle $(0 \to \sigma \to 0)$ of uniaxial stress, the work $\oint \sigma \mathrm{d}\gamma$ of the stress on the strain vanishes if the loading remains below the yield

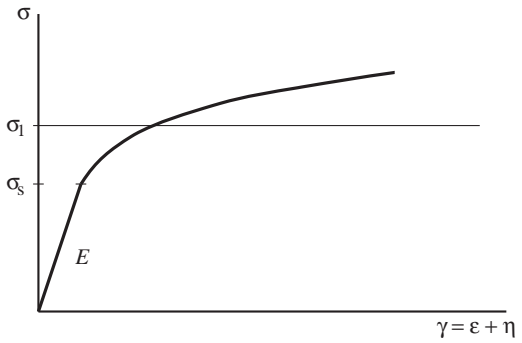

Figure 1.27: Problem 2.

stress ($\sigma < \sigma_s$), while it is given by $\int \sigma d\eta$ if the stress exceeds the yield stress ($\sigma > \sigma_s$).

4. For a material with yield stress σ_s in tension obeying the von Mises yield criterion, determine the stress σ at the elasticity limit for the following states of principal stress:

$$\sigma_1 = \sigma_2 = 0, \quad \sigma_3 = -\sigma,$$

$$\sigma_1 = 0, \quad \sigma_2 = \sigma_3 = -\sigma,$$

$$\sigma_1 = \sigma_2 = \sigma_3 = \sigma.$$

5. Under plane stress conditions, the von Mises yield locus in the σ_1, σ_2-plane is an ellipse. Determine the stress σ at the elasticity limit σ_s with the von Mises (and alternatively with the Tresca) yield criterion for the following states of plane stress:

$$\sigma_1 = \pm\sigma, \quad \sigma_2 = 0,$$

$$\sigma_2 = \pm\sigma, \quad \sigma_1 = 0,$$

$$\sigma_1 = \sigma_2 = \pm\sigma,$$

$$\sigma_1 = -\sigma_2 = \pm\sigma.$$

6. A spherical membrane (radius R, thickness t) is inflated by internal pressure of intensity p (Fig. 1.28). The elasticity limit in the membrane is attained at $p_s = 2t\sigma_s/R$.

In order to obtain a permanent expansion of the sphere, the pressure is increased to $p = \lambda p_s$. What is the associated permanent increase in radius and change in membrane thickness?

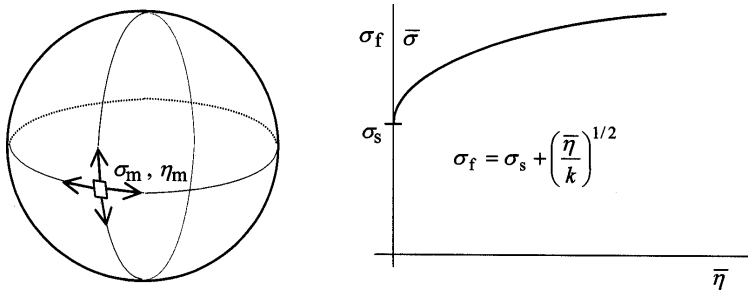

Figure 1.28: Problem 6.

In the present case, the plastic strain η_m along meridians and η_t across the thickness are related by $\eta_t = -2\eta_m$. Confirm that the equivalent plastic strain is given by $\bar{\eta} = 2\eta_m = |\eta_t|$.

References

[1] E. Kröner, Plastizität und Versetzungen, in *Vorlesungen über theoretische Physik*, Vol. II, A. Sommerfeld, Akademische Verlagsgesellschaft, Leipzig, 1970.

[2] J.H. Argyris, D.W. Scharpf and J.B. Spooner, Die elastoplastische Berechnung von allgemeinen Tragwerken und Kontinua, *Ing. Archiv* **37** (1969) 326–352.

[3] W. Prager, *Introduction to Mechanics of Continua*, Ginn, Boston, MA, 1961.

[4] M.T. Huber, Wlasciva praca odksztalcenia jako miara witezenia materialu. *Czas. Techn., Lwów* **22** (1904) 38–81. See also, J. Engel, Historical aspects of Huber's works, in *Huber's Yield Criterion in Plasticity*, M. Pietrzyk *et al.* (Eds), Akademia Górniczo-Hutnicza, Kraków, 1994.

[5] R. von Mises, Mechanik der festen Körper im plastisch deformablen Zustand, *Göttinger Nachrichten, Math. Phys. Kl.* (1913) 582–592.

[6] H. Tresca, Mémoire sur l'écoulement des corps solides soumis à de fortes pressions, *Compt. Rend. Acad. Sci. Paris* **59** (1864) 754.

[7] B. de Saint Vénant, Mémoire sur l'établissement des équations différentielles des mouvements intérieurs opérés dans les corps solides ductiles au delà des limites où l'élasticité pourrait les ramener à leur premier état, *Compt. Rend. Acad. Sci. Paris* **70** (1870) 473–480.

[8] M.L. Lévy, Mémoire sur les équations générales des mouvements intérieurs des corps solides ductiles au delá des limites où l'élasticité pourrait les ramener á leur premier état, *Compt. Rend. Acad. Sci. Paris* **70** (1870) 1323–1325.

[9] R. von Mises, Mechanik der plastischen Formänderung von Kristallen, *Z. Angew. Math. Mech. (ZAMM)* **8** (1928) 161–185.

[10] L. Prandtl, Spannungsverteilung in plastischen Körpern, *Proc. 1st. Int. Congr. Appl. Mech.*, Delft, Technische Boekhandel en Druckerij, J. Waltman Jr, 1924, pp. 43–54.

[11] E. Reuss, Berücksichtigung der elastischen Formänderungen in der Plastizitätstheorie, *Z. Angew. Math. Mech. (ZAMM)* **10** (1930) 266–274.

[12] R. Hill, *The Mathematical Theory of Plasticity*, Clarendon Press, Oxford, 1950.

[13] W. Prager, The theory of plasticity; a survey of recent achievements (James Clayton Lecture), *Proc. Inst. Mech. Engng* **169** (1955) 41–57.

[14] M. Feigen, Inelastic behavior under combined tension and torsion, *Proc. 2nd USA Congr. of Appl. Mech.*, 1954, pp. 469–476.

[15] Iu.I. Kadashevich and V.V. Novozhilov, The theory of plasticity which takes into account residual microstresses (*PMM* **22** (1958) 78–89) *TPMM* **22** (1959) 104–118.

[16] J.M. Corum, W.L. Greenstreet, K.C. Lin, C.E. Pugh and R.W. Swindeman, Interim guidelines for detailed inelastic analysis of high-temperature reactor system components, Oak Ridge National Laboratory, Tennessee, 1974.

[17] P.M. Naghdi, Stress–strain relations in plasticity and thermoplasticity, in *Plasticity, Proc. 2nd Symp. Naval Struc. Mech.*, E.H. Lee and P.S. Symonds (Eds), Pergamon Press, Oxford, 1960, pp. 121–169.

[18] W.T. Koiter, General theorems for elastic–plastic solids, in *Progress in Solid Mechanics*, Vol. 1, I.N. Sneddon and R. Hill (Eds), Chapter 4, North-Holland, Amsterdam, 1960, pp. 167–221.

[19] A. Paglietti, *Plasticity of Cold Worked Metals – A Deductive Approach*, WIT Press, Southampton, 2007.

This page intentionally left blank

CHAPTER 2

Elastoplastic response of structures and solids

2.1 Considerations on elastoplastic structures

2.1.1 Introductory remarks

General considerations
For simplicity of presentation, we consider a structure loaded by a single force P and denote the corresponding displacement (same location and orientation as the force) by u. The response of the structure to the applied force will be followed up in the force–displacement diagram.

The behaviour of the structure (Fig. 2.1) is linear elastic as long as the applied force P does not exceed the value P_s at which the stress somewhere in the structure first reaches the elasticity limit of the material. An increase of the applied force beyond P_s induces plastic flow in certain parts of the structure and is accompanied by decreasing stiffness. Unloading from a plastically deformed state takes place elastically, unless plastic flow sets in anew. Since geometric changes are considered negligible, plastic deformation does not modify the elastic properties of the structure. Therefore, elastic unloading from a plastically deformed state is governed by the stiffness of the original elastic structure.

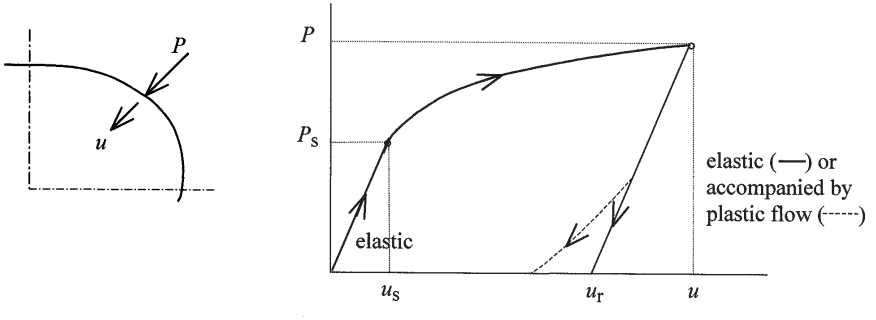

Figure 2.1: Elastoplastic force–displacement response of structure.

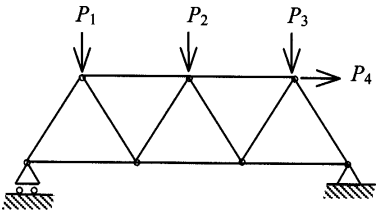

Figure 2.2: Example of statically determinate structure.

As long as the applied force induces stresses below the elasticity limit of the material everywhere in the structure, changes in the mechanical state are completely reversible and disappear upon removal of the loading. Loading beyond elasticity leads to permanent strains, and changes of the initial state are obtained after removal of the applied force. The plastic strains developed in the loading sequence are maintained after elastic unloading. Depending on the type, the integrity of the structure may necessitate the appearance of complementary elastic strains that establish kinematic compatibility. The resulting residual strains are compatible with the residual displacements. The residual stresses associated with the elastic strains in the unloaded structure constitute a self-equilibrated stress system.

Statically determinate systems
A characteristic of statically determinate systems is the possibility of obtaining the stresses from the condition of static equilibrium without reference to the material constitutive law and the kinematic compatibility. An example of a statically determinate structure is given in Fig. 2.2 in the form of a plane truss.

In such a system, the time history of the applied forces determines the temporal variation of the stresses by statics. Elastic and plastic parts of the strain are obtained by an evaluation of the respective material constitutive law. Removal of the applied forces implies vanishing of the stress everywhere in the system. Therefore, the residual state is characterized by the absence of stress and elastic strain. The residual strains are identical to the plastic strains developed during the loading sequence, which are compatible with the residual displacements. The plastic strains in a statically determinate system may be associated with admissible displacements, as may also the elastic strains on their own.

Kinematically determinate systems
In kinematically determinate systems the displacements are prescribed such that the strain can be completely determined. Figure 2.3 shows an example for a kinematically determinate truss structure.

Given the time history of the displacements imposed on the system, the strain variation is determined by kinematics. The associated stresses are

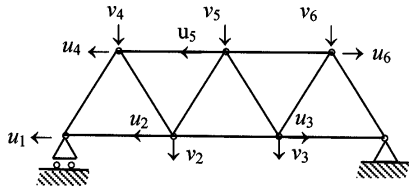

Figure 2.3: Example of a kinematically determinate structure.

obtained by an evaluation of the stress–strain relations for the elastoplastic material, and are continuously in equilibrium with the constraining forces.

In the present case, unloading stands for the removal of the imposed displacements. Therefore, the residual state is characterized by the absence of displacement and strain. The condition of vanishing residual strain implies that plastic strains are compensated by elastic strains which determine the residual stresses.

2.1.2 Simple elastic–perfectly plastic truss

The plane truss depicted in Fig. 2.4 consists of three bars of elastic–perfectly plastic material. Their mechanical response is characterized by the elastic modulus E and the yield stress σ_s. Since the dimensions (length l, cross-sectional area A) are identical for all three bars, their behaviour as structural members may be described uniquely by the force–elongation diagram in the figure. The bar force is defined as the stress resultant $S = \sigma A$, and the elongation is $\delta = \gamma l$. The elastic response of the individual bars is specified by the elastic stiffness $k = EA/l$, and is limited by $S_s = \sigma_s A$.

The truss is loaded by the force P applied at the junction point of the three bars and acts along the direction of the middle bar 1, the line of symmetry of the truss; the corresponding displacement is denoted by u. The side bars experience identical conditions of stress and strain ($S_3 = S_2, \delta_3 = \delta_2$). With reference to Fig. 2.5, we obtain, from the static equilibrium of the

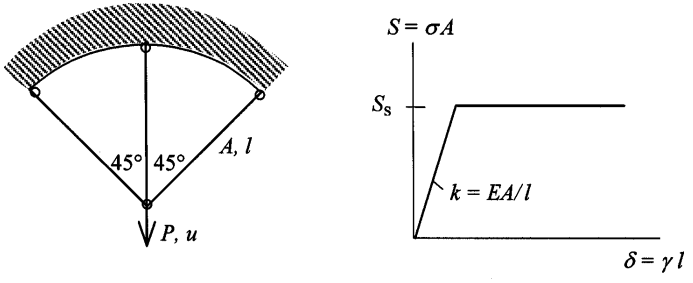

Figure 2.4: Elastic–perfectly plastic truss.

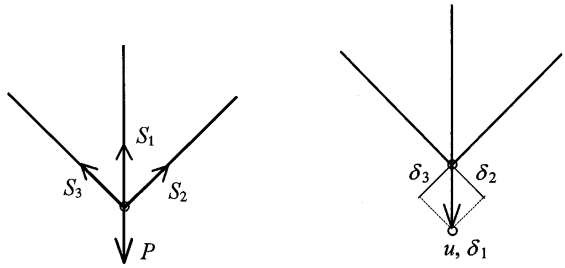

Figure 2.5: Statics and kinematics at the joint of the three bars.

forces at the application point of P, the relation

$$P = S_1 + \frac{\sqrt{2}}{2} S_2 + \frac{\sqrt{2}}{2} S_3 = S_1 + \sqrt{2} S_2. \tag{2.1}$$

Projection of the displacement u along the directions of the bars gives the elongations

$$\delta_1 = u, \quad \delta_2 = \delta_3 = \frac{\sqrt{2}}{2} u, \tag{2.2}$$

which ensure the kinematic compatibility of the truss.

Elastic response
The static condition, eqn (2.1), and the kinematic condition, eqn (2.2), do not rely on any particular response of the material. Within the elastic range, however, the force S in each bar is related to the elongation δ by the elastic stiffness k. We then have

$$S_1 = k\, \delta_1 = ku, \quad S_2 = k\, \delta_2 = \frac{\sqrt{2}}{2}\, ku. \tag{2.3}$$

Substitution in the equilibrium condition, eqn (2.1), gives the relation

$$P = 2ku, \tag{2.4}$$

from which the elastic stiffness of the truss system is seen to be $2k$. Equation (2.4) determines the displacement u for a given force P, and so the elongations of the bars follow from eqn (2.2) and the stress resultants from eqn (2.3):

$$S_1 = \frac{P}{2}, \quad S_2 = \frac{\sqrt{2}}{2}\, \frac{P}{2}. \tag{2.5}$$

Since the cross-sectional areas of all bars are the same, the stress magnitude is highest in the middle bar 1. This bar is therefore the first to attain the

yield stress σ_s when loading is increased starting from $P = 0$. We obtain the elastic limit load of the system for $S_1 = S_s$ in eqn (2.5) and the associated displacement by eqn (2.4) as

$$P_s = 2S_s, \quad u_s = \frac{P_s}{2k}. \tag{2.6}$$

Elastoplastic response

For loading in the elastoplastic regime ($P > P_s$) the force in bar 1 cannot be further increased and remains at S_s. The force in bars 2 and 3 is thus specified directly by the equilibrium condition, eqn (2.1), as a function of the applied force P. We then have for the stress resultants S in the bars

$$S_1 = S_s, \quad S_2 = \frac{\sqrt{2}}{2}\,(P - S_s). \tag{2.7}$$

The condition $S_1 = S_s$ imposed by the material on bar 1 during elastoplastic deformation enables us to determine the stress state in the truss from the static equilibrium alone. In this sense the originally simply redundant system becomes statically determinate for $P \geq P_s$.

Regarding next the deformations, as long as the side bars 2 and 3 are still below the elasticity limit S_s, the elastic relation in eqn (2.3) determines the elongation δ_2 with the stress resultant S_2 from eqn (2.7). This does not apply to the middle bar 1, which is in a plastic state. However, δ_1 can be obtained in terms of δ_2 by the kinematic compatibility, eqn (2.2). From the above,

$$\delta_2 = \frac{S_2}{k} = \frac{\sqrt{2}}{2k}\,(P - S_s), \quad \delta_1 = \sqrt{2}\delta_2 = \frac{P - S_s}{k}. \tag{2.8}$$

While the elongations $\delta_3 = \delta_2$ are entirely elastic, that of bar 1 reads

$$\delta_1 = \delta_{1e} + \delta_{1p} \tag{2.9}$$

and is composed of an elastic part δ_{1e} related to the stress resultant $S_1 = S_s$ by elasticity, and the plastic part δ_{1p}. The two constituents are given by

$$\begin{aligned} \delta_{1e} &= \frac{S_s}{k}, \\ \delta_{1p} &= \delta_1 - \delta_{1e} = \frac{P - 2S_s}{k}. \end{aligned} \tag{2.10}$$

In the elastoplastic range of the system we can relate the applied force P to the corresponding displacement u if we observe in eqn (2.1) for the equilibrium, the plasticity condition $S_1 = S_s = ku_s$ and the elastic relation of eqn (2.3) for S_2. We thus obtain

$$P = k(u_s + u) \quad \text{and} \quad P - P_s = k(u - u_s), \tag{2.11}$$

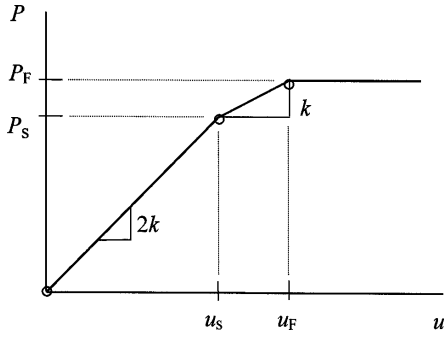

Figure 2.6: Load–displacement diagram for the truss.

where eqn (2.6) has been utilized in the second expression. It is noticed that the stiffness of the system is reduced from $2k$ in the elastic range to k in the elastoplastic range (Fig. 2.6).

Limit state
The force P can be increased further until the elasticity limit S_s is also reached in the side bars 2 and 3. Then the maximum value of P is obtained from eqn (2.1) as

$$P_F = (1 + \sqrt{2})\, S_s = \frac{1 + \sqrt{2}}{2}\, P_s. \tag{2.12}$$

At this state the displacement u follows from eqn (2.11) to

$$u_F = \sqrt{2}\, u_s, \tag{2.13}$$

and may be increased further while the applied force remains constant at $P = P_F$ (Fig. 2.6). The associated elongations of the bars can be determined by eqn (2.2) from the kinematics; their elastic parts are restricted to S_s/k by the material.

2.1.3 Loading–unloading cycle: residual state

The three-bar truss in Fig. 2.7 is considered a simplification of the supporting system for the main landing gear of a civil aircraft. Given the elastic design under regular loading conditions, it is of interest to assess the safety afforded by the elastoplastic range, and the residual state in the truss after unloading. For an estimation, the material of the bars is assumed elastic–perfectly plastic with elastic modulus E and yield stress σ_s.

Statics and kinematics
With reference to Fig. 2.8, the condition of equilibrium between the stress resultants in the three bars (the bar forces S_1, S_2, S_3) and the loading (vertical force P, horizontal force $Q = 0$) is derived as

$$S_2 + \sqrt{3}S_3 = 0\,, \quad 2S_1 + \sqrt{3}S_2 + S_3 = -2P \text{ or } \quad S_3 - S_1 = P. \tag{2.14}$$

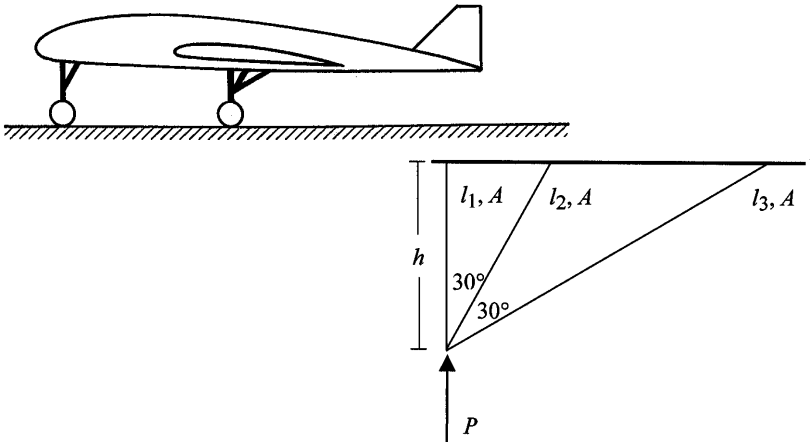

Figure 2.7: Landing gear support of aircraft (simplified).

From the kinematics, the displacement of the loading point by u and v in the vertical and horizontal directions, respectively, implies changes $\delta_1, \delta_2, \delta_3$ in the length of the bars given by

$$\delta_1 = -u, \quad \delta_2 = -\frac{\sqrt{3}}{2}u - \frac{1}{2}v, \quad \delta_3 = -\frac{1}{2}u - \frac{\sqrt{3}}{2}v. \tag{2.15}$$

Elimination of u and v supplies the condition of kinematic compatibility in the form

$$\delta_1 - \sqrt{3}\delta_2 + \delta_3 = 0. \tag{2.16}$$

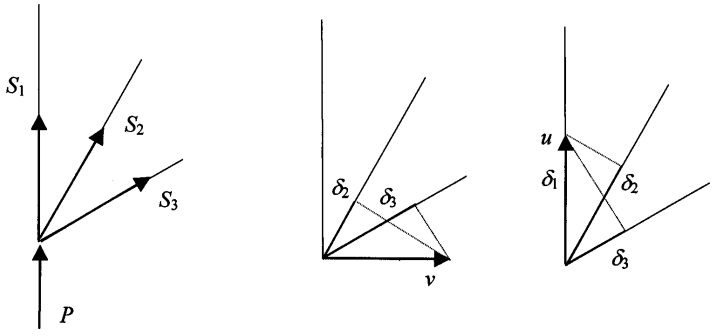

Figure 2.8: Statics and kinematics.

Elastic response
In the elastic range the bar forces are related to the elongations:

$$\begin{aligned} S_1 &= \frac{EA}{l_1}\delta_1 = \frac{EA}{h}\delta_1, \\ S_2 &= \frac{EA}{l_2}\delta_2 = \frac{\sqrt{3}}{2}\frac{EA}{h}\delta_2, \\ S_3 &= \frac{EA}{l_3}\delta_3 = \frac{1}{2}\frac{EA}{h}\delta_3. \end{aligned} \tag{2.17}$$

The bar lengths are l_1, l_2, l_3 and $h = l_1 = \sqrt{3}l_2/2 = l_3/2$ is the height of the truss. The cross-sections of all three bars have the same area A.

With the elastic relations of eqn (2.17), the kinematic compatibility condition, eqn (2.16), can be expressed in static terms,

$$\frac{1}{2}S_1 - S_2 + S_3 = 0, \tag{2.18}$$

and completes eqn (2.14) for the determination of the bar forces:

$$\begin{aligned} S_1 &= -2\frac{1+\sqrt{3}}{3+2\sqrt{3}}P, \\ S_2 &= -\frac{\sqrt{3}}{3+2\sqrt{3}}P, \\ S_3 &= \frac{1}{3+2\sqrt{3}}P. \end{aligned} \tag{2.19}$$

The elongations follow from eqn (2.17):

$$\begin{aligned} \delta_1 &= -2\frac{1+\sqrt{3}}{3+2\sqrt{3}}\frac{h}{EA}P, \\ \delta_2 &= -\frac{2}{3+2\sqrt{3}}\frac{h}{EA}P, \\ \delta_3 &= \frac{2}{3+2\sqrt{3}}\frac{h}{EA}P. \end{aligned} \tag{2.20}$$

A more systematic procedure uses the kinematic relations of eqn (2.15) in order to express the elongations $\delta_1, \delta_2, \delta_3$ in eqn (2.17) for the bar forces in terms of the displacement components u and v. After substitution in the equilibrium condition, eqn (2.14) is solved for the displacements which in turn determine bar elongations and stresses, also cf. Section 2.2.2.

The magnitude of the force is largest in the vertical bar 1. The yield stress σ_s is first reached in this element (this is not necessarily true for bars with different cross-section areas). From eqn (2.19) with $S_1 = \sigma_s A = S_s$, the load at the elasticity limit is obtained as

$$P_s = \frac{1}{2}\frac{3+2\sqrt{3}}{1+\sqrt{3}}S_s = \frac{3+\sqrt{3}}{4}S_s. \tag{2.21}$$

Elastoplastic range
In the elastoplastic range ($P > P_s$), the constitution of the non-hardening material maintains the bar force $S_1 = S_s$. The other two bar forces are obtained from the equilibrium condition, eqn (2.14). One has

$$\begin{aligned} S_1 &= -S_s, \\ S_3 &= P + S_1 = P - S_s, \\ S_2 &= -\sqrt{3}S_3 = -\sqrt{3}(P - S_s). \end{aligned} \tag{2.22}$$

Plastic limit
The load carrying capacity of the truss is exhausted when a second bar attains the yield stress. From eqn (2.22), the next to yield is bar 2, the intermediate oblique element. The bar forces at the plastic limit state are

$$S_1 = S_2 = -S_s\,, \quad S_3 = -\frac{\sqrt{3}}{3}S_2 = \frac{\sqrt{3}}{3}S_s \tag{2.23}$$

and eqn (2.14) determines the plastic limit (maximum) load

$$P_F = S_3 - S_1 = \frac{3+\sqrt{3}}{3}S_s. \tag{2.24}$$

Comparison with the elasticity limit in eqn (2.21) yields the safety factor $P_F/P_s = 4/3$.

At the plastic limit, bars 3 and 2 are still elastic. Their elongations are related to the stress resultants by eqn (2.17). This does not apply to bar 1, which has experienced plastic deformation. It satisfies, however, the kinematic compatibility by eqn (2.16). The elongations of the bars are:

$$\begin{aligned} \delta_3 &= \left(\frac{1}{2}\frac{EA}{h}\right)^{-1} S_3 = \sqrt{3}\frac{2}{3}\frac{h}{EA}S_s, \\ \delta_2 &= \left(\frac{\sqrt{3}}{2}\frac{EA}{h}\right)^{-1} S_2 = -\sqrt{3}\frac{2}{3}\frac{h}{EA}S_s, \\ \delta_1 &= \sqrt{3}\delta_2 - \delta_3 = -(3+\sqrt{3})\frac{2}{3}\frac{h}{EA}S_s. \end{aligned} \tag{2.25}$$

The elastic part of δ_1 is given by eqn (2.17) with $S_1 = -S_s$, and subtraction from eqn (2.25) furnishes the plastic elongation:

$$\delta_{p1} = \delta_1 - \left(\frac{EA}{h}\right)^{-1} S_1 = -\left(1 + \sqrt{3}\frac{2}{3}\right)\frac{h}{EA}S_s. \tag{2.26}$$

Residual state
Unloading from $P = P_F$ to $P = 0$ is associated with elastic changes in the mechanical state of the system. The residual state can be obtained by superposition of the solution for unloading to that for elastoplastic loading. To this end, the result of an elastic application of $P = -P_F$ is obtained from eqns (2.19) and (2.20). Alternatively, the state at the elasticity limit ($P = P_s$) may be multiplied by the load factor $-P_F/P_s = -4/3$.

For the residual force S_{1r} in bar 1, it is observed that $S_1 = -S_s$ at both the plastic limit $P = P_F$ and the elasticity limit $P = P_s$. The other two forces, S_{2r} and S_{3r}, are preferably obtained from the condition of equilibrium, eqn (2.14), with $P = 0$:

$$\begin{aligned} S_{1r} &= -S_s + \frac{4}{3}S_s = \frac{1}{3}S_s, \\ S_{3r} &= S_{1r} = \frac{1}{3}S_s, \\ S_{2r} &= -\sqrt{3}S_{3r} = -\frac{\sqrt{3}}{3}S_s. \end{aligned} \tag{2.27}$$

Regarding the residual deformations, the elongations of the elastic bars 3 and 2 are related to the residual stresses by eqn (2.17), as is also the elastic part of the residual elongation of bar 1 in the truss. Superposing the plastic part from eqn (2.26) we obtain

$$\begin{aligned} \delta_{1r} &= -(1 + \sqrt{3})\frac{2}{3}\frac{h}{EA}S_s, \\ \delta_{2r} &= -\frac{2}{3}\frac{h}{EA}S_s, \\ \delta_{3r} &= \frac{2}{3}\frac{h}{EA}S_s. \end{aligned} \tag{2.28}$$

Of course, the residual elongations satisfy the condition of kinematic compatibility. This condition could have been utilized for an alternative determination of δ_{1r} using δ_{2r} and δ_{3r}.

2.1.4 Beam under bending moment

The beam in Fig. 2.9 has a cross-section which is constant over the entire length l and symmetric with respect to the x- and the y-axis. The bending

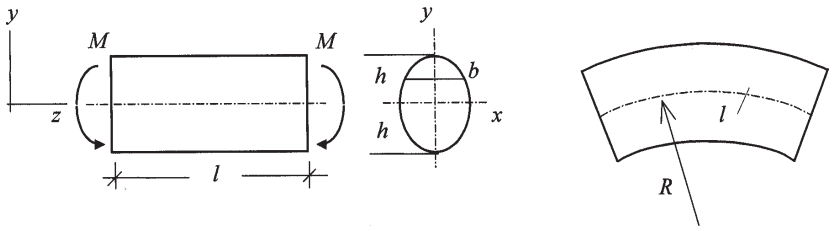

Figure 2.9: Beam under bending moment.

moment M applied at the end cross-sections acts in the y, z-plane, which is the plane of symmetry of the problem. Longitudinal fibres of the beam are bent parallel to this plane. The fibres in the x, z-plane are bent without extension to a curve with radius R, and define the neutral plane in the original configuration. Cross-sections of the beam remain plane and are rigidly connected to the neutral plane, thus following the rotation around the x-axis, the neutral axis of the cross-section.

The elongation δ of longitudinal fibres in the beam is then found to be proportional by the factor l/R to the distance y from the neutral axis. Accordingly, the axial strain γ reads

$$\gamma = \frac{\delta}{l} = \frac{y}{R}. \tag{2.29}$$

The above kinematics conforms to the elementary or engineer's theory of bending (ETB) which disregards in-plane deformation of the cross-section. It will be employed in the elastic and the elastoplastic range.

Elasticity
Within the elastic range of the material, $\gamma \equiv \varepsilon$ and the strain induces in each cross-section axial stresses

$$\sigma = E\varepsilon = \frac{E}{R}\, y, \tag{2.30}$$

linearly distributed along the y-axis. Stress and strain are zero on the neutral axis and attain their maximum intensities at the outmost fibres of the beam. The condition of a vanishing axial force

$$\int_A \sigma \mathrm{d}A = \frac{E}{R} \int_A y \mathrm{d}A = 0 \tag{2.31}$$

requires that the neutral axis passes through the centre of gravity of the cross-section with area A, and is here identically fulfilled for the x-axis of symmetry. For the bending moment we obtain

$$M = \int_A \sigma y \mathrm{d}A = \frac{E}{R} \int_A y^2 \mathrm{d}A = \frac{E}{R} I, \tag{2.32}$$

where

$$I = \int_A y^2 \mathrm{d}A = 2 \int_0^h b(y) y^2 \mathrm{d}y \tag{2.33}$$

defines the moment of inertia of the cross-section with respect to the x-axis. Evaluation of the second integral in eqn (2.33) requires the width b of the cross-section as a function of y.

The yield stress σ_s of the material limits the elastic response of the beam by the condition

$$\max |\sigma| \leq \sigma_\mathrm{s} \tag{2.34}$$

and is attained at the same time in the upper ($y = h$) and lower ($y = -h$) outmost fibres (Fig. 2.10). Denoting the bending moment at the elasticity limit by M_s, and combining eqn (2.32) with eqn (2.30) we deduce the expressions

$$M_\mathrm{s} = \frac{\sigma_\mathrm{s}}{h} I, \quad \frac{1}{R_\mathrm{s}} = \frac{M_\mathrm{s}}{EI} = \frac{\sigma_\mathrm{s}}{Eh}. \tag{2.35}$$

Elastoplastic range

For loading beyond M_s the strain is still given by eqn (2.29), while the stress is restricted by the flow characteristic of the material. If the material does not harden, the magnitude of the stress is limited by σ_s and the elastic strain by σ_s/E. The cross-section of the beam then exhibits an elastic core of extension 2ξ (Fig. 2.10), the remaining outer regions being in the plastic state, $|\sigma| = \sigma_\mathrm{s}$. The strain is entirely elastic within the core. In the outer regions the elastic strain is $\varepsilon = \varepsilon_\mathrm{s} = \sigma_\mathrm{s}/E$, the difference to the total strain γ from eqn (2.29) defines the plastic part η.

The antisymmetric stress distribution over the cross-section ensures that no axial force arises, as required. The bending moment can be determined as the sum of two parts. The bending moment pertaining to the elastic core

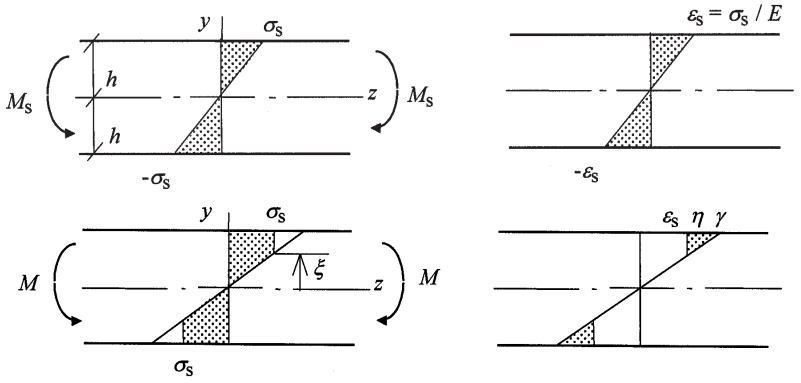

Figure 2.10: Stress and strain at and beyond the elasticity limit (lower).

is obtained by application of eqn (2.32) to this part of the cross-section and reads

$$M_{\mathrm{e}} = \frac{E}{R}\, I_{\mathrm{e}} = \frac{\sigma_{\mathrm{s}}}{\xi}\, I_{\mathrm{e}}. \tag{2.36}$$

Here,

$$I_{\mathrm{e}} = \int\limits_{A_{\mathrm{e}}} y^2 \mathrm{d}A = 2 \int\limits_{0}^{\xi} b(y) y^2 \mathrm{d}y \tag{2.37}$$

and eqn (2.30) was used to express the quotient E/R. The bending moment carried by the plastic regions of the cross-section ($|\sigma| = \sigma_{\mathrm{s}}$) is obtained as

$$M_{\mathrm{p}} = \int\limits_{A_{\mathrm{p}}} \sigma y \mathrm{d}A = \sigma_{\mathrm{s}} \int\limits_{\xi}^{h} y \mathrm{d}A - \sigma_{\mathrm{s}} \int\limits_{-\xi}^{-h} y \mathrm{d}A = \sigma_{\mathrm{s}} S_{\mathrm{p}}, \tag{2.38}$$

where

$$S_{\mathrm{p}} = \int\limits_{\xi}^{h} y \mathrm{d}A - \int\limits_{-\xi}^{-h} y \mathrm{d}A = 2 \int\limits_{\xi}^{h} y \mathrm{d}A = 2 \int\limits_{\xi}^{h} b(y)\, y \mathrm{d}y, \tag{2.39}$$

is twice the area moment of the upper plastic region of the cross-section.

In the elastoplastic range, bending moment and curvature are

$$\begin{gathered} M = M_{\mathrm{e}} + M_{\mathrm{p}} = \sigma_{\mathrm{s}} \left[\frac{I_{\mathrm{e}}(\xi)}{\xi} + S_{\mathrm{p}}(\xi) \right], \\ \frac{1}{R} = \frac{\sigma_{\mathrm{s}}}{E\xi}. \end{gathered} \tag{2.40}$$

For a given bending moment $M > M_{\mathrm{s}}$, eqn (2.40) determines the extension ξ of the elastic core; this, in turn, specifies the radius R of the bent beam. The extension of the elastic core, ξ, diminishes with increasing curvature of the beam or equivalently with decreasing radius R. Thereby, the contribution M_{e} to the bending moment M decreases while M_{p} increases.

Plastic limit

Ultimately, when $\xi = 0$, the bending moment is equilibrated exclusively in the plastic state characterized by $|\sigma| = \sigma_{\mathrm{s}}$ entirely in the cross-section:

$$M_{\mathrm{F}} = \sigma_{\mathrm{s}}\, S, \tag{2.41}$$

where

$$S = 2 \int\limits_{0}^{h} y \mathrm{d}A = 2 \int\limits_{0}^{h} b\,(y)\, y \mathrm{d}y. \tag{2.42}$$

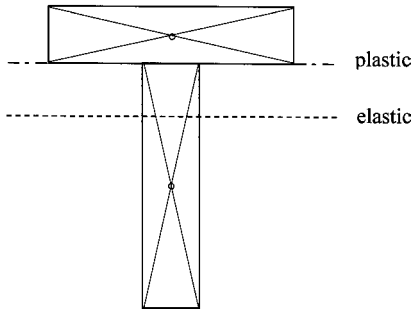

Figure 2.11: Neutral axis of a T-shaped beam in the elastic and plastic states.

Comparison of the above plastic limit with the elastic limit moment M_{s}, eqn (2.35), yields

$$\frac{M_{\mathrm{F}}}{M_{\mathrm{s}}} = \frac{hS}{I} > 1. \tag{2.43}$$

Although eqn (2.43) might be considered a satisfactory safety factor from the static point of view, it is seen from eqn (2.40) that the state $\xi = 0$ is associated with a vanishing curvature radius R, which implies an unacceptable permanent change in the shape of the beam.

It is worth noting that in the fully plastic state the elastic condition for a vanishing resultant of the axial stress, eqn (2.31), has to be replaced by the requirement

$$\int_A \sigma \mathrm{d}A = \int_{A_1} \sigma_{\mathrm{s}} \mathrm{d}A + \int_{A_2} (-\sigma_{\mathrm{s}}) \mathrm{d}A = \sigma_{\mathrm{s}}(A_1 - A_2) = 0. \tag{2.44}$$

By the elastic condition the neutral axis passes through the centre of gravity of the cross-section, while by the plastic condition it has to divide it into two equal areas. Consequently, the neutral axis translates from one position to the other during elastoplastic deformation, unless it is an axis of symmetry. As an example, Fig. 2.11 demonstrates the neutral axis in the elastic and plastic states of a T-shaped cross-section.

Rectangular cross-section
As a specific case, we consider a rectangular cross-section (height $2h$, width b) and obtain the characteristics

$$I = \frac{2}{3} b\, h^3, \quad S = b\, h^2. \tag{2.45}$$

For a varying elastic core:

$$I_{\mathrm{e}} = \frac{2}{3}\, b\, \xi^3, \quad S_{\mathrm{p}} = b(h^2 - \xi^2). \tag{2.46}$$

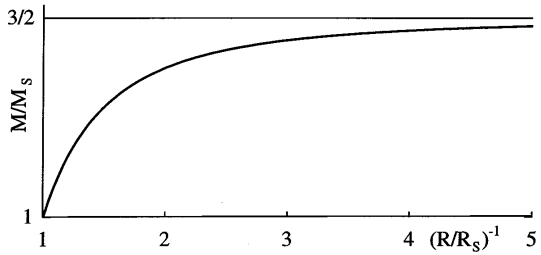

Figure 2.12: Bending moment vs radius of curvature for a beam of rectangular cross-section.

The bending moment in the elastoplastic range, eqn (2.40), becomes here

$$M = \left(1 - \frac{1}{3}\frac{\xi^2}{h^2}\right)\, b\, h^2\, \sigma_{\mathrm{s}}. \tag{2.47}$$

The elasticity limit is obtained for $\xi = h$, and the plastic limit for $\xi = 0$ as

$$M_{\mathrm{s}} = \frac{2}{3}\, b\, h^2\, \sigma_{\mathrm{s}} \quad \text{and} \quad M_{\mathrm{F}} = b\, h^2\, \sigma_{\mathrm{s}}, \tag{2.48}$$

respectively. For the rectangular cross-section, the quotient in eqn (2.43) assumes the value $M_{\mathrm{F}}/M_{\mathrm{s}} = 3/2$.

Equation (2.47) normalized by the moment at the elasticity limit reads

$$\frac{M}{M_{\mathrm{s}}} = \frac{3}{2}\left(1 - \frac{1}{3}\,\frac{\xi^2}{h^2}\right). \tag{2.49}$$

The ratio of the associated radii of curvature follows from eqns (2.35) and (2.40) as

$$\frac{R}{R_{\mathrm{s}}} = \frac{\xi}{h}, \tag{2.50}$$

and substitution in eqn (2.49) gives

$$\frac{M}{M_{\mathrm{s}}} = \frac{3}{2}\,\left(1 - \frac{1}{3}\,\frac{R^2}{R_{\mathrm{s}}^2}\right), \quad \frac{R_{\mathrm{s}}}{R} = \frac{\sqrt{3}}{3}\left(1 - \frac{2}{3}\,\frac{M}{M_{\mathrm{s}}}\right)^{-1/2}. \tag{2.51}$$

A graphical representation of the variation of curvature with bending moment is shown in Fig. 2.12.

Unloading

For an illustration of the residual stress in the rectangular cross-section, the bending moment is removed from $M = M_{\mathrm{F}}$ to $M = 0$. The stress distribution in the cross-section after unloading can be obtained by superposition of the elastoplastic solution at $M = M_{\mathrm{F}}$ and the elastic solution for

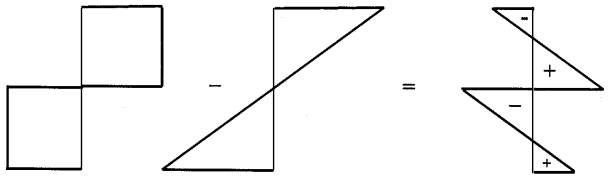

Figure 2.13: Residual stress after unloading from $M = M_{\mathrm{F}}$.

$M = -M_{\mathrm{F}}$. For the latter, the linear stress distribution at the elasticity limit $M = M_{\mathrm{s}}$ is multiplied by the load factor $-M_{\mathrm{F}}/M_{\mathrm{s}} = -3/2$. The magnitude of the unloading stress does not exceed the elastic range of the material ($3\sigma_{\mathrm{s}}/2 < 2\sigma_{\mathrm{s}}$). The process of superposition is demonstrated in Fig. 2.13, and results in a self-equilibrating system of residual stress at $M = 0$.

The kinematics of the bending model completely determines the strain once the curvature radius of the neutral plane is given. This is an example of a kinematically determinate system. Bending beyond the elasticity limit to a curvature $1/R > 1/R_{\mathrm{s}}$ induces plastic strain in the cross-section. Upon removal of the imposed bending deformation the plastic strain is compensated by an elastic part such that $\gamma_{\mathrm{r}} = \varepsilon_{\mathrm{r}} + \eta = 0$. This is illustrated in Fig. 2.14. The residual stress $\sigma_{\mathrm{r}} = -E\eta$ implies that a bending moment is associated with the unloaded state $1/R = 0$. Removal of deformation is elastic only if the plastic strain to be compensated is $|\eta| \leq \sigma_{\mathrm{s}}/E$.

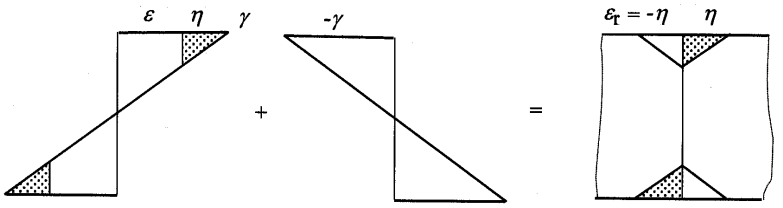

Figure 2.14: Kinematic unloading of an elastoplastic beam.

2.2 Elastoplastic analysis of solids

2.2.1 Static equilibrium and kinematics

With reference to Fig. 2.15 we consider the static equilibrium of a deformable body of solid material subjected to body forces

$$\mathbf{f} = \{f_{\mathrm{x}}\ f_{\mathrm{y}}\ f_{\mathrm{z}}\} \tag{2.52}$$

acting in the interior per unit volume V, and to surface forces

$$\mathbf{t} = \{t_{\mathrm{x}}\ t_{\mathrm{y}}\ t_{\mathrm{z}}\} \tag{2.53}$$

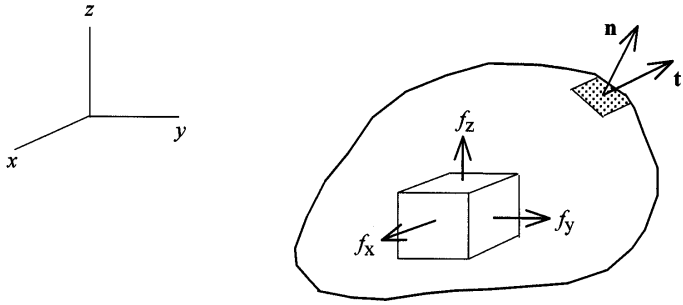

Figure 2.15: Body forces **f** and surface forces **t** acting on the solid.

acting per unit area on the surface S with local unit normal

$$\mathbf{n} = \{l\ m\ n\}. \tag{2.54}$$

The equilibrium condition for the stresses in the interior of the solid is expressed by the equilibrium equations for the force components along the coordinate axes:

$$\begin{aligned}
\frac{\partial \sigma_{xx}}{\partial x} + \frac{\partial \sigma_{yx}}{\partial y} + \frac{\partial \sigma_{zx}}{\partial z} + f_x = 0,\\
\frac{\partial \sigma_{xy}}{\partial x} + \frac{\partial \sigma_{yy}}{\partial y} + \frac{\partial \sigma_{zy}}{\partial z} + f_y = 0,\\
\frac{\partial \sigma_{xz}}{\partial x} + \frac{\partial \sigma_{yz}}{\partial y} + \frac{\partial \sigma_{zz}}{\partial z} + f_z = 0.
\end{aligned} \tag{2.55}$$

On the boundary of the solid the stresses must satisfy the condition

$$\begin{aligned}
l\sigma_{xx} + m\sigma_{yx} + n\sigma_{zx} = t_x,\\
l\sigma_{xy} + m\sigma_{yy} + n\sigma_{zy} = t_y,\\
l\sigma_{xz} + m\sigma_{yz} + n\sigma_{zz} = t_z.
\end{aligned} \tag{2.56}$$

The strains in the solid derive from the displacements

$$\mathbf{u} = \{u\ v\ w\}, \tag{2.57}$$

with components u, v and w along the coordinate axes as

$$\begin{aligned}
\gamma_{xx} &= \frac{\partial u}{\partial x}, \qquad \gamma_{xy} = \frac{\partial u}{\partial y} + \frac{\partial v}{\partial x},\\
\gamma_{yy} &= \frac{\partial v}{\partial y}, \qquad \gamma_{yz} = \frac{\partial v}{\partial z} + \frac{\partial w}{\partial y},\\
\gamma_{zz} &= \frac{\partial w}{\partial z}, \qquad \gamma_{xz} = \frac{\partial u}{\partial z} + \frac{\partial w}{\partial x}.
\end{aligned} \tag{2.58}$$

The displacement field satisfies the kinematic conditions imposed on the boundary and maintains the continuity of the solid. From the latter requirement, kinematic compatibility conditions can be deduced for the strains.

The utility of the above relations for the strains and the stresses can be summarized as follows. For a given displacement field the strains in the solid are uniquely determined by eqn (2.58). In matrix notation,

$$\boldsymbol{\gamma} = \boldsymbol{\partial}\mathbf{u}, \tag{2.59}$$

where the array

$$\boldsymbol{\partial} = \begin{bmatrix} \frac{\partial}{\partial x} & 0 & 0 \\ 0 & \frac{\partial}{\partial y} & 0 \\ 0 & 0 & \frac{\partial}{\partial z} \\ \frac{1}{\sqrt{2}}\frac{\partial}{\partial y} & \frac{1}{\sqrt{2}}\frac{\partial}{\partial x} & 0 \\ 0 & \frac{1}{\sqrt{2}}\frac{\partial}{\partial z} & \frac{1}{\sqrt{2}}\frac{\partial}{\partial y} \\ \frac{1}{\sqrt{2}}\frac{\partial}{\partial z} & 0 & \frac{1}{\sqrt{2}}\frac{\partial}{\partial x} \end{bmatrix} \tag{2.60}$$

defines the differential matrix operator applied to the displacement $\mathbf{u}(\mathbf{x})$ in order to obtain the strain $\boldsymbol{\gamma} = \{\gamma_{xx}\ \gamma_{yy}\ \gamma_{zz}\ \gamma_{xy}/\sqrt{2}\ \gamma_{yz}/\sqrt{2}\ \gamma_{xz}/\sqrt{2}\}$.

With the notation in eqn (2.60), the static condition, eqn (2.55), can be alternatively presented in matrix form,

$$\boldsymbol{\partial}^{\mathrm{t}}\boldsymbol{\sigma} + \mathbf{f} = \mathbf{0}, \tag{2.61}$$

which collectively expresses the equilibrium between body forces $\mathbf{f}$ in the solid and stresses $\boldsymbol{\sigma} = \{\sigma_{xx}\,\sigma_{yy}\,\sigma_{zz}\,\sqrt{2}\,\sigma_{xy}\,\sqrt{2}\,\sigma_{yz}\,\sqrt{2}\,\sigma_{xz}\}$.

For an analogous presentation of the static boundary condition, eqn (2.56), we introduce the 3×6 matrix,

$$\mathbf{N}^{\mathrm{t}} = \begin{bmatrix} l & 0 & 0 & m/\sqrt{2} & 0 & n/\sqrt{2} \\ 0 & m & 0 & l/\sqrt{2} & n/\sqrt{2} & 0 \\ 0 & 0 & n & 0 & m/\sqrt{2} & l/\sqrt{2} \end{bmatrix}, \tag{2.62}$$

arranging the components of the unit surface normal, and obtain instead

$$\mathbf{N}^{\mathrm{t}}\boldsymbol{\sigma} = \mathbf{t}. \tag{2.63}$$

The matrix $\mathbf{N}$ has the same pattern as $\boldsymbol{\partial}$, eqn (2.60), the direction cosines l, m and n taking the place of the differential operators $\partial/\partial x$, $\partial/\partial y$ and $\partial/\partial z$.

In contrast to the kinematics, the stress state cannot be derived from given forces $\mathbf{f}$ and $\mathbf{t}$ as the strains are derived from displacements. The static conditions, eqns (2.61) and (2.63), may rather be interpreted as operations accumulating a given stress field to resultant forces equilibrating $\mathbf{f}$

and $\mathbf{t}$. The inverse task, the determination of the stress state induced by the given forces, requires solution of eqn (2.61), the system of three differential equations with the associated boundary conditions in eqn (2.63), as will be outlined below.

2.2.2 Methods of elastoplastic analysis

As long as the mechanical state everywhere in the solid is below the elasticity limit, the stress $\boldsymbol{\sigma}$ in eqn (2.61) can be expressed in terms of the strain via Hooke's law. The elastic strain $\boldsymbol{\gamma} \equiv \boldsymbol{\varepsilon}$ is derived from the displacements by eqn (2.59) and therefore

$$\boldsymbol{\sigma} = \boldsymbol{\kappa}\boldsymbol{\varepsilon} = \boldsymbol{\kappa}\boldsymbol{\partial}\mathbf{u}. \tag{2.64}$$

The equilibrium condition, eqn (2.61), then becomes

$$\boldsymbol{\partial}^{\mathrm{t}}(\boldsymbol{\kappa}\boldsymbol{\partial}\mathbf{u}) + \mathbf{f} = \mathbf{0} \tag{2.65}$$

and is thus converted into a system of three differential equations for the three components of the displacement vector $\mathbf{u}$ in the solid. In this connection, the static boundary condition, eqn (2.114), is also expressed in terms of the unknown displacements by means of the elastic relation, eqn (2.64), while any kinematic constraints can be imposed directly on the displacements.

When regions in the solid undergo inelastic deformation, eqn (2.59) gives the compound strain $\boldsymbol{\gamma} = \boldsymbol{\varepsilon} + \boldsymbol{\eta}$ consisting of elastic and plastic parts. The elasticity relation is based on the elastic strain, and eqn (2.64) has to be modified accordingly. The expression for the stress reads

$$\boldsymbol{\sigma} = \boldsymbol{\kappa}[\boldsymbol{\gamma} - \boldsymbol{\eta}] = \boldsymbol{\kappa}[\boldsymbol{\partial}\mathbf{u} - \boldsymbol{\eta}]. \tag{2.66}$$

This requires knowledge of the plastic strain $\boldsymbol{\eta}$ in addition to the displacement field $\mathbf{u}$. Since plastic flow is described by stress-dependent incremental relations, an integration has to be carried out locally accounting for the time history of the stress up to the instant under consideration

$$\boldsymbol{\eta} = \int_0^t \dot{\boldsymbol{\eta}}\, \mathrm{d}t. \tag{2.67}$$

The above exposition suggests that beyond the elasticity limit the equilibrium problem is preferably stated in the incremental or rate form

$$\boldsymbol{\partial}^{\mathrm{t}}\dot{\boldsymbol{\sigma}} + \dot{\mathbf{f}} = \mathbf{0} \tag{2.68}$$

instead of eqn (2.61). *For typographical brevity we prefer to use here time rates* $\dot{(\ )} = \mathrm{d}(\ )/\mathrm{d}t$ *in place of differential changes* $\mathrm{d}(\ )$*, although plasticity is not a time-dependent phenomenon.*

In eqn (2.68) the rate of stress can be expressed by the rate form of eqn (2.66) which reads

$$\dot{\boldsymbol{\sigma}} = \boldsymbol{\kappa}\,[\dot{\boldsymbol{\gamma}} - \dot{\boldsymbol{\eta}}] = \boldsymbol{\kappa}\,[\boldsymbol{\partial}\dot{\mathbf{u}} - \dot{\boldsymbol{\eta}}]\,. \tag{2.69}$$

This gives the equilibrium equation in terms of the displacement velocity $\dot{\mathbf{u}}$ and the time rate of plastic strain $\dot{\boldsymbol{\eta}}$, as

$$\boldsymbol{\partial}^{\mathrm{t}}(\boldsymbol{\kappa}\boldsymbol{\partial}\dot{\mathbf{u}}) + [\dot{\mathbf{f}} - \boldsymbol{\partial}^{\mathrm{t}}(\boldsymbol{\kappa}\dot{\boldsymbol{\eta}})] = \mathbf{0}. \tag{2.70}$$

A comparison of eqn (2.70) with eqn (2.65) for the elastic case reveals that the elastoplastic problem may be interpreted as an elastic one for the displacement velocity $\dot{\mathbf{u}}$, with the body forces $\dot{\mathbf{f}}$ modified by the effect of stress-like terms originating from the plastic strain rate $\dot{\boldsymbol{\eta}}$. Analogous remarks apply to the static boundary conditions.

The elastoplastic problem as stated by eqn (2.70) suggests an iterative procedure, implying a sequence of elastic solutions along with the prediction and correction of the plastic strain rate (termed the method of successive elastic solutions in [1]). For isotropic hardening (Section 1.3.1) the algorithm for a single iteration cycle $i, i+1$ reads

$$\begin{aligned}
&\text{Predictor} \quad \dot{\boldsymbol{\eta}}_i \\
&\text{Determine} \quad \dot{\mathbf{u}}_i \quad \text{as from } \boldsymbol{\partial}^{\mathrm{t}}(\boldsymbol{\kappa}\boldsymbol{\partial}\dot{\mathbf{u}}_i) + [\dot{\mathbf{f}} - \boldsymbol{\partial}^{\mathrm{t}}(\boldsymbol{\kappa}\dot{\boldsymbol{\eta}}_i)] = \mathbf{0} \\
&\qquad\qquad \dot{\boldsymbol{\gamma}}_i = \boldsymbol{\partial}\dot{\mathbf{u}}_i, \quad \dot{\boldsymbol{\sigma}}_i = \boldsymbol{\kappa}[\dot{\boldsymbol{\gamma}}_i - \dot{\boldsymbol{\eta}}_i] \\
&\text{Corrector} \quad \dot{\boldsymbol{\eta}}_{i+1} = \frac{1}{h}\mathbf{s}\mathbf{s}^{\mathrm{t}}\dot{\boldsymbol{\sigma}}_i \quad \text{or} \quad \dot{\boldsymbol{\eta}}_{i+1} = \frac{2G}{h+3G}\mathbf{s}\mathbf{s}^{\mathrm{t}}\dot{\boldsymbol{\gamma}}_i.
\end{aligned} \tag{2.71}$$

The above recurrence scheme is activated anew with the corrected estimate for $\dot{\boldsymbol{\eta}}$ until convergence is achieved. The rate of convergence may depend on the expression determining $\dot{\boldsymbol{\eta}}_{i+1}$ in eqn (2.71). In particular, problems exhibiting a weak dependence of the stress on the plastic strain favour the determination of $\dot{\boldsymbol{\eta}}$ with $\dot{\boldsymbol{\sigma}}$, by eqn (1.154). If, on the other hand, the strain is the quantity less sensitive to variations of the plastic strain, $\dot{\boldsymbol{\gamma}}$ would be chosen for the calculation of $\dot{\boldsymbol{\eta}}$ in accordance with eqn (1.157). Implementation of kinematic hardening (Section 1.3.2) is straightforward.

Instead of eqn (2.69) an alternative expression for the rate of stress is based on the elastoplastic material stiffness from eqn (1.158):

$$\dot{\boldsymbol{\sigma}} = \left[\mathbf{I} - \frac{2G}{h+3G}\mathbf{s}\mathbf{s}^{\mathrm{t}}\right]\boldsymbol{\kappa}\dot{\boldsymbol{\gamma}} = \bar{\boldsymbol{\kappa}}\dot{\boldsymbol{\gamma}} = \bar{\boldsymbol{\kappa}}\boldsymbol{\partial}\dot{\mathbf{u}}. \tag{2.72}$$

Substitution in eqn (2.68) for the rate equilibrium leads to

$$\boldsymbol{\partial}^{\mathrm{t}}(\bar{\boldsymbol{\kappa}}\boldsymbol{\partial}\dot{\mathbf{u}}) + \dot{\mathbf{f}} = \mathbf{0}, \tag{2.73}$$

which can be formally viewed as an elastic problem for the displacement velocity $\dot{\mathbf{u}}$, with stress-dependent material coefficients. In addition, the rate

problem defined by eqn (2.73) is nonlinear since the actual entry of the material stiffness (elastoplastic $\bar{\boldsymbol{\kappa}}$ or elastic $\boldsymbol{\kappa}$) depends on the condition of plastic loading or unloading, thus requiring knowledge of the solution.

The complete treatment of an elastoplastic problem can be subdivided into two distinct parts. An elastic solution furnishes the mechanical state until the elasticity limit is attained first somewhere in the solid. Beyond this state incrementation requires a number of rate-type elastoplastic problems to be solved and the solutions to be accumulated in a sequence following the prescribed application of the external forces and/or displacements. In general, elastoplastic solutions require the employment of numerical computer techniques usually based on extensions of the elastic finite element or other methods to the elastoplastic range. These techniques will be discussed in Chapter 5. Independently, analytical solutions developed under certain simplifying assumptions give valuable insights into elastoplastic behaviour.

2.2.3 The residual state

As long as the applied force system does not lead to stresses beyond the elasticity limit of the material, all changes of the mechanical state in the solid are reversible and disappear after removal of the imposed action. Loading beyond the elasticity limit, on the other hand, leads to permanent strains and therefore changes of the mechanical state remain even after an elastic removal of the applied loads. Let $\mathbf{u}, \boldsymbol{\gamma}$ and $\boldsymbol{\sigma}$ denote the actual displacement field, the strains and the stresses, respectively, in the loaded solid, and $\boldsymbol{\eta}$ the plastic strains. If elasticity were unlimited, $\mathbf{u}_\mathrm{e}, \boldsymbol{\varepsilon}_\mathrm{e}$ and $\boldsymbol{\sigma}_\mathrm{e} = \boldsymbol{\kappa}\boldsymbol{\varepsilon}_\mathrm{e}$ would denote the mechanical fields associated with the same loads, while by definition $\boldsymbol{\eta} \equiv \mathbf{0}$. Since plastic flow does not modify the elastic properties, elastic unloading from a plastic state induces changes $-\mathbf{u}_\mathrm{e}, -\boldsymbol{\varepsilon}_\mathrm{e}, -\boldsymbol{\sigma}_\mathrm{e}$. The residual state may thus be obtained by simple superposition of the elastoplastic solution for the loading path and the elastic solution pertaining to the same ultimately applied loads as

$$\begin{aligned} \mathbf{u}_\mathrm{r} = \mathbf{u} - \mathbf{u}_\mathrm{e}, \quad \boldsymbol{\gamma}_\mathrm{r} = \boldsymbol{\gamma} - \boldsymbol{\varepsilon}_\mathrm{e} \\ \boldsymbol{\sigma}_\mathrm{r} = \boldsymbol{\sigma} - \boldsymbol{\sigma}_\mathrm{e} = \boldsymbol{\sigma} - \boldsymbol{\kappa}\boldsymbol{\varepsilon}_\mathrm{e}. \end{aligned} \tag{2.74}$$

Conversely, it follows from eqn (2.74) that if the residual state $\mathbf{u}_\mathrm{r}, \boldsymbol{\gamma}_\mathrm{r}, \boldsymbol{\sigma}_\mathrm{r}$ were known, an elastic solution yielding $\mathbf{u}_\mathrm{e}, \boldsymbol{\varepsilon}_\mathrm{e}, \boldsymbol{\sigma}_\mathrm{e}$ is sufficient for the determination of the actual elastoplastic state. In detail,

$$\mathbf{u} = \mathbf{u}_\mathrm{e} + \mathbf{u}_\mathrm{r}, \quad \boldsymbol{\gamma} = \boldsymbol{\varepsilon}_\mathrm{e} + \boldsymbol{\gamma}_\mathrm{r}, \quad \boldsymbol{\sigma} = \boldsymbol{\sigma}_\mathrm{e} + \boldsymbol{\sigma}_\mathrm{r}. \tag{2.75}$$

Whenever the plastic strain $\boldsymbol{\eta}$ developed during the course of the loading process remains unaffected by the unloading, the residual strain in eqn (2.74) can be expressed alternatively as

$$\boldsymbol{\gamma}_\mathrm{r} = \boldsymbol{\varepsilon}_\mathrm{r} + \boldsymbol{\eta}. \tag{2.76}$$

The plastic part of the strain will not necessarily be kinematically compatible and therefore complementary elastic strains $\boldsymbol{\varepsilon}_{\mathrm{r}}$ appear such that kinematic compatibility is restored by the compound residual strain $\boldsymbol{\gamma}_{\mathrm{r}}$. The residual stress,

$$\boldsymbol{\sigma}_{\mathrm{r}} = \boldsymbol{\kappa}\boldsymbol{\varepsilon}_{\mathrm{r}}, \tag{2.77}$$

constitutes a self-equilibrating stress system associated with vanishing applied forces.

2.2.4 Static and kinematic determinateness

The statically determinate system
As outlined previously, static determinateness implies that the stresses can be obtained from the conditions of static equilibrium without reference to the material constitutive law and the kinematic relations.

From the above, the stress and the time history of stress can be considered functions of the applied force system and its time history, independently of the behaviour of the particular material. The elastic strain is obtained at each instant t of the loading programme by Hooke's law:

$$\boldsymbol{\varepsilon}(t) = \boldsymbol{\kappa}^{-1}\boldsymbol{\sigma}(t). \tag{2.78}$$

Where yielding occurs, the rate of plastic strain (isotropic hardening) is

$$\dot{\boldsymbol{\eta}} = \frac{1}{h}\,\mathbf{s}\mathbf{s}^{\mathrm{t}}\dot{\boldsymbol{\sigma}}, \tag{2.79}$$

and integration with respect to time furnishes the plastic strain

$$\boldsymbol{\eta}(t) = \int_{t_{\mathrm{s}}}^{t} \frac{1}{h}\,\mathbf{s}\mathbf{s}^{\mathrm{t}}\dot{\boldsymbol{\sigma}}\,\mathrm{d}t. \tag{2.80}$$

At instant t_{s} the yield stress is first attained at the respective location. The strain $\boldsymbol{\gamma} = \boldsymbol{\varepsilon} + \boldsymbol{\eta}$ follows by the additive composition of the elastic and the permanent part. In the present case the strain $\boldsymbol{\gamma}$ obtained from the stress via the constitutive material law satisfies kinematic compatibility.

Since the stress is a function of the applied force only, unloading to zero force does not leave any stress, independently of previous plastic flow. For this reason, there is also no residual elastic strain

$$\boldsymbol{\sigma}_{\mathrm{r}} = \mathbf{0}, \quad \boldsymbol{\varepsilon}_{\mathrm{r}} = \mathbf{0}. \tag{2.81}$$

Consequently, the residual strain after an elastic unloading is identical to the plastic strain developed during the course of the loading process:

$$\boldsymbol{\gamma}_{\mathrm{r}} \equiv \boldsymbol{\eta}. \tag{2.82}$$

It follows from eqn (2.82) that, in the statically determinate case, the plastic strains satisfy the kinematic compatibility conditions and are associated with a field of permanent displacements. The same can be concluded for the elastic strains so that ultimately the displacement field may be separated here into an elastic and a plastic part.

The kinematically determinate case
Kinematically determinate problems are characterized by a prescribed displacement field $\mathbf{u}(t)$ from which the strain can be obtained everywhere in the system at any time instant t. One may thus start with the determination of the strain:

$$\boldsymbol{\gamma}(t) = \boldsymbol{\partial}\mathbf{u}(t), \tag{2.83}$$

and obtain the stress up to the elasticity limit by

$$\boldsymbol{\sigma}(t) = \boldsymbol{\kappa}\boldsymbol{\partial}\mathbf{u}(t). \tag{2.84}$$

Beyond the elasticity limit,

$$\boldsymbol{\sigma} = \boldsymbol{\kappa}[\boldsymbol{\gamma} - \boldsymbol{\eta}]. \tag{2.85}$$

For isotropic hardening, the rate of plastic strain during flow follows from an evaluation of the expression

$$\dot{\boldsymbol{\eta}} = \frac{2G}{h + 3G}\mathbf{s}\mathbf{s}^{\mathrm{t}}\dot{\boldsymbol{\gamma}}. \tag{2.86}$$

Integration with respect to time supplies the plastic strain

$$\boldsymbol{\eta} = \int_{t_{\mathrm{s}}}^{t} \frac{2G}{h + 3G}\mathbf{s}\mathbf{s}^{\mathrm{t}}\dot{\boldsymbol{\gamma}}\mathrm{d}t. \tag{2.87}$$

The direction $\mathbf{s}$ of plastic flow requires the stress from eqn (2.85). In the kinematically determinate case the stresses obtained via the material constitutive law from the prescribed strains satisfy static equilibrium.

Here unloading implies the removal of the imposed displacements. As a consequence, no residual strains are left in the system

$$\boldsymbol{\gamma}_{\mathrm{r}} = \boldsymbol{\varepsilon}_{\mathrm{r}} + \boldsymbol{\eta} = \mathbf{0}. \tag{2.88}$$

The appearance in eqn (2.88) of the plastic strain $\boldsymbol{\eta}$ developed during the course of loading presumes an elastic removal of the imposed displacements. The requirement of vanishing residual strains implies that plastic strains are compensated by elastic strains inducing residual stresses

$$\boldsymbol{\sigma}_{\mathrm{r}} = \boldsymbol{\kappa}\boldsymbol{\varepsilon}_{\mathrm{r}} = -\boldsymbol{\kappa}\boldsymbol{\eta}. \tag{2.89}$$

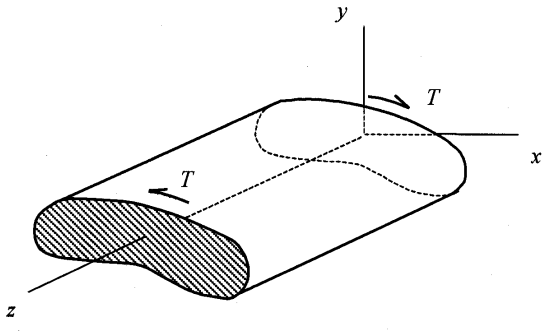

Figure 2.16: Cylindrical bar under torsion.

2.3 Distinct cases

2.3.1 Torsion of cylindrical bars

The case under consideration is described in Fig. 2.16. A cylindrical or prismatical bar of arbitrary cross-section is twisted by the application of a torsional moment T at the end cross-sections. As shown in the figure, the coordinate system of reference is defined such that the z-axis is directed along the bar, while cross-sections perpendicular to it are referred to the x, y-plane.

Kinematics
The kinematics of torsion is based on the Saint Vénant assumption that cross-sections perpendicular to the longitudinal axis undergo rotation without deformation in their plane (x, y-plane) and warping in the longitudinal direction (z-axis); see [2] for an historical account. For convenience, the z-axis is chosen to coincide with the axis of rotation.

The rigid rotation of cross-sections is specified by the angle of twist

$$\theta' = \frac{\mathrm{d}\theta}{\mathrm{d}z} = \text{constant}, \tag{2.90}$$

which is considered independent of the location along the longitudinal axis. The angle of rotation for a cross-section at position z in the longitudinal direction thus reads

$$\theta = \theta' z. \tag{2.91}$$

As a consequence of the rotation, material points P with coordinates x, y in the cross-section are displaced to a new position P' (Fig. 2.17).

For small angles, the displacements along the x- and the y-axes are

$$u = -\theta y = -\theta' z y, \quad v = \theta x = \theta' z x. \tag{2.92}$$

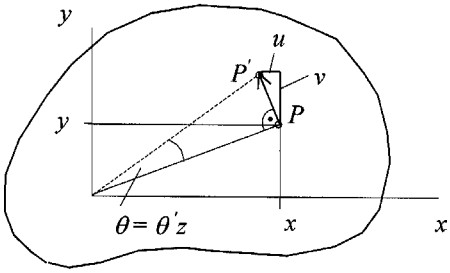

Figure 2.17: Displacement of point P due to rotation θ.

The longitudinal displacement is assumed to be independent of the position z:

$$w = w(x, y; \theta'). \tag{2.93}$$

It defines the warping w, which varies with location x, y in the cross-section. The angle of twist θ' affects the magnitude collectively.

From the displacement functions in eqns (2.92) and (2.93), it is seen that all direct strains vanish, $\gamma_{xx} = \gamma_{yy} = \gamma_{zz} = 0$. The shear strain in the plane of the cross-section also vanishes,

$$\gamma_{xy} = \frac{\partial u}{\partial y} + \frac{\partial v}{\partial x} = -\theta' z + \theta' z = 0 \tag{2.94}$$

and the functions in eqn (2.92) indeed do not produce any in-plane deformation. For the remaining two shear strain components, one derives

$$\begin{aligned} \gamma_{yz} &= \frac{\partial v}{\partial z} + \frac{\partial w}{\partial y} = \theta' x + \frac{\partial w}{\partial y}, \\ \gamma_{xz} &= \frac{\partial u}{\partial z} + \frac{\partial w}{\partial x} = -\theta' y + \frac{\partial w}{\partial x}. \end{aligned} \tag{2.95}$$

Differentiation of the shear strain $\gamma_{yz} = \gamma_{zy}$ with respect to x and of $\gamma_{xz} = \gamma_{zx}$ with respect to y gives

$$\begin{aligned} \frac{\partial \gamma_{zy}}{\partial x} &= \theta' + \frac{\partial^2 w}{\partial y\, \partial x}, \\ \frac{\partial \gamma_{zx}}{\partial y} &= -\theta' + \frac{\partial^2 w}{\partial x\, \partial y}. \end{aligned} \tag{2.96}$$

Assuming a continuous variation of w with x and y, the mixed second-order partial derivatives on the right-hand side of eqn (2.96) are independent

of the differentiation sequence and are therefore equal. Subtraction of the upper equation from the lower equation thus yields

$$\frac{\partial \gamma_{zx}}{\partial y} - \frac{\partial \gamma_{zy}}{\partial x} = -2\theta'. \tag{2.97}$$

Equation (2.97), derived from the deformation kinematics of the torsion problem, expresses a condition for kinematic compatibility in terms of the strains γ_{zx} and γ_{zy}.

Statics
The absence of the strain components $\gamma_{xx}, \gamma_{yy}, \gamma_{zz}$ and γ_{xy} implies, by virtue of the material law, the absence of the corresponding stress components. Therefore, $\sigma_{xx} = \sigma_{yy} = \sigma_{zz} = 0$ and $\sigma_{xy} = 0$ in the elastic as well as in the elastoplastic range. The remaining two components $\sigma_{zx} = \sigma_{xz}, \sigma_{zy} = \sigma_{yz}$ represent shear stresses. Their mode of action in the plane of the cross-section is indicated in Fig. 2.18. It is noticed that a resultant shear stress τ is obtained from

$$\tau^2 = \sigma_{zx}^2 + \sigma_{zy}^2. \tag{2.98}$$

Taking into account the vanishing stress components in conjunction with the fact that no body forces are present, the condition of static equilibrium for the stresses, eqn (2.55), reduces to

$$\begin{aligned} \frac{\partial \sigma_{zx}}{\partial z} &= \frac{\partial \sigma_{zy}}{\partial z} = 0, \\ \frac{\partial \sigma_{zx}}{\partial x} &+ \frac{\partial \sigma_{zy}}{\partial y} = 0. \end{aligned} \tag{2.99}$$

From the upper set of equations, the non-vanishing stress components σ_{zx} and σ_{zy} are independent of the location along the z-axis. The variation in the x, y-plane is governed by the lower equation.

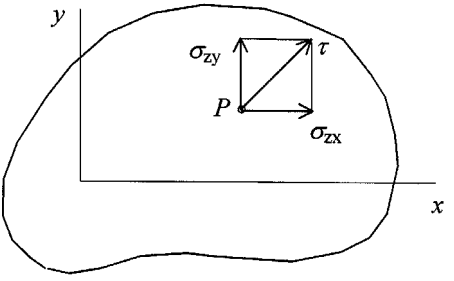

Figure 2.18: Components of the shear stress τ acting in the cross-section.

Prandtl's stress function [3]
If a function $F(x, y)$ is defined such that the shear stresses are

$$\sigma_{zx} = \frac{\partial F}{\partial y}, \qquad \sigma_{zy} = -\frac{\partial F}{\partial x}, \tag{2.100}$$

then the equilibrium condition in the x, y-plane, eqn (2.99), assumes the form

$$\frac{\partial^2 F}{\partial y\, \partial x} - \frac{\partial^2 F}{\partial x\, \partial y} = 0 \tag{2.101}$$

and is identically satisfied if F is a continuous function of x and y.

Substitution of the expressions for the shear stress components from eqn (2.100) in eqn (2.98) gives the resultant τ in terms of the stress function

$$\tau^2 = \left(\frac{\partial F}{\partial y}\right)^2 + \left(\frac{\partial F}{\partial x}\right)^2. \tag{2.102}$$

The stress function F may be visualized as a surface spanned over the x, y-plane. For isolines on the surface (F = constant, $\mathrm{d}F = 0$), with eqn (2.100),

$$\mathrm{d}F = \frac{\partial F}{\partial x}\mathrm{d}x + \frac{\partial F}{\partial y}\mathrm{d}y = -\sigma_{zy}\mathrm{d}x + \sigma_{zx}\mathrm{d}y = 0. \tag{2.103}$$

From the last equation it follows that,

$$\frac{\sigma_{zy}}{\sigma_{zx}} = \frac{\mathrm{d}y}{\mathrm{d}x} \tag{2.104}$$

and the resultant shear stress τ is thus tangential to the lines F = constant, which are known as shear stress trajectories (Fig. 2.19). Since the shear stress along the contour of the cross-section must be tangential to it, the contour is an isoline. This expresses the static boundary condition.

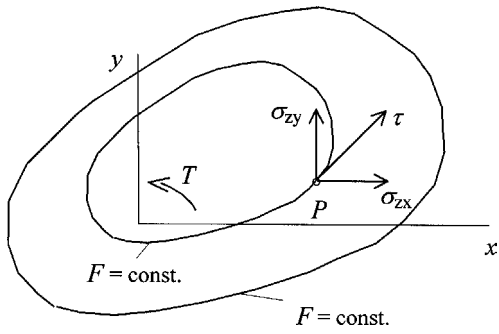

Figure 2.19: Isolines F = constant and shear stresses.

There are no resultant shear forces $(Q_{\rm x}, Q_{\rm y})$ in the cross-section. Because of $F =$ constant along the contour:

$$Q_{\rm x} = \int\int \sigma_{\rm zx} {\rm d}x{\rm d}y = \int \left(\int \frac{\partial F}{\partial y} {\rm d}y \right) {\rm d}x = 0.$$

Similarly, $Q_{\rm y} = 0$ for the other component. Integration is over the cross-section. It is noticed that $\int \frac{\partial F}{\partial y} {\rm d}y = \int \partial_{\rm y} F = \Delta F_{\rm c}$; the difference between contour values of the stress function, here at $x =$ constant, vanishes: $\Delta F_{\rm c} = 0$ (Fig. 2.20).

Calculation of the torsional moment (torque) from the shear stress leads to the integral

$$T = \int\int (\sigma_{\rm zy} x - \sigma_{\rm zx} y) {\rm d}x\, {\rm d}y = -\int\int \left(\frac{\partial F}{\partial x} x + \frac{\partial F}{\partial y} y \right) {\rm d}x\, {\rm d}y, \qquad (2.105)$$

which extends over the cross-section of the bar. The second expression is obtained by utilizing eqn (2.100) for the shear stress components. Application of partial integration in conjunction with the definition $F = 0$ along the contour gives the torque in terms of the stress function

$$T = 2\int\int F {\rm d}x\, {\rm d}y. \qquad (2.106)$$

This is twice the volume of the space between the surface $F(x, y)$ and the x, y-plane.

For the transformation of the integral on the right-hand side of eqn (2.105) by partial integration, we write the first term as

$$\int\int \frac{\partial F}{\partial x} x {\rm d}x\, {\rm d}y = \int \left(\int \frac{\partial F}{\partial x} x {\rm d}x \right) {\rm d}y, \qquad (2.107)$$

and using the relation

$$\frac{\partial}{\partial x}(Fx) = F + \frac{\partial F}{\partial x} x, \qquad (2.108)$$

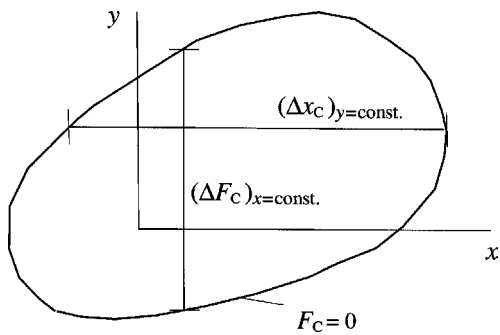

Figure 2.20: On integration over the cross-section.

we obtain

$$\int \frac{\partial F}{\partial x} x \mathrm{d}x = \int \frac{\partial}{\partial x}(Fx)\mathrm{d}x - \int F \mathrm{d}x. \tag{2.109}$$

Evaluation of the first integral on the right-hand side of eqn (2.109) for the cross-section yields

$$\int \frac{\partial}{\partial x}(Fx)\mathrm{d}x = \int \partial_{\mathrm{x}}(Fx) = F_{\mathrm{c}} \Delta x_{\mathrm{c}}, \tag{2.110}$$

where Δx_{c} denotes the difference of the x-coordinate of the contour at $y = \text{constant}$, and F_{c} is the contour value of the stress function (Fig. 2.20). The integral vanishes for the choice $F_{\mathrm{c}} = 0$ and therefore eqn (2.107) simplifies to

$$\int \int \frac{\partial F}{\partial x} x \mathrm{d}x\mathrm{d}y = -\int \int F \mathrm{d}x\, \mathrm{d}y. \tag{2.111}$$

An analogous treatment for the second term in the last integral in eqn (2.105) gives

$$\int \int \frac{\partial F}{\partial y} y \mathrm{d}y\mathrm{d}x = -\int \int F \mathrm{d}y\mathrm{d}x, \tag{2.112}$$

and eqn (2.106) for the torque follows by summation of eqns (2.111) and (2.112).

Specification of the stress function

Since the equations of static equilibrium are satisfied identically by the stress function, its specification must be based on different conditions. For a problem of *elastic torsion*, denote the stress function by F_{e}. Here, the stresses σ_{zx} and σ_{zy} are related to the strains $\gamma_{\mathrm{zx}} = \varepsilon_{\mathrm{zx}}$ and $\gamma_{\mathrm{zy}} = \varepsilon_{\mathrm{zy}}$ by the elastic shear modulus G. Using the expressions in eqn (2.100) for the stresses,

$$\gamma_{\mathrm{zx}} = \varepsilon_{\mathrm{zx}} = \frac{1}{G}\frac{\partial F_{\mathrm{e}}}{\partial y}, \quad \gamma_{\mathrm{zy}} = \varepsilon_{\mathrm{zy}} = -\frac{1}{G}\frac{\partial F_{\mathrm{e}}}{\partial x}. \tag{2.113}$$

Substitution of eqn (2.113) in the condition of kinematic compatibility, eqn (2.97), supplies a differential equation for the elastic stress function

$$\frac{\partial^2 F_{\mathrm{e}}}{\partial x^2} + \frac{\partial^2 F_{\mathrm{e}}}{\partial y^2} = -2G\theta' = \text{constant}. \tag{2.114}$$

Equation (2.114) has the same form as the differential equation governing the deflection of an elastic membrane subjected to pressure loading. On this basis, Ludwig Prandtl introduced a solution for the problem of elastic torsion of prismatical bars by analogy [3]. For experimental integration, an elastic membrane spanned over the contour of the cross-section of the bar is subjected to pressure loading. The deflection of the membrane can be interpreted as the stress function $F_{\mathrm{e}}(x, y)$. Specification of the stress function determines in turn the shear stress components σ_{zx} and σ_{zy}, the resultant shear stress τ, and the torque $T = T_{\mathrm{e}}$ according to the foregoing results. The components of shear strain are given by eqn (2.113).

Next, considering *plastic torsion* for materials obeying the von Mises yield condition we notice that the equivalent stress here is given by

$$\bar{\sigma}^2 = \frac{3}{2}\boldsymbol{\sigma}_{\mathrm{D}}^{\mathrm{t}}\,\boldsymbol{\sigma}_{\mathrm{D}} = 3(\sigma_{\mathrm{zx}}^2 + \sigma_{\mathrm{zy}}^2) = 3\tau^2. \tag{2.115}$$

In fact, the only non-zero entities of the deviatoric stress vector are $\sqrt{2}\,\sigma_{\mathrm{zx}}$ and $\sqrt{2}\,\sigma_{\mathrm{zy}}$, leading to the expression in eqn (2.115). In the cross-section the elasticity limit is reached where $\bar{\sigma} = \sigma_{\mathrm{s}}$, or on account of eqn (2.115), where

$$\tau = \frac{\sigma_{\mathrm{s}}}{\sqrt{3}} = \tau_{\mathrm{s}}. \tag{2.116}$$

This defines the yield stress τ_{s} of the material under shear and relates it to the tensile yield stress σ_{s} for the von Mises criterion.

We denote the stress function in the plastic case by F_{p}. If the cross-section is made of perfectly plastic material and has completely entered the plastic range, the shear stress τ is constrained everywhere by the yield stress of the material. With reference to eqn (2.100), we then obtain

$$\tau^2 = \left(\frac{\partial F_{\mathrm{p}}}{\partial x}\right)^2 + \left(\frac{\partial F_{\mathrm{p}}}{\partial y}\right)^2 = \frac{\sigma_{\mathrm{s}}^2}{3} = \text{constant}. \tag{2.117}$$

It is observed that $\partial F_{\mathrm{p}}/\partial x, \partial F_{\mathrm{p}}/\partial y$ are the components of the gradient of the stress function and thus eqn (2.117) states that the gradient length is constant. This defines the stress function $F_{\mathrm{p}}(x, y)$ as a surface of constant maximum inclination, spanned over the cross-section.

Once the stress function is specified, the shear stress components can be determined; their resultant is constant at $\tau = \tau_{\mathrm{s}}$. The torque $T = T_{\mathrm{p}}$ obtained as

$$T_{\mathrm{p}} = 2\int\int F_{\mathrm{p}}\mathrm{d}x\mathrm{d}y = T_{\mathrm{F}}, \tag{2.118}$$

determines the carrying capacity T_{F} of the plastic cross-section.

For an illustration, we consider the plastic torsion of a bar with circular cross-section made of perfectly plastic material with tensile yield stress σ_{s} (Fig. 2.21). The surface of constant maximum inclination spanned over the

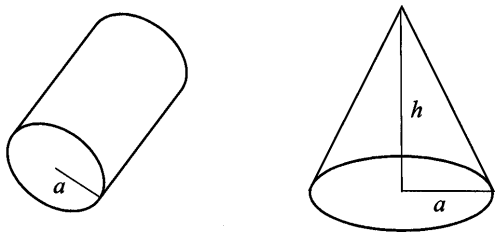

Figure 2.21: Plastic torsion of a circular bar.

circle is a cone and represents the stress function $F_{\mathrm{p}}(x, y)$ at full plastic yield. The slope is defined by the quotient of the height h of the cone to the radius a of the circle. With reference to eqn (2.117), it is specified by the yield stress of the material and reads

$$\frac{h}{a} = \frac{\sigma_{\mathrm{s}}}{\sqrt{3}}. \tag{2.119}$$

This determines $F_{\mathrm{p}}(x, y)$ and the plastic stress state completely. The plastic yield moment is given by twice the volume of the cone

$$T_{\mathrm{F}} = \frac{2}{3}\pi a^2 h = \frac{2}{3}\pi a^3 \frac{\sigma_{\mathrm{s}}}{\sqrt{3}}. \tag{2.120}$$

Of course, $\sigma_{\mathrm{s}}/\sqrt{3} = \tau_{\mathrm{s}}$, the yield stress of the material in shear.

For more complicated cross-sections, Nadai [4] proposed that surfaces of constant maximum slope can be obtained by forming a sand heap over the cross-section. This simple method is known as the sand-heap analogy to plastic torsion. Apart from the demonstration effect, the analogy might be utilized for a determination of the plastic stress function by simulating sand heap formation over the cross-section in question via analytical or computational techniques (Fig. 2.22; [5]).

The two extreme cases considered up to now, the elastic case with the stress function F_{e} governed by eqn (2.114) and the plastic case with the stress function F_{p} governed by eqn (2.117), have to be supplemented by the elastoplastic situation. Here, the cross-section is only partially at plastic yield while the core is still elastic (Fig. 2.23). The stress state in the elastic and the plastic regions is specified by the stress functions F_{e} and F_{p}, respectively, which may be determined as before. At the common boundary separating the two regions, the equality of the stress components requires

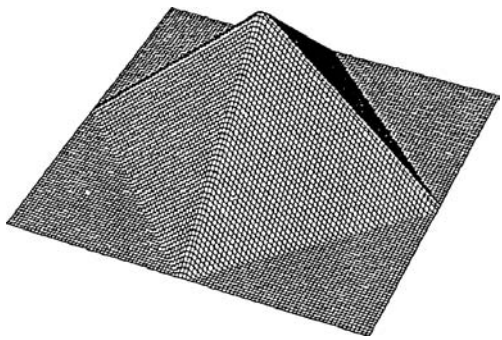

Figure 2.22: Computer generated sand heap over a quadratic cross-section.

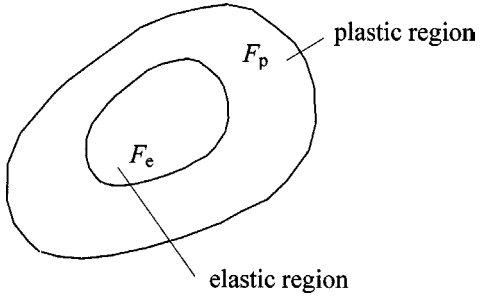

Figure 2.23: Part of the cross-section at plastic yield, the other part being elastic.

that the stress functions satisfy the continuity condition

$$\frac{\partial F_e}{\partial x} = \frac{\partial F_p}{\partial x}, \quad \frac{\partial F_p}{\partial y} = \frac{\partial F_p}{\partial y}, \tag{2.121}$$

by the partial derivatives and determines the location of the interior boundary as a function of the applied torque $T = T_e + T_p$.

At the elasticity limit ($T = T_s$) the stress function F_e still spans the entire cross-section. With increasing torque the elastic region shrinks and vanishes at the plastic limit ($T = T_F$). At the same time the plastic region grows from the contour into the interior of the cross-section. Ultimately, the function F_p alone governs the stress state.

2.3.2 Plane strain

Long cylindrical or prismatical bodies subjected to loads in the cross-section not varying along the axis deform under plane strain conditions if the axial displacement is suppressed at the ends. Choosing the z-axis in the longitudinal direction, cross-sections perpendicular to it lie in the x, y-plane (Fig. 2.24). Under plane strain conditions, the kinematics of deformation of the body is described by the displacements

$$u = u(x, y), \quad v = v(x, y), \quad w = 0. \tag{2.122}$$

The longitudinal displacement w vanishes completely, while the displacements u, v in the plane of the cross-section do not depend on the location along the z-axis. From the displacement functions in eqn (2.122), the strains γ_{xx}, γ_{yy} and γ_{xy} in the plane of the cross-section derive as functions of x and y. The out-of-plane strains vanish: $\gamma_{zz} = \gamma_{xz} = \gamma_{yz} = 0$.

With the shear strains, the shear stress components $\sigma_{xz} = \sigma_{zx}$ and $\sigma_{yz} = \sigma_{zy}$ are also zero, for an elastic as well as for an elastoplastic material. An axial stress component σ_{zz}, however, exists: in-plane deformation implies axial strain in elasticity and plasticity, and imposition of the plane

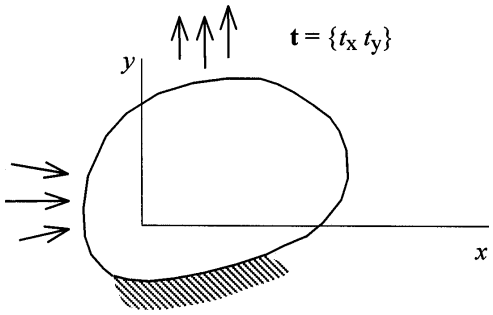

Figure 2.24: Cylindrical body in plane strain (cross-section).

strain condition induces axial stress. For the static equilibrium of the non-vanishing stress components eqn (2.55) reduces to

$$\begin{aligned} \frac{\partial \sigma_{\mathrm{xx}}}{\partial x} + \frac{\partial \sigma_{\mathrm{yx}}}{\partial y} + f_{\mathrm{x}} = 0, \\ \frac{\partial \sigma_{\mathrm{xy}}}{\partial x} + \frac{\partial \sigma_{\mathrm{yy}}}{\partial y} + f_{\mathrm{y}} = 0. \end{aligned} \tag{2.123}$$

These differential equations concern the distribution of the three stress components $\sigma_{\mathrm{xx}}, \sigma_{\mathrm{yy}}$ and σ_{xy} in the cross-section, while the requirement

$$\frac{\partial \sigma_{\mathrm{zz}}}{\partial z} = 0$$

establishes the constancy of σ_{zz} along the z-axis. The associated boundary conditions are

$$\begin{aligned} l\,\sigma_{\mathrm{xx}} + m\,\sigma_{\mathrm{yx}} = t_{\mathrm{x}}, \\ l\,\sigma_{\mathrm{xy}} + m\,\sigma_{\mathrm{yy}} = t_{\mathrm{y}}, \end{aligned} \tag{2.124}$$

where the components t_{x} and t_{y} of the surface forces acting perpendicular to the longitudinal axis are by definition independent of the z-coordinate.

Stationary elastic strain

In spite of the reduced dimensions, a solution of the elastoplastic problem under the condition of plane strain requires activation of the procedures described in Section 2.2.2. A particular situation arises when the elastic strains become stationary. Then $\dot{\varepsilon}_{\mathrm{zz}} = 0$ and the suppression of the axial deformation implies that the plastic strain rate $\dot{\eta}_{\mathrm{zz}}$ also vanishes:

$$\dot{\gamma}_{\mathrm{zz}} = \dot{\eta}_{\mathrm{zz}} = 0. \tag{2.125}$$

For this, the flow rule requires the deviatoric stress σ_{Dzz} to be zero,

$$\sigma_{\mathrm{Dzz}} = \sigma_{\mathrm{zz}} - \sigma_{\mathrm{H}} = 0, \tag{2.126}$$

and relates the axial stress to the in-plane stress components

$$\sigma_{\mathrm{zz}} = \sigma_{\mathrm{H}} = \frac{\sigma_{\mathrm{xx}} + \sigma_{\mathrm{yy}}}{2}. \tag{2.127}$$

The deviatoric stress components in the plane of the cross-section are

$$\begin{aligned} \sigma_{\mathrm{Dxx}} &= \sigma_{\mathrm{xx}} - \sigma_{\mathrm{H}} = \frac{\sigma_{\mathrm{xx}} - \sigma_{\mathrm{yy}}}{2}, \\ \sigma_{\mathrm{Dyy}} &= \sigma_{\mathrm{yy}} - \sigma_{\mathrm{H}} = \frac{\sigma_{\mathrm{yy}} - \sigma_{\mathrm{xx}}}{2}, \end{aligned} \tag{2.128}$$

and since $\sigma_{\mathrm{Dzz}} = 0$, they satisfy the condition

$$\sigma_{\mathrm{Dxx}} + \sigma_{\mathrm{Dyy}} = 0. \tag{2.129}$$

The equivalent deviatoric stress, eqn (1.98), becomes

$$\bar{\sigma}^2 = \frac{3}{2}(\sigma_{\mathrm{Dxx}}^2 + \sigma_{\mathrm{Dyy}}^2 + 2\sigma_{\mathrm{xy}}^2) = 3\left[\left(\frac{\sigma_{\mathrm{xx}} - \sigma_{\mathrm{yy}}}{2}\right)^2 + \sigma_{\mathrm{xy}}^2\right]. \tag{2.130}$$

For a perfectly plastic material which is completely in the plastic range, $\bar{\sigma} = \sigma_{\mathrm{s}}$ everywhere in the cross-section. In this case, eqn (2.130) provides us with an algebraic equation for the in-plane stress components:

$$\left(\frac{\sigma_{\mathrm{xx}} - \sigma_{\mathrm{yy}}}{2}\right)^2 + \sigma_{\mathrm{xy}}^2 = \frac{\sigma_{\mathrm{s}}^2}{3} = \tau_{\mathrm{s}}^2. \tag{2.131}$$

Either the tensile yield stress σ_{s} or the shear yield stress τ_{s} may be used for a limitation of the stress state. It is noticed that elimination of σ_{zz} by eqn (2.127) and the plastic condition for the three in-plane components of the stress, eqn (2.131), convert the equilibrium condition, eqn (2.123), to a system sufficient for determination of the stress state. The problem may then be considered statically determinate in that the kinematic compatibility condition is not required for the calculation of the stresses.

Regarding the plastic flow, we deduce from the flow rule – eqn (1.116) with eqn (1.118) – using eqn (2.128) for the deviatoric stresses, the strain rates

$$\begin{aligned} \dot{\eta}_{\mathrm{xx}} &= \frac{3}{4}\frac{\dot{\bar{\eta}}}{\bar{\sigma}}(\sigma_{\mathrm{xx}} - \sigma_{\mathrm{yy}}), \\ \dot{\eta}_{\mathrm{yy}} &= \frac{3}{4}\frac{\dot{\bar{\eta}}}{\bar{\sigma}}(\sigma_{\mathrm{yy}} - \sigma_{\mathrm{xx}}). \end{aligned} \tag{2.132}$$

Since $\dot{\eta}_{zz} = 0$, the in-plane components satisfy the isochoric condition

$$\dot{\eta}_{xx} + \dot{\eta}_{yy} = 0. \tag{2.133}$$

The plastic shear strain rate follows as

$$\dot{\eta}_{xy} = 3\frac{\dot{\bar{\eta}}}{\bar{\sigma}}\sigma_{xy}. \tag{2.134}$$

From eqn (2.132), the difference of the normal strain rate components is proportional to the difference of the normal stress components in the plane,

$$\dot{\eta}_{xx} - \dot{\eta}_{yy} = \frac{3}{2}\frac{\dot{\bar{\eta}}}{\bar{\sigma}}(\sigma_{xx} - \sigma_{yy}), \tag{2.135}$$

and dividing by eqn (2.134) we obtain the quotient

$$\frac{\dot{\eta}_{xx} - \dot{\eta}_{yy}}{\dot{\eta}_{xy}} = \frac{\sigma_{xx} - \sigma_{yy}}{2\sigma_{xy}}. \tag{2.136}$$

In the absence of elastic constituents, the plastic strain rate obeys the kinematic compatibility conditions.

2.3.3 Thick-walled cylinder under internal pressure

The thick-walled cylinder in Fig. 2.25 is subjected to internal pressure p under the condition of plane strain. The material is assumed elastic–perfectly plastic with yield stress in shear τ_s. In the present axisymmetric case, the use of a cylindrical reference system 0–$r\varphi z$ appears advantageous.

The stress state is defined in terms of the normal stress components σ_r, σ_φ in the plane and σ_z along the longitudinal axis. Because of the axial symmetry the shear stress vanishes and the normal stresses are independent of the angular location. The single equilibrium condition to be satisfied is along the radial direction. It is deduced as

$$\frac{\mathrm{d}\sigma_r}{\mathrm{d}r} + \frac{\sigma_r - \sigma_\varphi}{r} = 0. \tag{2.137}$$

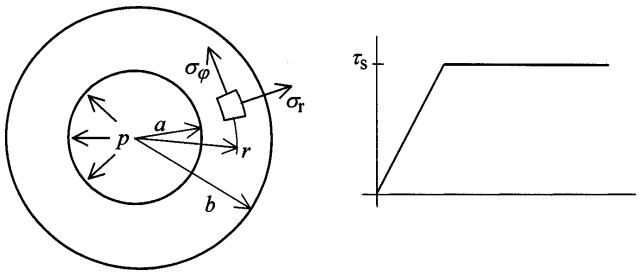

Figure 2.25: Elastic–perfectly plastic thick-walled cylinder.

The elastic solution of the problem given in [2] is

$$\sigma_{\mathrm{r}} = \frac{pa^2}{b^2 - a^2}\left(1 - \frac{b^2}{r^2}\right), \quad \sigma_{\varphi} = \frac{pa^2}{b^2 - a^2}\left(1 + \frac{b^2}{r^2}\right), \qquad \sigma_{\mathrm{z}} = 2\nu\frac{pa^2}{b^2 - a^2}, \tag{2.138}$$

where a and b denote the inner and the outer cylinder radii, respectively.

With eqn (2.138) for the stress components in conjunction with $\nu = 1/2$ for simplicity, the hydrostatic stress becomes

$$\sigma_{\mathrm{H}} = \frac{\sigma_{\mathrm{r}} + \sigma_{\varphi} + \sigma_{\mathrm{z}}}{3} = \frac{pa^2}{b^2 - a^2} = \sigma_{\mathrm{z}}, \tag{2.139}$$

and the deviatoric stress components are

$$\sigma_{\mathrm{Dz}} = \sigma_{\mathrm{z}} - \sigma_{\mathrm{H}} = 0, \qquad \sigma_{\mathrm{D}\varphi} = -\sigma_{\mathrm{Dr}} = \frac{pa^2}{b^2 - a^2}\frac{b^2}{r^2}. \tag{2.140}$$

The equivalent deviatoric stress, eqn (2.130), follows to

$$\bar{\sigma}(r) = \sqrt{\frac{3}{2}(\sigma_{\mathrm{Dr}}^2 + \sigma_{\mathrm{D}\varphi}^2)} = \sqrt{3}\frac{pa^2}{b^2 - a^2}\frac{b^2}{r^2}. \tag{2.141}$$

It is a function of the cylinder radius with the maximum at $r = a$, the interior boundary. The elasticity limit of the material is attained for $\bar{\sigma}(a) = \sqrt{3}\tau_{\mathrm{s}}$, and the associated pressure from eqn (2.141) is

$$p_{\mathrm{s}} = \frac{b^2 - a^2}{b^2}\tau_{\mathrm{s}}. \tag{2.142}$$

Beyond this pressure the deformation is elastoplastic. The plastic limit state is characterized by the stationarity of the stress, so the rate of elastic strain vanishes (see Chapter 3). The condition of plane strain then implies that $\dot{\eta}_{\mathrm{z}} = 0$, and $\sigma_{\mathrm{Dz}} = 0$. In this case, the von Mises yield condition is expressed by eqn (2.131). For the present axisymmetric stress state, presuming $\sigma_{\varphi} > \sigma_{\mathrm{r}}$ everywhere, there follows

$$\sigma_{\varphi} - \sigma_{\mathrm{r}} = 2\tau_{\mathrm{s}} = \text{constant}. \tag{2.143}$$

With the above yield state for the stresses in the entire cross-section the equilibrium condition, eqn (2.137), at the plastic limit reads

$$\frac{\mathrm{d}\sigma_{\mathrm{r}}}{\mathrm{d}r} - \frac{2\tau_{\mathrm{s}}}{r} = 0, \tag{2.144}$$

which can be integrated for the radial stress

$$\sigma_{\mathrm{r}} = 2\tau_{\mathrm{s}} \ln r + C. \tag{2.145}$$

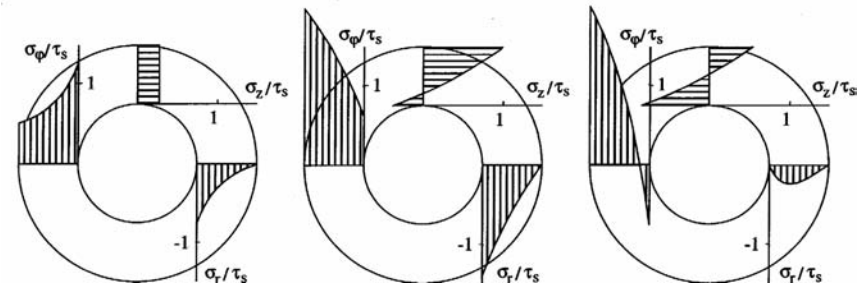

Figure 2.26: Radial distribution of stress components in the cylinder.

The integration constant C is obtained from the exterior boundary condition $\sigma_{\rm r}(b) = 0$, and specifies $\sigma_{\rm r}$ completely. The circumferential stress σ_φ satisfies the yield condition, eqn (2.143), and the axial stress $\sigma_{\rm z}$ equals the hydrostatic stress. The normal stress components are:

$$\begin{aligned} \sigma_{\rm r} &= 2\tau_{\rm s} \ln \frac{r}{b}, \\ \sigma_\varphi &= 2\tau_{\rm s} + \sigma_{\rm r} = 2\tau_{\rm s} \left(1 + \ln \frac{r}{b}\right), \\ \sigma_{\rm z} &= \frac{\sigma_{\rm r} + \sigma_\varphi}{2} = \tau_{\rm s} \left(1 + 2 \ln \frac{r}{b}\right). \end{aligned} \tag{2.146}$$

The interior boundary condition determines the plastic limit pressure

$$p_{\rm F} = -\sigma_{\rm r}(a) = 2\tau_{\rm s} \ln \frac{b}{a}. \tag{2.147}$$

Unloading from the plastic limit leaves residual stresses which can be obtained as the difference between the plastic solution, eqn (2.146), and elastic stresses, eqn (2.138), calculated for $p = p_{\rm F}$ from eqn (2.147). The result is:

$$\begin{aligned} (\sigma_{\rm r})_{\rm r} &= \sigma_{\rm r} - (\sigma_{\rm r})_{\rm e} = 2\tau_{\rm s} \left(\ln \frac{r}{b} - \frac{a^2}{r^2} \frac{b^2 - r^2}{b^2 - a^2} \ln \frac{a}{b}\right), \\ (\sigma_\varphi)_{\rm r} &= \sigma_\varphi - (\sigma_\varphi)_{\rm e} = 2\tau_{\rm s} \left(1 + \ln \frac{r}{b} + \frac{a^2}{r^2} \frac{b^2 + r^2}{b^2 - a^2} \ln \frac{a}{b}\right), \\ (\sigma_{\rm z})_{\rm r} &= \sigma_{\rm z} - (\sigma_{\rm z})_{\rm e} = 2\tau_{\rm s} \left(\frac{1}{2} + \ln \frac{r}{b} + \frac{a^2}{b^2 - a^2} \ln \frac{a}{b}\right). \end{aligned} \tag{2.148}$$

The above applies if the residual stress does not exceed the elasticity limit,

$$|(\sigma_\varphi - \sigma_{\rm r})_{\rm r}| = |(\sigma_\varphi - \sigma_{\rm r})_{\rm F} - (p_{\rm F}/p_{\rm s})(\sigma_\varphi - \sigma_{\rm r})_{\rm s}| \le 2\tau_{\rm s},$$

and implies $p_{\rm F}/p_{\rm s} \le 2$, or $b/a \le 2.22$. A graphical representation of the radial distribution of the stresses at $p = p_{\rm s}, = p_{\rm F}, = 0$ is given in Fig. 2.26.

2.3.4 Plane stress

The condition of plane stress is commonly ascribed to thin plates of constant thickness loaded by forces acting uniformly over the thickness along the periphery of the plate (Fig. 2.27). Since all out-of-plane stress components vanish, $\sigma_{zz} = \sigma_{xz} = \sigma_{yz} = 0$, the equilibrium condition, eqn (2.55), reduces to

$$\begin{aligned} \frac{\partial \sigma_{xx}}{\partial x} + \frac{\partial \sigma_{yx}}{\partial y} + f_x = 0, \\ \frac{\partial \sigma_{xy}}{\partial x} + \frac{\partial \sigma_{yy}}{\partial y} + f_y = 0. \end{aligned} \tag{2.149}$$

It concerns the variation of the in-plane components $\sigma_{xx}, \sigma_{yy}, \sigma_{xy}$ as functions of x and y. The static boundary conditions are as in eqn (2.124). The elastoplastic problem can be solved by an application of the algorithms described in Section 2.2.2, accounting for the fact that stresses in the z-direction are absent.

It is observed that for $\sigma_{zz} = 0$ the hydrostatic stress σ_H is given by

$$\sigma_H = \frac{\sigma_{xx} + \sigma_{yy}}{3}, \tag{2.150}$$

and leads to the deviatoric normal stresses

$$\begin{aligned} \sigma_{Dxx} = \sigma_{xx} - \sigma_H = \frac{2\sigma_{xx} - \sigma_{yy}}{3}, \\ \sigma_{Dyy} = \sigma_{yy} - \sigma_H = \frac{2\sigma_{yy} - \sigma_{xx}}{3}, \\ \sigma_{Dzz} = \quad -\sigma_H = -\frac{\sigma_{xx} + \sigma_{yy}}{3}. \end{aligned} \tag{2.151}$$

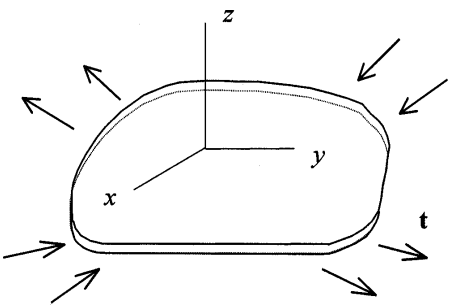

Figure 2.27: Plate under plane stress conditions.

With reference to Section 1.2.3 one obtains from eqn (1.97) for the equivalent deviatoric stress

$$\begin{aligned}\bar{\sigma}^2 = \frac{3}{2}\boldsymbol{\sigma}_{\mathrm{D}}^{\mathrm{t}}\boldsymbol{\sigma} &= \frac{3}{2}\left(\sigma_{\mathrm{Dxx}}\sigma_{\mathrm{xx}} + \sigma_{\mathrm{Dyy}}\sigma_{\mathrm{yy}} + 2\sigma_{\mathrm{xy}}^2\right) \\ &= \sigma_{\mathrm{xx}}^2 + \sigma_{\mathrm{yy}}^2 - \sigma_{\mathrm{xx}}\sigma_{\mathrm{yy}} + 3\sigma_{\mathrm{xy}}^2,\end{aligned} \tag{2.152}$$

where advantage has been taken of the fact that $\sigma_{\mathrm{zz}} = 0$ in evaluating the scalar product of the two stress vectors.

In the particular case of a perfectly plastic material, the completely plastic state is characterized by $\bar{\sigma} = \sigma_{\mathrm{s}}$ everywhere, and eqn (2.152) supplies an algebraic equation constraining the stress components. It can be used in conjunction with the differential equilibrium equations (2.149) in order to determine the plane stress state without reference to the kinematic compatibility. In this sense, the problem may be considered statically determinate.

The plastic strain rate exhibits three components in the plane $\dot{\eta}_{\mathrm{xx}}, \dot{\eta}_{\mathrm{yy}}$, $\dot{\eta}_{\mathrm{xy}}$ and one out-of-plane component $\dot{\eta}_{\mathrm{zz}}$, which determines the permanent change in thickness of the plate. From the isochoric condition

$$\dot{\eta}_{\mathrm{zz}} = -(\dot{\eta}_{\mathrm{xx}} + \dot{\eta}_{\mathrm{yy}}). \tag{2.153}$$

This relation is used in order to express the equivalent plastic strain rate in terms of the in-plane components. From eqn (1.115),

$$\begin{aligned}\dot{\bar{\eta}}^2 &= \frac{2}{3}\left(\dot{\eta}_{\mathrm{xx}}^2 + \dot{\eta}_{\mathrm{yy}}^2 + \dot{\eta}_{\mathrm{zz}}^2 + \frac{1}{2}\dot{\eta}_{\mathrm{xy}}^2\right) \\ &= \frac{4}{3}\left(\dot{\eta}_{\mathrm{xx}}^2 + \dot{\eta}_{\mathrm{yy}}^2 + \dot{\eta}_{\mathrm{xx}}\dot{\eta}_{\mathrm{yy}} + \frac{1}{4}\dot{\eta}_{\mathrm{xy}}^2\right).\end{aligned} \tag{2.154}$$

Solutions to plane stress problems (as well as to plane strain problems) can be found in the books by Kachanov [6] and Kaliszky [7], for example, along with detailed discussions. In terms of principal stresses σ_1 and σ_2, solutions of the form

$$\begin{aligned}\sigma_1 &= 2\tau_{\mathrm{s}}\cos\left(\omega - \frac{\pi}{6}\right), \\ \sigma_2 &= 2\tau_{\mathrm{s}}\cos\left(\omega + \frac{\pi}{6}\right),\end{aligned} \tag{2.155}$$

are seen to satisfy the yield condition $\bar{\sigma} = \sigma_{\mathrm{s}} = \sqrt{3}\tau_{\mathrm{s}}$ identically for the perfectly plastic material in the state of plane stress. This is confirmed by substitution in eqn (2.152) for the equivalent stress. The function $\omega = \omega(x, y)$ can be related to the hydrostatic stress σ_{H}. In fact, with eqn (2.155) we obtain

$$3\sigma_{\mathrm{H}} = \sigma_1 + \sigma_2 = 2\sqrt{3}\tau_{\mathrm{s}}\cos\omega = 2\sigma_{\mathrm{s}}\cos\omega. \tag{2.156}$$

The ultimate solution utilizes the equilibrium equations (2.149) for finding $\omega(x, y)$. If the problem does not exhibit natural principal directions, these constitute an additional variable.

The silently assumed constancy of the mechanical state over the plate thickness requires discussion. Solutions of plane stress problems that neglect variations over the thickness are approximate in nature and refer to thin plates; for a treatment of the elastic case see [2]. It is noted that eqn (2.149) for the equilibrium defines a problem for the stress distribution in the x, y-plane. Variations perpendicular to the plate along the z-direction must establish kinematic compatibility. In order to elucidate the argument recall that the vanishing of the out-of-plane stress components σ_{zz}, σ_{xz} and σ_{yz} implies $\gamma_{xz} = \gamma_{yz} = 0$ while $\gamma_{zz} \neq 0$. Focusing on the non-vanishing out-of-plane strain γ_{zz} we deduce from the strain kinematics, eqn (2.58), the relations

$$\begin{aligned} \frac{\partial^2 \gamma_{zz}}{\partial x^2} &= -\frac{\partial^2 \gamma_{xx}}{\partial z^2}, \\ \frac{\partial^2 \gamma_{zz}}{\partial y^2} &= -\frac{\partial^2 \gamma_{yy}}{\partial z^2}, \\ 2\frac{\partial^2 \gamma_{zz}}{\partial x \partial y} &= -\frac{\partial^2 \gamma_{xy}}{\partial z^2}. \end{aligned} \tag{2.157}$$

The above equation is based on a continuous displacement field and constitutes a part of the familiar conditions of kinematic compatibility, the remainder involved in the solution of eqn (2.149). The right-hand sides in eqn (2.157) vanish if variations over the plate thickness are not allowed. Then the left-hand sides of the equation require that the distributions $\gamma_{zz}(x, y)$ is not higher than linear. Otherwise, kinematic compatibility implies a dependence of the in-plane quantities on the thickness dimension, but of higher order. This leads to the conclusion that plane solutions are adequate for thin plates.

2.3.5 Reduced stress and strain space

The lower dimensionality of plane problems suggests representation of stress and strain by reduced 3×1 vectors comprising only in-plane components. Omitting particular indication, we write

$$\boldsymbol{\sigma} = \{\sigma_{xx}\, \sigma_{yy}\, \sqrt{2}\sigma_{xy}\}, \quad \boldsymbol{\gamma} = \left\{\gamma_{xx}\, \gamma_{yy}\, \frac{1}{\sqrt{2}}\gamma_{xy}\right\}. \tag{2.158}$$

The transition from the complete 6×1 vectors to the above 3×1 representation entails certain modifications in the elastic as well as the elastoplastic relations between stress and strain.

Plane stress
The reduced stress vector contains information on all non-vanishing components. Partitioning into hydrostatic and deviatoric constituents,

$$\sigma_{\mathrm{H}} = \frac{1}{3}\mathbf{e}_2^{\mathrm{t}}\boldsymbol{\sigma}, \quad \boldsymbol{\sigma}_{\mathrm{H}} = \sigma_{\mathrm{H}}\mathbf{e}_2 \quad (\mathbf{e}_2 = \{1\,1\,0\,\}) \tag{2.159}$$

and

$$\boldsymbol{\sigma}_{\mathrm{D}} = \boldsymbol{\sigma} - \boldsymbol{\sigma}_{\mathrm{H}}.$$

The reduced deviatoric stress vector lacks the axial component and therefore the sum of the in-plane components will in general not vanish:

$$\mathbf{e}_2^{\mathrm{t}}\boldsymbol{\sigma}_{\mathrm{D}} = \mathbf{e}_2^{\mathrm{t}}[\boldsymbol{\sigma} - \sigma_{\mathrm{H}}\mathbf{e}_2] = \sigma_{\mathrm{H}}. \tag{2.160}$$

For the same reason the reduced deviatoric and hydrostatic portions are not orthogonal:

$$\boldsymbol{\sigma}_{\mathrm{H}}^{\mathrm{t}}\boldsymbol{\sigma}_{\mathrm{D}} = \sigma_{\mathrm{H}}^2. \tag{2.161}$$

The in-plane strain vector does not contain complete information on the strain state because of the existence of an axial component. The condition of plane stress $\sigma_{zz} = 0$, however, establishes by elasticity a relation between the three normal components of the elastic strain, thus allowing elimination of ε_{zz}. The two-dimensional elasticity law for plane stress assumes the form

$$\boldsymbol{\sigma} = \boldsymbol{\kappa}[\boldsymbol{\gamma} - \boldsymbol{\eta}]$$

with

$$\boldsymbol{\kappa} = 2G\left[\mathbf{I}_3 + \frac{\nu}{1-\nu}\mathbf{e}_2\mathbf{e}_2^{\mathrm{t}}\right], \quad \boldsymbol{\kappa}^{-1} = \frac{1}{2G}\left[\mathbf{I}_3 - \frac{\nu}{1+\nu}\mathbf{e}_2\mathbf{e}_2^{\mathrm{t}}\right], \tag{2.162}$$

where $\mathbf{I}_3$ denotes the 3×3 identity matrix. The inverse of the material stiffness matrix could be simply deduced by reducing the three-dimensional operator to the in-plane entities.

In plasticity the equivalent stress can be obtained from

$$\bar{\sigma}^2 = \frac{3}{2}\boldsymbol{\sigma}_{\mathrm{D}}^{\mathrm{t}}\boldsymbol{\sigma} = \frac{3}{2}\left(\boldsymbol{\sigma}_{\mathrm{D}}^{\mathrm{t}}\boldsymbol{\sigma}_{\mathrm{D}} + \sigma_{\mathrm{H}}^2\right), \tag{2.163}$$

where the first expression takes advantage of the plane stress state. By differentiation,

$$\mathrm{d}\bar{\sigma} = \frac{3}{2}\frac{1}{\bar{\sigma}}\boldsymbol{\sigma}_{\mathrm{D}}^{\mathrm{t}}\mathrm{d}\boldsymbol{\sigma} = \mathbf{s}^{\mathrm{t}}\mathrm{d}\boldsymbol{\sigma} \qquad \left(\mathbf{s} = \frac{3}{2}\frac{1}{\bar{\sigma}}\boldsymbol{\sigma}_{\mathrm{D}}\right) \tag{2.164}$$

formally as before in the complete representation but with the reduced 3×1 vector $\mathbf{s}$. The latter defines the direction of flow in the x, y-plane for perfect plasticity as well as for isotropic hardening:

$$\mathrm{d}\boldsymbol{\eta} = \mathrm{d}\bar{\eta}\mathbf{s}, \quad \mathrm{d}\bar{\eta} = \frac{1}{h}\mathrm{d}\bar{\sigma} = \frac{1}{h}\mathbf{s}^{\mathrm{t}}\mathrm{d}\boldsymbol{\sigma}. \tag{2.165}$$

An alternative expression of the plastic strain increment in terms of the incremental strain is arrived at using the elastic relation for the stress increment in eqn (2.165), right,

$$\mathrm{d}\bar{\sigma} = \mathbf{s}^{\mathrm{t}}\mathrm{d}\boldsymbol{\sigma} = \mathbf{s}^{\mathrm{t}}\boldsymbol{\kappa}\mathrm{d}\boldsymbol{\gamma} - (\mathbf{s}^{\mathrm{t}}\boldsymbol{\kappa}\mathbf{s})\mathrm{d}\bar{\eta} \tag{2.166}$$

and solving for

$$\mathrm{d}\bar{\eta} = \frac{1}{h + \mathbf{s}^{\mathrm{t}}\boldsymbol{\kappa}\mathbf{s}}\mathbf{s}^{\mathrm{t}}\boldsymbol{\kappa}\mathrm{d}\boldsymbol{\gamma}. \tag{2.167}$$

The simplifications of the complete representation (Chapter 1) are not applicable. For the in-plane 3×1 vector $\mathbf{s}$ we notice the relations

$$\mathbf{e}_2^{\mathrm{t}}\mathbf{s} = \frac{3}{2}\frac{\sigma_{\mathrm{H}}}{\bar{\sigma}},\ \mathbf{s}^{\mathrm{t}}\mathbf{s} = \frac{3}{2}\left(1 - \frac{3}{2}\frac{\sigma_{\mathrm{H}}^2}{\bar{\sigma}^2}\right),\ \mathbf{s}^{\mathrm{t}}\boldsymbol{\kappa}\mathbf{s} = 3G\left(1 - \frac{3}{2}\frac{1-2\nu}{1-\nu}\frac{\sigma_{\mathrm{H}}^2}{\bar{\sigma}^2}\right), \tag{2.168}$$

which reduce to those for the 6×1 vectors ($\mathbf{e}^{\mathrm{t}}\mathbf{s} = 0, \mathbf{s}^{\mathrm{t}}\mathbf{s} = 3/2, \mathbf{s}^{\mathrm{t}}\boldsymbol{\kappa}\mathbf{s} = 3G$) only if $\sigma_{\mathrm{H}} = 0$ (i.e. for $\sigma_{\mathrm{xx}} = -\sigma_{\mathrm{yy}}$).

In the case of kinematic hardening (Section 1.3.2), the consideration of plastic flow can also be restricted to the in-plane components. The description of the yield condition, however, requires in the quantity $\bar{\sigma}_{\mathrm{K}}$ complete information on the translation of the yield surface. Since translation is by a deviatoric vector, in-plane representation by a 3×1 vector $\boldsymbol{\alpha} = \{\alpha_{\mathrm{xx}}\ \alpha_{\mathrm{yy}}\ \sqrt{2}\alpha_{\mathrm{xy}}\}$ does not contain complete information: the term $\alpha_{\mathrm{zz}} = -(\alpha_{\mathrm{xx}} + \alpha_{\mathrm{yy}})$ is missing. In order to retain the previous formulation in the reduced space, we introduce a plane translation vector $\boldsymbol{\beta}$ such that,

$$\boldsymbol{\beta} = [\mathbf{I}_3 + \mathbf{e}_2\mathbf{e}_2^{\mathrm{t}}]\boldsymbol{\alpha} \tag{2.169}$$

and

$$\boldsymbol{\beta}_{\mathrm{D}} = \boldsymbol{\alpha}, \quad \beta_{\mathrm{H}} = \mathbf{e}_2^{\mathrm{t}}\boldsymbol{\alpha} = -\alpha_{\mathrm{zz}}.$$

It is also seen that for the reduced vectors the equivalent stress $\bar{\sigma}_{\mathrm{K}}$ is

$$\bar{\sigma}_{\mathrm{K}}^2 = \frac{3}{2}[\boldsymbol{\sigma} - \boldsymbol{\beta}]_{\mathrm{D}}^{\mathrm{t}}[\boldsymbol{\sigma} - \boldsymbol{\beta}] = \frac{3}{2}\boldsymbol{\sigma}_{\mathrm{KD}}^{\mathrm{t}}\boldsymbol{\sigma}_{\mathrm{K}} \qquad (\boldsymbol{\sigma}_{\mathrm{K}} = \boldsymbol{\sigma} - \boldsymbol{\beta}). \tag{2.170}$$

Differentiating, we obtain the consistency condition in the form

$$\mathrm{d}\bar{\sigma}_{\mathrm{K}} = \mathbf{s}_{\mathrm{K}}^{\mathrm{t}}[\mathrm{d}\boldsymbol{\sigma} - \mathrm{d}\boldsymbol{\beta}] = 0 \qquad \left(\mathbf{s}_{\mathrm{K}} = \frac{3}{2}\frac{1}{\bar{\sigma}_{\mathrm{K}}}\boldsymbol{\sigma}_{\mathrm{KD}}\right). \tag{2.171}$$

Observing that

$$\mathbf{s}_{\mathrm{K}}^{\mathrm{t}}\mathrm{d}\boldsymbol{\beta} = \mathrm{d}\bar{\alpha} = h\mathrm{d}\bar{\eta}, \tag{2.172}$$

the magnitude $\mathrm{d}\bar{\eta}$ of the plastic strain increment follows as for the complete representation.

Plane strain

In plane strain the in-plane 3×1 strain vector contains complete information, but the reduced stress vector does not because of the existence of an axial component $\sigma_{zz} \neq 0$. Even for the strain, the argument does not apply to the elastic and plastic constituents separately, but to $\gamma_{zz} = \varepsilon_{zz} + \eta_{zz} = 0$.

In the elastic range the vanishing of the axial strain ($\varepsilon_{zz} = 0$) allows simple reduction of the complete elastic material stiffness to the in-plane components. It also establishes a relation between the normal stresses, used for the elimination of σ_{zz} when considering the inverse. The two-dimensional elasticity matrices for plane strain read

$$\boldsymbol{\kappa} = 2G\left[\mathbf{I}_3 + \frac{\nu}{1-2\nu}\mathbf{e}_2\mathbf{e}_2^{\mathrm{t}}\right], \quad \boldsymbol{\kappa}^{-1} = \frac{1}{2G}\left[\mathbf{I}_3 - \nu\mathbf{e}_2\mathbf{e}_2^{\mathrm{t}}\right]. \tag{2.173}$$

The transition from the plane stress expressions is obtained by substituting $\nu/(1-\nu)$ for ν.

In plasticity the non-vanishing axial elastic component restores the condition of plane strain: $\varepsilon_{zz} = -\eta_{zz}$, for isochoric plasticity $-\eta_{zz} = \eta_{xx} + \eta_{yy} = \mathbf{e}_2^{\mathrm{t}}\boldsymbol{\eta}$. This leads in the reduced space to the elastic stress–strain relations

$$\boldsymbol{\sigma} = \boldsymbol{\kappa}[\boldsymbol{\varepsilon} + \nu\varepsilon_{zz}\mathbf{e}_2] = \boldsymbol{\kappa}[\boldsymbol{\gamma} - \boldsymbol{\eta}^*] \tag{2.174}$$

with

$$\boldsymbol{\eta}^* = [\mathbf{I} - \nu\mathbf{e}_2\mathbf{e}_2^{\mathrm{t}}]\boldsymbol{\eta}.$$

The axial stress σ_{zz} is related to in-plane quantities by elasticity as follows

$$E\varepsilon_{zz} = \sigma_{zz} - \nu(\sigma_{xx} + \sigma_{yy}) = \sigma_{zz} - \nu\mathbf{e}_2^{\mathrm{t}}\boldsymbol{\sigma},$$

which gives

$$\sigma_{zz} = \mathbf{e}_2^{\mathrm{t}}[E\boldsymbol{\eta} + \nu\boldsymbol{\sigma}]. \tag{2.175}$$

Despite the principal possibility of space reduction, in plane strain the axial components of quantities involved in the description of plasticity are seen to play an active role. Determination of the plastic flow is therefore based conveniently on the three-dimensional formalism developed in Chapter 1 (Sections 1.2 and 1.3).

2.3.6 A note on the torsion of thin-walled cylindrical shells

The thin-walled shell depicted in Fig. 2.28 has an arbitrary cross-section with thickness possibly varying along the circumferential direction. The cross-section of the shell (and the distribution of thickness) is constant along the longitudinal axis. The shell is subjected to a torsional moment (torque) T acting at the ends, which are not constrained and are free to deform. The deformation is assumed to result from a rigid rotation of the cross-section

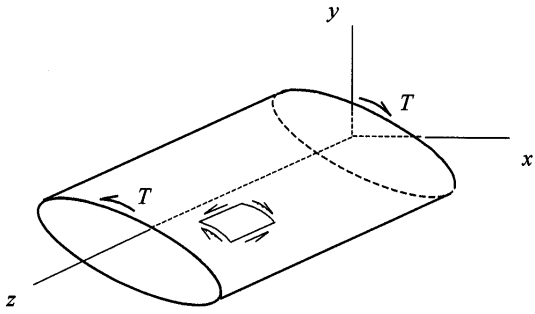

Figure 2.28: Torsion of a thin-walled cylindrical shell.

in its plane and warping along the longitudinal axis. Peripheral positions in the cross-section are specified by the mid-thickness coordinate s (Fig. 2.29); the shear stress τ is defined tangential to s. It is assumed that the shear stress is constant over the thickness $t(s)$. The shear flow

$$q = \tau t \tag{2.176}$$

defines a shear force per unit length.

The condition of equilibrium for an element of the shell (Fig. 2.30) reduces here to the requirements

$$\frac{\partial q}{\partial s} = 0, \quad \frac{\partial q}{\partial z} = 0, \tag{2.177}$$

which state that the shear flow q is constant in the cross-section, and does not depend on the axial position z. In view of eqn (2.176), the consequence of eqn (2.177) for the stress is

$$\frac{\partial \tau}{\partial s} + \frac{\tau}{t}\frac{\partial t}{\partial s} = 0, \quad \frac{\partial \tau}{\partial z} = 0, \tag{2.178}$$

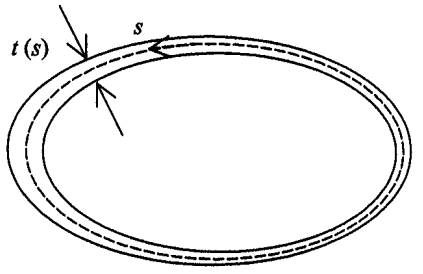

Figure 2.29: Geometry of ring cross-section.

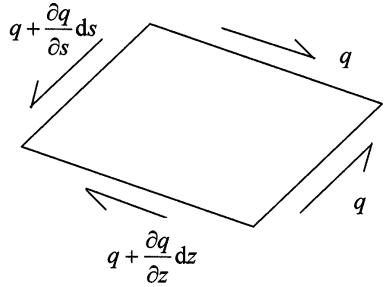

Figure 2.30: Equilibrium of a shell element.

since $t = t(s)$ and $\partial t/\partial z = 0$. The shear stress does not vary along the longitudinal direction; it is not constant within the cross-section if the thickness is variable.

The torsional moment equilibrated by the shear stress (Fig. 2.31) is

$$\mathrm{d}T = hq\mathrm{d}s = 2q\mathrm{d}A,$$

and by integration we obtain Bredt's formula [8]:

$$T = 2q \oint \mathrm{d}A = 2qA, \tag{2.179}$$

where A is the enclosed area. For $q =$ constant the components of the lateral shear force vanish:

$$Q_{\mathrm{x}} = \oint q\mathrm{d}x = q \oint \mathrm{d}x = 0$$

and

$$Q_{\mathrm{y}} = \oint q\mathrm{d}y = q \oint \mathrm{d}y = 0.$$

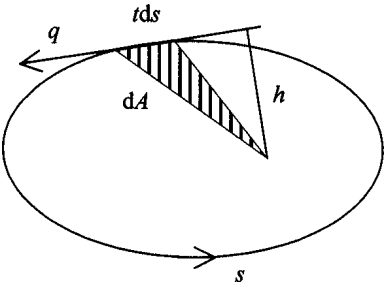

Figure 2.31: Torsional moment.

Regarding description in terms of the stress function F (Section 2.3.1), the condition of pure torsion requests that $F =$ constant along the outer and inner contours of the cross-section. The assumption of a constant shear stress over the thickness is equivalent to a linear variation of F between the contours limiting the cross-section. For convenience, let an example be constructed by considering the solution of the elastic problem for the solid cross-section and defining the inner contour of a ring along the isoline ($F =$ constant) next to the outer contour. The elastic solution for the ring cross-section is given by the surface F between the two contours and determines the equilibrated torque T. The assumption of a linear stress function based on the small thickness of the ring neglects variations in the tangent of the surface over the thickness.

The above simplification in elasticity may be transferred to the case of hardening plasticity [6]. In the fully plastic state, the assumption of a constant shear flow is, however, not compatible with the requirement $\tau = \tau_s =$ constant everywhere along the periphery unless the thickness of the cylindrical shell is constant. In the case of constant thickness ($t =$ constant) the plastic limit moment determined for an arbitrary cross-section from eqn (2.179) amounts to

$$T_F = 2\tau_s t A = 2q_s A. \tag{2.180}$$

The quantity

$$q_s = \tau_s t \tag{2.181}$$

defines a critical value for the shear flow q.

Conversely, if the stress distribution in a rod of solid (or thick-walled) cross-section allows representation by shear flow in an assembly of tubes of constant thickness, the torque at the plastic limit can be obtained from differential contributions by eqn (2.180). With reference to Fig. 2.32, the cross-section area of tube elements is $\mathrm{d}A = tS$, and therefore

$$\mathrm{d}T_F = 2\tau_s t A = 2\tau_s \frac{A}{S}\mathrm{d}A,$$

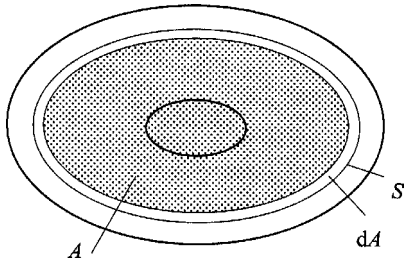

Figure 2.32: Representation of a solid cross-section.

where S denotes the length of the perimeter enclosing the area A. Integrating over the solid cross-section,

$$T_{\mathrm{F}} = 2\tau_{\mathrm{s}} \int \frac{A}{S} \mathrm{d}A, \tag{2.182}$$

which can be used as an alternative to eqn (2.106) under the specified restrictions.

2.4 Problems

1. The truss structure investigated in Section 2.1.3 exhibits in the elastic range the force–displacement relationship

$$P = \frac{3 + 2\sqrt{3}}{1 + \sqrt{3}} \frac{k}{2} u, \qquad k = \frac{EA}{h}.$$

In the elastoplastic range this becomes

$$P - P_{\mathrm{s}} = \frac{1}{1 + \sqrt{3}} \frac{k}{2} (u - u_{\mathrm{s}}),$$

where u_{s} is the vertical displacement of the loaded node at the elasticity limit $P = P_{\mathrm{s}}$. Arrive at the above result and compare the stiffness of the system below and beyond the elasticity limit.

2. The truss depicted in Fig. 2.33 is a modification of the case study in Section 2.1.3. In the present configuration the cross-sections of the bars

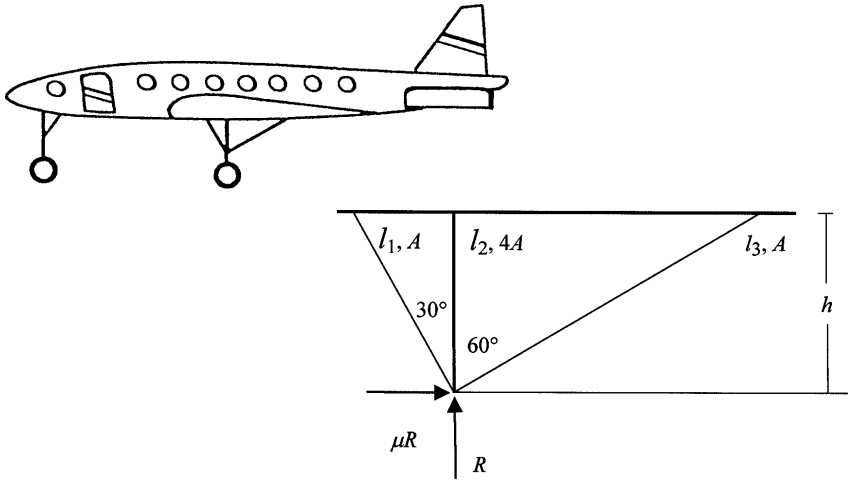

Figure 2.33: Problem 2.

differ, and therefore determination of the sequence of plastic yielding cannot be based on the bar forces but requires consideration of the stresses. Furthermore, the ground reaction force exhibits a vertical component R and a horizontal component $\mu R = R/2$ representing ground friction.

Obtain the elastic, elastoplastic and residual state in the bars after unloading from the plastic limit. To check the solution, the elastic limit and the plastic limit are given as

$$R_{\mathrm{s}} = 4\frac{3+2\sqrt{3}}{10+\sqrt{3}}S_{\mathrm{s}} \quad \text{and} \quad R_{\mathrm{F}} = (1+\sqrt{3})S_{\mathrm{s}},$$

respectively ($S_{\mathrm{s}} = \sigma_{\mathrm{s}} A$).

3. The background developed in Section 2.1.4 for the beam under pure bending will be utilized for the treatment of loading by a lateral force. If the effect of shear is neglected, the problem reduces to that of a bending moment varying along the longitudinal axis.

For the elastic–perfectly plastic beam shown in Fig. 2.34 (E, σ_{s}), the critical cross-section at $z = 0$ determines the elastic limit and the plastic limit as

$$P_{\mathrm{s}} = \frac{2}{3}\frac{bh^2}{l}\sigma_{\mathrm{s}} \quad \text{and} \quad P_{\mathrm{F}} = \frac{bh^2}{l}\sigma_{\mathrm{s}},$$

respectively. At $P = P_{\mathrm{F}}$, confirm that the extent of the plastified zone along the beam is $(z/l)_{\mathrm{p}} = 1/3$, and determine the elastic core ξ/h in the cross-sections as a function of the position z/l. Obtain the distribution of the residual stress in the end cross-section ($z = 0$) after unloading from P_{F}. Prepare a graphical representation of the above results.

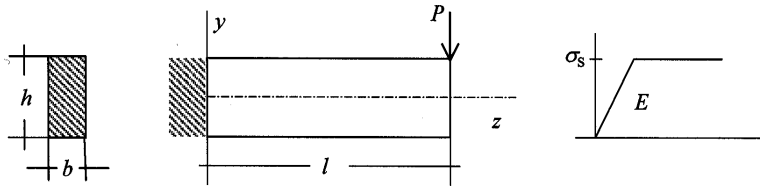

Figure 2.34: Problem 3.

4. As an extension of the case study in Section 1.2.5 for the laterally constrained plate ($\gamma_{\mathrm{yy}} = 0$) under tension, a shear stress is superposed here (Fig. 2.35). The loading at the vertical sides of the plate consists of the tensile stress $\sigma_{\mathrm{xx}} = \sigma\cos\varphi$ and the shear stress $\sigma_{\mathrm{xy}} = \sigma\sin\varphi\,(0 \le \varphi \le \pi/2)$. The material is modelled as elastic–perfectly plastic ($E, \nu, \tau_{\mathrm{s}}$).

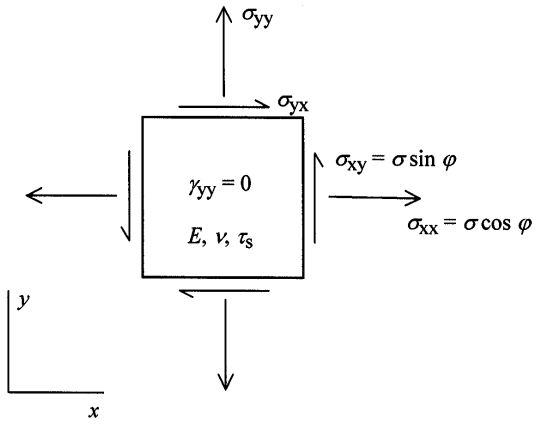

Figure 2.35: Problem 4.

Confirm that the von Mises yield criterion predicts the limits of the elastoplastic range as follows:

$$\frac{3}{(1-\nu+\nu^2)\cos^2\varphi+3\sin^2\varphi} \le \left(\frac{\sigma}{\tau_{\rm s}}\right)^2 \le \frac{1}{\sin^2\varphi+\frac{1}{4}\cos^2\varphi}.$$

For the choice $\nu = 0$, depict the elastic and plastic limits given above as a function of the parameter φ. Deduce an expression for the quotient $(\mathrm{d}\eta_{\rm xx} - \mathrm{d}\eta_{\rm yy})/\mathrm{d}\eta_{\rm xy}$ of the incremental plastic strain. Show that the stress state left after unloading from the plastic limit is defined by

$$(\sigma_{\rm xx})_{\rm r} = (\sigma_{\rm xy})_{\rm r} = 0\,, \quad (\sigma_{\rm yy})_{\rm r} = \frac{\left(\frac{1}{2}-\nu\right)\cos\varphi}{\left(\sin^2\varphi+\frac{1}{4}\cos^2\varphi\right)^{1/2}}\tau_{\rm s}.$$

5. The thin-walled circular cylinder shown in Fig. 2.36 is subjected to internal pressure p and a torque T. The material is assumed to be elastic–perfectly plastic $(E, \nu, \sigma_{\rm s})$ obeying the von Mises yield criterion. Only membrane stresses $(\sigma_{\varphi\varphi}, \sigma_{\rm zz}, \sigma_{{\rm z}\varphi})$ are considered; the longitudinal strain is suppressed $(\gamma_{\rm zz} = 0)$.

Determine the state of stress in the elastic range as

$$\sigma_{\varphi\varphi} = p\frac{a}{t}\,, \quad \sigma_{\rm zz} = \nu\sigma_{\varphi\varphi}\,, \quad \sigma_{{\rm z}\varphi} = \frac{T}{2\pi a^2 t}$$

and establish the relationship between the components $\sigma_{\varphi\varphi}$ and $\sigma_{{\rm z}\varphi}$ at the elasticity limit $\sigma_{\rm s}$. In the elastoplastic regime, deduce the axial stress $\sigma_{\rm zz}$ from the yield condition. Show that at the plastic limit $(\sigma_{\rm zz} = \sigma_{\varphi\varphi}/2)$ these components are related by

$$\frac{1}{4}\sigma_{\varphi\varphi}^2 + \sigma_{{\rm z}\varphi}^2 = \frac{\sigma_{\rm s}^2}{3}$$

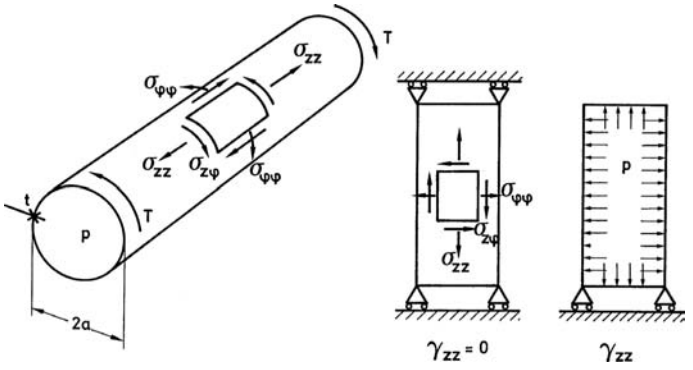

Figure 2.36: Problem 5.

and prepare a graphical representation of the $\sigma_{\varphi\varphi}, \sigma_{z\varphi}$ relationship at the elastic and plastic limits for $\nu = 0$.

Alternatively, for the unconstrained cylinder ($\gamma_{zz} \neq 0$) we have,

$$\sigma_{zz} = \frac{p}{2}\frac{a}{t} = \frac{1}{2}\sigma_{\varphi\varphi}$$

and the condition limiting the elastic range here coincides with the plastic limit of the previous constrained case. Also, the elastic and plastic limits are now unique since the system has become statically determinate.

Suppose in one loading programme, the elasticity limit is attained by the pressure p acting alone, and plastic flow is then induced by applying a torque at the rate $\dot{T}$ while $p =$ constant. In a different loading programme, the torque T is applied alone up to the elasticity limit, and plastic flow is then induced by the application of the pressure at the rate $\dot{p}$ while $T =$ constant. Study the momentary direction of the plastic flow in the two cases respectively.

6. (a) A rod of constant cross-section is subjected to torsion (perfectly plastic material, yield stress in shear τ_s). Discuss the Prandtl stress function in the fully plastic range and confirm the associated limit torque for the following cross-sections (Fig. 2.37):

$$\text{Quadratic (side length } a\text{):} \quad T_F = \frac{1}{3}a^3\tau_s,$$

$$\text{Circular ring (radius } a, b\text{):} \quad T_F = \frac{2}{3}\pi(b^3 - a^3)\tau_s,$$

$$\text{Circular shell (thickness } t\text{):} \quad T_F = 2\pi a^2 t\tau_s.$$

(b) In addition, consider a rectangular cross-section $a \times b$, a compound cross-section (hemicircle $a/2$, rectangle $a \times (b - a)$), a regular triangle with

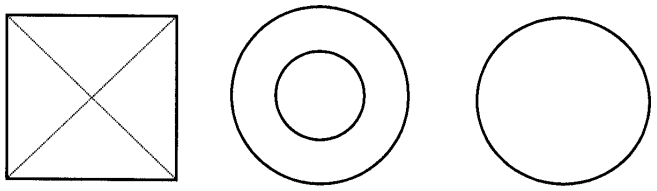

Figure 2.37: Problem 6(a).

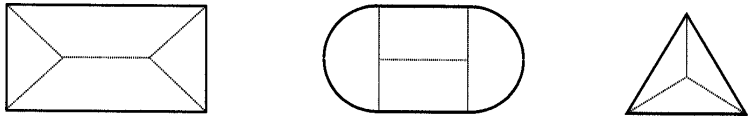

Figure 2.38: Problem 6(b).

side-length a (Fig. 2.38). Check the results by the alternative shear flow approach given in Section 2.3.6:

$$T_{\mathrm{F}} = \frac{1}{6}(3b-a)a^2\tau_{\mathrm{s}}, \quad T_{\mathrm{F}} = \left(2b+\pi\frac{a}{3}\right)\left(\frac{a}{2}\right)^2\tau_{\mathrm{s}}, \quad T_{\mathrm{F}} = \frac{2}{3}\left(\frac{a}{2}\right)^3\tau_{\mathrm{s}}.$$

7. Based on the geometrical interpretation of the stress function $F(x,y)$ in torsion as a surface, reflect on the transition from the elastic to the fully plastic state and discuss the meaning of the continuity condition given in eqn (2.121).

References

[1] A. Mendelson, *Plasticity – Theory and Application*, Macmillan, New York, 1968.

[2] S. Timoshenko and J.N. Goodier, *Theory of Elasticity*, 3rd edn, McGraw-Hill, New York, 1970.

[3] L. Prandtl, Zur Torsion von prismatischen Stäben, *Z. Physik* **4** (1903) 758–759.

[4] A. Nadai, *Theory of Flow and Fracture of Solids*, Vol. I, 2nd edn, McGraw-Hill, New York, 1950.

[5] H. Puhl, On the modelling of real sand piles, *Physica A* **182** (1992) 295–319.

[6] L.M. Kachanov, *Foundations of the Theory of Plasticity*, North-Holland, Amsterdam, 1971.

[7] S. Kaliszky, *Plasticity – Theory and Engineering Applications*, Studies in Applied Mechanics 21, Elsevier, Amsterdam, 1989.

[8] R. Bredt, *VDI* **40** (1896) 815.

This page intentionally left blank

CHAPTER 3

Load-carrying capacity of perfectly plastic systems

3.1 Introductory remarks

Perfectly plastic materials are characterized completely by the yield stress σ_s limiting the elastic range. In this case, the load-carrying capacity of a uniaxial tensile specimen is exhausted once the elasticity limit is reached. The specimen then exhibits a tendency to extend further by plastic flow at constant stress. Truss structures assembled from bar members do not reach the elastic limit of the material everywhere at the same time, and therefore the externally applied loads can be increased beyond the limit of incipient yield as long as the magnitude of the stress can still be increased in some members. Multiaxial stress in perfectly plastic solids at the state of yield can be subjected to variations under observance of the yield condition. The ability of the system to sustain an increasing loading is exhausted when stresses need not be changed for continuing plastic flow. Examples have been given in Chapters 1 and 2.

From the above considerations, it can be concluded that structures of perfectly plastic material are characterized by a limited load-carrying capacity. At limit load the structure may undergo plastic flow at constant applied forces. At the incipient stage of plastic deformation under investigation, the geometrical dimensions are assumed constant. An estimation of the load-carrying capacity of perfectly plastic structures will be based on two concepts, one concerning the system and the other the material. These are the principle of virtual work and Drucker's plasticity postulate, respectively.

3.1.1 The principle of virtual work

Consider a deformable body subjected to body forces $\mathbf{f}$ and to surface forces $\mathbf{t}$ (Chapter 2). Let $\widetilde{\boldsymbol{\sigma}}(\mathbf{x})$ denote a virtual stress field which satisfies the static equilibrium in the interior

$$\boldsymbol{\partial}^{\mathrm{t}}\widetilde{\boldsymbol{\sigma}} + \mathbf{f} = \mathbf{0}, \tag{3.1}$$

and the boundary condition

$$\mathbf{N}^{\mathrm{t}}\widetilde{\boldsymbol{\sigma}} = \mathbf{t}. \tag{3.2}$$

Since no further restrictions are imposed on the virtual stresses $\widetilde{\boldsymbol{\sigma}}$, there will generally exist more than one statically admissible stress distribution, satisfying the static equilibrium as stated by eqns (3.1) and (3.2). One of them is the actual stress field in the loaded system.

Independently, let $\dot{\underset{\sim}{\mathbf{u}}}(\mathbf{x})$ be a virtual velocity field compatible with the requirement to maintain the integrity of the body and with the kinematic boundary conditions. From the virtual velocity field, a strain rate can be derived as

$$\dot{\underset{\sim}{\boldsymbol{\gamma}}} = \boldsymbol{\partial}\dot{\underset{\sim}{\mathbf{u}}} \tag{3.3}$$

and is kinematically admissible for the system under consideration. The above requirements define in general a class of virtual velocities $\dot{\underset{\sim}{\mathbf{u}}}$ and associated strain rates $\dot{\underset{\sim}{\boldsymbol{\gamma}}}$, including the actual velocity field and strain rate.

The principle of virtual work, presented in the rate form, reads

$$\int_V \mathbf{f}^{\mathrm{t}}\dot{\underset{\sim}{\mathbf{u}}}\mathrm{d}V + \int_S \mathbf{t}^{\mathrm{t}}\dot{\underset{\sim}{\mathbf{u}}}\mathrm{d}S = \int_V \widetilde{\boldsymbol{\sigma}}^{\mathrm{t}}\dot{\underset{\sim}{\boldsymbol{\gamma}}}\mathrm{d}V. \tag{3.4}$$

Accordingly, the rate of work (power) performed by the applied forces $\mathbf{f}, \mathbf{t}$ on the virtual velocity equals the power of the virtual stress on the virtual strain rate in the body. It is pointed out that the virtual stress and virtual strain rate may be completely independent. The former must only establish the static equilibrium with the applied forces, while the latter is derived from an assumed velocity field which is kinematically admissible. In eqn (3.4) the rate of work of the distributed forces may have to be supplemented by the contribution $\sum_{j=1}^{K} \mathbf{P}_j^{\mathrm{t}}\dot{\underset{\sim}{\mathbf{u}}}_j$ of any loading represented by discrete forces $\mathbf{P}_j$ at single locations $j = 1, ..., K$; $\dot{\underset{\sim}{\mathbf{u}}}_j$ denotes the respective virtual velocity.

3.1.2 Drucker's plasticity postulate

The postulate refers to the material properties in plasticity and was formulated by Drucker [1], thus it bears his name. Figure 3.1 reproduces the uniaxial stress–strain diagram for an elastoplastic hardening material. In order to avoid any apparent assumption of particular conditions, let the tensile specimen have previously been deformed plastically and now be subjected to a certain stress level σ_{o} below the flow stress pertaining to the experienced plastic strain.

An additional loading programme increases the stress level in the specimen until the value σ where the actual yield limit is attained. Further increase by the stress increment $\mathrm{d}\sigma$ is then associated with plastic flow, producing the increment $\mathrm{d}\eta$ in plastic strain. Subsequently, the additional

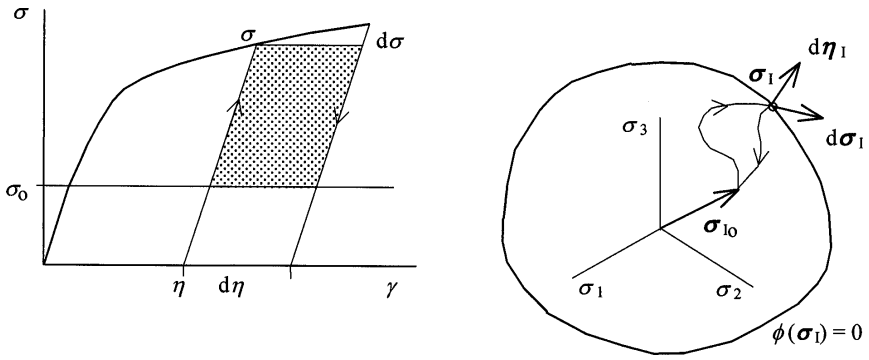

Figure 3.1: On the formulation of Drucker's plasticity postulate.

stress is removed and the original level σ_o is restored. The mechanical work dissipated in the cycle by the excess stress is given by the expression

$$dw = (\sigma - \sigma_o)d\eta + \frac{1}{2}\, d\sigma d\eta > 0. \tag{3.5}$$

The inequality sign in eqn (3.5) is a consequence of the dissipative nature of plastic deformation. For the particular choice $\sigma_o = \sigma$ it expresses the hardening property of the material:

$$d\sigma d\eta > 0 \quad \text{and} \quad \frac{d\sigma}{d\eta} > 0.$$

This property is associated with material stability in the sense that the increase in magnitude of the strain requires an increase in magnitude of the stress. In perfect plasticity deformation occurs at constant stress such that $d\sigma d\eta = 0$, which for $\sigma_o \neq \sigma$ modifies the requirement in eqn (3.5) to $dw = (\sigma - \sigma_o)d\eta > 0$.

The counterpart of eqn (3.5) under multiaxial conditions is obtained analogously starting at a stress state $\boldsymbol{\sigma}_o$ in the elastic domain, $\phi(\boldsymbol{\sigma}_o, ...) < 0$, of the material which might have already experienced plastic deformation (the dots '...' stand for the actual value of the hardening parameters). The material is then stressed to a plastic state $\boldsymbol{\sigma}$ where $\phi(\boldsymbol{\sigma}, ...) = 0$, and an additional increment in stress, $d\boldsymbol{\sigma}$, produces the incremental plastic strain $d\boldsymbol{\eta}$. Thereafter the original stress state $\boldsymbol{\sigma}_o$ is restored. A pictorial representation is given in Fig. 3.1 with reference to the deviatoric plane in principal space. Drucker's plasticity postulate requires the work of the additionally applied stresses in the cycle to be positive:

$$dw = [\boldsymbol{\sigma} - \boldsymbol{\sigma}_o]^t d\boldsymbol{\eta} + \frac{1}{2}\, d\boldsymbol{\sigma}^t d\boldsymbol{\eta} > 0. \tag{3.6}$$

The above refers to a hardening material. In perfect plasticity the second-order term is set equal to zero and the work may vanish. The postulate will be elucidated by a number of applications to follow.

Equation (3.6) contains fundamental statements of the mathematical theory of plasticity, which will be deduced below assuming smoothness of the yield function in stress space or of parts of it, and avoiding singular locations. Furthermore, the postulate will be utilized when discussing load-carrying capacity and shakedown.

Normality of plastic flow

The perfectly plastic case is defined by setting in eqn (3.6) the second-order term equal to zero

$$\mathrm{d}\boldsymbol{\sigma}^{\mathrm{t}}\mathrm{d}\boldsymbol{\eta} = 0, \tag{3.7}$$

from which the increment of plastic strain is orthogonal to the increment of stress. At the same time, the stress changes that induce plastic flow are here tangential to the yield surface $\phi(\boldsymbol{\sigma}) = 0$ such that $[\mathrm{d}\phi/\mathrm{d}\boldsymbol{\sigma}]\mathrm{d}\boldsymbol{\sigma} = 0$. Therefore, the strain increment in eqn (3.7) must be normal to the yield surface along the gradient of the yield function,

$$\mathrm{d}\boldsymbol{\eta} = \Lambda \left[\frac{\mathrm{d}\phi}{\mathrm{d}\boldsymbol{\sigma}}\right]^{\mathrm{t}}. \tag{3.8}$$

Interpretation of the first-order term in eqn (3.6) for $\boldsymbol{\sigma}_{\mathrm{o}} = \mathbf{0}$ along with eqn (3.8) gives

$$\mathrm{d}w = \boldsymbol{\sigma}^{\mathrm{t}}\mathrm{d}\boldsymbol{\eta} = \Lambda \frac{\mathrm{d}\phi}{\mathrm{d}\boldsymbol{\sigma}}\boldsymbol{\sigma} > 0. \tag{3.9}$$

This requires the plastic strain increment $\mathrm{d}\boldsymbol{\eta}$ at stress state $\boldsymbol{\sigma}$ to point outwards from the yield surface, and the scalar multiplier to be a positive quantity, $\Lambda > 0$.

For the hardening material, taking $\boldsymbol{\sigma}_{\mathrm{o}} = \boldsymbol{\sigma}$ in eqn (3.6), the plasticity postulate requires that

$$\mathrm{d}\boldsymbol{\sigma}^{\mathrm{t}}\mathrm{d}\boldsymbol{\eta} > 0, \tag{3.10}$$

which is satisfied by the normality statement for the incremental plastic strain, eqn (3.8). Here, $\phi(\boldsymbol{\sigma}, ...) = 0$ and

$$\mathrm{d}\boldsymbol{\eta} = \Lambda \left[\frac{\partial\phi}{\partial\boldsymbol{\sigma}}\right]^{\mathrm{t}}. \tag{3.11}$$

In fact, substituting eqn (3.11) in eqn (3.10), one confirms that

$$\mathrm{d}\boldsymbol{\sigma}^{\mathrm{t}}\mathrm{d}\boldsymbol{\eta} = \Lambda \frac{\partial\phi}{\partial\boldsymbol{\sigma}}\mathrm{d}\boldsymbol{\sigma} > 0. \tag{3.12}$$

The term $[\partial\phi/\partial\boldsymbol{\sigma}]\mathrm{d}\boldsymbol{\sigma}$ must be positive for the occurrence of plastic flow in the case of hardening, and $\Lambda > 0$ as stated previously.

If the plastic flow were allowed to possess a component $\mathrm{d}\boldsymbol{\eta}_\mathrm{t}$ tangential to the yield surface in addition to the normal one $\mathrm{d}\boldsymbol{\eta}_\mathrm{n}$ such that $\mathrm{d}\boldsymbol{\eta} = \mathrm{d}\boldsymbol{\eta}_\mathrm{n} + \mathrm{d}\boldsymbol{\eta}_\mathrm{t}$, then the work expression

$$\mathrm{d}\boldsymbol{\sigma}^\mathrm{t}\mathrm{d}\boldsymbol{\eta} = \mathrm{d}\boldsymbol{\sigma}^\mathrm{t}\mathrm{d}\boldsymbol{\eta}_\mathrm{n} + \mathrm{d}\boldsymbol{\sigma}^\mathrm{t}\mathrm{d}\boldsymbol{\eta}_\mathrm{t} \tag{3.13}$$

is not necessarily positive. The first term on the right-hand side of the equation is positive by the normality condition. However, the second contribution may be negative because the inducing stress increment $\mathrm{d}\boldsymbol{\sigma}$ can assume an arbitrary direction relative to $\mathrm{d}\boldsymbol{\eta}$, the direction of the latter being fixed by the stress state $\boldsymbol{\sigma}$.

A graphical interpretation of the normality condition is given in Fig. 3.2 for the deviatoric plane in principal stress space. Assuming a plastic state $\boldsymbol{\sigma}_\mathrm{I}$ defining a point on the yield surface $\phi = 0$, plastic flow is induced by stress increments $\mathrm{d}\boldsymbol{\sigma}_\mathrm{I}$ pointing out from the yield surface. According to the notion of the flow rule, the direction of the plastic strain increment depends on the stress state where the flow occurs but not on the stress increment inducing the flow. For this reason, only increments of plastic strain $\mathrm{d}\boldsymbol{\eta}_\mathrm{I}$ that are directed along the exterior normal to the yield surface at $\boldsymbol{\sigma}_\mathrm{I}$ satisfy eqn (3.10). For any other assumed direction of $\mathrm{d}\boldsymbol{\eta}_\mathrm{I}$, inducing stress increments $\mathrm{d}\boldsymbol{\sigma}_\mathrm{I}$ may be found for which eqn (3.10) is not satisfied.

Convexity of the yield surface

The satisfaction of eqn (3.10) by the normality condition for plastic flow allows the first term in the work expression of eqn (3.6) to be

$$[\boldsymbol{\sigma} - \boldsymbol{\sigma}_\mathrm{o}]^\mathrm{t}\mathrm{d}\boldsymbol{\eta} \geq 0. \tag{3.14}$$

The significance of eqn (3.14) for the yield surface is visualized by the vectorial representation of stress and plastic strains in principal space (Fig. 3.2 (right)). Let $\boldsymbol{\sigma}_\mathrm{I}$ be a stress state on the yield surface, $\phi(\boldsymbol{\sigma}_\mathrm{I}) = 0$, where plastic flow occurs as specified by the incremental plastic strain $\mathrm{d}\boldsymbol{\eta}_\mathrm{I}$ along the external normal. Different stress states $\boldsymbol{\sigma}_\mathrm{Io}$ on the yield surface, $\phi(\boldsymbol{\sigma}_\mathrm{Io}) = 0$, satisfy eqn (3.14) only if the vectors $\boldsymbol{\sigma}_\mathrm{Io}$ are within the interior side of the tangent plane at $\boldsymbol{\sigma}_\mathrm{I}$. As a consequence, the yield surface is locally convex.

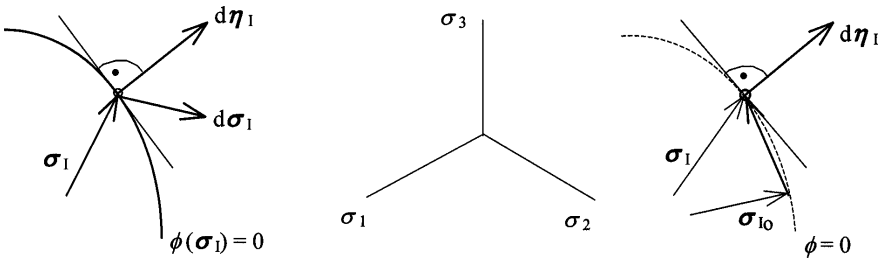

Figure 3.2: Normality of plastic flow and convexity of yield surface.

The same can be concluded for the vicinity of any other plastic state $\boldsymbol{\sigma}_\mathrm{I}$ and thus the yield surface is entirely convex.

3.1.3 Uniqueness of incremental elastoplastic solutions

The general principles presented so far will be utilized next to discuss the uniqueness of incremental elastoplastic solutions. For this purpose, we consider a certain instant in the course of the loading programme where the mechanical state in the solid is assumed to be uniquely known as a result of previous evolution. The momentary change of the applied loads at this state is specified by the time rates $\dot{\mathbf{f}}$ and $\dot{\mathbf{t}}$ of the body and surface forces, respectively. The solution of the elastoplastic problem furnishes the velocity $\dot{\mathbf{u}}$, strain rate $\dot{\boldsymbol{\gamma}}$ and stress rate $\dot{\boldsymbol{\sigma}}$ depending on the position in the solid. Stress rate and strain rate are linked by the constitutive law of the elastoplastic material.

For an examination of the uniqueness of the solution of the rate elastoplastic problem, we assume that apart from the one solution $\dot{\mathbf{u}}_1, \dot{\boldsymbol{\gamma}}_1, \dot{\boldsymbol{\sigma}}_1$, a different solution $\dot{\mathbf{u}}_2, \dot{\boldsymbol{\gamma}}_2, \dot{\boldsymbol{\sigma}}_2$ might exist. Since either stress rate, $\dot{\boldsymbol{\sigma}}_1$ and $\dot{\boldsymbol{\sigma}}_2$, is in equilibrium with the same force system $\dot{\mathbf{f}}, \dot{\mathbf{t}}$, their difference does not exhibit any resultant force. Therefore, considering the virtual work for the difference $[\dot{\boldsymbol{\sigma}}_2 - \dot{\boldsymbol{\sigma}}_1]$ the left-hand side of eqn (3.4) vanishes identically for any admissible velocity field, and the stress integral on the right-hand side is

$$\int_V [\dot{\boldsymbol{\sigma}}_2 - \dot{\boldsymbol{\sigma}}_1]^\mathrm{t} [\dot{\boldsymbol{\gamma}}_2 - \dot{\boldsymbol{\gamma}}_1] \mathrm{d}V = 0. \tag{3.15}$$

Use of the difference $[\dot{\boldsymbol{\gamma}}_2 - \dot{\boldsymbol{\gamma}}_1]$ as an admissible strain is justified since both $\dot{\boldsymbol{\gamma}}_1$ and $\dot{\boldsymbol{\gamma}}_2$ are assumed to be solutions and thus kinematically compatible. Utilization in expressing the virtual work statement for $\dot{\boldsymbol{\sigma}}_1$, $\dot{\boldsymbol{\sigma}}_2$ individually and subtraction also leads to the result of eqn (3.15).

The integrand in eqn (3.15) can be detailed as

$$\begin{aligned} &[\dot{\boldsymbol{\sigma}}_2 - \dot{\boldsymbol{\sigma}}_1]^\mathrm{t} [\dot{\boldsymbol{\gamma}}_2 - \dot{\boldsymbol{\gamma}}_1] \\ &\quad = [\dot{\boldsymbol{\sigma}}_2 - \dot{\boldsymbol{\sigma}}_1]^\mathrm{t} [\dot{\boldsymbol{\varepsilon}}_2 - \dot{\boldsymbol{\varepsilon}}_1] + [\dot{\boldsymbol{\sigma}}_2 - \dot{\boldsymbol{\sigma}}_1]^\mathrm{t} [\dot{\boldsymbol{\eta}}_2 - \dot{\boldsymbol{\eta}}_1]. \end{aligned} \tag{3.16}$$

The analysis of the strain rate in eqn (3.16) into elastic and plastic contributions helps to discuss the impact of the respective material properties separately. In isotropy, the term with the elastic part of the strain rate can be transformed by the relationships for deviatoric and hydrostatic quantities, eqns (1.44) and (1.42), to

$$\begin{aligned} &[\dot{\boldsymbol{\sigma}}_2 - \dot{\boldsymbol{\sigma}}_1]^\mathrm{t} [\dot{\boldsymbol{\varepsilon}}_2 - \dot{\boldsymbol{\varepsilon}}_1] \\ &\quad = \frac{1}{2G} [\dot{\boldsymbol{\sigma}}_2 - \dot{\boldsymbol{\sigma}}_1]_\mathrm{D}^\mathrm{t} [\dot{\boldsymbol{\sigma}}_2 - \dot{\boldsymbol{\sigma}}_1]_\mathrm{D} + \frac{1}{3K} [\dot{\boldsymbol{\sigma}}_2 - \dot{\boldsymbol{\sigma}}_1]_\mathrm{H}^\mathrm{t} [\dot{\boldsymbol{\sigma}}_2 - \dot{\boldsymbol{\sigma}}_1]_\mathrm{H} > 0. \end{aligned} \tag{3.17}$$

The right-hand side of eqn (3.17) consists of sums of quadratic terms multiplied by the elastic constants; it is positive unless $\dot{\boldsymbol{\sigma}}_2 = \dot{\boldsymbol{\sigma}}_1$, in which case

it vanishes. Isotropy is not a necessary assumption; the properties of the matrix $\boldsymbol{\kappa}$ ensure that the work of elastic deformation is positive such that $\boldsymbol{\sigma}^{\mathrm{t}}\boldsymbol{\varepsilon} = \boldsymbol{\varepsilon}^{\mathrm{t}}\boldsymbol{\kappa}\boldsymbol{\varepsilon} > 0$ for any $\boldsymbol{\sigma} = \boldsymbol{\kappa}\boldsymbol{\varepsilon} \neq \mathbf{0}$.

Next, considering locations where a plastic strain rate also appears in eqn (3.16), we write the respective term as

$$[\dot{\boldsymbol{\sigma}}_2 - \dot{\boldsymbol{\sigma}}_1]^{\mathrm{t}}[\dot{\boldsymbol{\eta}}_2 - \dot{\boldsymbol{\eta}}_1] = \dot{\boldsymbol{\sigma}}_2^{\mathrm{t}}\dot{\boldsymbol{\eta}}_2 - \dot{\boldsymbol{\sigma}}_2^{\mathrm{t}}\dot{\boldsymbol{\eta}}_1 - \dot{\boldsymbol{\sigma}}_1^{\mathrm{t}}\dot{\boldsymbol{\eta}}_2 + \dot{\boldsymbol{\sigma}}_1^{\mathrm{t}}\dot{\boldsymbol{\eta}}_1 \geq 0. \tag{3.18}$$

We restrict the verification of eqn (3.18) to perfect plasticity in which case $\dot{\boldsymbol{\sigma}}_1, \dot{\boldsymbol{\sigma}}_2$ are tangential to the yield surface at the plastic state considered, and $\dot{\boldsymbol{\eta}}_1, \dot{\boldsymbol{\eta}}_2$ are normal to it. Therefore, all scalar products in eqn (3.18) vanish. If one of the stress rates does not induce plastic flow, its scalar product with the other plastic strain rate is negative and makes the expression positive.

From the above discussion it follows that the integrand in eqn (3.15) is always positive, and the volume integral vanishes only if the solution for the stress rate is unique, $\dot{\boldsymbol{\sigma}}_2 = \dot{\boldsymbol{\sigma}}_1 = \dot{\boldsymbol{\sigma}}$.

Formally, perfect plasticity is characterized by the condition of a non-varying yield surface $\phi(\boldsymbol{\sigma}) = 0$:

$$\dot{\phi} = \frac{\mathrm{d}\phi}{\mathrm{d}\boldsymbol{\sigma}}\dot{\boldsymbol{\sigma}}_1 = \frac{\mathrm{d}\phi}{\mathrm{d}\boldsymbol{\sigma}}\dot{\boldsymbol{\sigma}}_2 = 0. \tag{3.19}$$

By the normality of plastic flow,

$$\dot{\boldsymbol{\eta}}_1 = \Lambda_1 \left[\frac{\mathrm{d}\phi}{\mathrm{d}\boldsymbol{\sigma}}\right]^{\mathrm{t}}, \quad \dot{\boldsymbol{\eta}}_2 = \Lambda_2 \left[\frac{\mathrm{d}\phi}{\mathrm{d}\boldsymbol{\sigma}}\right]^{\mathrm{t}}. \tag{3.20}$$

In the two cases, the derivative $\mathrm{d}\phi/\mathrm{d}\boldsymbol{\sigma}$ is unique since it refers to the same plastic state. Use of eqn (3.20) in eqn (3.18) and observance of eqn (3.19) reveals that either expression in eqn (3.18) vanishes and confirms the equality to zero. If at certain locations one of the rate solutions, say $\dot{\boldsymbol{\sigma}}_1$, induces plastic flow while the other causes elastic unloading, the set of equations (3.19) and (3.20) assumes the form

$$\frac{\mathrm{d}\phi}{\mathrm{d}\boldsymbol{\sigma}}\dot{\boldsymbol{\sigma}}_1 = 0, \qquad \frac{\mathrm{d}\phi}{\mathrm{d}\boldsymbol{\sigma}}\dot{\boldsymbol{\sigma}}_2 < 0 \tag{3.21}$$

and

$$\dot{\boldsymbol{\eta}}_1 = \Lambda_1 \left[\frac{\mathrm{d}\phi}{\mathrm{d}\boldsymbol{\sigma}}\right]^{\mathrm{t}}, \quad \dot{\boldsymbol{\eta}}_2 = \mathbf{0}. \tag{3.22}$$

This makes several terms in eqn (3.18) equal to zero except for a negative term $\dot{\boldsymbol{\sigma}}_2^{\mathrm{t}}\dot{\boldsymbol{\eta}}_1$ which causes the expression to be positive. The inequality sign in eqn (3.18) is thus justified. The treatment for hardening material is left as an exercise to the reader.

3.1.4 Plastic limit

We define the plastic limit as the mechanical state of an elastic–perfectly plastic system at which deformation may be momentarily continued while the applied forces are kept constant. In this sense the load-carrying capacity of the system is then exhausted, the applied forces constitute a *limit load* system (or collapse load). If the loading consists of body forces $\mathbf{f}$ and surface

forces $\mathbf{t}$, or is represented by discrete forces $\mathbf{P}_j\,(j=1,\ldots,K)$, their value at the plastic limit is denoted by $\mathbf{f}_{\mathrm{F}}, \mathbf{t}_{\mathrm{F}}$ and $\mathbf{P}_{\mathrm{F}j}$, respectively. At this state, a velocity field $\dot{\mathbf{u}}_{\mathrm{F}}$ will be found that deforms the body at constant applied forces: $\dot{\mathbf{P}}_{\mathrm{F}j}=\mathbf{0}, \dot{\mathbf{f}}_{\mathrm{F}}=\mathbf{0}, \dot{\mathbf{t}}_{\mathrm{F}}=\mathbf{0}$. The stress rate $\dot{\boldsymbol{\sigma}}_{\mathrm{F}}=\mathbf{0}$ can be associated with the vanishing rate of the external loading and, following previous discussion, it represents a unique solution to the rate problem. In conformity with the vanishing stress rate, the rate of elastic strain vanishes as well, and the rate of strain deduced from $\dot{\mathbf{u}}_{\mathrm{F}}$ is entirely plastic in nature:

$$\dot{\boldsymbol{\eta}}_{\mathrm{F}} \equiv \dot{\boldsymbol{\gamma}}_{\mathrm{F}} = \boldsymbol{\partial}\dot{\mathbf{u}}_{\mathrm{F}}. \tag{3.23}$$

The velocity field $\dot{\mathbf{u}}_{\mathrm{F}}$ is called a *yield* or *flow mechanism*; it is inherent to the plastic limit state.

Once the plastic strain rate $\dot{\boldsymbol{\eta}}$ is locally known, the gradient $\mathrm{d}\phi/\mathrm{d}\boldsymbol{\sigma}^{\mathrm{t}}$ of the yield function (directed along $\dot{\boldsymbol{\eta}}$) specifies the stress state $\boldsymbol{\sigma}$ at $\phi(\boldsymbol{\sigma})=0$ where plastic flow occurs. It can be concluded that the *power of dissipation* per unit volume (d) is a function of the plastic strain rate:

$$d = \boldsymbol{\sigma}^{\mathrm{t}}\dot{\boldsymbol{\eta}} = d(\dot{\boldsymbol{\eta}}) > 0. \tag{3.24}$$

The power of dissipation for a body of volume V is,

$$D = \int_V \boldsymbol{\sigma}^{\mathrm{t}}\dot{\boldsymbol{\eta}}\,\mathrm{d}V \tag{3.25}$$

For an assessment of a given level $\mathbf{f}, \mathbf{t}, \mathbf{P}_j\,(j=1,\ldots,K)$ of the applied forces with respect to the plastic limit, a *safety factor* n is introduced such that the set $n\mathbf{f}, n\mathbf{t}, n\mathbf{P}_j$ constitutes a limit load system. Thus

$$\mathbf{f}_{\mathrm{F}} = n\,\mathbf{f}, \quad \mathbf{t}_{\mathrm{F}} = n\,\mathbf{t}, \quad \mathbf{P}_{\mathrm{F}j} = n\mathbf{P}_j \quad (j=1,\ldots,K). \tag{3.26}$$

Accordingly, the system is loaded below the plastic limit if $n>1$. For $n<1$ the plastic limit is exceeded; $n=1$ reproduces the limit load.

The limit load theorems to follow in Sections 3.2 and 3.3 provide us with a means for estimating the safety of loaded perfectly plastic systems against collapse, without the necessity of a complete solution to the elastoplastic problem. An historical account on the subject is found in [2] along with a concise theoretical exposition.

Independently of the small strain assumption, the tendency of the system to deform may be of importance for the load carrying capacity. For an indication of the significance of the deforming geometry, we consider the tensile test under the force $P=\sigma A$ with both the stress σ and the cross-section area A varying during extension. Differentiating, stationary loading is characterized by the requirement

$$\frac{\mathrm{d}P}{P} = \frac{\mathrm{d}\sigma}{\sigma} + \frac{\mathrm{d}A}{A} = 0. \tag{i}$$

For constant volume $V = Al$ we simply have $\mathrm{d}A/A + \mathrm{d}l/l = 0$ where $\mathrm{d}l/l = \mathrm{d}\gamma$, the strain increment. Then from eqn (i),

$$\frac{\mathrm{d}\sigma}{\mathrm{d}\gamma} = \sigma. \tag{ii}$$

The above stationarity condition accounts for only instantaneous deformation; overall changes in geometry may be negligible. The tensile force attains a maximum at $\mathrm{d}P = 0$ for $\mathrm{d}\sigma/\mathrm{d}\gamma = \sigma > 0$, before the slope of the stress–strain diagram becomes zero. In perfect plasticity the condition of eqn (ii) is met at the yield stress, where the transition from elasticity with $\mathrm{d}\sigma/\mathrm{d}\gamma = E$ to plasticity with $\mathrm{d}\sigma/\mathrm{d}\gamma = 0$ occurs immediately.

Plastic flow of hollow cylinder

The plastic yielding of the thick-walled cylinder under internal pressure (inner radius a, outer radius b, Fig. 3.3) has been considered in Section 2.3.3; the solution of the plane strain problem was developed in terms of stress. In the following we explore the kinematics of the plastic flow at the limit state of the perfectly plastic solid, express the power of dissipation and determine the associated magnitude of the applied pressure.

Plane deformation of the axisymmetric problem is completely defined by the radial displacement u. Circumferential and axial components, along the φ-direction and the z-direction, are absent: $v = w = 0$. Description of the flow mechanism requires specification of the displacement velocity $\dot{u}(r) \equiv \dot{u}_{\mathrm{F}}(r)$ along the radius r. The strain deduced therefrom is entirely plastic in nature: $\dot{\boldsymbol{\gamma}} \equiv \dot{\boldsymbol{\eta}}$. The components of the strain rate in the radial and circumferential directions derive from the velocity of plastic flow as

$$\dot{\eta}_{\mathrm{r}} = \frac{\mathrm{d}\dot{u}}{\mathrm{d}r}, \quad \dot{\eta}_{\varphi} = \frac{\dot{u}}{r}; \tag{3.27}$$

the axial strain vanishes by definition. Substitution in the isochoric condition $\dot{\eta}_{\mathrm{r}} + \dot{\eta}_{\varphi} = 0$ constrains the velocity field $\dot{u}(r)$ by the differential equation

$$\frac{\mathrm{d}\dot{u}}{\mathrm{d}r} + \frac{\dot{u}}{r} = 0. \tag{3.28}$$

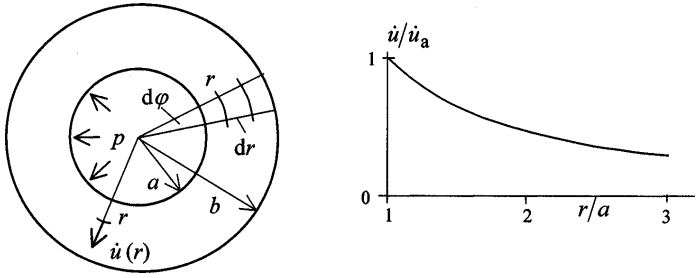

Figure 3.3: Yield mechanism for a hollow circular cylinder.

The above result is also arrived at by suppressing changes of the material volume element $r\mathrm{d}\varphi\mathrm{d}r\mathrm{d}z$ directly. With $\mathrm{d}r/\mathrm{d}t = \dot{r} = \dot{u}$,

$$\frac{\mathrm{d}}{\mathrm{d}t}(r\mathrm{d}\varphi\mathrm{d}r\mathrm{d}z) = (\dot{u}\mathrm{d}r + r\mathrm{d}\dot{u})\mathrm{d}\varphi\mathrm{d}z = 0. \tag{3.29}$$

This is equivalent to eqn (3.28) which supplies the velocity field as

$$\frac{\dot{u}}{\dot{u}_\mathrm{a}} = \frac{a}{r}. \tag{3.30}$$

The solution has been adapted to the (unknown) displacement velocity $\dot{u}_\mathrm{a}$ at inner radius $r = a$.

Use of eqn (3.30) in eqn (3.27) gives the strain components

$$\dot{\eta}_\varphi = \frac{a}{r}\frac{\dot{u}_\mathrm{a}}{r}, \quad \dot{\eta}_\mathrm{r} = -\frac{a}{r}\frac{\dot{u}_\mathrm{a}}{r} = -\dot{\eta}_\varphi. \tag{3.31}$$

The equivalent plastic strain rate becomes

$$\dot{\bar{\eta}} = \left[\frac{2}{3}(\dot{\eta}_\mathrm{r}^2 + \dot{\eta}_\varphi^2)\right]^{\frac{1}{2}} = \frac{2}{\sqrt{3}}\frac{a}{r}\frac{\dot{u}_\mathrm{a}}{r}. \tag{3.32}$$

With the flow mechanism as an admissible velocity field, the statement of virtual power for the cylinder of unit length subjected to the internal pressure p assumes the form

$$2\pi a p\dot{u}_\mathrm{a} = \int_a^b \boldsymbol{\sigma}^\mathrm{t}\dot{\boldsymbol{\eta}}(2\pi r\mathrm{d}r), \tag{3.33}$$

the stress $\boldsymbol{\sigma}$ being statically equivalent to the applied pressure. At limit state $p = p_\mathrm{F}$, the stress taken as the actual $\boldsymbol{\sigma} = \boldsymbol{\sigma}_\mathrm{F}$, the integral on the right-hand side of eqn (3.33) supplies the power of dissipation. Then, since $\boldsymbol{\sigma}$ and $\dot{\boldsymbol{\eta}}$ are associated by the flow rule, the specific power of dissipation (per unit volume) for the von Mises material becomes

$$\boldsymbol{\sigma}^\mathrm{t}\dot{\boldsymbol{\eta}} = \bar{\sigma}\dot{\bar{\eta}} = 2\tau_\mathrm{s}\frac{a}{r}\frac{\dot{u}_\mathrm{a}}{r}. \tag{3.34}$$

We expressed $\bar{\sigma} = \sigma_\mathrm{s} = \sqrt{3}\tau_\mathrm{s}$ by the yield stress in shear, and $\dot{\bar{\eta}}$ by eqn (3.32). With eqn (3.34) the power of dissipation per unit cylinder length follows to

$$D = 2\pi\int_a^b \boldsymbol{\sigma}^\mathrm{t}\dot{\boldsymbol{\eta}}r\mathrm{d}r = 4\pi a\tau_\mathrm{s}\dot{u}_\mathrm{a}\ln\frac{b}{a}. \tag{3.35}$$

Substituting for the integral in eqn (3.33) we obtain the pressure $p \equiv p_\mathrm{F}$ at the plastic limit as

$$p_\mathrm{F} = 2\tau_\mathrm{s}\ln\frac{b}{a},$$

which confirms the result given in Section 2.3.3.

3.2 Static limit load theorem

The static theorem examines the safety of the loaded structure (generally a deformable body) with respect to the plastic limit by means of virtual stress systems which are in equilibrium with the applied forces. The theorem reads: *The structure is capable of sustaining the given loading as long as a virtual stress system exists which is in equilibrium with the applied forces and is everywhere in the structure within the elastic range as defined by the yield condition. The structure will, on the other hand, not be able to sustain the given loading if a statically admissible stress system cannot be found for which the yield condition is not violated somewhere in the structure.*

For an elucidation of the theorem, let the loading be specified by the body forces $\mathbf{f}$ and the surface forces $\mathbf{t}$; the limit load is given as $\mathbf{f}_{\mathrm{F}} = n\mathbf{f}$ and $\mathbf{t}_{\mathrm{F}} = n\mathbf{t}$, respectively. Virtual, statically admissible stress systems $\widetilde{\boldsymbol{\sigma}}$ must satisfy the equilibrium conditions with $\mathbf{f}$ and $\mathbf{t}$. The static theorem then states that:

(i) if for a *single* system $\widetilde{\boldsymbol{\sigma}}$, $\phi(\widetilde{\boldsymbol{\sigma}}) < 0$ everywhere, then $n > 1$;
(ii) if for *all* systems $\widetilde{\boldsymbol{\sigma}}$, $\phi(\widetilde{\boldsymbol{\sigma}}) > 0$ somewhere, then $n < 1$.

For a proof of the second part of the theorem, we point out that (ii) also comprises the actual stress system so that no solution can be found for the applied forces which satisfies static equilibrium *and* the yield condition at the same time; the structure is loaded beyond its plastic limit.

Regarding the first part of the theorem, we complete the characterization of the plastic limit state by the definition of the flow mechanism $\dot{\mathbf{u}}_{\mathrm{F}}$, which produces exclusively plastic strains $\dot{\boldsymbol{\gamma}}_{\mathrm{F}} \equiv \dot{\boldsymbol{\eta}}_{\mathrm{F}}$. Furthermore, the actual stress system at the limit load is denoted by $\boldsymbol{\sigma}_{\mathrm{F}}$. Using the flow mechanism for the virtual kinematics required in order to link the statically associated quantities $\widetilde{\boldsymbol{\sigma}}$ and $\mathbf{f}, \mathbf{t}$ by the principle of virtual work, eqn (3.4), one has

$$\int_V \mathbf{f}^{\mathrm{t}} \dot{\mathbf{u}}_{\mathrm{F}} \mathrm{d}V + \int_S \mathbf{t}^{\mathrm{t}} \dot{\mathbf{u}}_{\mathrm{F}} \mathrm{d}S = \int_V \widetilde{\boldsymbol{\sigma}}^{\mathrm{t}} \dot{\boldsymbol{\eta}}_{\mathrm{F}} \mathrm{d}V \tag{3.36}$$

and at the plastic limit state with $\boldsymbol{\sigma}_{\mathrm{F}}$ and $\mathbf{f}_{\mathrm{F}}, \mathbf{t}_{\mathrm{F}}$,

$$\int_V \mathbf{f}_{\mathrm{F}}^{\mathrm{t}} \dot{\mathbf{u}}_{\mathrm{F}} \mathrm{d}V + \int_S \mathbf{t}_{\mathrm{F}}^{\mathrm{t}} \dot{\mathbf{u}}_{\mathrm{F}} \mathrm{d}S = \int_V \boldsymbol{\sigma}_{\mathrm{F}}^{\mathrm{t}} \dot{\boldsymbol{\eta}}_{\mathrm{F}} \mathrm{d}V. \tag{3.37}$$

Setting in eqn (3.37) $\mathbf{f}_{\mathrm{F}} = n\mathbf{f}, \mathbf{t}_{\mathrm{F}} = n\mathbf{t}$ and dividing by eqn (3.36) we obtain the safety factor n in the form

$$n = \frac{\int_V \boldsymbol{\sigma}_{\mathrm{F}}^{\mathrm{t}} \dot{\boldsymbol{\eta}}_{\mathrm{F}} \mathrm{d}V}{\int_V \widetilde{\boldsymbol{\sigma}}^{\mathrm{t}} \dot{\boldsymbol{\eta}}_{\mathrm{F}} \mathrm{d}V}. \tag{3.38}$$

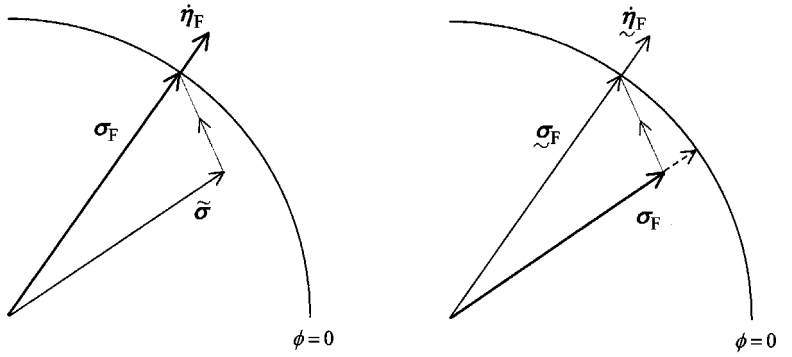

Figure 3.4: Drucker's plasticity postulate in the context of the limit load theorems (left: static theorem; right: kinematic theorem).

For an assessment of the safety factor, next we interpret the plasticity postulate, eqn (3.6), for the perfectly plastic material. Here $\boldsymbol{\sigma}_{\mathrm{F}}$ denotes the stress state at which the plastic flow $\dot{\boldsymbol{\eta}}_{\mathrm{F}}$ occurs, and takes the place of $\boldsymbol{\sigma}$ (Fig. 3.4). According to the static theorem, $\widetilde{\boldsymbol{\sigma}}$ is regarded an elastic stress state and plays the role of $\boldsymbol{\sigma}_{\mathrm{o}}$. Therefore, eqn (3.6) becomes

$$[\boldsymbol{\sigma}_{\mathrm{F}} - \widetilde{\boldsymbol{\sigma}}]^{\mathrm{t}}\, \dot{\boldsymbol{\eta}}_{\mathrm{F}} > 0, \tag{3.39}$$

where the strain rate has been used instead of the increment. Detailing the inequality and integrating over the volume,

$$\int_V \boldsymbol{\sigma}_{\mathrm{F}}^{\mathrm{t}} \dot{\boldsymbol{\eta}}_{\mathrm{F}} \mathrm{d}V > \int_V \widetilde{\boldsymbol{\sigma}}^{\mathrm{t}} \dot{\boldsymbol{\eta}}_{\mathrm{F}} \mathrm{d}V. \tag{3.40}$$

Thus from eqn (3.38) for the safety factor,

$$n > 1, \tag{3.41}$$

which means that the structure is loaded below the plastic limit. Since eqn (3.41) was deduced for a virtual stress system in the elastic range and in equilibrium with the applied forces, the first part of the static theorem is seen to be true.

The static theorem may be utilized in order to obtain a *lower limit* to the safety factor. For this purpose, let a virtual stress system $\widetilde{\sigma}_{\mathrm{F}}$ satisfy the yield condition everywhere in the structure such that $\phi(\widetilde{\sigma}_{\mathrm{F}}) \leq 0$, and be in equilibrium with a multiple of the applied forces: $\widetilde{n}\mathbf{f}, \widetilde{n}\mathbf{t}$. Linking the above static quantities by the principle of virtual work, as in eqn (3.36), we write

$$\widetilde{n} \left(\int_V \mathbf{f}^{\mathrm{t}} \dot{\mathbf{u}}_{\mathrm{F}} \mathrm{d}V + \int_S \mathbf{t}^{\mathrm{t}} \dot{\mathbf{u}}_{\mathrm{F}} \mathrm{d}S \right) = \int_V \widetilde{\boldsymbol{\sigma}}_{\mathrm{F}}^{\mathrm{t}} \dot{\boldsymbol{\eta}}_{\mathrm{F}} \mathrm{d}V \tag{3.42}$$

and division by eqn (3.37) gives the quotient

$$\frac{\widetilde{n}}{n} = \frac{\int\limits_V \widetilde{\boldsymbol{\sigma}}_{\mathrm{F}}^{\mathrm{t}} \dot{\boldsymbol{\eta}}_{\mathrm{F}} \mathrm{d}V}{\int\limits_V \boldsymbol{\sigma}_{\mathrm{F}}^{\mathrm{t}} \dot{\boldsymbol{\eta}}_{\mathrm{F}} \mathrm{d}V}. \tag{3.43}$$

In analogy to eqn (3.39), the plasticity postulate assumes in the present case the form

$$[\boldsymbol{\sigma}_{\mathrm{F}} - \widetilde{\boldsymbol{\sigma}}_{\mathrm{F}}]^{\mathrm{t}} \dot{\boldsymbol{\eta}}_{\mathrm{F}} \geq 0 \tag{3.44}$$

from which

$$\frac{\int\limits_V \widetilde{\sigma}_{\mathrm{F}}^{\mathrm{t}} \dot{\boldsymbol{\eta}}_{\mathrm{F}} \mathrm{d}V}{\int\limits_V \boldsymbol{\sigma}_{\mathrm{F}}^{\mathrm{t}} \dot{\boldsymbol{\eta}}_{\mathrm{F}} \mathrm{d}V} \leq 1 \tag{3.45}$$

and, comparing with eqn (3.43),

$$\widetilde{n} \leq n. \tag{3.46}$$

Accordingly, approximations $\widetilde{n}$ to the safety factor n by satisfaction of the static equilibrium and the yield condition supply only values not higher than the complete solution of the limit state problem.

3.3 Kinematic limit load theorem

The kinematic theorem examines the safety of the elastic–perfectly plastic structure or deformable body using virtual yield mechanisms which are compatible with the kinematics of the system. The theorem reads: *The structure is not able to carry the applied forces if for a single virtual yield mechanism the power of the applied forces is higher than the power of dissipation in the structure. The structure is, on the other hand, in the position to carry the loading if the power of the applied forces is lower than the power of dissipation for all possible virtual yield mechanisms.*

For an elucidation of the kinematic theorem, let the applied loading consist of body forces $\mathbf{f}$ and surface forces $\mathbf{t}$, the limit load being $\mathbf{f}_{\mathrm{F}} = n\mathbf{f}, \mathbf{t}_{\mathrm{F}} = n\mathbf{f}$. A virtual yield mechanism $\underset{\sim}{\dot{\mathbf{u}}}_{\mathrm{F}}$ is introduced as a kinematically compatible velocity field producing exclusively plastic strain rates: $\dot{\boldsymbol{\gamma}}_{\mathrm{F}} \equiv \dot{\boldsymbol{\eta}}_{\mathrm{F}}$. The stress locally associated with the virtual plastic flow $\dot{\boldsymbol{\eta}}_{\mathrm{F}}$ via the yield function is denoted $\underset{\sim}{\boldsymbol{\sigma}}_{\mathrm{F}}$. Extending the discussion of Section 3.1, the power of dissipation based on the virtual yield mechanism is

$$\underset{\sim}{D} = \int\limits_V d(\underset{\sim}{\dot{\boldsymbol{\eta}}}_{\mathrm{F}}) \mathrm{d}V = \int\limits_V \underset{\sim}{\boldsymbol{\sigma}}_{\mathrm{F}}^{\mathrm{t}} \underset{\sim}{\dot{\boldsymbol{\eta}}}_{\mathrm{F}} \mathrm{d}V > 0. \tag{3.47}$$

The power of the applied forces in conjunction with the virtual yield mechanism $\underset{\sim}{\dot{\mathbf{u}}}_{\mathrm{F}}$ reads

$$\underset{\sim}{L} = \int\limits_V \mathbf{f}^{\mathrm{t}} \underset{\sim}{\dot{\mathbf{u}}}_{\mathrm{F}} \mathrm{d}V + \int\limits_S \mathbf{t}^{\mathrm{t}} \underset{\sim}{\dot{\mathbf{u}}}_{\mathrm{F}} \mathrm{d}S. \tag{3.48}$$

The kinematic theorem may then be stated as:

(i) if for a *single* system $\underset{\sim}{\dot{\mathbf{u}}}_{\mathrm{F}}$, $\underset{\sim}{L} > \underset{\sim}{D}$, then $n < 1$;
(ii) if for *all* yield mechanisms $\underset{\sim}{\dot{\mathbf{u}}}_{\mathrm{F}}$, $\underset{\sim}{L} < \underset{\sim}{D}$, then $n > 1$.

For a proof of the kinematic limit load theorem, we first express the principle of virtual work for the limit load system $\mathbf{f}_{\mathrm{F}}, \mathbf{t}_{\mathrm{F}}$, which induces the stresses $\boldsymbol{\sigma}_{\mathrm{F}}$ in the structure. Using the virtual yield mechanism $\underset{\sim}{\dot{\mathbf{u}}}_{\mathrm{F}}$ as input for the kinematics in eqn (3.4), we write

$$\int_V \mathbf{f}_{\mathrm{F}}^{\mathrm{t}} \underset{\sim}{\dot{\mathbf{u}}}_{\mathrm{F}} \mathrm{d}V + \int_S \mathbf{t}_{\mathrm{F}}^{\mathrm{t}} \underset{\sim}{\dot{\mathbf{u}}}_{\mathrm{F}} \mathrm{d}S = \int_V \boldsymbol{\sigma}_{\mathrm{F}}^{\mathrm{t}} \underset{\sim}{\dot{\boldsymbol{\eta}}}_{\mathrm{F}} \mathrm{d}V. \tag{3.49}$$

Comparison of the left-hand side in eqn (3.49) with the right-hand expression in eqn (3.48) reveals that the former is n-times the latter since $\mathbf{f}_{\mathrm{F}} = n\mathbf{f}$ and $\mathbf{t}_{\mathrm{F}} = n\mathbf{t}$. Also, inspection of the right-hand side of eqn (3.49) and of the analogous expression in eqn (3.47) shows that, despite the same strain rate, the stress is different in each case. Therefore, the virtual power $\underset{\sim}{L}$ of the applied forces, eqn (3.48), and the power of dissipation $\underset{\sim}{D}$ of the virtual yield mechanism, eqn (3.47), may be linked by eqn (3.49) as follows:

$$n\underset{\sim}{L} = \int_V \boldsymbol{\sigma}_{\mathrm{F}}^{\mathrm{t}} \underset{\sim}{\dot{\boldsymbol{\eta}}}_{\mathrm{F}} \mathrm{d}V \neq \int_V \underset{\sim}{\boldsymbol{\sigma}}_{\mathrm{F}}^{\mathrm{t}} \underset{\sim}{\dot{\boldsymbol{\eta}}}_{\mathrm{F}} \mathrm{d}V = \underset{\sim}{D}. \tag{3.50}$$

The difference between the two quantities is

$$\underset{\sim}{D} - n\underset{\sim}{L} = \int_V [\underset{\sim}{\boldsymbol{\sigma}}_{\mathrm{F}} - \boldsymbol{\sigma}_{\mathrm{F}}]^{\mathrm{t}} \underset{\sim}{\dot{\boldsymbol{\eta}}}_{\mathrm{F}} \mathrm{d}V. \tag{3.51}$$

The integrand may be examined by means of the plasticity postulate, eqn (3.6). In the present case, $\underset{\sim}{\boldsymbol{\sigma}}_{\mathrm{F}}$ is defined as the local stress state at $\phi(\underset{\sim}{\boldsymbol{\sigma}}_{\mathrm{F}}) = 0$ associated with the virtual plastic flow $\underset{\sim}{\boldsymbol{\eta}}_{\mathrm{F}}$, and has to be treated like $\boldsymbol{\sigma}$ (Fig. 3.4). The stress $\boldsymbol{\sigma}_{\mathrm{F}}$ at the same location satisfies the yield condition $\phi(\boldsymbol{\sigma}_{\mathrm{F}}) \leq 0$ within the structure, but is not associated with the virtual plastic flow and takes the place of $\boldsymbol{\sigma}_{\mathrm{o}}$. Therefore, here eqn (3.6) assumes the form

$$[\underset{\sim}{\boldsymbol{\sigma}}_{\mathrm{F}} - \boldsymbol{\sigma}_{\mathrm{F}}]^{\mathrm{t}} \underset{\sim}{\dot{\boldsymbol{\eta}}}_{\mathrm{F}} \geq 0 \tag{3.52}$$

and establishes by eqn (3.51) the inequality

$$n\underset{\sim}{L} \leq \underset{\sim}{D} \quad \text{or} \quad n \leq \frac{\underset{\sim}{D}}{\underset{\sim}{L}}. \tag{3.53}$$

For $\underset{\sim}{D} < \underset{\sim}{L}$, it follows from eqn (3.53) that $n < 1$, which confirms the first part of the kinematic theorem. Regarding the second part, the safety factor $n > 1$ cannot be deduced immediately from the inequality in eqn (3.53) if

$\underset{\sim}{D} > \underset{\sim}{L}$. The theorem requires, however, that $\underset{\sim}{D} > \underset{\sim}{L}$ for all admissible yield mechanisms which also comprises the actual one at the plastic limit. Evaluation of the expressions in eqns (3.47), (3.48) and (3.49) for the mechanical power with the actual yield mechanism $\dot{\mathbf{u}}_{\mathrm{F}}$, the associated strain rate $\dot{\boldsymbol{\eta}}_{\mathrm{F}}$ and stress $\boldsymbol{\sigma}_{\mathrm{F}}$, converts eqn (3.50) to

$$nL = \int_V \mathbf{f}_{\mathrm{F}}^{\mathrm{t}} \dot{\mathbf{u}}_{\mathrm{F}} \mathrm{d}V + \int_S \mathbf{t}_{\mathrm{F}}^{\mathrm{t}} \dot{\mathbf{u}}_{\mathrm{F}} \mathrm{d}S = \int_V \boldsymbol{\sigma}_{\mathrm{F}}^{\mathrm{t}} \dot{\boldsymbol{\eta}}_{\mathrm{F}} \mathrm{d}V = D. \tag{3.54}$$

There follows:

$$n = \frac{D}{L} \tag{3.55}$$

and thus $n > 1$ if $D > L$ for the actual yield mechanism, which confirms the second part of the kinematic theorem. At the same time, failure as given by the first part is excluded for all other virtual yield mechanisms.

The kinematic limit load theorem may be utilized to determine an *upper limit* to the safety factor n. For this purpose, the rate of dissipation $\underset{\sim}{D}$ is obtained by eqn (3.47) using an admissible yield mechanism, and the virtual power $\underset{\sim}{L}$ of the applied forces by eqn (3.48). An approximation to the safety factor can then be defined by the quotient

$$\underset{\sim}{n} = \frac{\underset{\sim}{D}}{\underset{\sim}{L}} \geq n, \tag{3.56}$$

the inequality having already been established in eqn (3.53). Accordingly, approximations $\underset{\sim}{n}$ to the safety factor n based only on plastic flow kinematics and the yield condition supply values that are not lower than the complete solution of the limit state problem.

From eqns (3.56) and (3.46), it is concluded that, by the kinematic and the static limit load theorems, the safety factor of the structure at a given level of the loading is bounded as follows:

$$\widetilde{n} \leq n \leq \underset{\sim}{n}. \tag{3.57}$$

As a consequence, the actual safety factor n may be considered the *maximum* value of statically obtained trials $\widetilde{n}$, or the *minimum* of trials $\underset{\sim}{n}$ based on kinematics.

3.4 Simple applications of the limit load theorems

The purpose of the following simple examples is to illustrate the employment of the limit load theorems, and to demonstrate verification of their features to some extent. To this end, cases known from complete elastoplastic solutions in previous chapters will be the subject of direct load-carrying capacity considerations. For applications of practical interest to engineering

structures the reader is referred to Refs [3–5]; readers may also consult the monograph [6] on plastic limit analysis.

3.4.1 Plastic limit of three-bar truss

The three-bar truss under consideration has been investigated in Section 2.1.3. Here, the ultimate load of the elastic–perfectly plastic structure will be estimated by utilizing the limit load theorems.

An expression of the virtual work principle suitable for truss structures reads

$$L = \sum_{j=1}^{K} \mathbf{P}_j^{\mathrm{t}} \dot{\underset{\sim}{\mathbf{u}}}_j = \sum_{k=1}^{N} \widetilde{S}_k \dot{\underset{\sim}{\delta}}_k. \tag{3.58}$$

The left-hand side of the equation represents the rate of work that the forces $\mathbf{P}_j$, applied at the joints of the truss, perform on the respective virtual velocities $\dot{\underset{\sim}{\mathbf{u}}}_j$. The right-hand side gives the work of statically admissible stress resultants $\widetilde{S}_k = \widetilde{\sigma}_k A_k$ in the bar members (cross-section A_k, length l_k) with the rate of change in length $\dot{\underset{\sim}{\delta}}_k = \dot{\underset{\sim}{\gamma}}_k l_k$ induced by the virtual velocities at the joints. The power of dissipation in the truss is

$$D = \sum_{k=1}^{N} S_k \dot{\delta}_{\mathrm{p}k} = \sum_{k=1}^{N} S_{\mathrm{f}k} |\dot{\delta}_{\mathrm{p}k}|, \tag{3.59}$$

where $S_{\mathrm{f}k} = \sigma_{\mathrm{f}k} A_k$ is based on the actual flow stress $\sigma_{\mathrm{f}k}$ in the kth bar and $\dot{\delta}_{\mathrm{p}k} = \dot{\eta}_k l_k$ is the plastic part of the rate of change in length. In perfect plasticity, $S_{\mathrm{f}k} \Leftarrow S_{\mathrm{s}k} = \sigma_{\mathrm{s}} A_k$.

Evaluation of the expressions in eqns (3.58) and (3.59) for a virtual yield mechanism supplies the quantities $\underset{\sim}{L}$ and $\underset{\sim}{D}$, respectively, as defined for the system in Section 3.3.

Static approach

The static limit load theorem relies on stress states satisfying the condition of static equilibrium within the elastic range of the material (Fig. 3.5). From eqn (2.14), for the equilibrium of a virtual stress system

$$\widetilde{S}_2 + \sqrt{3}\widetilde{S}_3 = 0, \quad 2\widetilde{S}_1 + \sqrt{3}\widetilde{S}_2 + \widetilde{S}_3 = -2P, \tag{3.60}$$

and for bar stresses whithin the elastic limit

$$|\widetilde{S}_1| \le S_{\mathrm{s}}, \quad |\widetilde{S}_2| \le S_{\mathrm{s}}, \quad |\widetilde{S}_3| \le S_{\mathrm{s}}. \tag{3.61}$$

From eqn (3.60) left, bar 3 is in the elastic range as long as $|\widetilde{S}_2| \le S_{\mathrm{s}}$. For this reason, $\widetilde{S}_3$ can be eliminated in eqn (3.60) right, such that estimates of the limit load are obtained as

$$\widetilde{P}_{\mathrm{F}} = -\widetilde{S}_1 - \frac{\sqrt{3}}{3}\widetilde{S}_2. \tag{3.62}$$

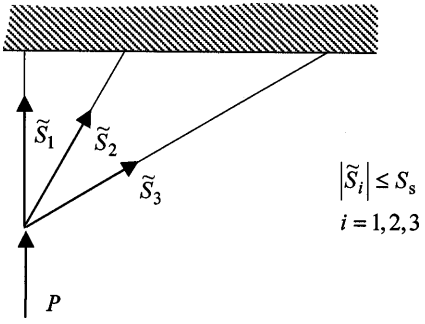

Figure 3.5: Three-bar truss: statics of virtual stresses.

This expression will attain a maximum value for $\widetilde{S}_1 = \widetilde{S}_2 = -S_s$, and supplies the limit load:

$$P_F = \max\left(-\widetilde{S}_1 - \frac{\sqrt{3}}{3}\widetilde{S}_2\right) = \frac{3+\sqrt{3}}{3}S_s. \tag{3.63}$$

From Section 2.1.3, this is in fact the limit load. Therefore, the admissible stress system maximizing the applied force is as for the complete solution. There are, of course, a variety of stress systems complying with the contents of the static theorem. They provide us, however, with values lower than the one determined above for the limit load. For instance, the stress state at the elasticity limit represents an admissible system which is associated with a lower magnitude of the applied force and therefore $\widetilde{P}_F = P_s < P_F$.

Kinematic approach

Fundamental to the kinematic limit load theorem are admissible yield mechanisms. These are characterized by the induction of exclusively plastic strain rates such that the applied load remains unchanged. In the three-bar truss a yield mechanism ($\underset{\sim}{\dot{u}} \equiv \underset{\sim}{\dot{u}}_F$) implies that two of the bars undergo plastic flow, the third remaining rigid (Fig. 3.6). Thereby, the displacement velocity of the point joining the three bars is perpendicular to the non-deforming bar. This member experiences momentarily a rotation about the fixed hinge. The (plastically) deforming bars are at yield: $|\underset{\sim}{S}_{Fi}| = S_s$. There are three alternative yield mechanisms possible in the truss, and they will be examined in the following with respect to the estimation of the limit load ($\underset{\sim}{P} \equiv \underset{\sim}{P}_F$).

Assuming the vertical bar 1 to be rigid, a virtual yield mechanism is defined by the horizontal velocity $\underset{\sim}{\dot{u}}$ of the joint of the bars. The oblique members deform plastically and contribute to a finite value of the power of dissipation $\underset{\sim}{D}$ defined as in eqn (3.59). The virtual power of the applied force, on the other hand, is $\underset{\sim}{L} = 0 \cdot \underset{\sim}{P}$. Equating, we obtain an estimate of the limit load from

$$\underset{\sim}{L} = 0 \cdot \underset{\sim}{P} = \underset{\sim}{D} \quad \text{and} \quad \underset{\sim}{P} = \infty. \tag{3.64}$$

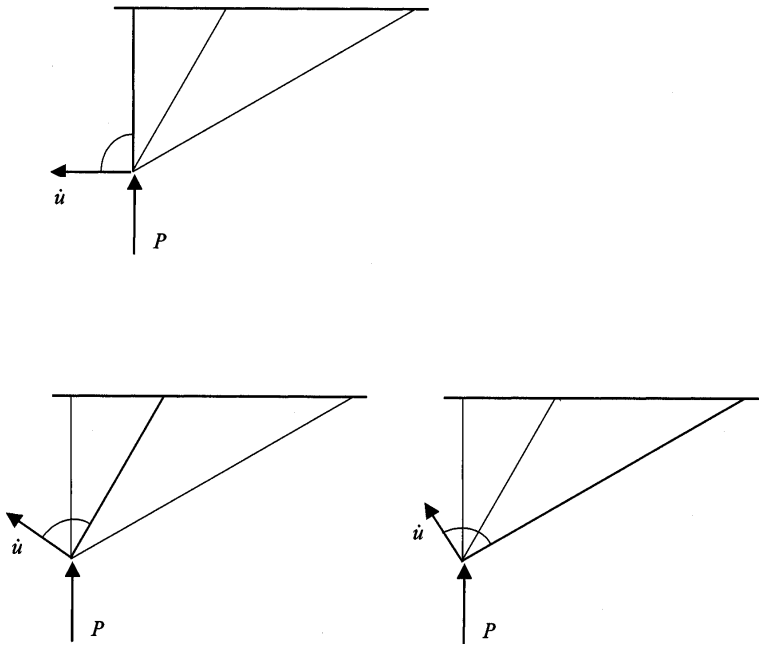

Figure 3.6: Three-bar truss: plastic yield mechanisms.

A second trial assumes bar 2 (middle) to be rigid, and the associated virtual yield mechanism is defined by a displacement velocity $\underset{\sim}{\dot{u}}$ of the joint, which is perpendicular to bar 2. The velocity possesses a vertical component $\underset{\sim}{\dot{u}}/2$ and imposes variations in length of the two other bars:

$$\underset{\sim}{\dot{\delta}}_1 = -\frac{1}{2}\underset{\sim}{\dot{u}}, \quad \underset{\sim}{\dot{\delta}}_3 = \frac{1}{2}\underset{\sim}{\dot{u}} \quad (\underset{\sim}{\dot{\delta}}_2 = 0).$$

The virtual power of dissipation and that of the applied force are obtained as

$$\underset{\sim}{D} = -S_{\mathrm{s}}\underset{\sim}{\dot{\delta}}_1 + S_{\mathrm{s}}\underset{\sim}{\dot{\delta}}_3 = S_{\mathrm{s}}\underset{\sim}{\dot{u}} \tag{3.65}$$

and

$$\underset{\sim}{L} = \frac{1}{2}\underset{\sim}{P}\underset{\sim}{\dot{u}},$$

respectively. Equating, the limit load is estimated as

$$\underset{\sim}{P} = 2S_{\mathrm{s}}, \tag{3.66}$$

which is lower than the first estimate.

The third yield mechanism deforms bars 1 and 2, while bar 3 is kept rigid. The displacement velocity $\underset{\sim}{\dot{u}}$ of the joint is perpendicular to bar 3. Its vertical projection is $\sqrt{3}\underset{\sim}{\dot{u}}/2$, the variations in length of the other bars are:

$$\underset{\sim}{\dot{\delta}}_1 = -\frac{\sqrt{3}}{2}\underset{\sim}{\dot{u}}, \quad \underset{\sim}{\dot{\delta}}_2 = -\frac{1}{2}\underset{\sim}{\dot{u}} \quad (\underset{\sim}{\dot{\delta}}_3 = 0).$$

The power of dissipation and the power of the applied force read

$$\underset{\sim}{D} = -S_{\mathrm{s}}\underset{\sim}{\dot{\delta}}_1 - S_{\mathrm{s}}\underset{\sim}{\dot{\delta}}_2 = \frac{1+\sqrt{3}}{2}S_{\mathrm{s}}\underset{\sim}{\dot{u}} \tag{3.67}$$

and

$$\underset{\sim}{L} = \frac{\sqrt{3}}{2}\underset{\sim}{P}\underset{\sim}{\dot{u}},$$

respectively. Equating, the limit load is estimated as

$$\underset{\sim}{P} = \frac{3+\sqrt{3}}{3}S_{\mathrm{s}}. \tag{3.68}$$

The last yield mechanism is seen to supply the lowest value for the limit load, which equals the exact one from the complete solution: $\underset{\sim}{P}_{\mathrm{F}} \equiv \underset{\sim}{P} = P_{\mathrm{F}}$.

3.4.2 Two plane examples

Ultimate bending of beam
The bending of a beam has been repeatedly referred to and is familiar to the reader. The simplest case is offered by the symmetric situation discussed in Section 2.1.4. Recalling the static theorem, it becomes obvious that the stress distribution shown in Fig. 3.7 (left) is associated with the maximum magnitude of the bending moment M_{F} given by eqn (2.41) with eqn (2.42). All other possible approximations complying with the requirement not to exceed the yield limit supply lower bending moments.

The yield mechanism employed for the application of the kinematic theorem is defined in Fig. 3.7 (right). The rate of the angle of rotation, $\underset{\sim}{\dot{\varphi}} \equiv \underset{\sim}{\dot{\varphi}}_{\mathrm{F}}$, induces exclusively plastic flow in the cross-section

$$\underset{\sim}{\dot{\eta}} = \underset{\sim}{\dot{\gamma}} = \frac{y}{l}\underset{\sim}{\dot{\varphi}}. \tag{3.69}$$

The virtual power of the bending moment $\underset{\sim}{M} \equiv \underset{\sim}{M}_{\mathrm{F}}$ and the dissipation rate are

$$\underset{\sim}{L} = \underset{\sim}{M}\underset{\sim}{\dot{\varphi}}$$

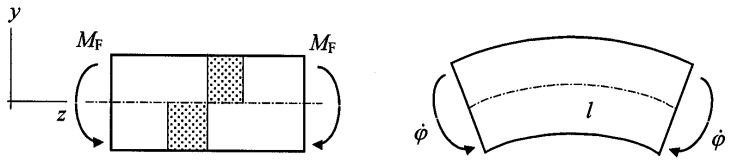

Figure 3.7: Limit bending moment of the beam.

and

$$\underset{\sim}{D} = \int_V \sigma_s \underset{\sim}{\dot{\eta}} \mathrm{d}V = 2\sigma_s \left(\int_0^h y b(y) \mathrm{d}y \right) \dot{\varphi}, \tag{3.70}$$

respectively. The latter expression for the dissipation rate makes use of the yield mechanism in eqn (3.69). Equating the expressions for $\underset{\sim}{L}$ and $\underset{\sim}{D}$ we obtain the limit moment

$$\underset{\sim}{M} = 2\sigma_s \int_0^h y b(y) \mathrm{d}y. \tag{3.71}$$

The estimate in eqn (3.71) is seen to be identical to the ultimate moment M_F from the complete solution, eqn (2.41) with eqn (2.42). This is due to the fact that the selected yield mechanism is the actual one.

Limit analysis of constrained plate

This is the example treated in Section 1.2.5, where the elastoplastic solution of the plane problem has been developed. Here, the maximum load pertaining to plastic collapse will be estimated directly by means of the limit load theorems for perfectly plastic systems.

The static approach observes the equilibrium condition and the yield limit. The former equates the longitudinal stress σ_1 in the plate to the applied stress, while the lateral stress σ_2 is a free quantity. Also, we recall the von Mises yield condition for the perfectly plastic material:

$$\sigma_1^2 + \sigma_2^2 - \sigma_1 \sigma_2 = \sigma_s^2. \tag{3.72}$$

An admissible stress state $\widetilde{\boldsymbol{\sigma}} \equiv \widetilde{\boldsymbol{\sigma}}_F$ estimating the limit can be obtained by substituting the elastic solution $\widetilde{\sigma}_2 = \nu \widetilde{\sigma}_1$ for the lateral stress in the yield condition and solving for $\widetilde{\sigma}_1 = (1 - \nu + \nu^2)^{1/2} \sigma_s$. This actually determines the stress state at incipient yield. In order to deduce the collapse load utilizing the static limit load theorem we seek the maximum $\widetilde{\sigma}_1$ satisfying the yield condition. To this end, differentiating eqn (3.72) we obtain the extremum condition

$$\frac{\mathrm{d}\widetilde{\sigma}_1}{\mathrm{d}\widetilde{\sigma}_2} = -\frac{2\widetilde{\sigma}_2 - \widetilde{\sigma}_1}{2\widetilde{\sigma}_1 - \widetilde{\sigma}_2} = 0. \tag{3.73}$$

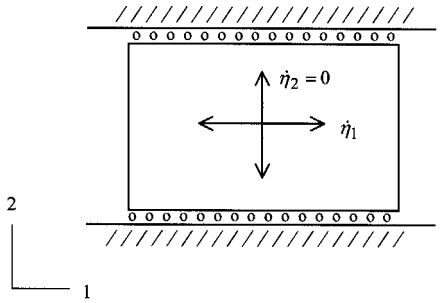

Figure 3.8: Limit analysis of a constrained plate.

The solution is $\widetilde{\sigma}_2 = \widetilde{\sigma}_1/2$, and from eqn (3.72)

$$\widetilde{\sigma}_1^2 = \frac{4}{3}\sigma_s^2, \tag{3.74}$$

which reproduces the result in Section 1.2.5.

For the kinematic approach we define a yield mechanism $\underset{\sim}{\dot{\boldsymbol{\eta}}} \equiv \underset{\sim}{\dot{\boldsymbol{\eta}}}_{\mathrm{F}}$ by the virtual set

$$\underset{\sim}{\dot{\eta}}_1, \quad \underset{\sim}{\dot{\eta}}_2 = 0, \quad \underset{\sim}{\dot{\eta}}_3 = -\underset{\sim}{\dot{\eta}}_1. \tag{3.75}$$

This satisfies the lateral constraint condition (Fig. 3.8) and the isochoric property of plastic flow. With eqn (3.75) the equivalent plastic strain rate is obtained as

$$\underset{\sim}{\dot{\bar{\eta}}}^2 = \frac{2}{3}\left(\underset{\sim}{\dot{\eta}}_1^{\,2} + \underset{\sim}{\dot{\eta}}_2^{\,2} + \underset{\sim}{\dot{\eta}}_3^{\,2}\right) = \frac{4}{3}\underset{\sim}{\dot{\eta}}_1^{\,2}. \tag{3.76}$$

The virtual power of the applied action and the virtual rate of dissipation for the plate with volume V are

$$\underset{\sim}{L} = \underset{\sim}{\sigma}_1 \underset{\sim}{\dot{\eta}}_1 V$$

and

$$\underset{\sim}{D} = \sigma_s \underset{\sim}{\dot{\bar{\eta}}} V = \frac{2}{\sqrt{3}}\sigma_s \underset{\sim}{\dot{\eta}}_1 V, \tag{3.77}$$

respectively. Equating, we obtain the same value for the limiting stress $\underset{\sim}{\sigma}_1$ as from eqn (3.74). The kinematic estimate coincides with the result of the complete solution because the yield mechanism employed is the actual one. Summarizing, $\widetilde{\sigma}_1 = \underset{\sim}{\sigma}_1 = \sigma_{1\mathrm{F}}$.

3.5 Problems

1. The bars of the trusses in Fig. 3.9 have a unique cross-section A and yield stress σ_s. Determine the limit load for a perfectly plastic material.

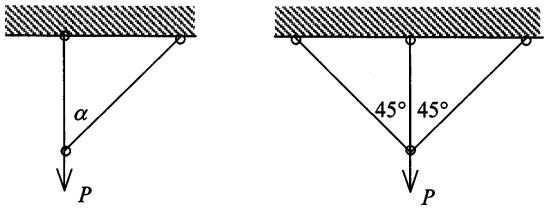

Figure 3.9: Problem 1.

2. As in 1. Indicate the bar determining the limit load (yielding first) in Fig. 3.10, and the momentary motion of the joint at this state for the loading cases (a), (b) and (c).

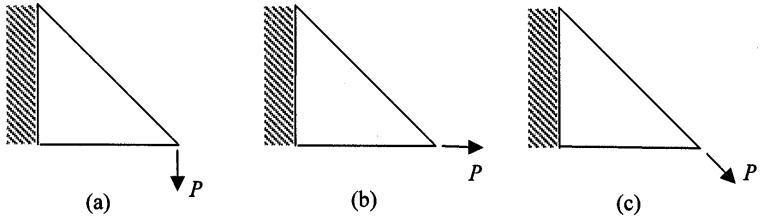

Figure 3.10: Problem 2.

3. Perform a rigorous transition from the continuum form of the virtual work principle, eqn (3.4), and the power of dissipation, eqn (3.25), to the discretized expressions presented for truss structures in Section 3.4.1 (eqns (3.58) and (3.59)).

4. Given that the elastic energy $(1/2)\boldsymbol{\sigma}^{\mathrm{t}}\boldsymbol{\varepsilon}$ is a positive quantity for any $\boldsymbol{\sigma} = \boldsymbol{\kappa}\boldsymbol{\varepsilon} \neq \mathbf{0}$, conclude that the statement $[\dot{\boldsymbol{\sigma}}_2 - \dot{\boldsymbol{\sigma}}_1]^{\mathrm{t}}[\dot{\boldsymbol{\varepsilon}}_2 - \dot{\boldsymbol{\varepsilon}}_1] > 0$ is a consequence of the positive definite form $\boldsymbol{\varepsilon}^{\mathrm{t}}\boldsymbol{\kappa}\boldsymbol{\varepsilon} > 0$ as a property of the elasticity matrix $\boldsymbol{\kappa}$, not restricted to the case of isotropy detailed in eqn (3.17).

5. Examine the inelastic work term in eqn (3.18) for hardening material. This is simple in case one of the stress rates does not induce plastic flow: the expression is seen to be positive based on arguments analogous to perfect plasticity. Otherwise, consider a yield condition $\phi(\boldsymbol{\sigma}, \boldsymbol{\eta}) = 0$. Therefrom, deducing the consistency of incremental changes and introducing the

normality rule for plastic flow, the multiplier Λ is determined such that the plastic strain rate becomes

$$\dot{\boldsymbol{\eta}} = -\left(\frac{\partial\phi}{\partial\boldsymbol{\eta}}\frac{\partial\phi}{\partial\boldsymbol{\sigma}^{\mathrm{t}}}\right)^{-1}\frac{\partial\phi}{\partial\boldsymbol{\sigma}^{\mathrm{t}}}\frac{\partial\phi}{\partial\boldsymbol{\sigma}}\dot{\boldsymbol{\sigma}}.$$

With this,

$$[\dot{\boldsymbol{\sigma}}_2 - \dot{\boldsymbol{\sigma}}_1]^{\mathrm{t}}[\dot{\boldsymbol{\eta}}_2 - \dot{\boldsymbol{\eta}}_1] = -\left(\frac{\partial\phi}{\partial\boldsymbol{\eta}}\frac{\partial\phi}{\partial\boldsymbol{\sigma}^{\mathrm{t}}}\right)^{-1}\left\{[\dot{\boldsymbol{\sigma}}_2 - \dot{\boldsymbol{\sigma}}_1]^{\mathrm{t}}\frac{\partial\phi}{\partial\boldsymbol{\sigma}^{\mathrm{t}}}\frac{\partial\phi}{\partial\boldsymbol{\sigma}}[\dot{\boldsymbol{\sigma}}_2 - \dot{\boldsymbol{\sigma}}_1]\right\} > 0$$

unless $\dot{\boldsymbol{\sigma}}_2 = \dot{\boldsymbol{\sigma}}_1$. Alternatively, utilize the general result for plastic flow obtained in Section 1.4.

In the above, the preset inverse multiplier is negative, while the expression in the braces assumes positive values as does the form

$$\mathbf{a}^{\mathrm{t}}(\mathbf{b}\mathbf{b}^{\mathrm{t}})\mathbf{a} = (\mathbf{a}^{\mathrm{t}}\mathbf{b})(\mathbf{b}^{\mathrm{t}}\mathbf{a}) = (\mathbf{b}^{\mathrm{t}}\mathbf{a})^{\mathbf{2}} \geq \mathbf{0},$$

as long as the vectors $\mathbf{a}, \mathbf{b}$ are not orthogonal and $\mathbf{a} \neq \mathbf{0}$.

References

[1] D.C. Drucker, A more fundamental approach to plastic stress–strain relations, *Proc. 1st US Natl Congr. Appl. Mech.* (Chicago, 1951), ASME, New York, 1952, pp. 487–91.

[2] W.T. Koiter, General theorems for elastic–plastic solids, in *Progress in Solid Mechanics*, Vol. 1, I.N. Sneddon and R. Hill (Eds), Chapter 4, North-Holland, Amsterdam, 1960, pp. 167–221.

[3] P.G. Hodge, Jr, *Plastic Analysis of Structures*, McGraw-Hill, New York, 1959.

[4] A. Sawczuk and Th. Jaeger, *Grenztragfähigkeitestheorie der Platten*, Springer-Verlag, Berlin, 1963.

[5] S. Kaliszky, *Plasticity – Theory and Engineering Applications*, Studies in Applied Mechanics 21, Elsevier, Amsterdam, 1989.

[6] J.A. Kamenjarzh, *Limit Analysis of Solids and Structures*, CRC Press, Boca Raton, 1996.

This page intentionally left blank

CHAPTER 4

Theory of shakedown

4.1 Structures under time-variant loading

So far, the structure has been loaded by forces that are increasing monotonically with time. Frequently the loading consists of a system of forces that may vary independently with time, alternating between limits in a regular or irregular manner. This time variation is assumed to be slow, still justifying a quasistatic description of the response of the structure.

As long as the stresses induced during the course of the loading programme remain below the elasticity limit of the material, the lifetime of the structure is determined by *elastic fatigue*, implying a high number of load cycles. If the loading causes plastic flow within the structure, failure can occur under various conditions. In conjunction with an elastic–perfectly plastic material, the combination of the forces may constitute at a certain instant a *limit load* system giving rise to plastic collapse. This case has already been covered by the limit load theory in Chapter 3. However, even if plastic limit states are not encountered during the course of the loading programme, repeated occurrence of plastic flow in the loading sequences may lead to deformations with magnitudes beyond specified tolerances by the *accumulation of plastic strains*. In the case of *alternating plastic flow*, deformations remain restricted, but the structure will fail by plastic fatigue after a low number of loading cycles.

It can be concluded that the structure is prone to failure as long as plastic flow continues to appear during the course of the load sequences. Therefore, safety demands that plastic flow ceases to occur after an initial period in the loading programme. This implies that plasticity must develop in the structure such that subsequent load sequences are accommodated elastically.

In this connection, let the loading programme of a structure or a deformable body, respectively, comprise time-variant body forces $\mathbf{f}(t)$ and surface forces $\mathbf{t}(t)$, inducing displacements $\mathbf{u}(t)$, strains $\boldsymbol{\gamma}(t)$ and stresses $\boldsymbol{\sigma}(t)$; analogously for discrete forces $\mathbf{P}_j(t)$ $(j = 1, \ldots, K)$. Where plastic flow occurs, the strain is composed of elastic and plastic parts: $\boldsymbol{\gamma}(t) = \boldsymbol{\varepsilon}(t) + \boldsymbol{\eta}(t)$. It is assumed that at each instant t unloading from the actual state

would take place elastically, and can be associated with an elastic solution $\mathbf{u}_{\mathrm{e}}(t), \boldsymbol{\varepsilon}_{\mathrm{e}}(t), \boldsymbol{\sigma}_{\mathrm{e}}(t)$ for the loads at the considered instant. Superposition of the actual elastoplastic solution and the elastic unloading solution will in general leave residual displacements $\mathbf{u}_{\mathrm{r}}(t)$, strains $\boldsymbol{\gamma}_{\mathrm{r}}(t)$ and stresses $\boldsymbol{\sigma}_{\mathrm{r}}(t)$ characteristic of this instant. Conversely, each actual elastoplastic state may be interpreted as a result of the superposition of the residual state and the elastic solution for the momentary loading system (cf. Section 2.2.3). For example, the stress $\boldsymbol{\sigma}$ at instant t can be presented everywhere in the structure as

$$\boldsymbol{\sigma}(t) = \boldsymbol{\sigma}_{\mathrm{r}}(t) + \boldsymbol{\sigma}_{\mathrm{e}}(t). \tag{4.1}$$

The residual stress $\boldsymbol{\sigma}_{\mathrm{r}}$ in eqn (4.1) is a consequence of the residual elastic strain $\boldsymbol{\varepsilon}_{\mathrm{r}}$, which is part of the residual strain

$$\boldsymbol{\gamma}_{\mathrm{r}}(t) = \boldsymbol{\varepsilon}_{\mathrm{r}}(t) + \boldsymbol{\eta}(t). \tag{4.2}$$

Shakedown of the structure is defined by the disappearance of plastic flow. Then $\dot{\boldsymbol{\eta}}$ vanishes and $\boldsymbol{\eta}$ does not vary anymore with time. Therefore, differentiation of eqn (4.2) with respect to time gives

$$\dot{\boldsymbol{\gamma}}_{\mathrm{r}} = \dot{\boldsymbol{\varepsilon}}_{\mathrm{r}}, \tag{4.3}$$

and thus $\dot{\boldsymbol{\varepsilon}}_{\mathrm{r}}$ is a kinematically compatible strain (rate) field. It is utilized in forming the virtual work expression for $\dot{\boldsymbol{\sigma}}_{\mathrm{r}}$, the time rate of the residual stress field, and yields

$$\int_V \dot{\boldsymbol{\sigma}}_{\mathrm{r}}^{\mathrm{t}} \dot{\boldsymbol{\varepsilon}}_{\mathrm{r}} \mathrm{d}V = 0. \tag{4.4}$$

The volume integral in eqn (4.4) vanishes because $\dot{\boldsymbol{\sigma}}_{\mathrm{r}}$ is a self-equilibrating stress system such that the resultant forces are zero. The integrand can be transformed by means of the elastic material law to

$$\dot{\boldsymbol{\sigma}}_{\mathrm{r}}^{\mathrm{t}} \dot{\boldsymbol{\varepsilon}}_{\mathrm{r}} = \dot{\boldsymbol{\varepsilon}}_{\mathrm{r}}^{\mathrm{t}} \boldsymbol{\kappa} \dot{\boldsymbol{\varepsilon}}_{\mathrm{r}} = \dot{\boldsymbol{\sigma}}_{\mathrm{r}}^{\mathrm{t}} \boldsymbol{\kappa}^{-1} \dot{\boldsymbol{\sigma}}_{\mathrm{r}} > 0. \tag{4.5}$$

It is a positive quantity, and therefore eqn (4.4) can be satisfied only if the time rates $\dot{\boldsymbol{\sigma}}_{\mathrm{r}}$ and $\dot{\boldsymbol{\varepsilon}}_{\mathrm{r}}$ are zero. Apart from this formal conclusion, if the plastic $\dot{\boldsymbol{\eta}}$ disappears there is no continuing kinematic incompatibility to compensate by elastic residual strains $\dot{\boldsymbol{\varepsilon}}_{\mathrm{r}}$ after unloading. It follows that, when the structure has shaken down, all residual quantities are no longer functions of time: the plastic strain $\boldsymbol{\eta}$ by definition, the elastic strain $\boldsymbol{\varepsilon}_{\mathrm{r}}$ as from the above discussion and the residual strain $\boldsymbol{\gamma}_{\mathrm{r}}$ by virtue of its constituents $\boldsymbol{\varepsilon}_{\mathrm{r}}$ and $\boldsymbol{\eta}$, eqn (4.2). Since with $\boldsymbol{\varepsilon}_{\mathrm{r}}$ also the residual stress $\boldsymbol{\sigma}_{\mathrm{r}}$ is time independent, the actual stress $\boldsymbol{\sigma}(t)$ in eqn (4.1) follows the temporal variation of the elastic solution $\boldsymbol{\sigma}_{\mathrm{e}}(t)$. It becomes

$$\boldsymbol{\sigma}(t) = \boldsymbol{\sigma}_{\mathrm{r}} + \boldsymbol{\sigma}_{\mathrm{e}}(t). \tag{4.6}$$

In conformity with the vanishing plastic flow, the stress must be within the elastic range everywhere in the structure. By means of the yield condition:

$$\phi\left(\boldsymbol{\sigma}(t), \dots\right) = \phi\left(\boldsymbol{\sigma}_{\mathrm{r}} + \boldsymbol{\sigma}_{\mathrm{e}}(t), \dots\right) < 0. \tag{4.7}$$

The shakedown issue is not restricted to perfectly plastic solids, but may concern hardening materials as well. The hardening property of the material will facilitate shakedown if the sign of the stress is maintained in the load sequences. The Baushinger effect appearing when stress reversals are encountered may reduce the benefit of hardening. In the yield condition, eqn (4.7), the hardening parameters (symbolized by the dots, ...) are taken at the level last attained by the preceding plastic deformation. In systems that do not build up residual stresses, the evolution of plastic deformation will stop once the elastic solution $\boldsymbol{\sigma}_{\mathrm{e}}(t)$ does not any more exceed locally the material yield limit pertaining to the actual state of hardening.

An historical account on the theory of shakedown is found in [1] along with a concise presentation of the theoretical background.

4.2 Static shakedown theorem (Melan)

Investigation of the capability of the structure to carry the given loading programme might be based on an elastoplastic analysis, completely accounting for the variation of the loading with time. Melan's static theorem [2, 3] helps to examine possible shakedown of the structure by a simplified consideration involving virtual self-equilibrating stress systems and the elastic solution for the transient stress during the course of the loading programme. The theorem can be stated as follows: *The structure will shake down during the course of the loading programme if a time-independent system of residual stresses exists which, superposed to the (fictitious) elastic solution, results to stress states below the yield limit everywhere in the structure for the entire loading programme. Shakedown is, on the other hand, not possible if no time-independent system of residual stresses exists for which the superposition of the elastic solution would not lead to a violation of the yield condition at a certain instant somewhere in the structure.*

For an elucidation of the static theorem, let $\widetilde{\boldsymbol{\sigma}}_{\mathrm{r}}$ denote a time-independent system of residual stresses, and $\boldsymbol{\sigma}_{\mathrm{e}}(t)$ the transient stress field pertaining to the elastic solution for the given loading programme. The stress $\widetilde{\boldsymbol{\sigma}}_{\mathrm{r}}$ represents a virtual, self-equilibrating stress system for the structure with no resultant forces. The virtual stress field

$$\widetilde{\boldsymbol{\sigma}}(t) = \widetilde{\boldsymbol{\sigma}}_{\mathrm{r}} + \boldsymbol{\sigma}_{\mathrm{e}}(t) \tag{4.8}$$

obtained by the superposition of $\widetilde{\boldsymbol{\sigma}}_{\mathrm{r}}$ and $\boldsymbol{\sigma}_{\mathrm{e}}(t)$ satisfies the static equilibrium conditions for the loading programme and follows the temporal variation of the elastically determined stresses $\boldsymbol{\sigma}_{\mathrm{e}}(t)$. The static shakedown theorem is

presented in short form as follows:

(i) The structure will shake down if a *single* $\widetilde{\boldsymbol{\sigma}}_{\mathrm{r}}$ exists such that $\phi\left(\widetilde{\boldsymbol{\sigma}}_{\mathrm{r}}+\boldsymbol{\sigma}_{\mathrm{e}}(t)\right)<0$.
(ii) Shakedown is not possible if *no* $\widetilde{\boldsymbol{\sigma}}_{\mathrm{r}}$ exists for which $\phi\left(\widetilde{\boldsymbol{\sigma}}_{\mathrm{r}}+\boldsymbol{\sigma}_{\mathrm{e}}(t)\right)\leq 0$.

A proof of the first part of the theorem is given by considering the temporal variation of the elastic energy of the difference between the actual residual stress system $\boldsymbol{\sigma}_{\mathrm{r}}(t)$ and the virtual one $\widetilde{\boldsymbol{\sigma}}_{\mathrm{r}}$ entering the static theorem. Defining for the structure the expression

$$\mathcal{E}=\int_{V}\frac{1}{2}\left[\boldsymbol{\sigma}_{\mathrm{r}}-\widetilde{\boldsymbol{\sigma}}_{\mathrm{r}}\right]^{\mathrm{t}}\boldsymbol{\kappa}^{-1}\left[\boldsymbol{\sigma}_{\mathrm{r}}-\widetilde{\boldsymbol{\sigma}}_{\mathrm{r}}\right]\mathrm{d}V>0, \tag{4.9}$$

we observe that the above energy is a positive quantity by virtue of the elastic properties of the material.

The time rate of $\mathcal{E}$ in eqn (4.9) is obtained as

$$\dot{\mathcal{E}}=\int_{V}\left[\boldsymbol{\sigma}_{\mathrm{r}}-\widetilde{\boldsymbol{\sigma}}_{\mathrm{r}}\right]^{\mathrm{t}}\boldsymbol{\kappa}^{-1}\dot{\boldsymbol{\sigma}}_{\mathrm{r}}\mathrm{d}V=\int_{V}\left[\boldsymbol{\sigma}_{\mathrm{r}}-\widetilde{\boldsymbol{\sigma}}_{\mathrm{r}}\right]^{\mathrm{t}}\dot{\boldsymbol{\varepsilon}}_{\mathrm{r}}\mathrm{d}V, \tag{4.10}$$

which considers that $\boldsymbol{\sigma}_{\mathrm{r}}$ is a function of time, while $\widetilde{\boldsymbol{\sigma}}_{\mathrm{r}}$ is not. The second expression for $\dot{\mathcal{E}}$ in eqn (4.10) is detailed by means of eqn (4.2) for the residual strain

$$\int_{V}\left[\boldsymbol{\sigma}_{\mathrm{r}}-\widetilde{\boldsymbol{\sigma}}_{\mathrm{r}}\right]^{\mathrm{t}}\dot{\boldsymbol{\varepsilon}}_{\mathrm{r}}\mathrm{d}V=\int_{V}\left[\boldsymbol{\sigma}_{\mathrm{r}}-\widetilde{\boldsymbol{\sigma}}_{\mathrm{r}}\right]^{\mathrm{t}}\dot{\boldsymbol{\gamma}}_{\mathrm{r}}\mathrm{d}V-\int_{V}\left[\boldsymbol{\sigma}_{\mathrm{r}}-\widetilde{\boldsymbol{\sigma}}_{\mathrm{r}}\right]^{\mathrm{t}}\dot{\boldsymbol{\eta}}\mathrm{d}V. \tag{4.11}$$

As neither $\boldsymbol{\sigma}_{\mathrm{r}}$ nor $\widetilde{\boldsymbol{\sigma}}_{\mathrm{r}}$ possess resultant forces and $\dot{\boldsymbol{\gamma}}_{\mathrm{r}}$ is a kinematically compatible strain field, the principle of virtual work shows that the first integral on the right-hand side of eqn (4.11) is equal to zero. In the second integral, the difference of the residual stresses $\boldsymbol{\sigma}_{\mathrm{r}}$ and $\widetilde{\boldsymbol{\sigma}}_{\mathrm{r}}$ can be substituted, with reference to eqns (4.1) and (4.8), by the difference of the stresses $\boldsymbol{\sigma}$ and $\widetilde{\boldsymbol{\sigma}}$. It follows for the integrand that

$$\left[\boldsymbol{\sigma}_{\mathrm{r}}-\widetilde{\boldsymbol{\sigma}}_{\mathrm{r}}\right]^{\mathrm{t}}\dot{\boldsymbol{\eta}}=\left[\boldsymbol{\sigma}-\widetilde{\boldsymbol{\sigma}}\right]^{\mathrm{t}}\dot{\boldsymbol{\eta}}>0, \tag{4.12}$$

the inequality being a consequence of Drucker's plasticity postulate (Section 3.1.2). Here, $\boldsymbol{\sigma}$ represents the stress state $\phi(\boldsymbol{\sigma})=0$ where the plastic strain rate $\dot{\boldsymbol{\eta}}$ occurs, whereas $\phi(\widetilde{\boldsymbol{\sigma}})<0$ as required by the static theorem (Fig. 4.1). As a consequence of eqns (4.11) and (4.12), the time rate of $\mathcal{E}$ in eqn (4.10) is negative:

$$\dot{\mathcal{E}}=-\int_{V}\left[\boldsymbol{\sigma}-\widetilde{\boldsymbol{\sigma}}\right]^{\mathrm{t}}\dot{\boldsymbol{\eta}}\mathrm{d}V<0. \tag{4.13}$$

Since $\mathcal{E}$ in eqn (4.9) must be positive ($\mathcal{E}>0$), the negative time rate ($\dot{\mathcal{E}}<0$) can exist only for a limited time, and therefore the plastic flow $\dot{\boldsymbol{\eta}}$

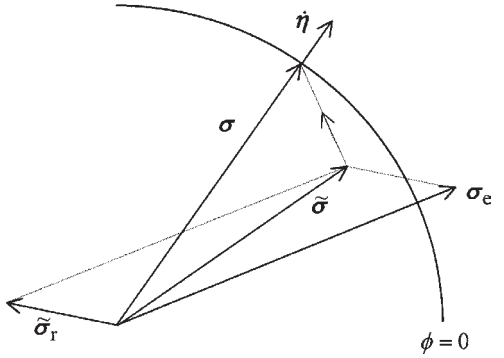

Figure 4.1: On the static shakedown theorem.

must cease to occur after a certain initial period in the loading programme. This conclusion has been based on the assumption of a time-independent residual stress system $\widetilde{\boldsymbol{\sigma}}_{\mathrm{r}}$ which, added to the (fictitious) elastic solution, results in stresses $\widetilde{\boldsymbol{\sigma}}$ representing elastic states of the material, $\phi(\widetilde{\boldsymbol{\sigma}}) < 0$. It thus verifies the first part of the static shakedown theorem.

The meaning of the second part of the theorem is that the establishment of a stationary residual stress system will actually not be possible because plastic flow does not cease to occur during the course of the loading programme.

4.3 Kinematic shakedown theorem (Koiter)

Koiter's kinematic theorem of shakedown [4] is associated with the notion of the virtual cycle or increment of plastic strain. In this connection, let an assumed distribution of plastic strain rate $\dot{\underline{\boldsymbol{\eta}}}(t)$ be imposed on the structure and be considered over a certain time interval T within the loading programme. As long as the plastic strain rate $\dot{\underline{\boldsymbol{\eta}}}$ is not kinematically admissible, it induces complementary elastic strains $\dot{\underline{\boldsymbol{\varepsilon}}}$ in order that the sum

$$\dot{\underset{\sim}{\boldsymbol{\gamma}}} = \dot{\underline{\boldsymbol{\varepsilon}}} + \dot{\underline{\boldsymbol{\eta}}} = \boldsymbol{\partial}\dot{\underset{\sim}{\mathbf{u}}}, \tag{4.14}$$

constitutes a virtual strain associated with the virtual velocity field $\dot{\underset{\sim}{\mathbf{u}}}$.

The velocity field $\dot{\underset{\sim}{\mathbf{u}}}(t)$ is not a plastic yield mechanism since the elastic constituent $\dot{\underline{\boldsymbol{\varepsilon}}}$ is present in eqn (4.14). The stress

$$\dot{\underline{\boldsymbol{\sigma}}} = \boldsymbol{\kappa}\dot{\underline{\boldsymbol{\varepsilon}}} = \boldsymbol{\kappa}[\dot{\underset{\sim}{\boldsymbol{\gamma}}} - \dot{\underline{\boldsymbol{\eta}}}], \tag{4.15}$$

related to the complementary elastic strain by the elastic properties of the material constitutes a self-equilibrating system.

The absence of stress resultants for $\dot{\underline{\boldsymbol{\sigma}}}$ can be stated by the virtual work principle in the form

$$\int_V \dot{\underset{\sim}{\gamma}}^{\mathrm{t}} \dot{\underline{\boldsymbol{\sigma}}} \mathrm{d}V = 0. \tag{4.16}$$

Expressing in eqn (4.16) the stress rate by the elastic relation, eqn (4.15), and deriving the strain rate $\dot{\underset{\sim}{\gamma}}$ from the virtual velocity field $\dot{\underset{\sim}{\mathbf{u}}}$ one obtains

$$\int_V (\boldsymbol{\partial} \dot{\underset{\sim}{\mathbf{u}}})^{\mathrm{t}} \boldsymbol{\kappa} \boldsymbol{\partial} \dot{\underset{\sim}{\mathbf{u}}} \mathrm{d}V = \int_V (\boldsymbol{\partial} \dot{\underset{\sim}{\mathbf{u}}})^{\mathrm{t}} \boldsymbol{\kappa} \dot{\underline{\boldsymbol{\eta}}} \mathrm{d}V, \tag{4.17}$$

which governs the virtual velocity $\dot{\underset{\sim}{\mathbf{u}}}$ as a consequence of the imposed plastic strain rate $\dot{\underline{\boldsymbol{\eta}}}$. A solution of eqn (4.17) furnishes $\dot{\underset{\sim}{\mathbf{u}}}$ from which $\dot{\underset{\sim}{\gamma}}$ is deduced, and $\dot{\underline{\boldsymbol{\varepsilon}}}$, $\dot{\underline{\boldsymbol{\sigma}}}$ are then obtained via eqns (4.14) and (4.15), respectively.

The *virtual cycle* or *increment of plastic strain* is defined as a kinematically compatible strain field given by the time integral

$$\underset{\sim}{\Delta} \boldsymbol{\eta} = \int_0^T \dot{\underline{\boldsymbol{\eta}}} \mathrm{d}t = \int_0^T \dot{\underset{\sim}{\gamma}} \, \mathrm{d}t = \underset{\sim}{\Delta} \boldsymbol{\gamma} \tag{4.18}$$

over the interval T. For an explanation of the definition of the virtual cycle of plastic strain rate by eqn (4.18), it is pointed out that the momentary $\dot{\underline{\boldsymbol{\eta}}}$ is incompatible, while its integral $\underset{\sim}{\Delta} \boldsymbol{\eta}$ over the time interval T is required to constitute a kinematically admissible strain field. It follows that the incremental plastic strain

$$\underset{\sim}{\Delta} \boldsymbol{\eta} = \int_0^T \boldsymbol{\partial} \dot{\underset{\sim}{\mathbf{u}}} \mathrm{d}t = \boldsymbol{\partial} \left[\int_0^T \dot{\underset{\sim}{\mathbf{u}}} \mathrm{d}t \right] = \boldsymbol{\partial} \left[\underset{\sim}{\Delta} \mathbf{u} \right] \tag{4.19}$$

derives from the displacement field,

$$\underset{\sim}{\Delta} \mathbf{u} = \int_0^T \dot{\underset{\sim}{\mathbf{u}}} \mathrm{d}t, \tag{4.20}$$

which may be considered an *incremental yield mechanism.*

The definition of the virtual increment of plastic strain as a compatible strain by means of eqn (4.18) implies that for the interval T the elastic strain from eqn (4.14) vanishes:

$$\int_0^T \dot{\underline{\boldsymbol{\varepsilon}}} \mathrm{d}t = \mathbf{0}, \tag{4.21}$$

as does the associated self-equilibrating stress

$$\int_0^T \underline{\dot{\boldsymbol{\sigma}}} \mathrm{d}t = \mathbf{0}. \tag{4.22}$$

Further to the above definitions, we introduce the work of the applied forces $\mathbf{f}(t), \mathbf{t}(t)$ on the virtual velocity $\underset{\sim}{\dot{\mathbf{u}}}(t)$ over the time interval T by the integral

$$\int_0^T \underset{\sim}{L} \mathrm{d}t = \int_0^T \left[\int_V \mathbf{f}^{\mathrm{t}} \underset{\sim}{\dot{\mathbf{u}}} \mathrm{d}V + \int_S \mathbf{t}^{\mathrm{t}} \underset{\sim}{\dot{\mathbf{u}}} \mathrm{d}S \right] \mathrm{d}t, \tag{4.23}$$

and the mechanical dissipation over the same interval due to the imposed plastic strain rate $\underline{\dot{\boldsymbol{\eta}}}(t)$ by the integral

$$\int_0^T \underline{D} \mathrm{d}t = \int_0^T \left[\int_V \underline{\boldsymbol{\sigma}}^{\mathrm{t}} \underline{\dot{\boldsymbol{\eta}}} \mathrm{d}V \right] \mathrm{d}t. \tag{4.24}$$

In eqn (4.24), $\underline{\boldsymbol{\sigma}}$ denotes the stress associated with the imposed plastic strain rate $\underline{\dot{\boldsymbol{\eta}}}$ via the flow rule. In eqn (4.23), a possible contribution $\sum_{j=1}^{K} \mathbf{P}_j^{\mathrm{t}} \underset{\sim}{\dot{\mathbf{u}}}_j$ on the right-hand side due to discrete forces $\mathbf{P}_j(t)$ is also subject to the time integration.

The kinematic shakedown theorem may be stated as follows:

(i) The structure will not shake down by adaptation to the loading programme if for an interval T a *single* virtual plastic strain increment

$$\underset{\sim}{\Delta \boldsymbol{\eta}} = \int_0^T \underline{\dot{\boldsymbol{\eta}}} \mathrm{d}t = \int_0^T \boldsymbol{\partial} \underset{\sim}{\dot{\mathbf{u}}} \mathrm{d}t, \tag{4.25}$$

can be found which satisfies the inequality

$$\int_0^T \underset{\sim}{L} \mathrm{d}t > \int_0^T \underline{D} \mathrm{d}t. \tag{4.26}$$

(ii) The structure will adapt itself to the loading programme if the above inequality can be reversed for *all* combinations of imposed plastic strain rates $\underline{\dot{\boldsymbol{\eta}}}(t)$ in the virtual cycle and loads $\mathbf{f}(t), \mathbf{t}(t)$ in the programme.

For a proof of the kinematic theorem, we assume the structure to shake down despite the inequality in eqn (4.26). According to the static theorem, a virtual system of stationary residual stress $\widetilde{\boldsymbol{\sigma}}_{\mathrm{r}}$ will then exist such that superposition of the (fictitious) elastic solution $\boldsymbol{\sigma}_{\mathrm{e}}(t)$ for the loading programme does not cause plastic flow. The mathematical expression for the above is

$$\widetilde{\boldsymbol{\sigma}}_{\mathrm{r}} + \boldsymbol{\sigma}_{\mathrm{e}}(t) = \widetilde{\boldsymbol{\sigma}}(t) \quad \text{and} \quad \phi(\widetilde{\boldsymbol{\sigma}}) < 0. \tag{4.27}$$

The static equivalence of the virtual stress $\widetilde{\boldsymbol{\sigma}}$ and the externally applied forces $\mathbf{f}, \mathbf{t}$ can be manifested by the virtual work principle. Since $\dot{\underset{\sim}{\mathbf{u}}}$ is a kinematically admissible velocity field and $\dot{\underset{\sim}{\boldsymbol{\gamma}}}$ the associated strain rate, we can write for the interval T,

$$\int_0^T \left[\int_V \mathbf{f}^{\mathrm{t}} \dot{\underset{\sim}{\mathbf{u}}} \mathrm{d}V + \int_S \mathbf{t}^{\mathrm{t}} \dot{\underset{\sim}{\mathbf{u}}} \mathrm{d}S \right] \mathrm{d}t = \int_0^T \left[\int_V \widetilde{\boldsymbol{\sigma}}^{\mathrm{t}} \dot{\underset{\sim}{\boldsymbol{\gamma}}} \mathrm{d}V \right] \mathrm{d}t, \tag{4.28}$$

where the original expression for the virtual rate of work has been integrated over the considered time interval.

The left-hand side of eqn (4.28) is identified as the work expression in eqn (4.23), the left-hand side in eqn (4.26). The right-hand side of eqn (4.28) is further investigated in the following. In this respect, the volume integral is detailed by means of the strain composition of eqn (4.14) to read

$$\int_V \widetilde{\boldsymbol{\sigma}}^{\mathrm{t}} \dot{\underset{\sim}{\boldsymbol{\gamma}}} \mathrm{d}V = \int_V \widetilde{\boldsymbol{\sigma}}^{\mathrm{t}} \dot{\underline{\boldsymbol{\eta}}} \mathrm{d}V + \int_V \widetilde{\boldsymbol{\sigma}}^{\mathrm{t}} \dot{\underline{\boldsymbol{\varepsilon}}} \mathrm{d}V. \tag{4.29}$$

Also, using the definition of $\widetilde{\boldsymbol{\sigma}}$ in eqn (4.27),

$$\int_V \widetilde{\boldsymbol{\sigma}}^{\mathrm{t}} \dot{\underline{\boldsymbol{\varepsilon}}} \mathrm{d}V = \int_V \widetilde{\boldsymbol{\sigma}}_{\mathrm{r}}^{\mathrm{t}} \dot{\underline{\boldsymbol{\varepsilon}}} \mathrm{d}V + \int_V \boldsymbol{\sigma}_{\mathrm{e}}^{\mathrm{t}} \dot{\underline{\boldsymbol{\varepsilon}}} \mathrm{d}V. \tag{4.30}$$

The integrand in the second expression on the right-hand side of eqn (4.30) is transformed by the law of elasticity to

$$\boldsymbol{\sigma}_{\mathrm{e}}^{\mathrm{t}} \dot{\underline{\boldsymbol{\varepsilon}}} = \boldsymbol{\sigma}_{\mathrm{e}}^{\mathrm{t}} \boldsymbol{\kappa}^{-1} \dot{\underline{\boldsymbol{\sigma}}} = \boldsymbol{\varepsilon}_{\mathrm{e}}^{\mathrm{t}} \dot{\underline{\boldsymbol{\sigma}}}. \tag{4.31}$$

As the elastic solution supplies kinematically compatible strains $\boldsymbol{\varepsilon}_{\mathrm{e}}$, and $\dot{\underline{\boldsymbol{\sigma}}}$ is a self-equilibrating stress system, the principle of virtual work states that

$$\int_V \boldsymbol{\sigma}_{\mathrm{e}}^{\mathrm{t}} \dot{\underline{\boldsymbol{\varepsilon}}} \mathrm{d}V = \int \boldsymbol{\varepsilon}_{\mathrm{e}}^{\mathrm{t}} \dot{\underline{\boldsymbol{\sigma}}} \mathrm{d}V = 0. \tag{4.32}$$

The result of eqn (4.32) simplifies eqn (4.30) for use in eqn (4.29). Accordingly, the time integral in eqn (4.28) now reads

$$\int_0^T \left[\int_V \widetilde{\boldsymbol{\sigma}}^{\mathrm{t}} \dot{\underset{\sim}{\boldsymbol{\gamma}}} \mathrm{d}V \right] \mathrm{d}t = \int_0^T \left[\int_V \widetilde{\boldsymbol{\sigma}}^{\mathrm{t}} \dot{\underline{\boldsymbol{\eta}}} \mathrm{d}V \right] \mathrm{d}t + \int_0^T \left[\int_V \widetilde{\boldsymbol{\sigma}}_{\mathrm{r}}^{\mathrm{t}} \dot{\underline{\boldsymbol{\varepsilon}}} \mathrm{d}V \right] \mathrm{d}t. \tag{4.33}$$

Since the virtual stress field $\widetilde{\boldsymbol{\sigma}}_{\mathrm{r}}$ was assumed to be time independent, we deduce for the second term on the right-hand side in eqn (4.33)

$$\int_0^T \left[\int_V \widetilde{\boldsymbol{\sigma}}_{\mathrm{r}}^{\mathrm{t}} \dot{\underline{\boldsymbol{\varepsilon}}} \mathrm{d}V \right] \mathrm{d}t = \int_V \widetilde{\boldsymbol{\sigma}}_{\mathrm{r}}^{\mathrm{t}} \left[\int_0^T \dot{\underline{\boldsymbol{\varepsilon}}} \mathrm{d}t \right] \mathrm{d}V = 0. \tag{4.34}$$

The vanishing of the integral for the elastic strain rate over the time interval T is by definition a property of the virtual plastic strain cycle.

Considering eqn (4.33) with eqn (4.34) in eqn (4.28), we conclude that

$$\int_0^T \underset{\sim}{L} \mathrm{d}t = \int_0^T \left[\int_V \widetilde{\boldsymbol{\sigma}}^{\mathrm{t}} \underline{\dot{\boldsymbol{\eta}}} \mathrm{d}V \right] \mathrm{d}t. \tag{4.35}$$

Equation (4.35) which results from the assumption of shakedown will be contrasted with the inequality in eqn (4.26) stated in the theorem. For this purpose, we recall that the fictitious stress $\underline{\boldsymbol{\sigma}}$ in eqn (4.24) is associated with the imposed strain rate $\underline{\dot{\boldsymbol{\eta}}}$ by means of the plastic flow rule, while $\widetilde{\boldsymbol{\sigma}}$ in eqn (4.35) is not. In this case the plasticity postulate may be interpreted as

$$[\underline{\boldsymbol{\sigma}} - \widetilde{\boldsymbol{\sigma}}]^{\mathrm{t}} \underline{\dot{\boldsymbol{\eta}}} > 0 \quad \text{or} \quad \widetilde{\boldsymbol{\sigma}}^{\mathrm{t}} \underline{\dot{\boldsymbol{\eta}}} < \underline{\boldsymbol{\sigma}}^{\mathrm{t}} \underline{\dot{\boldsymbol{\eta}}}. \tag{4.36}$$

Integration for the volume of the structure and over the time interval T leads to the inequality

$$\int_0^T \left[\int_V \widetilde{\boldsymbol{\sigma}}^{\mathrm{t}} \underline{\dot{\boldsymbol{\eta}}} \, \mathrm{d}V \right] \mathrm{d}t < \int_0^T \left[\int_V \underline{\boldsymbol{\sigma}}^{\mathrm{t}} \underline{\dot{\boldsymbol{\eta}}} \, \mathrm{d}V \right] \mathrm{d}t = \int_0^T \underline{D} \, \mathrm{d}t. \tag{4.37}$$

The consequence for eqn (4.35) is

$$\int_0^T \underset{\sim}{L} \mathrm{d}t < \int_0^T \underline{D} \mathrm{d}t. \tag{4.38}$$

It follows that the assumption of shakedown is contradictory to the inequality stated by the theorem in eqn (4.26). The structure will not adapt to the prescribed loading programme. This confirms the first part of the kinematic theorem. Regarding the second part of the theorem, it is concluded by reasoning that if eqn (4.38) is unconditionally valid, the static theorem is satisfied and therefore the structure will shake down. For a rigorous mathematical proof of the second part the reader is referred to [1].

4.4 Application of shakedown theory

4.4.1 Shakedown of rod under torsion and tension

Utilization of the static theorem will be illustrated by the cylindrical rod of circular cross-section (Fig. 4.2) subjected to the axial tensile force P and the torque T; the material is elastic–perfectly plastic. The simple example treated in [5] is well suited for the purpose of demonstration.

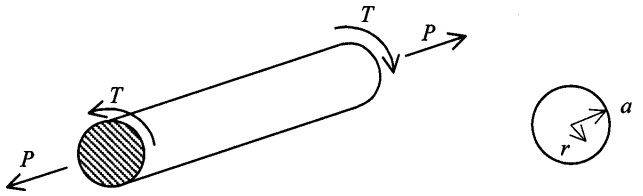

Figure 4.2: Rod under torsion and tension.

We notice the elastic solution for the axial stress σ and the shear stress τ

$$\begin{aligned} \sigma_{\mathrm{e}} &= \frac{P}{\pi a^2}, \\ \tau_{\mathrm{e}} &= \tau_{\mathrm{a}} \frac{r}{a} = \frac{2T}{\pi a^3} \frac{r}{a}, \end{aligned} \tag{4.39}$$

where τ_{a} denotes the value of the shear stress at the periphery ($r = a$). In eqn (4.39) the shear stress has been related to the torque

$$T = 2\pi \int_0^a \tau \, r^2 \mathrm{d}r. \tag{4.40}$$

In the elastic range the integral is evaluated for a linear variation of τ along the radius. The elasticity limit is attained when $\tau_{\mathrm{a}} = \tau_{\mathrm{s}}$, the yield stress of the material in shear. Then,

$$T_{\mathrm{s}} = \frac{\pi a^3}{2} \tau_{\mathrm{s}}. \tag{4.41}$$

The plastic limit state is given for $\tau = \tau_{\mathrm{s}}$ in the entire cross-section. The associated torque is

$$T_{\mathrm{F}} = \frac{2\pi a^3}{3} \tau_{\mathrm{s}} = \frac{4}{3} T_{\mathrm{s}}. \tag{4.42}$$

The homologous quantities of axial force are

$$P_{\mathrm{s}} = \pi a^2 \sigma_{\mathrm{s}} = P_{\mathrm{F}}, \tag{4.43}$$

where $\sigma_{\mathrm{s}} = \sqrt{3} \tau_{\mathrm{s}}$ is the yield stress of the material in tension.

An obvious system of stationary residual stresses is defined by the quantities

$$\begin{aligned} \widetilde{\sigma}_{\mathrm{r}} &= 0, \\ \widetilde{\tau}_{\mathrm{r}} &= \lambda \left(1 - \frac{4}{3} \frac{r}{a} \right) \tau_{\mathrm{s}}. \end{aligned} \tag{4.44}$$

The residual stresses are taken as by elastic unloading from the fully plastic state. The multiplier λ is a free parameter.

The virtual stresses entering Melan's theorem are

$$\begin{aligned} \widetilde{\sigma} &= \sigma_{\mathrm{e}} + \widetilde{\sigma}_{\mathrm{r}} = \frac{P}{\pi a^2}, \\ \widetilde{\tau} &= \tau_{\mathrm{e}} + \widetilde{\tau}_{\mathrm{r}} = \frac{2T}{\pi a^3}\frac{r}{a} + \lambda\left(1 - \frac{4}{3}\frac{r}{a}\right)\tau_{\mathrm{s}}. \end{aligned} \tag{4.45}$$

For shakedown the above stress state must be below the yield limit of the material. With the von Mises yield criterion:

$$\widetilde{\sigma}^2 + 3\widetilde{\tau}^2 < \sigma_{\mathrm{s}}^2,$$

or normalizing by the yield stress,

$$\left(\frac{\widetilde{\sigma}}{\sigma_{\mathrm{s}}}\right)^2 + \left(\frac{\widetilde{\tau}}{\tau_{\mathrm{s}}}\right)^2 < 1. \tag{4.46}$$

Loading factors for the axial force and the torque are defined with reference to the values at the elastic limit, a dimensionless radial distance is introduced:

$$\begin{aligned} p &= \frac{P}{P_{\mathrm{s}}} = \frac{1}{\sigma_{\mathrm{s}}}\frac{P}{\pi a^2}, \\ q &= \frac{T}{T_{\mathrm{s}}} = \frac{1}{\tau_{\mathrm{s}}}\frac{2T}{\pi a^3}, \\ \rho &= \frac{r}{a}. \end{aligned} \tag{4.47}$$

With the above quantities the elastic constituents σ_{e} and τ_{e} in eqn (4.45) can be referred to the elasticity limit in tension and shear, respectively. Then one obtains

$$\frac{\widetilde{\sigma}}{\sigma_{\mathrm{s}}} = p, \quad \frac{\widetilde{\tau}}{\tau_{\mathrm{s}}} = q\rho + \lambda\left(1 - \frac{4}{3}\rho\right). \tag{4.48}$$

The yield locus from eqn (4.46) can now be expressed in the form

$$q\rho + \lambda\left(1 - \frac{4}{3}\rho\right) = \pm\sqrt{1 - p^2} \tag{4.49}$$

and bounds the shakedown region.

For pure torsion ($p = 0$) eqn (4.49) suggests representation in the q, λ-plane (Fig. 4.3). Since $0 \le \rho \le 1$, eqn (4.49) bounds the shakedown region by a parallelogram:

$$\rho = 0\colon \ \lambda = \pm 1, \quad \rho = 1\colon \ q - \lambda/3 = \pm 1.$$

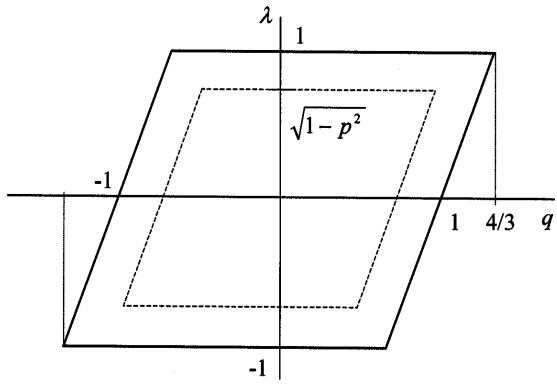

Figure 4.3: Shakedown diagram for the rod.

The loading cycles associated with $\lambda = 0$ are symmetric: $(-1 < q < 1)$, no yield. For $\lambda = 1$ shakedown is ensured if $-2/3 < q < 4/3$; the maximum torque coincides with the plastic limit moment for the twisted rod. Independently of the value of the parameter λ the shakedown interval for q is bounded by $q_{\max} - q_{\min} = 2$.

Combination with the axial force $(p \neq 0)$ is seen to reduce the shakedown region while maintaining the shape of a parallelogram:

$$\lambda = \pm\sqrt{1-p^2}, \quad q - \lambda/3 = \pm\sqrt{1-p^2}.$$

The maximum torque is now given by $q_{\max} = (4/3)\sqrt{1-p^2}$, and the shakedown interval is $q_{\max} - q_{\min} = 2\sqrt{1-p^2}$ independently of the value of the parameter λ.

4.4.2 Further reading

A survey on the shakedown analysis of elastoplastic structures is given in [6]. In this paper, shakedown analysis is positioned within a classification of elastoplastic problems, the shakedown theory is extended to account for thermal effects and some applications are presented. In addition, reference is made to additional literature dealing with specific issues of shakedown analysis of structures and structural members. The literature on variable loads in plasticity surveyed in [7] goes beyond basic assumptions of the present classical theory. The continuing development of the subject is reflected by the individual articles in [8].

References

[1] W.T. Koiter, General theorems for elastic–plastic solids, in *Progress in Solids Mechanics*, Vol. 1, I.N. Sneddon and R. Hill (Eds), Chapter 4, North-Holland, Amsterdam, 1960, pp. 167–221.

[2] E. Melan, Der Spannungszustand eines Hencky-Mises'schen Kontinuums bei veränderlicher Belastung, *Sitz. Ber. Ak. Wiss. Wien*, IIa, **147** (1938) 73.

[3] E. Melan, Zur Plastizität des räumlichen Kontinuums, *Ing. Arch.* **9** (1938) 116.

[4] W.T. Koiter, A new general theorem on shakedown of elastic–plastic structures, *Proc. Kon. Ned. Ak. Wet.* B **59** (1956) 24.

[5] L.M. Kachanov, *Foundations of the Theory of Plasticity*, North-Holland, Amsterdam, 1971.

[6] A. Sawczuk, Shakedown analysis of elastic–plastic structures, *Nucl. Engng Des.* **28** (1974) 121–136.

[7] J.A. König and G. Maier, Shakedown analysis of elastoplastic structures: A review of recent developments, *Nucl. Engng Des.* **66** (1981) 81–95.

[8] D. Weichert and G. Maier (Eds), *Inelastic Analysis of Structures under Variable Loads*, Solid Mechanics and its Applications 83, Kluwer, Dordrecht, 2000/Springer, Berlin, 2001.

This page intentionally left blank

CHAPTER 5

Development of finite element solution methods

5.1 The systematics of the finite element method

The finite element method is described here to the extent required for the present purpose. For complete information on the subject, the reader is referred to the standard textbook by Zienkiewicz *et al.* [1].

The development of finite element methods for the numerical analysis of solids and structures relies on the virtual work principle presented in Chapter 3. It is expressed as

$$\sum_{l=1}^{K} \underset{\sim}{\mathbf{u}}_l^{\mathrm{t}} \mathbf{P}_l + \int_S \underset{\sim}{\mathbf{u}}^{\mathrm{t}} \mathbf{t} \mathrm{d}S + \int_V \underset{\sim}{\mathbf{u}}^{\mathrm{t}} \mathbf{f} \mathrm{d}V = \int_V \underset{\sim}{\boldsymbol{\gamma}}^{\mathrm{t}} \boldsymbol{\sigma} \mathrm{d}V. \tag{5.1}$$

The quantities $\underset{\sim}{\mathbf{u}}$ and $\underset{\sim}{\boldsymbol{\gamma}}$ refer to the virtual displacement field and the associated strain, respectively, $\mathbf{P}_l$ denotes a point force vector, $\mathbf{t}$ the surface forces acting on the surface S, $\mathbf{f}$ the body forces in the volume V. The above equivalence of the inner stresses and applied forces is an alternative statement of the equilibrium conditions (Chapter 2).

Next, the domain of integration in eqn (5.1) is divided into a number of finite elements (*nel*) defined by a mesh with N nodal points (Fig. 5.1). The geometry of the finite element model is described by the coordinates $\mathbf{x}_i = \{x\, y\, z\}_i$ of the N nodal points. They are collected in the $3N \times 1$ vector array

$$\mathbf{X} = \{\mathbf{x}_1\, \mathbf{x}_2 \cdots \mathbf{x}_i \cdots \mathbf{x}_N\}. \tag{5.2}$$

Each individual finite element is specified by n element nodal points. The respective coordinates can be grouped from the vector in eqn (5.2)

$$\mathbf{X}_q = \{\mathbf{x}_1 \cdots \mathbf{x}_j \cdots \mathbf{x}_n\}_q = \mathbf{a}_q \mathbf{X}. \tag{5.3}$$

The $3n \times 1$ vector array $\mathbf{X}_q$ comprises the coordinates of the qth element; the incidence matrix $\mathbf{a}_q$ symbolizes the grouping operation. Between nodal

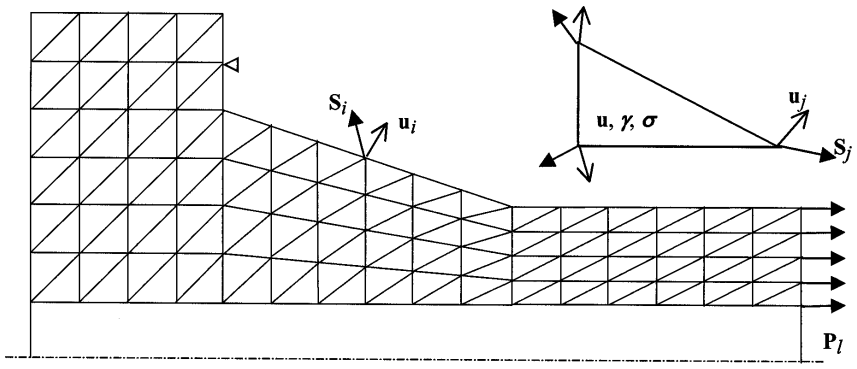

Figure 5.1: Discretization by finite elements.

points the coordinates vary in accordance with the prescribed geometric characteristics of the element.

The displacement vector of the system is defined in analogy to eqn (5.2) as

$$\mathbf{U} = \{\mathbf{u}_1\, \mathbf{u}_2 \cdots \mathbf{u}_i \cdots \mathbf{u}_N\} \tag{5.4}$$

and $\mathbf{u}_i = \{u\, v\, w\}_i$ denotes the displacement of the ith mesh nodal point. Grouping for individual elements is as in eqn (5.3):

$$\mathbf{U}_q = \{\mathbf{u}_1 \cdots \mathbf{u}_j \cdots \mathbf{u}_n\}_q = \mathbf{a}_q \mathbf{U}. \tag{5.5}$$

The variation of the displacement $\mathbf{u} = \{u\, v\, w\}$ within the element is presented in the form

$$\mathbf{u}(\mathbf{x}) = \boldsymbol{\omega}(\mathbf{x})\mathbf{U}_q. \tag{5.6}$$

The $3 \times 3n$ matrix $\boldsymbol{\omega}$ contains interpolation functions pertaining to the finite element approximation of the deformation kinematics. From eqn (5.6), the strain within the element can be obtained analogously to eqn (2.59) with the differential operator of eqn (2.60),

$$\boldsymbol{\gamma}(\mathbf{x}) = \boldsymbol{\partial}(\boldsymbol{\omega}\mathbf{U}_q) = \boldsymbol{a}(\mathbf{x})\mathbf{U}_q. \tag{5.7}$$

The $6 \times 3n$ matrix $\boldsymbol{a}(\mathbf{x})$ denotes the strain operator for the finite element associated with the displacement distribution by the function $\boldsymbol{\omega}(\mathbf{x})$.

The piecewise (i.e. within the domain of single elements) function defined by eqn (5.6) is utilized for the virtual displacements on the left-hand side of the work expression in eqn (5.1). The virtual work of the applied forces can be obtained as the sum of contributions from the individual finite element

domains. For a single finite element

$$\sum_{k=1}^{L} \underset{\sim}{\mathbf{u}}_k^{\mathrm{t}} \mathbf{P}_k + \int_{S_q} \underset{\sim}{\mathbf{u}}^{\mathrm{t}} \mathbf{t} \mathrm{d}S + \int_{V_q} \underset{\sim}{\mathbf{u}}^{\mathrm{t}} \mathbf{f} \mathrm{d}V$$

$$= \underset{\sim}{\mathbf{U}}_q^{\mathrm{t}} \left[\sum_{k=1}^{L} \boldsymbol{\omega}_k^{\mathrm{t}} \mathbf{P}_k + \int_{S_q} \boldsymbol{\omega}^{\mathrm{t}} \mathbf{t} \mathrm{d}S + \int_{V_q} \boldsymbol{\omega}^{\mathrm{t}} \mathbf{f} \mathrm{d}V \right] = \underset{\sim}{\mathbf{U}}_q^{\mathrm{t}} \mathbf{P}_q. \tag{5.8}$$

This defines the $3n \times 1$ vector array

$$\mathbf{P}_q = \{\mathbf{P}_1 \cdots \mathbf{P}_j \cdots \mathbf{P}_n\}_q$$

$$= \sum_{k=1}^{L} \boldsymbol{\omega}_k^{\mathrm{t}} \mathbf{P}_k + \int_{S_q} \boldsymbol{\omega}^{\mathrm{t}} \mathbf{t} \mathrm{d}S + \int_{V_q} \boldsymbol{\omega}^{\mathrm{t}} \mathbf{f} \mathrm{d}V \tag{5.9}$$

of forces $\mathbf{P}_j = \{P_{\mathrm{x}}\, P_{\mathrm{y}}\, P_{\mathrm{z}}\}_j$ at the element nodal points, which are equivalent to the actually applied ones, $\mathbf{P}_k$ $(k = 1, \ldots, L)$, $\mathbf{t}$ and $\mathbf{f}$. The forces applied at single points in the element are denoted by $\mathbf{P}_k$, and $\boldsymbol{\omega}_k = \boldsymbol{\omega}(\mathbf{x}_k)$ is the value of the interpolation function at the point of application with coordinates $\mathbf{x}_k = \{x\, y\, z\}_k$. Note that tractions transmitted between elements do not appear in eqn (5.8). They cancel one another in the sum if the kinematic approximation guarantees the continuity of the velocity across the element boundaries.

The summation of eqn (5.8) over all finite element contributions furnishes the virtual work of the forces in the entire discretized domain:

$$\sum_{l=1}^{K} \underset{\sim}{\mathbf{u}}_l^{\mathrm{t}} \mathbf{P}_l + \int_{S} \underset{\sim}{\mathbf{u}}^{\mathrm{t}} \mathbf{t} \mathrm{d}S + \int_{V} \underset{\sim}{\mathbf{u}}^{\mathrm{t}} \mathbf{f} \mathrm{d}V = \sum_{q=1}^{nel} \underset{\sim}{\mathbf{U}}_q^{\mathrm{t}} \mathbf{P}_q. \tag{5.10}$$

Introduction of the hypervectors

$$\mathbf{U}_{\mathrm{E}} = \{\mathbf{U}_1\, \mathbf{U}_2 \cdots \mathbf{U}_q \cdots \mathbf{U}_{nel}\}$$

$$\mathbf{P}_{\mathrm{E}} = \{\mathbf{P}_1\, \mathbf{P}_2 \cdots \mathbf{P}_q \cdots \mathbf{P}_{nel}\}$$

allows symbolic representation of the sum in eqn (5.10) as a scalar product

$$\sum_{q=1}^{nel} \underset{\sim}{\mathbf{U}}_q^{\mathrm{t}} \mathbf{P}_q = \underset{\sim}{\mathbf{U}}_{\mathrm{E}}^{\mathrm{t}} \mathbf{P}_{\mathrm{E}}.$$

With eqn (5.5) for the individual elements in the hypervector $\mathbf{U}_{\mathrm{E}}$, one obtains collectively between elemental and mesh nodal point displacements:

$$\mathbf{U}_{\mathrm{E}} = \begin{bmatrix} \vdots \\ \mathbf{U}_q \\ \vdots \end{bmatrix} = \begin{bmatrix} \vdots \\ \mathbf{a}_q \\ \vdots \end{bmatrix} \mathbf{U} = \mathbf{a}\mathbf{U}. \tag{5.11}$$

This ordering operation applies equally to virtual displacements. The virtual work expression in eqn (5.10) becomes

$$\underset{\sim}{\mathbf{U}}{}^{\mathrm{t}}_{\mathrm{E}}\mathbf{P}_{\mathrm{E}} = \underset{\sim}{\mathbf{U}}{}^{\mathrm{t}}\mathbf{a}^{\mathrm{t}}\mathbf{P}_{\mathrm{E}} = \underset{\sim}{\mathbf{U}}{}^{\mathrm{t}}\mathbf{P}. \tag{5.12}$$

This formally defines the $3N \times 1$ vector,

$$\mathbf{P} = \{\mathbf{P}_1\, \mathbf{P}_2 \cdots \mathbf{P}_i \cdots \mathbf{P}_N\} = \mathbf{a}^{\mathrm{t}}\mathbf{P}_{\mathrm{E}} \tag{5.13}$$

comprising the forces $\mathbf{P}_i = \{P_{\mathrm{x}}\, P_{\mathrm{y}}\, P_{\mathrm{z}}\}_i$ at the mesh nodal points, equivalent to those actually applied to the system. The matrix operation in eqn (5.13) stands for their formation effected by accumulating element contributions from $\mathbf{P}_{\mathrm{E}}$ following the pattern of the incidence matrix $\mathbf{a}$ (see eqn (5.18) below).

For an analogous hierarchical evaluation of the virtual work of the stresses on the right-hand side of eqn (5.1), we consider a single element in conjunction with the approximation for the virtual strain in eqn (5.7)

$$\int_{V_q} \underset{\sim}{\boldsymbol{\gamma}}{}^{\mathrm{t}}\boldsymbol{\sigma}\mathrm{d}V = \underset{\sim}{\mathbf{U}}{}^{\mathrm{t}}_{q} \int_{V_q} \boldsymbol{a}^{\mathrm{t}}\boldsymbol{\sigma}\mathrm{d}V = \underset{\sim}{\mathbf{U}}{}^{\mathrm{t}}_{q}\mathbf{S}_q. \tag{5.14}$$

The $3n \times 1$ vector

$$\mathbf{S}_q = \{\mathbf{S}_1\ \cdots \mathbf{S}_j \cdots \mathbf{S}_n\}_q = \int_{V_q} \boldsymbol{a}^{\mathrm{t}}\boldsymbol{\sigma}\mathrm{d}V \tag{5.15}$$

comprises the forces $\mathbf{S}_j = \{S_{\mathrm{x}}\, S_{\mathrm{y}}\, S_{\mathrm{z}}\}_j$ resulting at each element nodal point from the stress $\boldsymbol{\sigma}$ in the element.

The virtual work of the stresses in the entire discretized domain is obtained by summation of all element contributions from eqn (5.14):

$$\int_{V} \underset{\sim}{\boldsymbol{\gamma}}{}^{\mathrm{t}}\boldsymbol{\sigma}\mathrm{d}V = \sum_{q=1}^{nel} \underset{\sim}{\mathbf{U}}{}^{\mathrm{t}}_{q}\mathbf{S}_q$$

and

$$\sum_{q=1}^{nel} \underset{\sim}{\mathbf{U}}{}^{\mathrm{t}}_{q}\mathbf{S}_q = \underset{\sim}{\mathbf{U}}{}^{\mathrm{t}}_{\mathrm{E}}\mathbf{S}_{\mathrm{E}} = \underset{\sim}{\mathbf{U}}{}^{\mathrm{t}}\mathbf{S}. \tag{5.16}$$

Summation over elements has been substituted by the scalar product of the hypervectors $\underset{\sim}{\mathbf{U}}_{\mathrm{E}}$ and

$$\mathbf{S}_{\mathrm{E}} = \begin{bmatrix} \vdots \\ \mathbf{S}_q \\ \vdots \end{bmatrix} = \{\mathbf{S}_q\} \quad (q = 1, \ldots, nel).$$

The association of elemental and mesh nodal point displacements by eqn (5.11) is implied in the transition to the last expression in eqn (5.16). Analogously to eqn (5.13), the vector

$$\mathbf{S} = \{\mathbf{S}_1\, \mathbf{S}_2 \cdots \mathbf{S}_i \cdots \mathbf{S}_N\} = \mathbf{a}^{\mathrm{t}}\mathbf{S}_{\mathrm{E}} \tag{5.17}$$

defines a $3N \times 1$ array comprising the stresses resulting at the nodal points of the finite element assembly. These are effectively determined by accumulation of element contributions:

$$\mathbf{S} = \mathbf{a}^{\mathrm{t}}\mathbf{S}_{\mathrm{E}} = \sum_{q=1}^{nel} \mathbf{a}_q^{\mathrm{t}}\mathbf{S}_q. \tag{5.18}$$

Equation (5.18) for the assembled $\mathbf{S}$ along with eqn (5.15) for the elemental $\mathbf{S}_q$ may be interpreted as the integral

$$\mathbf{S} = \int_V \boldsymbol{a}^{\mathrm{t}}\boldsymbol{\sigma}\mathrm{d}V = \sum_{q=1}^{nel} \mathbf{a}_q^{\mathrm{t}} \int_{V_q} \boldsymbol{a}^{\mathrm{t}}\boldsymbol{\sigma}\mathrm{d}V$$

evaluated by means of the finite element systematics.

Analysis of the virtual work of the stress in the discretized system into finite element contributions is summarized in the following compressed form

$$\int_V \underset{\sim}{\boldsymbol{\gamma}}^{\mathrm{t}}\boldsymbol{\sigma}\mathrm{d}V = \sum_{q=1}^{nel} \underset{\sim}{\mathbf{U}}_q^{\mathrm{t}} \int_{V_q} \boldsymbol{a}^{\mathrm{t}}\boldsymbol{\sigma}\mathrm{d}V = \underset{\sim}{\mathbf{U}}^{\mathrm{t}} \sum_{q=1}^{nel} \mathbf{a}_q^{\mathrm{t}} \int_{V_q} \boldsymbol{a}^{\mathrm{t}}\boldsymbol{\sigma}\mathrm{d}V.$$

The above utilizes finite element kinematics, and the sum in the last expression supplies the stress resultants $\mathbf{S}$ at the nodal points of the mesh.

With eqns (5.10) and (5.12) for the contribution of the applied forces and eqn (5.16) for that of the stresses, the virtual work equality in eqn (5.1) is expressed in the finite element representation of the problem as

$$\underset{\sim}{\mathbf{U}}^{\mathrm{t}}\mathbf{P} = \underset{\sim}{\mathbf{U}}^{\mathrm{t}}\mathbf{S}.$$

This establishes at the nodal points of the finite element mesh the equilibrium condition

$$\mathbf{P} = \mathbf{S} \tag{5.19}$$

between the applied loads in the vector array $\mathbf{P}$ and the stress resultants in the vector array $\mathbf{S}$.

5.2 Elastic computation procedure

Equation (5.19) expresses the condition of static equilibrium for the discretized finite element system utilizing kinematic compatibility of displacements and strains. A complete description of the deformation problem requires specification of the stress–strain relations, and their introduction into the finite element equation. Within the elastic range, the stress–strain relations are as in eqns (1.47) and (2.64). The strain $\boldsymbol{\varepsilon} \equiv \boldsymbol{\gamma}$ derived from the finite element approximation is given by eqn (5.7), and substitution in the elasticity law supplies the stress within a finite element

$$\boldsymbol{\sigma} = \boldsymbol{\kappa}\boldsymbol{\varepsilon} = \boldsymbol{\kappa}\boldsymbol{a}\mathbf{U}_q. \tag{5.20}$$

Use in eqn (5.15) relates stress resultants and displacements at the nodal points of the element

$$\mathbf{S}_q = \left[\int_{V_q} \boldsymbol{a}^{\mathrm{t}}\boldsymbol{\kappa}\boldsymbol{a}\mathrm{d}V\right]\mathbf{U}_q = \mathbf{k}_q\mathbf{U}_q. \tag{5.21}$$

The symmetric matrix

$$\mathbf{k}_q = \int_{V_q} \boldsymbol{a}^{\mathrm{t}}\boldsymbol{\kappa}\boldsymbol{a}\mathrm{d}V \tag{5.22}$$

is known as the stiffness matrix of the elastic element. It determines the forces $\mathbf{S}_q$ resulting from displacements $\mathbf{U}_q$ imposed on the element nodal points. Higher-order elements require a numerical evaluation of the volume integral in eqn (5.22) based on values of the integrand at a number of integration points. For all elements collectively eqn (5.21) becomes

$$\mathbf{S}_{\mathrm{E}} = \lceil\mathbf{k}_q\rfloor\mathbf{U}_{\mathrm{E}} = \mathbf{k}\mathbf{U}_{\mathrm{E}} \tag{5.23}$$

with the diagonal matrix

$$\mathbf{k} = \begin{bmatrix} \ddots & & \\ & \mathbf{k}_q & \\ & & \ddots \end{bmatrix} \quad (q = 1, \ldots, nel).$$

The relation between stress resultants and displacements for individual elements enters the analogous relation for the assembled discretized system. With eqn (5.11) for the element displacements in eqn (5.23) and substituting in eqn (5.17), we obtain

$$\mathbf{S} = \mathbf{a}^{\mathrm{t}}\mathbf{k}\mathbf{a}\mathbf{U} = \mathbf{K}\mathbf{U}. \tag{5.24}$$

The symmetric matrix

$$\mathbf{K} = \mathbf{a}^{\mathrm{t}}\mathbf{k}\mathbf{a} \tag{5.25}$$

is known as the stiffness matrix of the elastic finite element system formed by accumulating element contributions (refer to eqns (5.18), (5.21) and (5.5)):

$$\mathbf{K} = \sum_{q=1}^{nel} \mathbf{a}_q^{\mathrm{t}}\mathbf{k}_q\mathbf{a}_q = \int_V \boldsymbol{a}^{\mathrm{t}}\boldsymbol{\kappa}\boldsymbol{a}\mathrm{d}V.$$

It may be formally considered an extension of the elemental stiffness, eqn (5.22), and determines the forces $\mathbf{S}$ resulting from displacements $\mathbf{U}$ imposed at the mesh nodal points.

With eqn (5.24) for the stress resultants eqn (5.19), the finite element equation determines the displacements in the elastic system

$$\mathbf{S} = \mathbf{K}\mathbf{U} = \mathbf{P} \quad \text{and} \quad \mathbf{U} = \mathbf{K}^{-1}\mathbf{P}. \tag{5.26}$$

The solution of eqn (5.26) is not unique unless the system is fixed against arbitrary motion. Suppression of the degrees of freedom (displacements) at the supports implies elimination of the respective positions in the matrix equation. This leaves a reduced system of equations possessing a unique solution. Analogously, displacement values may be prescribed at a number of nodal points.

After the solution step, the displacements $\mathbf{U}_q$ of the individual elements are grouped from the complete vector $\mathbf{U}$, eqn (5.5). Evaluation of the strains $\boldsymbol{\varepsilon} \equiv \boldsymbol{\gamma}$, eqn (5.7), and the stresses $\boldsymbol{\sigma}$, eqn (5.20), at defined locations in the finite element terminates the elastic computation.

5.3 Algorithms for plastic flow

5.3.1 Basic schemes

For an introductory discussion on solution algorithms accounting for plastic flow, we first refer to momentary response described by the time rates of the variables. Where necessary, specification will refer to isotropic hardening (Chapter 1). The issue of incrementation will be treated separately later. It is observed that the equation of virtual work and the finite element formalism developed in Section 5.1 transfer equally to the time rates of applied forces, inner stresses, displacements and strains. This can be proved by incrementing the relationships in question (or forming the time rate) for a fixed geometry of the system, as assumed here.

The tangential stiffness method

An immediate extension of the previous elastic algorithm to the present elastoplastic case can be based on the stress–strain relation of eqn (2.72).

The finite element form is derived by utilizing eqn (5.7) for the strain rate in

$$\dot{\boldsymbol{\sigma}} = \bar{\boldsymbol{\kappa}}\dot{\boldsymbol{\gamma}} = \bar{\boldsymbol{\kappa}}\boldsymbol{a}\dot{\mathbf{U}}_q, \tag{5.27}$$

where $\bar{\boldsymbol{\kappa}}$ denotes the momentary elastoplastic stiffness of the material in loading. Otherwise $\bar{\boldsymbol{\kappa}} = \boldsymbol{\kappa}$, the elastic material stiffness.

The stress resultants at the element nodal points are obtained by utilizing eqn (5.27) in the rate form of eqn (5.15) as

$$\dot{\mathbf{S}}_q = \left[\int_{V_q} \boldsymbol{a}^{\mathrm{t}}\bar{\boldsymbol{\kappa}}\boldsymbol{a}\mathrm{d}V\right]\dot{\mathbf{U}}_q = \bar{\mathbf{k}}_q\dot{\mathbf{U}}_q, \tag{5.28}$$

which defines the momentary elastoplastic stiffness matrix $\bar{\mathbf{k}}_q$ of the element. Then, with reference to eqn (5.18) for the stress resultants at the mesh nodal points

$$\dot{\mathbf{S}} = \mathbf{a}^{\mathrm{t}}\bar{\mathbf{k}}\mathbf{a}\dot{\mathbf{U}} = \bar{\mathbf{K}}\dot{\mathbf{U}}. \tag{5.29}$$

This defines the symmetric stiffness matrix $\bar{\mathbf{K}}$ of the elastoplastic system at the considered instant. It relates rate quantities and is formed in a manner similar to that for the elastic case in eqn (5.25), but with the element contribution $\bar{\mathbf{k}}$ instead of $\mathbf{k}$.

From the finite element equation, eqn (5.19),

$$\dot{\mathbf{S}} = \bar{\mathbf{K}}\dot{\mathbf{U}} = \dot{\mathbf{P}} \quad \text{and} \quad \dot{\mathbf{U}} = \bar{\mathbf{K}}^{-1}\dot{\mathbf{P}}. \tag{5.30}$$

The uniqueness of the solution implies appropriate elimination of degrees of freedom fixing the system. Subsequent computation of the strain rate $\dot{\boldsymbol{\gamma}}$ and the stress rate $\dot{\boldsymbol{\sigma}}$, eqn (5.27), from the displacement velocity $\dot{\mathbf{U}}$ completes the momentary elastoplastic solution. The procedure resembles the elastic one and is considered a direct solution in contrast to the iterative algorithms outlined subsequently, except for the check on the plastic loading condition (Section 2.2.2). Since the procedure is based on the momentary elastoplastic stiffness matrix of the system, it is known as the tangential stiffness method. The sequence of instructions for this algorithm is summarized in Scheme 5.1.

Predictor $\quad \dot{\mathbf{U}}$

Element loop, $\quad q = 1, nel$

Integration points

$\dot{\boldsymbol{\gamma}} \Leftarrow \boldsymbol{a}\dot{\mathbf{U}} \quad , \quad \bar{\boldsymbol{\kappa}} \Leftarrow \boldsymbol{\kappa}(\text{elastic})$

Plastic flow $\quad (\phi(\boldsymbol{\sigma}) = 0 \text{ and } \mathbf{s}^{\mathrm{t}}\dot{\boldsymbol{\gamma}} > 0): \quad \bar{\boldsymbol{\kappa}} \Leftarrow \bar{\boldsymbol{\kappa}}\,(\text{elastoplastic})$

Element stiffness: $\quad \bar{\mathbf{k}}_q \Leftarrow \int\limits_{V_q} \boldsymbol{a}^{\mathrm{t}}\bar{\boldsymbol{\kappa}}\boldsymbol{a}\mathrm{d}V$

End integration

Contribution to system matrix $\quad \bar{\mathbf{K}} \Leftarrow \bar{\mathbf{K}} + \mathbf{a}_q^{\mathrm{t}}\bar{\mathbf{k}}_q\mathbf{a}_q$

End elements

Corrector $\quad \dot{\mathbf{U}} \Leftarrow \bar{\mathbf{K}}^{-1}\dot{\mathbf{P}}$

Scheme 5.1: Tangential stiffness algorithm.

The loop over the integration points calculates the volume integral for the elastoplastic element stiffness using a numerical approximation except for finite elements allowing analytical evaluation. The loop over the elements performs the accumulation into the stiffness matrix of the system. Computer implementation, particularly with vector arithmetic, favours long loops. This is achieved by reversing the order of the element and the integration loop. Thereby, each integration point is processed for a specified number of elements adapted to the vector length of the hardware.

Initial load methods

Alternative solution schemes are inherently iterative. They are based on eqn (2.69), the form of the constitutive relation that requires explicit determination of the plastic strain rate $\dot{\boldsymbol{\eta}}$. In the finite element approximation,

$$\dot{\boldsymbol{\sigma}} = \boldsymbol{\kappa}\left[\dot{\boldsymbol{\gamma}} - \dot{\boldsymbol{\eta}}\right] = \boldsymbol{\kappa}\left[\boldsymbol{a}\dot{\mathbf{U}}_q - \dot{\boldsymbol{\eta}}\right] \tag{5.31}$$

where $\boldsymbol{\kappa}$ denotes the elastic stiffness matrix of the material. In regions deforming elastically, $\dot{\boldsymbol{\eta}} = \mathbf{0}$ and $\dot{\boldsymbol{\gamma}} \equiv \dot{\boldsymbol{\varepsilon}}$.

With eqn (5.31), the rate of the stress resultants at the element nodal points is obtained from eqn (5.15) as

$$\dot{\mathbf{S}}_q = \left[\int\limits_{V_q} \boldsymbol{a}^{\mathrm{t}}\boldsymbol{\kappa}\boldsymbol{a}\mathrm{d}V\right]\dot{\mathbf{U}}_q - \int\limits_{V_q} \boldsymbol{a}^{\mathrm{t}}\boldsymbol{\kappa}\dot{\boldsymbol{\eta}}\,\mathrm{d}V = \mathbf{k}_q\dot{\mathbf{U}}_q + \dot{\mathbf{J}}_q. \tag{5.32}$$

Comparison with eqn (5.28) shows that employment of the elastic element stiffness $\mathbf{k}_q$ instead of the elastoplastic one implies compensation by the

additional nodal loads

$$\dot{\mathbf{J}}_q = -\int_{V_q} \boldsymbol{a}^{\mathrm{t}} \boldsymbol{\kappa} \dot{\boldsymbol{\eta}} \mathrm{d}V, \tag{5.33}$$

which account for the plastic strain rate $\dot{\boldsymbol{\eta}}$ where plastic flow occurs. With the element contributions from eqn (5.32) in eqn (5.18), the stress resultants at the mesh nodal points are obtained as

$$\dot{\mathbf{S}} = \mathbf{a}^{\mathrm{t}} \mathbf{k} \mathbf{a} \dot{\mathbf{U}} + \mathbf{a}^{\mathrm{t}} \dot{\mathbf{J}}_{\mathrm{E}} = \mathbf{K} \dot{\mathbf{U}} + \dot{\mathbf{J}} \tag{5.34}$$

and

$$\dot{\mathbf{J}}_{\mathrm{E}} = \{ \cdots \dot{\mathbf{J}}_q \cdots \} \quad (q = 1, \ldots, nel).$$

This defines the nodal loads

$$\dot{\mathbf{J}} = \mathbf{a}^{\mathrm{t}} \dot{\mathbf{J}}_{\mathrm{E}} = \sum_{q=1}^{nel} \mathbf{a}_q^{\mathrm{t}} \dot{\mathbf{J}}_q$$

required in conjunction with the elastic stiffness matrix $\mathbf{K}$ for the description of the momentary response of the elastoplastic system.

The finite element equation (5.19) now becomes

$$\dot{\mathbf{S}} = \mathbf{K} \dot{\mathbf{U}} + \dot{\mathbf{J}} = \dot{\mathbf{P}} \quad \text{and} \quad \dot{\mathbf{U}} = \mathbf{K}^{-1} [\dot{\mathbf{P}} - \dot{\mathbf{J}}], \tag{5.35}$$

the solution referring to the appropriately fixed system. Given the displacement rate, computation of the strain rate $\dot{\boldsymbol{\gamma}}$, eqn (5.7), and stress rate $\dot{\boldsymbol{\sigma}}$, eqn (5.31), completes the momentary solution, in principle. It has to be recalled, however, that the solution relies on the plastic strain rate as an input, which is not a datum. It must be estimated prior to the solution, and can be obtained *a posteriori* using either the computed rate of strain or stress (see eqn (2.71)). The two alternative expressions for the plastic strain rate in terms of the finite element approximation are

$$\dot{\boldsymbol{\eta}} = \frac{1}{h} \mathbf{s} \mathbf{s}^{\mathrm{t}} \dot{\boldsymbol{\sigma}} = \frac{1}{h} \mathbf{s} \mathbf{s}^{\mathrm{t}} \boldsymbol{\kappa} \left[\boldsymbol{a} \dot{\mathbf{U}}_q - \dot{\boldsymbol{\eta}} \right], \tag{5.36}$$

with

$$\mathbf{s}^{\mathrm{t}} \dot{\boldsymbol{\sigma}} = \mathbf{s}^{\mathrm{t}} \boldsymbol{\kappa} \left[\boldsymbol{a} \dot{\mathbf{U}}_q - \dot{\boldsymbol{\eta}} \right] \geq 0,$$

and

$$\dot{\boldsymbol{\eta}} = \frac{1}{h + 3G} \mathbf{s} \mathbf{s}^{\mathrm{t}} (\boldsymbol{\kappa} \dot{\boldsymbol{\gamma}}) = \frac{1}{h + 3G} \mathbf{s} \mathbf{s}^{\mathrm{t}} (\boldsymbol{\kappa} \boldsymbol{a} \dot{\mathbf{U}}_q), \tag{5.37}$$

with

$$\mathbf{s}^{\mathrm{t}} (\boldsymbol{\kappa} \dot{\boldsymbol{\gamma}}) = \mathbf{s}^{\mathrm{t}} (\boldsymbol{\kappa} \boldsymbol{a} \dot{\mathbf{U}}_q) \geq 0.$$

The evaluation of either of the above expressions under observance of the respective plastic loading condition furnishes new estimates for a subsequent

iteration cycle. Instead of simplifying the product $\boldsymbol{\kappa}\mathbf{s} \Leftarrow 2G\mathbf{s}$ we retained the original form for two reasons: not to exclude special cases like plane stress/plane strain (see Section 2.3.5) and to leave $(\boldsymbol{\kappa}\dot{\boldsymbol{\gamma}})$ in eqn (5.37) in the form of a stress in case strains are not computed explicitly by the particular software. In such a case, the plastic strain rate in eqn (5.36) also enters eqn (5.33) for the compensation loads as the combination $(\boldsymbol{\kappa}\dot{\boldsymbol{\eta}})$.

If the strains $\boldsymbol{\eta}$ were not the result of plastic flow but prescribed, the solution is associated with given initial strains and the vector $\mathbf{J}$ comprises the initial loads. Accounting for initial strains (e.g. thermal strains) is a standard option in finite element analysis of elastic systems. It can be utilized in plasticity in conjunction with the iterative determination of strains from plastic flow [2]. The initial load method can be executed in either the *initial strain* mode [3] based on plastic flow in terms of the stress rate, eqn (5.36), or in the *initial stress* mode [4] based on the strain rate, eqn (5.37). The computation steps of the initial load iteration are indicated in Scheme 5.2.

Predictor $\quad \dot{\mathbf{U}}$

Element loop, $\quad q = 1, nel$

Integration points

Predictor $\dot{\boldsymbol{\eta}}:\quad \dot{\boldsymbol{\sigma}}^* = \boldsymbol{\kappa}\dot{\boldsymbol{\gamma}} \Leftarrow \boldsymbol{\kappa}\boldsymbol{a}\dot{\mathbf{U}}_q, \quad \dot{\boldsymbol{\sigma}} \Leftarrow \dot{\boldsymbol{\sigma}}^* - (\boldsymbol{\kappa}\dot{\boldsymbol{\eta}})$

$$\text{Corrector} \begin{cases} \dot{\boldsymbol{\eta}} \Leftarrow \frac{1}{h+3G}\mathbf{s}\mathbf{s}^{\mathrm{t}}\dot{\sigma}^* & \text{(initial stress)} \\ \dot{\boldsymbol{\eta}} \Leftarrow \frac{1}{h}\mathbf{s}\mathbf{s}^{\mathrm{t}}\dot{\boldsymbol{\sigma}} & \text{(initial strain)} \end{cases}$$

$$\text{Initial load (element):} \quad \dot{\mathbf{J}}_q \Leftarrow -\int_{V_q} \boldsymbol{a}^{\mathrm{t}}\boldsymbol{\kappa}\dot{\boldsymbol{\eta}}\mathrm{d}V$$

End integration

Initial load (system) $\quad \dot{\mathbf{J}} \Leftarrow \dot{\mathbf{J}} + \mathbf{a}_q^{\mathrm{t}}\dot{\mathbf{J}}_q$

End elements

Corrector $\quad \dot{\mathbf{U}} \Leftarrow \mathbf{K}^{-1}\left[\dot{\mathbf{P}} - \dot{\mathbf{J}}\right]$

Scheme 5.2: Initial load iteration with elastic stiffness $\mathbf{K}$ (initial stress/initial strain version).

The general remarks on the function of the loops in Scheme 5.1 apply here as well. In both cases, the sequence of operations has been selected such that the element loop is activated only once. This will necessitate some caution regarding the first iteration cycle. In Scheme 5.2 (initial load iteration) the formation of the elastic stiffness matrix of the system is not shown explicitly. The elastic stiffness matrix is not affected by plastic deformation; it is considered available once and for all. The argument also concerns the

factorization of the matrix required in the solution step for the displacements. This fact attains significance in a complete elastoplastic analysis extending over a sequence of several incremental loading steps (Section 5.5).

The etymology of the historical denotations initial stress and initial strain goes back to deviations from elasticity [5]. The elastoplastic stress–strain relation $\dot{\boldsymbol{\sigma}} = \bar{\boldsymbol{\kappa}}\dot{\boldsymbol{\gamma}}$ can be alternatively expressed as

$$\dot{\boldsymbol{\sigma}} = \boldsymbol{\kappa}\dot{\boldsymbol{\gamma}} + [\bar{\boldsymbol{\kappa}} - \boldsymbol{\kappa}]\,\dot{\boldsymbol{\gamma}} = \boldsymbol{\kappa}\dot{\boldsymbol{\gamma}} + \dot{\boldsymbol{\tau}} \tag{5.38}$$

in terms of the elasticity matrix $\boldsymbol{\kappa}$ and an initial stress,

$$\dot{\boldsymbol{\tau}} = [\bar{\boldsymbol{\kappa}} - \boldsymbol{\kappa}]\,\dot{\boldsymbol{\gamma}}, \tag{5.39}$$

accounting for the deviation from elastic response. The initial stress term $\dot{\boldsymbol{\tau}}$ is a function of the strain rate $\dot{\boldsymbol{\gamma}}$. Analogously, the inverse elastoplastic stress–strain relation $\dot{\boldsymbol{\gamma}} = \bar{\boldsymbol{\kappa}}^{-1}\dot{\boldsymbol{\sigma}}$ can be brought into the form

$$\dot{\boldsymbol{\gamma}} = \boldsymbol{\kappa}^{-1}\dot{\boldsymbol{\sigma}} + \left[\bar{\boldsymbol{\kappa}}^{-1} - \boldsymbol{\kappa}^{-1}\right]\dot{\boldsymbol{\sigma}} = \boldsymbol{\kappa}^{-1}\dot{\boldsymbol{\sigma}} + \dot{\boldsymbol{\eta}}. \tag{5.40}$$

Here, the initial strain

$$\dot{\boldsymbol{\eta}} = \left[\bar{\boldsymbol{\kappa}}^{-1} - \boldsymbol{\kappa}^{-1}\right]\dot{\boldsymbol{\sigma}} \tag{5.41}$$

accounts for the deviation from elasticity as a function of the stress rate $\dot{\boldsymbol{\sigma}}$. Comparing eqns (5.38) and (5.40), we obtain between $\dot{\boldsymbol{\tau}}$ and $\dot{\boldsymbol{\eta}}$ the relationship

$$\dot{\boldsymbol{\tau}} + \boldsymbol{\kappa}\dot{\boldsymbol{\eta}} = \mathbf{0}. \tag{5.42}$$

Accordingly, implementation of plasticity via initial stress or initial strain is a matter of the functions available in the computer software. The most significant issue is the dependence of each quantity on either the strain rate, eqn (5.39), or the stress rate, eqn (5.41), which influences the numerical behaviour. Favourable employment of each form has been investigated by Dieter Scharpf [6], and will be discussed subsequently.

5.3.2 Convergence of the iterative solution technique

In the following, the convergence properties of the iterative initial load method of solution are discussed for either the initial stress or the initial strain mode of execution. For this purpose, referring first to the initial strain formalism in Scheme 5.2, an iteration cycle for the plastic strain rate can be defined by the recursive instruction

$$\begin{bmatrix} \vdots \\ \dot{\boldsymbol{\eta}}_k \\ \vdots \end{bmatrix}_{i+1} = \begin{bmatrix} \ddots & & \\ & \left(\dfrac{1}{h}\mathbf{s}\mathbf{s}^{\mathrm{t}}\right)_k & \\ & & \ddots \end{bmatrix} \begin{bmatrix} \vdots \\ \dot{\boldsymbol{\sigma}}_k \\ \vdots \end{bmatrix}_i \qquad \text{or} \tag{5.43}$$

$$\{\dot{\boldsymbol{\eta}}_k\}_{i+1} = \left[\left(\frac{2G}{h}\mathbf{s}\mathbf{s}^{\mathrm{t}}\right)_k\right] \boldsymbol{\alpha}\,\{\dot{\boldsymbol{\eta}}_k\}_i \quad (k = 1, \ldots, nip \times nel).$$

In eqn (5.43), the vector arrays extend over the locations where stresses and strains are evaluated. Commonly, these locations are the integration points (nip) in each element amounting to a total number of $nip \times nel$ in the entire finite element system. The size of the vector arrays thus is $(noc \times nip \times nel) \times 1$, where noc denotes the number of components in each $\boldsymbol{\eta}$ or $\boldsymbol{\sigma}$. In accordance with Scheme 5.2, $\dot{\boldsymbol{\eta}}_{i+1}$ is the corrector, and $\dot{\boldsymbol{\sigma}}_i$ the result of the predictor step. The transition to the second expression in eqn (5.43) relies on the transformation

$$\{\dot{\boldsymbol{\sigma}}_l\} = \frac{\partial\{\boldsymbol{\sigma}_l\}}{\partial\{\boldsymbol{\eta}_k\}}\{\dot{\boldsymbol{\eta}}_k\} = \lceil \boldsymbol{\kappa}_l \rfloor \boldsymbol{\alpha}\{\dot{\boldsymbol{\eta}}_k\} \qquad (l,k = 1,\ldots,nip \times nel). \tag{5.44}$$

The matrix

$$\boldsymbol{\alpha} = \lceil \boldsymbol{\kappa}_l^{-1} \rfloor \frac{\partial\{\boldsymbol{\sigma}_l\}}{\partial\{\boldsymbol{\eta}_k\}} = \frac{\partial\{\boldsymbol{\varepsilon}_l\}}{\partial\{\boldsymbol{\eta}_k\}} \tag{5.45}$$

globally describes the sensitivity of the stress (more precisely that of the elastic strain $\boldsymbol{\varepsilon}$) to the plastic strain. It is a quadratic matrix with dimensions $(noc \times nip \times nel)^2$.

In a statically determinate system where $\boldsymbol{\sigma}$ is fixed by the applied forces, $\boldsymbol{\alpha} = \mathbf{0}$. The matrix $\boldsymbol{\alpha}$ can be expressed alternatively in terms of the strain $\boldsymbol{\gamma}$ as

$$\boldsymbol{\alpha} = \frac{\partial\{\boldsymbol{\varepsilon}_l\}}{\partial\{\boldsymbol{\eta}_k\}} = \frac{\partial\{\boldsymbol{\gamma}_l\}}{\partial\{\boldsymbol{\eta}_k\}} - \mathbf{I} \qquad (l,k = 1,\ldots,nip \times nel), \tag{5.46}$$

and in a kinematically determinate system where $\boldsymbol{\gamma}$ is fixed by the external action, $\boldsymbol{\alpha} = -\mathbf{I}$. Under more general conditions the matrix $\boldsymbol{\alpha}$ is to be derived from the computational steps determining the stress $\boldsymbol{\sigma}$ for a given strain $\boldsymbol{\gamma}$. At this place, it is worth noticing that in Scheme 5.2 the organization of the instructions reflects the programmer's point of view. The essential task performed by the algorithm, however, is the determination of the plastic strain rate $\dot{\boldsymbol{\eta}}$ by the recursive operation of eqn (5.43). This can be easily revealed by just another interpretation of the iteration cycle.

A convergent solution of eqn (5.43) implies that $\dot{\boldsymbol{\eta}}_{i+1} = \dot{\boldsymbol{\eta}}_i = \dot{\boldsymbol{\eta}}$ everywhere in the system. Iterates will deviate from the solution $\dot{\boldsymbol{\eta}}$ by a quantity $\boldsymbol{\delta}$. Thus,

$$\dot{\boldsymbol{\eta}}_i = \dot{\boldsymbol{\eta}} + \boldsymbol{\delta}_i, \qquad \dot{\boldsymbol{\eta}}_{i+1} = \dot{\boldsymbol{\eta}} + \boldsymbol{\delta}_{i+1} \tag{5.47}$$

and from eqn (5.43) the deviations during consecutive iterations are governed by

$$\{\boldsymbol{\delta}_k\}_{i+1} = \left\lceil \left(\frac{2G}{h}\mathbf{s}\mathbf{s}^{\mathrm{t}}\right)_k \right\rfloor \boldsymbol{\alpha}\{\boldsymbol{\delta}_k\}_i \quad (k = 1,\ldots,nip \times nel). \tag{5.48}$$

For convergence of the iterative procedure, the deviation from the solution must diminish. In the statically determinate case ($\boldsymbol{\alpha} = \mathbf{0}$) no deviations arise; the solution can be obtained at once. In the other special case, the

kinematically determinate system ($\boldsymbol{\alpha} = -\mathbf{I}$), eqn (5.48) assumes at each evaluation point $k = 1, \ldots, nip \times nel$ the form

$$(\boldsymbol{\delta}_k)_{i+1} = -\left(\frac{2G}{h}\mathbf{s}\mathbf{s}^{\mathrm{t}}\right)_k (\boldsymbol{\delta}_k)_i = -\left(\frac{3G}{h}\right)_k (\boldsymbol{\delta}_k)_i. \tag{5.49}$$

The transition to the last expression observes that the deviations are proportional to the vector $\mathbf{s}$: at each point $\boldsymbol{\delta}_i = (\dot{\bar{\eta}}_i - \dot{\bar{\eta}})\mathbf{s}$. At the same time, this fact reduces the essential task to the convergence of the equivalent plastic strain rate $\dot{\bar{\eta}}$.

From eqn (5.49), the sign of the deviation vector $\{\boldsymbol{\delta}_k\}$ will alternate during the course of the iteration. Its magnitude will diminish if all coefficients $3G/h$ are less than unity. Accordingly, a condition for convergence can be stated as

$$\max_k \left(\frac{3G}{h}\right)_k < 1. \tag{5.50}$$

It is seen from eqn (5.50) that the initial strain procedure becomes divergent for the kinematically determinate system when $h < 3G$. Moreover, the initial strain formalism fails entirely in the case of perfect plasticity ($h = 0$) as explained earlier.

Next, following in Scheme 5.2 the initial stress option, the iteration cycle for the plastic strain rate is

$$\begin{aligned}\{\dot{\boldsymbol{\eta}}_k\}_{i+1} &= \left\lceil \left(\frac{2G}{h+3G}\mathbf{s}\mathbf{s}^{\mathrm{t}}\right)_k \right\rfloor \{\dot{\gamma}_k\}_i \\ &= \left\lceil \left(\frac{2G}{h+3G}\mathbf{s}\mathbf{s}^{\mathrm{t}}\right)_k \right\rfloor \boldsymbol{\beta}\,\{\dot{\boldsymbol{\eta}}_k\}_i \quad (k = 1, \ldots, nip \times nel).\end{aligned} \tag{5.51}$$

The matrix

$$\boldsymbol{\beta} = \frac{\partial\{\boldsymbol{\gamma}_l\}}{\partial\{\boldsymbol{\eta}_k\}} = \boldsymbol{\alpha} + \mathbf{I} \tag{5.52}$$

globally describes the sensitivity of the strain $\boldsymbol{\gamma}$ to the plastic strain $\boldsymbol{\eta}$. It is analogous to the matrix $\boldsymbol{\alpha}$, eqn (5.45), and is related to it by eqn (5.46). For a kinematically determinate system, $\boldsymbol{\beta} = \mathbf{0}$, whereas $\boldsymbol{\beta} = \mathbf{I}$ in the statically determinate case ($\boldsymbol{\alpha} = \mathbf{0}$).

An examination of convergence can be based on the behaviour of the deviation $\boldsymbol{\delta}_i$ of the ith iterate from the solution, cf. eqn (5.47). With reference to eqn (5.51), the deviations of consecutive iterations are here governed by

$$\{\boldsymbol{\delta}_k\}_{i+1} = \left\lceil \left(\frac{2G}{h+3G}\mathbf{s}\mathbf{s}^{\mathrm{t}}\right)_k \right\rfloor \boldsymbol{\beta}\{\boldsymbol{\delta}_k\}_i \qquad (k = 1, \ldots, nip \times nel). \tag{5.53}$$

If the system is kinematically determinate ($\boldsymbol{\beta} = \mathbf{0}$), the deviation vanishes and the solution is obtained at once. In the statically determinate case

($\boldsymbol{\beta} = \mathbf{I}$) eqn (5.53) can be written for each evaluation point individually:

$$(\boldsymbol{\delta}_k)_{i+1} = \left(\frac{2G}{h+3G}\mathbf{s}\mathbf{s}^{\mathrm{t}}\right)_k (\boldsymbol{\delta}_k)_i = \left(\frac{3G}{h+3G}\right)_k (\boldsymbol{\delta}_k)_i. \tag{5.54}$$

As in eqn (5.49), the transition to the second expression in eqn (5.54) relies on the proportionality of $\boldsymbol{\delta}_i = (\dot{\bar{\eta}}_i - \dot{\bar{\eta}})\mathbf{s}$ to the direction vector $\mathbf{s}$.

From eqn (5.54), the sign of the deviations $\boldsymbol{\delta}_i$ remains the same during the course of the iteration. Its magnitude will diminish if all coefficients $3G/(h+3G)$ are less than unity. Therefore, the condition for convergence can be stated as

$$\max_k \left(\frac{3G}{h+3G}\right)_k < 1. \tag{5.55}$$

For a diminishing value of the hardening parameter h, the quotient in eqn (5.55) increases and attains unity at $h = 0$. Consequently, the initial stress formalism is always convergent also under statically determinate conditions, but for the case of perfect plasticity. The failure of the iterative algorithm then, is due to the fact that in a perfectly plastic material variations in stress cannot be imposed arbitrarily.

Summarizing, the initial strain formalism furnishes immediately the solution to the plastic flow problem under controlled stress conditions (statically determinate case). Under controlled strain conditions (kinematically determinate case) its range of convergence is quite limited, cf. eqn (5.50). The initial strain formalism fails completely for perfectly plastic material ($h = 0$). The initial stress version furnishes immediately the solution to the plastic flow problem under controlled strain conditions (kinematically determinate case). Under controlled stress conditions (statically determinate case) its range of convergence extends up to the case of perfect plasticity which at the same time limits the existence of solutions.

Apart from the special cases considered, the deduction of explicit convergence criteria is not that simple under more general conditions. For either scheme the evolution of the deviations $\boldsymbol{\delta}_i$ during iteration can be written as

$$\{\boldsymbol{\delta}_k\}_{i+1} = \mathbf{M}\{\boldsymbol{\delta}_k\}_i. \tag{5.56}$$

The magnification matrix $\mathbf{M}$ of the deviations $\boldsymbol{\delta}_i$ in eqn (5.56) is specified as from eqn (5.48) for the initial strain mode of the iteration algorithm, and from eqn (5.53) for the initial stress mode. Convergence is tested with the Euclidean norm $\|\{\boldsymbol{\delta}_k\}\|$ of the vector array $\{\boldsymbol{\delta}_k\}$. This norm is defined by the sum of squares of the vector components

$$\|\{\boldsymbol{\delta}_k\}\|^2 = \{\boldsymbol{\delta}_k\}^{\mathrm{t}}\{\boldsymbol{\delta}_k\}. \tag{5.57}$$

For convergence, it is requested that $\|\{\boldsymbol{\delta}_k\}_{i+1}\| < \|\{\boldsymbol{\delta}_k\}_i\|$, or with eqn (5.56)

$$\|\mathbf{M}\{\boldsymbol{\delta}_k\}_i\| \leq \|\mathbf{M}\|\,\|\{\boldsymbol{\delta}\}_i\| < \|\{\boldsymbol{\delta}_k\}_i\|. \tag{5.58}$$

The scalar quantity $\|\mathbf{M}\| = \sigma(\mathbf{M})$ is known as the *spectral norm* of the matrix $\mathbf{M}$. It conforms with the Euclidean norm of the vector $\{\boldsymbol{\delta}_k\}$ by satisfying the first inequality in eqn (5.58). The convergence condition is deduced from the second inequality, and reads

$$\|\mathbf{M}\| = \sigma(\mathbf{M}) < 1. \tag{5.59}$$

The spectral norm $\sigma(\mathbf{M})$ of the real matrix $\mathbf{M}$ is defined as the positive square root of the maximum eigenvalue λ_i of the product $\mathbf{M}^{\mathrm{t}}\mathbf{M}$. It reads

$$\sigma(\mathbf{M}) = \sqrt{\max\lambda_i(\mathbf{M}^{\mathrm{t}}\mathbf{M})}. \tag{5.60}$$

The above formulation can be specified for the previous cases and leads to the same convergence conditions as before. This is left as an exercise to the reader. Furthermore, since the direction $\mathbf{s}$ of the plastic strain rate $\dot{\boldsymbol{\eta}} = \dot{\bar{\eta}}\mathbf{s}$ remains fixed with the stress state during iteration, the proof for convergence can be limited to the magnitude $\dot{\bar{\eta}}$.

5.4 Integration of inelastic stress–strain relations

Inelastic analysis is actually carried out for a given loading programme and is concerned with the determination of displacements, strains and stresses rather than the momentary variation of these quantities. Since the constitutive equations of plastic flow refer merely to the strain rate $\dot{\boldsymbol{\eta}}$ or the infinitesimal increment $\mathrm{d}\boldsymbol{\eta}$, respectively, the inelastic strain $\boldsymbol{\eta}$ has to be obtained by integration

$$\boldsymbol{\eta} = \int_0^{\mathrm{t}} \dot{\boldsymbol{\eta}}\mathrm{d}t. \tag{5.61}$$

Evaluation of the integral in the above equation demands an approximate incremental procedure for which *accuracy* is an obvious requirement. Besides, if the integrand itself depends on the inelastic strain, integration effects the solution of a differential equation $\dot{\boldsymbol{\eta}} = \mathbf{f}(\boldsymbol{\eta})$. Then, the *stability* of the numerical scheme becomes important. This issue has been addressed by the author in [7].

Various approximate schemes are feasible for the integration of the inelastic strain. Given a finite increment in time (or another appropriate progress parameter) leading from state t_n to state t_{n+1}, the integral in eqn (5.61) is written as

$$\boldsymbol{\eta}_{n+1} = \boldsymbol{\eta}_n + \int_n^{n+1} \dot{\boldsymbol{\eta}}\mathrm{d}t \tag{5.62}$$

and the task to be performed is the approximation within the increment.

5.4.1 Subincrementation

Given the stress increment $\boldsymbol{\sigma}_\Delta$ such that $\boldsymbol{\sigma}_{n+1} = \boldsymbol{\sigma}_n + \boldsymbol{\sigma}_\Delta$, ns equal subincrements are specified by

$$\delta\boldsymbol{\sigma} = \frac{1}{ns}\boldsymbol{\sigma}_\Delta \tag{5.63}$$

and define within the increment the stress states (Fig. 5.2)

$$\boldsymbol{\sigma}_k = \boldsymbol{\sigma}_n + k\delta\boldsymbol{\sigma} \qquad (k = 1, \ldots, ns). \tag{5.64}$$

Subincrements of the plastic strain can be obtained by the initial strain expression in Scheme 5.2 as

$$\delta\boldsymbol{\eta}_k = \left(\frac{1}{h}\mathbf{s}\mathbf{s}^{\mathrm{t}}\right)_{k-1} \delta\boldsymbol{\sigma}. \tag{5.65}$$

Here, the notation allocates the quantities h and $\mathbf{s}$ to the stress stage $k-1$ at the beginning of the subincrement, but specification at k or any other location in between is equally possible. The approximation of the plastic strain within the actual increment then reads

$$\boldsymbol{\eta}_\Delta = \int_n^{n+1} \mathrm{d}\boldsymbol{\eta} \quad \Leftarrow \quad \sum_{k=1}^{ns} \delta\boldsymbol{\eta}_k. \tag{5.66}$$

Alternatively, a strain increment $\boldsymbol{\gamma}_\Delta$ given such that $\boldsymbol{\gamma}_{n+1} = \boldsymbol{\gamma}_n + \boldsymbol{\gamma}_\Delta$, is partitioned in ns subincrements

$$\delta\boldsymbol{\gamma} = \frac{1}{ns}\boldsymbol{\gamma}_\Delta, \tag{5.67}$$

which determine the intermediate states of a fictitious stress quantity

$$\boldsymbol{\sigma}_k^* = \boldsymbol{\sigma}_n + k(\boldsymbol{\kappa}\delta\boldsymbol{\gamma}) \qquad (k = 1, \ldots, ns). \tag{5.68}$$

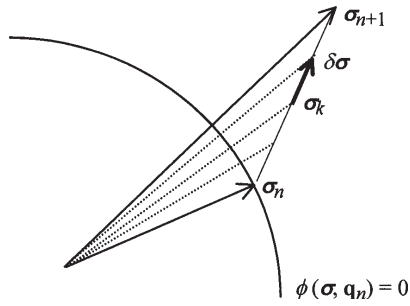

Figure 5.2: Subincrementation in stress space.

Obviously, $\boldsymbol{\sigma}_n \equiv \boldsymbol{\sigma}^*$ at the beginning of the increment while specification of the stress at the subincremental stations requires knowledge of the plastic strain. From the initial stress expression in Scheme 5.2,

$$\delta\boldsymbol{\eta}_k = \left(\frac{1}{h+3G}\mathbf{s}\mathbf{s}^{\mathrm{t}}\right)_{k-1}(\boldsymbol{\kappa}\delta\boldsymbol{\gamma}), \tag{5.69}$$

and the stress sequence within the increment is obtained as

$$\boldsymbol{\sigma}_k = \boldsymbol{\sigma}_k^* - \sum_{i=1}^{k}(\boldsymbol{\kappa}\delta\boldsymbol{\eta})_i \qquad (k = 1, \ldots, ns). \tag{5.70}$$

The stress determined at station k is utilized in the calculation of the next subincremental plastic strain $\delta\boldsymbol{\eta}_{k+1}$. This defines a sequential procedure for the explicit evaluation of eqn (5.69). The use of any other stress state within the subincrement requires in general an iterative procedure for $\delta\boldsymbol{\eta}_k$. Accumulation to $\boldsymbol{\eta}_\Delta$ as in eqn (5.66) supplies the approximation to the actual plastic strain within the entire increment.

It can be seen, in retrospect, that in both cases the approximation to the incremental plastic strain is performed in accordance with

$$\int_n^{n+1} \mathrm{d}\boldsymbol{\eta} = \int_n^{n+1} \mathbf{s}\mathrm{d}\bar{\eta} \quad \Leftarrow \quad \sum_{k=1}^{ns} \mathbf{s}_{k-1}\delta\bar{\eta}_k. \tag{5.71}$$

The individual schemes – initial strain and initial stress – differ in the computation of the scalar equivalent quantity $\delta\bar{\eta}_k$ by

$$\delta\bar{\eta}_k = \left(\frac{1}{h}\mathbf{s}^{\mathrm{t}}\right)_{k-1}\delta\boldsymbol{\sigma} \quad \text{and} \quad \delta\bar{\eta}_k = \left(\frac{1}{h+3G}\mathbf{s}^{\mathrm{t}}\right)_{k-1}(\boldsymbol{\kappa}\delta\boldsymbol{\gamma}), \tag{5.72}$$

respectively.

5.4.2 Incremental approximation

For a discussion of approximations based exclusively on the end points of the increment, we consider the following integration scheme:

$$\boldsymbol{\eta}_\Delta = \int_n^{n+1} \mathrm{d}\boldsymbol{\eta} = \int_n^{n+1} \mathbf{s}\mathrm{d}\bar{\eta} = \mathbf{s}_\zeta\bar{\eta}_\Delta \tag{5.73}$$

with $\bar{\eta}_\Delta = \bar{\eta}_{n+1} - \bar{\eta}_n$. Equation (5.73) reflects the mid-value theorem of integral calculus, where $\mathbf{s}_\zeta$ indicates specification of the flow direction $\mathbf{s}$ at position ζ. The normalized quantity $0 \le \zeta \le 1$ is known as the collocation parameter. In terms of the integration variable $\bar{\eta}$,

$$\zeta = \frac{\bar{\eta} - \bar{\eta}_n}{\bar{\eta}_{n+1} - \bar{\eta}_n},$$

but formulation in other progress variables is also feasible. It defines locations within the increment such that $\zeta = 0$ marks the beginning, $\zeta = 1$ the end of the incremental step.

In general, the flow direction will depend on both the stress and the hardening state: $\mathbf{s}(\boldsymbol{\sigma}, \mathbf{q})$, but only dependence on the stress $\boldsymbol{\sigma}$ will be exemplified in what follows. Integration by eqn (5.73) can be effected in conjunction with an assumed linear relationship of the stress within the increment $n, n+1$,

$$\boldsymbol{\sigma}_\zeta = (1-\zeta)\boldsymbol{\sigma}_n + \zeta\boldsymbol{\sigma}_{n+1}, \tag{5.74}$$

which gives as an approximation to the incremental plastic strain

$$\boldsymbol{\eta}_\Delta = \mathbf{s}(\boldsymbol{\sigma}_\zeta)\bar{\eta}_\Delta = \mathbf{s}_\zeta\bar{\eta}_\Delta. \tag{5.75}$$

The value of the collocation parameter ζ in eqns (5.75) and (5.73) can be chosen so as to satisfy specific requirements related to simplicity of the computation, accuracy of the approximation and stability of the integration.

Since the equivalent plastic strain $\bar{\eta}$ constitutes the integration parameter in eqn (5.73), the magnitude $\bar{\eta}_\Delta$ of the incremental plastic strain is considered a given quantity while the direction $\mathbf{s}_\zeta$ is subject to selection. In an explicit, forward Euler scheme it is taken at the beginning of the increment: $\mathbf{s}_{\zeta=0} = \mathbf{s}_n$. In a fully implicit, backward Euler procedure the direction $\mathbf{s}_{\zeta=1} = \mathbf{s}_{n+1}$ is employed, pertaining to the end of the increment. A superior accuracy is usually achieved for values within the interval. At the same time, this requires storage of two stress states $\boldsymbol{\sigma}_n$ and $\boldsymbol{\sigma}_{n+1}$ at each evaluation point in the system.

Actually, incremental changes of plastic strain have to be considered for a given increment in stress or strain, not for $\bar{\eta}_\Delta$. This is pursued below for the case of isotropic hardening. To this end, we extend the mid-value argument to the integration of eqn (1.152) for $\mathrm{d}\bar{\eta}$ and obtain

$$\bar{\eta}_\Delta = \int_n^{n+1} \frac{1}{h}\mathbf{s}^{\mathrm{t}}\mathrm{d}\boldsymbol{\sigma} = \frac{1}{h_\zeta}\mathbf{s}_\zeta^{\mathrm{t}}\boldsymbol{\sigma}_\Delta \qquad (\boldsymbol{\sigma}_\Delta = \boldsymbol{\sigma}_{n+1} - \boldsymbol{\sigma}_n). \tag{5.76}$$

In terms of the incremental strain from eqn (1.156),

$$\bar{\eta}_\Delta = \int_n^{n+1} \frac{2G}{h+3G}\mathbf{s}^{\mathrm{t}}\mathrm{d}\boldsymbol{\gamma} = \frac{2G}{h_\zeta+3G}\mathbf{s}_\zeta^{\mathrm{t}}\boldsymbol{\gamma}_\Delta \qquad (\boldsymbol{\gamma}_\Delta = \boldsymbol{\gamma}_{n+1} - \boldsymbol{\gamma}_n), \tag{5.77}$$

or, alternatively,

$$\bar{\eta}_\Delta = \frac{1}{h_\zeta+3G}\mathbf{s}_\zeta^{\mathrm{t}}\boldsymbol{\sigma}_\Delta^*, \tag{5.78}$$

where the quantity

$$\boldsymbol{\sigma}_\Delta^* = \boldsymbol{\kappa}\boldsymbol{\gamma}_\Delta$$

may be interpreted as a fictitious stress increment. We notice that with eqns (5.76) and (5.77) in conjunction with eqn (5.75), the relations between the differentials in eqns (1.154) and (1.157) simply transfer to the present case of finite incremental changes. The test on plastic loading is interpreted analogously.

Elastic–plastic transition

The above considerations on incremental plastic strain assume both the beginning and the end of the transition $n, n+1$ located in the plastic regime. If a plastic state $n+1$ is reached from an elastic state n, then only part of the increment is associated with plastic flow, the transition up to the yield limit being elastic (Fig. 5.3). The state n' where plastic flow initiates is defined by the condition $\phi(\boldsymbol{\sigma}_{n'}, \mathbf{q}_n) = 0$, which determines the stress $\boldsymbol{\sigma}_{n'}$. The quantity $\mathbf{q}_n$ represents the value of the hardening parameters prior to the incremental change. Assuming a linear variation of stress within the increment as by eqn (5.74), we have $\boldsymbol{\sigma}_{n'} = (1-\zeta')\boldsymbol{\sigma}_n + \zeta'\boldsymbol{\sigma}_{n+1}$, and the value of ζ' can be obtained from the yield condition. In the expressions for incremental plastic flow, the stress $\boldsymbol{\sigma}_{n'}$ takes the place of $\boldsymbol{\sigma}_n$, and the relevant increment in stress is $\boldsymbol{\sigma}_{n+1} - \boldsymbol{\sigma}_{n'} = (1-\zeta')\boldsymbol{\sigma}_\Delta$.

As an example of the linear variation, the equivalent stress $\bar{\sigma}_{n'}$ is given by

$$\begin{aligned}\bar{\sigma}^2_{n'} &= \frac{3}{2}[(1-\zeta')\boldsymbol{\sigma}_{\mathrm{D}n} + \zeta'\boldsymbol{\sigma}_{\mathrm{D}n+1}]^{\mathrm{t}}[(1-\zeta')\boldsymbol{\sigma}_{\mathrm{D}n} + \zeta'\boldsymbol{\sigma}_{\mathrm{D}n+1}] \\ &= (1-\zeta')^2\bar{\sigma}^2_n + (\zeta')^2\bar{\sigma}^2_{n+1} + 3(1-\zeta')\zeta'\boldsymbol{\sigma}^{\mathrm{t}}_{\mathrm{D}n}\boldsymbol{\sigma}_{\mathrm{D}n+1}. \qquad (5.79)\end{aligned}$$

The von Mises yield condition with isotropic hardening, eqn (1.150), in the form $\bar{\sigma}^2_{n'} = \sigma^2_{fn}$ becomes a quadratic equation for the parameter ζ'. Analogously, in the case of kinematic hardening eqn (1.159) or eqn (1.161), respectively, used in conjunction with the linear variation of $\boldsymbol{\sigma}_{\mathrm{D}}$ within the increment determines the value of ζ'. The hardening variable here is $\mathbf{q}_n = \boldsymbol{\alpha}_n$, taken at the state prior to the incremental change.

Computational finite element procedures effectively deal with the increment of strain rather than with the increment of stress. A fictitious stress

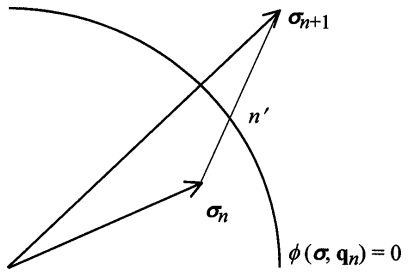

Figure 5.3: Elastic–plastic transition.

defined in this connection within the increment as

$$\boldsymbol{\sigma}^* = \boldsymbol{\sigma}_n + \boldsymbol{\kappa}[\boldsymbol{\gamma} - \boldsymbol{\gamma}_n] \tag{5.80}$$

assumes at the limit points the values

$$\boldsymbol{\sigma}^*_n = \boldsymbol{\sigma}_n \quad \text{and} \quad \boldsymbol{\sigma}^*_{n+1} = \boldsymbol{\sigma}_n + \boldsymbol{\kappa}\boldsymbol{\gamma}_\Delta. \tag{5.81}$$

If state $\boldsymbol{\sigma}_n$ at the beginning of the increment is within the elastic range, we have $\boldsymbol{\sigma}^*_{n'} \equiv \boldsymbol{\sigma}_{n'}$ at the yield limit. Then the condition $\phi(\boldsymbol{\sigma}^*_{n'}, \mathbf{q}_n) = 0$ for $\boldsymbol{\sigma}^*_{n'}$ determines the initiation of plastic flow, as does the condition $\phi(\boldsymbol{\sigma}_{n'}, \mathbf{q}_n) = 0$ in terms of $\boldsymbol{\sigma}_{n'}$. With a linear approximation for $\boldsymbol{\sigma}^*$ within the increment:

$$\boldsymbol{\sigma}^*_{n'} = (1 - \zeta')\boldsymbol{\sigma}^*_n + \zeta'\boldsymbol{\sigma}^*_{n+1}. \tag{5.82}$$

It turns out that the value of the parameter ζ' at incipient plastic flow in the increment can be obtained from the yield condition as before (with $\boldsymbol{\sigma}^*_{n+1}$ in place of $\boldsymbol{\sigma}_{n+1}$), but the result is different. In the present case ζ' is used to define the part $\boldsymbol{\gamma}_{n+1} - \boldsymbol{\gamma}_{n'} = (1 - \zeta')\boldsymbol{\gamma}_\Delta$ or $(1 - \zeta')\boldsymbol{\sigma}^*_\Delta$ respectively, of the incremental strain associated with plastic flow instead of the incremental stress in the former case.

An accuracy study

We consider approximate computation of the plastic strains in the rectangular plate under tension discussed analytically in Section 1.2.5. The plane problem can be represented by the reduced stress and strain vectors,

$$\boldsymbol{\sigma} = \begin{bmatrix} \sigma_1 \\ \sigma_2 \end{bmatrix}, \quad \boldsymbol{\gamma} = \begin{bmatrix} \gamma_1 \\ \gamma_2 \end{bmatrix}, \quad \boldsymbol{\eta} = \begin{bmatrix} \eta_1 \\ \eta_2 \end{bmatrix}, \tag{i}$$

with components along the sides of the rectangular plate. The elastic relationship between stress and strains reads

$$\begin{bmatrix} \sigma_1 \\ \sigma_2 \end{bmatrix} = \frac{E}{1-\nu^2} \begin{bmatrix} 1 & \nu \\ \nu & 1 \end{bmatrix} \begin{bmatrix} \gamma_1 - \eta_1 \\ \gamma_2 - \eta_2 \end{bmatrix}, \quad \begin{bmatrix} \gamma_1 - \eta_1 \\ \gamma_2 - \eta_2 \end{bmatrix} = \frac{1}{E} \begin{bmatrix} 1 & -\nu \\ -\nu & 1 \end{bmatrix} \begin{bmatrix} \sigma_1 \\ \sigma_2 \end{bmatrix}. \tag{ii}$$

The deviatoric stresses in the plane define the direction of plastic flow

$$\boldsymbol{\sigma}_{\mathrm{D}} = \begin{bmatrix} 2\sigma_1 - \sigma_2 \\ 2\sigma_2 - \sigma_1 \end{bmatrix} \quad \text{and} \quad \mathbf{s} = \frac{3}{2}\frac{1}{\bar{\sigma}}\boldsymbol{\sigma}_{\mathrm{D}}. \tag{iii}$$

Starting at the elastic limit, the state of stress is advanced incrementally such that

$$\boldsymbol{\sigma}_{n+1} = \boldsymbol{\sigma}_n + \boldsymbol{\sigma}_\Delta \quad \text{and} \quad \boldsymbol{\sigma}_\Delta = \begin{bmatrix} \sigma_{1\Delta} \\ \nu\sigma_{1\Delta} - E\eta_{2\Delta} \end{bmatrix}. \tag{iv}$$

In the incremental stress vector in eqn (iv), the component $\sigma_{1\Delta}$ is imposed in each step as a prescribed loading condition. The expression for $\sigma_{2\Delta}$ arises from the suppression of the lateral strain component, $\gamma_{2\Delta} = 0$ in the incremental form of eqn (ii), and requires knowledge of the plastic strain increment.

The incremental plastic strain $\boldsymbol{\eta}_\Delta$ is approximated by eqn (5.75), but eqn (5.77) for $\bar{\eta}_\Delta$ relies on the complete three-dimensional definitions of stress and strain and

cannot be used in conjunction with the present reduced vector arrays. For this purpose, we state an incremental condition of perfect plasticity in the form

$$\mathbf{s}_\zeta^{\mathrm{t}} \boldsymbol{\sigma}_\Delta = \mathbf{s}_\zeta^{\mathrm{t}} \boldsymbol{\kappa} [\boldsymbol{\gamma}_\Delta - \boldsymbol{\eta}_\Delta] = 0, \tag{v}$$

with the elasticity matrix $\boldsymbol{\kappa}$ as from eqn (ii). Then with eqn (5.75),

$$\bar{\eta}_\Delta = \frac{1}{\mathbf{s}_\zeta^{\mathrm{t}} \boldsymbol{\kappa} \mathbf{s}_\zeta} \mathbf{s}_\zeta^{\mathrm{t}} \boldsymbol{\kappa} \boldsymbol{\gamma}_\Delta \quad \text{and} \quad \boldsymbol{\eta}_\Delta = \bar{\eta}_\Delta \mathbf{s}_\zeta. \tag{vi}$$

An iterative treatment of the incremental elastoplastic problem starts each iteration cycle with an estimate $\boldsymbol{\eta}_{\Delta i} = \bar{\eta}_{\Delta i} \mathbf{s}_{\zeta i}$ of the plastic strain increment. Computation of the increment of stress $\boldsymbol{\sigma}_\Delta$, and of strain $\boldsymbol{\gamma}_\Delta$, determines the direction $\mathbf{s}_{\zeta i+1}$ and the magnitude $\bar{\eta}_{\Delta i+1}$ of the incremental plastic strain $\boldsymbol{\eta}_{\Delta i+1} = \bar{\eta}_{\Delta i+1} \mathbf{s}_{\zeta i+1}$, which enters as a new estimate in the next iteration cycle.

The actual numerical investigation [5] refers to the case $\nu = 0$ and covers loading from the elastic limit within the range $1 \leq \sigma_1/\sigma_\mathrm{s} \leq 1.13$. Results are alternatively obtained with the explicit scheme ($\zeta = 0$) and the mid-step approximation ($\zeta = 1/2$). In terms of a Taylor series expansion, the above schemes correspond to a first- and second-order approximation within the increment, respectively.

The accuracy of the two approximations is demonstrated in Fig. 5.4 by a comparison with the longitudinal stress–plastic strain plot of the analytical solution. Numerical results are shown for two different incrementations: five steps leading to the ultimately applied stress, or single-step computation. As expected, the accuracy of the second-order integration scheme is superior to the linearized one; remarkably good results are obtained with the latter by applying the loading in a single step.

Figure 5.5 indicates convergence of the numerical approximation to the analytical value for a diminishing size of the load increments. For this purpose, the normalized deviation of the numerical result η_1 from the analytical 'exact' value $\eta_{1\mathrm{e}}$ at ultimate load is depicted as a function of the number of load increments employed. It is seen that the rate of convergence is higher for the second-order

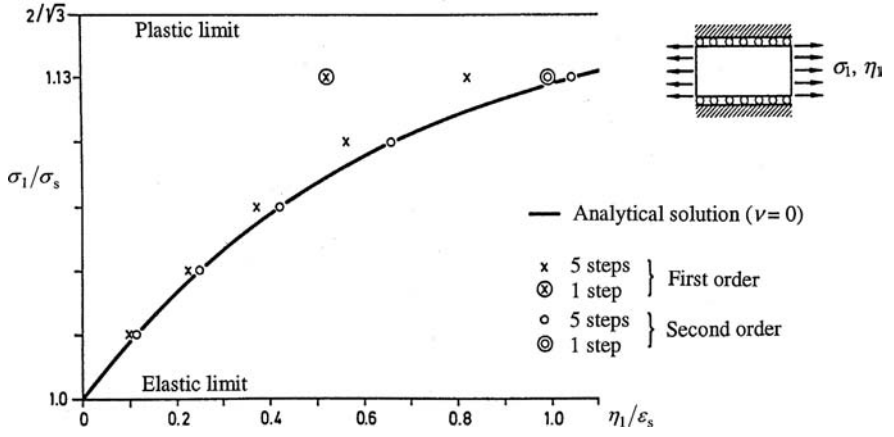

Figure 5.4: Approximate vs analytical solution for a perfectly plastic plate.

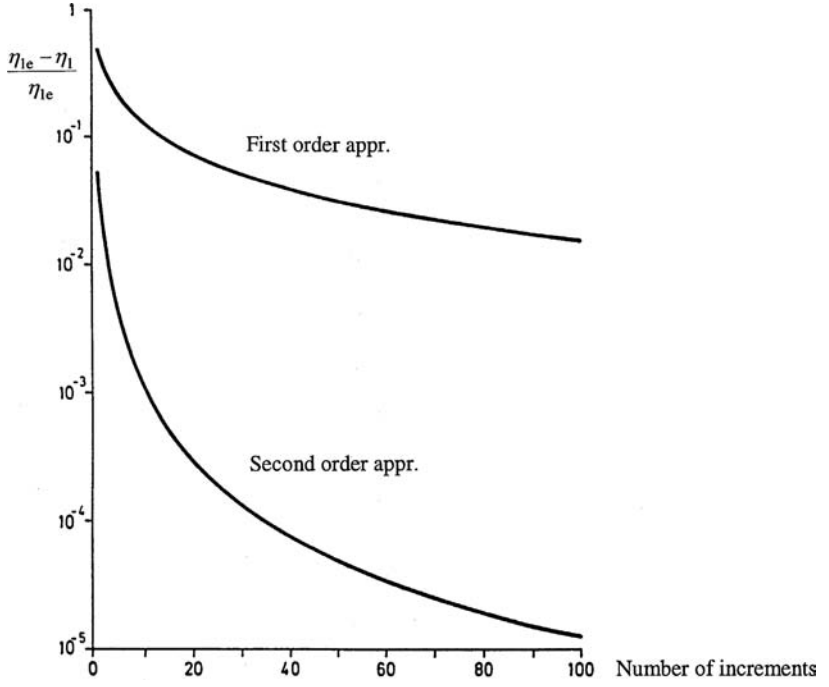

Figure 5.5: Error in plastic strain at final load depending on increment size.

approximation. In order to achieve a high-quality solution in the increments, the convergence criterion allowed only a relative deviation of $\leq 10^{-14}$ in the iterated variables. The number of iterations in the step appears to be insensitive to the step size, and therefore the number of iterations for the entire computation follows closely the variation in the number of loading increments.

5.4.3 Stability of integration

For the integration of the plastic strain

$$\boldsymbol{\eta} = \int \mathrm{d}\boldsymbol{\eta} = \int \mathbf{s}\mathrm{d}\bar{\eta},$$

the integrand $\mathbf{s}(\boldsymbol{\sigma})$ requires the stress $\boldsymbol{\sigma}$ as a prescribed function of the parameter $\bar{\eta}$. If such a relationship is given, the incremental approximation concerns the evaluation of the integral and raises merely the question of accuracy. If, on the other hand, the strain $\boldsymbol{\gamma}$ is assumed to be known as a function of $\bar{\eta}$, then the direction of plastic flow has to be interpreted as $\mathbf{s}(\boldsymbol{\kappa}[\boldsymbol{\gamma} - \boldsymbol{\eta}])$, and

$$\mathrm{d}\boldsymbol{\eta} = \mathbf{s}\left(\boldsymbol{\kappa}[\boldsymbol{\gamma} - \boldsymbol{\eta}]\right)\mathrm{d}\bar{\eta} \tag{5.83}$$

represents a differential equation for the plastic strain $\boldsymbol{\eta}$. The incremental approximation to its solution raises the issue of numerical stability, which concerns the propagation of perturbations.

The differential equation to be solved will be studied in a model form by the analogy,

$$\frac{1}{\mathrm{d}\bar{\eta}}\mathrm{d}\boldsymbol{\eta} - \mathbf{s}(\boldsymbol{\eta}) = \mathbf{0} \quad \Rightarrow \quad \dot{\mathbf{x}} + \mathbf{f}(\mathbf{x}) = \mathbf{0}, \tag{5.84}$$

where $\dot{\mathbf{x}} = (1/\mathrm{d}t)\mathrm{d}\mathbf{x}$ denotes the rate of change of the variable $\mathbf{x}$ with respect to the progress parameter t. For integration analogous to eqns (5.73) and (5.75), we obtain from eqn (5.84),

$$\mathbf{x}_{n+1} = \mathbf{x}_n - \tau\mathbf{f}(\mathbf{x}_\zeta), \tag{5.85}$$

with $\tau = t_{n+1} - t_n$ defining the incremental step. In addition, we state a linear variation of $\mathbf{x}$ within the increment,

$$\mathbf{x}_\zeta = (1-\zeta)\mathbf{x}_n + \zeta\mathbf{x}_{n+1}, \tag{5.86}$$

where $\zeta = (t - t_n)/\tau$.

The stability of the approximate integration concerns sensitivity of the solution to numerical perturbations. A perturbation $\delta\mathbf{x}$ to the solution $\mathbf{x}$ implies a variation of the integrand $\mathbf{f}(\mathbf{x})$. From eqn (5.85),

$$\delta\mathbf{x}_{n+1} = \delta\mathbf{x}_n - \tau\delta\mathbf{f}(\mathbf{x}_\zeta), \qquad \delta\mathbf{f} = \frac{\mathrm{d}\mathbf{f}}{\mathrm{d}\mathbf{x}}\delta\mathbf{x} = \mathbf{N}\delta\mathbf{x}. \tag{5.87}$$

With eqn (5.86) we obtain $\delta\mathbf{x}$, and

$$\delta\mathbf{f}(\mathbf{x}_\zeta) = \mathbf{N}_\zeta\left[(1-\zeta)\delta\mathbf{x}_n + \zeta\delta\mathbf{x}_{n+1}\right] \qquad \left(\mathbf{N}_\zeta = \left.\frac{\mathrm{d}\mathbf{f}}{\mathrm{d}\mathbf{x}}\right|_\zeta\right).$$

Substituting in eqn (5.87), we deduce for the propagation of perturbations the relation

$$[\mathbf{I} + \zeta\tau\mathbf{N}_\zeta]\delta\mathbf{x}_{n+1} = [\mathbf{I} - (1-\zeta)\tau\mathbf{N}_\zeta]\delta\mathbf{x}_n. \tag{5.88}$$

Ultimately, eqn (5.88) can be written as

$$\delta\mathbf{x}_{n+1} = \mathbf{A}\delta\mathbf{x}_n, \tag{5.89}$$

where the matrix

$$\mathbf{A} = [\mathbf{I} + \zeta\tau\mathbf{N}_\zeta]^{-1}[\mathbf{I} - (1-\zeta)\tau\mathbf{N}_\zeta] \tag{5.90}$$

is the amplification matrix for the perturbation.

In order to study the sensitivity of the integration scheme, the perturbation $\delta\mathbf{x}_n$ is represented as a linear combination of the m eigenvectors $\mathbf{y}_i(\mathbf{A})$ of the amplification matrix $\mathbf{A}$,

$$\delta\mathbf{x}_n = \sum_{i=1}^{m} c_i\mathbf{y}_i \quad \text{and} \quad \delta\mathbf{x}_{n+1} = \sum_{i=1}^{m} c_i\lambda_i\mathbf{y}_i. \tag{5.91}$$

Repeated application of eqn (5.91) over k consecutive integration steps following an initial perturbation $\delta\mathbf{x}_0$ gives

$$\delta\mathbf{x}_k = \mathbf{A}^k\delta\mathbf{x}_0 = \sum_{i=1}^{m} c_i\lambda_i^k\mathbf{y}_i. \tag{5.92}$$

Since the exponent k increases during the course of the incremental integration, the perturbation will diminish if all eigenvalues λ_i of the matrix $\mathbf{A}$ are absolutely less than unity. Stability requires that perturbations are not amplified. A sufficient condition therefore can be given in terms of the spectral radius ρ of the matrix $\mathbf{A}$ as

$$\rho(\mathbf{A}) = \max|\lambda_i(\mathbf{A})| < 1. \tag{5.93}$$

In eqn (5.90), the amplification matrix $\mathbf{A}$ is a rational function of the matrix $\mathbf{N}$. Then, the eigenvalues $\lambda_i(\mathbf{A})$ exhibit the same functional dependence:

$$\lambda_i(\mathbf{A}) = \frac{1-(1-\zeta)\tau\lambda_i(\mathbf{N}_\zeta)}{1+\zeta\tau\lambda_i(\mathbf{N}_\zeta)} = 1 - \frac{\tau\lambda_i(\mathbf{N}_\zeta)}{1+\zeta\tau\lambda_i(\mathbf{N}_\zeta)}. \tag{5.94}$$

The stability requirement of eqn (5.93) restricts the eigenvalues to $|\lambda_i(\mathbf{A})| < 1$, and hence

$$-1 < 1 - \frac{\tau\lambda_i(\mathbf{N}_\zeta)}{1+\zeta\tau\lambda_i(\mathbf{N}_\zeta)} < 1. \tag{5.95}$$

From eqn (5.95), there follows

$$0 < \tau\lambda_i(\mathbf{N}_\zeta) < \frac{2}{1-2\zeta}. \tag{5.96}$$

Accordingly, the stability of the integration requires the eigenvalues of the matrix $\mathbf{N}$ to be positive, $\lambda_i(\mathbf{N}) > 0$, and the incremental step τ to be limited by

$$\tau < \frac{2}{(1-2\zeta)\rho(\mathbf{N}_\zeta)} \qquad \left(0 \le \zeta < \frac{1}{2}\right). \tag{5.97}$$

Here, $\rho(\mathbf{N}) = \max \lambda_i(\mathbf{N})$ denotes the spectral radius of the matrix $\mathbf{N}$.

For $\zeta = 0$ the integration is explicit, and for stability $\tau < 2/\rho(\mathbf{N})$. For $0 < \zeta \le 1$ the integration involves quantities at the end of the increment, and is termed implicit. In the interval $0 \le \zeta < 1/2$, the integration is stable for finite values of the increment τ complying with the condition of eqn (5.97). The transition from conditional stability to unconditional stability is at $\zeta = 1/2$, so that $\tau \to \infty$ for $1/2 \le \zeta < 1$. Within this interval, the integration is insensitive to perturbations independently of the choice for the incremental step τ.

The stability requirement, eqn (5.93), ensures damping of the perturbation which was represented by eqn (5.92). If the eigenvalues of the amplification matrix $\mathbf{A}$ are positive, the damping is effected monotonously. For negative eigenvalues the sign of contributions from individual eigenvectors changes consecutively. Thus, the sign of the eigenvalues of $\mathbf{A}$ given by eqn (5.94) defines an oscillation limit in terms of the incremental step τ.

Stability is associated with the nature of the expected solution. Assuming linearity in eqn (5.84), we obtain for the evolution of the variable $\mathbf{x}$ the differential equation

$$\dot{\mathbf{x}} + \mathbf{N}\mathbf{x} = \mathbf{0}. \tag{5.98}$$

The solution of the above equation is

$$\begin{aligned} \mathbf{x} &= \exp(-t\mathbf{N})\mathbf{x}_0 \\ &= \mathbf{x}_0 - t\mathbf{N}\mathbf{x}_0 + \frac{t^2}{2!}\mathbf{N}^2\mathbf{x}_0 - \frac{t^3}{3!}\mathbf{N}^3\mathbf{x}_0 + \cdots, \end{aligned} \tag{5.99}$$

where the second expression results from the power series expansion of the exponential. Representation of the initial vector $\mathbf{x}_0$ as a linear combination of the

eigenvectors $\mathbf{y}_i(\mathbf{N})$ of the matrix $\mathbf{N}$,

$$\mathbf{x}_0 = \sum_{i=1}^{m} c_i \mathbf{y}_i, \tag{5.100}$$

transforms the power series in eqn (5.99) as follows:

$$\mathbf{x}_0 - t\mathbf{N}\mathbf{x}_0 + \frac{t^2}{2!}\mathbf{N}^2\mathbf{x}_0 - \frac{t^3}{3!}\mathbf{N}^3\mathbf{x}_0 + \cdots$$

$$= \sum_{i=1}^{m} \left(c_i \mathbf{y}_i - c_i t \lambda_i \mathbf{y}_i + c_i \frac{t^2 \lambda_i^2}{2!}\mathbf{y}_i - c_i \frac{t^3 \lambda_i^3}{3!}\mathbf{y}_i + \cdots \right). \tag{5.101}$$

Here, $\lambda_i(\mathbf{N})$ are the eigenvalues of the matrix $\mathbf{N}$, and the solution of eqn (5.98) can be expressed as

$$\mathbf{x} = \sum_{i=1}^{m} e^{-\mathrm{t}\lambda_i} c_i \mathbf{y}_i. \tag{5.102}$$

Since stability requires $\lambda_i(\mathbf{N}) > 0$, cf. eqn (5.96), it is associated with a decaying function $\mathbf{x}(t)$ as from eqn (5.102).

The incremental transition for $t_{n+1} \Leftarrow t_n + \tau$ obtained from eqn (5.99) reads

$$\mathbf{x}_{n+1} = \mathbf{x}_n - \tau\mathbf{N}\mathbf{x}_n + \frac{\tau^2}{2!}\mathbf{N}^2\mathbf{x}_n - \frac{\tau^3}{3!}\mathbf{N}^3\mathbf{x}_n + \cdots. \tag{5.103}$$

The linear part,

$$\mathbf{x}_{n+1} = [\mathbf{I} - \tau\mathbf{N}]\mathbf{x}_n \tag{5.104}$$

is identical to the explicit integration ($\zeta = 0$) of eqn (5.98) by the incremental scheme of eqn (5.85). Conversely, the explicit form of the integration scheme models exactly the linear part of the solution for the incremental step in eqn (5.103).

The above considerations on stability of the model equation can be immediately transferred to the equation of plastic flow on the left-hand side of eqn (5.84) by the substitution

$$\mathbf{x} \Leftarrow \boldsymbol{\eta}, \quad \mathbf{f}(\mathbf{x}) \Leftarrow -\mathbf{s}(\boldsymbol{\eta}). \tag{5.105}$$

Also implied is the assumption of a linear variation of the stress within the increment, eqn (5.74), and determination of $\mathbf{s}_\zeta = \mathbf{s}(\boldsymbol{\sigma}_\zeta)$ in eqn (5.75).

Perturbations in $\boldsymbol{\eta}$ are propagated by the incremental update $\boldsymbol{\eta}_{n+1} \Leftarrow \boldsymbol{\eta}_n + \boldsymbol{\eta}_\Delta$ in accordance with

$$\delta\boldsymbol{\eta}_{n+1} = \delta\boldsymbol{\eta}_n + \bar{\eta}_\Delta \delta\mathbf{s}_\zeta. \tag{5.106}$$

The direction of plastic flow

$$\mathbf{s} = \frac{3}{2}\frac{1}{\bar{\sigma}}\boldsymbol{\sigma}_\mathrm{D} = \frac{3}{2}\left(\frac{3}{2}\boldsymbol{\sigma}_\mathrm{D}^\mathrm{t}\boldsymbol{\sigma}_\mathrm{D}\right)^{-1/2}\boldsymbol{\sigma}_\mathrm{D}, \tag{5.107}$$

is a function of the deviatoric stress

$$\boldsymbol{\sigma}_\mathrm{D} = 2G[\boldsymbol{\gamma}_\mathrm{D} - \boldsymbol{\eta}] \quad \text{and} \quad \delta\boldsymbol{\sigma}_\mathrm{D} = -2G\delta\boldsymbol{\eta}. \tag{5.108}$$

The strain $\boldsymbol{\gamma}$ is considered free of perturbations such that these are introduced exclusively by the plastic strain $\boldsymbol{\eta}$. Therefore,

$$\delta\mathbf{s} = \frac{\mathrm{d}\mathbf{s}}{\mathrm{d}\boldsymbol{\sigma}_\mathrm{D}}\delta\boldsymbol{\sigma}_\mathrm{D} = -2G\frac{\mathrm{d}\mathbf{s}}{\mathrm{d}\boldsymbol{\sigma}_\mathrm{D}}\delta\boldsymbol{\eta} = -\mathbf{N}\delta\boldsymbol{\eta}. \tag{5.109}$$

The matrix

$$\mathbf{N} = -\frac{\partial\mathbf{s}}{\partial\boldsymbol{\eta}} = 2G\frac{\mathrm{d}\mathbf{s}}{\mathrm{d}\boldsymbol{\sigma}_\mathrm{D}} = \frac{3G}{\bar{\sigma}}\left[\mathbf{I} - \frac{2}{3}\mathbf{s}\mathbf{s}^\mathrm{t}\right] \tag{5.110}$$

is defined in analogy to eqn (5.87). From eqn (5.107) by differentiation,

$$\frac{\mathrm{d}\mathbf{s}}{\mathrm{d}\boldsymbol{\sigma}_\mathrm{D}} = \frac{3}{2}\frac{1}{\bar{\sigma}}\left[\mathbf{I} - \frac{2}{3}\mathbf{s}\mathbf{s}^\mathrm{t}\right], \tag{5.111}$$

which leads to the last expression for $\mathbf{N}$.

Noticing that

$$\begin{aligned}\delta\boldsymbol{\sigma}_{\mathrm{D}\zeta} &= (1-\zeta)\delta\boldsymbol{\sigma}_{\mathrm{D}n} + \zeta\delta\boldsymbol{\sigma}_{\mathrm{D}n+1} \\ &= -2G[(1-\zeta)\delta\boldsymbol{\eta}_n + \zeta\delta\boldsymbol{\eta}_{n+1}] = -2G\delta\boldsymbol{\eta}_\zeta,\end{aligned} \tag{5.112}$$

we obtain with eqn (5.109)

$$\delta\mathbf{s}_\zeta = -\mathbf{N}_\zeta\delta\boldsymbol{\eta}_\zeta = -\mathbf{N}_\zeta[(1-\zeta)\delta\boldsymbol{\eta}_n + \zeta\delta\boldsymbol{\eta}_{n+1}], \tag{5.113}$$

the matrix $\mathbf{N}$ to be specified at position ζ.

Substitution of eqn (5.113) in eqn (5.106) and rearrangement of terms gives

$$[\mathbf{I} + \zeta\bar{\eta}_\Delta\mathbf{N}_\zeta]\delta\boldsymbol{\eta}_{n+1} = [\mathbf{I} - (1-\zeta)\bar{\eta}_\Delta\mathbf{N}_\zeta]\delta\boldsymbol{\eta}_n \tag{5.114}$$

in place of eqn (5.88) pertaining to the model problem, with all related arguments applicable. In particular, interpretation of the stability condition of eqn (5.97) for the numerical integration of the equation of plastic flow leads to

$$\bar{\eta}_\Delta < \frac{2}{(1-2\zeta)3G/\bar{\sigma}}. \tag{5.115}$$

Here, $\tau \Leftarrow \bar{\eta}_\Delta$ and $\rho(\mathbf{N}) \Leftarrow 3G/\bar{\sigma}$ for the spectral radius as from eqn (5.110).

Interpretation of stability

Assuming plastic flow under monotonically increasing loading to be governed by isotropic hardening, the equivalent stress follows the uniaxial hardening characteristic of the material: $\bar{\sigma} = \sigma_\mathrm{f}(\bar{\eta})$ and $\bar{\sigma}_\Delta = h\bar{\eta}_\Delta$ where h can be referred to as a mid-value or a secant adapted to the finite incremental relationship. Then eqn (5.115) defines a stability condition in terms of the increment of equivalent stress $\bar{\sigma}_\Delta$. However, since the discussion concerns rather a prescribed strain history, we notice that $\dot{\bar{\sigma}} = \mathbf{s}^\mathrm{t}\dot{\boldsymbol{\sigma}} = 2G\mathbf{s}^\mathrm{t}[\dot{\boldsymbol{\gamma}} - \dot{\boldsymbol{\eta}}]$ from which the quantity $\dot{\bar{\sigma}}^* = 2G\mathbf{s}^\mathrm{t}\dot{\boldsymbol{\gamma}} = (h+3G)\dot{\bar{\eta}}$ is deduced as a fictitious equivalent stress rate in terms of the strain rate. Taking finite increments $\bar{\sigma}^*_\Delta = (h+3G)\bar{\eta}_\Delta$ with h as defined above, the stability condition in

eqn (5.115) can be used to restrict the quantity $\bar{\sigma}^*_\Delta = 2G\mathbf{s}^{\mathrm{t}}_\zeta \boldsymbol{\gamma}_\Delta$ and thus control the strain increment $\boldsymbol{\gamma}_\Delta$.

It is recalled that stability ensures damping of disturbances $\delta\boldsymbol{\eta}$ propagated by the incremental integration, eqn (5.106). In the integration scheme, $\bar{\eta}_\Delta$ is considered a fixed quantity and thus disturbances in $\boldsymbol{\eta}$ are constrained. In fact, from eqn (5.75) with $\mathbf{s}^{\mathrm{t}}\mathbf{s} = 3/2$ we observe that

$$\boldsymbol{\eta}^{\mathrm{t}}_\Delta \boldsymbol{\eta}_\Delta = \frac{3}{2}\bar{\eta}^2_\Delta = \text{ constant} \quad \text{and} \quad \boldsymbol{\eta}^{\mathrm{t}}_\Delta \delta\boldsymbol{\eta}_\Delta = 0. \tag{5.116}$$

The second equality in eqn (5.116), obtained by differentiation, expresses the orthogonality between $\boldsymbol{\eta}_\Delta$ and $\delta\boldsymbol{\eta}_\Delta$ as a consequence of the fixed magnitude. This implies that

$$\boldsymbol{\eta}^{\mathrm{t}}_\Delta[\delta\boldsymbol{\eta}_{n+1} - \delta\boldsymbol{\eta}_n] = 0 \quad \Rightarrow \quad \mathbf{s}^{\mathrm{t}}_\zeta \delta\mathbf{s}_\zeta = 0. \tag{5.117}$$

The final result in the above equation makes use of eqns (5.106) and (5.75). It concerns the direction of incremental plastic flow and shows that disturbances induce a rotation in the vector $\mathbf{s}_\zeta$, maintaining the constancy of its length.

5.4.4 Radial return

The term was introduced in [8] in connection with incrementation of perfectly plastic flow. The following presentation uses the formalism of the account in [9].

After application of an increment in strain $\boldsymbol{\gamma}_\Delta$ the stress can be obtained as

$$\boldsymbol{\sigma}_{n+1} = \boldsymbol{\sigma}_n + \boldsymbol{\kappa}[\boldsymbol{\gamma}_\Delta - \boldsymbol{\eta}_\Delta] = \boldsymbol{\sigma}^*_{n+1} - 2G\boldsymbol{\eta}_\Delta. \tag{5.118}$$

The fictitious stress

$$\boldsymbol{\sigma}^*_{n+1} = \boldsymbol{\sigma}_n + \boldsymbol{\kappa}\boldsymbol{\gamma}_\Delta \tag{5.119}$$

predicted under the assumption of elasticity must be corrected by the contribution of the incremental plastic strain $\boldsymbol{\eta}_\Delta$ such that the stress $\boldsymbol{\sigma}_{n+1}$ meets the yield surface (Fig. 5.6). In isochoric plasticity, this procedure affects only the deviatoric state of stress since plastic strains do not exhibit volumetric parts.

Perfect plasticity and isotropic hardening
The direction of the incremental plastic strain is specified here by the stress $\boldsymbol{\sigma}_{n+1}$ at the end of the increment

$$\boldsymbol{\eta}_\Delta = \bar{\eta}_\Delta \mathbf{s}_{n+1} \quad \text{with} \quad \mathbf{s}_{n+1} = \frac{3}{2}\frac{1}{\bar{\sigma}_{n+1}}\boldsymbol{\sigma}_{Dn+1}. \tag{5.120}$$

Then, from eqn (5.118) for the deviatoric part,

$$\boldsymbol{\sigma}^*_{\mathrm{D}n+1} = \boldsymbol{\sigma}_{\mathrm{D}n+1} + 2G\boldsymbol{\eta}_\Delta = \left(1 + 3G\frac{\bar{\eta}_\Delta}{\bar{\sigma}_{n+1}}\right)\boldsymbol{\sigma}_{\mathrm{D}n+1}, \tag{5.121}$$

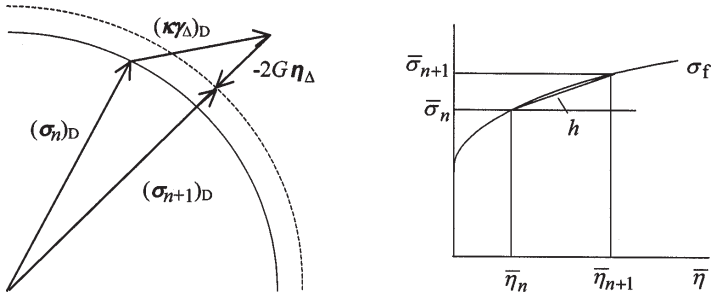

Figure 5.6: Radial return to the yield surface.

and therefore the directions of $\boldsymbol{\sigma}_{Dn+1}$ and $\boldsymbol{\sigma}^*_{Dn+1}$ are identical:

$$\mathbf{s}_{n+1} = \frac{3}{2}\frac{1}{\bar{\sigma}_{n+1}}\boldsymbol{\sigma}_{Dn+1} = \frac{3}{2}\frac{1}{\bar{\sigma}^*_{n+1}}\boldsymbol{\sigma}^*_{Dn+1} = \mathbf{s}^*_{n+1}. \tag{5.122}$$

Thus, in eqn (5.118), the correction by $2G\boldsymbol{\eta}_\Delta$ up to the yield surface is along $\boldsymbol{\sigma}^*_{Dn+1}$, which suggests the denotation radial return for this technique.

From eqn (5.120) right, the equivalent deviatoric stress $\bar{\sigma}_{n+1}$ can be expressed as

$$\bar{\sigma}_{n+1} = \mathbf{s}^{\mathrm{t}}_{n+1}\boldsymbol{\sigma}_{Dn+1} = \mathbf{s}^{\mathrm{t}}_{n+1}\boldsymbol{\sigma}_{n+1}. \tag{5.123}$$

With eqn (5.118) for $\boldsymbol{\sigma}_{n+1}$, eqn (5.120) for $\boldsymbol{\eta}_\Delta$ and $\mathbf{s}_{n+1} = \mathbf{s}^*_{n+1}$ from eqn (5.122),

$$\bar{\sigma}_{n+1} = \mathbf{s}^{*\mathrm{t}}_{n+1}\boldsymbol{\sigma}^*_{n+1} - 3G\bar{\eta}_\Delta = \bar{\sigma}^*_{n+1} - 3G\bar{\eta}_\Delta. \tag{5.124}$$

In perfect plasticity the condition to be observed in inelastic deformation is $\phi_{n+1} = \bar{\sigma}_{n+1} - \sigma_s = 0$, and with eqn (5.124) the equivalent plastic strain increment follows to

$$\bar{\eta}_\Delta = \frac{1}{3G}(\bar{\sigma}^*_{n+1} - \sigma_s) \geq 0. \tag{5.125}$$

The quantity $\bar{\sigma}^*_{n+1}$ is computed as an equivalent stress with the fictitious stress $\boldsymbol{\sigma}^*_{n+1}$, and σ_s denotes the uniaxial yield stress. Backsubstitution in eqn (5.120) for $\boldsymbol{\eta}_\Delta$ with $\mathbf{s}_{n+1} = \mathbf{s}^*_{n+1}$, and in eqn (5.118) completes the determination of the stress state $\boldsymbol{\sigma}_{n+1}$ at the end of the increment.

The above formalism follows as a special case of the technique developed in [9] independently for hardening plasticity. For isotropic hardening (Section 1.3.1), plastic states at the end of the increment comply with

$$\phi_{n+1} = \bar{\sigma}_{n+1} - \sigma_{fn+1} = 0. \tag{5.126}$$

From the uniaxial flow curve in Fig. 5.6, the yield stress of the material can be expressed as

$$\sigma_{fn+1} = \sigma_{fn} + h\bar{\eta}_\Delta, \tag{5.127}$$

where h is an estimated incremental average or a secant slope computed during the course of an iteration procedure.

With eqn (5.124) for $\bar{\sigma}_{n+1}$ and eqn (5.127) for $\sigma_{\mathrm{f}n+1}$, the equivalent plastic strain increment follows from eqn (5.126):

$$\bar{\eta}_\Delta = \frac{1}{h+3G}(\bar{\sigma}^*_{n+1} - \sigma_{\mathrm{f}n}) \geq 0. \tag{5.128}$$

This expression for $\bar{\eta}_\Delta$ incorporates the incremental plastic loading condition $(\bar{\sigma}^*_{n+1} - \sigma_{\mathrm{f}n}) > 0$, and reduces to eqn (5.125) for a perfectly plastic material ($h = 0$). In conjunction with $\mathbf{s}_{n+1} = \mathbf{s}^*_{n+1}$ as a consequence of the radial return technique, eqn (5.128) determines the plastic strain increment $\boldsymbol{\eta}_\Delta$ in eqn (5.120) using the fictitious stress $\boldsymbol{\sigma}^*_{n+1}$ as input, and completes the computation of the stress $\boldsymbol{\sigma}_{n+1}$ by eqn (5.118). The incremental quantity at the origin of eqn (5.128) is the strain $\boldsymbol{\gamma}_\Delta$, as for the *initial stress* version for the plastic strain increment.

If the stress increment $\boldsymbol{\sigma}_\Delta$ is given instead of the incremental strain, the input is the stress $\boldsymbol{\sigma}_{n+1} = \boldsymbol{\sigma}_n + \boldsymbol{\sigma}_\Delta$. The task then reduces to the computation of the equivalent plastic strain increment in eqn (5.120). The condition $\phi_{n+1} = 0$, eqn (5.126), along with eqn (5.127) for the yield stress gives

$$\bar{\eta}_\Delta = \frac{1}{h}(\bar{\sigma}_{n+1} - \sigma_{\mathrm{f}n}) \geq 0. \tag{5.129}$$

The hardening parameter h can be specified such that the uniaxial flow diagram is exactly reproduced, for which reason eqn (5.129) may be considered superfluous. It conforms, however, with the overall formalism and pertains to the *initial strain* version for $\boldsymbol{\eta}_\Delta$.

Kinematic hardening
Referring to Section 1.3.2, plastic states satisfy the condition

$$\phi_{\mathrm{K}n+1} = \bar{\sigma}_{\mathrm{K}n+1} - \sigma_{\mathrm{s}} = 0, \tag{5.130}$$

where analogously to eqn (5.123) for the equivalent stress

$$\bar{\sigma}_{\mathrm{K}n+1} = \mathbf{s}^{\mathrm{t}}_{\mathrm{K}n+1}\boldsymbol{\sigma}_{\mathrm{K}n+1} \quad \text{with} \quad \mathbf{s}_{\mathrm{K}n+1} = \frac{3}{2}\frac{1}{\bar{\sigma}_{\mathrm{K}n+1}}\boldsymbol{\sigma}_{\mathrm{KD}n+1}. \tag{5.131}$$

In the 'kinematic' stress vector,

$$\boldsymbol{\sigma}_{\mathrm{K}n+1} = [\boldsymbol{\sigma}_n + \boldsymbol{\sigma}_\Delta] - [\boldsymbol{\alpha}_n + \boldsymbol{\alpha}_\Delta] = \boldsymbol{\sigma}'_{\mathrm{K}n+1} - \boldsymbol{\alpha}_\Delta, \tag{5.132}$$

the part

$$\begin{aligned} \boldsymbol{\sigma}'_{\mathrm{K}n+1} &= [\boldsymbol{\sigma}_n + \boldsymbol{\sigma}_\Delta] - \boldsymbol{\alpha}_n = \boldsymbol{\sigma}_{n+1} - \boldsymbol{\alpha}_n \\ &= \boldsymbol{\sigma}_{\mathrm{K}n} + \boldsymbol{\sigma}_\Delta \end{aligned} \tag{5.133}$$

can be determined once the stress increment $\boldsymbol{\sigma}_\Delta$ is given.

The incremental translation $\boldsymbol{\alpha}_\Delta$ of the yield surface is assumed to point along the direction $\mathbf{s}_{\mathrm{K}n+1}$, and can be written as

$$\boldsymbol{\alpha}_\Delta = \frac{2}{3}\bar{\alpha}_\Delta \mathbf{s}_{\mathrm{K}n+1} = \frac{\bar{\alpha}_\Delta}{\bar{\sigma}_{\mathrm{K}n+1}}\boldsymbol{\sigma}_{\mathrm{KD}n+1}. \tag{5.134}$$

Therefore, from eqn (5.132) for deviatoric parts,

$$\boldsymbol{\sigma}'_{\mathrm{KD}n+1} = \boldsymbol{\sigma}_{\mathrm{KD}n+1} + \boldsymbol{\alpha}_\Delta = \left(1 + \frac{\bar{\alpha}_\Delta}{\bar{\sigma}_{\mathrm{K}n+1}}\right)\boldsymbol{\sigma}_{\mathrm{KD}n+1}, \tag{5.135}$$

and the directions of $\boldsymbol{\sigma}'_{\mathrm{KD}n+1}$ and $\boldsymbol{\sigma}_{\mathrm{KD}n+1}$ are identical, i.e. $\mathbf{s}_{\mathrm{K}n+1} = \mathbf{s}'_{\mathrm{K}n+1}$.

Thus, with eqn (5.132) for $\boldsymbol{\sigma}_{\mathrm{K}n+1}$ and eqn (5.134) for $\boldsymbol{\alpha}_\Delta$ we obtain for the equivalent stress in eqn (5.131),

$$\bar{\sigma}_{\mathrm{K}n+1} = (\mathbf{s}'_{\mathrm{K}n+1})^{\mathrm{t}}\boldsymbol{\sigma}'_{\mathrm{K}n+1} - (\mathbf{s}'_{\mathrm{K}n+1})^{\mathrm{t}}\boldsymbol{\alpha}_\Delta = \bar{\sigma}'_{\mathrm{K}n+1} - \bar{\alpha}_\Delta, \tag{5.136}$$

where $\bar{\sigma}'_{\mathrm{K}n+1}$ is determined by applying the equivalent stress operation to the vector $\boldsymbol{\sigma}'_{\mathrm{K}n+1}$, and

$$\bar{\alpha}_\Delta = h\bar{\eta}_\Delta.$$

The condition $\phi_{\mathrm{K}n+1} = 0$, eqn (5.130), then furnishes for $\bar{\eta}_\Delta$ the *initial strain* form,

$$\bar{\eta}_\Delta = \frac{1}{h}(\bar{\sigma}'_{\mathrm{K}n+1} - \sigma_{\mathrm{s}}) \geq 0, \tag{5.137}$$

and for the incremental plastic strain,

$$\boldsymbol{\eta}_\Delta = \bar{\eta}_\Delta \mathbf{s}_{\mathrm{K}n+1} = \bar{\eta}_\Delta \mathbf{s}'_{\mathrm{K}n+1}. \tag{5.138}$$

If, alternatively, the strain increment $\boldsymbol{\gamma}_\Delta$ is given (Fig. 5.7), use of the elastic relation $\boldsymbol{\sigma}_\Delta = \boldsymbol{\kappa}[\boldsymbol{\gamma}_\Delta - \boldsymbol{\eta}_\Delta]$ in eqn (5.132) leads to the expression

$$\begin{aligned}\boldsymbol{\sigma}_{\mathrm{K}n+1} &= [\boldsymbol{\sigma}_n + \boldsymbol{\kappa}\boldsymbol{\gamma}_\Delta] - [\boldsymbol{\alpha}_n + \boldsymbol{\alpha}_\Delta] - 2G\boldsymbol{\eta}_\Delta \\ &= \boldsymbol{\sigma}^{*\prime}_{\mathrm{K}n+1} - [\boldsymbol{\alpha}_\Delta + 2G\boldsymbol{\eta}_\Delta].\end{aligned} \tag{5.139}$$

Here, the part

$$\begin{aligned}\boldsymbol{\sigma}^{*\prime}_{\mathrm{K}n+1} &= [\boldsymbol{\sigma}_n + \boldsymbol{\kappa}\boldsymbol{\gamma}_\Delta] - \boldsymbol{\alpha}_n = \boldsymbol{\sigma}^*_{n+1} - \boldsymbol{\alpha}_n \\ &= \boldsymbol{\sigma}_{\mathrm{K}n} + \boldsymbol{\kappa}\boldsymbol{\gamma}_\Delta\end{aligned} \tag{5.140}$$

is available from the incremental finite element solution and the state at the beginning of the increment. Since both $\boldsymbol{\alpha}_\Delta$ and $\boldsymbol{\eta}_\Delta$ are assumed to be directed along $\mathbf{s}_{\mathrm{K}n+1}$, an argument analogous to eqn (5.135) shows that $\mathbf{s}_{\mathrm{K}n+1} = \mathbf{s}^{*\prime}_{\mathrm{K}n+1}$.

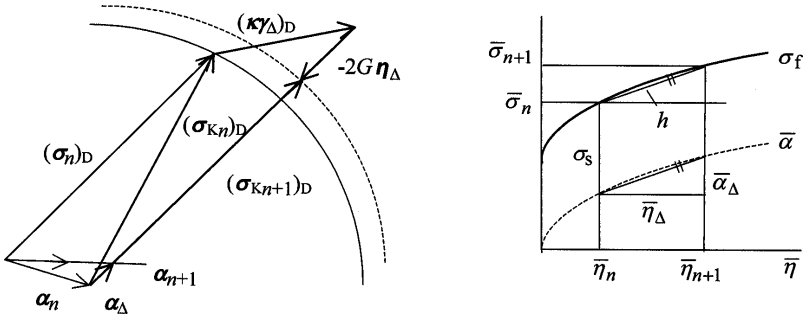

Figure 5.7: Radial return for kinematic hardening.

Then, with eqn (5.139) for $\boldsymbol{\sigma}_{Kn+1}$ the equivalent stress quantity from eqn (5.131) becomes

$$\begin{aligned}\bar{\sigma}_{Kn+1} &= (\mathbf{s}^{*\prime}_{Kn+1})^t \boldsymbol{\sigma}^{*\prime}_{K+1} - (\mathbf{s}^{*\prime}_{Kn+1})^t [\boldsymbol{\alpha}_\Delta + 2G\boldsymbol{\eta}_\Delta] \\ &= \bar{\sigma}^{*\prime}_{Kn+1} - (\bar{\alpha}_\Delta + 3G\bar{\eta}_\Delta), \end{aligned} \tag{5.141}$$

where $\bar{\alpha}_\Delta = h\bar{\eta}_\Delta$. Utilization in the condition $\phi_{Kn+1} = 0$ of eqn (5.130) gives for $\bar{\eta}_\Delta$ the *initial stress* form

$$\bar{\eta}_\Delta = \frac{1}{h+3G}(\bar{\sigma}^{*\prime}_{Kn+1} - \sigma_s) \geq 0, \tag{5.142}$$

instead of eqn (5.137). The quantity $\bar{\sigma}^{*\prime}_{Kn+1}$ is computed as an equivalent deviatoric stress with the vector $\boldsymbol{\sigma}^{*\prime}_{Kn+1}$, eqn (5.140). The direction $\mathbf{s}^{*\prime}_{Kn+1}$ of its deviatoric part completes the specification of the incremental plastic strain $\boldsymbol{\eta}_\Delta$, eqn (5.138), and of the translation $\boldsymbol{\alpha}_\Delta$, eqn (5.134).

In retrospect we notice that fundamental to the radial return technique is the employment of the flow direction at final state, for the entire incremental step. This selection corresponds to the fully implicit, backward Euler scheme of the incremental approximation with $\mathbf{s}_{\zeta=1} = \mathbf{s}_{n+1}$.

5.4.5 A more general return technique

In case that the material behaviour is not isotropic and when the plastic flow is not directed along the stress deviator, techniques different from radial return are required to adapt the elastic excess stress in the increment to the yield surface. The algorithm developed in [10] for this purpose may be referred to the generalized formalism of Section 1.4 with the yield condition $\phi(\boldsymbol{\sigma}, \mathbf{q}) \leq 0$, and will be outlined in the following.

Let the strain increment $\boldsymbol{\gamma}_\Delta$ pertaining to the transition $n \to n+1$ be given. If the stress $\boldsymbol{\sigma}^*_{n+1} = \boldsymbol{\sigma}_n + \boldsymbol{\kappa}\boldsymbol{\gamma}_\Delta$ from the elastic prediction violates the yield condition such that $\phi(\boldsymbol{\sigma}^*_{n+1}, \mathbf{q}_n) > 0$, it is fictitious and must be

corrected by accounting for the effect of plastic flow on the hardening parameters $\mathbf{q}$ until

$$\phi_{n+1} = \phi(\boldsymbol{\sigma}_{n+1}, \mathbf{q}_{n+1}) = 0. \tag{5.143}$$

The correction is performed iteratively. Entering an iteration cycle with estimates $(\boldsymbol{\sigma}_{n+1})_i$, $(\mathbf{q}_{n+1})_i$ for which $(\phi_{n+1})_i > 0$, improved estimates

$$\begin{aligned} (\boldsymbol{\sigma}_{n+1})_{i+1} &= (\boldsymbol{\sigma}_{n+1})_i + \delta\boldsymbol{\sigma}_i, \\ (\mathbf{q}_{n+1})_{i+1} &= (\mathbf{q}_{n+1})_i + \delta\mathbf{q}_i, \end{aligned} \tag{5.144}$$

are required to satisfy the yield condition in the form

$$(\phi_{n+1})_{i+1} \cong (\phi_{n+1})_i + \left.\frac{\partial\phi}{\partial\boldsymbol{\sigma}}\right|_{n+1,i} \delta\boldsymbol{\sigma}_i + \left.\frac{\partial\phi}{\partial\mathbf{q}}\right|_{n+1,i} \delta\mathbf{q}_i = 0, \tag{5.145}$$

which is obtained by linearization at state $(\boldsymbol{\sigma}_{n+1})_i, (\mathbf{q}_{n+1})_i$. Since the correction process takes place at constant strain $\boldsymbol{\gamma}_n + \gamma_\Delta$, elasticity gives for the stress variation in eqn (5.145)

$$\delta\boldsymbol{\sigma}_i = -\boldsymbol{\kappa}\delta\boldsymbol{\eta}_i. \tag{5.146}$$

The variation of the hardening parameters is

$$\delta\mathbf{q}_i = (\boldsymbol{\mathcal{H}}_{n+1})_i \delta\boldsymbol{\eta}_i, \tag{5.147}$$

while the variation in plastic strain is assumed given by the flow rule as

$$\delta\boldsymbol{\eta}_i = \Lambda_i \left[\frac{\partial\phi}{\partial\boldsymbol{\sigma}}\right]^{\mathrm{t}}_{n+1,i}. \tag{5.148}$$

After substitution, eqn (5.145) is solved for

$$\Lambda_i = \left(\frac{\partial\phi}{\partial\boldsymbol{\sigma}}\boldsymbol{\kappa}\frac{\partial\phi}{\partial\boldsymbol{\sigma}^{\mathrm{t}}} - \frac{\partial\phi}{\partial\mathbf{q}}\boldsymbol{\mathcal{H}}\frac{\partial\phi}{\partial\boldsymbol{\sigma}^{\mathrm{t}}}\right)^{-1}_{n+1,i} (\phi_{n+1})_i. \tag{5.149}$$

This determines $\delta\boldsymbol{\eta}_i$ and $\delta\mathbf{q}_i, \delta\boldsymbol{\sigma}_i$ for the new estimates $(\boldsymbol{\sigma}_{n+1})_{i+1}, (\mathbf{q}_{n+1})_{i+1}$ in eqn (5.144). In place of eqn (5.148) for the variation in plastic strain we might use the alternative representation

$$\delta\boldsymbol{\eta}_i = \delta\bar{\eta}_i(\mathbf{s}_{n+1})_i,$$

but this introduces inhomogeneity in the formalism.

The iterative return is started with

$$\begin{aligned} (\boldsymbol{\sigma}_{n+1})_1 &= \boldsymbol{\sigma}_n + \boldsymbol{\kappa}\boldsymbol{\gamma}_\Delta = \boldsymbol{\sigma}^*_{n+1} \\ (\mathbf{q}_{n+1})_1 &= \mathbf{q}_n. \end{aligned}$$

At the end of the iteration, when the yield condition is met after rit iteration cycles, the increment of plastic strain is

$$\boldsymbol{\eta}_\Delta = \sum_{i=1}^{rit} \delta\boldsymbol{\eta}_i = \sum_{i=1}^{rit} \delta\bar{\eta}_i(\mathbf{s}_{n+1})_i.$$

When the conditions are met the procedure effects radial return since $(\mathbf{s}_{n+1})_i = \mathbf{s}^*_{n+1} = \text{constant}$, and $\boldsymbol{\eta}_\Delta = (\sum_{i=1}^{rit} \delta\bar{\eta}_i)\mathbf{s}^*_{n+1}$.

5.5 Elastoplastic computation

5.5.1 Incrementation

The numerical finite element analysis of elastoplastic systems for a specified history of slowly applied loads is based on the consideration of the condition of quasistatic equilibrium at a series of stages. It combines an elastic solution until initial yield (Section 5.2) with a sequence of incremental solutions in the plastic range. Beyond the elastic limit the algorithm is controlled by a stepwise application of the loading. This is necessitated by the path-dependent nature of the elastoplastic stress–strain relations, which imply incremental approximation. Referring to the transition from stage n to stage $n+1$, the statement of static equilibrium between applied loads $\mathbf{P}$ at the mesh nodal points and stress resultants $\mathbf{S}$ as expressed by eqn (5.19) taken at $n+1$, the end of the loading step, reads

$$\mathbf{P}_{n+1} = \mathbf{P}_n + \mathbf{P}_\Delta = \mathbf{S}_n + \mathbf{S}_\Delta = \mathbf{S}_{n+1}. \tag{5.150}$$

Since equilibrium has been established at stage n, we are left with an incremental equation for the displacement $\mathbf{U}_\Delta$:

$$\mathbf{P}_\Delta = \mathbf{S}_\Delta(\mathbf{U}_\Delta). \tag{5.151}$$

Non-equilibrated numerical residuals at stage n can be accounted for in the subsequent incremental solution by modifying the increment of the applied loads to

$$\mathbf{P}_\Delta \Leftarrow [\mathbf{P}_{n+1} - \mathbf{P}_n] + [\mathbf{P}_n - \mathbf{S}_n] = \mathbf{P}_{n+1} - \mathbf{S}_n.$$

Under the assumption that displacements do not modify appreciably the geometry of the system, $\mathbf{S}_\Delta$ is obtained with the incremental stresses $\boldsymbol{\sigma}_\Delta$ in exactly the same manner as $\mathbf{S}$ is obtained with the stress $\boldsymbol{\sigma}$. The above can be concluded from the finite element formalism in Section 5.1. The functional dependence on the incremental displacement $\mathbf{U}_\Delta$ is a result of the approximate integration of the elastoplastic stress–strain relations, which provides us with a relationship between the increment of stress and the

increment of strain. To be specific, the strain increment required there is determined by the finite element kinematics as

$$\boldsymbol{\gamma}_\Delta = \boldsymbol{a}\mathbf{U}_{q\Delta} = \boldsymbol{a}\mathbf{a}_q\mathbf{U}_\Delta.$$

The principle of the incremental computer procedure can be summarized as shown in Scheme 5.3.

Elastic limit state	$\max\ \phi(\boldsymbol{\sigma}_\mathrm{e}, \sigma_\mathrm{s}) = 0 :\ \mathbf{P}_\mathrm{s}$
	$\mathbf{P}_0 \Leftarrow \mathbf{P}_\mathrm{s}, \mathbf{U}_0 \Leftarrow \mathbf{U}_\mathrm{s}, \boldsymbol{\sigma}_0 \Leftarrow \boldsymbol{\sigma}_\mathrm{s}$
Loading loop:	$n = 0, ninc$
Load increment	$\mathbf{P}_\Delta :\ \mathbf{P}_{n+1} = \mathbf{P}_n + \mathbf{P}_\Delta$
Elastoplastic solution	$\mathbf{U}_\Delta :\ \mathbf{U}_{n+1} = \mathbf{U}_n + \mathbf{U}_\Delta$
	$\boldsymbol{\sigma}_\Delta :\ \boldsymbol{\sigma}_{n+1} = \boldsymbol{\sigma}_n + \boldsymbol{\sigma}_\Delta$
End loading	

Scheme 5.3: Incremental elastoplastic algorithm.

At the beginning of an elastoplastic computation stands the specification of the elastic limit state. This is the state at which the elasticity limit of the material is first attained locally in the system. Frequently, the loading $\mathbf{P}$ can be assumed to be proportional, varying by a factor from a reference level $\mathbf{P}_\mathrm{R}$: $\mathbf{P} = \lambda\mathbf{P}_\mathrm{R}$. Determination of the elastic limit state then requires a single elastic solution and scaling by the factor λ_s obtained from the condition of initial yield:

$$\max\ \phi(\lambda_\mathrm{s}\boldsymbol{\sigma}_\mathrm{R}) = \lambda_\mathrm{s}(\max\ \bar{\sigma}_\mathrm{R}) - \sigma_\mathrm{s} = 0.$$

The maximum is searched for within the system. In the case of a different, arbitrary loading history, either incrementation is started at the origin or the elastic limit state is obtained iteratively.

The subsequent loading is applied in increments $\mathbf{P}_\Delta$. The choice of the size of the loading increment is guided merely by two aspects: the linearization error and the convergence of a possible iterative solution. The expressions for incremental plastic flow developed in Section 5.4.2 are homologous to those for the time rates in the algorithms of Section 5.3. Therefore, the basic solution schemes are equally applicable to finite increments, in principle. Modifications arise from higher-order incremental approximation and elastoplastic transition.

It is worth noticing that both issues, higher-order approximation in the incremental step and transition, affect the direct nature of the tangential stiffness method and necessitate iteration. On the contrary, accommodation in the initial load technique is straightforward. A simple solution algorithm

for the elastoplastic increment in Scheme 5.3 is obtained with the assumption that the stress state at the end specifies the direction of plastic flow (radial return, Section 5.4.4).

Incremental solution
Scheme 5.4 demonstrates employment of the initial load technique stated previously in Scheme 5.2 for the rate problem. The algorithm refers to the radial return approximation associated with the initial stress approach. The scheme can be easily modified for the analogous initial strain procedure. Since the scheme is then based on the stress at the end of the increment, the computation of $\boldsymbol{\sigma}_{n+1}$ must be placed prior to that of $\bar{\eta}_\Delta$ by eqn (5.129). This necessitates a prediction for $\boldsymbol{\eta}_\Delta = \bar{\eta}_\Delta \mathbf{s}$ when entering each iteration cycle. The reader will realize that implementation of kinematic hardening as from Section 5.4.4 in the incremental Scheme 5.4 is straightforward. All instructions can be used without modification by changing the input to the appropriate quantities for kinematic hardening. This requires storage and incremental update of the translation vector $\boldsymbol{\alpha}$ of the yield surface. Incorporation of mixed isotropic–kinematic hardening is also simple.

In Scheme 5.4, the sequence of operations is listed from the programmer's point of view. The essential iteration concerns, however, the incremental plastic strain $\boldsymbol{\eta}_\Delta$ and its magnitude $\bar{\eta}_\Delta$, and convergence is tested with this quantity.

Input: $\mathbf{P}_\Delta, \boldsymbol{\sigma}_n$

Predictor $\mathbf{U}_\Delta$

Element loop : $q = nel$

Integration points

$$\boldsymbol{\sigma}^*_\Delta = \boldsymbol{\kappa}\boldsymbol{\gamma}_\Delta \Leftarrow \boldsymbol{\kappa}\boldsymbol{a}\mathbf{U}_{\Delta q}\,,\ \boldsymbol{\sigma}^*_{n+1} \Leftarrow \boldsymbol{\sigma}_n + \boldsymbol{\sigma}^*_\Delta$$

$$\bar{\eta}_\Delta \Leftarrow \frac{1}{h+3G}(\bar{\sigma}^*_{n+1} - \sigma_{\mathrm{f}n}) \geq 0$$

$$\boldsymbol{\eta}_\Delta \Leftarrow \bar{\eta}_\Delta \mathbf{s}^*_{n+1}\,, \quad \boldsymbol{\sigma}_{n+1} \Leftarrow \boldsymbol{\sigma}^*_{n+1} - \boldsymbol{\kappa}\boldsymbol{\eta}_\Delta$$

Initial load (element) $\mathbf{J}_{\Delta q} \Leftarrow -\int_{V_q} \boldsymbol{a}^{\mathrm{t}} \boldsymbol{\kappa} \boldsymbol{\eta}_\Delta \mathrm{d}V$

End integration

Initial load (system) $\mathbf{J}_\Delta \Leftarrow \mathbf{J}_\Delta + \mathbf{a}_q^{\mathrm{t}} \mathbf{J}_{\Delta q}$

End elements

Corrector $\mathbf{U}_\Delta \Leftarrow \mathbf{K}^{-1}[\mathbf{P}_\Delta - \mathbf{J}_\Delta]$

Scheme 5.4: Initial load algorithm for radial return.

5.5.2 Overview of algorithms

We arrive at a unified fashion of incremental algorithms by considering the solution of the vector equation

$$\mathbf{R}_\Delta(\mathbf{U}_\Delta) = \mathbf{P}_\Delta - \mathbf{S}_\Delta(\mathbf{U}_\Delta) = \mathbf{0}, \tag{5.152}$$

which is the residual form of eqn (5.151).

An iteration cycle for $\mathbf{U}_\Delta$ in eqn (5.152) starts with an estimate $\mathbf{U}_{\Delta i}$ for which, in general, $\mathbf{R}_\Delta(\mathbf{U}_{\Delta i}) \neq \mathbf{0}$, and supplies the next estimate $\mathbf{U}_{\Delta i+1}$ by solving the linearized equation:

$$\mathbf{R}_\Delta(\mathbf{U}_{\Delta i+1}) \cong \mathbf{R}_\Delta(\mathbf{U}_{\Delta i}) + \left[\frac{\mathrm{d}\mathbf{R}_\Delta}{\mathrm{d}\mathbf{U}_\Delta}\right]_i [\mathbf{U}_{\Delta i+1} - \mathbf{U}_{\Delta i}] = \mathbf{0}. \tag{5.153}$$

From the above equation,

$$\mathbf{U}_{\Delta i+1} = \mathbf{U}_{\Delta i} - \left[\frac{\mathrm{d}\mathbf{R}_\Delta}{\mathrm{d}\mathbf{U}_\Delta}\right]_i^{-1} \mathbf{R}_\Delta(\mathbf{U}_{\Delta i}), \tag{5.154}$$

which is known as the Newton–Raphson iteration technique for the solution of nonlinear equation systems. If the system is linear, the solution is obtained in a single cycle.

For the residual vector in eqn (5.152) the recursive scheme of eqn (5.154) assumes the form

$$\mathbf{U}_{\Delta i+1} = \mathbf{U}_{\Delta i} + \left[\frac{\mathrm{d}\mathbf{S}_\Delta}{\mathrm{d}\mathbf{U}_\Delta}\right]_i^{-1} [\mathbf{P}_\Delta - \mathbf{S}_\Delta(\mathbf{U}_{\Delta i})]. \tag{5.155}$$

With reference to the finite element formalism in Section 5.1, the stress resultants in eqn (5.155) are obtained from element contributions in $\mathbf{S}_{\Delta\mathrm{E}} = \{\mathbf{S}_{\Delta q}\}$ $(q = 1, \ldots, nel)$ by accumulation:

$$\mathbf{S}_\Delta = \mathbf{a}^{\mathrm{t}}\mathbf{S}_{\Delta\mathrm{E}} \quad \text{and} \quad \mathbf{S}_{\Delta q} = \int_{V_q} \boldsymbol{a}^{\mathrm{t}}\boldsymbol{\sigma}_\Delta \mathrm{d}V. \tag{5.156}$$

The derivative with respect to the displacement increment reads

$$\frac{\mathrm{d}\mathbf{S}_\Delta}{\mathrm{d}\mathbf{U}_\Delta} = \mathbf{a}^{\mathrm{t}}\frac{\mathrm{d}\mathbf{S}_{\Delta\mathrm{E}}}{\mathrm{d}\mathbf{U}_\Delta} = \mathbf{a}^{\mathrm{t}}\frac{\mathrm{d}\mathbf{S}_{\Delta\mathrm{E}}}{\mathrm{d}\mathbf{U}_{\Delta\mathrm{E}}}\mathbf{a}, \tag{5.157}$$

where

$$\mathbf{U}_{\Delta\mathrm{E}} = \mathbf{a}\mathbf{U}_\Delta, \quad \frac{\mathrm{d}\mathbf{U}_{\Delta\mathrm{E}}}{\mathrm{d}\mathbf{U}_\Delta} = \mathbf{a}.$$

The entry of individual elements in the gradient matrix in eqn (5.157) is given by

$$\frac{\mathrm{d}\mathbf{S}_{\Delta\mathrm{E}}}{\mathrm{d}\mathbf{U}_{\Delta\mathrm{E}}} = \left[\frac{\mathrm{d}\mathbf{S}_{\Delta q}}{\mathrm{d}\mathbf{U}_{\Delta q}}\right],$$

and in the diagonal hypermatrix

$$\frac{\mathrm{d}\mathbf{S}_{\Delta q}}{\mathrm{d}\mathbf{U}_{\Delta q}} = \int_{V_q} \boldsymbol{a}^{\mathrm{t}} \frac{\mathrm{d}\boldsymbol{\sigma}_\Delta}{\mathrm{d}\boldsymbol{\gamma}_\Delta} \boldsymbol{a} \mathrm{d}V. \tag{5.158}$$

From finite element kinematics,

$$\boldsymbol{\gamma}_\Delta = \boldsymbol{a}\mathbf{U}_{\Delta q}, \quad \frac{\mathrm{d}\boldsymbol{\gamma}_\Delta}{\mathrm{d}\mathbf{U}_{\Delta q}} = \boldsymbol{a}.$$

Application of the Newton–Raphson technique, eqn (5.155), ultimately requires the stress increment as a function of the incremental strain in eqn (5.156), which enters the residual and leads to the system gradient in eqn (5.157) via the element contributions of eqn (5.158). The system gradient exhibits the structure of the momentary elastoplastic stiffness matrix as in eqn (5.29), but is different. It results as a derivative from the incremental approximation of the elastoplastic problem (Section 5.4.2), and is determined at the state pertaining to the ith iteration cycle.

The stress increment can be written as

$$\boldsymbol{\sigma}_\Delta = \boldsymbol{\kappa}[\boldsymbol{\gamma}_\Delta - \boldsymbol{\eta}_\Delta] = \bar{\boldsymbol{\kappa}}_\zeta \boldsymbol{\gamma}_\Delta, \tag{5.159}$$

where, with eqns (5.75) and (5.77) for the plastic strain increment, the coefficient matrix is

$$\bar{\boldsymbol{\kappa}}_\zeta = \boldsymbol{\kappa}\left[\mathbf{I} - \frac{2G}{h_\zeta + 3G}\mathbf{s}_\zeta \mathbf{s}_\zeta^{\mathrm{t}}\right]. \tag{5.160}$$

Substitution in eqn (5.156) and tracing back the finite element hierarchy transfers the incremental constitutive description to the discretized system

$$\mathbf{S}_\Delta = \mathbf{K}\mathbf{U}_\Delta + \mathbf{J}_\Delta = \bar{\mathbf{K}}_\zeta \mathbf{U}_\Delta. \tag{5.161}$$

The relation between incremental stress $\boldsymbol{\sigma}_\Delta$ and incremental strain $\boldsymbol{\gamma}_\Delta$, eqn (5.159) in conjunction with eqn (5.160), resembles the elastoplastic relation between infinitesimal quantities in eqn (1.158); it is nonlinear as long as $\zeta > 0$. The matrix $\bar{\boldsymbol{\kappa}}_\zeta$ can be used as an approximation to $\mathrm{d}\boldsymbol{\sigma}_\Delta/\mathrm{d}\boldsymbol{\gamma}_\Delta$; employment of the associated system matrix $\bar{\mathbf{K}}_\zeta$ as an approximation to the gradient $\mathrm{d}\mathbf{S}_\Delta/\mathrm{d}\mathbf{U}_\Delta$ in eqn (5.155) gives

$$\mathbf{U}_{\Delta i+1} = \mathbf{U}_{\Delta i} + \bar{\mathbf{K}}_{\zeta i}^{-1}[\mathbf{P}_\Delta - \mathbf{S}_\Delta(\mathbf{U}_{\Delta i})]. \tag{5.162}$$

It can be seen, with the second expression for $\mathbf{S}_\Delta$ in eqn (5.161), that eqn (5.162) is equivalent to an iterative secant solution for the increment

$$\mathbf{U}_{\Delta i+1} = \bar{\mathbf{K}}_{\zeta i}^{-1}\mathbf{P}_\Delta, \tag{5.163}$$

which is homologous to the tangential stiffness technique, eqn (5.30).

Alternatively, if the recursive scheme of eqn (5.155) is operated with the stiffness matrix $\mathbf{K}$ of the elastic system as another approximation to the system gradient, we have

$$\mathbf{U}_{\Delta i+1} = \mathbf{U}_{\Delta i} + \mathbf{K}^{-1}[\mathbf{P}_\Delta - \mathbf{S}_\Delta(\mathbf{U}_{\Delta i})]. \tag{5.164}$$

This is, by the first expression for $\mathbf{S}_\Delta$ in eqn (5.161), equivalent to the initial load iteration

$$\mathbf{U}_{\Delta i+1} = \mathbf{K}^{-1}[\mathbf{P}_\Delta - \mathbf{J}_\Delta(\mathbf{U}_{\Delta i})]. \tag{5.165}$$

The dependence of the initial load vector $\mathbf{J}_\Delta$ on the incremental displacement $\mathbf{U}_\Delta$ is not explicit, but via the incremental plastic strain $\boldsymbol{\eta}_\Delta$, which may be computed by either the initial strain or the initial stress version.

It is worth noticing that both solution techniques, the initial load iteration, eqn (5.165), and the secant (or tangential) solution, eqn (5.163), can be developed from the incremental equation of equilibrium, eqn (5.151), in conjunction with the alternative expressions for the stress resultants in eqn (5.161). For a linear (explicit) approximation of the incremental plastic strain, the secant technique supplies the solution directly (with caution regarding the condition of plastic loading), while the initial load method requires iteration even in the linearized case.

5.5.3 Summary

Due to the nature of the elastoplastic stress–strain relations and the path dependence of plastic deformation, elastoplastic analysis requires a stepwise application of the loading when in the system the yield stress of the material is exceeded and plastic flow sets in. The incrementation of the process demands caution with regard to the stability of the numerical integration. The incremental solutions in the loading sequence may be performed either directly by the tangential stiffness approach or iteratively by the initial load technique. The former is based on a system matrix that varies while plasticity progresses; the latter solves repeatedly an elastic problem within each step with corrective loads accounting for the effect of plasticity, and poses the task of convergence. The initial strain and the initial stress mode of evaluation of the incremental plastic strain entering the corrective loads, one based on the stress and the second on the strain increment, exhibit different convergence behaviour.

Methods of elastoplastic analysis have been exemplified so far on the background of the finite element methodology. Implementation may be effected, in principle, as an extension of computer codes designed for the analysis of elastic systems. At this place, we would like to mention discretization methods other than finite elements. The reader may be interested in learning about the boundary element method [11] and its early application to plasticity [12], a subject whose scope is still extending. In addition, numerical approaches not making use of a mesh as required by the finite element

method are making steady progress [13]; see also [14] for a comprehensive survey. Each particular discretization technique necessitates an appropriate implementation of plasticity. However, this affects neither the numerical treatment at the material constitutive level nor the overall solution algorithms presented in this chapter.

References

[1] O.C. Zienkiewicz, R.L. Taylor and J.Z. Zhu, *The Finite Element Method: Its Basis and Fundamentals*, 6th edn, Elsevier, Amsterdam, 2005.

[2] J.H. Argyris, Elasto-plastic matrix displacement analysis of three-dimensional continua, *J. R. Aeron. Soc.* **69** (1965) 633–636.

[3] J.H. Argyris, D.W. Scharpf and J.B. Spooner, Die elastoplastische Berechnung von allgemeinen Tragwerken und Kontinua, *Ing. Archiv* **37** (1969) 326–352.

[4] O.C. Zienkiewicz, S. Valliapan and I.P. King, Elasto-plastic solutions of engineering problems – initial stress, finite element approach, *Int. J. Numer. Meth. Engng* **1** (1969) 75–100.

[5] I.St. Doltsinis and H.A. Balmer, Bemerkungen zur elastoplastischen Berechnung von Tragwerken, ISD-Report No. 169, University of Stuttgart 1974.

[6] J.H. Argyris and D.W. Scharpf, Methods of elastoplastic analysis, *Z. Angew. Math. Phys.* (*ZAMP*) **23** (1972) 517–551.

[7] J.H. Argyris and I.St. Doltsinis, On the integration of inelastic stress-strain relations – Part 1: Foundations of method, *Res Mech. Lett.* **1** (1981), 343–348; Part 2: Developments of method, *Res Mech. Lett.* **1** (1981), 349–355.

[8] M.L. Wilkins, Calculation of elastic–plastic flow, in *Methods of Computational Physics*, Vol. 3, B. Alter *et al.* (Eds), Academic Press, New York, 1964.

[9] H. Balmer, I.St. Doltsinis and M. König, Elastoplastic and creep analysis with the ASKA program system, *Comput. Meths Appl. Mech. Engng* **3** (1974) 87–104.

[10] M. Ortiz and J.C. Simo, An analysis of a new class of integration algorithms for elastoplastic constitutive relations, *Int. J. Numer. Meth. Engng* **23** (1986) 353–366.

[11] C.A. Brebbia, *The Boundary Element Method for Engineers*, Rentech Press, London/Halstead Press, New York, 1978.

[12] J.C.F. Telles, *The Boundary Element Method Applied to Inelastic Problems*, Lecture Notes in Engineering 1, Springer, Berlin Heidelberg, 1983.

[13] G.R. Liu and Y.T. Gu, *An Introduction to Meshfree Methods and Their Programming*, Springer, Dordrecht, 2005.

[14] S.Li and W.K. Lin, *Meshfree Particle Methods*, Springer, Berlin and Heidelberg, 2004.

CHAPTER 6

Extension of inelastic description

6.1 Influence of temperature

Thermoelasticity
Stress analysis under non-isothermal conditions (temporally or spatially) necessitates a description of the mechanical response of the material to temperature variations. In the elastic range, the appearance of thermal strains

$$\boldsymbol{\eta}_{\mathrm{T}} = \alpha(T - T_{\mathrm{o}})\mathbf{e} \tag{6.1}$$

is a major effect. Here, α denotes the coefficient of linear thermal expansion, T the actual absolute temperature, and T_{o} the reference temperature from which the thermal strain is measured. In an isotropic material thermal expansion (or contraction) is a volumetric effect, and therefore the vector $\boldsymbol{\eta}_{\mathrm{T}}$ is proportional to $\mathbf{e} = \{1\,1\,1\,0\,0\,0\}$, cf. Section 1.2.1.

Under the combined action of stress and change in temperature the measured strain $\boldsymbol{\gamma}$ is composed as

$$\boldsymbol{\gamma} = \boldsymbol{\varepsilon} + \boldsymbol{\eta}_{\mathrm{T}} = \boldsymbol{\kappa}^{-1}\boldsymbol{\sigma} + \alpha(T - T_{\mathrm{o}})\mathbf{e}, \tag{6.2}$$

where $\boldsymbol{\varepsilon}$ denotes the part associated with the stress $\boldsymbol{\sigma}$. The stress then reads

$$\boldsymbol{\sigma} = \boldsymbol{\kappa}[\boldsymbol{\gamma} - \boldsymbol{\eta}_{\mathrm{T}}] = \boldsymbol{\kappa}\boldsymbol{\gamma} - 3K\alpha(T - T_{\mathrm{o}})\mathbf{e} \tag{6.3}$$

and is zero at $\boldsymbol{\gamma} = \mathbf{0}$, $T = T_{\mathrm{o}}$ or if the thermal action is unconstrained. It should be noticed that both the elastic constants in the matrix $\boldsymbol{\kappa}$ and the coefficient α can be temperature-dependent quantities.

The significance of the thermoelastic stress–strain relations for the continuum is as follows. Using in eqn (6.3) the kinematic relation of eqn (2.59) for the strain $\boldsymbol{\gamma}$, and substituting in eqn (2.61) for the static equilibrium (Chapter 2), we obtain instead

$$\boldsymbol{\partial}^{\mathrm{t}}(\boldsymbol{\kappa}\boldsymbol{\partial}\mathbf{u}) + [\mathbf{f} - \boldsymbol{\partial}^{\mathrm{t}}(\boldsymbol{\kappa}\boldsymbol{\eta}_{\mathrm{T}})] = \mathbf{0} \tag{6.4}$$

as a differential equation for the displacements $\mathbf{u}$. Accordingly, thermal strains can be taken into account by a modification of the body forces in

the equilibrium condition, cf. eqn (2.65) for the isothermal case. Determination of the additional 'pseudo' body forces presumes knowledge of the distribution of the thermal strain or the temperature respectively, within the domain of the problem. The presence of the thermal strain in eqn (6.3) also modifies the expression of the static boundary condition, eqn (2.63), in terms of the displacements.

Regarding thermoelastic analysis by finite elements, we notice that the stress in eqn (5.20) now reads

$$\boldsymbol{\sigma} = \boldsymbol{\kappa}[\boldsymbol{a}\mathbf{U}_q - \boldsymbol{\eta}_{\mathrm{T}}] \tag{6.5}$$

and therefore the stress resultants in the element, eqn (5.21), are

$$\mathbf{S}_q = \mathbf{k}_q\mathbf{U}_q + \mathbf{J}_q(\boldsymbol{\eta}_{\mathrm{T}}), \quad \mathbf{J}_q(\boldsymbol{\eta}_{\mathrm{T}}) = -\int_{V_q} \boldsymbol{a}\boldsymbol{\kappa}\boldsymbol{\eta}_{\mathrm{T}}\mathrm{d}V. \tag{6.6}$$

The origin of the initial loads $\mathbf{J}_q$ in the finite element is here the thermal strain $\boldsymbol{\eta}_{\mathrm{T}}$.

Accordingly, on the level of the discretized system,

$$\mathbf{S} = \mathbf{K}\mathbf{U} + \mathbf{J}(\boldsymbol{\eta}_{\mathrm{T}}) = \mathbf{P} \quad \text{and} \quad \mathbf{U} = \mathbf{K}^{-1}[\mathbf{P} - \mathbf{J}(\boldsymbol{\eta}_{\mathrm{T}})] \tag{6.7}$$

in place of the isothermal eqn (5.26).

Non-isothermal elastoplasticity

Plastic flow adds to the non-elastic part of the strain such that the elastic stress–strain relation becomes

$$\boldsymbol{\sigma} = \boldsymbol{\kappa}[\boldsymbol{\gamma} - \boldsymbol{\eta}_{\mathrm{T}} - \boldsymbol{\eta}_{\mathrm{P}}]$$

and in differential form

$$\mathrm{d}\boldsymbol{\sigma} = \boldsymbol{\kappa}[\mathrm{d}\boldsymbol{\gamma} - \mathrm{d}\boldsymbol{\eta}_{\mathrm{T}} - \mathrm{d}\boldsymbol{\eta}_{\mathrm{P}}] + \mathrm{d}\boldsymbol{\kappa}[\boldsymbol{\gamma} - \boldsymbol{\eta}_{\mathrm{T}} - \boldsymbol{\eta}_{\mathrm{P}}]. \tag{6.8}$$

The subscript 'P' denotes the plastic contribution.

In the differential expression for the stress in eqn (6.8), the second term is a consequence of temperature dependent elastic parameters:

$$\boldsymbol{\kappa} = \boldsymbol{\kappa}(T) \quad \text{and} \quad \mathrm{d}\boldsymbol{\kappa} = \mathrm{d}T\boldsymbol{\kappa}'.$$

Therefore, expressing the strain in terms of the stress

$$\mathrm{d}\boldsymbol{\kappa}[\boldsymbol{\gamma} - \boldsymbol{\eta}_{\mathrm{T}} - \boldsymbol{\eta}_{\mathrm{P}}] = \mathrm{d}T\boldsymbol{\kappa}'\boldsymbol{\kappa}^{-1}\boldsymbol{\sigma}. \tag{6.9}$$

In the first part of eqn (6.8), the variation in thermal strain is obtained from eqn (6.1) as

$$\mathrm{d}\boldsymbol{\eta}_{\mathrm{T}} = \beta\mathrm{d}T\mathbf{e} \quad \text{with} \quad \beta = \alpha + \alpha'(T - T_{\mathrm{o}}) \tag{6.10}$$

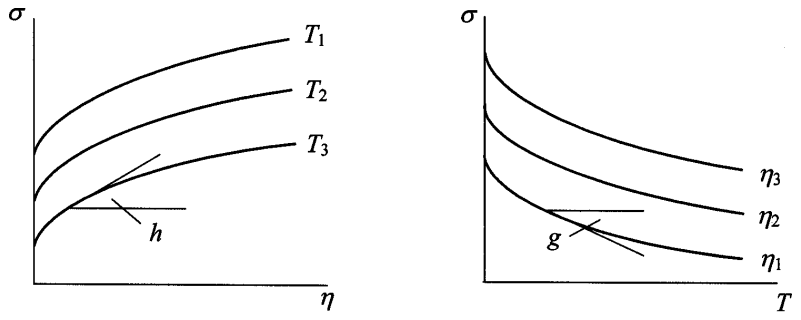

Figure 6.1: Temperature dependence of the yield stress.

and is determined by the temperature variation $\mathrm{d}T$ with the differential coefficient of thermal expansion β. Combining eqns (6.10) and (6.9) in the differential stress–strain relation, eqn (6.8), we obtain instead

$$\mathrm{d}\boldsymbol{\sigma} = \boldsymbol{\kappa}[\mathrm{d}\boldsymbol{\gamma} - \mathrm{d}\boldsymbol{\eta}^*_{\mathrm{T}} - \mathrm{d}\boldsymbol{\eta}_{\mathrm{P}}], \tag{6.11}$$

where the quantity

$$\mathrm{d}\boldsymbol{\eta}^*_{\mathrm{T}} = [\beta\mathbf{e} - \boldsymbol{\kappa}^{-1}\boldsymbol{\kappa}'\boldsymbol{\kappa}^{-1}\boldsymbol{\sigma}]\mathrm{d}T = \boldsymbol{\beta}^*\mathrm{d}T \tag{6.12}$$

summarizes the effect of temperature variations on the elastic response.

In plasticity, variations of temperature modify the yield stress of the material such that σ_{f} diminishes if the temperature is elevated (Fig. 6.1). Formally, the yield stress depends on plastic strain and temperature

$$\sigma_{\mathrm{f}} = \sigma_{\mathrm{f}}(\bar{\eta}_{\mathrm{P}}, T), \quad \mathrm{d}\sigma_{\mathrm{f}} = h\mathrm{d}\bar{\eta}_{\mathrm{P}} + g\mathrm{d}T. \tag{6.13}$$

The coefficients in the differential expression are

$$h = \partial\sigma_{\mathrm{f}}/\partial\bar{\eta}_{\mathrm{P}} > 0 \quad \text{and} \quad g = \partial\sigma_{\mathrm{f}}/\partial T < 0.$$

For isotropic hardening refer to Section 1.3.1. Employing eqn (6.13) in the consistency condition of plasticity ($\mathrm{d}\phi = \mathrm{d}\bar{\sigma} - \mathrm{d}\sigma_{\mathrm{f}} = 0$), the equivalent plastic strain increment follows as

$$\mathrm{d}\bar{\eta}_{\mathrm{P}} = \frac{1}{h}(\mathrm{d}\bar{\sigma} - g\mathrm{d}T) = \frac{1}{h}(\mathbf{s}^{\mathrm{t}}\mathrm{d}\boldsymbol{\sigma} - g\mathrm{d}T) \geq 0. \tag{6.14}$$

Since the coefficient g is a negative quantity, elevation of the temperature, $\mathrm{d}T > 0$, enhances the magnitude of plastic flow. For the same reason, the plastic loading condition $\mathrm{d}\bar{\eta}_{\mathrm{P}} > 0$ can be satisfied even if $\mathrm{d}\bar{\sigma} = \mathbf{s}^{\mathrm{t}}\mathrm{d}\boldsymbol{\sigma} < 0$.

Using eqn (6.14) for the plastic strain increment $\mathrm{d}\boldsymbol{\eta}_{\mathrm{P}} = \mathrm{d}\bar{\eta}_{\mathrm{P}}\mathbf{s}$ in eqn (6.11), we obtain the strain increment in terms of the incremental stress and temperature:

$$\mathrm{d}\boldsymbol{\gamma} = \boldsymbol{\kappa}^{-1}\mathrm{d}\boldsymbol{\sigma} + \mathrm{d}\boldsymbol{\eta}^*_{\mathrm{T}} + \mathrm{d}\boldsymbol{\eta}_{\mathrm{P}} = \left[\mathbf{I} + \frac{2G}{h}\mathbf{s}\mathbf{s}^{\mathrm{t}}\right]\boldsymbol{\kappa}^{-1}\mathrm{d}\boldsymbol{\sigma} + \left[\boldsymbol{\beta}^* - \frac{g}{h}\mathbf{s}\right]\mathrm{d}T. \tag{6.15}$$

The stress increment can be deduced from eqn (6.15) by inversion, but instead we derive first an alternative expression for the magnitude of the incremental plastic strain in terms of the strain increment, along the lines of Section 1.3.1. To this end, substituting eqn (6.11) for $\mathrm{d}\boldsymbol{\sigma}$ in eqn (6.14) and solving for $\mathrm{d}\bar{\eta}_\mathrm{P}$ we obtain

$$\begin{aligned}\mathrm{d}\bar{\eta}_\mathrm{P} &= \frac{2G}{h+3G}\mathbf{s}^\mathrm{t}[\mathrm{d}\boldsymbol{\gamma} - \mathrm{d}\boldsymbol{\eta}^*_\mathrm{T}] - \frac{g}{h+3G}\mathrm{d}T \\ &= \frac{2G}{h+3G}\left(\mathbf{s}^\mathrm{t}\mathrm{d}\boldsymbol{\gamma} + \frac{\bar{\sigma}G'/G - g}{2G}\mathrm{d}T\right) \geq 0. \end{aligned} \tag{6.16}$$

For the transition to the second expression, note with eqn (6.12) that

$$\mathbf{s}^\mathrm{t}\mathrm{d}\boldsymbol{\eta}^*_\mathrm{T} = \mathbf{s}^\mathrm{t}[\beta\mathbf{e} - \boldsymbol{\kappa}^{-1}\boldsymbol{\kappa}'\boldsymbol{\kappa}^{-1}\boldsymbol{\sigma}]\mathrm{d}T = -\frac{\bar{\sigma}}{2G}\frac{G'}{G}\mathrm{d}T. \tag{6.17}$$

In fact, since $\mathbf{s}$ is deviatoric we have: $\mathbf{s}^\mathrm{t}\mathbf{e} = 0$, $\mathbf{s}^\mathrm{t}\boldsymbol{\kappa}^{-1} = \mathbf{s}^\mathrm{t}/2G$, $\mathbf{s}^\mathrm{t}\boldsymbol{\kappa}' = 2G'\mathbf{s}^\mathrm{t}$, and $\mathbf{s}^\mathrm{t}\boldsymbol{\sigma} = \bar{\sigma}$.

Building in the stress–strain relation the incremental plastic strain $\mathrm{d}\boldsymbol{\eta}_\mathrm{P} = \mathrm{d}\bar{\eta}_\mathrm{P}\mathbf{s}$ with eqn (6.16), and with eqn (6.12) for the thermoelastic contribution, we arrive at the relation

$$\mathrm{d}\boldsymbol{\sigma} = \left[\mathbf{I} - \frac{2G}{h+3G}\mathbf{s}\mathbf{s}^\mathrm{t}\right]\boldsymbol{\kappa}\mathrm{d}\boldsymbol{\gamma} - \boldsymbol{\kappa}\left[\boldsymbol{\beta}^* + \frac{\bar{\sigma}G'/G - g}{h+3G}\mathbf{s}\right]\mathrm{d}T. \tag{6.18}$$

This determines the variation in stress for a specified variation in strain and temperature in the presence of plastic flow. Also, $\bar{\sigma} = \sigma_\mathrm{f}$ by the yield condition.

For kinematic hardening (Section 1.3.2) the consistency condition during plastic flow reads

$$\mathrm{d}\phi_\mathrm{K} = \mathbf{s}^\mathrm{t}_\mathrm{K}[\mathrm{d}\boldsymbol{\sigma} - \mathrm{d}\boldsymbol{\alpha}] - \mathrm{d}\sigma_\mathrm{s} = 0. \tag{6.19}$$

It is stated here that temperature variations should not affect the position $\boldsymbol{\alpha}$ of the yield surface, and therefore $\mathrm{d}\boldsymbol{\alpha} = (2/3)h\mathrm{d}\boldsymbol{\eta}_\mathrm{P}$, $\mathbf{s}^\mathrm{t}_\mathrm{K}\mathrm{d}\boldsymbol{\alpha} = \mathrm{d}\bar{\alpha} = h\mathrm{d}\bar{\eta}$ as in the isothermal case. The effect of temperature on the extent of the yield surface is accounted for by the quantity σ_s, which now follows the temperature dependence of the yield stress σ_f: $\mathrm{d}\sigma_\mathrm{s} = g\mathrm{d}T$. Then, from eqn (6.19),

$$\mathrm{d}\bar{\eta}_\mathrm{P} = \frac{1}{h}(\mathbf{s}^\mathrm{t}_\mathrm{K}\mathrm{d}\boldsymbol{\sigma} - g\mathrm{d}T) \geq 0. \tag{6.20}$$

The expression in eqn (6.20) is homologous to eqn (6.14) associated with isotropic hardening except for the vector $\mathbf{s}_\mathrm{K}$ in place of $\mathbf{s}$, which also specifies the direction of plastic flow for kinematic hardening: $\mathrm{d}\boldsymbol{\eta}_\mathrm{P} = \mathrm{d}\bar{\eta}_\mathrm{P}\mathbf{s}_\mathrm{K}$.

It is seen that the kinematic hardening model does not formally modify the plastic and elastoplastic stress–strain relations developed for isotropic hardening. Because of the appearance of $\mathbf{s}_\mathrm{K}$ in place of $\mathbf{s}$, we also have

to replace $\bar{\sigma} = \mathbf{s}^{\mathrm{t}}\boldsymbol{\sigma}$ by $\mathbf{s}_{\mathrm{K}}^{\mathrm{t}}\boldsymbol{\sigma}$ in eqns (6.16) and (6.18). Finally, the effect of temperature on the position of the yield surface – excluded above – can be introduced within the framework of the mixed kinematic–isotropic hardening model, described by the yield condition of eqn (1.170). With the mixed model the influence of temperature on $\sigma_{\mathrm{f}}(\bar{\eta}, T)$ can be partitioned between the location $\boldsymbol{\alpha}$ and the extent $\sigma_{\mathrm{is}}(\bar{\eta}, T)$ of the yield surface, similar to the effect of the plastic strain in the isothermal case, cf. eqns (1.171) and (1.172). Thereby, the essential formalism for the incremental stress–strain relations is not affected.

The statement of the momentary elastoplastic problem for the solid under non-isothermal conditions follows the lines of the isothermal case in Section 2.2.2. First, eqn (6.18) is presented as a relation between time rates,

$$\dot{\boldsymbol{\sigma}} = \bar{\boldsymbol{\kappa}}\dot{\boldsymbol{\gamma}} - \bar{\boldsymbol{\beta}}\dot{T} = \bar{\boldsymbol{\kappa}}\boldsymbol{\partial}\dot{\mathbf{u}} - \bar{\boldsymbol{\beta}}\dot{T}, \tag{6.21}$$

where the expressions symbolized by $\bar{\boldsymbol{\kappa}}$ and $\bar{\boldsymbol{\beta}}$ can be easily identified. We notice the mechanical (deformation) and the thermal (temperature) part of the relation. Second, substituting in the rate equilibrium condition for the stress, eqn (2.68), we obtain the differential equation for the velocity field $\dot{\mathbf{u}}(\mathbf{x})$:

$$\boldsymbol{\partial}^{\mathrm{t}}(\bar{\boldsymbol{\kappa}}\boldsymbol{\partial}\dot{\mathbf{u}}) + \left[\dot{\mathbf{f}} - \boldsymbol{\partial}^{\mathrm{t}}(\bar{\boldsymbol{\beta}}\dot{T})\right] = \mathbf{0}. \tag{6.22}$$

Comparison with the isothermal counterpart, eqn (2.73), based on the elastoplastic material stiffness reveals that the action of a prescribed temperature rate can be simply accounted for by a modification of the body forces $\dot{\mathbf{f}}$.

Alternatively, an implicit form analogous to eqn (2.70) based on the elastic material stiffness is obtained with the stress–strain relation of eqn (6.11). The plastic strain rate $\dot{\boldsymbol{\eta}}_{\mathrm{P}} = \dot{\bar{\eta}}_{\mathrm{P}}\mathbf{s}$ from either eqn (6.14) or eqn (6.16) exhibits one part emanating from the mechanical action and another part induced by the thermal action. The mechanical part is subjected to the iteration procedure defined in eqn (2.71) while the thermal part contributes along with the thermoelastic rate effects to the modification of the body force $\dot{\mathbf{f}}$. Summarizing, instead of eqn (6.21) we have for the stress rate the relation

$$\dot{\boldsymbol{\sigma}} = \boldsymbol{\kappa}[\dot{\boldsymbol{\gamma}} - \dot{\boldsymbol{\eta}}_{\mathrm{P}}|_{\mathrm{T}}] - \bar{\boldsymbol{\beta}}\dot{T},$$

where $\dot{\boldsymbol{\eta}}_{\mathrm{P}}|_{\mathrm{T}}$ denotes the part of the plastic strain rate associated with the mechanical actions at constant temperature. This modifies the condition of static equilibrium in eqn (6.22) to

$$\boldsymbol{\partial}^{\mathrm{t}}(\boldsymbol{\kappa}\boldsymbol{\partial}\dot{\mathbf{u}}) + [\dot{\mathbf{f}} - \boldsymbol{\partial}^{\mathrm{t}}(\bar{\boldsymbol{\beta}}\dot{T}) - \boldsymbol{\partial}^{\mathrm{t}}(\boldsymbol{\kappa}\,\dot{\boldsymbol{\eta}}_{\mathrm{P}}|_{\mathrm{T}})] = \mathbf{0},$$

with the elastic material stiffness $\boldsymbol{\kappa}$ in place of the elastoplastic $\bar{\boldsymbol{\kappa}}$.

Incremental computation
The isothermal case has been treated in Section 5.5. Equilibrium of the finite element system at loading stage $\mathbf{P}_{n+1}$ requires

$$\mathbf{P}_{n+1} = \mathbf{S}_{n+1} \qquad \text{with} \quad \mathbf{S}_{n+1} = \int_V \boldsymbol{a}^{\mathrm{t}} \boldsymbol{\sigma}_{n+1} \mathrm{d}V. \tag{6.23}$$

The resultants $\mathbf{S}_{n+1}$ of the internal stresses $\boldsymbol{\sigma}_{n+1}$ are actually formed by accumulation of element contributions at the mesh nodal points (Section 5.1).

Under non-isothermal conditions the stress reads

$$\begin{aligned} \boldsymbol{\sigma}_{n+1} &= \boldsymbol{\kappa}_{n+1}[\boldsymbol{\gamma}_{n+1} - \boldsymbol{\eta}_{\mathrm{P}n+1} - \boldsymbol{\eta}_{\mathrm{T}n+1}] \\ &= \boldsymbol{\kappa}_{n+1}[\boldsymbol{\gamma}_n - \boldsymbol{\eta}_{Pn} - \boldsymbol{\eta}_{\mathrm{T}n+1}] + \boldsymbol{\kappa}_{n+1}[\boldsymbol{\gamma}_\Delta - \boldsymbol{\eta}_{\mathrm{P}\Delta}]. \end{aligned} \tag{6.24}$$

The local temperature T_{n+1} determines the actual elastic material stiffness and the thermal strain:

$$\boldsymbol{\kappa}_{n+1} = \boldsymbol{\kappa}(T_{n+1}), \qquad \boldsymbol{\eta}_{\mathrm{T}n+1} = \alpha(T_{n+1})(T_{n+1} - T_{\mathrm{o}})\mathbf{e}.$$

In eqn (6.24), the quantities $\boldsymbol{\gamma}_n$ and $\boldsymbol{\eta}_{\mathrm{P}n}$ are known from past analysis, the difference $[\boldsymbol{\gamma}_n - \boldsymbol{\eta}_{\mathrm{P}n}]$ can be stored. The quantities to compute are the strain increment $\boldsymbol{\gamma}_\Delta$ and the incremental plastic strain $\boldsymbol{\eta}_{\mathrm{P}\Delta}$; the latter necessitates in fact the incrementation. Note that a temperature dependence of the thermoelastic properties of the material does not favour representation of the stress as $\boldsymbol{\sigma}_{n+1} = \boldsymbol{\sigma}_n + \boldsymbol{\sigma}_\Delta$, since the expression for $\boldsymbol{\sigma}_\Delta$ appears inconvenient, cf. eqn (6.8).

With eqn (6.24), the stress resultants in eqn (6.23) become

$$\mathbf{S}_{n+1} = \mathbf{J}_0 + \mathbf{K}_{n+1}\mathbf{U}_\Delta + \mathbf{J}_\Delta(\boldsymbol{\eta}_{\mathrm{P}\Delta}), \tag{6.25}$$

where $\mathbf{K}_{n+1}$ denotes the stiffness matrix of the elastic system for the thermal state at the end of the increment and $\mathbf{J}_\Delta$ the initial loads accounting for the incremental plastic strain. Past effects and thermal strain are considered by the vector

$$\mathbf{J}_0 = \int_V \boldsymbol{a}^{\mathrm{t}} \boldsymbol{\kappa}_{n+1}[\boldsymbol{\gamma}_n - \boldsymbol{\eta}_{\mathrm{P}n} - \boldsymbol{\eta}_{\mathrm{T}n+1}]\mathrm{d}V, \tag{6.26}$$

assembled from element contributions. For its interpretation, it is worth noticing the case of temperature-insensitive elastic properties, where

$$\begin{aligned} \mathbf{J}_0 &= \int_V \boldsymbol{a}^{\mathrm{t}} \boldsymbol{\kappa}[\boldsymbol{\gamma}_n - \boldsymbol{\eta}_{\mathrm{P}n} - \boldsymbol{\eta}_{\mathrm{T}n}]\mathrm{d}V + \int_V \boldsymbol{a}^{\mathrm{t}} \boldsymbol{\kappa} \boldsymbol{\eta}_{\mathrm{T}\Delta} \mathrm{d}V \\ &= \mathbf{S}_n + \mathbf{J}_\Delta(\boldsymbol{\eta}_{\mathrm{T}\Delta}). \end{aligned} \tag{6.27}$$

Utilizing eqn (6.25) for the stress resultants in the equilibrium condition of eqn (6.23), and solving for the incremental displacement:

$$\mathbf{U}_\Delta = \mathbf{K}_{n+1}^{-1}[\mathbf{P}_{n+1} - \mathbf{J}_0 - \mathbf{J}_\Delta(\boldsymbol{\eta}_{\mathrm{P}\Delta})] = \mathbf{K}_{n+1}^{-1}[\mathbf{P}_\Delta^* - \mathbf{J}_\Delta(\boldsymbol{\eta}_{\mathrm{P}\Delta})]. \tag{6.28}$$

As the plastic strain increment $\boldsymbol{\eta}_{\mathrm{P}\Delta}$ depends on $\mathbf{U}_\Delta$, eqn (6.28) suggests an iterative algorithm for the solution of the incremental problem.

The load vector $\mathbf{P}_\Delta^*$ introduced in eqn (6.28) is defined as

$$\mathbf{P}_\Delta^* = \mathbf{P}_{n+1} - \mathbf{J}_0 = [\mathbf{P}_{n+1} - \mathbf{S}_n] - \mathbf{J}_\Delta(\boldsymbol{\eta}_{\mathrm{T}\Delta}) = \mathbf{P}_\Delta - \mathbf{J}_\Delta(\boldsymbol{\eta}_{\mathrm{T}\Delta}). \tag{6.29}$$

The second expression refers to temperature-insensitive elastic properties, eqn (6.27), in the last expression $\mathbf{P}_\Delta = \mathbf{P}_{n+1} - \mathbf{S}_n$ comprises numerical residuals $\mathbf{P}_n - \mathbf{S}_n$ not equilibrated at stage n. Then, eqn (6.28) reduces to

$$\mathbf{U}_\Delta = \mathbf{K}^{-1}[\mathbf{P}_\Delta - \mathbf{J}_\Delta(\boldsymbol{\eta}_{\mathrm{T}\Delta}) - \mathbf{J}_\Delta(\boldsymbol{\eta}_{\mathrm{P}\Delta})]. \tag{6.30}$$

This is the incremental version of the thermoelastic finite element solution, eqn (6.7); except for the plastic contribution, or – equally – the isothermal elastoplastic initial load form, eqn (5.165), except for the thermal contribution.

Incrementation of the plastic strain considers satisfaction of the yield condition. For isotropic hardening in the non-isothermal case

$$\phi_{n+1} = \bar{\sigma}_{n+1} - \sigma_{\mathrm{f}}(\bar{\eta}_{n+1}, T_{n+1}) \leq 0. \tag{6.31}$$

The temperature T_{n+1} is a given quantity, and therefore we write

$$\sigma_{\mathrm{f}}(\bar{\eta}_{n+1}, T_{n+1}) = \sigma_{\mathrm{f}}(\bar{\eta}_n, T_{n+1}) + h\bar{\eta}_\Delta, \tag{6.32}$$

which means that transition from temperature T_n to T_{n+1} is performed beforehand (cf. Fig. 6.2). Then from eqn (6.31) we obtain for the equivalent plastic strain increment the familiar initial strain form

$$\bar{\eta}_{\mathrm{P}\Delta} = \frac{1}{h}[\bar{\sigma}_{n+1} - \sigma_{\mathrm{f}}(\bar{\eta}_{\mathrm{P}n}, T_{n+1})] \leq 0 \tag{6.33}$$

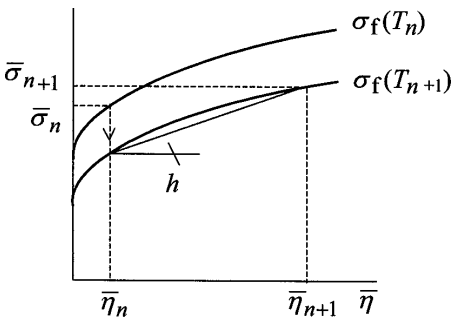

Figure 6.2: Scheme for non-isothermal transition.

in terms of actual stress, which specifies the incremental plastic strain $\boldsymbol{\eta}_\Delta = \bar{\eta}_{\mathrm{P}\Delta}\mathbf{s}_\zeta$ in conjunction with the selected flow direction $\mathbf{s}_\zeta$.

For an alternative expression of the incremental plastic strain in terms of overall strain we separate the stress in eqn (6.24) as in Section 5.4.4

$$\begin{aligned}\boldsymbol{\sigma}_{n+1} &= \boldsymbol{\kappa}_{n+1}[\boldsymbol{\gamma}_{n+1} - \boldsymbol{\eta}_{\mathrm{T}n+1} - \boldsymbol{\eta}_{\mathrm{P}n}] - \boldsymbol{\kappa}_{n+1}\boldsymbol{\eta}_{\mathrm{P}\Delta} \\ &= \boldsymbol{\sigma}^*_{n+1} - 2G_{n+1}\boldsymbol{\eta}_{\mathrm{P}\Delta}. \end{aligned} \tag{6.34}$$

This is similar to eqn (5.118), but the fictitious stress quantity is defined here as

$$\boldsymbol{\sigma}^*_{n+1} = \boldsymbol{\kappa}_{n+1}[\boldsymbol{\gamma}_{n+1} - \boldsymbol{\eta}_{\mathrm{T}n+1} - \boldsymbol{\eta}_{\mathrm{P}n}], \tag{6.35}$$

and for temperature-insensitive elastic properties:

$$\boldsymbol{\sigma}^*_{n+1} = \boldsymbol{\sigma}_n + \boldsymbol{\kappa}[\boldsymbol{\gamma}_\Delta - \boldsymbol{\eta}_{\mathrm{T}\Delta}].$$

The deviatoric part of $\boldsymbol{\sigma}^*_{n+1}$ reads

$$\boldsymbol{\sigma}^*_{\mathrm{D}n+1} = 2G_{n+1}[\boldsymbol{\gamma}_{\mathrm{D}n+1} - \boldsymbol{\eta}_{\mathrm{P}n}] = \boldsymbol{\sigma}_{\mathrm{D}n+1} + 2G_{n+1}\boldsymbol{\eta}_{\mathrm{P}\Delta} \tag{6.36}$$

as in eqn (5.121), and for the radial return technique where $\boldsymbol{\eta}_{\mathrm{P}\Delta} = \bar{\eta}_{\mathrm{P}\Delta}\mathbf{s}_{n+1} = \bar{\eta}_{\mathrm{P}\Delta}(3/2\bar{\sigma})\boldsymbol{\sigma}_{\mathrm{D}n+1}$, it is proportional to $\boldsymbol{\sigma}_{\mathrm{D}n+1}$; therefore, $\mathbf{s}_{n+1} = \mathbf{s}^*_{n+1}$. The volumetric thermal strain does not contribute to the deviatoric quantities.

With the above, the equivalent stress in the yield condition in eqn (6.31) can be presented as in eqn (5.124) except for the definition of $\boldsymbol{\sigma}^*_{n+1}$ by eqn (6.35). Using also eqn (6.32) for the uniaxial yield stress, we obtain from $\phi_{n+1} = 0$ the magnitude of the incremental plastic strain

$$\bar{\eta}_{\mathrm{P}\Delta} = \frac{1}{h + 3G_{n+1}}[\bar{\sigma}^*_{n+1} - \sigma_{\mathrm{f}}(\bar{\eta}_{\mathrm{P}n}, T_{n+1})] \geq 0. \tag{6.37}$$

This is formally the same as the isothermal initial stress form eqn (5.128), but implies temperature update of the yield stress σ_{f} and of the elastic shear modulus. The scalar quantity $\bar{\sigma}^*_{n+1}$ is obtained as an equivalent stress with the fictitious stress $\boldsymbol{\sigma}^*_{n+1}$ from eqn (6.35). In this connection, volumetric thermal strains can be discarded since they do not affect deviatoric quantities; equally for the flow direction $\mathbf{s}^*_{n+1} = (3/2\bar{\sigma}^*_{n+1})\boldsymbol{\sigma}^*_{\mathrm{D}n+1}$ in the relation $\boldsymbol{\eta}_{\mathrm{P}\Delta} = \bar{\eta}_{\mathrm{P}\Delta}\mathbf{s}^*_{n+1}$ for the incremental plastic strain.

This completes the formalism for the initial load method and an iterative solution by the successive approximation of eqn (6.28). A Newton-like procedure as in Section 5.5.2 may be applied to the residual form of the equilibrium condition in eqn (6.23)

$$\mathbf{P}_{n+1} - \mathbf{S}_{n+1}(\mathbf{U}_\Delta) = \mathbf{0}. \tag{6.38}$$

In analogy to eqn (5.155) the recursive scheme for $\mathbf{U}_\Delta$ is written as

$$\mathbf{U}_{\Delta i+1} = \mathbf{U}_{\Delta i} + \left[\frac{\mathrm{d}\mathbf{S}_{n+1}}{\mathrm{d}\mathbf{U}_\Delta}\right]_i^{-1} \left[\mathbf{P}_{n+1} - \mathbf{S}_{n+1}(\mathbf{U}_{\Delta i})\right]. \tag{6.39}$$

With reference to the definition of the stress resultants in eqn (6.23), the system gradient matrix is symbolically given by

$$\frac{\mathrm{d}\mathbf{S}_{n+1}}{\mathrm{d}\mathbf{U}_\Delta} = \int_V \boldsymbol{a}^{\mathrm{t}} \frac{\mathrm{d}\boldsymbol{\sigma}_{n+1}}{\mathrm{d}\boldsymbol{\gamma}_\Delta} \boldsymbol{a} \mathrm{d}V. \tag{6.40}$$

The actual formation of the gradient matrix follows the operations in eqn (5.157) with the elemental contributions of eqn (5.158), which here rely on the differential quotient $\mathrm{d}\boldsymbol{\sigma}_{n+1}/\mathrm{d}\boldsymbol{\gamma}_\Delta$ in the element. From eqn (6.24) for the stress $\boldsymbol{\sigma}_{n+1}$, we deduce

$$\frac{\mathrm{d}\boldsymbol{\sigma}_{n+1}}{\mathrm{d}\boldsymbol{\gamma}_\Delta} = \boldsymbol{\kappa}_{n+1} \left[\mathbf{I} - \frac{\mathrm{d}\boldsymbol{\eta}_{\mathrm{P}\Delta}}{\mathrm{d}\boldsymbol{\gamma}_\Delta}\right] \cong \bar{\boldsymbol{\kappa}}_{n+1,\zeta}. \tag{6.41}$$

Here, the matrix

$$\bar{\boldsymbol{\kappa}}_{n+1,\zeta} = \boldsymbol{\kappa}_{n+1} \left[\mathbf{I} - \frac{2G_{n+1}}{h_\zeta + 3G_{n+1}} \mathbf{s}_\zeta \mathbf{s}_\zeta^{\mathrm{t}}\right] \tag{6.42}$$

can be computed as an elastoplastic material stiffness, cf. eqn (6.18), at temperature T_{n+1} and position $0 \le \zeta \le 1$ within the step. The expression in eqn (6.42) is obtained as an approximation of the differential quotient in eqn (6.41) using eqn (6.16) in $\boldsymbol{\eta}_{\mathrm{P}\Delta} = \bar{\eta}_{\mathrm{P}\Delta}\mathbf{s}_\zeta$ for the plastic strain increment. If, on the other hand, the variation of $\boldsymbol{\eta}_{\mathrm{P}\Delta}$ with $\boldsymbol{\gamma}_\Delta$ is neglected in eqn (6.41) the elastic material stiffness $\boldsymbol{\kappa}_{n+1}$ can be used as an alternative approximation to the differential quotient. In each case, the iteration scheme of eqn (6.39) is operated with

$$\frac{\mathrm{d}\mathbf{S}_{n+1}}{\mathrm{d}\mathbf{U}_\Delta} \Leftarrow \bar{\mathbf{K}}_{n+1,\zeta} \qquad \text{or} \qquad \frac{\mathrm{d}\mathbf{S}_{n+1}}{\mathrm{d}\mathbf{U}_\Delta} \Leftarrow \mathbf{K}_{n+1} \tag{6.43}$$

in place of the system gradient. The matrices $\bar{\mathbf{K}}_{n+1,\zeta}$ and $\mathbf{K}_{n+1}$ are the global counterparts of the local approximations: the elastoplastic $\bar{\boldsymbol{\kappa}}_{n+1,\zeta}$ and the elastic $\boldsymbol{\kappa}_{n+1}$, respectively. Employment in eqn (6.39) of the elastic stiffness matrix $\mathbf{K}_{n+1}$ of the system is equivalent to the initial load technique, eqn (6.28).

Kinematic hardening

A description of incremental plastic flow in conjunction with the kinematic hardening model has been developed in Section 5.4.4 for isothermal conditions. The extension to the non-isothermal case assumes that variation of temperature modifies the size of the yield surface but not its position. This is

accounted for by an elastic limit $\sigma_{\rm s}(T)$ reproducing the temperature dependence of the uniaxial yield stress $\sigma_{\rm f}(\bar\eta, T)$ at constant plastic deformation (Fig. 6.2). For the incremental transition $n, n+1$,

$$\sigma_{\rm s}(T_{n+1}) - \sigma_s(T_n) = \sigma_{\rm f}(\bar\eta_n, T_{n+1}) - \sigma_{\rm f}(\bar\eta_n, T_n). \tag{6.44}$$

Variation of position $\boldsymbol{\alpha}$ is exclusively due to plastic deformation,

$$\bar\alpha_\Delta = h\bar\eta_\Delta = \sigma_{\rm f}(\bar\eta_{n+1}, T_{n+1}) - \sigma_{\rm f}(\bar\eta_n, T_{n+1}). \tag{6.45}$$

With the above definitions, the magnitude of the incremental plastic strain, eqn (5.137), changes in the non-isothermal case to

$$\bar\eta_\Delta = \frac{1}{h}[\bar\sigma'_{{\rm K}n+1} - \sigma_{\rm s}(T_{n+1})] \geq 0. \tag{6.46}$$

It relies on the stress $\boldsymbol{\sigma}_{n+1}$ which determines the vector $\boldsymbol{\sigma}'_{{\rm K}n+1} = \boldsymbol{\sigma}_{n+1} - \boldsymbol{\alpha}_n$, eqn (5.133), and the direction of incremental flow taken as $\mathbf{s}_{{\rm K}n+1} = \mathbf{s}'_{{\rm K}n+1}$.

Similarly, for the radial return algorithm, the non-isothermal expression of the initial stress form, eqn (5.142), can be written as

$$\bar\eta_\Delta = \frac{1}{h + 3G_{n+1}}[\bar\sigma^{*\prime}_{{\rm K}n+1} - \sigma_{\rm s}(T_{n+1})] \geq 0. \tag{6.47}$$

It is based on the fictitious kinematic stress

$$\boldsymbol{\sigma}^{*\prime}_{{\rm K}n+1} = \boldsymbol{\kappa}_{n+1}[\boldsymbol{\gamma}_{n+1} - \boldsymbol{\eta}_{{\rm T}n+1} - \boldsymbol{\eta}_{{\rm P}n}] - \boldsymbol{\alpha}_n = \boldsymbol{\sigma}^*_{n+1} - \boldsymbol{\alpha}_n, \tag{6.48}$$

defined as the isothermal one, eqn (5.140), but with $\boldsymbol{\sigma}^*_{n+1}$ from eqn (6.35) for non-isothermal conditions. The stress vector of eqn (6.48) specifies the direction of the increment $\boldsymbol{\eta}_\Delta = \bar\eta_\Delta \mathbf{s}^{*\prime}_{{\rm K}n+1}$ for the radial return to the yield surface.

Introduction of the above quantities allows the treatment of kinematic hardening by the initial load technique either as in the successive approximation by eqn (6.28) or in the Newton-like fashion, eqn (6.39), with the elastic stiffness $\mathbf{K}_{n+1}$ of the discretized system as an iteration matrix. A closer approximation to the gradient matrix of the system is obtained along the lines indicated for the isotropic hardening material on the basis of elastoplastic relations referring to finite increments, cf. eqns (6.40)–(6.42).

6.2 Viscoelasticity and creep

Viscosity

Metals loaded at elevated temperature undergo, in addition to the instantaneous deformation caused by the thermal and mechanical loading, time-dependent inelastic deformation due to activation of viscous processes.

Viscosity is attributed to the amorphous constituents of the material, whereas plastic flow is related to the microscopic structure [1]. A description of time-dependent material response is necessary in order to account for creep (progressing deformation at constant stress) and relaxation processes (stress release at constant strain), which may determine the useful lifetime of systems operated at elevated temperature. The dependence of the material behaviour on the rate of deformation or the rate of loading is, on the other hand, of great significance when the transient response of a structure or a component is to be investigated.

The uniaxial response of the viscous material is described by the relation

$$\sigma = 3\mu\dot{\eta}_{\mathrm{V}}, \tag{6.49}$$

where μ is the viscosity coefficient. It follows that the stress σ is induced by a temporal variation $\dot{\eta}_{\mathrm{V}}$ of the viscous inelastic strain. The relation given in eqn (6.49) pertains to a linear viscous solid. A nonlinear dependence of the stress on the strain rate can still be represented in the form of eqn (6.49), but with viscosity coefficient $\mu(\dot{\eta}_{\mathrm{V}})$. For instance, the frequently encountered power law form

$$\sigma = k\dot{\eta}_{\mathrm{V}}^{m} \quad \text{or} \quad \frac{\sigma}{\sigma_{\mathrm{o}}} = \left(\frac{\dot{\eta}_{\mathrm{V}}}{\dot{\eta}_{\mathrm{Vo}}}\right)^{m} \tag{6.50}$$

(relating positive quantities or magnitudes) can be accommodated in eqn (6.49) via the viscosity coefficient:

$$3\mu = k\dot{\eta}_{\mathrm{V}}^{m-1} = \frac{\sigma_{\mathrm{o}}}{\dot{\eta}_{\mathrm{Vo}}^{m}}\dot{\eta}_{\mathrm{V}}^{m-1}. \tag{6.51}$$

In eqn (6.50), the values $\sigma_{\mathrm{o}}, \dot{\eta}_{\mathrm{Vo}}$ specify a reference state while $\sigma, \dot{\eta}_{\mathrm{V}}$ are variable quantities.

In either case, the linear or the nonlinear, the stress is a consequence of the rate of strain and vanishes if the strain is kept temporarily constant. The exponent m in eqn (6.50) is known as the rate sensitivity of the stress. It is defined by the differential quotient

$$m = \frac{\mathrm{dln}\sigma}{\mathrm{dln}\dot{\eta}_{\mathrm{V}}}, \tag{6.52}$$

referring to the logarithmic form of the equation. For metals $0 \leq m \leq 1$, the lower limit pertaining rather to a perfectly plastic solid ($\sigma = k$), the upper limit to a linear viscous material.

Viscoelastic material

Viscoelastic response can be modelled by assembling viscous and elastic material constituents (elements) in various ways. We restrict ourselves in the following to two essential combinations of linear constituents.

The parallel assembly of an elastic element (spring) and a viscous element (dashpot; Fig. 6.3), is known as the viscoelastic Kelvin–Voigt solid.

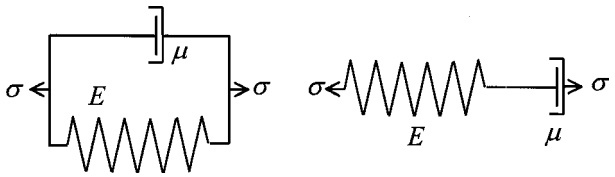

Figure 6.3: Viscoelastic Kelvin–Voigt model (left) and Maxwell element (right).

The stress required for straining the model is composed of two additive contributions

$$\sigma = E\gamma + 3\mu\dot{\gamma}. \tag{6.53}$$

The first term on the right-hand side of eqn (6.53) is from the elastic part, the second from the viscous part. Both constituents undergo the same strain: $\gamma = \varepsilon$ enters the elastic relation, $\dot{\gamma} = \dot{\eta}_{\mathrm{V}}$ the viscous.

In the viscoelastic model, a constant strain ($\dot{\gamma} = 0$) is associated with a constant stress as from elasticity, while the viscous contribution vanishes. The stress increases when the strain rate is increased. If the solid is subject to a constant stress σ_0 applied at time $t = 0$, integration of eqn (6.53) furnishes the strain

$$\gamma = \frac{\sigma_0}{E}\left[1 - \exp\left(-\frac{Et}{3\mu}\right)\right], \tag{6.54}$$

which is seen to evolve from initially $\gamma_0 = 0$ towards the asymptotic limit $\gamma_\infty = \sigma_0/E$.

An assembly of the elastic and the viscous element in series leads to the Maxwell model (Fig. 6.3). In this case the stress conditions are uniform in both constituents, but the strain of the compound element is additively composed. Thus for the strain rate

$$\dot{\gamma} = \frac{\dot{\sigma}}{E} + \frac{\sigma}{3\mu}. \tag{6.55}$$

A constant stress induces a constant strain rate associated with the viscous constituent. Instantaneous application of the stress σ_0 (high stress rate, $\sigma/3\mu$ negligible) immediately produces a strain $\gamma_0 = \sigma_0/E = \varepsilon_0$ in the elastic constituent. If the strain is fixed at γ_0 ($\dot{\gamma} = 0$), integration of eqn (6.55) gives the stress

$$\sigma = \sigma_0 \exp\left(-\frac{Et}{3\mu}\right). \tag{6.56}$$

At constant strain the stress is relaxing with time from initially σ_0 towards ultimately zero. The quotient $3\mu/E$ in eqn (6.56) is called the relaxation time.

It can be concluded that, independently of other properties, the Kelvin–Voigt model is suitable in describing the temporal evolution of the strain at

given stress, while the Maxwell model appears to be convenient for describing the stress relaxation at given strain.

Creep of metals
The creep strain rate $\dot{\eta}_C$ is superposed to the elastic strain rate $\dot{\varepsilon} = \dot{\sigma}/E$ such that

$$\dot{\gamma} = \frac{\dot{\sigma}}{E} + \dot{\eta}_C, \tag{6.57}$$

which is a combination of the Maxwell type. A relationship between creep strain rate and stress is frequently attempted in the power-law form

$$\frac{\dot{\eta}_C}{\dot{\eta}_{Co}} = \left(\frac{\sigma}{\sigma_o}\right)^n. \tag{6.58}$$

This can be interpreted as an inverse relation to eqn (6.50) with $n = 1/m$. Since the exponent n assumes values higher than unity, the effect of stress variations on the creep strain rate is significant.

Further to eqn (6.58), functional fitting of uniaxial creep data obtained experimentally at different levels of constant stress and temperature (Fig. 6.4) can be employed for establishing the creep law in the form of a functional dependence

$$\dot{\eta}_C = f(\sigma, T, t, \eta_C), \tag{6.59}$$

where η_C is the accumulated creep strain. The question arises then regarding the utilization of such a data set and the associated functional description, under transient, i.e. time varying stress and temperature. The rules postulated in this regard are referred to as hardening rules [2].

The *time hardening* rule assumes that the creep rate at any instant is defined by a functional dependence of the form

$$\dot{\eta}_C = f(\sigma, T, t). \tag{6.60}$$

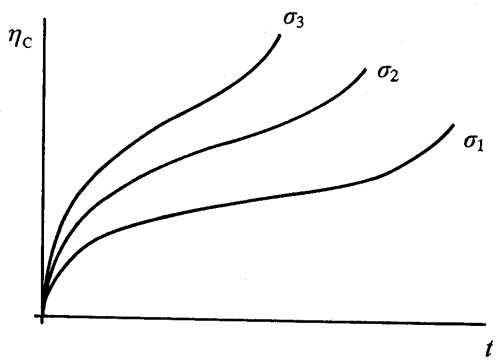

Figure 6.4: Uniaxial creep curves.

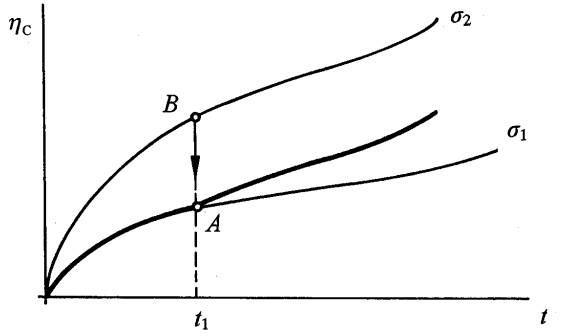

Figure 6.5: Hardening rules for creep: time hardening.

Following eqn (6.60), if the stress is changed from σ_1 to σ_2 at time t_1, the creep rate $\dot{\eta}_{C2}$ is determined for stress σ_2, at fixed instant t_1 (Fig. 6.5).

The *strain hardening* rule assumes the creep rate at any instant to be given by the functional dependence

$$\dot{\eta}_C = f(\sigma, T, \eta_C). \tag{6.61}$$

This implies that, by changing the stress from σ_1 to σ_2 at strain η_{C1}, the updated creep rate $\dot{\eta}_{C2}$ is determined for stress σ_2 keeping the strain η_{C1} constant (Fig. 6.6). Regarding variations in temperature, they are treated analogously to the change of stress for both hardening rules.

Under multiaxial conditions, the creep strain rate in metals can be written as

$$\dot{\boldsymbol{\eta}}_C = \dot{\bar{\eta}}_C \mathbf{s} \qquad \text{with} \quad \mathbf{s} = \frac{3}{2}\frac{1}{\bar{\sigma}}\boldsymbol{\sigma}_D, \tag{6.62}$$

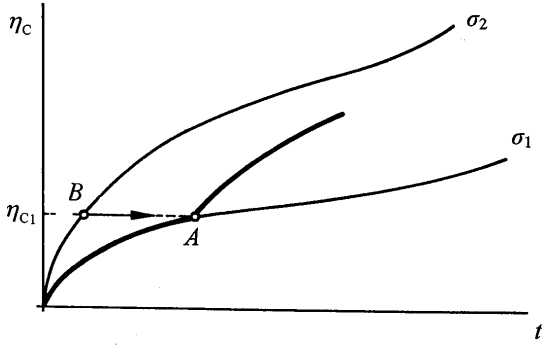

Figure 6.6: Hardening rules for creep: strain hardening.

in formal analogy to plastic flow. The magnitude of the creep strain rate is defined by

$$\dot{\bar{\eta}}_{\mathrm{C}}^2 = \frac{2}{3}\dot{\boldsymbol{\eta}}_{\mathrm{C}}^{\mathrm{t}}\dot{\boldsymbol{\eta}}_{\mathrm{C}} \tag{6.63}$$

and is specified in eqn (6.62) using the function of eqn (6.59) from uniaxial data with equivalent quantities as arguments: $\dot{\bar{\eta}}_{\mathrm{C}} = f(\bar{\sigma}, T, t, \bar{\eta}_{\mathrm{C}})$. The vector $\mathbf{s}$ defines the direction of $\dot{\boldsymbol{\eta}}_{\mathrm{C}}$, which is assumed along the deviatoric stress $\boldsymbol{\sigma}_{\mathrm{D}}$; the creep strain is isochoric.

The representation of the creep strain rate in eqn (6.62) is equivalent to the description of the viscous material constituent by

$$\boldsymbol{\sigma}_{\mathrm{D}} = 2\mu\dot{\boldsymbol{\eta}}_{\mathrm{C}}, \tag{6.64}$$

the multiaxial analogue to eqn (6.49). For scalar equivalent quantities the relation of eqn (6.64) assumes the form

$$\bar{\sigma} = 3\mu\dot{\bar{\eta}}_{\mathrm{C}}, \tag{6.65}$$

which can be compared with uniaxial material characteristics. Utilizing eqn (6.59) for $\dot{\bar{\eta}}_{\mathrm{C}}$ in eqn (6.65) specifies the viscosity coefficient:

$$3\mu = \frac{\bar{\sigma}}{f(\bar{\sigma}, T, t, \bar{\eta}_{\mathrm{C}})}. \tag{6.66}$$

Incrementation

Inspection of eqns (6.49) and (6.50) describing viscous materials, suggests that the stress dependence is of primary importance for the strain rate. Therefore, we investigate incrementation of the functional form $\dot{\eta}_{\mathrm{C}} = f(\sigma)$ within the time interval $\tau = t_{n+1} - t_n$:

$$\eta_{\mathrm{C}\Delta} = \eta_{\mathrm{C}n+1} - \eta_{\mathrm{C}n} = \int_{t_n}^{t_{n+1}} f(\sigma)\mathrm{d}t. \tag{6.67}$$

For a given temporal variation of the stress within the interval, the integral in eqn (6.67) can be evaluated either analytically or, most likely, numerically.

By the mid-value theorem,

$$\eta_{\mathrm{C}\Delta} = \tau f(\sigma_\zeta) \qquad (0 \le \zeta \le 1), \tag{6.68}$$

where a linear variation of the stress σ within the increment as in eqn (5.74) may be assumed in order to express σ_ζ in terms of σ_n, σ_{n+1} and of the collocation parameter $\zeta = (t - t_{n+1})/\tau$. Then the incremental transition of the creep strain is performed by

$$\eta_{\mathrm{C}n+1} = \eta_{\mathrm{C}n} + \tau f(\sigma_\zeta), \quad \sigma_\zeta = (1-\zeta)\sigma_n + \zeta\sigma_{n+1}. \tag{6.69}$$

If the history of the stress σ is considered prescribed in the process, numerical perturbations $\delta\eta_{\mathrm{C}}$ at stage n are transmitted to stage $n+1$ without any modification by the integration scheme. If, on the other hand, the history of the strain γ is prescribed, the stress $\sigma = E(\gamma - \eta_{\mathrm{C}})$ is affected by perturbations in the creep strain. As a consequence, the incremental approximation by eqn (6.68) can alter numerical perturbations introducing either amplification or damping, and raises the question of stability.

Incrementation of eqn (6.69) gives

$$\begin{aligned}\delta\eta_{\mathrm{C}n+1} &= \delta\eta_{\mathrm{C}n} + \tau \left.\frac{\mathrm{d}f}{\mathrm{d}\sigma}\right|_{\zeta} \delta\sigma_{\zeta} \\ &= \delta\eta_{\mathrm{C}n} - \tau E f'_{\zeta} \left[(1-\zeta)\delta\eta_{\mathrm{C}n} + \zeta\delta\eta_{\mathrm{C}n+1}\right], \end{aligned} \tag{6.70}$$

where $f' = \mathrm{d}f/\mathrm{d}\sigma$, and since $\gamma =$ constant, $\delta\sigma = -E\delta\eta_{\mathrm{C}}$. From eqn (6.70), numerical perturbations in the creep strain propagate in accordance with

$$\delta\eta_{\mathrm{C}n+1} = \left(1 - \frac{\tau E f'_{\zeta}}{1 + \zeta\tau E f'_{\zeta}}\right) \delta\eta_{\mathrm{C}n}. \tag{6.71}$$

For stability $|\delta\eta_{\mathrm{C}n+1}| < |\delta\eta_{\mathrm{C}n}|$, and from eqn (6.71)

$$0 < \tau E f'_{\zeta} < \frac{2}{1-2\zeta}. \tag{6.72}$$

This requires $f' > 0$ on the one hand, and restricts the time increment to

$$\tau < \frac{2}{(1-2\zeta)E f'_{\zeta}} \qquad \text{for} \quad 0 \le \zeta \le \frac{1}{2} \tag{6.73}$$

on the other hand. Unconditional stability is obtained for $1/2 < \zeta \le 1$. From eqn (6.71), the sign of perturbations will not alternate as long as the time step is below the oscillation limit

$$\tau < \frac{1}{(1-\zeta)E f'_{\zeta}}. \tag{6.74}$$

The stability limit for τ, eqn (6.73), and the oscillation limit, eqn (6.74), are plotted as a function of the collocation parameter ζ in Fig. 6.7.

For illustration, we consider the uniaxial case of a rod specimen having experienced the creep strain $\eta_{\mathrm{C}0}$. At time $t = 0$ let the specimen be constrained to $\gamma = 0$. This produces a stress $\sigma = -E\eta_{\mathrm{C}}$ and induces a strain rate $\dot{\eta_{\mathrm{C}}} = \sigma/3\mu$. The model problem is governed by the equation

$$\dot{\eta}_{\mathrm{C}} + \frac{E}{3\mu}\eta_{\mathrm{C}} = 0. \tag{6.75}$$

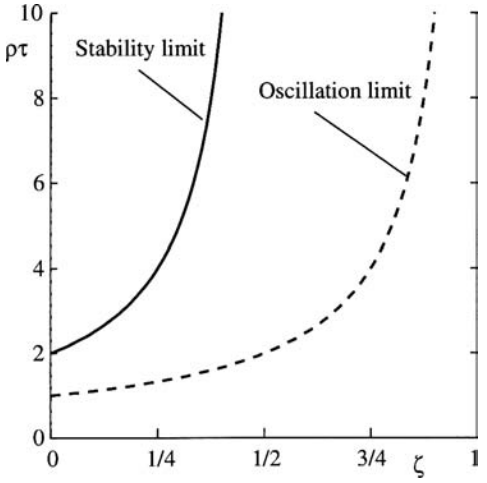

Figure 6.7: Limitation of the time increment by numerical stability.

Integration of eqn (6.75) furnishes the solution

$$\frac{\eta_{\mathrm{C}}}{\eta_{\mathrm{C}0}} = \exp\left(-\frac{Et}{3\mu}\right). \tag{6.76}$$

The creep strain is decaying asymptotically from initially $\eta_{\mathrm{C}0}$ to $\eta_{\mathrm{C}\infty} = 0$.

Approximate integration as by eqn (6.69) with

$$f = \frac{\sigma}{3\mu} = -\frac{E}{3\mu}\eta_{\mathrm{C}} \tag{6.77}$$

leads to the incremental transformation

$$\eta_{\mathrm{C}n+1} = \left(1 - \frac{\tau E/3\mu}{1 + \zeta\tau E/3\mu}\right)\eta_{\mathrm{C}n}, \tag{6.78}$$

which can be compared with eqn (6.71). In the present linear case, approximate solutions and perturbations progress in the same manner. Both quantities are seen to decay as long as the stability condition of eqn (6.72) is observed:

$$0 < \tau\frac{E}{3\mu} < \frac{2}{1-2\zeta}. \tag{6.79}$$

Instability and oscillatory behaviour, eqn (6.73), can be confirmed. Figure 6.8 demonstrates the significance of the collocation parameter ζ for the accuracy of the incremental approximation.

In the multiaxial case the creep rate is given by eqn (6.62). This relationship can be written as

$$\dot{\boldsymbol{\eta}}_{\mathrm{C}} - \mathbf{f}(\boldsymbol{\sigma}_{\mathrm{D}}) = \mathbf{0}. \tag{6.80}$$

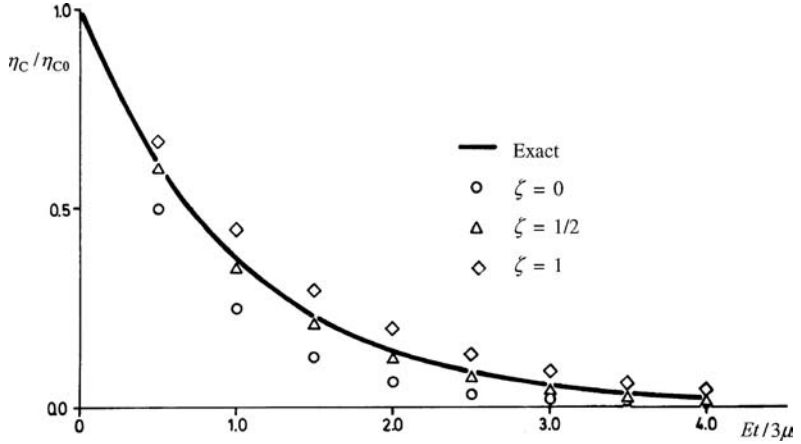

Figure 6.8: Accuracy of numerical integration.

The function $\mathbf{f}(\boldsymbol{\sigma}_\mathrm{D})$ presumes a dependence $\dot{\bar{\eta}}_\mathrm{C} = f(\bar{\sigma})$ such that

$$\mathbf{f}(\boldsymbol{\sigma}_\mathrm{D}) = \dot{\bar{\eta}}_\mathrm{C}\mathbf{s} = f(\bar{\sigma})\mathbf{s}(\boldsymbol{\sigma}_\mathrm{D}). \tag{6.81}$$

Incremental integration is effected by

$$\boldsymbol{\eta}_{\mathrm{C}n+1} = \boldsymbol{\eta}_{\mathrm{C}n} + \boldsymbol{\eta}_{\mathrm{C}\Delta} \qquad \text{with} \qquad \boldsymbol{\eta}_{\mathrm{C}\Delta} = \tau\mathbf{f}(\boldsymbol{\sigma}_{\mathrm{D}\zeta}), \tag{6.82}$$

where $\boldsymbol{\sigma}_{\mathrm{D}\zeta}$ is obtained at the selected instant ζ assuming a linear variation of the stress within the increment, eqn (5.74). If stresses $\boldsymbol{\sigma}$ are prescribed, the scheme in eqn (6.82) performs an approximate evaluation of the integral for the creep strain. For prescribed strain $\boldsymbol{\gamma}$, the stress varies with the creep strain:

$$\boldsymbol{\sigma}_\mathrm{D} = 2G[\boldsymbol{\gamma}_\mathrm{D} - \boldsymbol{\eta}_\mathrm{C}], \quad \frac{\mathrm{d}\boldsymbol{\sigma}_\mathrm{D}}{\mathrm{d}\boldsymbol{\eta}_\mathrm{C}} = -2G\mathbf{I}.$$

Then eqn (6.80) becomes a differential equation in $\boldsymbol{\eta}_\mathrm{C}$, and eqn (6.82) is applied to its numerical solution.

An investigation of stability follows [3] and the lines of Section 5.4.3, leading to the condition of eqn (5.97) for the time increment τ. The matrix $\mathbf{N}$ defined in eqn (5.87) is specified in the case of eqn (6.80) by the relationship

$$\delta\mathbf{f} = \frac{\mathrm{d}\mathbf{f}}{\mathrm{d}\boldsymbol{\sigma}_\mathrm{D}}\frac{\mathrm{d}\boldsymbol{\sigma}_\mathrm{D}}{\mathrm{d}\boldsymbol{\eta}_\mathrm{C}}\delta\boldsymbol{\eta}_\mathrm{C} = -\mathbf{N}\delta\boldsymbol{\eta}_\mathrm{C},$$

to

$$\mathbf{N} = -\frac{\mathrm{d}\mathbf{f}}{\mathrm{d}\boldsymbol{\sigma}_\mathrm{D}}\frac{\mathrm{d}\boldsymbol{\sigma}_\mathrm{D}}{\mathrm{d}\boldsymbol{\eta}_\mathrm{C}} = 2G\frac{\mathrm{d}\mathbf{f}}{\mathrm{d}\boldsymbol{\sigma}_\mathrm{D}}. \tag{6.83}$$

With reference to eqn (6.81),

$$\frac{\mathrm{d}\mathbf{f}}{\mathrm{d}\boldsymbol{\sigma}_{\mathrm{D}}} = f\frac{\mathrm{d}\mathbf{s}}{\mathrm{d}\boldsymbol{\sigma}_{\mathrm{D}}} + f'\mathbf{s}\frac{\mathrm{d}\bar{\sigma}}{\mathrm{d}\boldsymbol{\sigma}_{\mathrm{D}}}$$
$$= \frac{3}{2}\frac{f}{\bar{\sigma}}\left[\mathbf{I} - \frac{2}{3}\left(1 - \frac{f'\bar{\sigma}}{f}\right)\mathbf{s}\mathbf{s}^{\mathrm{t}}\right], \tag{6.84}$$

where eqns (1.119) and (5.111) have been considered. It is noticed that the second term in the parentheses in eqn (6.84) vanishes if $f(\bar{\sigma})$ is linearly proportional to $\bar{\sigma}$.

The spectral radius of the matrix $\mathbf{N}$, eqns (6.83) and (6.84), reads

$$\rho(\mathbf{N}) = 3G\frac{f}{\bar{\sigma}}\rho. \tag{6.85}$$

Here, ρ denotes the spectral radius of the bracket expression in eqn (6.84). The non-zero eigenvalues of this matrix are 1 and $f'\bar{\sigma}/f$. For the power-law form, eqn (6.58), $f'\bar{\sigma}/f = n > 1$, which defines ρ in this case. Assuming $\rho = f'\bar{\sigma}/f$, the stability condition for the time increment is deduced from eqn (5.97) as

$$\tau < \frac{2}{(1-2\zeta)3Gf'_{\zeta}}, \tag{6.86}$$

and is comparable to eqn (6.74) for the uniaxial case.

In Section 5.4.3, the stability of incremental plastic strain was investigated for a prescribed magnitude $\bar{\eta}_{\Delta}$. Since the physical origin of $\bar{\eta}_{\Delta}$ turns out to be irrelevant in this respect, the stability limit of eqn (5.115) can be interpreted for the present case of creep. With $\bar{\eta}_{\mathrm{C}\Delta} = \tau f(\bar{\sigma}_{\zeta})$, the time increment is restricted by eqn (5.115) to

$$\tau < \frac{2}{(1-2\zeta)3G(f/\bar{\sigma})_{\zeta}} \quad \text{for} \quad 0 \le \zeta \le \frac{1}{2}. \tag{6.87}$$

The above differs from eqn (6.86) because here the magnitude of the incremental creep strain is not subject to perturbations. The two limits are seen to coincide if $f(\bar{\sigma})$ is linearly proportional to $\bar{\sigma}$. The result is applicable to a series model of the Maxwell type, immaterial of the nature of the viscous constituent which specifies the relationship $\dot{\bar{\eta}} = f(\bar{\sigma})$.

Algorithmic implementation

In a straightforward approach to problems involving history- and rate-dependent material behaviour, the inelastic strain is assumed to be composed of an instantaneous and a time-dependent part which are described separately. The instantaneous contribution is governed by the theory of plasticity, while the time-dependent contribution is the result of creep. Bearing

in mind that, in metals, creep is associated with elevated temperatures and possibly non-isothermal conditions, the stress is given as

$$\boldsymbol{\sigma} = \boldsymbol{\kappa}[\boldsymbol{\gamma} - \boldsymbol{\eta}_{\mathrm{T}} - \boldsymbol{\eta}_{\mathrm{P}} - \boldsymbol{\eta}_{\mathrm{C}}], \tag{6.88}$$

which extends the stress–strain relation in eqn (6.8) by the creep strain.

For the incremental computation, the stress at state $n+1$ is written in the form

$$\boldsymbol{\sigma}_{n+1} = \boldsymbol{\kappa}_{n+1}[\boldsymbol{\gamma}_n - \boldsymbol{\eta}_{\mathrm{P}n} - \boldsymbol{\eta}_{\mathrm{T}n+1} - \boldsymbol{\eta}_{\mathrm{C}n+1}] + \kappa_{n+1}[\boldsymbol{\gamma}_\Delta - \boldsymbol{\eta}_{\mathrm{P}\Delta}], \tag{6.89}$$

following eqn (6.24). The incremental creep strain $\boldsymbol{\eta}_{\mathrm{C}\Delta}$ is not directly proportional to the increment of stress or strain as is the incremental plastic strain $\boldsymbol{\eta}_{\mathrm{P}\Delta}$. Therefore, it can be estimated with the currently available thermomechanical state for a given time increment τ, and is accumulated to the creep strain $\boldsymbol{\eta}_{\mathrm{C}n+1} = \boldsymbol{\eta}_{\mathrm{C}n} + \boldsymbol{\eta}_{\mathrm{C}\Delta}$. After that, the creep strain is formally treated in the same manner as the thermal strain. The creep strain is, however, deviatoric and completely different in nature from the volumetric thermal expansion. Furthermore, if the incrementation scheme for $\boldsymbol{\eta}_{\mathrm{C}\Delta}$ is not explicit and involves quantities at the end of the incremental step, the creep strain $\boldsymbol{\eta}_{\mathrm{C}n+1}$ has to be updated following the course of the iterative solution.

By eqn (6.89) for the stress $\boldsymbol{\sigma}_{n+1}$, the algorithmic issues presented previously in Section 6.1 remain essentially unmodified, in particular the determination of the incremental plastic strain. The update of the creep strain $\boldsymbol{\eta}_{\mathrm{C}n+1} = \boldsymbol{\eta}_{\mathrm{C}n} + \boldsymbol{\eta}_{\mathrm{C}\Delta}$ and superposition to the thermal strain $\boldsymbol{\eta}_{\mathrm{T}n+1}$ are the only alterations. Simplifications in the case of isothermal conditions are obvious, and allow an exclusive consideration of incremental quantities, see Section 5.5. Finally, in case creep is considered exclusively, the plasticity branch of the algorithm is not active.

6.3 Viscoplasticity

An alternative approach to rate- and history-dependent material phenomena does not distinguish between viscous and plastic contributions to the inelastic flow. The simplest form of the viscoplastic model for a state of uniaxial tensile stress is

$$\sigma = \sigma_{\mathrm{s}} + 3\mu\dot{\eta}_{\mathrm{V}}. \tag{6.90}$$

The model apparently consists of the parallel assembly of a perfectly plastic constituent with yield stress σ_{s} and a linear viscous one (Fig. 6.9, left). It accounts for the fact that certain materials do not exhibit viscous flow below a defined stress level ($\sigma \leq \sigma_{\mathrm{s}}$). Equation (6.90) is ascribed to a linear Bingham medium [4]. The relationship was extended to multiaxial situations by Hohenemser and Prager [5]; an additional discussion by Prager is found in [6].

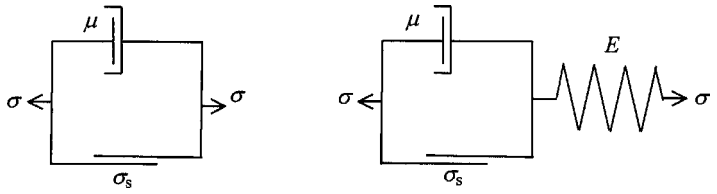

Figure 6.9: Viscoplastic (left) and elastic–viscoplastic models (right).

An elastic–viscoplastic model is obtained by the superposition of an elastic constituent. This element is joined in series (Fig. 6.9, right) such that the rate of overall strain is given by

$$\dot{\gamma} = \frac{\dot{\sigma}}{E} + \frac{\sigma - \sigma_{\mathrm{s}}}{3\mu}. \tag{6.91}$$

In eqn (6.91), $\dot{\sigma}/E$ represents the elastic contribution, while the second term is the viscoplastic part from eqn (6.90).

If the specimen is deformed at a constant strain rate ($\dot{\gamma} = \text{constant}$), the solution of eqn (6.91) for the stress is

$$\sigma = \sigma_{\mathrm{s}} + \left[1 - \exp\left(-\frac{Et}{3\mu}\right)\right] 3\mu\dot{\gamma}. \tag{6.92}$$

Equation (6.92) describes the interaction of elastic and inelastic response in the transient part of the deformation. With increasing time, the exponential in the parentheses diminishes and the expression for the stress tends to eqn (6.90) of the viscoplastic constituent. The effect of elasticity loses significance with time, and the stress ultimately becomes stationary (Fig. 6.10). The time scale of the phenomenon is defined by the relaxation constant

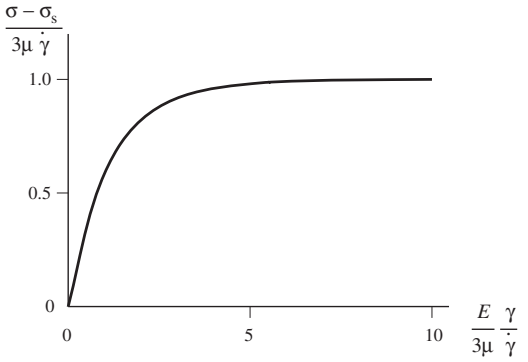

Figure 6.10: Transition to stationary stress.

$3\mu/E$. Since $\dot{\gamma} = \text{constant}$, the time can be measured in terms of deformation as $t = \gamma/\dot{\gamma}$.

An obvious generalization of the viscoplastic model defined by eqn (6.90) reads

$$\sigma = \sigma_{\mathrm{f}}(\eta_{\mathrm{V}}) + k\dot{\eta}_{\mathrm{V}}^{m}. \tag{6.93}$$

The quantity $\sigma_{\mathrm{f}}(\eta_{\mathrm{V}})$ describes the yield stress as a function of the inelastic (viscoplastic) strain specified by the hardening characteristic of the material in the absence of viscous effects. The second term is the power-law form of a nonlinear viscous constituent.

From eqn (6.93), the rate of viscoplastic strain is

$$\dot{\eta}_{\mathrm{V}} = \left(\frac{\sigma - \sigma_{\mathrm{f}}}{k}\right)^{n} \geq 0 \qquad \left(n = \frac{1}{m}\right). \tag{6.94}$$

It follows that viscoplastic flow occurs as soon as an 'overstress' $\sigma - \sigma_{\mathrm{f}}$ exists, or, alternatively, as long as the yield condition $\sigma - \sigma_{\mathrm{f}} \leq 0$ remains unsatisfied. Thus, in contrast to inviscid plasticity, viscoplastic flow is not governed by the satisfaction of the yield condition (consistency condition).

A constitutive framework for rate sensitive plastic materials has been presented by Perzyna in [7]. In our notation, the viscoplastic strain rate under multiaxial conditions is stated as

$$\dot{\boldsymbol{\eta}}_{\mathrm{V}} = \dot{\bar{\eta}}_{\mathrm{V}}\mathbf{s} \qquad \text{with} \quad \mathbf{s} = \frac{3}{2}\frac{1}{\bar{\sigma}}\boldsymbol{\sigma}_{\mathrm{D}}, \tag{6.95}$$

which is homologous to the presentation of plastic flow and creep. The direction $\mathbf{s}$ of viscoplastic flow is still specified by the deviatoric stress. The magnitude $\dot{\bar{\eta}}_{\mathrm{V}}$, defined as usual, is determined by the relationship

$$\dot{\bar{\eta}}_{\mathrm{V}} = \frac{1}{\bar{\mu}}F(\bar{\phi}) \geq 0. \tag{6.96}$$

In this case the viscous characteristics of the material are represented by the parameter $\bar{\mu}$. The function F depends on $\bar{\phi}$, the von Mises yield function, as known from inviscid plastic flow standardized by the yield stress of the material. Thus, including the temperature as a variable quantity

$$\bar{\phi} = \frac{\bar{\sigma} - \sigma_{\mathrm{f}}(\bar{\eta}_{\mathrm{V}}, T)}{\sigma_{\mathrm{f}}(\bar{\eta}_{\mathrm{V}}, T)}. \tag{6.97}$$

The discontinuity of the function $F(\bar{\phi})$ ensures that viscoplastic flow does not occur for $F(\bar{\phi}) \leq 0$.

The above description of the magnitude of viscoplastic flow can be associated with the notion of a rate-dependent yield function. To this end, we introduce for the function $F(\bar{\phi})$ in eqn (6.96) the specific form

$$F(\bar{\phi}) = \bar{\phi}^{n}. \tag{6.98}$$

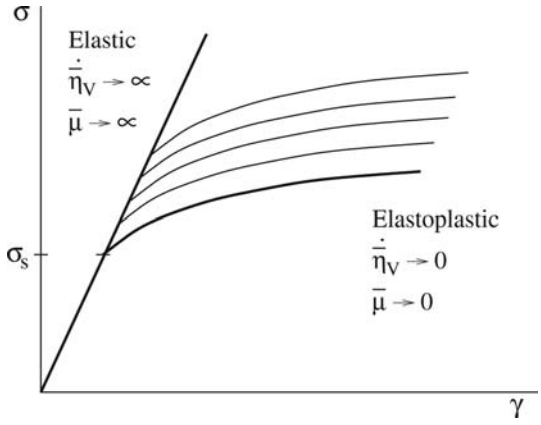

Figure 6.11: Range of elastic–viscoplastic response.

Then, rearranging we obtain

$$\bar{\sigma} - \left[1 + (\bar{\mu}\dot{\bar{\eta}}_{\mathrm{V}})^m\right] \sigma_{\mathrm{f}} = 0 \qquad \left(m = \frac{1}{n}\right). \tag{6.99}$$

This relation may be interpreted as expressing the effect of viscous phenomena on the static von Mises yield function with isotropic hardening. In particular, the second term can be viewed as a dynamic yield stress. It follows an increase or decrease of the viscosity $\bar{\mu}$ and rate of strain $\dot{\bar{\eta}}_{\mathrm{V}}$. In the limiting case of infinite viscosity ($\bar{\mu} \to \infty$) or for sudden deformation ($\dot{\bar{\eta}}_{\mathrm{V}} \to \infty$) the value of the equivalent stress $\bar{\sigma}$ is not restricted by eqn (6.99). At the other end, in the absence of viscosity ($\bar{\mu} \to 0$) or for very slow deformation ($\dot{\bar{\eta}}_{\mathrm{V}} \to 0$) eqn (6.99) reduces to the inviscid yield limit for which $\bar{\sigma}$ is bounded by the static yield stress $\sigma_{\mathrm{f}}(\bar{\eta}_{\mathrm{V}})$ (Fig. 6.11).

Elasto-viscoplastic analysis requires the stress in terms of strain,

$$\boldsymbol{\sigma} = \boldsymbol{\kappa}[\boldsymbol{\gamma} - \boldsymbol{\eta}_{\mathrm{T}} - \boldsymbol{\eta}_{\mathrm{V}}], \tag{6.100}$$

where the viscoplastic strain $\boldsymbol{\eta}_{\mathrm{V}}$ takes the place of the creep and plastic strain in the previous model. For the computational treatment by incrementation, refer to Section 6.1. At stage $n+1$, the stress is

$$\begin{aligned} \boldsymbol{\sigma}_{n+1} &= \boldsymbol{\kappa}_{n+1}[\boldsymbol{\gamma}_{n+1} - \boldsymbol{\eta}_{\mathrm{V}n+1} - \boldsymbol{\eta}_{\mathrm{T}n+1}] \\ &= \boldsymbol{\kappa}_{n+1}[\boldsymbol{\gamma}_n - \boldsymbol{\eta}_{\mathrm{V}n} - \boldsymbol{\eta}_{\mathrm{T}n+1}] + \boldsymbol{\kappa}_{n+1}[\boldsymbol{\gamma}_\Delta - \boldsymbol{\eta}_{\mathrm{V}\Delta}] \end{aligned} \tag{6.101}$$

and the present task reduces to the specification of the incremental viscoplastic strain $\boldsymbol{\eta}_{\mathrm{V}\Delta}$ instead of the plastic $\boldsymbol{\eta}_{\mathrm{P}\Delta}$ in eqn (6.24).

Incrementation of the viscoplastic strain is performed according to

$$\boldsymbol{\eta}_{\mathrm{V}\Delta} = \bar{\eta}_{\mathrm{V}\Delta}\mathbf{s}_\zeta. \tag{6.102}$$

The flow direction $\mathbf{s}_\zeta = \mathbf{s}(\boldsymbol{\sigma}_{\mathrm{D}\zeta})$ is determined at position ζ; in conformity with the radial return in plasticity, it is taken as $\mathbf{s}_{\zeta=1} = \mathbf{s}_{n+1}$. Regarding the magnitude of the incremental inelastic strain we consider the specific case $F(\bar{\phi}) = \bar{\phi}$ in eqn (6.96). For the time increment τ we obtain

$$\bar{\eta}_{\mathrm{V}\Delta} = \frac{\tau}{\bar{\mu}\sigma_{\mathrm{f}}(\bar{\eta}_{\mathrm{V}n}, T_{n+1})} \left[\bar{\sigma}_{n+1} - \sigma_{\mathrm{f}}\left(\bar{\eta}_{\mathrm{V}n}, T_{n+1}\right)\right] \geq 0, \tag{6.103}$$

which can be compared with eqn (6.33) for conventional plasticity.

It is seen that a complete analogy between the plastic and viscoplastic models is established by the substitution

$$\frac{1}{h} \Leftarrow \frac{\tau}{\bar{\mu}\sigma_{\mathrm{f}}(\bar{\eta}_{\mathrm{V}n}, T_{n+1})}. \tag{6.104}$$

This analogy allows the treatment of viscoplastic flow by the standard algorithms for plasticity except for the satisfaction of the yield condition. Implementation of different functions $F(\bar{\phi})$ requires additional modifications. Conversely, the viscoplastic material model may be employed for the solution of problems in plasticity [8]. For this purpose, fictitious viscoplastic flow is activated in the loading increment as by eqn (6.103) with the overstress from the elastic solution. The time increment τ and the viscosity coefficient $\bar{\mu}$ are selected in compliance with the actual plastic hardening parameter h as in eqn (6.104), such that the stress is not reduced below the yield limit. At loading stage $n+1$ the incremental viscoplastic process is maintained until the relaxed stress fulfils everywhere the static yield condition $\bar{\sigma}_{n+1} = \sigma_{\mathrm{f}}(\bar{\eta}_{n+1}, T_{n+1})$ to a satisfactory degree, and inelastic flow ceases. The accumulated viscoplastic flow in the step $[n, n+1]$ is taken as the plastic strain increment $\boldsymbol{\eta}_\Delta$. For a given strain increment $\boldsymbol{\gamma}_\Delta =$ constant, the technique performs stress relaxation to the yield surface along the deviatoric stress $\boldsymbol{\sigma}_{\mathrm{D}n+1}$, thus effecting radial return. The procedure may be employed in conjunction with a viscoplastic model referring to more general, non-deviatoric flow conditions, in which case it is comparable with the return technique described in Section 5.4.5 for plasticity.

Summarizing, an extended form of deviatoric viscoplasticity can be simply referred to eqn (6.90). Covering multiaxial conditions by the equivalent scalar quantities, we write

$$\bar{\sigma} = \sigma_{\mathrm{f}} + 3\mu\dot{\bar{\eta}}_{\mathrm{V}}.$$

The yield stress $\sigma_{\mathrm{f}}(\bar{\eta}_{\mathrm{V}}, T)$ provided by the hardening characteristic of the material for vanishing viscosity describes the plastic constituent of the model. The viscous constituent is specified by the coefficient $\mu(\dot{\bar{\eta}}_{\mathrm{V}}, \bar{\eta}_{\mathrm{V}}, T)$, which may accommodate nonlinearity and strain dependence in addition to the temperature.

For a given stress, the above equation determines the equivalent strain rate $\dot{\bar{\eta}}_{\mathrm{V}}$; the multiaxial strain rate $\dot{\boldsymbol{\eta}}_{\mathrm{V}}$ is obtained by eqn (6.95). If the inelastic strain rate

is a given quantity, the viscoplastic model defines a dynamic yield stress as

$$\sigma_{\mathrm{fV}} = \left(1 + \frac{3\mu\dot{\bar{\eta}}_{\mathrm{V}}}{\sigma_{\mathrm{f}}}\right)\sigma_{\mathrm{f}},$$

which compares with eqn (6.99).

6.4 Effects of inertia

6.4.1 Continuum level

In a number of problems the loading is applied within a short interval of time, or it is rapidly varied. Thereby, the property of inertia of the mass introduces the effect of time in the diffusion of the action of the loading in the solid. For a comprehensive presentation of dynamic plasticity problems the reader is referred to [9]. The following elementary introduction is restricted to the propagation of uniaxial waves; further mathematical details can be found in [10].

Let us consider the uniaxial case of the rod in Fig. 6.12, which is assumed to deform under negligible changes of geometry. The equation of motion along the longitudinal axis of the rod is obtained by equating the resultant of the stresses on a differential element to the inertia force due to the acceleration. The result is

$$\frac{\partial\sigma}{\partial x} = \varrho\frac{\partial^2 u}{\partial t^2}, \tag{6.105}$$

where $u(x,t)$ denotes the displacement along the longitudinal x-axis, $\sigma(x,t)$ is the normal stress in the same direction and ϱ is the density of the material (assumed constant).

Stating the stress $\sigma(\gamma)$ as a function of the longitudinal strain $\gamma(x,t)$, we obtain

$$\frac{\partial\sigma}{\partial x} = \frac{\mathrm{d}\sigma}{\mathrm{d}\gamma}\frac{\partial\gamma}{\partial x}, \qquad \gamma = \frac{\partial u}{\partial x}$$

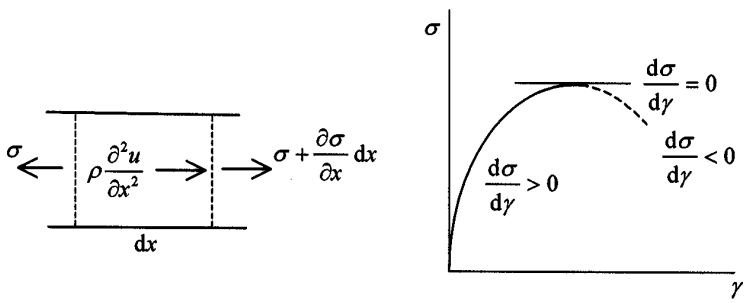

Figure 6.12: Dynamics of uniaxial motion (left) and material behaviour (right).

and from eqn (6.105)

$$\frac{\partial^2 u}{\partial t^2} = \frac{1}{\varrho}\frac{\mathrm{d}\sigma}{\mathrm{d}\gamma}\frac{\partial^2 u}{\partial x^2} = c^2\frac{\partial^2 u}{\partial x^2}. \tag{6.106}$$

The quantity

$$c = \left(\frac{1}{\varrho}\frac{\mathrm{d}\sigma}{\mathrm{d}\gamma}\right)^{1/2}, \tag{6.107}$$

known as the local speed of sound, characterizes the local velocity of propagation of perturbations. The propagation speed follows the variation of the slope $0 \le \mathrm{d}\sigma/\mathrm{d}\gamma \le E$ of the stress–strain characteristic of the material. It is high in the elastic range and diminishes as the slope decreases with progressing plastic strain.

Linear second-order differential expressions of the form

$$A\frac{\partial^2 u}{\partial t^2} + 2B\frac{\partial^2 u}{\partial t \partial x} + C\frac{\partial^2 u}{\partial x^2}$$

are classified in accordance with the sign of the discriminant $AC - B^2$. The differential expression is:

$$\begin{aligned} &\text{hyperbolic for} && AC - B^2 < 0,\\ &\text{parabolic for} && AC - B^2 = 0,\\ &\text{elliptic for} && AC - B^2 > 0. \end{aligned}$$

In eqn (6.106): $A = 1, B = 0, C = -c^2$, and

$$AC - B^2 = -c^2 = -\frac{1}{\varrho}\frac{\mathrm{d}\sigma}{\mathrm{d}\gamma}.$$

Hence, the differential equation of motion is of the hyperbolic type as long as $\mathrm{d}\sigma/\mathrm{d}\gamma > 0$ (hardening), becomes parabolic for $\mathrm{d}\sigma/\mathrm{d}\gamma = 0$ (perfect plasticity), and would be elliptic for $\mathrm{d}\sigma/\mathrm{d}\gamma < 0$ (softening), Fig. 6.12.

Introducing the particle velocity $v = \partial u/\partial t$ and the strain $\gamma = \partial u/\partial x$ as alternative variables, eqn (6.106), which is of the second order in u, can be substituted by a system of two first-order differential equations for $v(x,t)$ and $\gamma(x,t)$:

$$\begin{aligned} \frac{\partial v}{\partial t} &= c^2\frac{\partial \gamma}{\partial x},\\ \frac{\partial \gamma}{\partial t} &= \frac{\partial v}{\partial x}. \end{aligned} \tag{6.108}$$

The second equation reflects kinematic compatibility and relies on a continuous function $u(x,t)$.

With the definitions

$$\mathbf{v} = \begin{bmatrix} v \\ \gamma \end{bmatrix}, \qquad \mathbf{A} = \begin{bmatrix} 0 & c^2 \\ 1 & 0 \end{bmatrix},$$

the equation system can be written in the matrix form

$$\frac{\partial \mathbf{v}}{\partial t} - \mathbf{A}\frac{\partial \mathbf{v}}{\partial x} = \mathbf{0}. \tag{6.109}$$

Wave propagation

As long as the stress in the rod remains within the elastic range of the material, the wave speed is constant, $c = (E/\varrho)^{1/2} = c_0$, and solutions of eqn (6.106) for the displacement wave can be given in the form

$$u = f(x - c_0 t) + g(x + c_0 t). \tag{6.110}$$

The wave solution satisfies eqn (6.106) for arbitrary functions f and g, which must be adapted to the initial and boundary conditions of the problem. From the arguments, function f pertains to a wave moving along the positive direction of the x-axis (positive or right-hand side wave) and function g to a wave along the negative x-axis (negative or left-hand side wave).

Considering a positive wave, we obtain the strain and velocity by differentiation as

$$\gamma = \frac{\partial u}{\partial x} = f', \quad v = \frac{\partial u}{\partial t} = -c_0 f',$$

and

$$\sigma = -\frac{E}{c_0} v = -\varrho c_0 v \tag{6.111}$$

for the stress ($\sigma = E\varepsilon$, $\varepsilon \equiv \gamma$). From eqn (6.111), particles move in a compressive wave ($\sigma < 0$) in the same direction as the wave ($v > 0$). In an expansion wave ($\sigma > 0$) the particle motion is opposed to the wave direction ($v < 0$). The same conclusion can be drawn for a negative wave.

If a semi-infinite rod ($0 \le x \le \infty$) is subject to an impact stress $-\sigma_0$ at $x = 0$, $t = 0$, the motion of the initiated positive wave is described by

$$u = f(x - c_0 t) = -\frac{\sigma_0}{E}(x - c_0 t). \tag{6.112}$$

Strain and particle velocity derive from eqn (6.112) as

$$\gamma = \frac{\partial u}{\partial x} = -\frac{\sigma_0}{E} = \varepsilon, \qquad v = \frac{\partial u}{\partial t} = \frac{\sigma_0}{E} c_0 \tag{6.113}$$

and it is seen that the strain complies with the stress boundary condition via the elasticity law.

The solution in eqn (6.112) can be interpreted in the x, t plane (Fig. 6.13) as follows. The line $x = c_0 t$ separates the region ($x > c_0 t$) which is still at rest from the already disturbed region ($x < c_0 t$). It defines the motion of the wave front along the axis of the rod. In the undisturbed region, in front of the wave, the displacement, velocity and strain are zero. In the region $x < c_0 t$, behind the wave front, the displacement u is given by eqn (6.112).

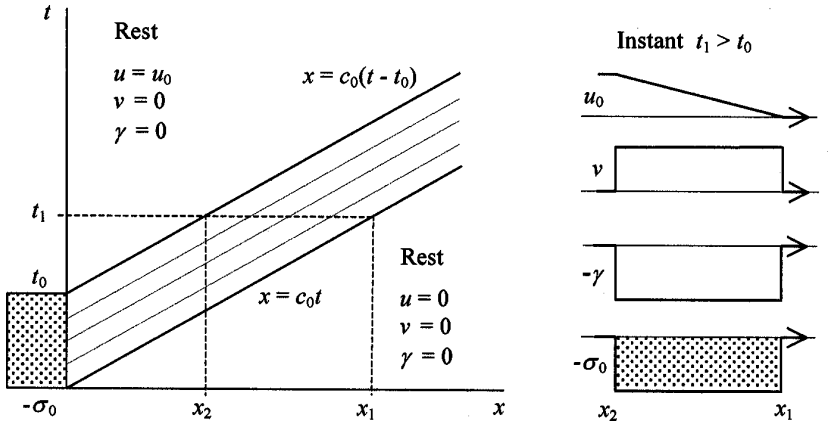

Figure 6.13: Propagation of stress pulse in an elastic rod.

At fixed instant t, it is linearly distributed along x. Its first derivatives with respect to space and time, the strain $\gamma < 0$ and the particle velocity $v > 0$, are constant, exhibiting a discontinuity at the wave front.

If the impact stress $-\sigma_0$ is applied in the form of a constant pulse of duration t_0, loading waves propagate from $x = 0$ until an unloading wave sets in at $t = t_0$ (Fig. 6.13). Superposition establishes a state of rest behind the second wave front which is defined by the line $x = c_0(t - t_0)$. As a result, the stress pulse propagates with velocity c_0 along the elastic rod.

The end $x = l$ of a rod of finite extension may be subject to various boundary conditions. For a fixed end the boundary condition reads

$$u(l,t) = 0, \quad v(l,t) = \left.\frac{\partial u}{\partial t}\right|_{x=l,t} = 0$$

and is seen to be satisfied by the superposition of a negative wave such that from the end

$$u = f(\chi - c_0 t) + g(\chi + c_0 t) \qquad (\chi = x - l). \tag{6.114}$$

The negative wave describes a reflection at the fixed end, and is defined by the property

$$g(\chi + c_0 t) = -f(-\chi - c_0 t),$$

which merely reverses the sign of wave and particle velocity. The nature of the wave (compressive, expansive) is not altered by the reflection.

At the fixed end ($\chi = x - l = 0$):

$$u(0,t) = f(-c_0 t) - f(-c_0 t) = 0$$

for the displacement, and

$$v(0,t) = \left.\frac{\partial u}{\partial t}\right|_{\chi=0,t} = -c_0 f'(-c_0 t) + c_0 f'(-c_0 t) = 0$$

for the velocity. The strain at reflection is

$$\gamma(0,t) = \left.\frac{\partial u}{\partial x}\right|_{\chi=0,t} = f'(-c_0 t) + f'(-c_0 t) = 2f'(-c_0 t)$$

and amounts to twice the value of the arriving wave. The same effect is experienced by the stress in the elastic solid.

A free end is characterized by the condition of a vanishing stress, and strain. Thus,

$$\gamma(l,t) = \left.\frac{\partial u}{\partial x}\right|_{x=l,t} = 0,$$

which can be effected by the superposition at $x = l$ of a negative wave in eqn (6.114) with the property

$$g(\chi + c_0 t) = f(-\chi - c_0 t).$$

This negative wave does not reverse the sign of the particle velocity. Therefore, compressive waves are reflected at the free end as expansion waves and vice versa.

The strain at the free end ($\chi = x - l = 0$) is obtained by

$$\gamma(0,t) = \left.\frac{\partial u}{\partial x}\right|_{\chi=0,t} = f'(-c_0 t) - f'(-c_0 t) = 0.$$

Velocity and displacement at the free end are deduced as

$$v(0,t) = \frac{\partial}{\partial t}(f+g)_{\chi=0,t} = -2c_0 f'(-c_0 t)$$

and

$$u(0,t) = f(-c_0 t) + g(c_0 t) = 2f(-c_0 t),$$

respectively. Reflection at the free end is seen to double the value of velocity and displacement pertaining to the arriving wave $u = f(x - c_0 t)$.

Propagation of elastic–plastic waves

Let the semi-infinite rod ($0 \le x \le \infty$) be made of elastoplastic material with elastic limit σ_s and a linear hardening characteristic (Fig. 6.14) described by the relations

$$\sigma = E\varepsilon \qquad \text{for} \quad |\sigma| \le \sigma_s,$$

$$\sigma = \frac{E}{E+h}(\sigma_s + h\gamma) \quad \text{for} \quad |\sigma| \ge \sigma_s.$$

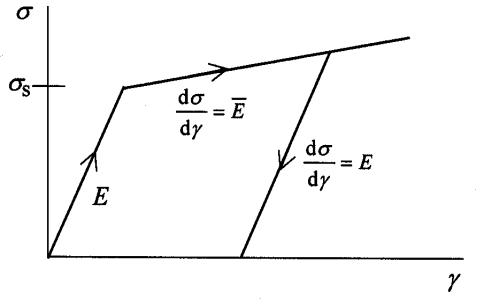

Figure 6.14: Linearly hardening elastoplastic material.

Application of an impact stress σ_0 not exceeding the range $-\sigma_s \le \sigma_0 \le \sigma_s$ induces an elastic wave which can be analysed as before. Suppose at time $t = 0$ the rod possesses a prestress $\sigma_0 = -\sigma_s$ equal to the elastic limit of the material. Application of an additional impact stress $-\sigma_{0\Delta}$ at $x = 0$, initiates a wave along the positive x-axis. Since the induced stress is beyond the elastic limit, we have $d\sigma/d\gamma = Eh/(E + h) = \bar{E}$.

In the linear hardening material the elastoplastic wave propagates with constant velocity $\bar{c} = (\bar{E}/\varrho)^{1/2} < c_0$, and can be described analogously to the previous elastic case. If the stress increment $-\sigma_{0\Delta}$ is a pulse of duration t_0, an unloading wave starts to propagate to the right at $x = 0, t = t_0$. Since unloading takes place elastically ($d\sigma/d\gamma = E$), the wave velocity is c_0. The faster elastic wave overtakes the elastoplastic one at

$$x = \frac{\bar{c}c_0}{c_0 - \bar{c}}t_0, \quad t = \frac{c_0}{c_0 - \bar{c}}t_0$$

and from then on the elastoplastic wave is eliminated.

An impact stress $-\sigma_0$ beyond the elastic limit ($|\sigma_0| > \sigma_s$) applied to the stress-free rod at $x = 0$, $t = 0$ originates two distinct deformation waves

$$u = -\frac{\sigma_s}{E}(x - c_0 t) - \frac{\sigma_0 - \sigma_s}{E}(x - \bar{c}t),$$

one propagating with the elastic wave speed c_0 and the other with the elastoplastic speed $\bar{c} < c_0$. With reference to the x, t-diagram (Fig. 6.15), the material is at rest below the line $x = c_0 t$ defining the position of the elastic wave front, and $\sigma = 0$ in this region. Below the line $x = \bar{c}t$ defining the position of the elastoplastic wave front, the elastic limit is not exceeded and $|\sigma| < \sigma_s$ here. Elastoplastic deformation occurs above the elastoplastic line, $x < \bar{c}t$. At the elastic and elastoplastic wave fronts the stress and the strain are discontinuous.

The elastoplastic wave extends with time according to $\bar{x} = \bar{c}t$, the elastic according to $x_0 = c_0 t$. The smaller the ratio $\bar{x}/x_0 = \bar{c}/c_0$, the flatter the hardening characteristic of the material. In the perfectly plastic case

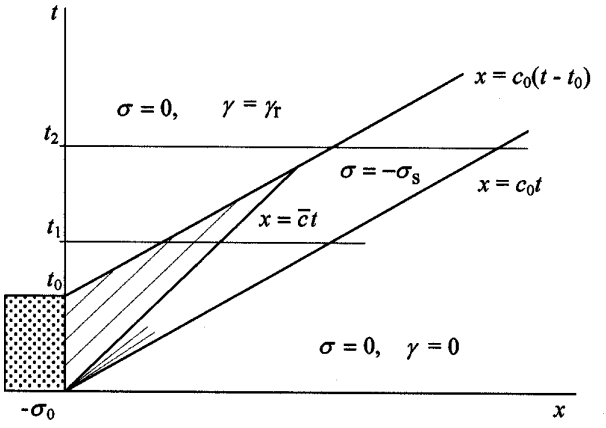

Figure 6.15: Elastic and elastoplastic wave.

$(\mathrm{d}\sigma/\mathrm{d}\gamma = 0)$, the speed of the elastoplastic wave vanishes as well as its extent $(\bar{c} = 0, \bar{x} = 0)$. As a consequence, only the strain associated with the limit stress σ_s is propagated by an elastic wave, while any deformation beyond the elastic limit cannot be transmitted along the rod but is localized at the point of application. If the material characteristic is curvilinear, several waves initiate as indicated in Fig. 6.15 by the fan from the origin.

In the case of a stress pulse of duration t_0, an unloading wave sets in at $x = 0$, $t = t_0$ and propagates with the elastic wave speed c_0. In front of the unloading wave the material state is that induced by the elastoplastic loading wave; behind the front the material is at rest. Since $c_0 > \bar{c}$, the unloading wave overtakes the elastoplastic loading wave. From then on, the pulse propagating along the rod is defined by the elastic loading and unloading fronts.

Nonlinear material

For completeness, we pay attention to issues concerning nonlinear materials for which the differential quotient $\mathrm{d}\sigma/\mathrm{d}\gamma$ depends on the strain γ, and therefore the wave speed is variable

$$c = c(\gamma)$$

The equation of motion, eqn (6.106), becomes nonlinear, and solutions are attempted by a linearization of the equivalent system in eqn (6.108) or its matrix form, eqn (6.109). To this end, the equations are decoupled by a transformation of variables. The spectral decomposition of the coefficient matrix $\mathbf{A}$ in eqn (6.109) gives

$$\mathbf{A} = \mathbf{C}\mathbf{\Lambda}\mathbf{C}^{-1}, \quad \mathbf{\Lambda} = \begin{bmatrix} c & 0 \\ 0 & -c \end{bmatrix}, \quad \mathbf{C} = \begin{bmatrix} c & c \\ 1 & -1 \end{bmatrix},$$

where the diagonal matrix $\mathbf{\Lambda}$ comprises the eigenvalues of $\mathbf{A}$ as the diagonal elements, and the matrix $\mathbf{C}$ is composed of the eigenvectors in its columns.

Utilization in eqn (6.109) supplies instead

$$\frac{\partial \boldsymbol{\xi}}{\partial t} - \boldsymbol{\Lambda}\frac{\partial \boldsymbol{\xi}}{\partial x} = \mathbf{0}, \tag{6.115}$$

which is a system of two differential equations for the transformed variables

$$\boldsymbol{\xi} = 2c\mathbf{C}^{-1}\mathbf{v} \quad \text{or} \quad \begin{bmatrix} \xi \\ \eta \end{bmatrix} = \begin{bmatrix} 1 & c \\ 1 & -c \end{bmatrix} \begin{bmatrix} v \\ \gamma \end{bmatrix}.$$

Since the coefficient matrix $\boldsymbol{\Lambda}$ in eqn (6.115) is diagonal, the two differential equations are uncoupled. Because of $c(\gamma)$, the system is nonlinear. It can be linearized by an inversion (or interchange) of dependent and independent variables. It then assumes the form

$$\frac{\partial x}{\partial \xi} - c\frac{\partial t}{\partial \xi} = 0, \quad \frac{\partial x}{\partial \eta} + c\frac{\partial t}{\partial \eta} = 0, \tag{6.116}$$

known as the canonical system. The canonical system is not equivalent to the original one in eqn (6.108). The reason is that the inversion of the variables requires a non-zero functional determinant,

$$\Delta = \begin{vmatrix} \dfrac{\partial \xi}{\partial x} & \dfrac{\partial \xi}{\partial t} \\ \dfrac{\partial \eta}{\partial x} & \dfrac{\partial \eta}{\partial t} \end{vmatrix} \neq 0,$$

and thereby solutions pertaining to $\Delta = 0$ are lost. These solutions are known as simple waves; they can be constructed by a discussion of the condition

$$\Delta(\xi, \eta) = 2c\frac{\partial \xi}{\partial x}\frac{\partial \eta}{\partial x} = -\frac{2}{c}\frac{\partial \xi}{\partial t}\frac{\partial \eta}{\partial t} = 0. \tag{6.117}$$

The expressions in eqn (6.117) are obtained with the aid of eqn (6.115), and reveal that the following cases satisfy the equation:

(i) $\xi =$ constant and $\eta =$ constant;
(ii) $\xi =$ constant or $\eta =$ constant.

A further analysis is not within the scope of this text but it can be found in [10]. In summary, it can be stated that in an elastoplastic material the velocity of propagation of waves starts at the elastic c_0 and decreases as deformation increases beyond the elastic limit. Since higher strains are transmitted with lower velocities by the material, a constant impact stress $|\sigma_0| > \sigma_\mathrm{s}$ (or strain) will not propagate as applied (Fig. 6.16). The elastic wave produces a discontinuous front defined by $|\sigma| = \sigma_\mathrm{s}$, while the overstress $|\sigma_0 - \sigma_\mathrm{s}|$ (or overstrain) attains a smooth distribution along the axis of the rod. This is a consequence of the lower signal velocity pertaining to each higher stress (or strain), which can be concluded from an extended discussion of the linearly hardening material.

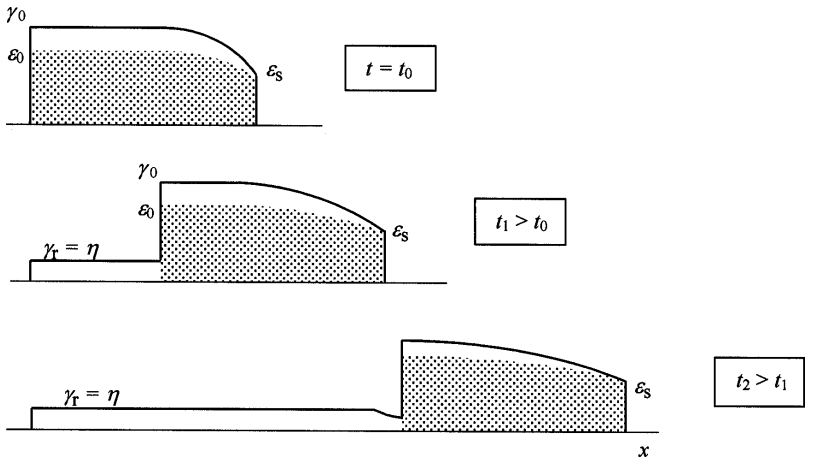

Figure 6.16: Distortion of impact stress profile propagating in nonlinear material

For the inversion of the variables to $x = x(\xi, \eta)$, $t = t(\xi, \eta)$ consider the functional dependence

$$\boldsymbol{\xi} = \boldsymbol{\xi}(\mathbf{x}) \quad \text{with} \quad \mathbf{x} = \begin{bmatrix} x \\ t \end{bmatrix}, \quad \boldsymbol{\xi} = \begin{bmatrix} \xi \\ \eta \end{bmatrix}.$$

Differentiating, we verify the identity

$$\mathrm{d}\boldsymbol{\xi} = \frac{\mathrm{d}\boldsymbol{\xi}}{\mathrm{d}\mathbf{x}}\mathrm{d}\mathbf{x} = \frac{\mathrm{d}\boldsymbol{\xi}}{\mathrm{d}\mathbf{x}}\frac{\mathrm{d}\mathbf{x}}{\mathrm{d}\boldsymbol{\xi}}\mathrm{d}\boldsymbol{\xi} \quad \text{or} \quad \frac{\mathrm{d}\boldsymbol{\xi}}{\mathrm{d}\mathbf{x}}\frac{\mathrm{d}\mathbf{x}}{\mathrm{d}\boldsymbol{\xi}} = \mathbf{I}.$$

This provides us with an equation for the partial derivatives in the matrix $\mathrm{d}\mathbf{x}/\mathrm{d}\boldsymbol{\xi}$:

$$\begin{bmatrix} \dfrac{\partial \xi}{\partial x} & \dfrac{\partial \xi}{\partial t} \\ \dfrac{\partial \eta}{\partial x} & \dfrac{\partial \eta}{\partial t} \end{bmatrix} \begin{bmatrix} \dfrac{\partial x}{\partial \xi} & \dfrac{\partial x}{\partial \eta} \\ \dfrac{\partial t}{\partial \xi} & \dfrac{\partial t}{\partial \eta} \end{bmatrix} = \begin{bmatrix} 1 & 0 \\ 0 & 1 \end{bmatrix}.$$

The solution is

$$\begin{bmatrix} \dfrac{\partial x}{\partial \xi} & \dfrac{\partial x}{\partial \eta} \\ \dfrac{\partial t}{\partial \xi} & \dfrac{\partial t}{\partial \eta} \end{bmatrix} = \frac{1}{\Delta} \begin{bmatrix} \dfrac{\partial \eta}{\partial t} & -\dfrac{\partial \xi}{\partial t} \\ -\dfrac{\partial \eta}{\partial x} & \dfrac{\partial \xi}{\partial x} \end{bmatrix}$$

and relies on a non-zero functional determinant ($\Delta \neq 0$). The components of the vector quantities $\partial\boldsymbol{\xi}/\partial t$, $\partial\boldsymbol{\xi}/\partial x$ in eqn (6.115) are

$$\begin{bmatrix} \dfrac{\partial \xi}{\partial t} \\ \dfrac{\partial \eta}{\partial t} \end{bmatrix} = \Delta \begin{bmatrix} -\dfrac{\partial x}{\partial \eta} \\ \dfrac{\partial x}{\partial \xi} \end{bmatrix}, \quad \begin{bmatrix} \dfrac{\partial \xi}{\partial x} \\ \dfrac{\partial \eta}{\partial x} \end{bmatrix} = \Delta \begin{bmatrix} \dfrac{\partial t}{\partial \eta} \\ -\dfrac{\partial t}{\partial \xi} \end{bmatrix},$$

and substitution leads to the linearized differential system of eqn (6.116).

Unloading wave
From the above, even a constant impact on an elastoplastic rod induces variations of stress and strain along the axis behind the discontinuous wave front. A pulse will initiate unloading at $x = 0$, $t = t_0$ which propagates as an elastic wave through previously strained regions of the rod.

The changes in stress and strain by the unloading are elastic,

$$\sigma - \sigma_{\mathrm{f}} = E(\gamma - \gamma_{\mathrm{f}}).$$

Here σ_{f} and γ_{f} refer to the plastic state at the instant before unloading, and are to be considered as functions of the location x along the rod. This is significant for the stress term in eqn (6.105) for the motion:

$$\frac{\partial \sigma}{\partial x} = E\frac{\partial \gamma}{\partial x} + \frac{\partial}{\partial x}(\sigma_{\mathrm{f}} - E\gamma_{\mathrm{f}}),$$

and instead of the homogeneous eqn (6.106) one obtains

$$\frac{\partial^2 u}{\partial t^2} - c_0^2 \frac{\partial^2 u}{\partial x^2} = \frac{1}{\varrho}\frac{\partial}{\partial x}(\sigma_{\mathrm{f}} - E\gamma_{\mathrm{f}}). \tag{6.118}$$

The unloading wave is thus governed by an inhomogeneous differential equation with the right-hand side known from the solution for the elastoplastic loading wave.

Three-dimensional continuum
The equations of motion for the three-dimensional continuum can be obtained from the equations of static equilibrium by simply considering the inertia force $-\varrho\ddot{\mathbf{u}}$ in addition to any other applied body forces. The matrix form of the equation of motion as from eqn (2.61) reads

$$\boldsymbol{\partial}^{\mathrm{t}}\boldsymbol{\sigma} + [\mathbf{f} - \varrho\ddot{\mathbf{u}}] = \mathbf{0}. \tag{6.119}$$

It is a collective representation of the component equations

$$\frac{\partial \sigma_{\mathrm{xx}}}{\partial x} + \frac{\partial \sigma_{\mathrm{yx}}}{\partial y} + \frac{\partial \sigma_{\mathrm{zx}}}{\partial z} + \left(f_{\mathrm{x}} - \varrho\frac{\partial^2 u}{\partial t^2}\right) = 0,$$

$$\frac{\partial \sigma_{\mathrm{xy}}}{\partial x} + \frac{\partial \sigma_{\mathrm{yy}}}{\partial y} + \frac{\partial \sigma_{\mathrm{zy}}}{\partial z} + \left(f_{\mathrm{y}} - \varrho\frac{\partial^2 v}{\partial t^2}\right) = 0,$$

$$\frac{\partial \sigma_{\mathrm{xz}}}{\partial x} + \frac{\partial \sigma_{\mathrm{yz}}}{\partial y} + \frac{\partial \sigma_{\mathrm{zz}}}{\partial z} + \left(f_{\mathrm{z}} - \varrho\frac{\partial^2 w}{\partial t^2}\right) = 0,$$

cf. eqn (2.55). The partial derivatives with respect to time are taken for fixed particles, which are usually defined by their spatial coordinates in the undeformed solid. Since deformations are assumed to be infinitesimally small, they do not affect the particle position. Also, the density ϱ is assumed

to be independent of deformation, but it may vary within an inhomogeneous solid, $\varrho = \varrho(\mathbf{x})$.

The body forces and the surface forces are defined as functions of time, $\mathbf{f}(t)$ and $\mathbf{t}(t)$, as are any kinematic boundary conditions. Here, not only the displacement $\mathbf{u}$, but also the velocity $\dot{\mathbf{u}}$ and acceleration $\ddot{\mathbf{u}}$ can be subject to restrictions during the course of the motion. In addition to the boundary conditions, definition of the transient problem requires specification of the state of motion at time $t = 0$ by initial conditions for the displacement or the velocity in the solid.

6.4.2 Finite element solution

Instead of a discussion on possible analytical solutions for particular cases, we describe the extension of the numerical finite element approach (Chapter 5) to dynamic analysis. It is noticed that the inertia forces have to be accounted for in the formulation of the virtual work principle. They modify eqn (5.1) to:

$$\sum_{l=1}^{K} \underset{\sim}{\mathbf{u}}_l^{\mathrm{t}} \mathbf{P}_l + \int_S \underset{\sim}{\mathbf{u}}^{\mathrm{t}} \mathbf{t} \mathrm{d}S + \int_V \underset{\sim}{\mathbf{u}}^{\mathrm{t}} \mathbf{f} \mathrm{d}V = \int_V \underset{\sim}{\boldsymbol{\gamma}}^{\mathrm{t}} \boldsymbol{\sigma} \mathrm{d}V + \int_V \varrho \underset{\sim}{\mathbf{u}}^{\mathrm{t}} \ddot{\mathbf{u}} \mathrm{d}V, \tag{6.120}$$

which refers to instant t, all variables representing functions of time.

The displacement $\mathbf{u}$ is a function of spatial position and time. This can be stated explicitly in the formalism of the finite element kinematics in eqn (5.6) by writing

$$\mathbf{u}(\mathbf{x}, t) = \boldsymbol{\omega}(\mathbf{x}) \mathbf{U}_q(t). \tag{6.121}$$

The separation of the spatial and temporal variables via the product form in eqn (6.121) has been presumed implicitly in previous parts of the text. It ensures that time derivatives (velocity $\dot{\mathbf{u}}$ and acceleration $\ddot{\mathbf{u}}$) are distributed within the finite element by the same functions $\boldsymbol{\omega}(\mathbf{x})$ as the displacements $\mathbf{u}$.

The inertia term in eqn (6.120) modifies the quasistatic eqn (5.19) to

$$\mathbf{P}(t) = \mathbf{S} + \mathbf{M}\ddot{\mathbf{U}}, \tag{6.122}$$

which is the equation of motion for the finite element system. The symmetric matrix,

$$\mathbf{M} = \sum_{q=1}^{nel} \mathbf{a}_q^{\mathrm{t}} \mathbf{m}_q \mathbf{a}_q = \mathbf{a}^{\mathrm{t}} \mathbf{m} \mathbf{a},$$

$$\mathbf{m} = \begin{bmatrix} \ddots & & \\ & \mathbf{m}_q & \\ & & \ddots \end{bmatrix} \qquad (q = 1, \ldots, nel),$$

is the mass matrix of the finite element system. It is composed of the element contributions

$$\mathbf{m}_q = \int_{V_q} \varrho \boldsymbol{\omega}^{\mathrm{t}} \boldsymbol{\omega} \mathrm{d}V. \tag{6.123}$$

A numerical analysis of dynamic problems in elastoplasticity is based on the incremental integration of the equations of motion with respect to time. For transition from instant t_n to t_{n+1} separated by the incremental step τ, an approximate integration can be performed by the scheme:

$$\begin{aligned} &\text{Acceleration} \quad \ddot{\mathbf{U}}_{n+1} \\ &\text{Velocity} \quad \dot{\mathbf{U}}_{n+1} = \dot{\mathbf{U}}_n + \tau \left[a_1 \ddot{\mathbf{U}}_n + a_2 \ddot{\mathbf{U}}_{n+1} \right] \\ &\text{Displacement} \quad \mathbf{U}_{n+1} = \mathbf{U}_n + \tau \dot{\mathbf{U}}_n + \tau^2 \left[b_1 \ddot{\mathbf{U}}_n + b_2 \ddot{\mathbf{U}}_{n+1} \right]. \end{aligned} \tag{6.124}$$

The four coefficients a_1, a_2, b_1, b_2 can be selected such that various time integration schemes known in the literature ([11, 12]) are reproduced. Their specification influences the numerical properties of the approximation.

The numerical analysis of the dynamic problem starts at state $t = t_0$ with given initial conditions. In an implicit integration scheme the equation of motion, eqn (6.122), is stated at each subsequent instant t_{n+1}, and the residual form

$$\mathbf{R}(\ddot{\mathbf{U}}_{n+1}) = \mathbf{P}_{n+1} - \mathbf{S}_{n+1} - \mathbf{M}\ddot{\mathbf{U}}_{n+1} = \mathbf{0} \tag{6.125}$$

is solved. An iterative solution technique can be based on the instruction

$$\ddot{\mathbf{U}}_{n+1,i+1} = \ddot{\mathbf{U}}_{n+1,i} - \left[\frac{\mathrm{d}\mathbf{R}}{\mathrm{d}\ddot{\mathbf{U}}} \right]_i^{-1} \mathbf{R}\left(\ddot{\mathbf{U}}_{n+1,i} \right), \tag{6.126}$$

for the transition from the ith iteration to iteration $i + 1$. Execution requires computation of the residual vector $\mathbf{R}(\ddot{\mathbf{U}}_{n+1})$ and of the gradient matrix $\mathrm{d}\mathbf{R}/\mathrm{d}\ddot{\mathbf{U}}$ of the system, or an approximation to it.

The residual vector in eqn (6.125) comprises the inertia forces

$$\mathbf{M}\ddot{\mathbf{U}} = \begin{bmatrix} \cdots & \mathbf{a}_q^{\mathrm{t}} & \cdots \end{bmatrix} \begin{bmatrix} \vdots \\ \mathbf{m}_q \ddot{\mathbf{U}}_q \\ \vdots \end{bmatrix} \qquad (q = 1, \ldots, nel)$$

as an additional entry to the static case. They are computed by element contributions with $\ddot{\mathbf{U}}_{q,n+1} = \mathbf{a}_q \ddot{\mathbf{U}}_{n+1}$ from the ith iteration cycle. The computation of the stress resultants $\mathbf{S}_{n+1}$ utilizes quasistatic procedures for elastoplasticity, creep or viscoplasticity. The incremental displacement $\mathbf{U}_\Delta = \mathbf{U}_{n+1} - \mathbf{U}_n$, required as an input for $\mathbf{S}_{n+1}$, is obtained by the approximation of eqn (6.124) using the $\ddot{\mathbf{U}}_{n+1}$ currently available.

The gradient of the residual function $\mathbf{R}(\ddot{\mathbf{U}}_{n+1})$, eqn (6.125), is deduced as

$$\frac{\mathrm{d}\mathbf{R}}{\mathrm{d}\ddot{\mathbf{U}}_{n+1}} = -\frac{\mathrm{d}\mathbf{S}_{n+1}}{\mathrm{d}\mathbf{U}_{n+1}}\frac{\mathrm{d}\mathbf{U}_{n+1}}{\mathrm{d}\ddot{\mathbf{U}}_{n+1}} - \mathbf{M} = -\tau^2 b_2 \frac{\mathrm{d}\mathbf{S}_{n+1}}{\mathrm{d}\mathbf{U}_{n+1}} - \mathbf{M}.$$

In obtaining the gradient, the applied forces $\mathbf{P}_{n+1}$ at instant t_{n+1} are assumed to be fixed, and use has been made of eqn (6.124) for the displacement $\mathbf{U}_{n+1}$. Approximations to the differential quotient $\mathrm{d}\mathbf{S}_{n+1}/\mathrm{d}\mathbf{U}_{n+1}$ are as in eqn (6.43) for the quasistatic analysis.

More sophisticated integration schemes employ higher order time derivatives. Instead of the acceleration and higher order time derivatives of the motion it is more convenient to work with the inertia forces and their time rates

$$\mathbf{F} = \mathbf{M}\ddot{\mathbf{U}} = \mathbf{P} - \mathbf{S}, \quad \dot{\mathbf{F}} = \dot{\mathbf{P}} - \dot{\mathbf{S}}.$$

With regard to the right-hand side of the equation for $\dot{\mathbf{F}}$, inclusion of higher order derivatives of the inertia forces does not appear reasonable. An accurate representation of both the applied loading and the internal stress term will present a difficult task.

Under the above aspect, approximations for the velocity and displacement at the end of the time increment will be accommodated in the scheme

$$\dot{\mathbf{U}}_{n+1} = \dot{\mathbf{U}}_n + \tau\mathbf{M}^{-1}\left[a_1\mathbf{F}_n + a_2\dot{\mathbf{F}}_n + a_3\mathbf{F}_{n+1} + a_4\dot{\mathbf{F}}_{n+1}\right],$$

$$\mathbf{U}_{n+1} = \mathbf{U}_n + \tau\dot{\mathbf{U}}_n + \tau^2\mathbf{M}^{-1}\left[b_1\mathbf{F}_n + b_2\dot{\mathbf{F}}_n + b_3\mathbf{F}_{n+1} + b_4\dot{\mathbf{F}}_{n+1}\right].$$

The coefficients $a_1, \ldots, a_4$ and $b_1, \ldots, b_4$ may express independent approximations of velocity and displacement in terms of the accelerations at the beginning and the end of the time increment, or can be consistently derived for an assumed variation of the acceleration (or the inertia force) within the increment. For a systematic exposition we refer to [11]. Here, illustrative examples are given following [13] with reference to Fig. 6.17.

A linear Taylor expansion of the inertia force

$$\mathbf{F}(\zeta) = \mathbf{F}_n + \zeta\tau\dot{\mathbf{F}}_n \quad (0 \le \zeta \le 1)$$

as a function of the normalized temporal variable $\zeta = (t - t_n)/\tau$, gives by integration

$$\dot{\mathbf{U}}_{n+1} = \dot{\mathbf{U}}_n + \tau\mathbf{M}^{-1}\left[\mathbf{F}_n + \frac{\tau}{2}\dot{\mathbf{F}}_n\right],$$

$$\mathbf{U}_{n+1} = \mathbf{U}_n + \tau\dot{\mathbf{U}}_n + \frac{\tau^2}{2}\mathbf{M}^{-1}\left[\mathbf{F}_n + \frac{\tau}{3}\dot{\mathbf{F}}_n\right].$$

Taylor expansions are based on values at the beginning of the time increment and lead to explicit forms of the integration scheme. Implicit variants can be obtained by Hermitean approximations [14] which employ sets of values at both the beginning and the end of the increment (Fig. 6.17). A linear Hermitean approximation of the inertia force (or acceleration) in the increment

$$\mathbf{F}(\zeta) = (1 - \zeta)\mathbf{F}_n + \zeta\mathbf{F}_{n+1},$$

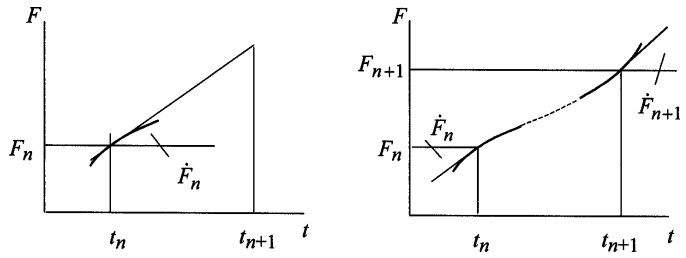

Figure 6.17: Taylor expansion of the inertia force (left) and Hermitean approximation (right).

gives for velocity and displacement the expressions

$$\dot{\mathbf{U}}_{n+1} = \dot{\mathbf{U}}_n + \frac{\tau}{2}\mathbf{M}^{-1}\left[\mathbf{F}_n + \mathbf{F}_{n+1}\right],$$

$$\mathbf{U}_{n+1} = \mathbf{U}_n + \tau\dot{\mathbf{U}}_{n+1} + \frac{\tau^2}{6}\mathbf{M}^{-1}\left[2\mathbf{F}_n + \mathbf{F}_{n+1}\right].$$

This is also covered by the general integration scheme, the respective coefficients a_1–a_4 and b_1–b_4 reproducing Newmark's linear acceleration method [15].

The next higher Hermitean polynomial is of the third degree in time:

$$\mathbf{F}(\zeta) = (1 - 3\zeta^2 + 2\zeta^3)\mathbf{F}_n + (\zeta - 2\zeta^2 + \zeta^3)\tau\dot{\mathbf{F}}_n + (3\zeta^2 - 2\zeta^3)\mathbf{F}_{n+1} + (-\zeta^2 + \zeta^3)\tau\dot{\mathbf{F}}_{n+1}.$$

It leads to velocity and displacement as follows

$$\dot{\mathbf{U}}_{n+1} = \dot{\mathbf{U}}_n + \frac{\tau}{12}\mathbf{M}^{-1}\left[6\mathbf{F}_n + \tau\dot{\mathbf{F}}_n + 6\mathbf{F}_{n+1} - \tau\dot{\mathbf{F}}_{n+1}\right],$$

$$\mathbf{U}_{n+1} = \mathbf{U}_n + \tau\dot{\mathbf{U}}_n + \frac{\tau^2}{60}\mathbf{M}^{-1}\left[21\mathbf{F}_n + 3\tau\dot{\mathbf{F}}_n + 9\mathbf{F}_{n+1} - 2\tau\dot{\mathbf{F}}_{n+1}\right],$$

and can be represented by the general integration scheme with an appropriate specification of the coefficients a_1–a_4 and b_1–b_4.

The numerical applications presented subsequently in the text utilize the cubic Hermitean approximation of the acceleration as above. Since the scheme is based on both $\mathbf{F} = \mathbf{M}\ddot{\mathbf{U}}$ and $\dot{\mathbf{F}}$, it requires solution of the rate equation

$$\dot{\mathbf{P}}_{n+1} - \dot{\mathbf{S}}_{n+1} - \dot{\mathbf{F}}_{n+1} = \mathbf{0}$$

at instant t_{n+1} in addition to eqn (6.125) for the motion. Here, the time rate of the applied forces has to be derived from their functional dependence on time, that of the stress resultants relies on the rate form of the stress–strain relations.

Cosine pulse in elastoplastic free rod

The following example demonstrates a simple application of the finite element technique and illustrates propagation of uniaxial elastoplastic waves. The description follows the original numerical study by the author included in [16]. The example has been conceived such that the rod has a length

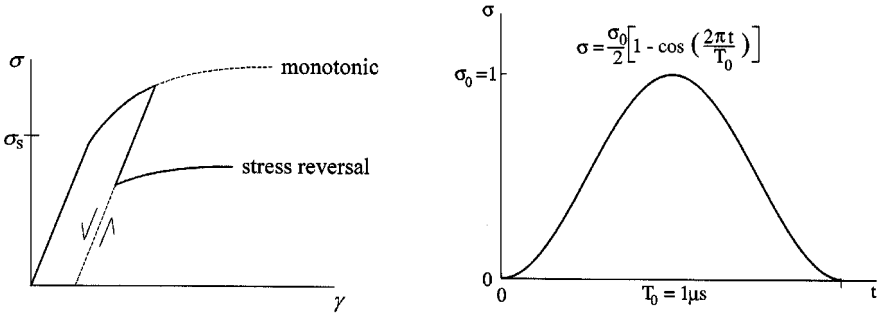

Figure 6.18: Cosine pulse and elastoplastic properties.

of $l = 0.4$ units, unit cross-section and unit density. The elastic modulus amounts to $E = 2.25 \cdot 10^{10}$, the initial yield stress is $\sigma_s = 0.75$. The plastic behaviour of the material is specified by a monotonic stress–plastic strain dependence in conjunction with kinematic hardening under stress reversal (Fig. 6.18). The stress pulse applied at the left end of the rod is characterized by a cosine shape of duration $T_0 = 1\,\mu s$ and magnitude $\sigma_0 = 1$ exceeding the elastic limit of the material. Figure 6.19 demonstrates the stress distribution in the elastoplastic rod at $2\,\mu s$ after initiation of the impact. The agreement between the coarser and finer discretizations in space and time is good.

Figure 6.20 illustrates the effect of plasticity by comparing with the elastic wave. The elastic solution is easily confirmed. The elastoplastic solution shows the interaction of several phenomena. At $2\,\mu s$, hardening has allowed

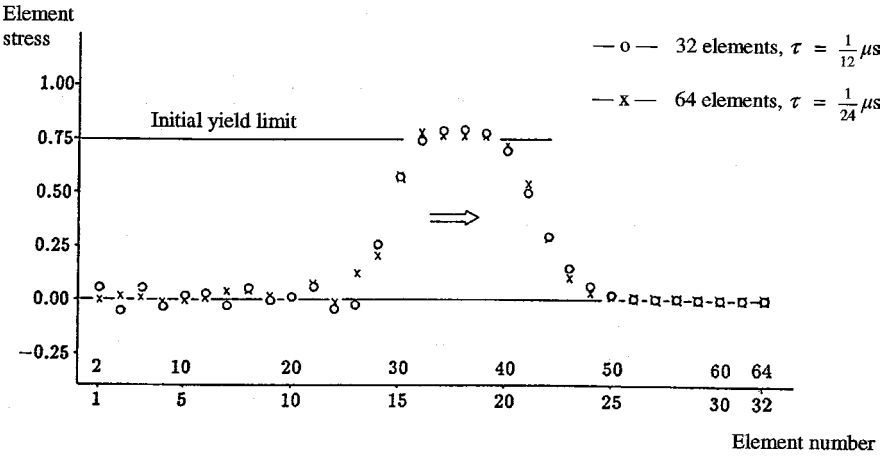

Figure 6.19: Results after $2\,\mu s$ for two different discretizations in space and time.

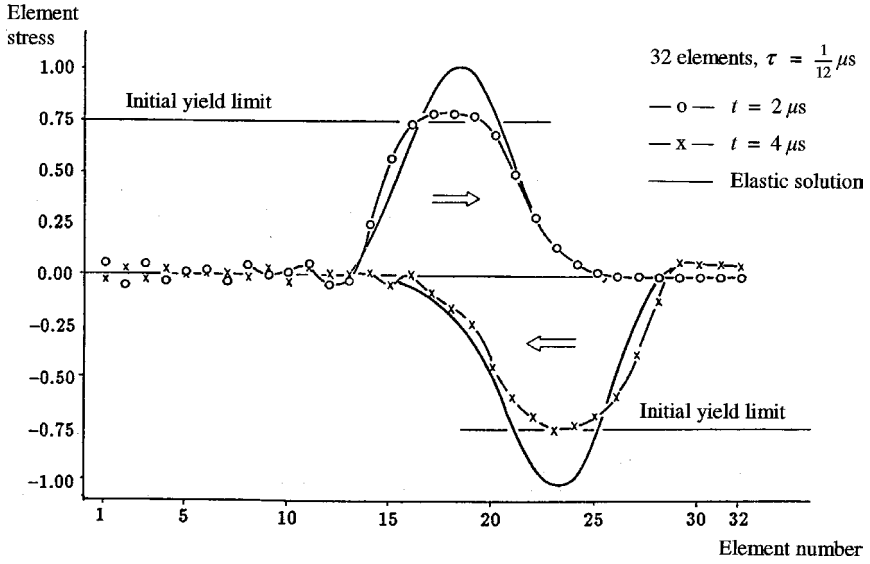

Figure 6.20: Elastoplastic vs elastic solution after 2 and 4 μs.

the stress to increase beyond the initial yield stress of the material, but this is limited by the unloading part of the stress pulse which sets in after 0.5 μs. In addition, the profile of the pulse is distorted due to the slower wave motion in the elastoplastic range.

After reflection at the other free end of the rod, the yield stress is diminished below the initial value by the kinematic hardening rule. The state after 4 μs shows that the front of the reflected wave propagates as the elastic one. The rising stress–plastic strain characteristic allows the stress to exceed the new yield stress ($\sigma_f < \sigma_s$), while elastic unloading moderates this effect. The distortion of the profile by the delaying elastoplastic motion is visible.

6.5 Pressure sensitive materials

6.5.1 Porous solids

Introductory remarks

The development of modern powder-metallurgy alloys aims at the achievement of properties superior to those found in alloys produced by ingot metallurgy. The employment of products of this type in engineering necessitates the description of their mechanical behaviour. The plastic behaviour of ductile porous materials, such as sintered or hot-pressed metal powders, is sensitive to the hydrostatic stress. This sensitivity requires a modification of the yield condition, on the one hand, and implies permanent changes in volume, on the other hand.

We consider elastoplastic deformation of an isotropic solid which contains microscopic pores distributed homogeneously within the basic matrix material. The local pore volume fraction (porosity)

$$\chi = \frac{V - V_\mathrm{o}}{V} \quad (0 \le \chi \le 1)$$

relates the pore volume $(V - V_\mathrm{o})$ to the volume V of the material element. The solid matrix occupies the volume V_o with fraction $(1 - \chi)$. The constitutive description of such a solid is attempted by suitable modification of standard relations. The yield condition for the porous material may be formally stated as

$$\phi(\bar{\sigma}, \sigma_\mathrm{H}, \sigma_\mathrm{f}, \chi) \le 0.$$

Here, the yield function ϕ depends on the equivalent deviatoric stress $\bar{\sigma}$ and the hydrostatic stress σ_H. The parameters σ_f and χ are the actual yield stress of the solid matrix and the porosity, respectively. For vanishing porosity $(\chi = 0)$ the yield function must reproduce that of the compact material. From the consistency condition $(\mathrm{d}\phi = 0)$ during plastic flow

$$\frac{\partial \phi}{\partial \bar{\sigma}} \mathrm{d}\bar{\sigma} + \frac{\partial \phi}{\partial \sigma_\mathrm{H}} \mathrm{d}\sigma_\mathrm{H} = -\frac{\partial \phi}{\partial \sigma_\mathrm{f}} \mathrm{d}\sigma_\mathrm{f} - \frac{\partial \phi}{\partial \chi} \mathrm{d}\chi.$$

Plastic flow is assumed to obey the normality rule

$$\mathrm{d}\boldsymbol{\eta} = \Lambda \left[\frac{\partial \phi}{\partial \boldsymbol{\sigma}} \right]^\mathrm{t} = \Lambda \left[\frac{\partial \phi}{\partial \bar{\sigma}} \mathbf{s} + \frac{1}{3} \frac{\partial \phi}{\partial \sigma_\mathrm{H}} \mathbf{e} \right].$$

In

$$\left[\frac{\partial \boldsymbol{\phi}}{\partial \boldsymbol{\sigma}} \right]^\mathrm{t} = \left[\frac{\partial \phi}{\partial \bar{\sigma}} \frac{\mathrm{d}\bar{\sigma}}{\mathrm{d}\boldsymbol{\sigma}} + \frac{\partial \phi}{\partial \sigma_\mathrm{H}} \frac{\mathrm{d}\sigma_\mathrm{H}}{\mathrm{d}\boldsymbol{\sigma}} \right]^\mathrm{t},$$

the expressions $\mathrm{d}\bar{\sigma}/\mathrm{d}\boldsymbol{\sigma}^\mathrm{t} = (3/2\bar{\sigma})\boldsymbol{\sigma}_\mathrm{D} = \mathbf{s}$, $\mathrm{d}\sigma_\mathrm{H}/\mathrm{d}\boldsymbol{\sigma}^\mathrm{t} = (1/3)\mathbf{e}$ have been substituted for the differential quotients. The vectors $\mathbf{s}$ and $\mathbf{e}$ are orthogonal. The deviatoric and volumetric parts of the plastic strain increment can be distinguished as follows:

$$\mathrm{d}\boldsymbol{\eta}_\mathrm{D} = \Lambda \frac{\partial \phi}{\partial \bar{\sigma}} \mathbf{s}, \qquad \mathrm{d}\boldsymbol{\eta}_\mathrm{V} = \frac{\Lambda}{3} \frac{\partial \phi}{\partial \sigma_\mathrm{H}} \mathbf{e}.$$

The permanent change in volume is associated with a modified porosity:

$$\mathrm{d}\chi = (1 - \chi)\mathbf{e}^\mathrm{t} \mathrm{d}\boldsymbol{\eta} = (1 - \chi)\Lambda \frac{\partial \phi}{\partial \sigma_\mathrm{H}}.$$

Hardening of the solid matrix material implies a dependence $\sigma_{\rm f}(\bar{\eta}_{\rm o})$ of the flow stress on the equivalent plastic strain $\bar{\eta}_{\rm o}$ in the matrix. For incremental variations

$$\mathrm{d}\sigma_{\rm f} = h_{\rm o}\mathrm{d}\bar{\eta}_{\rm o} = \frac{h_{\rm o}}{(1-\chi)\sigma_{\rm f}}\boldsymbol{\sigma}^{\rm t}\mathrm{d}\boldsymbol{\eta},$$

where $h_{\rm o}$ denotes the uniaxial hardening parameter. The matrix material (index 'o') is assumed to undergo isochoric plastic flow governed by the conventional von Mises yield condition. The transition to the second expression makes use of the equivalence

$$\boldsymbol{\sigma}^{\rm t}\mathrm{d}\boldsymbol{\eta} = (1-\chi)\bar{\sigma}_{\rm o}\mathrm{d}\bar{\eta}_{\rm o} \quad (\bar{\sigma}_{\rm o} = \sigma_{\rm f}),$$

which states that the plastic work referred to the porous solid is a result of the plastic flow in the compact matrix with volume fraction $(1-\chi)$.

Substituting the expressions for the hardening ($\mathrm{d}\sigma_{\rm f}$) and change in porosity ($\mathrm{d}\chi$) along with the flow rule for $\mathrm{d}\boldsymbol{\eta}$ in the consistency condition, we deduce the proportionality factor Λ as

$$\Lambda = \frac{1}{h}\left(\frac{\partial\phi}{\partial\bar{\sigma}}\mathrm{d}\bar{\sigma} + \frac{\partial\phi}{\partial\sigma_{\rm H}}\mathrm{d}\sigma_{\rm H}\right) = \frac{1}{h}\frac{\partial\phi}{\partial\boldsymbol{\sigma}}\mathrm{d}\boldsymbol{\sigma} = \frac{1}{h^*}\frac{\partial\phi}{\partial\boldsymbol{\sigma}}\boldsymbol{\kappa}\mathrm{d}\boldsymbol{\gamma} \geq 0.$$

The last expression in terms of the strain increment implies the use of the elasticity relation $\mathrm{d}\boldsymbol{\sigma} = \boldsymbol{\kappa}[\mathrm{d}\boldsymbol{\gamma} - \mathrm{d}\boldsymbol{\eta}]$. In addition, we have introduced the abbreviations,

$$h = -\frac{h_{\rm o}}{(1-\chi)\sigma_{\rm f}}\left(\frac{\partial\phi}{\partial\bar{\sigma}}\bar{\sigma} + \frac{\partial\phi}{\partial\sigma_{\rm H}}\sigma_{\rm H}\right)\frac{\partial\phi}{\partial\sigma_{\rm f}} - (1-\chi)\frac{\partial\phi}{\partial\sigma_{\rm H}}\frac{\partial\phi}{\partial\chi}$$

and

$$h^* = h + \frac{\partial\phi}{\partial\boldsymbol{\sigma}}\boldsymbol{\kappa}\left[\frac{\partial\phi}{\partial\boldsymbol{\sigma}}\right]^{\rm t}.$$

This completes the determination of the plastic strain increment

$$\mathrm{d}\boldsymbol{\eta} = \frac{1}{h}\left[\frac{\partial\phi}{\partial\boldsymbol{\sigma}}\right]^{\rm t}\frac{\partial\phi}{\partial\boldsymbol{\sigma}}\mathrm{d}\boldsymbol{\sigma} = \frac{1}{h^*}\left[\frac{\partial\phi}{\partial\boldsymbol{\sigma}}\right]^{\rm t}\frac{\partial\phi}{\partial\boldsymbol{\sigma}}\boldsymbol{\kappa}\mathrm{d}\boldsymbol{\gamma}.$$

In conjunction with the elastic stress–strain relation we obtain

$$\mathrm{d}\boldsymbol{\gamma} = \left\{\boldsymbol{\kappa}^{-1} + \frac{1}{h}\left[\frac{\partial\phi}{\partial\boldsymbol{\sigma}}\right]^{\rm t}\frac{\partial\phi}{\partial\boldsymbol{\sigma}}\right\}\mathrm{d}\boldsymbol{\sigma}$$

between incremental stress and incremental strain. The inverse reads

$$\mathrm{d}\boldsymbol{\sigma} = \left\{\boldsymbol{\kappa} - \frac{1}{h^*}\boldsymbol{\kappa}\left[\frac{\partial\phi}{\partial\boldsymbol{\sigma}}\right]^{\rm t}\frac{\partial\phi}{\partial\boldsymbol{\sigma}}\boldsymbol{\kappa}\right\}\mathrm{d}\boldsymbol{\gamma}.$$

The formalism follows [17] and is suitable to $\partial\phi/\partial\sigma_{\mathrm{f}} = -1$. In this case, the hardening parameter h reduces to h_{o} of the compact solid for $\chi = 0$ and $\partial\phi/\partial\chi = 0$. In the porous solid, the additional term accounts for the effect of permanent changes in porosity.

Specification of the approach

Various yield conditions proposed for porous solids in the literature are surveyed in [18] along with an assessment of appropriateness and performance. The following description of a single approach serves as an example.

The simple extension of the von Mises yield condition to pressure sensitive solids proposed by Green [19] can be stated as

$$\phi = \left[\left(\frac{\bar{\sigma}}{a}\right)^2 + \left(\frac{3\sigma_{\mathrm{H}}}{2b}\right)^2\right]^{1/2} - \sigma_{\mathrm{f}} \leq 0. \tag{6.127}$$

The above shows explicitly the dependence on the equivalent deviatoric stress $\bar{\sigma}$ and the hydrostatic stress σ_{H} (Fig. 6.21); σ_{f} denotes the uniaxial yield stress of the material. The coefficients,

$$0 \leq a(\chi) \leq 1, \qquad 0 \leq b(\chi) \leq \infty$$

depend on the porosity χ and can be adjusted to experimental data. An assumed relationship is

$$a = (1-\chi)^2, \quad b = -\ln\chi.$$

The pair $a = 1$ and $b = \infty$ pertains to the pressure insensitive yield condition. The yield locus from eqn (6.127) defines a relationship between the equivalent stress $\bar{\sigma}$ and the hydrostatic stress σ_{H}. For plastic states we obtain

$$\left(\frac{\bar{\sigma}}{a\sigma_{\mathrm{f}}}\right)^2 + \left(\frac{3\sigma_{\mathrm{H}}}{2b\sigma_{\mathrm{f}}}\right)^2 = 1,$$

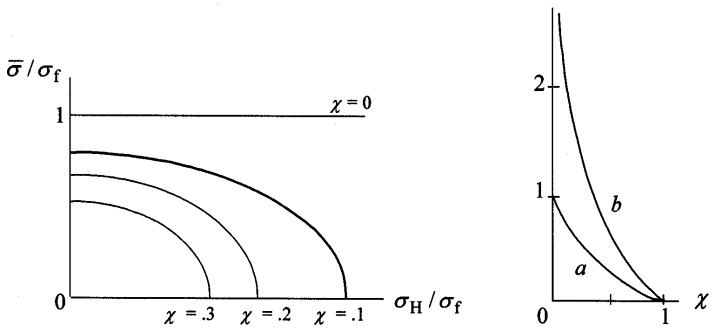

Figure 6.21: Yield model for porous solids.

which describes ellipses in the $\bar{\sigma}, \sigma_{\mathrm{H}}$-plane (Fig. 6.21). The von Mises yield locus is represented by the straight line $\bar{\sigma}/\sigma_{\mathrm{f}} = 1$.

For the yield function of eqn (6.127) we obtain the partial derivatives

$$\frac{\partial \phi}{\partial \bar{\sigma}} = \frac{1}{a^2}\frac{\bar{\sigma}}{\sigma_{\mathrm{G}}}, \qquad \frac{\partial \phi}{\partial \sigma_{\mathrm{H}}} = \left(\frac{3}{2b}\right)^2 \frac{\sigma_{\mathrm{H}}}{\sigma_{\mathrm{G}}}.$$

The quantity σ_{G} is an abbreviation defined by

$$\sigma_{\mathrm{G}}^2 = \left(\frac{\bar{\sigma}}{a}\right)^2 + \left(\frac{3\sigma_{\mathrm{H}}}{2b}\right)^2. \tag{6.128}$$

It represents a scalar equivalent stress pertaining to the *Green* yield condition for the porous solid.

The flow rule for the plastic strain specified by the normality condition reads

$$\mathrm{d}\boldsymbol{\eta} = \Lambda \left[\frac{\partial \phi}{\partial \boldsymbol{\sigma}}\right]^{\mathrm{t}} = \Lambda \left[\frac{1}{a^2}\boldsymbol{\sigma}_{\mathrm{D}} + \frac{1}{2b^2}\boldsymbol{\sigma}_{\mathrm{H}}\right], \tag{6.129}$$

the deviatoric and volumetric parts of the deformation being obvious. The proportionality factor Λ deriving from the consistency condition as

$$\Lambda = \frac{1}{h}\frac{3}{2}\frac{1}{\sigma_{\mathrm{G}}}\left[\frac{1}{a^2}\boldsymbol{\sigma}_{\mathrm{D}} + \frac{1}{2b^2}\boldsymbol{\sigma}_{\mathrm{H}}\right]^{\mathrm{t}} \mathrm{d}\boldsymbol{\sigma},$$

can be alternatively expressed in terms of the strain increment $\mathrm{d}\boldsymbol{\gamma}$. If the influence of permanent deformation on porosity can be neglected, the hardening parameter h becomes

$$h = \frac{h_{\mathrm{o}}}{(1-\chi)}\frac{\sigma_{\mathrm{G}}}{\sigma_{\mathrm{f}}}. \tag{6.130}$$

6.5.2 Soil materials

Drucker–Prager linear Mohr–Coulomb generalization

Problems of material failure in soil mechanics are often modelled following the theory of plasticity. The pertinent yield condition exhibits a dependence on the hydrostatic pressure different from that for porous metals. Material description in soil or rock mechanics is frequently based on the Mohr–Coulomb hypothesis. Its generalization due to Drucker and Prager [20] may be interpreted as a linear Mohr envelope for plane strain failure, and expresses in principle a linear dependence of the deviatoric equivalent stress $\bar{\sigma}$ on the hydrostatic stress σ_{H}:

$$\phi_{\mathrm{Y}} = \bar{\sigma} + \alpha_{\mathrm{Y}}\sigma_{\mathrm{H}} - b \leq 0. \tag{6.131}$$

With Fig. 6.22 the parameters in the yield condition can be interpreted as

$$\alpha_{\mathrm{Y}} = \frac{b}{a} \quad \text{and} \quad b = \sigma_{\mathrm{s}},\ a = p_{\mathrm{s}}.$$

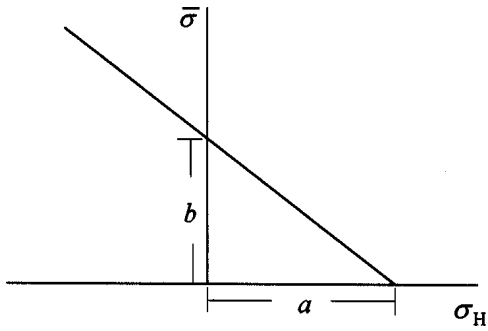

Figure 6.22: Linear Mohr–Coulomb generalization.

The quantities σ_s and p_s define limiting states of strength under purely deviatoric and hydrostatic stresses, respectively. The parameter

$$\alpha_Y = \frac{b - \bar{\sigma}}{\sigma_H}$$

defines the inclination of the yield line in the $\bar{\sigma}, \sigma_H$-plane. The yield condition has to be understood here rather as a failure criterion, and hence the introduction of a hardening ability does not appear meaningful. The material is assumed to be perfectly plastic, such that the parameters α_Y and b are not affected by plastic flow.

Permanent deformation of Mohr–Coulomb type materials cannot necessarily be associated with the yield function by the normality rule. A non-associated flow rule can be derived from the function

$$\phi_F = \bar{\sigma} + \alpha_F \sigma_H, \tag{6.132}$$

which reproduces the associated flow rule for $\alpha_F = \alpha_Y$. Plastic flow is then described by

$$\mathrm{d}\boldsymbol{\eta} = \Lambda \left[\frac{\mathrm{d}\phi_F}{\mathrm{d}\boldsymbol{\sigma}}\right]^t. \tag{6.133}$$

The proportionality factor Λ is determined by satisfying the consistency condition

$$\mathrm{d}\phi_Y = \frac{\mathrm{d}\phi_Y}{\mathrm{d}\boldsymbol{\sigma}} \mathrm{d}\boldsymbol{\sigma} = \frac{\mathrm{d}\phi_Y}{\mathrm{d}\boldsymbol{\sigma}} \boldsymbol{\kappa} \left[\mathrm{d}\boldsymbol{\gamma} - \mathrm{d}\boldsymbol{\eta}\right] = 0.$$

Employing the flow rule, eqn (6.133), for $\mathrm{d}\boldsymbol{\eta}$, we obtain

$$\Lambda = \frac{1}{h^*} \frac{\mathrm{d}\phi_Y}{\mathrm{d}\boldsymbol{\sigma}} \boldsymbol{\kappa} \mathrm{d}\boldsymbol{\gamma} \geq 0 \tag{6.134}$$

with the abbreviation

$$h^* = \frac{\mathrm{d}\phi_Y}{\mathrm{d}\boldsymbol{\sigma}} \boldsymbol{\kappa} \left[\frac{\mathrm{d}\phi_F}{\mathrm{d}\boldsymbol{\sigma}}\right]^t.$$

Ultimately,

$$\mathrm{d}\boldsymbol{\eta} = \frac{1}{h^*}\left[\frac{\mathrm{d}\phi_\mathrm{F}}{\mathrm{d}\boldsymbol{\sigma}}\right]^\mathrm{t}\frac{\mathrm{d}\phi_\mathrm{Y}}{\mathrm{d}\boldsymbol{\sigma}}\boldsymbol{\kappa}\mathrm{d}\gamma. \tag{6.135}$$

The elastoplastic relation between incremental stress and strain follows as

$$\mathrm{d}\boldsymbol{\sigma} = \boldsymbol{\kappa}\left\{\mathbf{I} - \frac{1}{h^*}\left[\frac{\mathrm{d}\phi_\mathrm{F}}{\mathrm{d}\boldsymbol{\sigma}}\right]^\mathrm{t}\frac{\mathrm{d}\phi_\mathrm{Y}}{\mathrm{d}\boldsymbol{\sigma}}\boldsymbol{\kappa}\right\}\mathrm{d}\gamma \tag{6.136}$$

and is not symmetric because of the introduction of a non-associated flow rule.

The gradients of the functions ϕ_F and ϕ_Y are easily obtained:

$$\left[\frac{\mathrm{d}\phi_\mathrm{F}}{\mathrm{d}\boldsymbol{\sigma}}\right]^\mathrm{t} = \mathbf{s} + \frac{\alpha_\mathrm{F}}{3}\mathbf{e}, \quad \left[\frac{\mathrm{d}\phi_\mathrm{Y}}{\mathrm{d}\boldsymbol{\sigma}}\right]^\mathrm{t} = \mathbf{s} + \frac{\alpha_\mathrm{Y}}{3}\mathbf{e}.$$

The first defines the direction of plastic flow and distinguishes the deviatoric and the volumetric part of the incremental plastic strain in eqn (6.133). Permanent volumetric changes are given by

$$3\mathrm{d}\eta_\mathrm{V} = \mathbf{e}^\mathrm{t}\mathrm{d}\boldsymbol{\eta} = \Lambda\alpha_\mathrm{F},$$

independently of the stress state. An increase in volume is obtained as long as α_F is a positive quantity ($\alpha_\mathrm{F} > 0$). The second gradient enters the determination of the proportionality factor Λ in eqn (6.134) either directly or via the expression

$$\frac{\mathrm{d}\phi_\mathrm{Y}}{\mathrm{d}\boldsymbol{\sigma}}\boldsymbol{\kappa} = \left[2G\mathbf{s} + \alpha_\mathrm{Y}K\mathbf{e}\right]^\mathrm{t},$$

with the elastic shear modulus G and the modulus of volume expansion K. We also notice the expression

$$h^* = \frac{\mathrm{d}\phi_\mathrm{Y}}{\mathrm{d}\boldsymbol{\sigma}}\boldsymbol{\kappa}\frac{\mathrm{d}\phi_\mathrm{F}}{\mathrm{d}\boldsymbol{\sigma}} = 3G + \alpha_\mathrm{Y}\alpha_\mathrm{F}K.$$

The scalar quantity

$$\sigma_\mathrm{L} = \bar{\sigma} + \alpha_\mathrm{Y}\sigma_\mathrm{H}$$

may be viewed as an equivalent stress pertaining to the *linearly* pressure sensitive yield condition, eqn (6.131).

The Coulomb rule considers the magnitude of the shear stress τ required for slip in the soil to depend upon the cohesion c of the material and to be linearly related to the normal pressure σ acting on the slip plane,

$$|\tau| = c - \sigma\tan\varphi,$$

where $\tan\varphi$ is known as the coefficient of internal friction. This limiting condition is represented by two straight lines in the τ, σ-plane (Fig. 6.23). The Mohr–Coulomb hypothesis of soil slip or yielding is illustrated in the figure for plane conditions. All combinations of normal and shear stress encountered at a point on planes of different orientations lie on the Mohr circle. The radius of the circle as specified by the stress state at the point under investigation is

$$R = \left[\left(\frac{\sigma_{xx} - \sigma_{yy}}{2} \right)^2 + \sigma_{xy}^2 \right]^{1/2}$$

and is equal to the maximum shearing stress. It is assumed that the material behaves elastically up to a certain state of stress at which yielding occurs. The limiting lines from the Coulomb rule determine the radius of the Mohr's circle at slip as

$$R = c \cos\varphi - \frac{\sigma_{xx} + \sigma_{yy}}{2} \sin\varphi.$$

This relates the maximum shearing stress to the cohesion c of the material, the angle φ of the linear envelope of the Mohr's circles and the mean normal stress $(\sigma_{xx} + \sigma_{yy})/2$ in the plane. For three-dimensional states the shear/normal stress combinations at a point are characterized by three Mohr circles. The above limiting condition then refers to the largest one.

Drucker and Prager [20] have shown that in the case of plane strain the generalized yield condition in eqn (6.131) reduces to the Mohr–Coulomb rule. To this end, it is assumed that the incremental plastic strains $\mathrm{d}\eta_{zz}, \mathrm{d}\eta_{xz}, \mathrm{d}\eta_{yz}$ vanish. By the (associated $\alpha_F = \alpha_Y = \alpha$) flow rule, eqn (6.133), the shear stresses σ_{xz}, σ_{yz} are zero, and

$$\sigma_{Dzz} = -\frac{2}{9}\alpha\bar{\sigma}$$

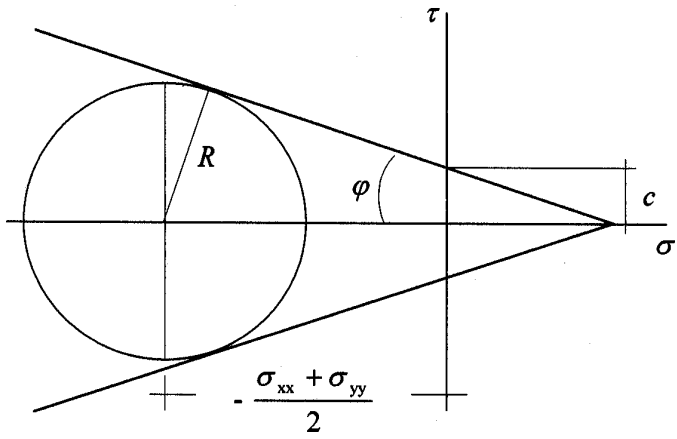

Figure 6.23: Mohr–Coulomb hypothesis.

for the deviatoric stress component. The hydrostatic stress then becomes

$$\sigma_{\mathrm{H}} = \frac{\sigma_{\mathrm{xx}} + \sigma_{\mathrm{yy}}}{2} - \frac{\alpha}{9}\bar{\sigma}$$

and the equivalent deviatoric stress is given by

$$\bar{\sigma}^2 = \frac{3}{1 - \frac{\alpha^2}{9}} \left[\left(\frac{\sigma_{\mathrm{xx}} - \sigma_{\mathrm{yy}}}{2} \right)^2 + \sigma_{\mathrm{xy}}^2 \right].$$

Substitution in the yield condition, eqn (6.131), and comparison with the Mohr–Coulomb hypothesis shows that an identity is established by setting

$$b = \frac{3c\,\cos\varphi}{(3 + \sin^2\varphi)^{1/2}}, \quad \alpha = \frac{3\,\sin\varphi}{(3 + \sin^2\varphi)^{1/2}}.$$

Parabolic Mohr–Coulomb generalization

More elaborated forms of failure surfaces for soil and rock mechanics can be found in [21]; the reader may consult also the articles in [22] and the references therein. Materials of the Mohr–Coulomb type mostly exhibit a curved Mohr envelope rather than a rectilinear one. It may therefore be difficult to model the material behaviour appropriately with the above linear approximation, if the hydrostatic pressure is subject to a strong variation. A yield condition in terms of the equivalent deviatoric stress $\bar{\sigma}$ and the hydrostatic stress σ_{H}, which in the case of plane strain failure leads to a parabolic Mohr envelope, is described by

$$\phi_{\mathrm{Y}} = \left(\bar{\sigma}^2 + \alpha_{\mathrm{Y}} \sigma_{\mathrm{H}} \right)^{1/2} - b \leq 0. \tag{6.137}$$

The parameters are defined with reference to Fig. 6.24 as

$$\alpha_{\mathrm{Y}} = b^2/a \quad \text{and} \quad b = \sigma_{\mathrm{s}},\ a = p_{\mathrm{s}}.$$

The physical interpretation of the constants a and b is identical to that for the linear model. For a non-associated flow rule, the function in eqn (6.137)

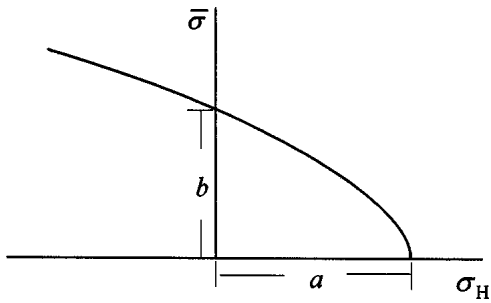

Figure 6.24: Parabolic Mohr–Coulomb generalization.

can be modified via the parameter α:

$$\phi_{\mathrm{F}} = \left(\bar{\sigma}^2 + \alpha_{\mathrm{F}}\sigma_{\mathrm{H}}\right)^{1/2}. \tag{6.138}$$

The formalism developed for the previous linear case is applicable here as well, but for the different specific functions and their derivatives.

We notice that for the functional type in eqns (6.137) and (6.138),

$$\frac{\partial\phi}{\partial\bar{\sigma}} = \frac{\bar{\sigma}}{\sigma_{\mathrm{P}}}, \quad \frac{\partial\phi}{\partial\sigma_{\mathrm{H}}} = \frac{\alpha}{2\sigma_{\mathrm{P}}} \qquad (\alpha = \alpha_{\mathrm{F}}, \alpha_{\mathrm{Y}}).$$

The scalar quantity σ_{P} defined by

$$\sigma_{\mathrm{P}}^2 = \bar{\sigma}^2 + \alpha\sigma_{\mathrm{H}}, \tag{6.139}$$

may be regarded as an equivalent stress associated with the *parabolic* condition. The complete gradient of the yield function with respect to the stress is obtained as

$$\left[\frac{\mathrm{d}\phi}{\mathrm{d}\boldsymbol{\sigma}}\right]^{\mathrm{t}} = \frac{\partial\phi}{\partial\bar{\sigma}}\mathbf{s} + \frac{1}{3}\frac{\partial\phi}{\partial\sigma_{\mathrm{H}}}\mathbf{e} = \frac{\bar{\sigma}}{\sigma_{\mathrm{P}}}\mathbf{s} + \frac{\alpha}{\sigma_{\mathrm{P}}}\mathbf{e} \qquad (\alpha = \alpha_{\mathrm{F}}, \alpha_{\mathrm{Y}})$$

and specifies the expressions for the incremental plastic strain and the elastoplastic stress–strain relation. The permanent change in volume results here in:

$$3\mathrm{d}\eta_{\mathrm{V}} = \mathbf{e}^{\mathrm{t}}\mathrm{d}\boldsymbol{\eta} = \Lambda\frac{\alpha_{\mathrm{F}}}{2\sigma_{\mathrm{P}}}.$$

It is seen to depend on the stress state by the equivalent stress quantity σ_{P}. The volume increases as long as the parameter α_{F} is positive ($\alpha_{\mathrm{F}} > 0$).

An analytical example

In order to demonstrate the significance of the hydrostatic stress on plastic yielding, consider the rectangular plate of uniform thickness under biaxial tension or compression treated in Section 1.2.5. The state of stress is specified by the principal stresses σ_1 and σ_2, whereby the longitudinal stress σ_1 is directly exerted on the plate. The lateral strain γ_2 is suppressed so that the longitudinal strain γ_1 alone defines the state of strain.

The elastic solution $\sigma_2 = \nu\sigma_1$ derives immediately from the prevention of the lateral contraction. The elastoplastic solution developed before for perfect plasticity with the von Mises yield condition shall be extended here to the pressure-dependent yield models.

From the elastic solution, the loading path in the $\bar{\sigma}, \sigma_{\mathrm{H}}$-plane prior to yielding is described by either of the straight lines

$$\bar{\sigma} = \pm 3\frac{\sqrt{1-\nu+\nu^2}}{1+\nu}\sigma_{\mathrm{H}}, \tag{6.140}$$

where the upper sign refers to loading in tension and the lower to loading in compression – considered to be the standard case. This convention shall also hold in subsequent relations. Beyond yielding, the elastic lines, eqn (6.140), must be replaced by the respective yield condition, which then describes the relationship between $\bar{\sigma}$ and σ_{H}.

From the yield condition, eqn (6.131) – *linear* dependence of the equivalent deviatoric stress on the hydrostatic stress ($b = \sigma_{\mathrm{s}}, \alpha_{\mathrm{Y}} = \alpha$) – we obtain

$$\bar{\sigma} = \sigma_{\mathrm{s}} - \alpha\sigma_{\mathrm{H}}. \tag{6.141}$$

The intersection of the two straight lines given by eqns (6.140) and (6.141) determines the elastic limit of the plate (Fig. 6.25). If the applied stress is compressive, plastic yielding occurs only as long as the elastic path, eqn (6.140), is steeper than the yield locus, eqn (6.141). The steepest elastic path is $\bar{\sigma}/\sigma_{\mathrm{H}} = -3$ (for $\nu = 0$), and therefore the yield line defined by $\alpha = 3$ represents a limit, at and above which no plastic yielding is possible for any value of $\nu \geq 0$.

The explicit form of the yield condition, eqn (6.131), reads in the present case

$$\phi = \sqrt{\sigma_1^2 + \sigma_2^2 - \sigma_1\sigma_2} + \frac{\alpha}{3}(\sigma_1 + \sigma_2) - \sigma_{\mathrm{s}} = 0.$$

In conjunction with the elastic solution ($\sigma_2 = \nu\sigma_1$) it determines the elastic limit for σ_1 as above. In the plastic range of loading, it establishes a relation for the lateral stress:

$$\sigma_2 = \frac{\left(\frac{1}{2} + \frac{\alpha^2}{9}\right)\sigma_1 - \frac{\alpha}{3}\sigma_{\mathrm{s}} \mp \sqrt{\sigma_{\mathrm{s}}^2 - \left(\frac{3}{4} - \frac{\alpha^2}{3}\right)\sigma_1^2 - \alpha\sigma_{\mathrm{s}}\sigma_1}}{1 - \frac{\alpha^2}{9}}.$$

A zero discriminant indicates that an upper limit load has been attained. Thus, the plastic range is found to be bounded as follows:

$$\frac{1}{\left|(1+\nu)\frac{\alpha}{3} \pm \sqrt{1 - \nu + \nu^2}\right|} \leq \frac{|\sigma_1|}{\sigma_{\mathrm{s}}} \leq \frac{1}{2}\left|\frac{-\alpha \pm \sqrt{3 - \frac{\alpha^2}{3}}}{\frac{3}{4} - \frac{\alpha^2}{3}}\right|. \tag{6.142}$$

In the case of compressive loading, the upper limit approaches infinity for $\alpha = 3/2$ and becomes meaningless for higher values.

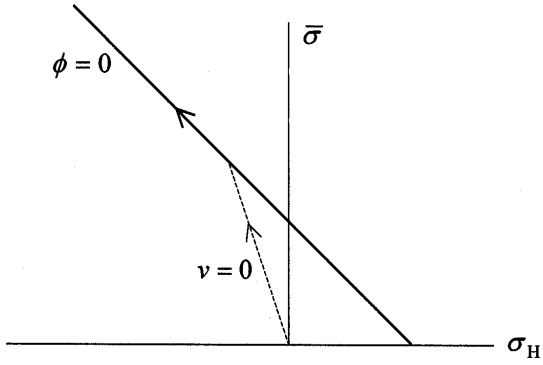

Figure 6.25: Elastic path and pressure-dependent yield limit.

Beyond the elastic limit, knowledge of the stresses σ_1 and σ_2 is utilized in obtaining the elastic strains

$$\left(1-\frac{\alpha^2}{9}\right)\frac{E\varepsilon_1}{\sigma_s} = \left[1-\frac{\nu}{2}-(1+\nu)\frac{\alpha^2}{9}\right]\frac{\sigma_1}{\sigma_s} + \nu\frac{\alpha}{3} \pm \nu\sqrt{1-\left(\frac{3}{4}-\frac{\alpha^2}{3}\right)\frac{\sigma_1^2}{\sigma_s^2}-\alpha\frac{\sigma_1}{\sigma_s}}$$

and

$$\left(1-\frac{\alpha^2}{9}\right)\frac{E\varepsilon_2}{\sigma_s} = \left[\frac{1}{2}-\nu+(1+\nu)\frac{\alpha^2}{9}\right]\frac{\sigma_1}{\sigma_s} - \frac{\alpha}{3} \mp \sqrt{1-\left(\frac{3}{4}-\frac{\alpha^2}{3}\right)\frac{\sigma_1^2}{\sigma_s^2}-\alpha\frac{\sigma_1}{\sigma_s}}.$$

The lateral constraint implies $\eta_2 = -\varepsilon_2$; for the longitudinal plastic strain the associated flow rule ($\alpha_F = \alpha_Y = \alpha$) gives

$$\mathrm{d}\eta_1 = \frac{\left(1-\frac{\alpha^2}{9}\right)\sigma_1 - \left(\frac{1}{2}+\frac{\alpha^2}{9}\right)\sigma_2 + \frac{\alpha}{3}\sigma_s}{\left(1-\frac{\alpha^2}{9}\right)\sigma_2 - \left(\frac{1}{2}+\frac{\alpha^2}{9}\right)\sigma_1 + \frac{\alpha}{3}\sigma_s}\mathrm{d}\eta_2.$$

Expressing the right-hand side of the differential relation in terms of σ_1, and integrating:

$$\left(1-\frac{\alpha^2}{9}\right)^2\frac{E\eta_1}{\sigma_s}=\left\{-\frac{1+\nu}{2}+\frac{\alpha^2}{9}\left[4-\frac{\nu}{2}+(1+\nu)\frac{\alpha^2}{9}\right]\right\}\frac{\sigma_1}{\sigma_s}$$
$$\mp\left[1-\nu+(2+\nu)\frac{\alpha^2}{9}\right]\sqrt{1-\left(\frac{3}{4}-\frac{\alpha^2}{3}\right)\frac{\sigma_1^2}{\sigma_s^2}-\alpha\frac{\sigma_1}{\sigma_s}}$$
$$+\frac{1}{4}\sqrt{3-\frac{\alpha^2}{3}}\ln\frac{\sqrt{3-\frac{\alpha^2}{3}}+\alpha+2\left(\frac{3}{4}-\frac{\alpha^2}{3}\right)\frac{\sigma_1}{\sigma_s}}{\sqrt{3-\frac{\alpha^2}{3}}-\alpha-2\left(\frac{3}{4}-\frac{\alpha^2}{3}\right)\frac{\sigma_1}{\sigma_s}}. \tag{6.143}$$

As long as σ_1/σ_s is below the elasticity limit, eqn (6.142) left, $\eta_1=\eta_2=0$.

Considering next a *parabolic* relation between the equivalent deviatoric and hydrostatic stress, we start with the explicit form of the yield condition, eqn (6.137),

$$\phi=\sqrt{\sigma_1^2+\sigma_2^2-\sigma_1\sigma_2+\frac{\alpha}{3}(\sigma_1+\sigma_2)}-\sigma_s=0$$

and proceed analogously to the above linear hydrostatic dependence.

The lateral stress in the plastic range is

$$\sigma_2=\frac{1}{2}\left(\sigma_1-\frac{\alpha}{3}\right)\mp\sqrt{\sigma_s^2-\frac{3}{4}\sigma_1^2-\frac{\alpha}{2}\sigma_1+\frac{\alpha^2}{36}},$$

and the plastic range is bounded by

$$\frac{\left|-(1+\nu)\alpha\pm\sqrt{(1+\nu)^2\alpha^2+36(1-\nu+\nu^2)\sigma_s^2}\right|}{6(1-\nu+\nu^2)}$$
$$\le|\sigma_1|\le\frac{1}{3}\left|-\alpha\pm2\sqrt{3\sigma_s^2+\frac{\alpha^2}{3}}\right|. \tag{6.144}$$

The elastic part of the longitudinal strain, ε_1, is obtained as

$$E\varepsilon_1=\left(1-\frac{\nu}{2}\right)\sigma_1+\nu\frac{\alpha}{6}\pm\nu\sqrt{\sigma_s^2-\frac{3}{4}\sigma_1^2-\frac{\alpha}{2}\sigma_1+\frac{\alpha^2}{36}},$$

and that of the lateral strain, ε_2, is

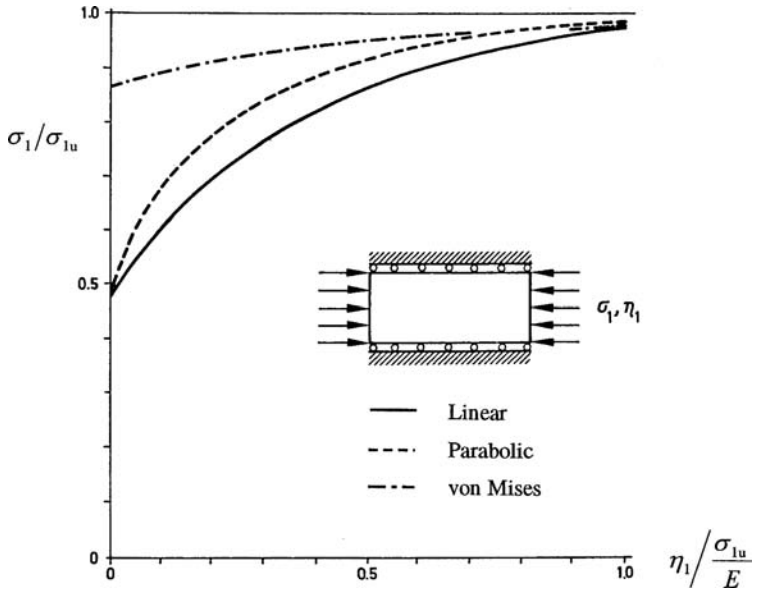

Figure 6.26: Influence of hydrostatic stress dependence on axial stress–plastic strain diagram.

$$E\varepsilon_2 = \left(\frac{1}{2} - \nu\right)\sigma_1 - \frac{\alpha}{6} \mp \sqrt{\sigma_s^2 - \frac{3}{4}\sigma_1^2 - \frac{\alpha}{2}\sigma_1 + \frac{\alpha^2}{36}}.$$

For the plastic parts we have $\eta_2 = -\varepsilon_2$ from the lateral constraint $\gamma_2 = 0$, and with the associated flow rule:

$$\mathrm{d}\eta_1 = \frac{2\sigma_1 - \sigma_2 + \dfrac{\alpha}{3}}{2\sigma_2 - \sigma_1 + \dfrac{\alpha}{3}}\mathrm{d}\eta_2.$$

The plastic longitudinal strain η_1 follows by integration in terms of σ_1 as

$$E\eta_1 = -\frac{1+\nu}{2}\sigma_1 \mp (1-\nu)\sqrt{\sigma_s^2 - \frac{3}{4}\sigma_1^2 - \frac{\alpha}{2}\sigma_1 + \frac{\alpha^2}{36}}$$
$$+ \frac{1}{4}\sqrt{3\sigma_s^2 + \frac{\alpha^2}{3}}\ln\frac{\sqrt{3\sigma_s^2 + \dfrac{\alpha^2}{3}} + \dfrac{\alpha}{2} + \dfrac{3}{2}\sigma_1}{\sqrt{3\sigma_s^2 + \dfrac{\alpha^2}{3}} - \dfrac{\alpha}{2} - \dfrac{3}{2}\sigma_1}. \qquad (6.145)$$

The relationships in eqns (6.143) and (6.145) pertaining to the linear and parabolic generalization of the Mohr–Coulomb hypothesis, respectively, are depicted in Fig. 6.26 along with the pressure independent von Mises

case. The results refer to an evaluation for $\nu = 0$. The Drucker–Prager yield condition has been based on a 45° slope of the yield locus (straight line) and $\sigma_s \neq 0$. In the second yield condition, the parabola has been determined such that the bounds of the plastic range coincide with those of the first. The quantities in the figure have been normalized by the maximum attainable compressive stress σ_{1u}, and start at the state of first yielding which defines the lower limit for the evaluation of η_1 in eqns (6.143) and (6.145).

References

[1] E. Kröner, Plastizität und Versetzungen, in A. Sommerfeld, *Vorlesungen über theoretische Physik*, Vol. II, Akademische Verlagsgesellschaft, Leipzig, 1970.

[2] Yu.N. Rabotnov, *Creep Problems in Structural Members*, North-Holland, Amsterdam, 1969.

[3] J.H. Argyris and I.St. Doltsinis, On the integration of inelastic stress-strain relations – Part 1: Foundations of method, *Res Mech. Lett.* **1** (1981), 343–348; Part 2: Developments of method, *Res Mech. Lett.* **1** (1981), 349–355.

[4] E.C. Bingham, *Fluidity and Plasticity*, McGraw-Hill, New York, 1922.

[5] K. Hohenemser and W. Prager, Über die Ansätze der Mechanik isotroper Kontinua, *Z. Angew. Math. Mech.* (*ZAMM*) **12** (1932) 216–226.

[6] W. Prager, *Einführung in die Kontinuumsmechanik*, Birkhäuser, Basel, 1961.

[7] P. Perzyna, The constitutive equations for rate sensitive plastic materials, *Q.Appl. Math.* **20** (1962) 321–332.

[8] J. Argyris, I. Doltsinis and M. Kleiber, Incremental formulation in nonlinear mechanics and large strain elasto–plasticity – Natural approach. Part II, *Comput. Meths Appl. Mech. Engng* **14** (1978) 259–294.

[9] N. Cristescu, *Dynamic Plasticity*, North-Holland, Amsterdam, 1967.

[10] L.M. Kachanov, *Foundations of the Theory of Plasticity*, North-Holland, Amsterdam, 1971.

[11] J. Argyris and H.-P. Mlejnek, *Dynamics of Structures*, Elsevier, Amsterdam, 1991.

[12] K.K. Tamma, X. Zhou and D. Sha, The time dimension: a theory towards the evolution, classification, characterization and design of computational algorithms for transient/dynamic applications, *Archives of Computational Methods in Engineering* **7** (2000) 67–290.

[13] J.H. Argyris and I.St. Doltsinis, On the large strain inelastic analysis in natural formulation. Part II. Dynamic problems, *Comput. Meths Appl. Mech. Engng.* **21** (1980) 81–128.

[14] J.H. Argyris, P.C. Dunne and Th. Angelopoulos, Nonlinear oscillations using the finite element technique, *Comput. Meths Appl. Mech. Engng* **2** (1973) 203–250.

[15] N.M. Newmark, A method of computation for structural dynamics, *Proc. ASCE* **85**, EMS (1959) 67–94.

[16] J.H. Argyris and P.C. Dunne, Some contributions to nonlinear solid mechanics, *Colloque IRIA* (Versailles, 1973), Springer, Berlin, 1974.

[17] I.St. Doltsinis, Nonlinear concepts in the analysis of solids and structures, in *Advances in Computational Nonlinear Mechanics*, International Centre for Mechanical Sciences (CISM), Courses and Lectures No. 300, Springer, Wien, 1989.

[18] S.M. Doraivelu, H.L. Gegel, J.S. Gunasekera, J.C. Malas, J.T. Morgan and J.F. Thomas, Jr, A new yield function for compressible P/M materials, *Int. J. Mech. Sci.* **26** (1984) 527–535.

[19] R.J. Green, A plasticity theory for porous solids, *Int. J. Mech. Sci.* **14** (1972) 215–224.

[20] D.C. Drucker and W. Prager, Soil mechanics and plastic analysis or limit design, *Q. Appl. Math.* **10** (1952) 157–165.

[21] O.C. Zienkiewicz and G.N. Pande, Some useful forms of isotropic yield surfaces for soil and rock mechanics, in *Finite Elements in Geomechanics*, G. Gudehus (Ed.), John Wiley, Chichester, 1977.

[22] H.B. Mühlhaus (Ed.), *Continuum Models for Materials with Microstructure*, John Wiley, Chichester, 1995.

This page intentionally left blank

CHAPTER 7

Application of finite element analysis

7.1 Remarks on numerical solutions

Computational techniques based on the finite element method prove to be suitable in providing appropriate numerical solutions to elastoplastic problems relevant to engineering practice. Relevance to practice implies complexity in geometry and boundary conditions, and in the material properties. Reasonable simplifications may facilitate the treatment by increasing the transparency and possibly reducing the effort of the computation. They are, however, not necessary to the degree requested in the context of analytical approaches. Conversely, some issues simplifying theoretical analysis may pose difficulties to the numerical model.

Numerical procedures favour the employment of analytical yield conditions like the Huber/von Mises one, despite the nonlinear form. Singular forms like Tresca's are well suited in theoretical analysis, when advantage can be taken of the piecewise linearity of the yield locus. The perfectly plastic approximation, a frequent assumption in developing analytical solutions, was a critical issue at the early stage of the evolution of numerical techniques. Perfectly plastic behaviour of the inelastic material constituent cannot, of course, be approached as the limiting case of plastic hardening material relying on the increment of stress. It requires an appropriate formalism in terms of the increment in strain, as detailed in Chapter 1. Besides, for smooth numerical properties, it is important that the formalism for the incremental plastic strain [1, 2] also encompasses the plastic loading condition [3]. An elegant approach was developed in Chapter 5 within the framework of the radial return technique.

The elastic constituent is essential to the algorithmic concept of elastoplastic computation, since it determines the stress. Analytical solutions based on the approximation of vanishing elastic strain (rigid–plastic approach) cannot, therefore, be treated by this numerical procedure. However, the case of small-strain plasticity and small-scale yielding considered here is characterized by the dominance of elasticity. At the plastic limit state of structures and structural parts made from elastic–perfectly plastic

materials, the stresses become stationary and changes in elastic strain do not occur; the variation in strain is entirely plastic. Although this does not pose serious algorithmic difficulties, problems may arise from the finite element representation. To be specific, the finite element kinematics are not necessarily able to reproduce an isochoric displacement field as required by the flow mechanism at the plastic limit.

For an elucidation, we recall that the deviatoric and hydrostatic parts of the stress rate in the elastoplastic material read

$$\dot{\boldsymbol{\sigma}}_{\mathrm{D}} = 2G\left[\dot{\boldsymbol{\gamma}}_{\mathrm{D}} - \dot{\boldsymbol{\eta}}\right], \quad \dot{\boldsymbol{\sigma}}_{\mathrm{H}} = 3K\dot{\boldsymbol{\gamma}}_{\mathrm{V}} \qquad (\dot{\boldsymbol{\eta}}_{\mathrm{V}} = \mathbf{0}).$$

In the case that finite element kinematics do not allow isochoric deformation we may have $\dot{\boldsymbol{\gamma}}_{\mathrm{D}} \Rightarrow \dot{\boldsymbol{\eta}}$ but $\dot{\boldsymbol{\gamma}}_{\mathrm{V}} \neq \mathbf{0}$ on the penalty of elastic strains as the plastic limit state approaches. As a consequence, variations in stress are still present and the applied load does not become stationary. This deficiency of finite element approximations becomes apparent at the limit load, although it can be inherent to finite element kinematics. The isochoric issue of plasticity was first investigated in [4].

A simple way out is to weaken the significance of the volumetric response of the finite element. For this purpose, the stress resultants at the element nodal points (Section 5.1) are determined by two separate volume integrals:

$$\mathbf{S}_q = \int_{V_q} \boldsymbol{a}^{\mathrm{t}}\boldsymbol{\sigma}\mathrm{d}V = \int_{V_q} \boldsymbol{a}_{\mathrm{D}}^{\mathrm{t}}\boldsymbol{\sigma}_{\mathrm{D}}\mathrm{d}V + \int_{V_q} \boldsymbol{a}_{\mathrm{V}}^{\mathrm{t}}\boldsymbol{\sigma}_{\mathrm{H}}\mathrm{d}V.$$

The deviatoric part makes use of the original element kinematics $\boldsymbol{a}_{\mathrm{D}} \equiv \boldsymbol{a}$ while the hydrostatic part $\boldsymbol{a}_{\mathrm{V}}$ follows a lower-order approximation (see [5]; for instance, linear variation of deviatoric quantities, constant hydrostatic/volumetric ones). Analogously, numerical evaluation of the two integrals is based on full integration of the deviatoric part and a reduced integration rule for the hydrostatic part. This transfers equally to the formation of all other element characteristics, like incremental stress resultants, element stiffness, initial loads.

As an overall remark, finite element elastoplastic computations cannot necessarily reproduce classical analytical solutions, but are capable of a more realistic modelling. On the other hand, each numerical solution represents a single event associated with a specific set of problem parameters. Analytical solutions, even if simplified, allow a discussion regarding the significance of the parameters of the problem.

The following applications of finite element inelastic analysis utilize, in their majority, standardized software for large-scale engineering problems [3, 12]. Unless stated otherwise, plasticity is governed by the von Mises yield condition with isotropic hardening. In the numerical model, incrementation of the plastic strain relies on the radial return technique (Section 5.4.4).

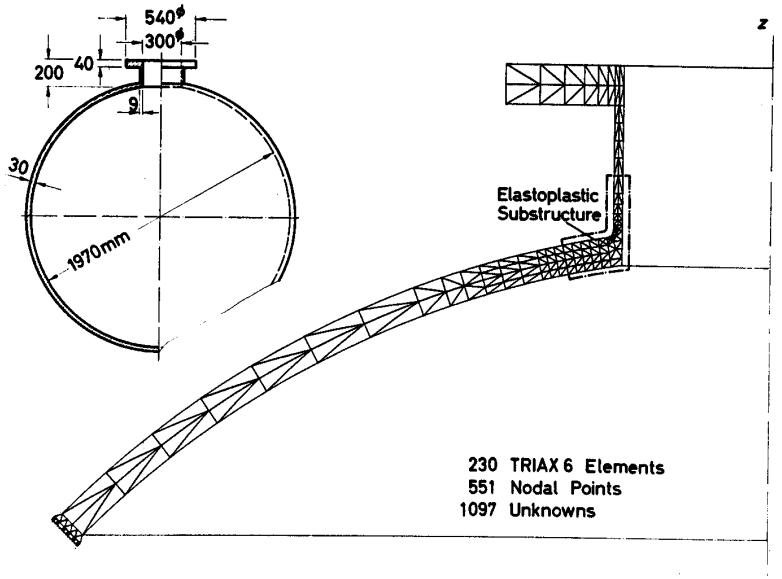

Figure 7.1: Pressure vessel with nozzle: geometry and finite element model.

7.2 Pressure vessel with nozzle

This example introduces the substructuring technique and demonstrates its application in elastoplastic finite element analysis [3].

The spherical vessel with a radial nozzle depicted in Fig. 7.1 is subjected to internal pressure increasing beyond the elastic range. For the finite element analysis, the upper quarter of the meridional section of the structure is represented by 230 triangular axisymmetric six-node elements. The properties of the vessel material are specified in Fig. 7.2. In the computation, an initial elastic solution determines the pressure $p_s = 3.413\,\text{MPa}$ at which the stress in the structure first attains the elasticity limit of the material $\sigma_s = 255\,\text{MPa}$. Subsequently, the pressure is increased to twice this value ($p = 2p_s$) by the application of 10 equal increments of loading.

Plasticity develops at the junction between the spherical part of the vessel and the nozzle, as depicted in Fig. 7.3 (left). The extent of the plastic zone at the final pressure $p = 2p_s = 6.826\,\text{MPa}$ is shown in Fig. 7.3 (right) along with the distribution of the equivalent deviatoric stress $\bar{\sigma}$ in the region of the junction. It is observed that the domain of plastic deformation is confined. It appears only at the junction, a fact that is predictable in the present case. Since a large part of the structure remains elastic, the computational effort of elastoplastic analysis can be reduced by defining an elastic and an elastoplastic domain (Fig. 7.1), and applying the substructuring technique.

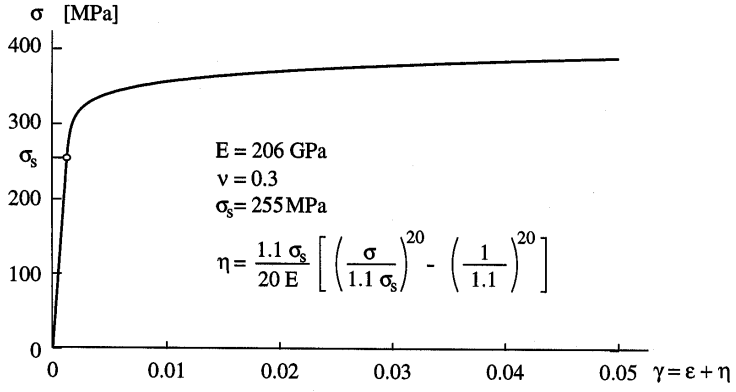

Figure 7.2: Uniaxial characteristics of the elastoplastic material.

Substructuring [6] is a solution technique that has been used for many years in large-scale finite element applications – even in elasticity – on computers with restricted capacity. It has attained new importance in the context of parallel computing, because it offers a systematic scheme for the distributed treatment of the problem on several processing units [7]. In this connection, classical substructuring may be considered a domain

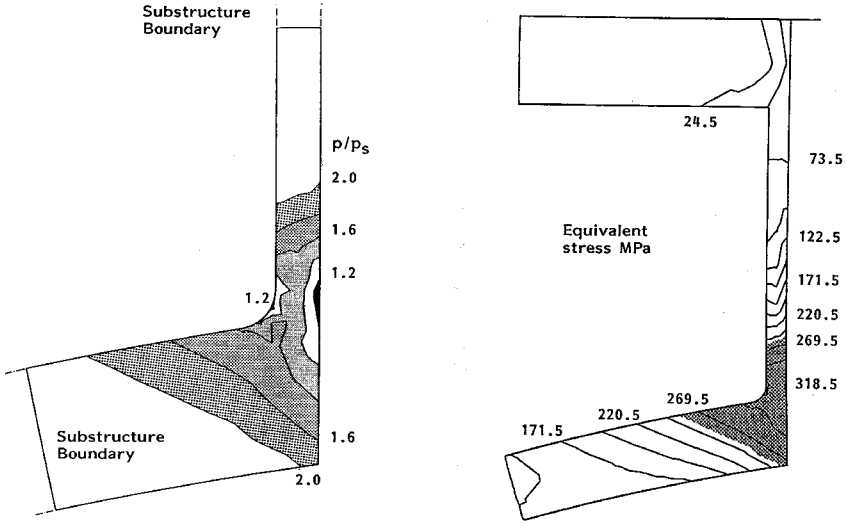

Figure 7.3: Development of the plastic zone in the elastoplastic substructure.

decomposition method [8]. In elastoplastic analysis, it can be utilized for a separation of purely elastic and elastoplastic operations in the domain of computation.

With reference to the finite element mesh in Fig. 7.1, we define three subdomains or substructures covering in the sum the entire model. Nodal points lying on the interior boundaries thus created, connect neighbouring substructures and define a subset $\mathbf{U}_\mathrm{C}$ of the displacements. In the three substructures, the displacements are grouped as

$$\mathbf{U}_1 = \{\mathbf{U}_\mathrm{I}\,\mathbf{U}_\mathrm{B}\}_1\,, \quad \mathbf{U}_2 = \{\mathbf{U}_\mathrm{I}\,\mathbf{U}_\mathrm{B}\}_2\,, \quad \mathbf{U}_3 = \{\mathbf{U}_\mathrm{I}\,\mathbf{U}_\mathrm{B}\}_3\,.$$

Each set $\mathbf{U}_\mathrm{B}$ comprises the displacements of the nodal points at the connecting boundary, $\mathbf{U}_\mathrm{I}$ all other displacements in the substructure. The $\mathbf{U}_\mathrm{B}$s can be related to $\mathbf{U}_\mathrm{C}$ by the symbolic ordering operation

$$\mathbf{U}_{\mathrm{B}1} = \mathbf{a}_1\,\mathbf{U}_\mathrm{C}, \;\; \mathbf{U}_{\mathrm{B}2} = \mathbf{a}_2\,\mathbf{U}_\mathrm{C}, \;\; \mathbf{U}_{\mathrm{B}3} = \mathbf{a}_3\,\mathbf{U}_\mathrm{C},$$

and the $\mathbf{a}_i$s denote incidence matrices. Collectively,

$$\mathbf{U}_\mathrm{B} = \{\mathbf{U}_{\mathrm{B}1}\,\mathbf{U}_{\mathrm{B}2}\,\mathbf{U}_{\mathrm{B}3}\} = \mathbf{a}\,\mathbf{U}_\mathrm{C}.$$

The stress resultants in the individual substructures are grouped analogously

$$\mathbf{S}_1 = \{\mathbf{S}_\mathrm{I}\,\mathbf{S}_\mathrm{B}\}_1\,, \quad \mathbf{S}_2 = \{\mathbf{S}_\mathrm{I}\,\mathbf{S}_\mathrm{B}\}_2\,, \quad \mathbf{S}_3 = \{\mathbf{S}_\mathrm{I}\,\mathbf{S}_\mathrm{B}\}_3\,.$$

Accumulation at the connecting nodes supplies the quantities in

$$\mathbf{S}_\mathrm{C} = \mathbf{a}^\mathrm{t}\,\mathbf{S}_\mathrm{B}, \quad \mathbf{S}_\mathrm{B} = \{\mathbf{S}_{\mathrm{B}1}\,\mathbf{S}_{\mathrm{B}2}\,\mathbf{S}_{\mathrm{B}3}\}\,,$$

which are equilibrated by the external forces acting at the same positions: $\mathbf{S}_\mathrm{C} = \mathbf{P}_\mathrm{C}$. If forces $\mathbf{P}_\mathrm{B}$ are defined at the connecting boundary in the substructures, accumulation to $\mathbf{P}_\mathrm{C}$ is as for the stress resultants.

Each subdomain can be viewed as a structural unit. The incremental equation of equilibrium for the elastoplastic substructure from eqn (5.34) reads

$$\begin{bmatrix} \mathbf{S}_{\Delta\mathrm{I}} \\ \mathbf{S}_{\Delta\mathrm{B}} \end{bmatrix} = \begin{bmatrix} \mathbf{K}_\mathrm{II} & \mathbf{K}_\mathrm{IB} \\ \mathbf{K}_\mathrm{BI} & \mathbf{K}_\mathrm{BB} \end{bmatrix} \begin{bmatrix} \mathbf{U}_{\Delta\mathrm{I}} \\ \mathbf{U}_{\Delta\mathrm{B}} \end{bmatrix} + \begin{bmatrix} \mathbf{J}_{\Delta\mathrm{I}} \\ \mathbf{J}_{\Delta\mathrm{B}} \end{bmatrix} = \begin{bmatrix} \mathbf{P}_{\Delta\mathrm{I}} \\ \mathbf{P}_{\Delta\mathrm{B}} \end{bmatrix}.$$

In the above detailed form $\mathbf{K}$ denotes the elastic stiffness and $\mathbf{J}_\Delta$ the initial loads originating from the plastic strain increment. The external forces $\mathbf{P}_\Delta$ are here equivalent to the applied increment of pressure. The connecting boundary can be loaded at the assembled state, in which case we set $\mathbf{P}_{\Delta\mathrm{B}} = \mathbf{0}$.

From the upper equation in the matrix

$$\mathbf{U}_{\Delta\mathrm{I}} = \mathbf{K}_\mathrm{II}^{-1}\,[\mathbf{P}_{\Delta\mathrm{I}} - \mathbf{J}_{\Delta\mathrm{I}} - \mathbf{K}_\mathrm{IB}\mathbf{U}_{\Delta\mathrm{B}}] \tag{i}$$

and substituting in the second row

$$\mathbf{S}_{\Delta\mathrm{B}} = \underbrace{\left[\mathbf{K}_\mathrm{BB} - \mathbf{K}_\mathrm{BI}\mathbf{K}_\mathrm{II}^{-1}\mathbf{K}_\mathrm{IB}\right]}_{\mathbf{K}^*}\mathbf{U}_{\Delta\mathrm{B}} + \underbrace{\mathbf{J}_{\Delta\mathrm{B}} + \mathbf{K}_\mathrm{BI}\mathbf{K}_\mathrm{II}^{-1}\,[\mathbf{P}_{\Delta\mathrm{I}} - \mathbf{J}_{\Delta\mathrm{I}}]}_{\mathbf{J}_\Delta^*}. \tag{ii}$$

In the elastic substructures, plastic strains are absent, $\mathbf{J}_{\Delta\mathrm{B}} = \mathbf{0}, \mathbf{J}_{\Delta\mathrm{I}} = \mathbf{0}$:

$$\mathbf{S}_{\Delta\mathrm{B}} = \mathbf{K}^*\mathbf{U}_{\Delta\mathrm{B}} + \mathbf{J}_\Delta^* \quad \text{with} \;\; \mathbf{J}_\Delta^* = \mathbf{K}_\mathrm{BI}\mathbf{K}_\mathrm{II}^{-1}\mathbf{P}_{\Delta\mathrm{I}}.$$

Accumulation of the contributions from the substructures to the stress resultants at the common nodal points yields

$$\mathbf{S}_{\Delta C} = \left[\mathbf{a}^{\mathrm{t}}\mathbf{K}\mathbf{a}\right]\mathbf{U}_{\Delta C} + \mathbf{a}^{\mathrm{t}}\mathbf{J}_{\Delta} = \mathbf{P}_{\Delta C} \qquad \text{(iii)}$$

with

$$\mathbf{a} = \begin{bmatrix} \mathbf{a}_1 \\ \mathbf{a}_2 \\ \mathbf{a}_3 \end{bmatrix}, \quad \mathbf{K} = \begin{bmatrix} \mathbf{K}_1^* & & \\ & \mathbf{K}_2^* & \\ & & \mathbf{K}_3^* \end{bmatrix}, \quad \mathbf{J}_{\Delta} = \begin{bmatrix} \mathbf{J}_{\Delta 1}^* \\ \mathbf{J}_{\Delta 2}^* \\ \mathbf{J}_{\Delta 3}^* \end{bmatrix}.$$

The solution of the reduced system (iii) for $\mathbf{U}_{\Delta C}$ supplies the $\mathbf{U}_{\Delta B}$s in the substructures. The $\mathbf{U}_{\Delta I}$ for the elastoplastic substructure follows from eqn (i), in the elastic substructures $\mathbf{J}_{\Delta I} = \mathbf{0}$. This completes the solution of the problem, in principle. Iteration with $\mathbf{J}_{\Delta}$ requires determination of the incremental plastic strain in the elastoplastic substructure, and evaluation of a new $\mathbf{J}_{\Delta}^*$, eqn (ii). Since all other entries in eqn (iii) remain unchanged, the iteration process is restricted to operations within the elastoplastic substructure and repeated solution of the reduced system (iii) with a modified right-hand side but constant coefficient matrix. The computational effort is reduced by this technique.

7.3 Aluminium sheet with circular hole: comparison of analysis with experiment

A comparison of the results of the numerical computation with experimental measurements is useful for several purposes. It permits a verification of the algorithmic procedure and the software implementation, on the one

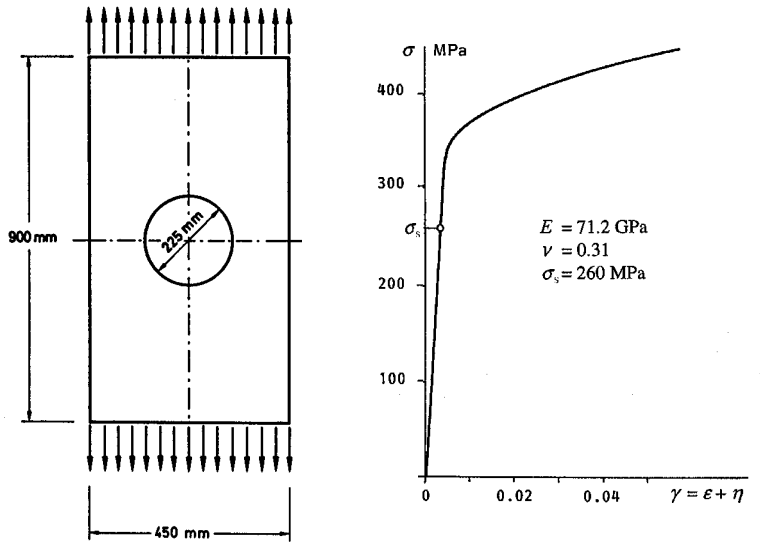

Figure 7.4: Sheet with circular hole: geometry and material properties.

hand, and an examination of the appropriateness of the material description on the other hand. Validation of the computational model, however, has to account for the random nature of some of the parameters and involves statistical comparison techniques [9]. The purpose here is just to demonstrate the performance of the elastoplastic finite element approach. Therefore, a description of the numerical analysis and a comparison with measurements follows [10] without entering details about the experimental technique used in the large-scale test.

The material is a flat 2 mm aluminium sheet cut to form a rectangle (900 mm × 450 mm) with a circular hole (225 mm ⌀). The geometry of the sheet is defined in Fig. 7.4 along with the material characteristics of the AL 2024-T3 aviation sheet employed. For the numerical simulation of the test by elastoplastic computation, the hardening characteristic relating the yield stress to the plastic strain is deduced from the experimental stress–strain diagram. A fairly accurate approximation has been obtained by an exponential function in the lower range of the curve and a fifth-order polynomial in the upper range of the curve.

Figure 7.5 shows the finite element discretization for the elastoplastic analysis. The discretization is performed by triangular plane stress elements with six nodes, and is not particularly fine. The double symmetry of the problem allows consideration of one quarter of the sheet.

In the numerical simulation the specimen is loaded by an axial tensile force P distributed uniformly over the horizontal edge of the sheet. The load at the elasticity limit of the material $\sigma_s = 260\,\text{MPa}$ is $P_s = 53.22\,\text{kN}$.

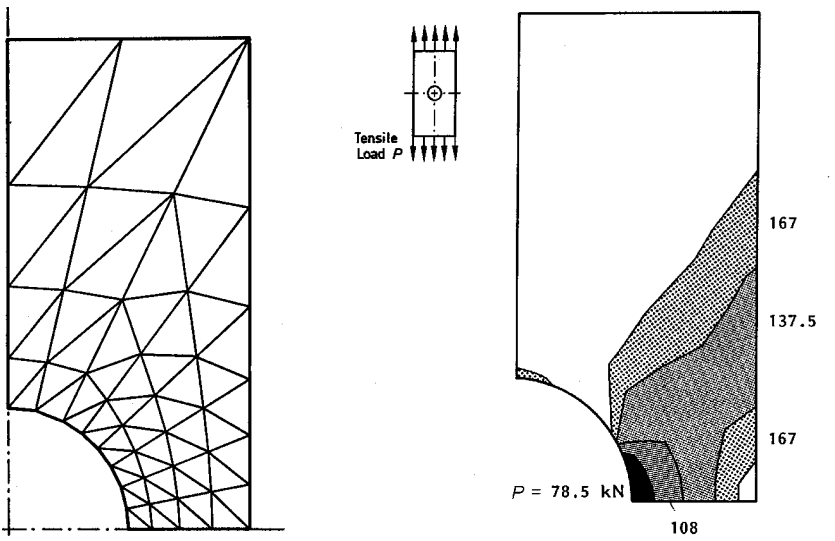

Figure 7.5: Finite element representation and progress of plastification.

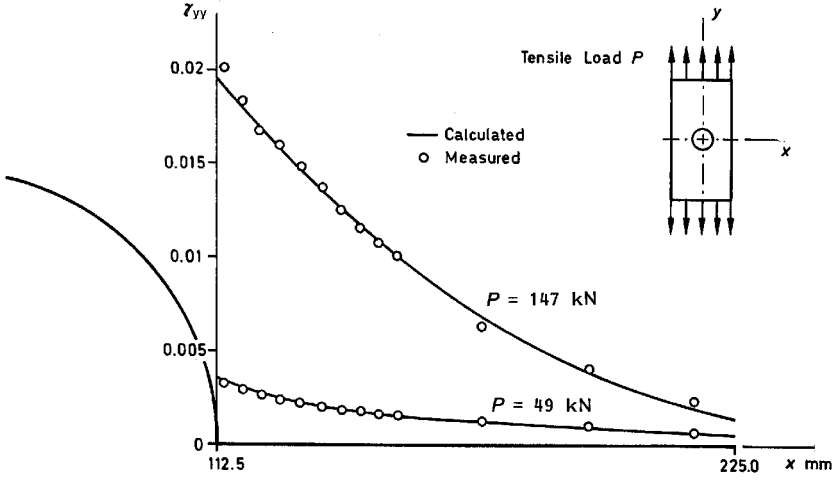

Figure 7.6: Distribution of axial strain along the weakest cross-section. Comparison of numerical results with measured data at two levels of loading.

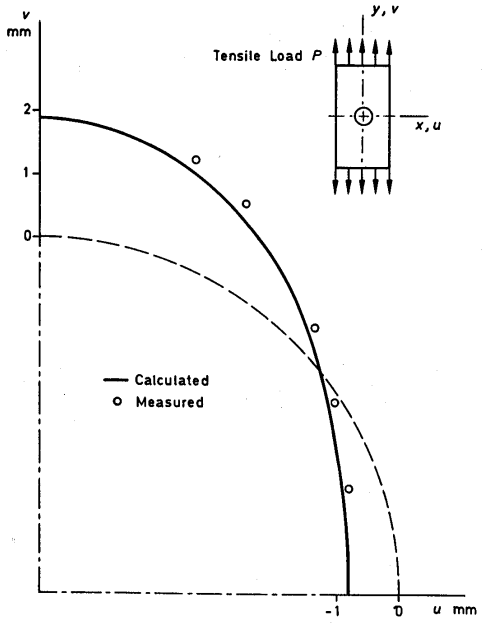

Figure 7.7: Deformation of the hole at final load $P = 167\,\mathrm{kN}$. Comparison of numerical results with photogrammetric laboratory measurements.

Subsequently, the loading is increased up to $P = 167\,\text{kN}$ using 11 incremental steps gradually diminishing in size. In the elastoplastic computation, plastic flow sets in at the weakest cross-section. The region where the material has deformed plastically expands from the boundary of the hole to the vertical edge of the sheet as the loading increases (Fig. 7.5).

In Fig. 7.6 a comparison is given between the computed and the measured longitudinal strain at the weakest cross-section along the horizontal axis of symmetry. The agreement is equally good in the elastic range ($P = 49\,\text{kN}$) and in the plastic range ($P = 147\,\text{kN}$). Figure 7.7 compares at the end load ($P = 167\,\text{kN}$) the deformation of the periphery of the hole as a result of the numerical simulation, with the displacements of distinct points obtained by photogrammetrical measurements. In order to enhance visibility, the scale of the displacements has been magnified considerably.

7.4 Heat shrink fitting of a wheel

As an application of thermal stress analysis involving plasticity we consider the process of heat shrink fitting of a wheel for a rail road vehicle [10]. The computation can be carried out in two separate steps. First, a heat conduction analysis determines the temperature distribution in the wheel at consecutive instants. Then, the incremental elastoplastic stress analysis is performed employing the obtained variation of the temperature distribution as an input. The above treatment of the thermomechanical problem relies on the assumption that the changes of the mechanical state do not induce appreciable thermal phenomena.

The wheel is made up of two parts, the hub and the rim (Fig. 7.8), each defining a substructure in the finite element representation (Fig. 7.9). Its

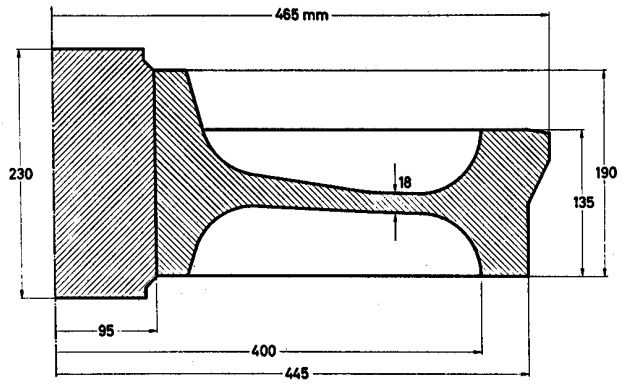

Figure 7.8: Rail road wheel: description of geometry.

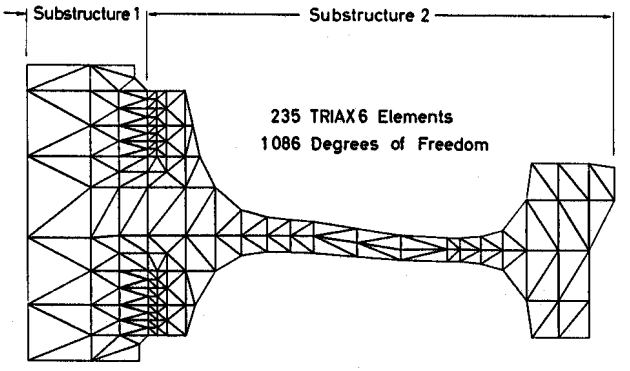

Figure 7.9: Finite element model and definition of two substructures.

meridional section is discretized by triangular axisymmetric six-node elements. Identical discretizations are used for both thermal and elastoplastic analysis.

Initially, the temperature of the hub is uniformly 20°C, the same as the ambient air temperature. At that stage, the temperature of the rim is 140°C. The difference of 120°C corresponds to the required original oversize of the hub relative to the bore of the rim. The two parts, rim and hub, are in ideal contact without exerting any pressure on each other. From this state the structure cools down, the process involving heat exchange between the rim and the hub by conduction and heat transfer to the surrounding air. The computed temporal variation of temperature is depicted for a number of locations in Fig. 7.10.

The elastoplastic analysis is based on the following material data:

$$E = 206\,\mathrm{GPa}, \quad \nu = 0.3, \quad \alpha = 1.7 \cdot 10^{-5} \left[1 - 0.412 \left(1 - \frac{\vartheta}{720}\right)^2\right] {}^{\circ}\mathrm{C}^{-1}$$

$$\sigma_\mathrm{f} = \sigma_\mathrm{s} \left[1 + 122.3 \frac{E}{\sigma_\mathrm{s}} \eta_\mathrm{P}\right]^{1/20}, \quad \sigma_\mathrm{s} = 255 \left[1 - \left(\frac{\vartheta}{850}\right)^2\right] \mathrm{MPa}.$$

The elasticity limit σ_s of the material and the coefficient of thermal expansion α are temperature dependent; ϑ denotes the temperature in °C.

The transient temperature loading necessitates an incremental computation to be carried out from the start. The elastoplastic procedure is activated automatically as soon as plastic flow sets in. Since the stress level in the hub is considerably lower than the elasticity limit of the material within the temperature range in question, the elastoplastic computation can be confined to the rim substructure. As a result of the numerical analysis, Fig. 7.11 shows the temporal variation of the radial stress σ_rr, the axial stress σ_zz and

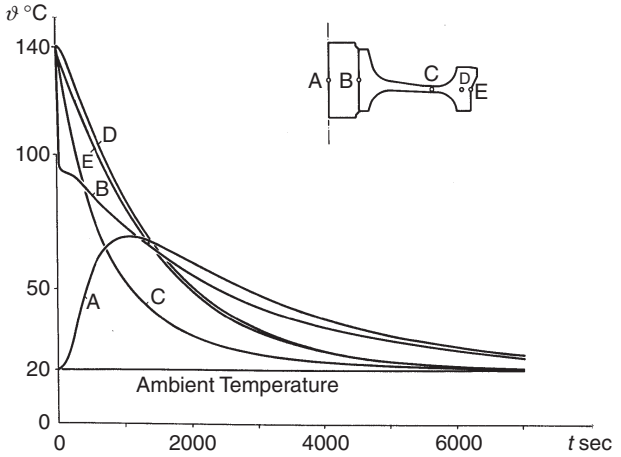

Figure 7.10: Temporal variation of temperature at different locations in the wheel during cooling down.

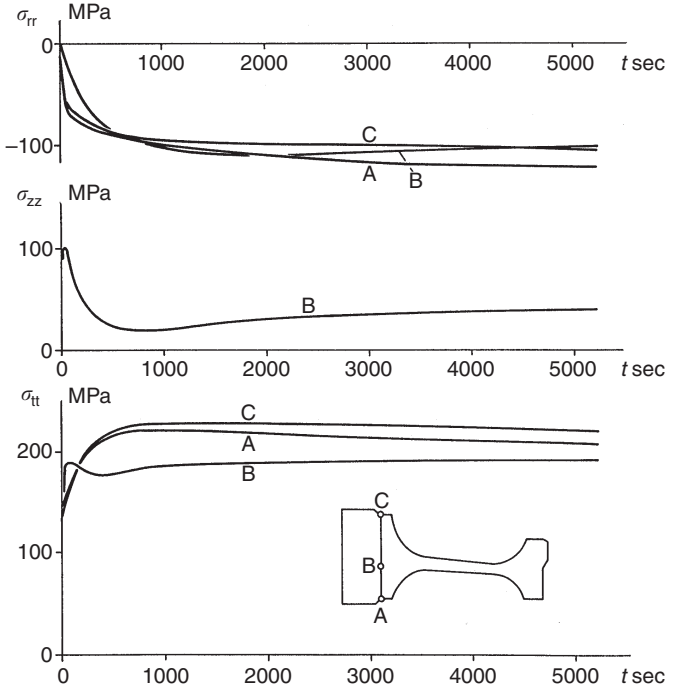

Figure 7.11: Temporal variation of stress along the bore of the rim.

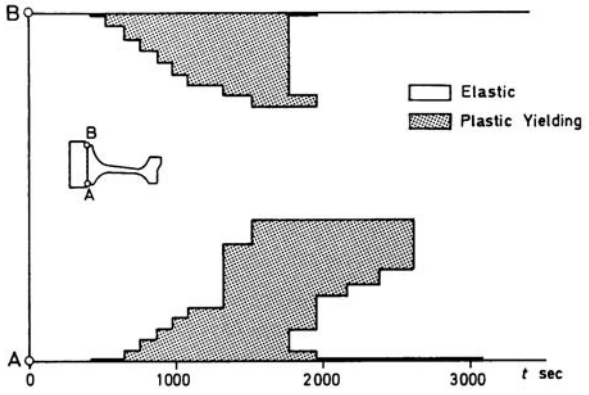

Figure 7.12: Evolution of plastic yielding along the bore of the rim.

the circumferential component σ_{tt} at different positions along the bore of the rim during the course of cooling down. The axial stress at the edges practically complies with the boundary condition $\sigma_{zz} = 0$ and therefore is not plotted. The development of plastic yielding along the bore of the rim is demonstrated in Fig. 7.12. The shaded areas specify the axial extent of plastic flow along the bore at each time increment during cooling of the wheel.

7.5 Thermal cycling of cylindrical container

The study refers to a nuclear reactor component: the fuel rod operating under the combined action of internal gas pressure and intermittent heat flux. The case can be treated as a long cylinder in a state of generalized plane strain. This implies that the axial strain does not vanish, but it is constant over the radius and does not vary along the axis.

The computational model reduces to a single layer of axisymmetric elements (triangular six node elements, Fig. 7.13). The condition of plane strain requires that the axial displacement is unique over each cross-section. Therefore, axial displacements are suppressed in the lower row of nodal points while a single axial freedom is allowed in the upper row. The radial displacements of the nodal points in the upper row are equal to those in the lower row.

Initially in the loading programme (Fig. 7.13), the pressure p is raised proportional to the temperature gradient T_Δ up to $p_{max} = 900\,\text{psi}, T_{\Delta\,max} = 170\,^\circ\text{F}$ ($1\,\text{in} = 2.54\,\text{cm}$, $1\,\text{psi} = 6.895\,\text{kPa}$, $1^\circ\text{F} = 1/1.8\,\text{K}$). Subsequently the pressure is kept constant while cycling the temperature gradient between zero and the maximum value. The temperature distribution over the wall thickness is almost linear. The radial pressure on the interior surface is accompanied by an axial force $P = pR_i^2\pi$ due to the end closure.

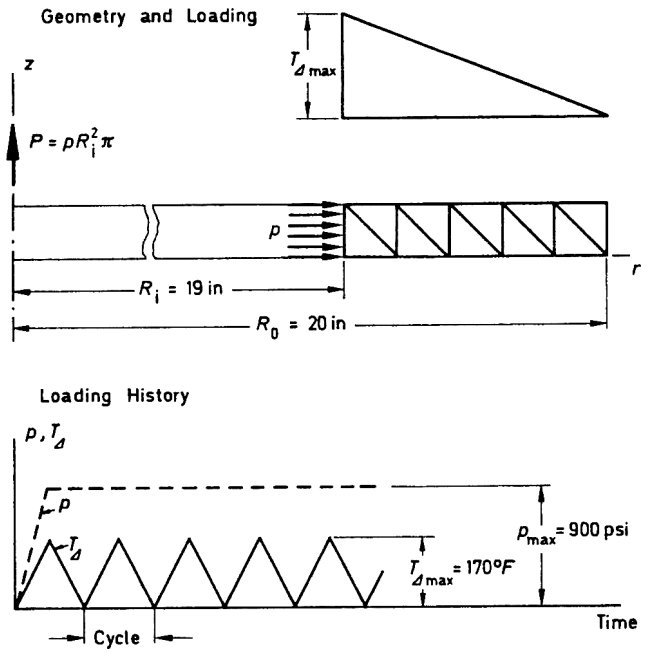

Figure 7.13: Description of the fuel rod problem.

The thermoelastic properties of the rod material (SA 240/304 steel) and the yield stress are taken at an average temperature of 400°F (477.59 K) as

$$E = 25 \cdot 10^6 \text{ psi}, \ \nu = 0.3, \ \alpha = 9.4 \cdot 10^{-6} \, 1/°\text{F},$$
$$\sigma_s = 1.7 \cdot 10^4 \text{ psi}.$$

The uniaxial hardening characteristic of the material is described by the functional dependence given in Fig. 7.2, Section 7.2. The cyclic loading suggests employment of the kinematic hardening rule.

Figure 7.14 demonstrates the representative stress–strain response of the rod in terms of the axial components. Following the numerical simulation of the process, shakedown is not attained completely. In that case, the stress–strain diagram in Fig. 7.14 would be limited by a straight line fixed on the strain axis. It is seen in Fig. 7.15 that the value of T_Δ at which plastic yielding sets in does not reach the limit of 170°F in loading or 0°F in unloading. It is worth noting that alternately the inner or outer region of the rod yields plastically; the inner in the unloading phase of the thermal cycle, the outer in the loading phase.

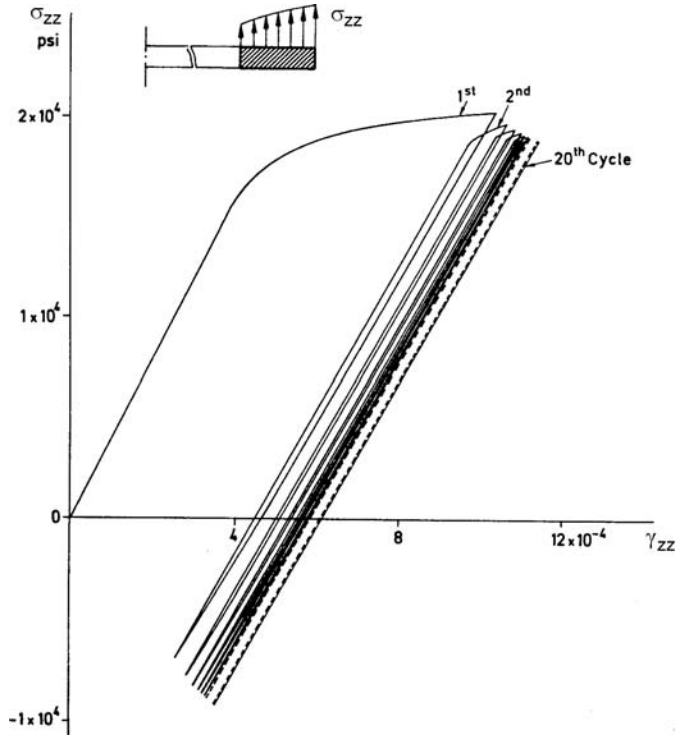

Figure 7.14: Axial stress at the outer radius versus axial strain.

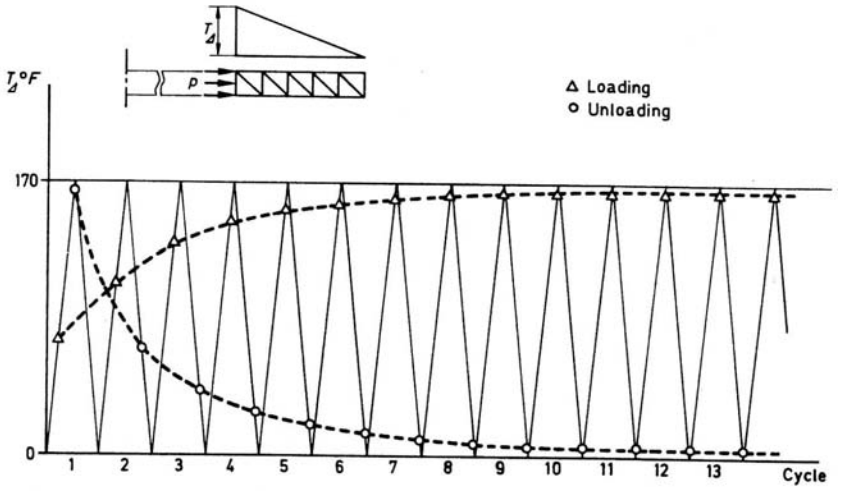

Figure 7.15: Gradient T_Δ at which yielding sets in during thermal cycling.

7.6 Vessel for liquid zinc

During the heating phase of vessels for liquid zinc, cracking may occur induced by stress corrosion. In order to explore the origin of stress corrosion induced cracks and identify locations prone to failure, a detailed stress analysis of the process is necessary [11].

The vessel under investigation has the dimensions $7.6 \times 1.3 \times 2.55\,\mathrm{m}^3$ and a capacity of 140 tons of zinc (Fig. 7.16). It stands on a grid of concrete beams and its side walls lean against three horizontal supports. The latter should prevent bulging of the side walls during operation. The vessel is heated by four burners at the upper third of the side walls, and the zinc melts. During the heating time of 255 h, temperature and displacements were measured at several points as indicated in Fig. 7.16.

The double symmetry of the vessel allows consideration of only one quarter of the structure in the finite element analysis. The discretized representation is shown in Fig. 7.17. The computation mesh comprises layered triangular shell elements modelling the walls and layered beam elements representing the rim stiffener. These bending elements presume the customary linear variation of strain, but the layers allow to account for the development of plasticity across the thickness [12].

The loading of the vessel is a result of the transient temperature distribution during heating and of the interior pressure from the melting zinc. In addition, forces are transmitted by the horizontal supports. In the computation model, the action of the horizontal supports is accounted for by displacements prescribed at the respective locations according to the measurements. The temperature distribution in the walls of the vessel has been modelled on the basis of the temperatures recorded hourly at the measurement points. The assumption on the temporal variation of the internal pressure from the melting zinc follows the development of the temperature field.

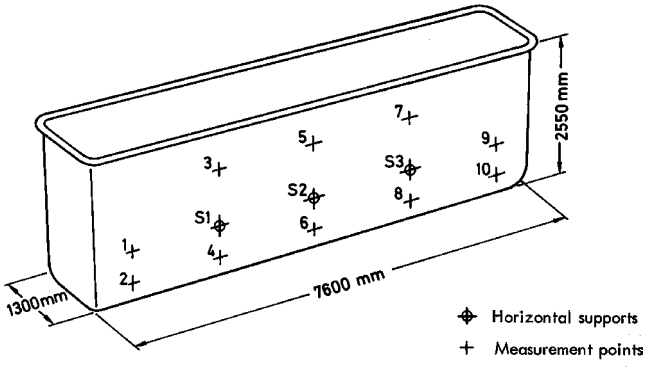

Figure 7.16: Vessel for liquid zinc: geometrical description.

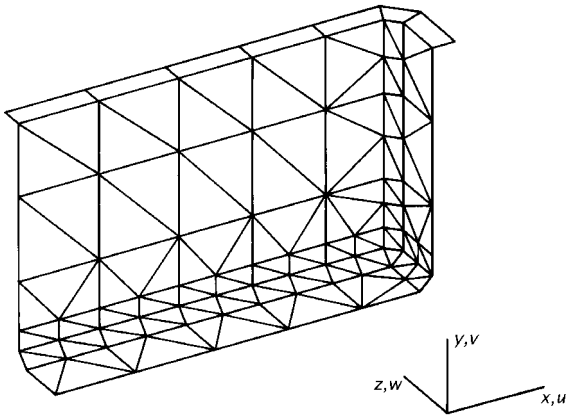

Figure 7.17: Finite element representation of a symmetric quarter of the vessel.

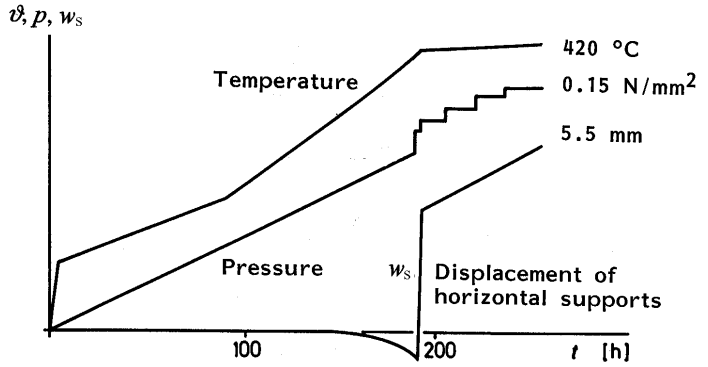

Figure 7.18: History of thermal and mechanical loading (schematic): heating up temperature ϑ, internal pressure p, displacement of horizontal supports w_s.

The vessel is initially filled with 100 tons of zinc, this amount is assumed to be melted after 190 h; subsequently 40 tons are added gradually. The history of the thermal and mechanical loading applied in the elastoplastic analysis of the heating process is shown schematically in Fig. 7.18.

The thermal and elastic material properties (modulus of elasticity, Poisson's ratio, coefficient of thermal expansion) are depicted in Fig. 7.19 as functions of the temperature. The figure also shows the uniaxial stress–strain characteristic of the material in the plastic range as derived from laboratory data at different temperatures.

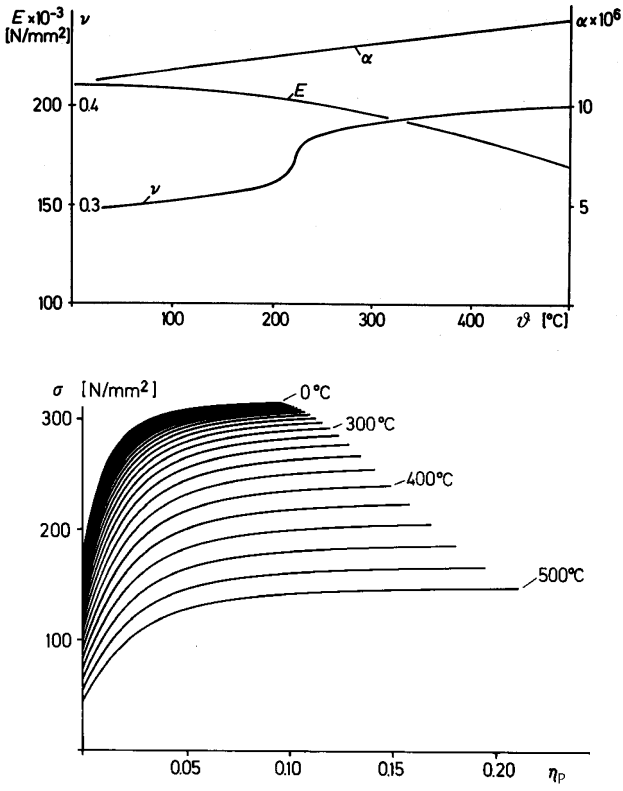

Figure 7.19: Temperature-dependent thermoelastic properties (upper) and plastic hardening characteristics (lower).

In the elastoplastic computation of the non-isothermal problem, the analysis of the heating phase has been executed in 15 intervals of time by applying the respective loading conditions. During the first 50 h of the heating process the supporting conditions at the bottom of the vessel change due to the induced deformations. In particular, at that time the vessel is seen standing only at the front end regions (Fig. 7.20). The arising contact problem is solved by a suitable iteration technique.

As a result of the computer simulation of the heating process of the vessel, Fig. 7.20 shows the deformation (40× magnified) of the finite element model at four instants of interest. The development of the region where the material undergoes plastic deformation is demonstrated in Fig. 7.21. Marked differences are visible between the interior surface and the exterior surface of the vessel walls. Figures 7.22 and 7.23 display the distribution of the principal stresses σ_1 and σ_2, respectively. They refer to the inner surface

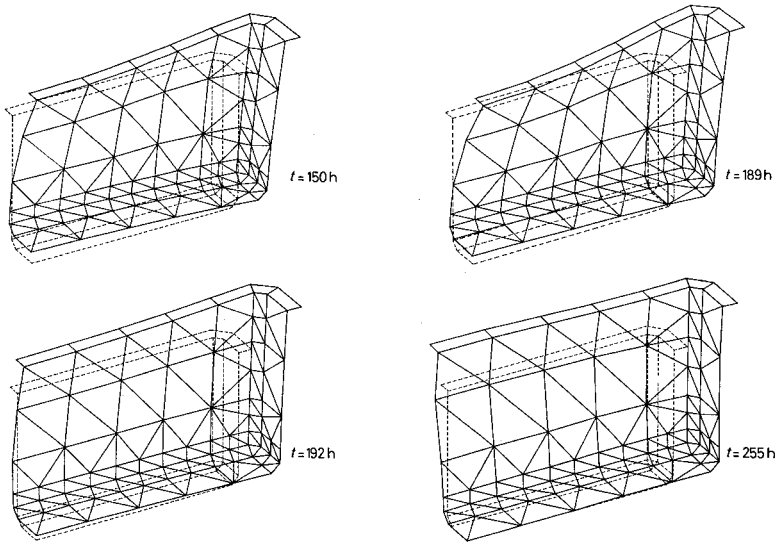

Figure 7.20: Deformation of the finite element model at various stages during heating up (magnified).

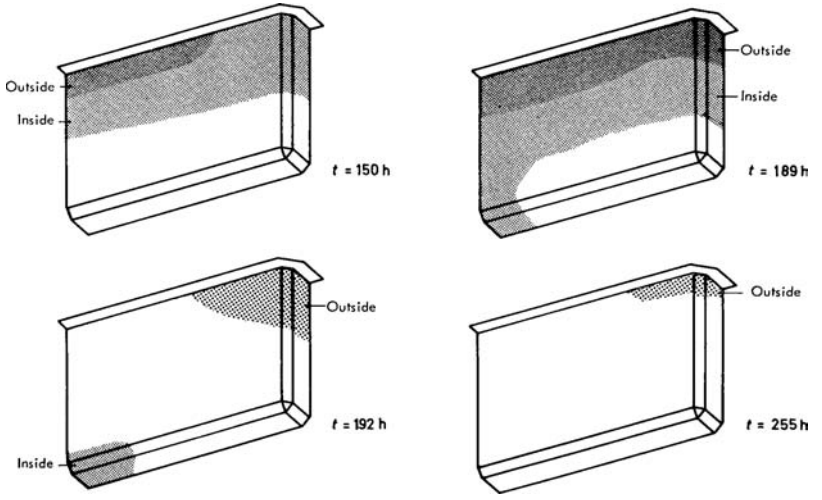

Figure 7.21: Plastic flow domain on the inside and outside of the vessel at various instants.

of the vessel since this is the one prone to stress corrosion cracking. Maximum stresses appear after 150 h near the rim stiffener and at the transition between the side walls and the bottom. The shear stress in the vessel walls is negligible.

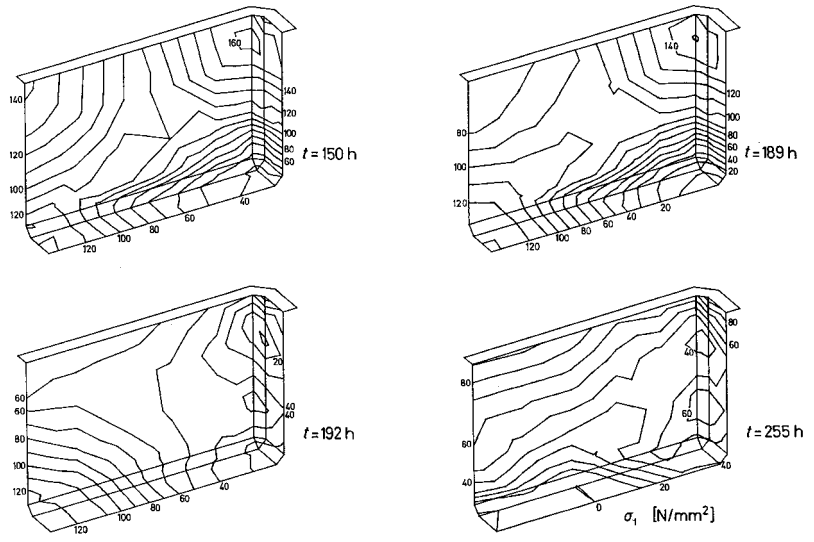

Figure 7.22: Distribution of principal stress σ_1 on the inside of the vessel.

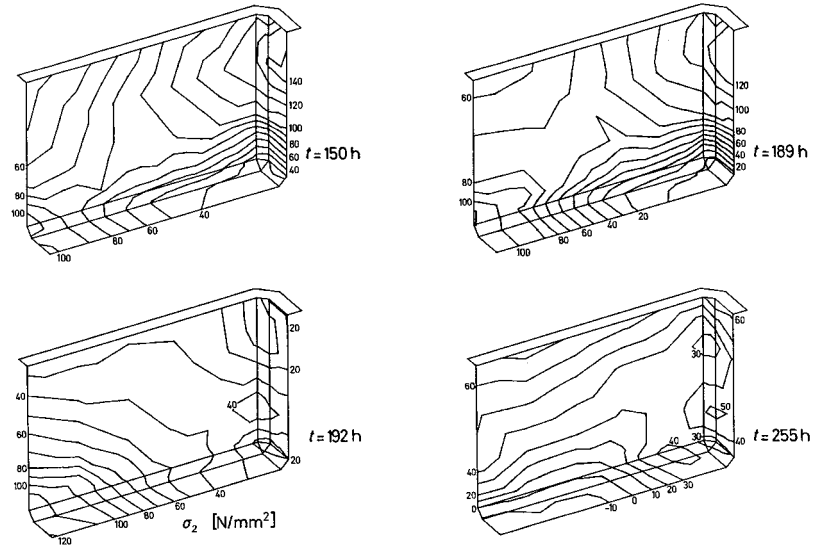

Figure 7.23: Distribution of principal stress σ_2 on the inside of the vessel.

7.7 Creep behaviour of pressure vessel

A thick-walled pressure vessel with spherical end closure (Fig. 7.24) is exposed to internal pressure. The magnitude of the uniformly applied pressure amounts to $p = 445$ psi, which deforms the material below the elasticity

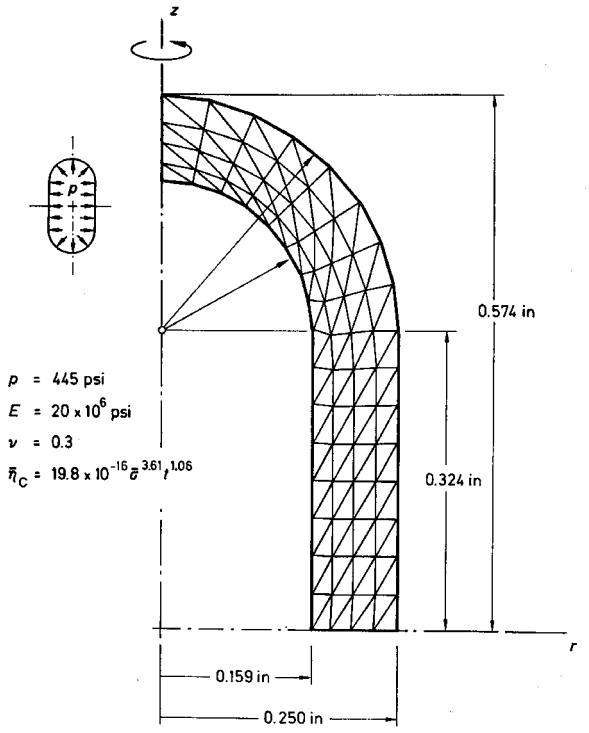

Figure 7.24: Geometry of pressure vessel and finite element model.

limit; plasticity does not arise. The vessel is operated at elevated uniform temperature such that creep strains develop with the passage of time. The study considers the effect of creep on the stress distribution in the material at constant pressure [10].

For the computational analysis the vessel has been discretized by triangular, axisymmetric, six-node finite elements. The finite element layout is shown in Fig. 7.24, and takes advantage of the longitudinal symmetry of the problem. In the present case, the task of inelastic analysis is restricted to the consideration of creep strains as described in Section 6.2. The creep law employed reads

$$\dot{\bar{\eta}}_{\mathrm{C}} = 21 \cdot 10^{-16}\, \bar{\sigma}^{3.61} t^{0.06} = f(\bar{\sigma}, t)$$

and is of the time hardening type, cf. eqn (6.60). Plastic strains as well as thermal strains do not enter the computation.

An elastic solution for the pressure $p = 445\,\mathrm{psi}$ supplies the stress distribution in the vessel as an initial condition to the subsequent incremental computation of the evolving creep strain. In the inelastic investigation the

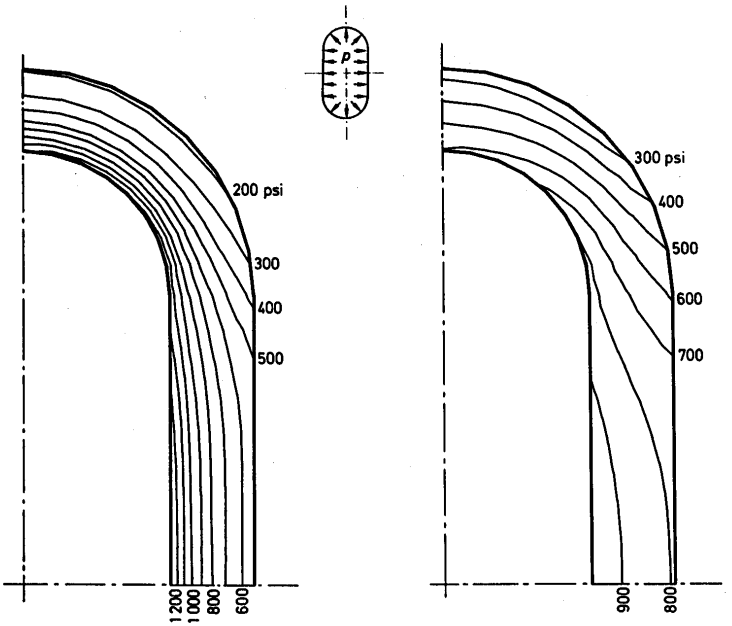

Figure 7.25: Contours of equivalent deviatoric stress $\bar{\sigma}$ for the elastic solution (left) and at stationary creep conditions (right).

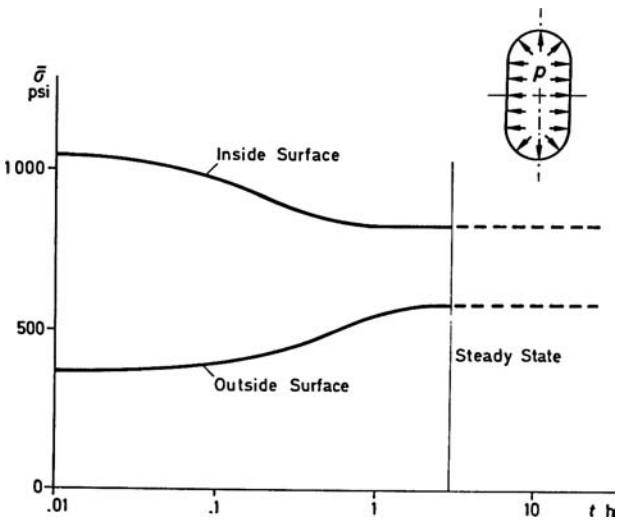

Figure 7.26: Relaxation of stress at the junction of the cylinder and the end closure.

pressure is kept constant while the increments of creep strain are accounted for by initial loads applied consecutively. The time stepping of the creep strain follows the explicit forward scheme.

The results of the numerical analysis are presented in Figs 7.25 and 7.26. Figure 7.25 gives the equivalent stress contours for the elastic solution (start of creep, $t = 0$) and the contours after approximately 3 h of creep. The plots demonstrate the redistribution of the stress as a consequence of creep, resulting in an overall smoothing of the stress pattern. After about 3 h, the stress has reached practically stationary conditions. This is seen in Fig. 7.26, illustrating the variation with time of the equivalent stress at the junction of the cylinder and the spherical end closure.

7.8 Viscoplastic analysis of a thermal shock problem

Emergency cooling in machine parts and nuclear reactor components introduces temporarily high temperature gradients responsible for local stress concentrations and irreversible deformations. The respective structural components are designed so as to sustain several cooling events of this kind in addition to the operational loading. The permanent straining accumulated during repeated cooling shock enbrittles the material and induces extensive cracking (Fig. 7.27).

The following study [13] deals with the thermomechanical processes associated with the local cooling of a metal block at a temperature of 320°C (Fig. 7.28). This configuration was the subject of experimental laboratory tests, where a water jet of 20°C struck the surface of the metal block over a contact area of 10 mm diameter. Evaporation of the water moderates the shock effect. In modelling the thermomechanical problem, it is assumed that the mechanical dissipation does not appreciably modify the development of temperature in the solid and that in the mechanical part inertia effects are negligible, justifying quasistatic analysis.

A description of the problem is given in Fig. 7.28, and the specification of the finite element discretization in Fig. 7.29. The numerical model is reduced to a two-dimensional mesh layout of the mid-plane of a part of the block,

Figure 7.27: Crack pattern after 22,000 thermal shock cycles.

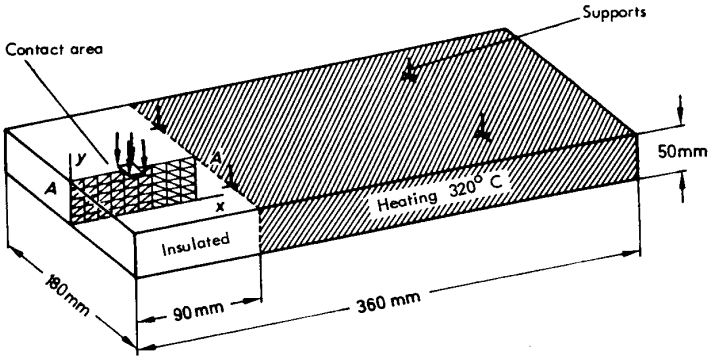

Figure 7.28: Description of the thermal shock problem.

while the effect of the remaining portions is substituted by appropriate boundary conditions for the temperature, that is, the stress analysis. A first computation performs the numerical simulation of the thermal process considering heat transfer to the surrounding air as well as to the water vapour. Without going into details of the thermal analysis, we only mention that the transient process has been traced incrementally up to a time of 1200 s with time steps increasing gradually from 0.002 s at the beginning to 1 s, 10 s and ultimately 600 s. After 10 s, no appreciable variations in temperature occurred, which signifies that stationary conditions are achieved rather quickly. The stationary temperature distribution is plotted in Fig. 7.30 for the analysed mid-section below the area impinged by the water jet.

The second part of the computation performs the transient stress analysis with the obtained temperature history as an input. The assumption of plane strain is taken here as an upper bound to the three-dimensional state of stress. The thermoelastic properties of the material depend on the

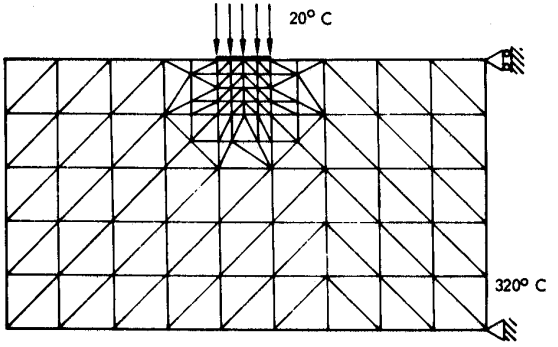

Figure 7.29: Finite element model of the mid-cross-section.

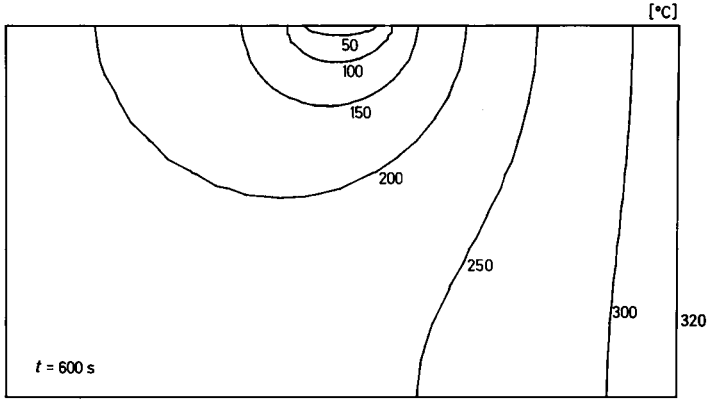

Figure 7.30: Contour plot of temperature in the cross-section at steady state ($t = 600\,\mathrm{s}$).

temperature and are as specified in Section 7.5. The hardening characteristic also depends on the temperature (Fig. 7.31). Although the functional dependence is as for the material referred to in Section 7.5, the elasticity limit is now higher by 74% and the ultimate stress by 41%.

Since the present material exhibits rate dependence, the inelastic response is modelled by the viscoplastic approach described in Section 6.3. The time rate of the equivalent viscoplastic strain is given by the relation

$$\dot{\bar{\eta}}_{\mathrm{V}} = \frac{1}{\bar{\mu}} \frac{\bar{\sigma} - \sigma_{\mathrm{f}}(\bar{\eta}_{\mathrm{V}}, T)}{\sigma_{\mathrm{f}}(\bar{\eta}_{\mathrm{V}}, T)},$$

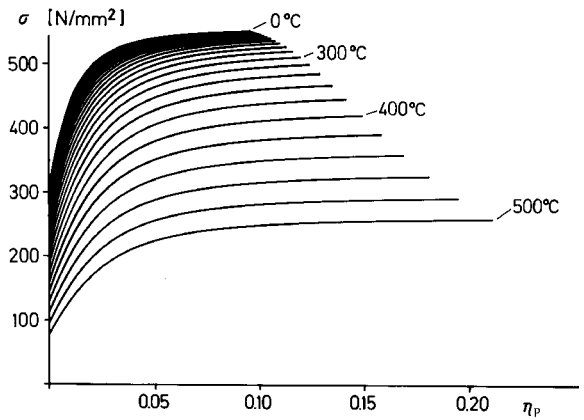

Figure 7.31: Plastic hardening characteristic of the material at different temperatures.

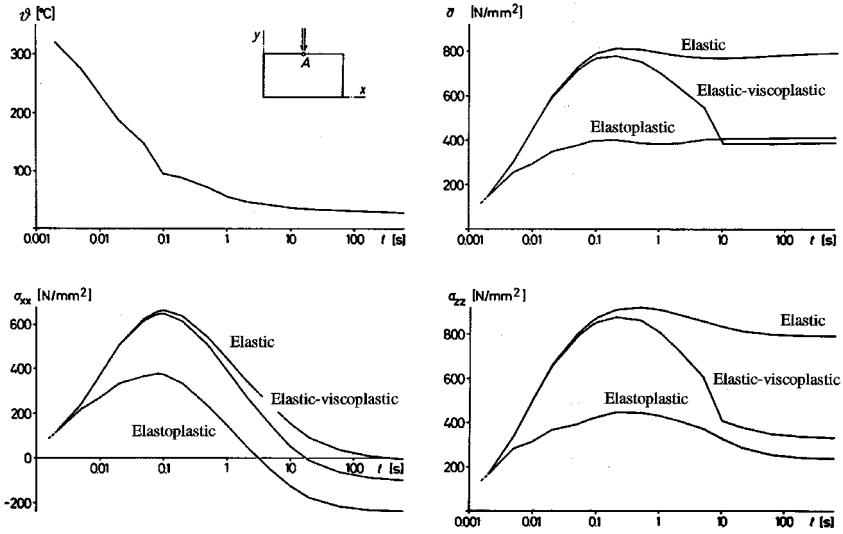

Figure 7.32: Temporal variation of temperature and stress at point A.

where the flow stress $\sigma_{\mathrm{f}}(\bar{\eta}_{\mathrm{V}}, T)$ follows the diagram in Fig. 7.31. Complete specification of the material model requires knowledge of the coefficient $\bar{\mu}$. This parameter is determined from the expression for $\dot{\bar{\eta}}_{\mathrm{V}}$ by utilizing the information that in the tensile test a 25% increase of the static yield stress to $\sigma = 1.25\sigma_{\mathrm{f}}$ is observed at the strain rate $\dot{\eta}_{\mathrm{V}} = 1.08 \cdot 10^{-2}\,\mathrm{s}^{-1}$. Therefore, $\bar{\mu} = (0.25/1.08)10^2\,\mathrm{s} = 23.148\,\mathrm{s}$.

The stress distribution due to the transient temperature field is traced numerically up to the appearance of stationary conditions. The incrementation of the viscoplastic strain is performed by the explicit forward scheme. Since the overstress governing the evolution of viscoplastic strain diminishes to zero as stationary conditions approach, the incremental time step is increased accordingly. As a result of the incremental computation, Fig. 7.32 indicates the development of the stresses at the central point of the impingement of the water jet. The viscoplastic solution is compared with the elastic and the plastic ones. At the beginning of the sudden cooling process, the viscoplastic stresses develop close to the elastic stress state. The two solutions diverge as inelastic deformation progresses. At the end of the transient process the plastic solution does not reproduce the stationary state of the viscoplastic response except (approximately) for the equivalent deviatoric stress $\bar{\sigma}$. As a matter of fact, the equivalent deviatoric stress is bounded by the flow stress of the material in both cases, but $\sigma_{\mathrm{f}}(\bar{\eta}, T)$ is not the same in the two solutions because the evolution of the inelastic strain differs. This is documented in Fig. 7.33. As a consequence of the difference in permanent strain, the individual stress components deviate markedly for plastic and viscoplastic response.

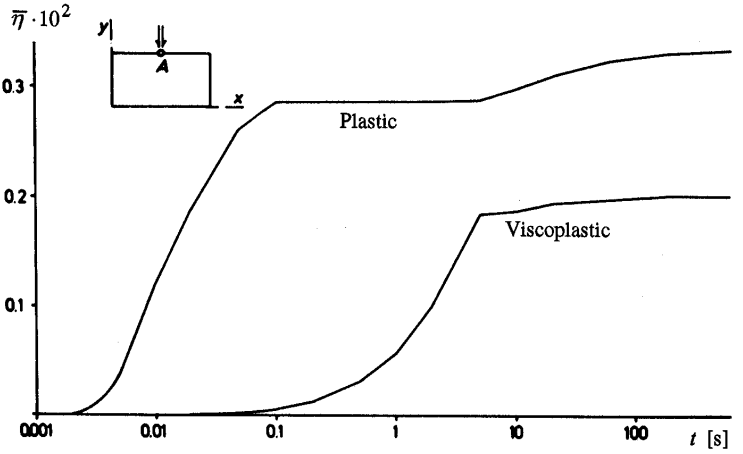

Figure 7.33: Development of the equivalent inelastic strain at impingement point A.

A contour plot of the equivalent deviatoric stress for the elastic–viscoplastic model is given in Fig. 7.34 at the instant of maximum stress ($t = 0.2\,\mathrm{s}$) and in Fig. 7.35 at steady state ($t = 600\,\mathrm{s}$). It is seen that the steep stress gradient formed at the location of the impingement is smoothed out with progressing viscoplastic deformation in the passage of time.

The study allows some conclusions to be drawn regarding the design of mechanical components subject to thermal shock. The comparison with the viscoplastic analysis shows that the elastic approach overestimates the stress

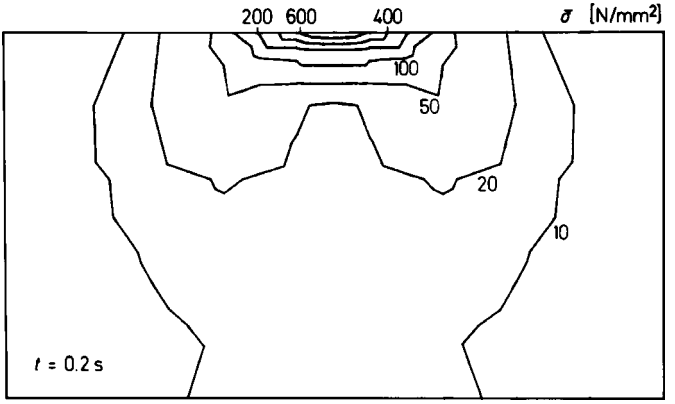

Figure 7.34: Elastic–viscoplastic approach: contour plot of the equivalent deviatoric stress at $t = 0.2\,\mathrm{s}$ (highest values attained).

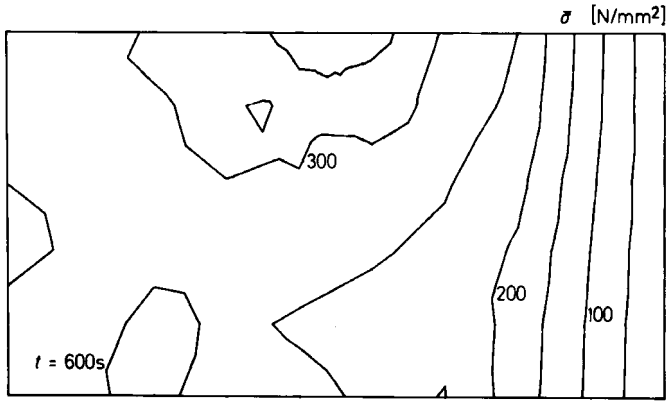

Figure 7.35: Elastic–viscoplastic approach: contour plot of the equivalent deviatoric stress at $t = 600\,\mathrm{s}$ (stationary conditions).

and is therefore conservative for design relying on a maximum stress criterion. Plasticity, on the other hand, overestimates the inelastic deformation and is conservative for design based on maximum strain.

7.9 Dynamic response of a beam under impact loading

The simply supported beam ($4 \times 0.32 \times 0.32\,\mathrm{m}^3$) described in Fig. 7.36 is subjected to impact loading by a vertical force $P(t)$ applied at mid-length. The short time pulse acts over a period of $T_0 = 0.1\,\mathrm{s}$, the temporal variation of the impact force simulating aircraft crash. The initial increase up to the lower level of the loading is associated with the impact of the deformable fuselage. The second, higher level is a consequence of the retarded impact of less flexible parts, like the engines.

The beam is made of steel-reinforced concrete exhibiting a rather complex inelastic behaviour, demonstrated by the bending moment–curvature diagram in Fig. 7.37. Laboratory measurements indicate a slight dependence of the response on the rate of loading, but a preliminary exploration relies on the simplifying assumption of an elastic–perfectly plastic overall behaviour of the beam in bending [14]. The elastic properties of the beam cross-section and the material density are specified as

$$EI = 5863.6\,\mathrm{kNm}^2 \quad \text{and} \quad \varrho = 2.4 \cdot 10^3\,\mathrm{kgm}^{-3}.$$

Taking advantage of the symmetry, half of the problem is discretized by two beam elements (Figs 7.38 and 7.41). The dynamic response of the beam to the pulse loading is traced by an incremental time integration of the equation of motion for the discretized system. The results of the computation are plotted in Figs 7.39 and 7.40, comparing the elastic–perfectly

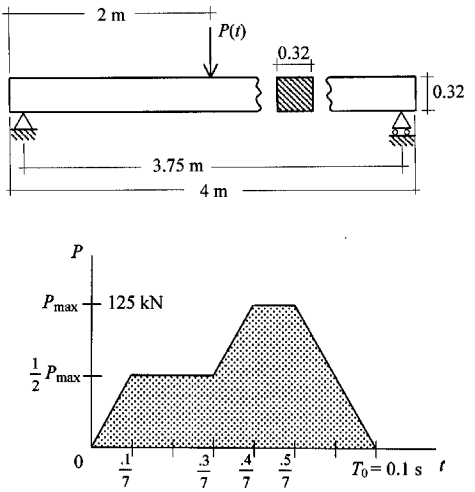

Figure 7.36: Simply supported beam subjected to impact loading.

plastic response to the purely elastic behaviour. Figure 7.39 displays the deflection at the mid-point of the beam where the impact force acts. After the passage of the pulse, the elastic beam is seen to undergo free vibrations following the natural frequency of the system. The plastic beam continues to deform after the passage of the pulse, elastic vibrations setting in subsequently. They occur with respect to the new position of rest attained by the preceding permanent deflection of the beam. As seen in Fig. 7.40, the bending moment opposed to the motion follows the bending deformation of the elastic beam, whereas the perfectly plastic approach restricts the value of the bending moment independently of the deformation. The study also reveals that the initial assumption of small deflections is not justified.

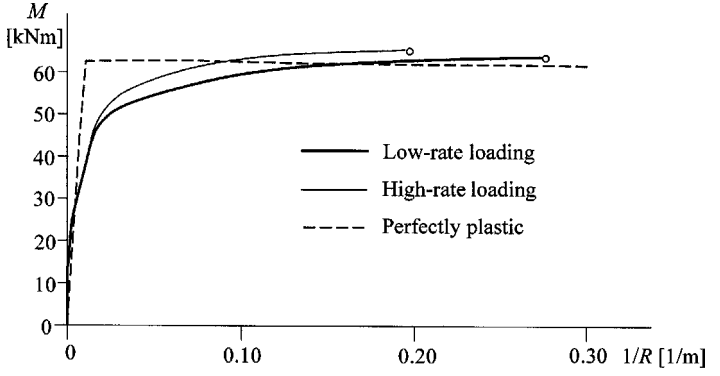

Figure 7.37: Bending moment–curvature diagrams from laboratory data, and elastic–perfectly plastic simplification.

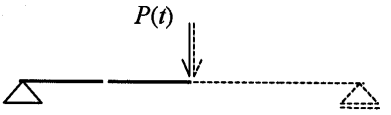

Figure 7.38: Discretized representation of half of the symmetric beam by two elements.

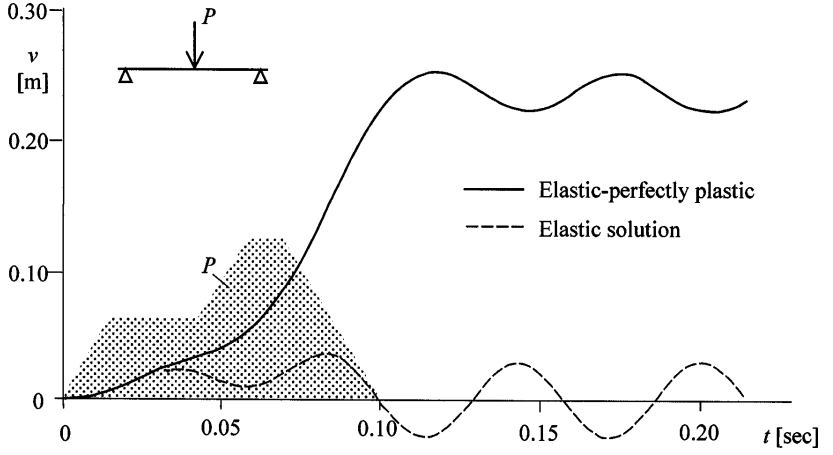

Figure 7.39: Deflection at mid-length of the impacted beam.

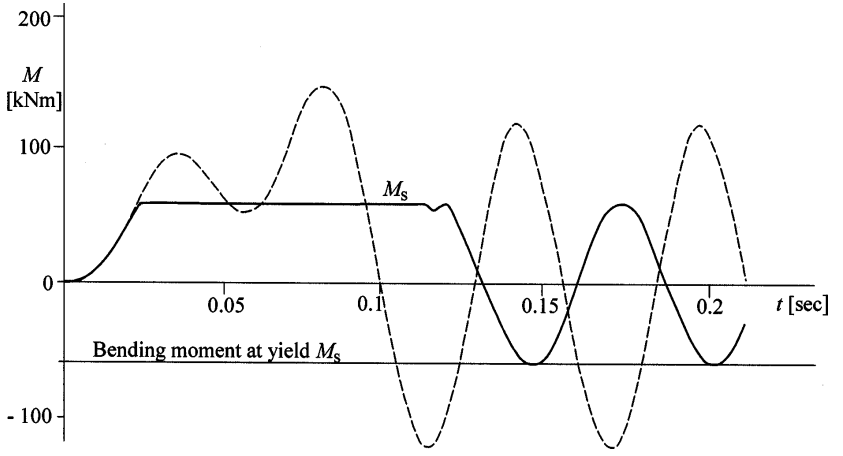

Figure 7.40: Bending moment at mid-length of the impacted beam.

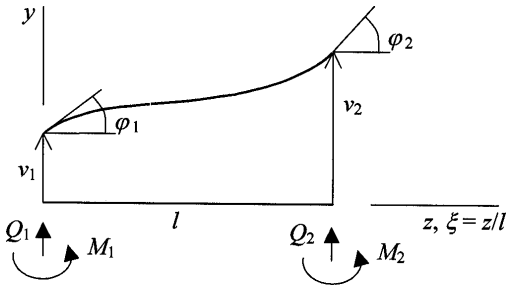

Figure 7.41: Definition of beam element.

The beam element in Fig. 7.41 bends in the z, y-plane following the symmetry of the cross-section. Ignoring the influence of shearing, its deformation is defined by the deflection $v(z)$, which determines the rotation angle φ and the curvature $1/R$. For small rotations,

$$\varphi = \frac{\mathrm{d}v}{\mathrm{d}z} = \frac{1}{l}\frac{\mathrm{d}v}{\mathrm{d}\xi}, \quad \frac{1}{R} = \frac{\mathrm{d}^2 v}{\mathrm{d}z^2} = \frac{1}{l^2}\frac{\mathrm{d}^2 v}{\mathrm{d}\xi^2},$$

and $\xi = z/l$ is a normalized distance along the axis.

Representation of the deformation of the beam by the deflections v_1, v_2 and the rotations φ_1, φ_2 at the end points defines a third-degree Hermitean polynomial for the variation of v along the beam axis

$$v(\xi) = \omega_1(\xi)v_1 + \omega_2(\xi)l\varphi_1 + \omega_3(\xi)v_2 + \omega_4(\xi)l\varphi_2.$$

The distribution functions are

$$\omega_1 = 1 - 3\xi^2 + 2\xi^3, \quad \omega_2 = \xi - 2\xi^2 + \xi^3, \quad \omega_3 = 3\xi^2 - 2\xi^3, \quad \omega_4 = -\xi^2 + \xi^3.$$

The kinematics of the beam element can be summarized in matrix form as follows:

$$\begin{bmatrix} v \\ \varphi \\ 1/R \end{bmatrix} = \begin{bmatrix} \omega_1 & \omega_2 l & \omega_3 & \omega_4 l \\ \omega_1'/l & \omega_2' & \omega_3'/l & \omega_4' \\ \omega_1''/l^2 & \omega_2''/l & \omega_3''/l^2 & \omega_4''/l \end{bmatrix} \begin{bmatrix} v_1 \\ \varphi_1 \\ v_2 \\ \varphi_2 \end{bmatrix}, \tag{i}$$

where $\omega_i' = \mathrm{d}\omega_i/\mathrm{d}\xi$, $\omega_i'' = \mathrm{d}^2\omega_i/\mathrm{d}\xi^2$ $(i = 1, \ldots, 4)$.

The static quantities corresponding to v_1, v_2 and φ_1, φ_2 are the lateral forces Q_1, Q_2 and bending moments M_1, M_2 at the end points of the beam, respectively. For moment equilibrium,

$$Q_1 = -Q_2 = \frac{M_1 + M_2}{l},$$

while the bending moments in the elastic range are

$$M_1 = -\frac{EI}{R_1}, \quad M_2 = \frac{EI}{R_2}.$$

The quantity EI represents the flexural stiffness of the beam in the plane of bending, I denoting the moment of inertia of the cross-section.

The matrix relation between stress resultants at the end cross-sections of the beam and the kinematic quantities reads

$$\underbrace{\begin{bmatrix} Q_1 \\ M_1 \\ Q_2 \\ M_2 \end{bmatrix}}_{\mathbf{S}_q} = \frac{EI}{l} \begin{bmatrix} -1 & 1 \\ -l & 0 \\ 1 & -1 \\ 0 & l \end{bmatrix} \begin{bmatrix} 1/R_1 \\ 1/R_2 \end{bmatrix} = \underbrace{\frac{2EI}{l^3} \begin{bmatrix} 6 & 3l & -6 & 3l \\ 3l & 2l^2 & -3l & l^2 \\ -6 & -3l & 6 & -3l \\ 3l & l^2 & -3l & 2l^2 \end{bmatrix}}_{\mathbf{k}_q} \underbrace{\begin{bmatrix} v_1 \\ \varphi_1 \\ v_2 \\ \varphi_2 \end{bmatrix}}_{\mathbf{U}_q}.$$

The last relationship takes account of the element kinematics,

$$\begin{bmatrix} 1/R_1 \\ 1/R_2 \end{bmatrix} = \frac{2}{l^2} \begin{bmatrix} -3 & -2l & 3 & -l \\ 3 & l & -3 & 2l \end{bmatrix} \begin{bmatrix} v_1 \\ \varphi_1 \\ v_2 \\ \varphi_2 \end{bmatrix},$$

and defines the elastic stiffness matrix $\mathbf{k}_q$ of the beam element.

In the elastoplastic regime the bending moment–curvature diagram (Fig. 7.37) suggests the relation

$$M = EI\left(\frac{1}{R} - \frac{1}{R_\mathrm{p}}\right),$$

where $1/R_\mathrm{p}$ denotes the residual curvature due to permanent deformation. It gives rise to the initial loads

$$\mathbf{J}_q = \begin{bmatrix} J_{\mathrm{Q}1} \\ J_{\mathrm{M}1} \\ J_{\mathrm{Q}2} \\ J_{\mathrm{M}2} \end{bmatrix} = -\frac{EI}{l} \begin{bmatrix} -1 & 1 \\ -l & 0 \\ 1 & -1 \\ 0 & l \end{bmatrix} \begin{bmatrix} 1/R_{\mathrm{p}1} \\ 1/R_{\mathrm{p}2} \end{bmatrix},$$

which have to be superposed to the previously defined stress resultants:

$$\mathbf{S}_q = \mathbf{k}_q \mathbf{U}_q + \mathbf{J}_q.$$

The evolution of permanent deformation is modelled as for plastic flow. The yield condition reads

$$\phi = \bar{M} - M_\mathrm{f} \leq 0.$$

Here $\bar{M} = |M|$, and the yield moment M_f of the cross-section is assumed to be a function of the accumulated magnitude of permanent curvature $\overline{R_\mathrm{p}^{-1}}$:

$$\mathrm{d}M_\mathrm{f} = H\mathrm{d}(\overline{R_\mathrm{p}^{-1}}).$$

From the consistency condition $\phi = 0$ during plastic flow, and with the flow rule in the form

$$\mathrm{d}(R_\mathrm{p}^{-1}) = \frac{M}{\bar{M}}\mathrm{d}(\overline{R_\mathrm{p}^{-1}}),$$

we obtain

$$\mathrm{d}(R_{\mathrm{p}}^{-1}) = \frac{1}{H}\mathrm{d}M = \frac{EI}{EI+H}\mathrm{d}(R^{-1}).$$

The first expression reflects hardening cross-section with the parameter $H > 0$. The second expression also encompasses the non-hardening case $H = 0$, as in the present application. It defines an increment of fictitious bending moment $\mathrm{d}M^* = EI\mathrm{d}(R^{-1})$, associated with the change in curvature $\mathrm{d}(R^{-1})$ of the beam.

For finite transitions, $n \to n+1$, the incremental permanent deformation can be derived from the yield condition $\phi_{n+1} = 0$ as

$$(R_{\mathrm{p}}^{-1})_\Delta = \frac{M_{n+1}}{\bar{M}_{n+1}}\frac{\bar{M}_{n+1} - M_{\mathrm{f}n}}{H} = \frac{M^*_{n+1}}{\bar{M}^*_{n+1}}\frac{\bar{M}^*_{n+1} - M_{\mathrm{f}n}}{EI+H}. \qquad \text{(ii)}$$

The test quantities are from

$$M^*_{n+1} = M_n + EI(R^{-1})_\Delta, \quad M_{n+1} = M^*_{n+1} - EI(R_{\mathrm{p}}^{-1})_\Delta,$$

in full correspondence with previous definitions for stresses (Section 5.4.4). The differences in eqn (ii) must be greater than zero or vanish, in accordance with the condition for plastic loading. The quantities $M_{n+1}/\bar{M}_{n+1}$, $M^*_{n+1}/\bar{M}^*_{n+1}$ define the sign of the incremental permanent deformation.

Instead of the employed semi-direct technique, the stiffness matrix of the beam element in the elastic range could have been obtained by a formal application of the finite element method. This will be exemplified for the element mass matrix in the following. Local motion of the beam is described collectively for the cross-section by the generalized displacements v and φ. They are associated with the translational mass $\varrho A\mathrm{d}z$ and rotational mass $\varrho I\mathrm{d}z$, respectively, over the length $\mathrm{d}z$ (cross-section area A, moment of inertia I). The inertia forces are locally

$$\left(\mathbf{m}'\mathrm{d}z\right)\ddot{\mathbf{u}} = \varrho\begin{bmatrix} A & \\ & I \end{bmatrix}\begin{bmatrix} \ddot{v} \\ \ddot{\varphi} \end{bmatrix}\mathrm{d}z, \qquad \mathbf{u} = \begin{bmatrix} v \\ \varphi \end{bmatrix},$$

and from the virtual work equivalence for the element

$$\underset{\sim}{\mathbf{U}}{}^{\mathrm{t}}_q\mathbf{m}_q\ddot{\mathbf{U}}_q = \int_{l_q}\underset{\sim}{\mathbf{u}}{}^{\mathrm{t}}\mathbf{m}'\ddot{\mathbf{u}}\mathrm{d}z, \qquad \mathbf{U}_q = \{\mathbf{u}_1\mathbf{u}_2\}_q.$$

Employing the element kinematics, eqn (i), in the form $\mathbf{u} = \boldsymbol{\omega}\mathbf{U}_q$ the mass matrix of the beam is obtained as

$$\mathbf{m}_q = \int_{l_q}\boldsymbol{\omega}^{\mathrm{t}}\mathbf{m}'\boldsymbol{\omega}\mathrm{d}z = l\int_0^1\boldsymbol{\omega}^{\mathrm{t}}(\xi)\mathbf{m}'\boldsymbol{\omega}(\xi)\mathrm{d}\xi.$$

The matrix $\boldsymbol{\omega}$ collects the interpolation functions for the displacements $\mathbf{u} = \{v\,\varphi\}$ or equally for their time derivatives in terms of the normalized coordinate ξ.

In the present example some attention must be paid to the parts of the beam extending over the supports (Fig. 7.36). These parts can be omitted in the static solution, but they add to the inertia. They are accounted for by suitably modifying the rotational mass at the supported points. This completes the description of the discretized representation of the impacted beam. The incremental integration of the resulting equations of motion follows the lines of Section 6.4.2.

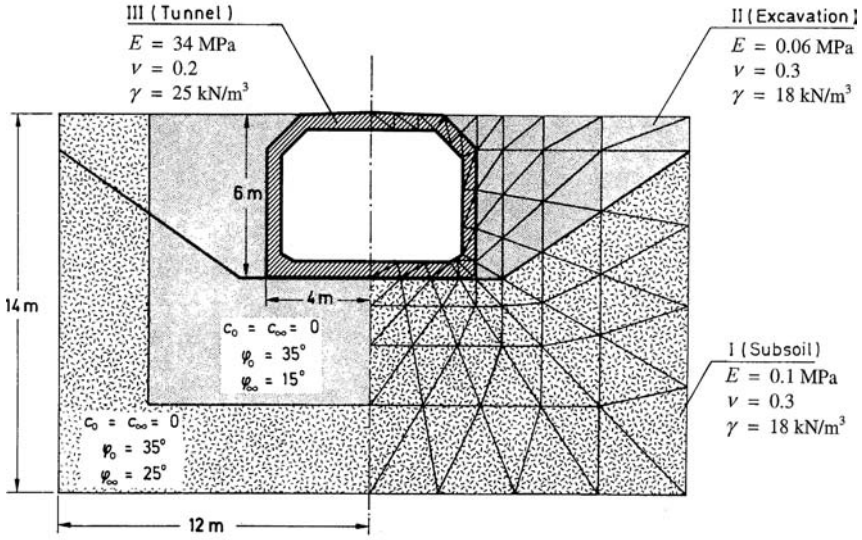

Figure 7.42: Cross-section of a traffic tunnel: definition of the problem, finite element representation and material parameters.

7.10 Soil stresses connected with the construction and operation of a traffic tunnel

This application refers to an actual case taken from geo-engineering practice [12]. It demonstrates the employment of elastoplastic analysis in soil mechanics in conjunction with the Mohr–Coulomb hypothesis of failure. The particular task to be investigated concerns the states of stress in the soil surrounding the tunnel. A description of the problem is shown in Fig. 7.42. The construction of the tunnel essentially consists of the following stages to be simulated consecutively. After excavating the soil at the site, the tunnel is constructed on the subsoil and the space remaining on both sides of the tunnel is filled up with soil. Subsequently, the top of the tunnel and the soil surface are subjected to pressure, and the traffic through the tunnel is started. Although the actual load due to traffic can be neglected, the ensuing vibrations effect a reduction of the soil friction, and thus induce a redistribution of the stress. Once stationary conditions have been attained, the surface pressure is removed.

The elastoplastic problem is considered two-dimensional under the condition of plane strain. Figure 7.42 shows the discretization mesh selected for the investigated configuration; the finite element type employed is a triangle with six nodes. The separation into substructures facilitates handling the removal and addition of material. For the purpose of an elementary demonstration of the numerical solution technique, the problem has been kept

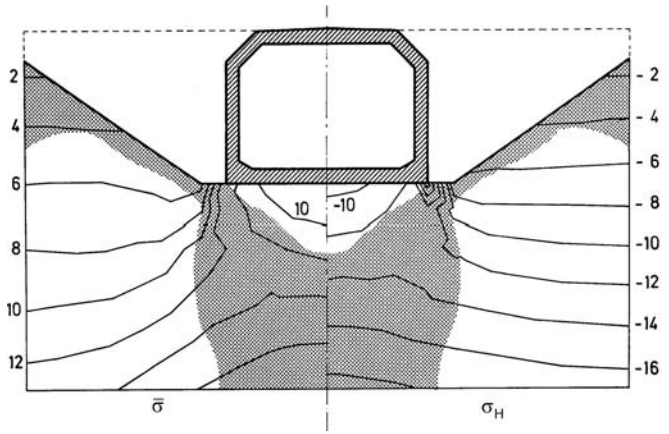

Figure 7.43: Stress state in the subsoil and yield region due to the weight of the tunnel (σ in 10^4 Pa).

intentionally within limits. Aside from the coarseness and reduced extent of the finite element mesh, the experienced engineer will also notice the omission of certain transition zones between the concrete tunnel and the surrounding soil.

The material constants for the different domains and stages of construction are specified in Fig. 7.42. The cohesion coefficient c and angle of internal friction φ define the Mohr–Coulomb condition of failure, which is approached by a plasticity model via the Drucker–Prager linear generalization (Section 6.5.2). For this purpose the constants of the model have to be related to the parameters c and φ. In the present case of plane strain, the relation is as given in Section 6.5.2.

Originally, the soil carries the stresses

$$\sigma_{zz} = -\gamma z, \quad \sigma_{xx} = \sigma_{yy} = \lambda \sigma_{zz}$$

due to its own weight. Here, γ denotes the specific weight of the soil material; the vertical z-coordinate, measured from the ground level, is positive when pointing downwards. For lack of better information the lateral earth pressure coefficient λ is taken as

$$\lambda = \frac{\nu}{1-\nu}.$$

The above stress distribution gives rise to equivalent loads at the nodal points of the finite element mesh simulating the dead weight. This is the only load acting on the subsoil remaining just after the excavation (Substructure I). The additional load applied subsequently due to the weight of the tunnel (Substructure III) induces inelastic deformation (Fig. 7.43). In the third

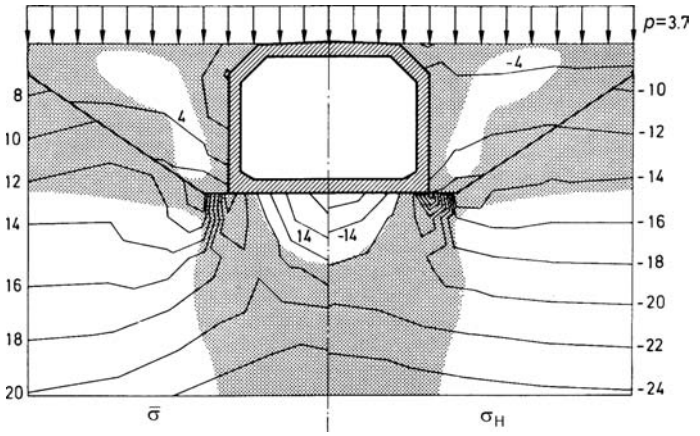

Figure 7.44: State of stress (in 10^4 Pa) and yield region after application of surface pressure $p = 3.7 \cdot 10^4$ Pa.

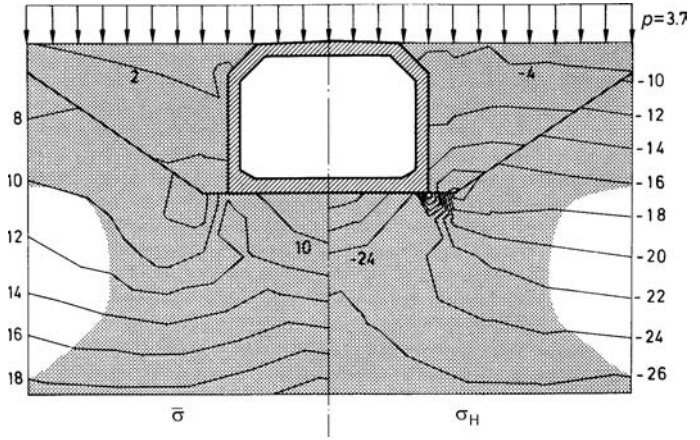

Figure 7.45: Distribution of stress (in 10^4 Pa) and yield region after reduction of the soil friction ($\varphi_0 \to \varphi_\infty$) under constant load.

stage of the numerical simulation, the empty space on both sides of the tunnel (Substructure II) is refilled with soil.

The fourth, fifth and sixth stages are concerned with the application of the surface pressure (Fig. 7.44), the reduction of the soil friction (angle φ) at constant load (Fig. 7.45) and the removal of the surface pressure. Thereby, material is neither added nor taken away. The results of the computational analysis shown in Figs 7.43–7.45 comprise plots of the distribution of the deviatoric equivalent stress $\bar{\sigma}$ and of the hydrostatic stress σ_H. Also depicted are the regions of permanent deformation in the soil. Figure 7.45 shows

that handling the graphical representation of the stress individually within substructures leads to discontinuities along the boundaries which are pronounced because of the coarse finite element discretization.

References

[1] O.C. Zienkiewicz, S. Valliapan and I.P. King, Elasto-plastic solution of engineering problems, initial stress, finite element approach, *Int. J. Numer. Meths Engng* **1** (1969) 75–100.

[2] J.H. Argyris and D.W. Scharpf, Methods of elastoplastic analysis, *ZAMP* **23** (1972) 517–551.

[3] H. Balmer, I.St. Doltsinis and M. König, Elastoplastic and creep analysis with the ASKA program system, *Comput. Meths Appl. Mech. Engng* **3** (1974) 87–104.

[4] J.C. Nagtegaal, D.M. Parks and J.R. Rice, On numerically accurate finite element solutions in the fully plastic range, *Comput. Meths Appl. Mech. Engng* **4** (1974) 153–177.

[5] R.L. Taylor and O.C. Zienkiewicz, Mixed finite element solution of fluid flow problems, in *Finite Elements in Fluids*, Vol. 4, R.H. Gallagher *et al.* (Eds), Wiley, New York, 1982.

[6] J. Argyris and H.-P. Mlejnek, *Die Methode der Finiten Elemente*, Vol. I, Friedrich Vieweg, Braunschweig, 1987.

[7] I.St. Doltsinis and S. Nölting, Generation and decomposition of finite element models for parallel computations, *Comput. Systems Engng* **2**(1992) 427–449.

[8] I.St. Doltsinis, Solution of coupled problems by distinct operators, *Engng Comput.* **14** (1997) 829–868.

[9] I.St. Doltsinis (Ed.), *Stochastic Analysis of Multivariate Systems in Computational Mechanics and Engineering*, CIMNE, Barcelona, 1999.

[10] J.H. Argyris, H. Balmer and I.St. Doltsinis, Material non-linearities in the finite element analysis, ISD-Lecture held at Jablonna, Poland (Polish Academy of Sciences, Institute of Fundamental Technological Research), September 22–28, 1974, ISD-Report no. 174, Stuttgart, 1974.

[11] I.St. Doltsinis and H. Wüstenberg, Festigkeitsberechnungen bei inelastischem Verhalten und zeitabhängiger thermischer und mechanischer Belastung, ISD-Report no. 238, Stuttgart, 1978.

[12] H.A. Balmer and I.St. Doltsinis, Extensions to the elastoplastic analysis with the ASKA program system, *Comput. Meths Appl. Mech. Engng* **13** (1978) 363–402.

[13] J.H. Argyris, I.St. Doltsinis and K.J. Willam, New developments in the inelastic analysis of quasistatic and dynamic problems, *Int. J. Numer. Meths Engng* **14** (1979) 1813–1850.

[14] I.St. Doltsinis and G. Frik, A Numerical study of beam under pulse loading, Internal Report, ISD, Stuttgart, 1976.

Index

This page intentionally left blank

This page intentionally left blank

Tribology and Design

Edited by: ***M. HADFIEL,*** *Bournemouth University, UK,* ***C.A. BREBBIA****, Wessex Institute of Technology, UK and* ***J. SEABRA,*** *University of Porto, Portugal*

Tribology and Design 2010 is the 3rd International Conference in the series which originated with two meetings held at Bournemouth University, UK in 2005 and 2007. The Tribology and Design Conference explores the role of technology and design in the broader sense. It aims to bring together colleagues from different disciplines interested in problems of surface interaction and design. The range of applications covers from geomechanics to nano problems and from sustainability issues to advanced materials. It has never been so important for the designer to consider product and system durability in relation to reliability and sustainability issues. The topics for discussion also cover studies of tribology in nature and how the resulting lessons can be applied by the designers. Another important theme is the application of tribology in biomechanics, a field in which surface mechanics in general is of fundamental importance.

This book contains the papers presented at the Third International Conference, arranged into the following subject areas: Tribology in Space Applications; Reliability in Product Design; Nano-Tribology and Design; Tribology Under Extreme Conditions; Tribology in Geo-Mechanics; Energy Applications; Surface Measurements; Tribology in Biomechanics; Life-Oriented Design; Tribology and Nature; Design Tools; Surface Engineering; Lubricant Design; Test Methods; Advanced Materials; Analytical Studies; Sustainability and Tribology; Product Reliability; Corrosion Problems

WIT Transactions on Engineering Sciences, Vol 66
ISBN: 978-1-84564-440-6 eISBN: 978-1-84564-441-3
Forthcoming / apx400pp / apx£152.00/US$274.00/€198.00

WIT*Press*
Ashurst Lodge, Ashurst, Southampton,
SO40 7AA, UK
Tel: 44 (0) 238 029 3223
Fax: 44 (0) 238 029 2853
E-Mail: witpress@witpress.com

This page intentionally left blank

This page intentionally left blank

This page intentionally left blank

This page intentionally left blank

This page intentionally left blank

This page intentionally left blank

This page intentionally left blank

This page intentionally left blank